Asymmetric Suzuki-Miyaura couplings of acyclic allylic systems

Violeta Stojalnikova

University of Oxford

A thesis presented in partial fulfilment of
the requirements for the award of the degree of
Doctor of Philosophy

Trinity 2023

Author's Declaration

This thesis describes work carried out in the Chemistry Research Laboratory, Oxford, between October 2018 and December 2022 under the supervision of Prof. Stephen Fletcher. The thesis is a result of my own work, except when clearly stated otherwise, and has not been submitted for any other degree at this or any other university.

Violeta Stojalnikova

July 2023

Abstract

The objective of this thesis is to investigate and develop Rh(I)-catalysed Suzuki-Miyaura cross-couplings of acyclic allylic species with arylboronic acids. While our group has achieved an asymmetric Rh-catalyzed Suzuki-Miyaura cross-coupling of cyclic racemic allylic halides and boronic acids, the catalyst-controlled stereoselective coupling of more complex acyclic unsymmetrical molecules has not been explored.

In this thesis, we present our efforts towards the development of a Rh-catalyzed enantioselective Suzuki-Miyaura cross-coupling with racemic acyclic substrates that have few or no symmetry elements. This approach represents an unprecedented advance that significantly broadens the applicability of this reaction.

We discuss the development of an enantioconvergent Suzuki-Miyaura cross-coupling of acyclic allylic systems in Chapter 2, while Chapter 3 explores the asymmetric formation of all-carbon quaternary stereocenters *via* the developed Suzuki-Miyaura cross-coupling of acyclic allylic systems. Additionally, Chapter 4 focuses on Suzuki-Miyaura couplings using terminal acyclic allylic systems and outlines a modular asymmetric synthesis of 3-aryl-α-tetralones *via* sequential double arylation.

Overall, the thesis addresses the challenges associated with synthesising acyclic C(sp^3)-rich compounds using novel asymmetric Suzuki-Miyaura couplings, with the aim of developing more efficient methods for producing enantioenriched small molecules.

Acknowledgements

I would like to thank Professor Stephen P. Fletcher for the opportunity to conduct research in his group and for continuous advice, leadership, understanding, patience, and unwavering support during my time in the lab.

I am grateful to all members of the group for constant guidance and for making my projects enjoyable. Thank you to the Fletcher group for being a supportive, engaging, and collaborative environment.

This thesis builds on the research and methodologies developed by other members of Fletcher group. I would like to express my gratitude to my collaborators, Ke Liu, Stephen Webster, and Callum Martin whose work, help and feedback I have relied on in the course of this research.

Finally, thanks to all my dear friends and loved ones whose support made my DPhil possible. In particular, I'd like to acknowledge my mother Vera, and the people who stood beside me throughout my DPhil, Konstantinos, Alkisti, Elena, Panos, and Radu.

List of Abbreviations

°	degree
4CzIPN	1,2,3,5-tetrakis(carbazol-9-yl)-4,6-dicyanobenzene
δ	chemical shift in ppm
λ	wavelength
μ	micro
ν	wavenumber
AAA	asymmetric allylic alkylation
AAAr	asymmetric allylic arylation
APCI	atmospheric-pressure chemical ionization
aq.	aqueous
Ar	aromatic
BINAP	2,2′-bis(diphenylphosphino)-1,1′-binaphthyl
Boc	tert-butyloxycarbonyl
br.	broad
BTFM	3,5-bis(trifluoromethyl)phenyl
c	centi
C	celsius
cod	cycloocta-1,5-diene
COSY	correlation spectroscopy experiment

d	day(s); doublet
det.	determined
d.r.	diastereomeric ratio
DTBM	3,5-di-*tert*-butyl-4-methoxyphenyl
DYKAT	dynamic kinetic transformation
ee	enantiomeric excess
EI	electron ionization
eq.	equivalent(s)
e.r.	enantiomeric ratio
ESI	electrospray ionization
FC	flash column chromatography
g	gram(s)
GC	gas chromatography
h	hour(s) or hextet
HMBC	Heteronuclear Multiple Bond Correlation experiment
HPLC	high pressure liquid chromatography
HR	high resolution
HSQC	Heteronuclear Single Quantum Coherence experiment
Hz	Hertz
IR	infrared spectroscopy

J	coupling constant (NMR) in Hz
KR	kinetic resolution
L	liter
m	milli; medium; multiplet
M	molar
m.p.	melting point
m/z	mass over charge ratio
min.	minute(s)
MS	mass spectrometry
N	normal
NMR	nuclear magnetic resonance
Ph	phenyl
ppm	parts per million
r.r.	regioisomeric ratio
q	quartet; quaternary
s	strong; singlet
sat.	saturated
SFC	supercritical fluid chromatography
t	triplet
THF	tetrahydrofuran

Tol	4-methylphenyl
Xyl	3,5-dimethylphenyl
vol	volume
w	weak
wt	weight

Table of Contents

Author's Declaration ... iii
Abstract ... iv
Acknowledgements ... v
List of Abbreviations ... vi
1 An introduction to asymmetric Suzuki-Miyaura couplings ... 1
1.1 Role of chirality in the design of biologically relevant molecules ... 2
1.2 Palladium-catalysed asymmetric Suzuki-Miyaura cross-couplings ... 6
1.3 Iridium-catalysed asymmetric Suzuki-Miyaura cross-couplings ... 10
1.4 Nickel-catalysed asymmetric Suzuki-Miyaura cross-couplings ... 12
1.5 Copper-catalysed asymmetric Suzuki-Miyaura cross-couplings ... 17
1.6 Rhodium-catalysed asymmetric Suzuki-Miyaura cross-couplings ... 22
1.7 Conclusions and thesis outline ... 24
2 Enantioconvergent Suzuki-Miyaura cross-coupling of acyclic allylic systems ... 29
2.1 Introduction ... 30
2.1.1 Regioselectivity in Rh-catalysed asymmetric Suzuki-Miyaura couplings ... 30
2.1.2 Additional challenges of using acyclic substrates ... 32
2.1.3 Stereocentres in acyclic molecules ... 32
2.1.4 Project aims ... 35
2.2 Results and Discussion ... 36
2.2.1 Reaction optimisation ... 36
2.2.2 Scope of the enantioconvergent arylation with acyclic substrates ... 43
2.2.3 Product derivatisation ... 49
2.2.4 Mechanistic studies ... 57
2.2.5 Proposed mechanism ... 61
2.2.6 Synthesis of an anticancer agent Lasofoxifene ... 62
2.3 Conclusions ... 64
2.4 Future directions ... 65
2.4.1 Asymmetric Suzuki-Miyaura coupling with vinylboronic acids ... 65
2.4.2 Synthesis of acyclic compounds with three contiguous stereocenters ... 67
2.4.3 Synthesis of chiral indane derivatives ... 69
3 Studies towards asymmetric formation of all-carbon quaternary stereocenters *via* Suzuki-Miyaura cross-coupling of acyclic allylic systems ... 73
3.1 Introduction ... 74

3.1.1 All-carbon quaternary stereocenters in acyclic systems 74
3.1.2 Project aims 75
3.2 Results and Discussion 76
3.2.1 Synthesis of tertiary allylic substrates 76
3.2.2 Preliminary results for Rh-catalysed arylation to form quaternary stereocentres 77
3.2.3 Synthesis of a simplified model substrate 79
3.2.4 Rh-catalysed arylation of a substrate with reduced complexity 79
3.3 Conclusions 85
3.4 Future directions 86
3.4.1 Employing amide as a directing group 86
3.4.2 Sythesis of bioactive substances containing remote quaternary stereocenters 87
4 Modular asymmetric synthesis of 3-aryl-α-tetralones *via* sequential double arylation 91
4.1 Introduction 92
4.1.1 Initial project aims 92
4.1.1 Initial experiments 93
4.1.2 The importance and current syntheses of α-tetralones 94
4.1.1 Revised project aims 98
4.2 Results and Discussion 100
4.2.1 Preparation of primary allylic substrate 100
4.2.1 Rh-catalysed arylation of primary substrate 100
4.2.1 Rh-catalysed arylation using two distinct boron nucleophiles 102
4.2.2 Application in synthesis of biologically active compounds 107
4.3 Conclusions 107
4.4 Future directions 109
4.4.1 Approaches to increasing enantioselectivity 109
4.4.2 Double functionalisation using vinylboronic acids 110
5 Experimental 114
5.1 General Methods 115
5.2 Experimental for Chapter 1 115
5.3 Experimental for Chapter 2 123
5.3.1 Procedures for the synthesis of starting materials 123
5.3.2 Procedures for the rhodium-catalysed reactions 134

5.3.3 Procedures for the product derivatization 183
5.3.4 Reaction optimisation 198
5.3.5 Procedures for the synthesis of substrates for mechanistic studies 201
5.3.6 Mechanistic studies 209
5.4 Experimental for Chapter 3 213
5.4.1 Procedures for the synthesis of the starting materials 213
5.4.2 Procedures for the rhodium-catalysed reactions 220
5.5 Experimental for Chapter 4 222
5.5.1 Procedures for the synthesis of starting materials 222
5.5.2 Procedures for the rhodium-catalysed reactions 224
6 Supplementary Information 237
6.1 NMR spectra 238
6.2 SFC traces 329
7 References 353

1 An introduction to asymmetric Suzuki-Miyaura couplings

1.1 Role of chirality in the design of biologically relevant molecules

Despite significant progress in comprehending disease biology and remarkable technological advancements, developing and introducing new drugs to the market remains a protracted and expensive process. The high cost of drug discovery is primarily due to the high attrition rate in clinical trials.[1] Therefore, it is crucial to develop innovative approaches and revised perspectives on drug discovery to deliver medicines to more patients and at a lower cost.

One such approach that has been extensively used in the past two decades is high-throughput screening (HTS). So far, the scope of easily accessible fragments for HTS has been skewed towards essentially planar molecules that lack three-dimensionality by well-developed and reliable $C(sp^2)$-$C(sp^2)$ couplings[2,3]; Suzuki-Miyaura reaction being dominant in medicinal chemistry. However, the use of $C(sp^2)$-rich (flat) scaffolds as potential drug candidates in the generation of HTS libraries has some disadvantages. Increased molecular planarity (mostly two-dimensional) provides limited shape diversity and less efficient interaction toward a three-dimensional target binding site.[4] Among other disadvantages, molecules with highly planar characteristics tend to pack tightly in a three-dimensional periodic lattice *via* π-stacking, leading to poor aqueous solubility.[5] Also, such compounds are considered metabolically labile as flat structures are prone to unhindered metabolically labile sites.[6]

In recent years, there has been a growing interest in synthesizing $C(sp^3)$-rich compounds as potential pharmaceutical agents. Evidence suggests that $C(sp^3)$-rich compounds have a higher chance of success in clinical trials compared to their $C(sp^2)$-rich counterparts.[7] For example, research has indicated that when small molecules have a higher $C(sp^3)$

count, they exhibit decreased promiscuity and a capacity to inhibit drug metabolizing enzymes such as CYP450.[8]

Furthermore, C(sp^3)-containing compounds can possess chiral centres, leading to differences in efficacy between enantiomers and diastereomers. In some cases, these stereoisomers may exhibit completely different pharmacological properties, making it important to identify and produce the correct stereoisomer in drug development.[9]

As a result, drug discovery endeavours have been focused on integrating C(sp^3) carbon centers to enable more efficient exploration of a greater portion of chemical space and enhance on-target selectivity. A significant proportion of drugs approved by the FDA from 1951 to 2021, specifically over 60%, comprise one or more stereocenters (Figure 1.1).

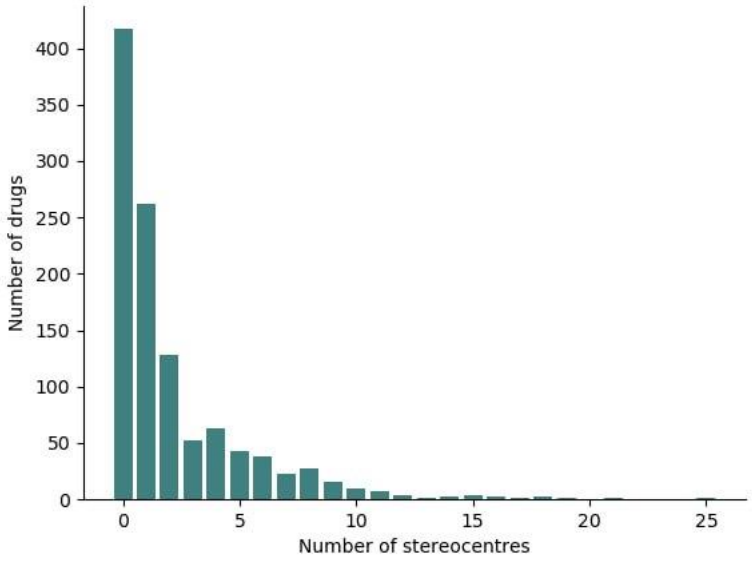

Figure 1.1. A frequency bar plot of the overall number of stereocentres in FDA approved pharmaceutical drugs.[10]

Many of these drugs are derived from natural products or their derivatives, which generally exhibit higher molecular complexity and, on average, contain more stereocenters. In fact, over the years chemical information density, largely arising from chiral centres has increased in FDA approved drugs (Figure 1.2).

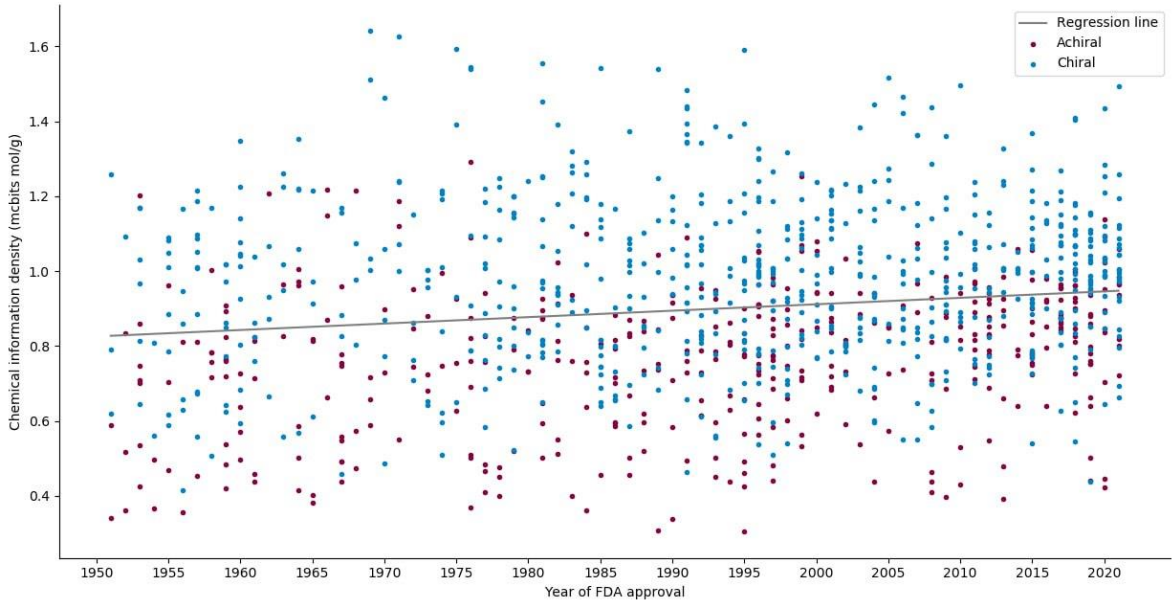

Figure 1.2 A scatter plot representing the change of chemical information density in FDA approved chiral and achiral pharmaceutical drugs over time, with an overall line of best fit. Complex drugs tend to have a high information density, which is primarily due to the presence of multiple stereocenters.[10]

Although it may appear intuitive that chiral drugs generally exhibit higher complexity and have more information density, a more in-depth analysis of the distribution of molecular complexity and information density (both of these measures quantify the complexity of chemical systems[11-13]) based on the number of stereocenters provides distinct evidence of the impact of chirality on molecular complexity and chemical information density in molecules within the dataset of FDA approved drugs (1951-2021).[10] The Bottcher group introduced the concept of molecular complexity[11] (C_m) which is predicated on Shannon's information theory[14], and it is quantified in molecular bits or mcbits. Molecular complexity captures the cumulative impact of the information content in a molecule[12], and small variations in the numerical value of C_m correspond to relatively greater changes in the underlying structural complexity. Typically, larger molecules exhibit higher complexity. Accordingly, to facilitate meaningful comparisons of molecular complexity, it is advantageous to consider molecular weight, and therefore it is recommended to

incorporate molecular weight, and express the result as information density in mcbit mol/g. From the performed analysis, it is clear that as the number of stereocenters increases in drugs so does their molecular complexity and information density (Figure 1.3).

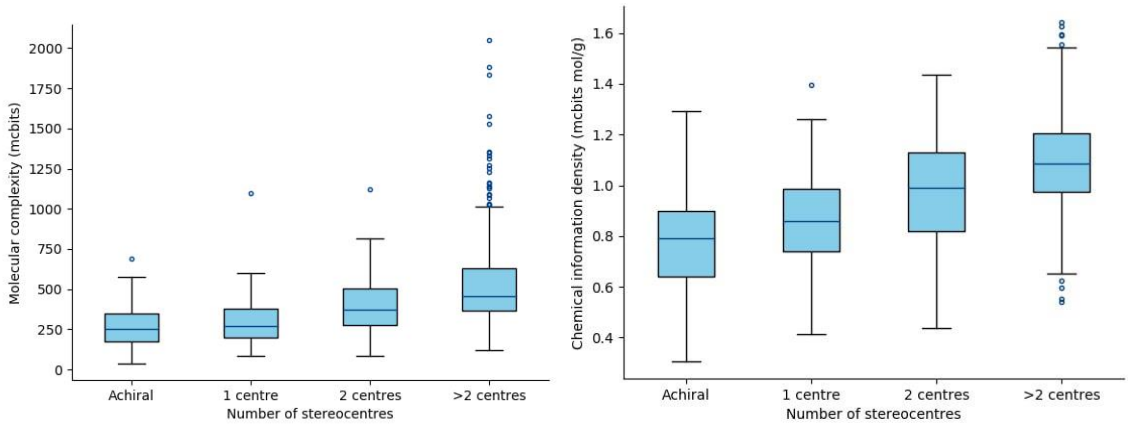

Figure 1.3 A box plot of the distribution of molecular complexity (in mcbits) (left) and chemical information density (in mcbits mol/g) (right) for compounds with different numbers of stereogenic centres. In the provided visualization, the median is depicted by a dark horizontal bar, while the interquartile range (IQR) is represented by a box. The whiskers extend to 1.5 times the IQR, marking the maximum and minimum values. Any dots present in the visualization are considered outliers, as they fall outside of this range on either side of the box.[10]

As such, there is a significant demand for new efficient methods to produce enantioenriched small molecules. In this chapter, we investigate existing methods for the enantioselective production of C(sp^3) chiral centers using asymmetric Suzuki-Miyaura couplings, with the aim of facilitating the efficient enantioselective synthesis of small molecules.

1.2 Palladium-catalysed asymmetric Suzuki-Miyaura cross-couplings

The Suzuki-Miyaura coupling is a crucial carbon-carbon bond-forming reaction, especially for constructing $C(sp^2)$-$C(sp^2)$ bonds (Figure 1.4, a).[15] It finds extensive application in in drug discovery and natural product synthesis due to its broad applicability, high functional group tolerance, and availability of boronic acids.[16]

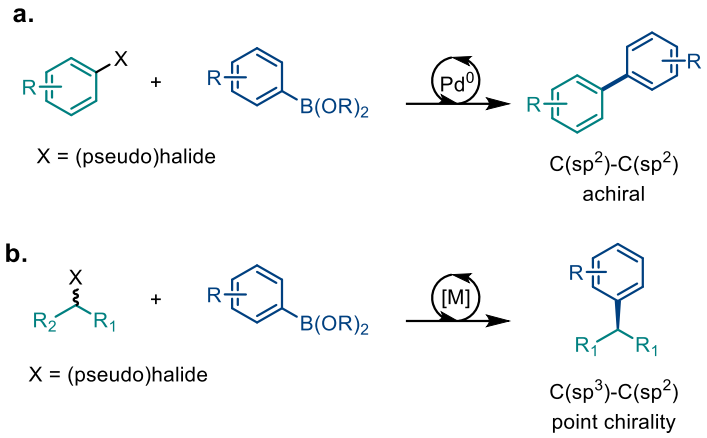

Figure 1.4 A general illustration of Suzuki-Miyaura cross-coupling reactions. a, A $C(sp^2)$-$C(sp^2)$ coupling between two aryl fragments. b, An asymmetric $C(sp^3)$-$C(sp^2)$ Suzuki-Miyaura cross coupling.

As discussed in the previous section, it is widely acknowledged that compounds featuring a higher degree of C-saturation and possessing chiral elements are more likely to succeed throughout the various stages of drug discovery. Accordingly, generating molecules with three-dimensional characteristics has become an area of significant interest in the pharmaceutical industry. Asymmetric versions of Suzuki-Miyaura couplings are therefore advantageous, and below we list efforts towards achieving this goal (Figure 1.4, b).

Palladium-catalyzed cross-coupling reactions have become an essential tool in organic synthesis, providing access to a wide range of valuable compounds. Among these reactions, the coupling of allylic nucleophiles with aryl and alkenyl electrophiles has

received considerable attention due to the potential for the formation of complex and diverse C(sp^3)-rich molecular architectures. Miyaura and colleagues demonstrated a palladium-catalyzed coupling of terminal allylic potassium trifluoroborates with aryl and alkenyl bromides (Figure 1.5). They also achieved an asymmetric version of the reaction using a MandyPhos ligand (L1), which yielded γ-substitution products in good yields, moderate to excellent regioselectivities (depending on the bromide coupling partner), and good enantioselectivities (up to 90% ee).[17] Mechanistic studies on this transformation revealed that the S_N2' transmetalation of the allylboron species to the aryl-palladium complex was followed by fast reductive elimination before any π-σ-π isomerization of the allyl-Pd(II) species could occur.[18] This mechanism accounts for the observed regioselectivity and was supported by experimental and computational studies.

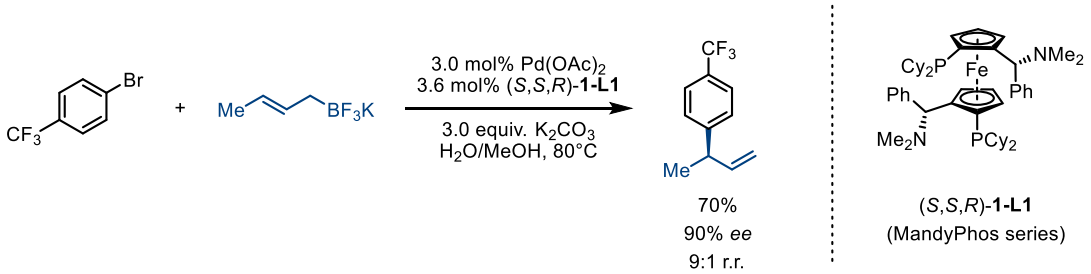

Figure 1.5 Pd-catalysed asymmetric cross-coupling of terminal allylic potassium trifluoroborates couple and aryl bromides.

The Morken research group has made significant contributions to the development of Pd-catalyzed enantioselective cross couplings of allylic electrophiles and allylic boron pinacol esters (Figure 1.6). Notably, the group has demonstrated that the catalytic system consisting of palladium and MeO-furyl-BIPHEP (L2) displays exceptional regioselectivities, good yields and enantioselectivities (87–91% ee) in the cross couplings of terminal allylic electrophiles and allylic boron pinacol esters.[19] The group has also demonstrated that both branched and linear (terminal) allyl carbonates can be employed

in cross-couplings with boron pinacol esters, resulting in the formation of quaternary all-carbon stereocenters.[20,21]

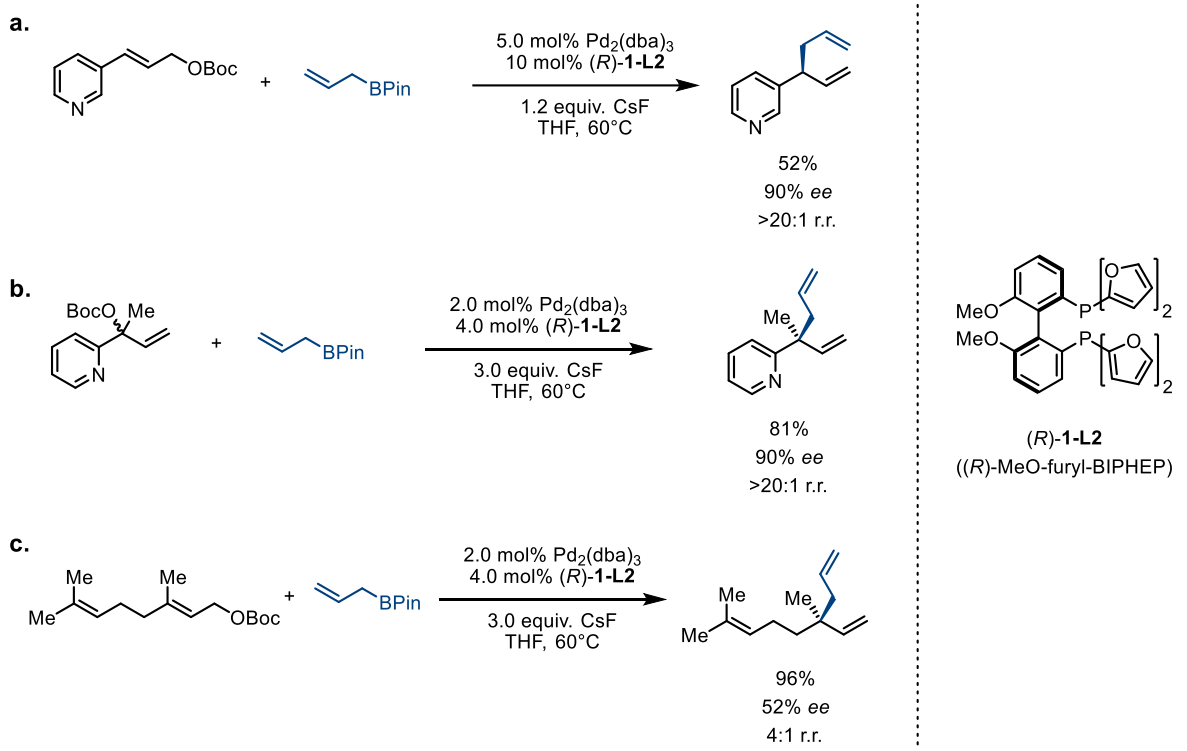

Figure 1.6 a, Pd-catalysed enantioselective cross coupling of terminal allylic electrophiles and allylic boron pinacol esters . b, Asymmetric allyl-allyl cross-coupling furnishing quaternary centres. c, Enantioselective Suzuki-Miyaura cross-coupling of terminal allylic electrophiles and allylic boron pinacol esters yielding quaternary all-carbon stereocenters.

In addition, the Morken group has demonstrated that similar transformations can be carried out in a diastereoselective manner (Figure 1.7), where substitution on the allylboronic ester allows for the introduction of adjacent chiral centers with good diastereocontrol and enantioselectivities ranging from good to excellent.[22] This methodology has potential for wide application in the synthesis of bioactive compounds, as demonstrated by its use in a concise asymmetric total synthesis of (*R*)-cuparenone.

In contrast to Miyaura's mechanistic conclusion, the Morken group proposes that rapid Pd-allyl isomerization occurs prior to the enantiodetermining reductive elimination in

these cross-coupling reactions.[21] These findings contribute significantly to the development of enantioselective cross-coupling reactions and highlight their utility in the synthesis of complex molecular structures.

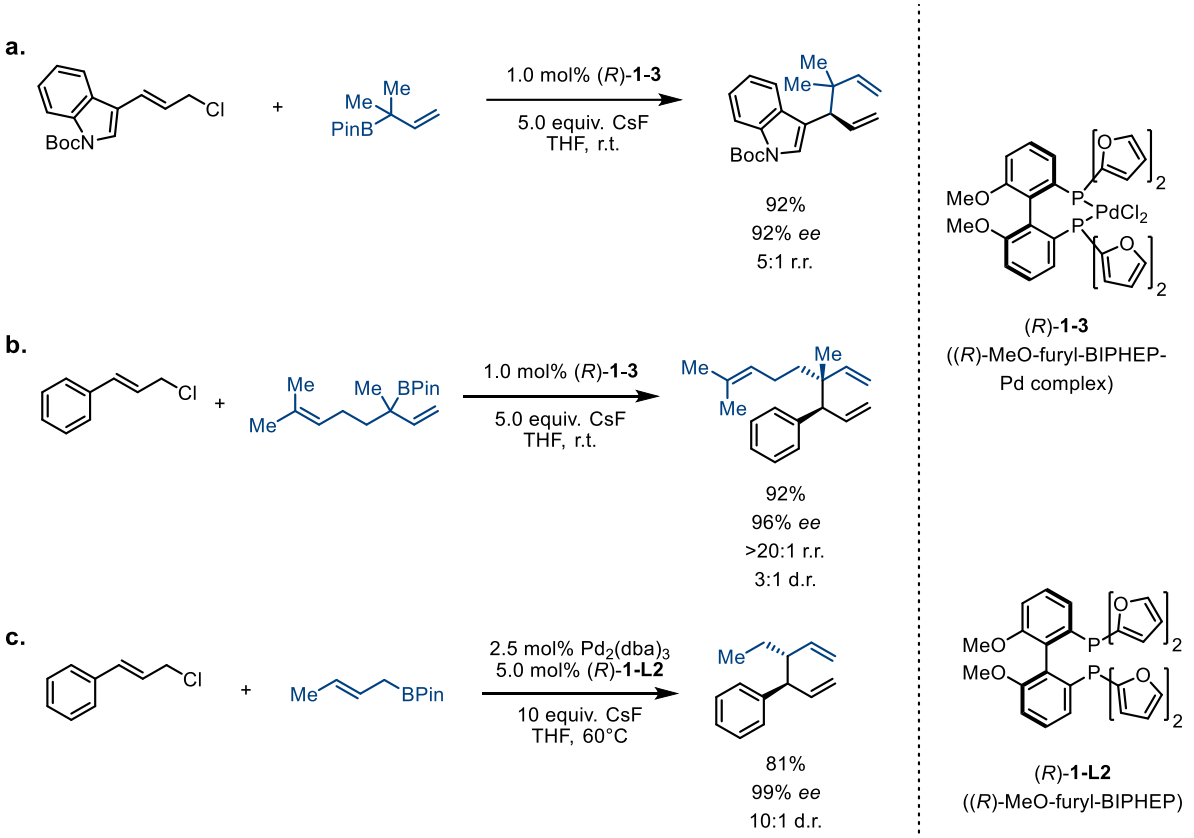

Figure 1.7 Couplings of terminal allyl chlorides and various allylboronic acid pinacol esters developed by Morken group.

The Ding group recently reported a palladium-catalyzed asymmetric allyl-allyl cross-coupling reaction of acetates of racemic Morita-Baylis-Hillman adducts and allylB(pin).[23] The reaction produced of a series of chiral 1,5-dienes bearing a vinylic ester functionality in good yields, high branched regioselectivities, and consistently excellent enantioselectivities (Figure 1.8). Downstream reactions of the allylation products led to the novel efficient synthesis of chiral polycyclic lactones and lactams, including the antidepressant (-)-Paroxetine.[23]

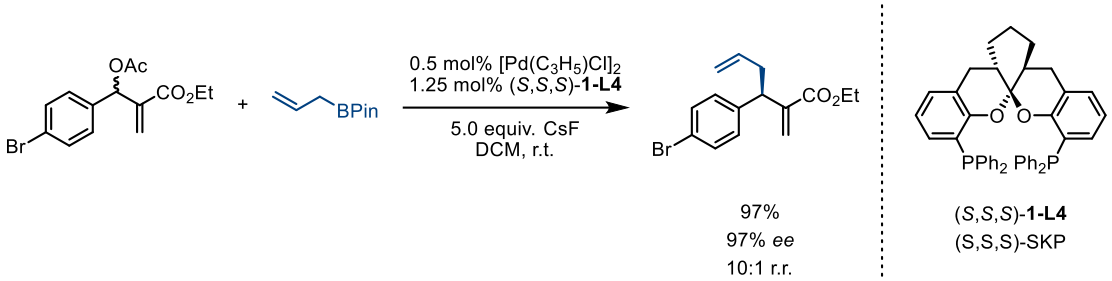

Figure 1.8 Asymmetric allylic allylation of racemic Morita-Baylis-Hillman adducts with allylic boron pinacol esters by Ding and co-workers.

1.3 Iridium-catalysed asymmetric Suzuki-Miyaura cross-couplings

The Carreira research group has made significant contributions to the field of Ir-catalyzed cross-coupling reactions through the development of a methodology for the coupling of allylic alcohols with boron nucleophiles (Figure 1.9).[24] The reaction can successfully be performed with vinyl[25] and alkynyl[26] trifluoroborates, furnishing branched products in good yields and excellent enantioselectivities. The proposed mechanism for this reaction involves the rapid isomerization of two allyl-Ir intermediates, allowing for the utilization of racemic starting materials.[27] The presence of an acid is necessary to promote substitution of the alcohol substrate, while a fluoride activator is required for the activation of the boronate.

Through the application of this methodology, the Carreira group has successfully synthesized a variety of biologically active complex molecules, such as nyasol and hinikiresinol.[25]

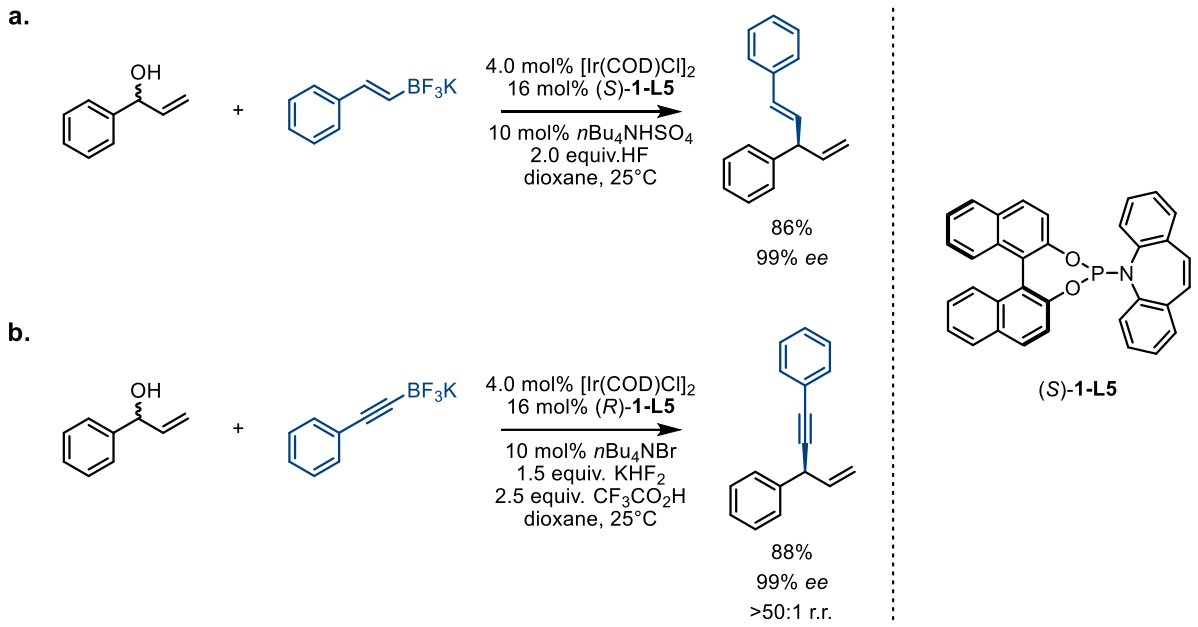

Figure 1.9 Carreira's iridium-catalysed Suzuki-Miyaura couplings of racemic terminal allylic alcohols and organoboron reagents. a, Vinyl boronate as a coupling partner. b, Phenethynyl boronate as a coupling partner.

In a similar transformation, Yang and co-workers disclosed that an allyl-allyl coupling can also be achieved in good yields, and excellent regio- and enantioselectivities (Figure 1.10).[28]

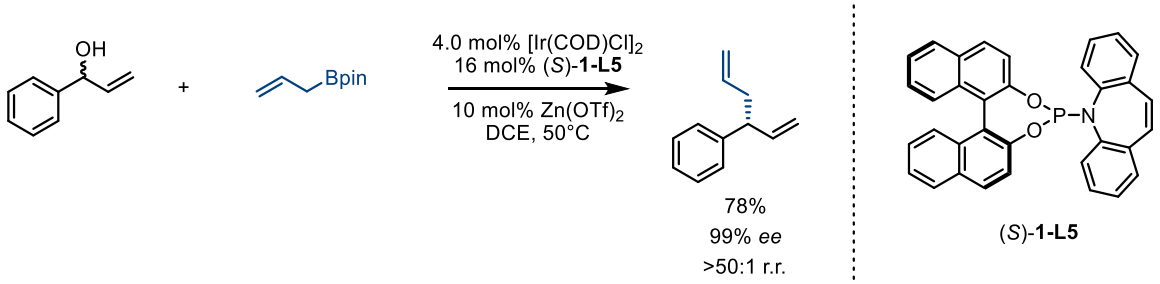

Figure 1.10 Iridium-catalysed enantioselective coupling of allylic boron pinacol esters and racemic terminal allylic alcohols by Yang and co-workers.

In a related study, Niu and co-workers reported the regio- and enantioselective coupling of allylic carbonates with a diborylmethane reagent (Figure 1.11).[29] They attributed the improved selectivity of the reaction to the presence of silver additives, which facilitate the transmetalation step.

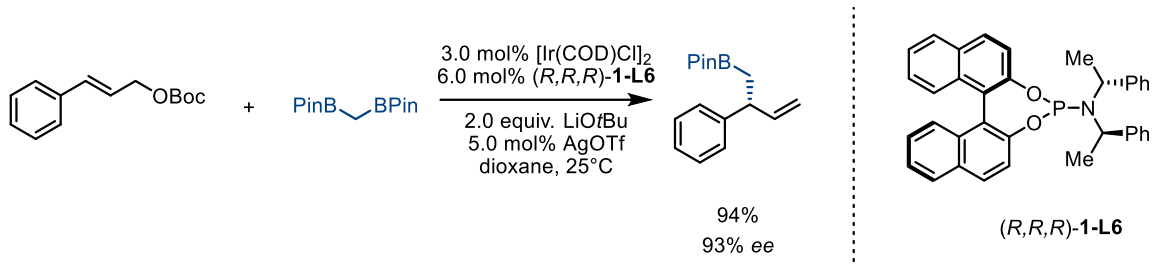

Figure 1.11 Iridium-catalysed enantioselective Suzuki-Miyaura coupling, assisted by silver triflate.

These findings represent important advancements in the field of Ir-catalyzed cross-coupling reactions and highlight the versatility and efficiency of this methodology for the synthesis of complex biologically active molecules.

1.4 Nickel-catalysed asymmetric Suzuki-Miyaura cross-couplings

The Fu group has developed numerous Ni-catalysed cross-couplings. In their enantioconvergent arylation of racemic α-chloroamides with arylboron nucleophiles, they achieved excellent enantioselectivities and yields (Figure 1.12a).[30] In addition to the use of C(sp^2) hybridised aryl nucleophilic partners, the Fu group has also been at the forefront of developing a variety of Ni-catalysed asymmetric C(sp^3)-C(sp^3) cross-couplings between secondary alkyl halides and alkylboron compounds (Figure 1.12b).[31] These Ni-catalysed asymmetric reactions usually require a directing group in the alkyl halide coupling partner, with a diverse range of directing groups including amines and amides being applicable. Fu and Zultanski also reported on an enantioselective nickel-catalyzed arylation of γ-chloroamides, in moderate to high yields but an improvement in enantioselectivity would be desirable (generally up to 90% ee) (Figure 1.12c).[32] Fu and Saito also reported the first asymmetric alkylation of racemic homobenzylic bromides and alkyl-(9-BBN) species, where proper positioning of the aromatic group is crucial for good enantioselectivity, as the catalyst system seems to differentiate between the CH_2Ar

group and the alkyl group of the homobenzylic bromide (Figure 1.12d).[33] In a more exotic development, the Fu group reported a cross-coupling reaction between arylboronic nucleophiles and a tethered olefin, where transmetallation was followed by Ni-catalyzed cyclization to produce 2,3-dihydrobenzofuran products (Figure 1.12e).[34] This method was successfully applied in the synthesis of the core of the drug candidate, fasiglifam.[34]

The proposed mechanism for the asymmetric alkylation of β-haloamines involves transmetalation, followed by single-electron transfer oxidative addition of the racemic alkyl halide and subsequent reductive elimination to form the alkyl-alkyl coupling product. The Fu group suggests that transmetalation followed by single-electron transfer oxidative addition is the enantiodetermining step in β-haloamines,[31] while DFT calculations by Kozlowski and co-workers suggest that reductive elimination is enantiodetermining.[35]

In conclusion, the Fu group's development of Ni-catalyzed cross-coupling reactions has made a significant impact in synthetic organic chemistry, providing an efficient and selective method for the formation of C-C bonds.

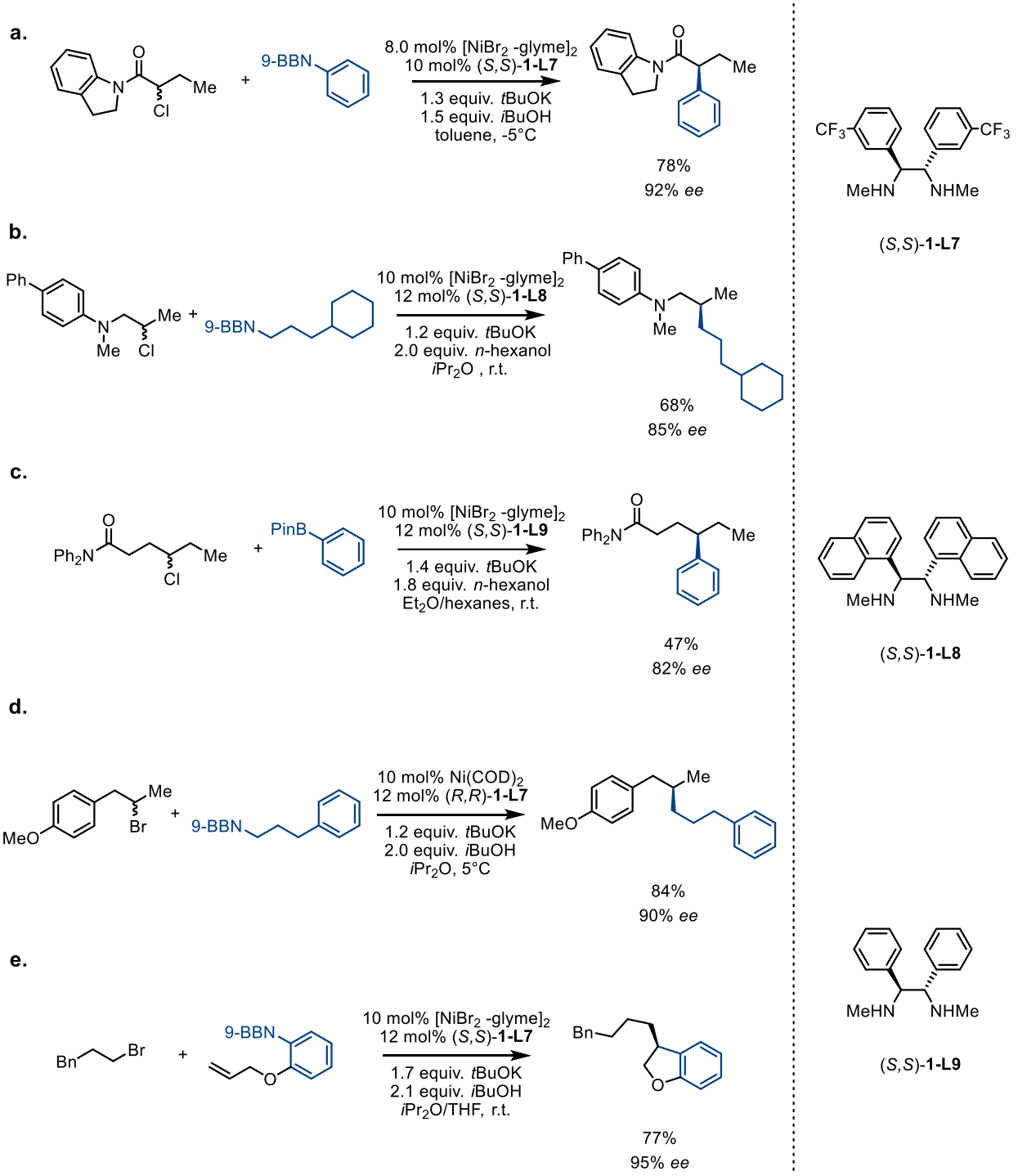

Figure 1.12 Fu's asymmetric cross couplings with aryl- and alkylborons. a, Enantioselective coupling of α-chloroamides. b, Asymmetric amine-directed Suzuki reactions of secondary alkyl chlorides c, Stereoconvergent coupling of a γ-chloroamide. d, Enantioselective Suzuki-Miyaura cross-couplings of unactivated homobenzylic bromide. e, Enantioselective C(sp^3)-generating cyclisation and cross-coupling cascade involving arylborons.

The Molander group has made a seminal contribution to the field of asymmetric cross-coupling reactions through the development of a photoredox/nickel dual catalytic methodology for the coupling of C(sp^3)-hybridized organoboron reagents.[36] This approach represents a new paradigm in the reactivity of alkylmetallic reagents in transition-metal-catalyzed processes. In a demonstration of the asymmetric utility of this methodology, a racemic trifluoroborate was subjected to cross-coupling with methyl 3-bromobenzoate in the presence of chiral ligand (*S,S*)-**1**-**L10**. This resulted in the synthesis of 1,1-diarylethane product in 52% yield and a promising enantiomeric excess of 50% (Figure 1.13).

The stereochemical outcome of the single-electron transmetalation is dictated by the facial selectivity of the addition of a prochiral alkyl radical to a ligated Ni center. The observed stereoconvergence provides strong evidence for the proposed mechanism, in which the organotrifluoroborate serves as a carbon radical precursor that is intercepted by the ligated Ni complex, leading to C-C bond formation *via* reductive elimination. This preliminary result implies that high levels of stereoselectivity can be achieved in the photoredox cross-coupling of secondary alkyl nucleophiles through appropriate modifications of reaction conditions and ligand structure. A follow-up study published by the same group provides further insights into the mechanism of this transformation, revealing an unexpected pathway for stereoinduction involving dynamic kinetic resolution (DKR) of a Ni(III) intermediate.[35] The stereodetermining step in this process is reductive elimination.

The refinement of this approach to asymmetric cross-coupling reactions has the potential to provide a significant advancement in the field by alleviating the need for the synthesis of enantioenriched organoboron reagents.

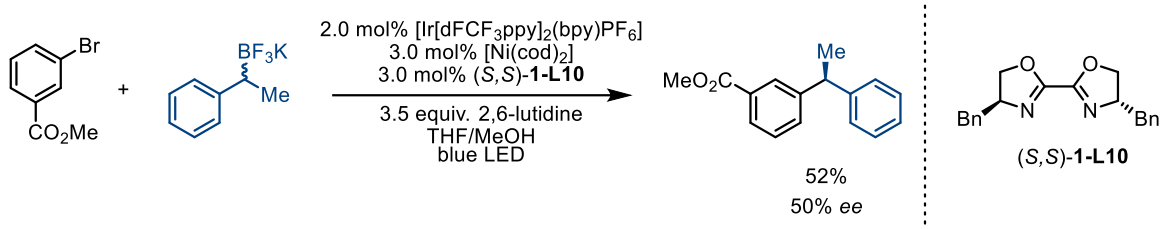

Figure 1.13 Enantioselective Suzuki-Miyaura coupling involving iridium/nickel photocatalysis by Molander group.

In a recent study, Shen and co-workers reported a novel approach for the installation of trifluoromethoxylated stereogenic centers in Ni-catalyzed C(sp^2)–C(sp^3) cross-couplings.[37] The researchers utilized α-trifluoromethoxylated benzyl bromides in the couplings with different aryl lithium organoborates, resulting in good yields and enantioselectivities (Figure 1.14). The study highlighted the importance of the choice of the reaction partner, with the use of a more reactive lithium organoborate over an arylboronic acid being crucial for the successful transmetalation below room temperature, which led to high levels of enantioselectivity. This research represents a valuable contribution to the field, providing a new and efficient method for the installation of trifluoromethoxylated stereogenic centers in C(sp^2)–C(sp^3) cross-couplings.

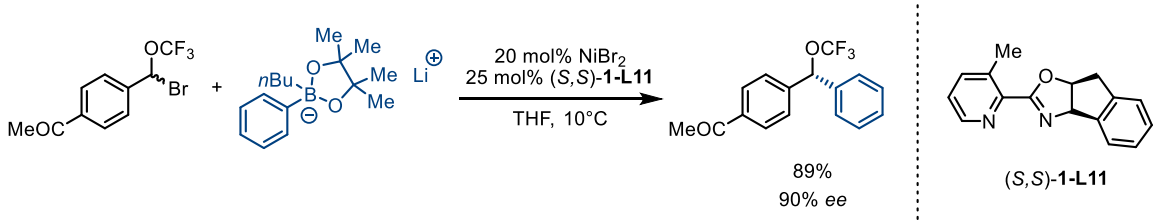

Figure 1.14 Nickel-catalysed C(sp^3)-C(sp^2) cross-coupling of benzyl bromides developed by Shen group.

In 2014, the Doyle group reported a Ni-catalyzed cross-coupling reaction between arylboroxines and allylic N,O-acetals situated within quinolines (Figure 1.15).[38] This

approach provides modular access to the important pharmaceutical scaffold of 2-aryl-1,2-dihydroquinolines with moderate to high levels of enantioselectivity. The catalytic, asymmetric arylation of quinolinium ions represents an underutilized but highly attractive method for accessing this motif, due to the ready availability of quinolinium precursors. This study is also a rare example of an enantioselective cross-coupling of a racemic electrophile bearing an oxygen leaving group. According to the group's mechanistic studies, the enantioselective arylation of quinolinium ions relies on the Ni-iminium activation mode.[39]

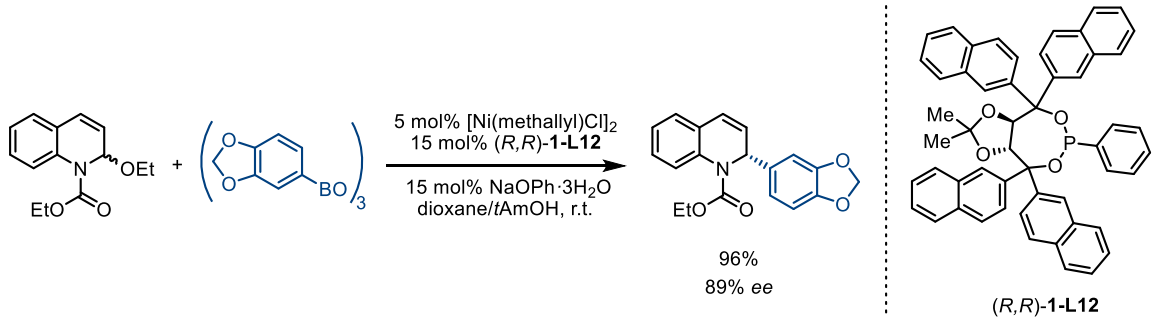

Figure 1.15 Nickel-catalysed enantioselective Suzuki-Miyaura cross-coupling of quinoliniums.

1.5 Copper-catalysed asymmetric Suzuki-Miyaura cross-couplings

Copper salts have long been recognised for their cost-effectiveness and stability, and have thus been widely used as catalysts. The synthetic chemistry community has therefore shown great interest in the area of asymmetric copper-catalyzed reactions.[40]

The Sawamura group has achieved a significant milestone by developing the first copper-catalyzed catalytic enantioselective allylic substitution reaction with alkylboron compounds (Figure 1.16).[41] Under the catalysis of a Cu(I) and DTBM-SegPhos system, the reaction between alkyl-9-BBN reagents and primary allylic chlorides exhibited excellent γ-selectivities (Figure 1.16a). The reaction yielded a branched product with an allylic

stereogenic center in good yields and moderate to good enantioselectivities, even with functionalized sp^3-alkyl groups. The group later expanded this methodology to include γ,γ-disubstituted primary allyl chlorides as substrates, enabling the generation of quaternary carbon stereogenic centers (Figure 1.16b).[42] The proposed reaction mechanism involves the addition-elimination of a neutral alkyl-copper(I) species.

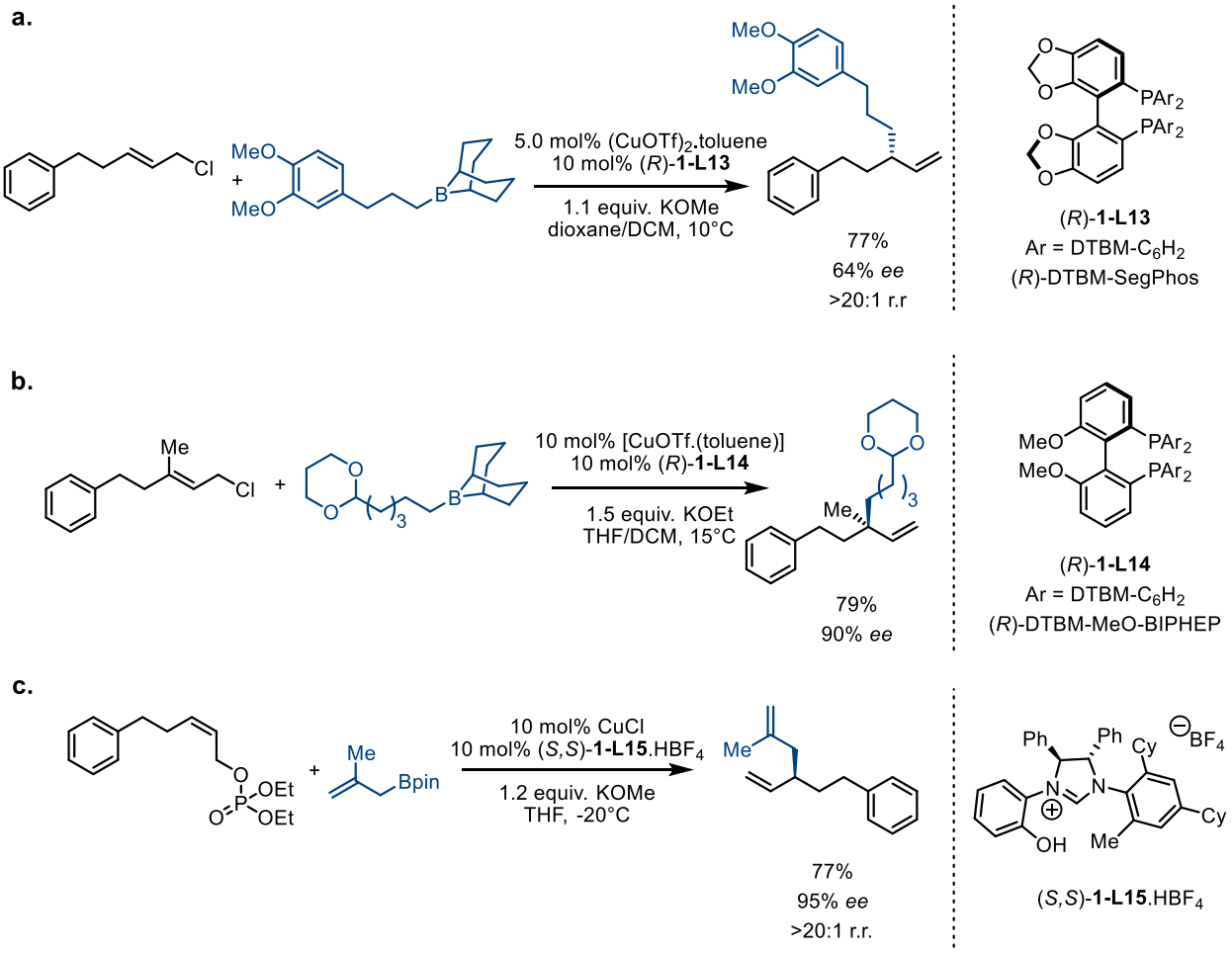

Figure 1.16 Cu-catalysed C(sp^3)-C(sp^3) forming asymmetric reactions by Sawamura and colleagues. a, Terminal allylic chlorides and alkylborons. b, Terminal allylic phosphates and allyl boronates. c, Quaternary-centre-forming coupling of prochiral allyl chlorides and alkylboronates.

The same group also reported copper-catalysed enantioselective allyl-allyl couplings between allylboronates and either *Z*-acyclic or cyclic allylic phosphates.[43] This reaction was accomplished using a new chiral NHC ligand bearing a phenolic hydroxy group. The

reaction exhibited exceptional S_N2'-type regioselectivities, delivering chiral 1,5-dienes (Figure 1.16c).

The Hayashi group has reported a method for the asymmetric allylic substitution of prochiral terminal allylic phosphates with organoboronates, catalyzed by a copper and N-heterocyclic carbene system.[44] The reaction provides the desired γ-substitution products with high enantioselectivity (Figure 1.17). Similar transformation using γ,γ-disubstituted allyl phosphates with arylboronates constructs quaternary stereocenters.[45]

The use of a hydroxy-bearing chiral N-heterocyclic carbene ligand is essential for achieving high enantioselectivity, as it stabilizes the copper intermediate and controls the stereochemistry of the reaction. Mechanistically, the reaction proceeds with near-perfect 1,3-anti stereochemistry and both *E*- and *Z*-substrates produce the same enantiomer as the major product.

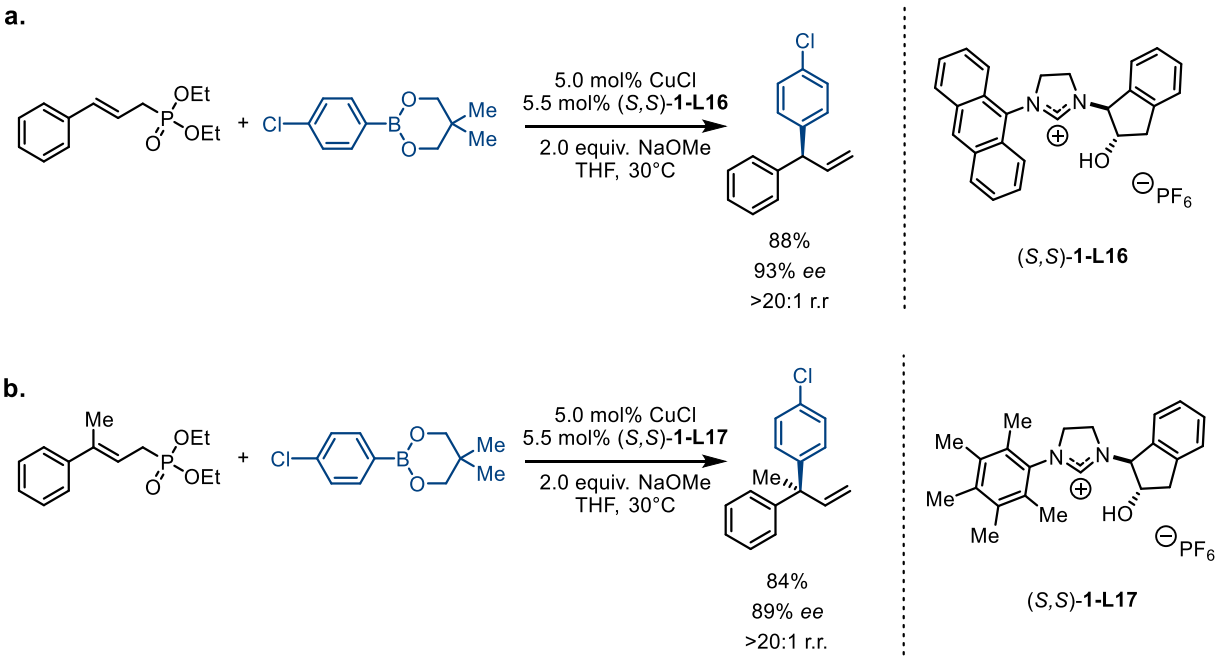

Figure 1.17 Copper-NHC catalysed asymmetric couplings of terminal allylic phosphates and arylboron reagents.

Overall, this method provides a powerful tool for the synthesis of enantioenriched gamma-substituted products and quaternary stereocenters, with broad substrate scope and high selectivity.

The Hoveyda group has made significant contributions to the field of copper and N-heterocyclic carbene catalysed enantioselective couplings (Figure 1.18). In particular, they have developed a cross-coupling method that allows for the generation of quaternary carbon stereogenic centers from terminal allylic phosphates and commercially available vinylboron reagents.[46] The group has also identified catalytic conditions that enable the addition of allenyl groups to similar allylic electrophiles, resulting in the formation of tertiary or quaternary chiral centers.[47] These transformations are facilitated by a copper/sulfonate-bridged bidentate N-heterocyclic carbene system and proceed with good yields and enantioselectivities.

In addition, the Hoveyda group has demonstrated the asymmetric coupling of terminal allylic phosphates and diborylmethane, leading to the formation of valuable products that contain both a stereogenic center and a boron pinacolate handle for further functionalisation.[48] The usefulness of this approach has been showcased through its application in the synthesis of rhopaloic acid A, a natural product. Propargylic boronic acids can serve as a coupling partners in the cross-coupling reaction for the formation of quaternary centers too.[49]

These examples represent only a fraction of the numerous asymmetric copper-catalyzed methodologies that the Hoveyda group has developed. Overall, their research has greatly expanded the scope of synthetic chemistry and has opened new avenues for the creation of chiral molecules with high enantioselectivity.[50,51]

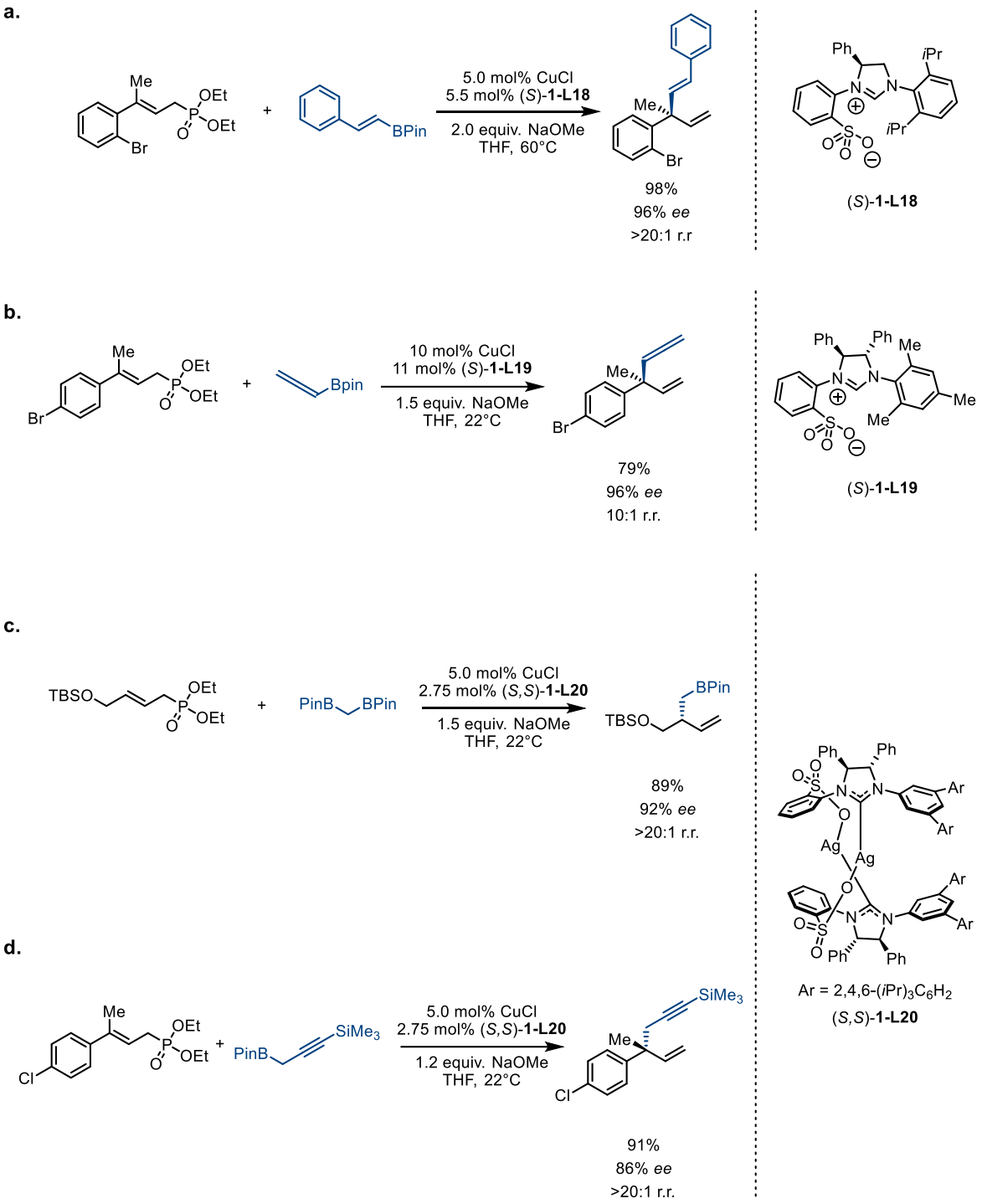

Figure 1.18 a. Quaternary-centre-forming enantioselective coupling between terminal allylic phosphates and vinylboronic acid pinacolate esters. b. Enantioselective S_N2' coupling of terminal allylic phosphates and allenylboron species. c. Asymmetric coupling of terminal allylic phosphates and diborylmethane. d. Propargylic boronic acid is utilised as a coupling partner in quaternary centre forming cross-coupling reaction.

1.6 Rhodium-catalysed asymmetric Suzuki-Miyaura cross-couplings

The use of rhodium as a metal catalyst in conjunction with organoboron reagents has been widely employed in catalytic asymmetric Suzuki-Miyaura couplings. In a report published by Lautens and colleagues, it was demonstrated that the addition of arylboronic acids to allylic dicarbonates could be catalyzed by rhodium with high levels of enantio- and regioselectivity (Figure 1.19).[52] The authors proposed that a 1,2 σ-enyl Rh intermediate was formed during the reaction, which could then undergo reductive elimination to give the major regioisomer observed. They suggested that the slow rate of isomerization of this intermediate enabled excellent regiocontrol. In a subsequent study, the authors demonstrated that it was also possible to access the alternative regioisomer by changing the ligand used, although with reduced levels of regiocontrol.[53]

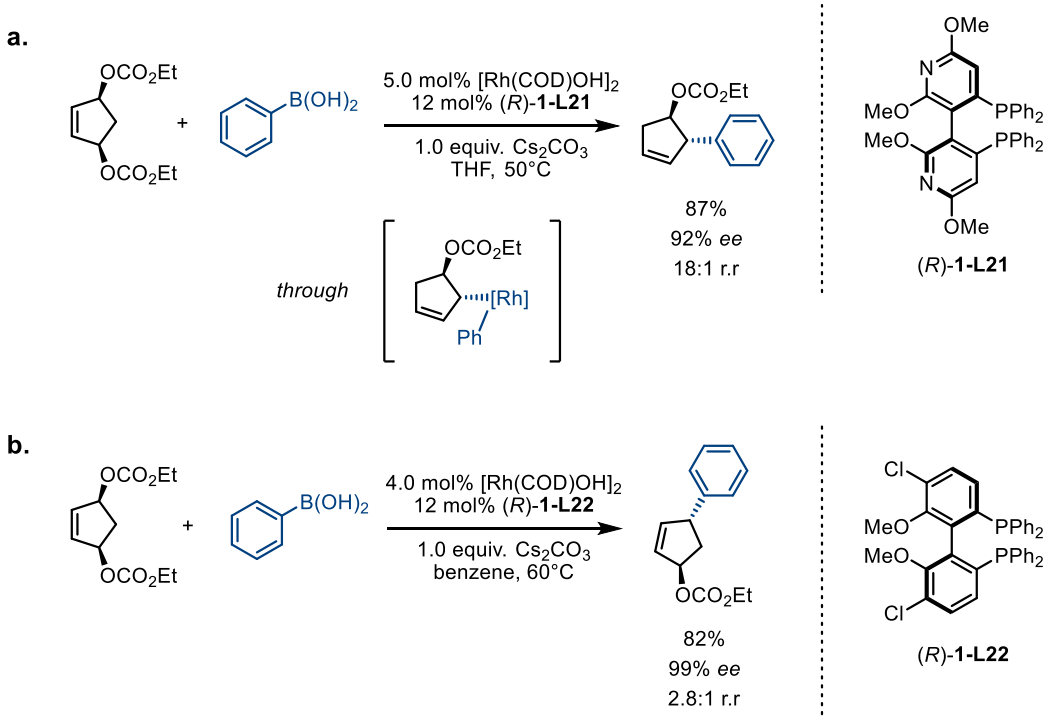

Figure 1.19 Rh-catalysed desymmetrisation of cyclic meso-bisphosphates.

In addition, the Lautens group demonstrated that the protocol can be successfully extended to acyclic terminal allylic systems, specifically acyclic *meso*-biscarbonates (Figure 1.20).[54]

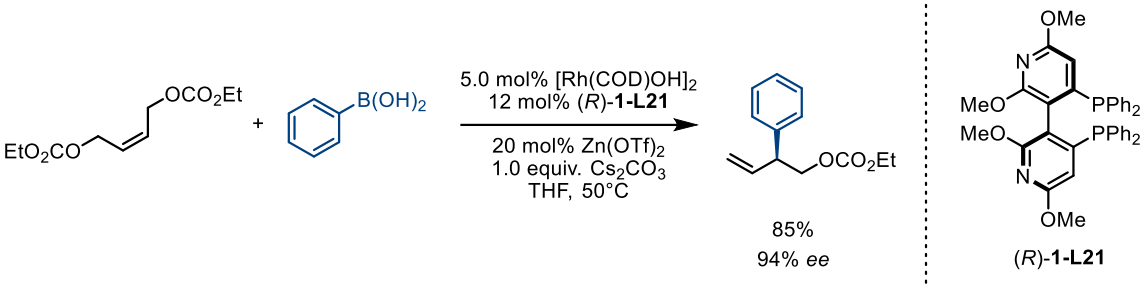

Figure 1.20 Rh-catalysed desymmetrisation of cyclic meso-bisphosphates.

In one of the studies, Gong and colleagues reported the use of Rh-catalysis in the asymmetric allylic arylation of nitroallyl acetate with phenylboronic acid (Figure 1.21).[55] This work builds upon the team's previous research on 1,4-addition reactions and suggests that the reaction occurs *via* a 1,4-addition process, leading to the β-elimination of the acetate group and the formation of the final product.

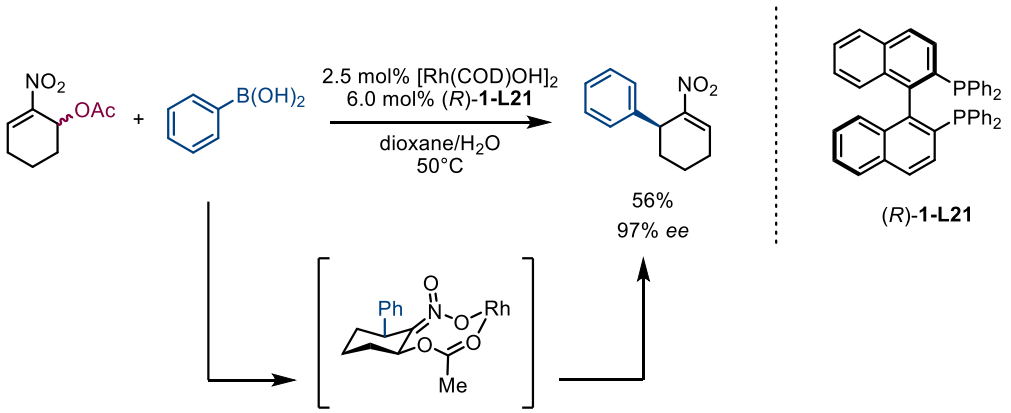

Figure 1.21 Suzuki-Miyaura coupling of nitroallyl acetate and phenylboronic acid.

Oi and coworkers reported on the use of Rh-catalysis in the regioselective cross-coupling of terminal acyclic allylic ethers with arylboronic acids (Figure 1.22).[56] This reaction demonstrates good yield and excellent enantiocontrol.

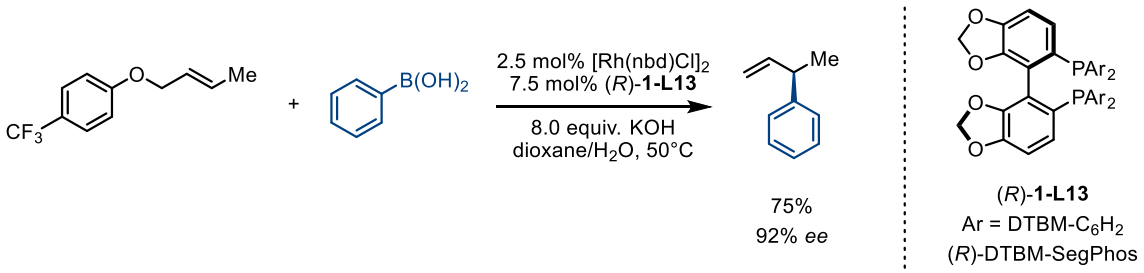

Figure 1.22 Regioselective arylation of terminal acyclic allylic ethers.

1.7 Conclusions and thesis outline

This chapter has overviewed the progress made in development of asymmetric Suzuki-Miyaura cross-couplings over the past two decades and their crucial role in the synthesis of biologically significant compounds. Ongoing research in this area leads to novel methods constantly being reported.[57-59] The transformations thus far reported in the literature have contributed to the development of enantioselective cross-couplings and enabled the synthesis of several pharmaceutical agents and natural products. Despite the vast amount of asymmetric Suzuki-Miyaura couplings being constantly developed, the existing procedures are too substrate specific, many of them work only with prochiral/achiral starting materials. These procedures fail when non-terminal allylic systems or non-prochiral starting materials are employed. Hence, racemic allylic systems where both termini of the allylic species contain substituents are often absent as electrophiles in the reported literature procedures. Given that theoretically the amount of potential racemic electrophiles is much greater than that of prochiral,[60] this represents a significant lack of generality. In addition, many reactions are limited to using unfunctionalized aromatic and aliphatic boronic acid derivatives, and do not tolerate heteroaromatic and other nucleophiles containing important functional groups, such nitrogen. Heteroaryl fragments are prominent pharmacophores in various drug discovery programmes, small structurally well-defined rings are commonly incorporated

in pharmaceutical agents too.[61-63] Methods that do not tolerate heteroaryl or saturated nitrogen containing coupling partners are less likely to adopted by the medicinal chemistry community and employed in drug discovery campaigns.

These shortcomings have encouraged the rapid development of new stereoconvergent reactions that can start from the racemic mixture of chiral substrate and offer powerful opportunities. In particular, there is an aim to address the limitations associated with the utilisation of terminal allylic electrophiles, thereby enabling access to a diverse array of racemic coupling partners. Nevertheless, these aspects of catalytic asymmetric C(sp^3) forming cross-coupling reactions have remained almost completely unexplored until our group developed several rhodium catalysed methodologies to couple racemic allylic electrophiles and aryl or heteroaryl boronic acids.[64,65] We have continued to expand our Rh-catalysed asymmetric Suzuki-Miyaura coupling method in recent years and these methodologies will be discussed in detail in the next chapter. Enantioselective procedures on simple cyclic benchmark substrates are now reasonably well established and they pave the way for further exploration in this area of research. However, the catalyst-controlled stereoselective coupling of more complex, especially acyclic unsymmetrical molecules is virtually unknown. Developing a Rh-catalysed enantioselective Suzuki-Miyaura cross-coupling with racemic acyclic substrates that have few or no symmetry elements would represent an unprecedented advance and would significantly expand the applicability of this reaction.

To tackle these exciting challenges, we developed an enantioconvergent Suzuki-Miyaura cross-coupling of acyclic allylic systems and we discuss it in Chapter 2 (Figure 1.23).

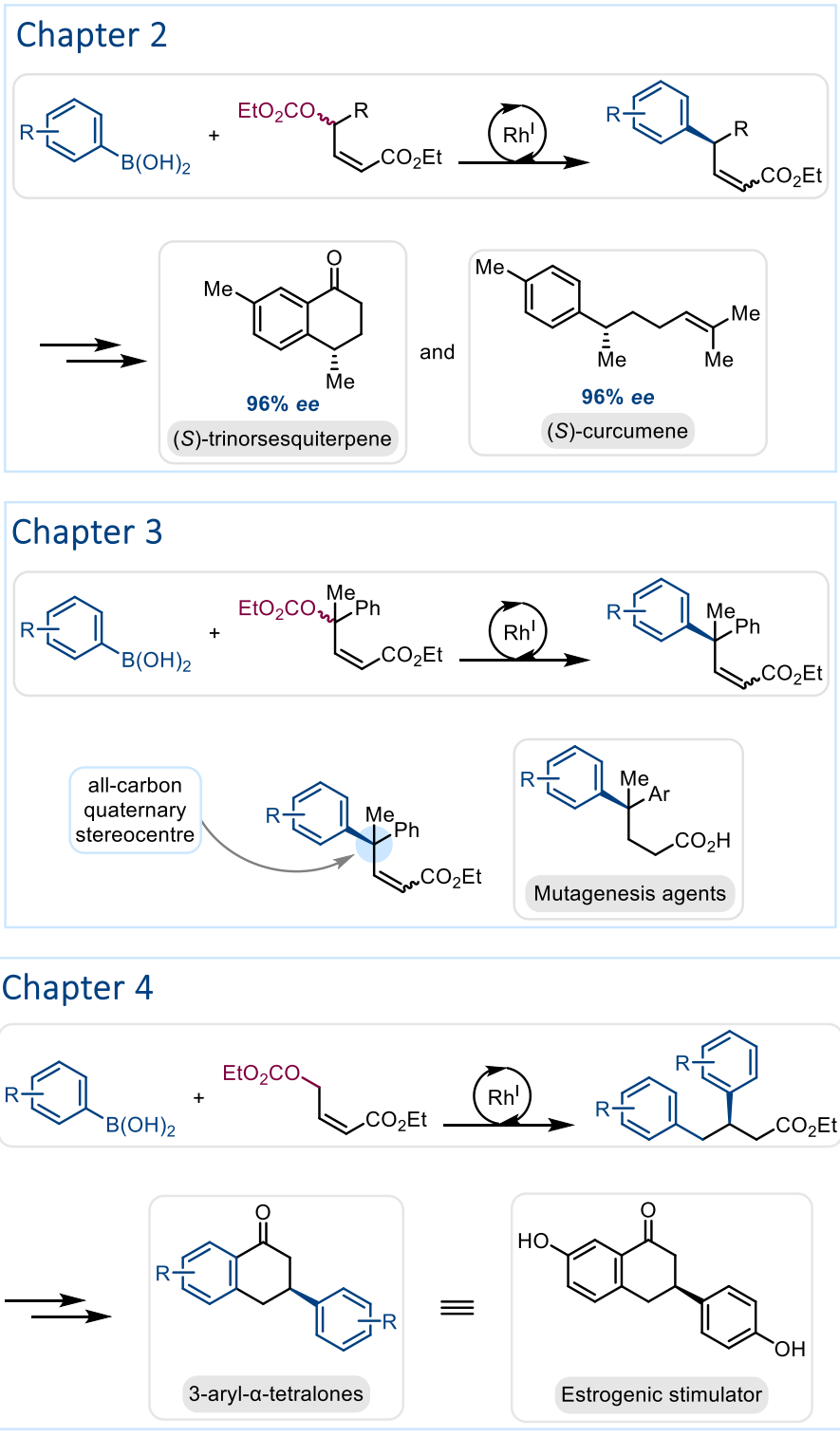

Figure 1.23 Outline of the work presented in the thesis. Chapter 2 discusses the development of enantioconvergent Suzuki-Miyaura cross-couplings of acyclic allylic systems. Chapter 3 explores the asymmetric formation of all-carbon quaternary stereocenters using the developed Suzuki-Miyaura cross-coupling of acyclic allylic systems. Chapter 4 focuses on Suzuki-Miyaura couplings using terminal acyclic allylic systems and uncovers a modular asymmetric synthesis of 3-aryl-α-tetralones *via* sequential double arylation.

Chapter 3 explores the asymmetric formation of all-carbon quaternary stereocenters *via* the developed Suzuki-Miyaura cross-coupling of acyclic allylic systems. Chapter 4 focuses on Suzuki-Miyaura couplings using terminal acyclic allylic systems and uncovers a modular asymmetric synthesis of 3-aryl-α-tetralones *via* sequential double arylation.

In summary, this thesis aims to address the challenges associated with synthesizing C(sp^3)-rich compounds *via* novel asymmetric Suzuki-Miyaura couplings and developing efficient methods to produce enantioenriched small molecules. By doing so, we hope to contribute to the development of more successful drug candidates and increase the chances of bringing new and effective drugs to market. We anticipate that this work will inspire progress in asymmetric catalysis, and that methodologies developed, and trends described here will be the key to solving other challenges in the field.

2 Enantioconvergent Suzuki-Miyaura cross-coupling of acyclic allylic systems

2.1 Introduction

2.1.1 Regioselectivity in Rh-catalysed asymmetric Suzuki-Miyaura couplings

As mentioned in Chapter 1, asymmetric Suzuki-Miyaura couplings with racemates have been reported scarcely. Our group has developed several methodologies for enantioselective Suzuki-Miyaura cross-couplings using cyclic allylic substrates and (hetero)arylboronic acids (Figure 2.1).[64,66,67]

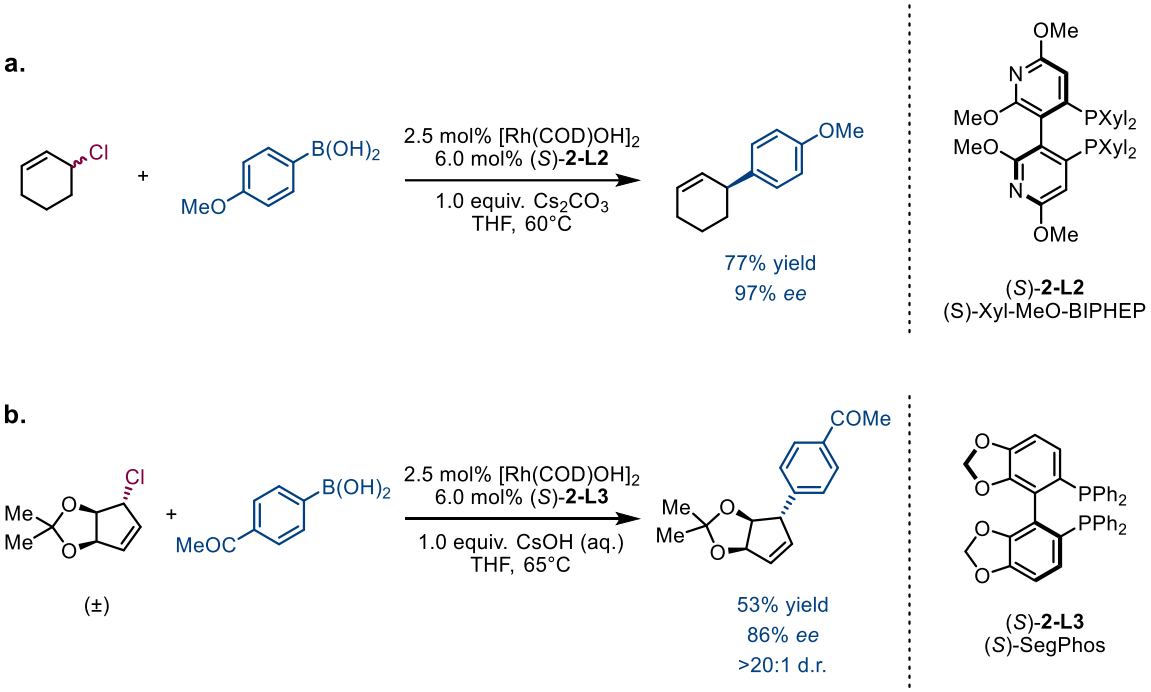

Figure 2.1 Examples of asymmetric rhodium-catalysed Suzuki–Miyaura couplings of racemic allyl chlorides and arylboronic acids developed by our group.

These reactions are restricted to electrophiles that are symmetrical about the allyl unit upon cleavage of the carbon-leaving group bond (also known as pseudosymmetric electrophiles). Furthermore, our experiments have demonstrated that the reaction is only successful with cyclic substrates where the double bond is fixed in the *Z* configuration (Figure 2.2).

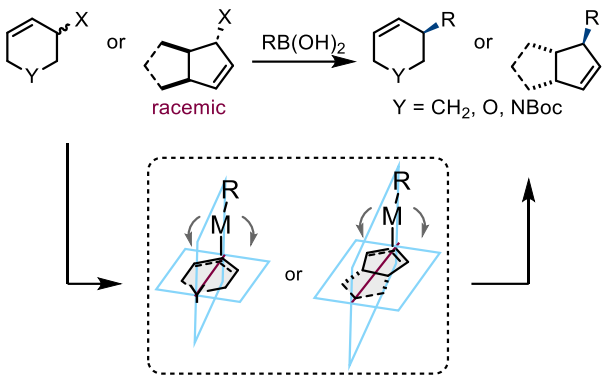

Figure 2.2 Previous work in the Fletcher group: cyclic allylic electrophiles.

In the cases where our Rh-catalysed Suzuki-Miyaura cross-coupling methodology was attempted with substrates that cannot form a pseudo-C2 symmetric intermediate, a mixture of regioisomers, each formed in excellent enantioselectivity (99% and 98% *ee*), was observed[67]. Regioisomeric ratio of almost 1:1 suggests that the process underway is an enantioselective regiodivergent arylation – each enantiomer of the starting material is converted into a different product (with high *ee*) by the same catalyst (Figure 2.3). This process could potentially be useful at synthesis of diverse libraries of enantiopure compounds, however it fails at regioconvergence.

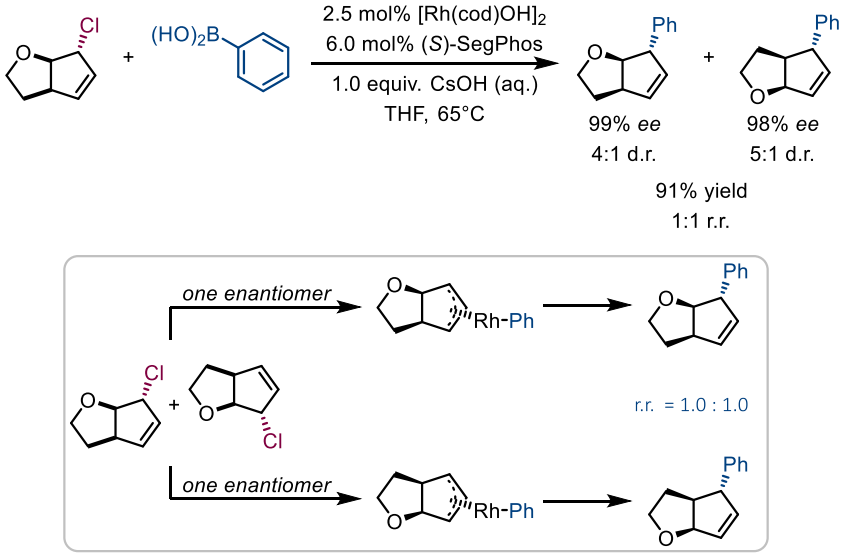

Figure 2.3 Rh-catalysed asymmetric Suzuki-Miyaura couplings with a substrate not containing pseudosymmetry.

2.1.2 Additional challenges of using acyclic substrates

As the conformational flexibility of the substrates increases, additional issues may arise. One possible problem stemming from the use of acyclic substrates is that the double bond geometry is not constrained by the ring. In this case, the allylic system can undergo π-σ-π interconversion in combination with rotation about a single bond to form either a *Z* or *E* double bond after reductive elimination.[68] This results in a minimum of eight stereoisomers with potentially similar energies for the catalytic system to distinguish between (Figure 2.4).

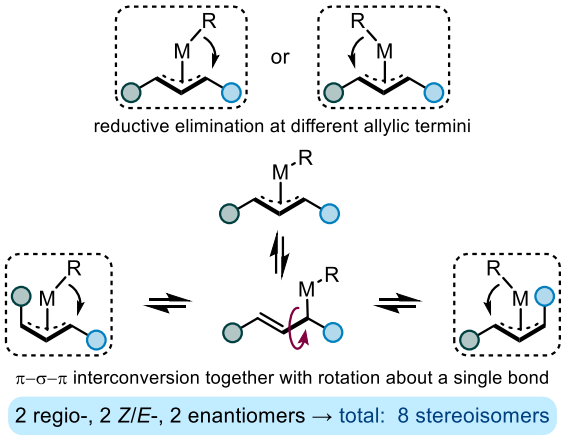

Figure 2.4 Selectivity challenges in acyclic non-symmetric systems.

Regio-, *E*/*Z*-, and enantioselective couplings of acyclic internal allylic electrophiles and arylboronic acids remain elusive but are highly sought after.

2.1.3 Stereocentres in acyclic molecules

Acyclic compounds containing C(sp^3) stereocentres are prevalent in natural products and biologically active compounds (Figure 2.5). These compounds often have unique structural features that make them attractive targets for synthesis in the pharmaceutical and fine chemical industries. Some of the best-in-class drugs contain a C(sp^3) stereocenter attached to an acyclic chain of carbon atoms, such as the anti-asthma drug (+)-AA2414[69] and the antioxidant aspergilol A[70], which have a diaryl stereocenter in an

acyclic system. In addition to these synthetic compounds, several natural products also contain an aryl-methyl stereocenter, including (*S*)-curcumene, neonulicin B, and shellolic acid E[71]. Of these, neonulicin B[72] has been shown to have antioxidant properties, making it a potentially interesting compound for biomedical research. Similar structural motif is also present in the patented Janus kinase inhibitor[73] and natural products chloranholide B[74] and baccharisketone.

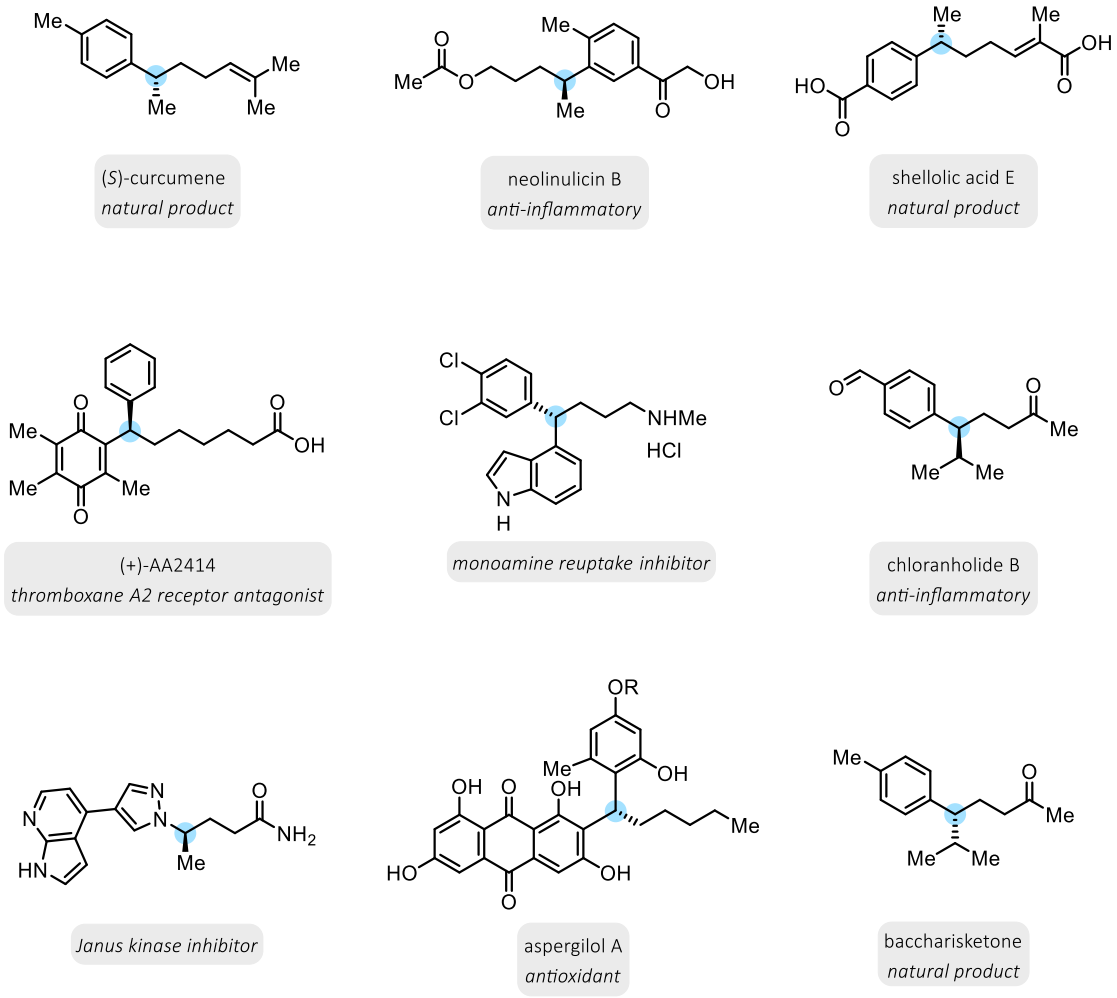

Figure 2.5 Natural products and bioactive compounds containing a carbon stereocentre in an acyclic system.

However, the synthesis of these compounds can be challenging as many are derived from chiral pool natural products or require lengthy multi-step linear syntheses.[75-78]

Fragments similar to those present in these bioactive compounds could be potentially accessed more efficiently *via* aforementioned asymmetric Suzuki-Miyaura couplings of acyclic allylic systems.

Stereospecific variant of the regioselective coupling of acyclic allylic electrophiles and boronic acids has been reported. For example, the Bouzbouz group disclosed that enantioenriched allylic fluorides undergo arylation with boronic acids with excellent α- to γ-chirality transfer to yield *Z*-alkenyl-unsaturated amides using $[Cp^*RhCl_2]_2$ as a precatalyst (Figure 2.6)[79]. To our knowledge, Bouzbouz group's work with allylic fluorides is the only regioselective example of Suzuki-Miyaura coupling with internal acyclic allylic electrophiles.

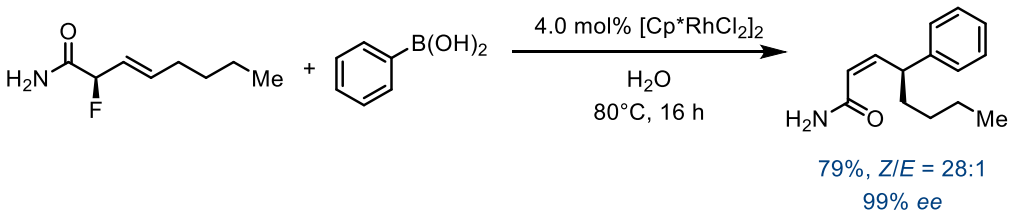

Figure 2.6 Stereospecific coupling of arylboronic acids and acyclic internal allylic electrophiles.

However, when it comes to regioselective Suzuki-Miyaura couplings of acyclic racemic electrophiles no reliable methods have been established. A Ni-catalysed cross-coupling of acyclic allylic acetates and boronic acids has been reported by Uemura[80] but the procedure suffers from a moderate yield and low ee (Figure 2.7).

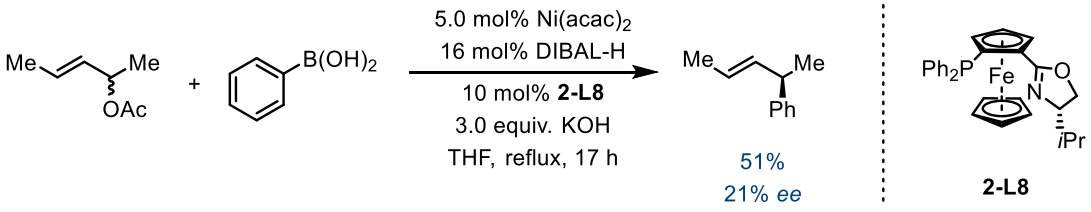

Figure 2.7 An example of an enantioselective coupling of an arylboronic acid and an acyclic internal allylic acetate.

Overall, the enantioselective generation of stereocenters in acyclic systems through asymmetric coupling of acyclic internal allylic systems and corresponding aryl boron nucleophiles is a major challenge in modern synthetic chemistry. As such, there is a need for reliable and modular asymmetric Suzuki-Miyaura couplings that can regioselectively form a new C(sp^3)-C(sp^2) stereocenter in an acyclic system.

2.1.4 Project aims

As discussed above, the use of racemic starting materials in asymmetric synthetic chemistry is often limited by the lack of methods for deracemising complex racemic compounds.[81,82] However, the development of such methods is attractive, as it allows circumvention of the problem of suitable substrates being restricted to prochiral and meso materials. In previous work, our group demonstrated the use of racemic starting materials in the synthesis of simple coupling products from cyclic pseudosymmetric substrates[64,66,67]. In this study, we aimed to expand the scope of these asymmetric Suzuki-Miyaura cross-couplings to acyclic substrates that do not possess pseudosymmetry. The goal of this project was to design a reliable and versatile asymmetric Rh-catalysed C(sp^2)-C(sp^3) cross-coupling that would generate the desired product with high enantio-, regio-, and Z/E-selectivity from a racemic starting material through the formation of Rh-π-allyl complexes (Figure 2.8).

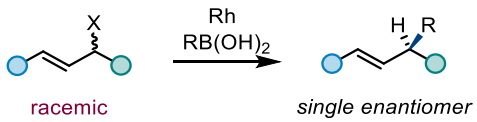

Figure 2.8 Envisaged Rh-catalysed enantioconvergent arylation of acyclic allylic species.

2.2 Results and Discussion

2.2.1 Reaction optimisation

In an attempt to test whether our Suzuki-Miyaura cross-coupling reaction is possible to perform on internal allylic electrophiles we chose several model substrates with equivalent allylic termini. We sought to first focus on the formation of a "pseudo-symmetric" intermediates through oxidative addition to circumvent the potential formation of complex mixtures of regioisomers that could be difficult to analyse. However, we encountered difficulties with the majority of the prototypical allylic chlorides examined that have this feature, as they were either unreactive, hydrolysed or underwent side reactions to yield an inseparable complex mixture (Figure 2.9).

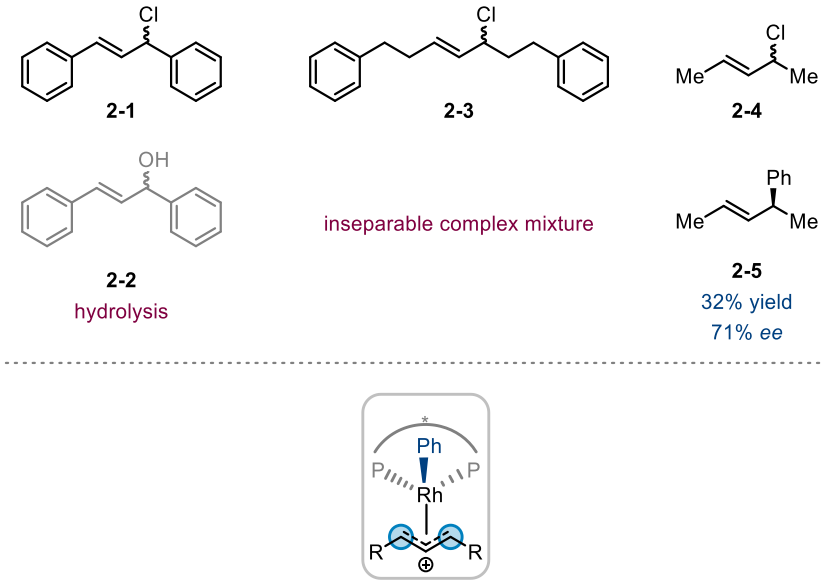

Figure 2.9 Substrates initially tried as electrophiles in the asymmetric Suzuki-Miyaura coupling.

While the methyl-substituted allylic chloride **2-4** did afford the desired product in low yield and moderate enantiomeric excess, we ultimately decided not to pursue this substrate further due to the high volatility of the starting material and the pentadiene byproduct (following elimination), as well as difficulties in purification and analysis of

the product mixtures, and the limited electrophile scope that the reaction would almost inevitably have.

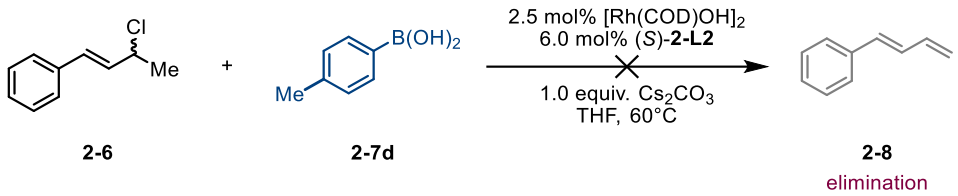

Figure 2.10 Non-pseudosymmetric substrate tried as an electrophile in the asymmetric Suzuki-Miyaura coupling.

We then attempted the reaction on an internal allylic system with inequivalent termini to check whether our catalytic system could somehow distinguish the two ends and result in a regioselective arylation. Unfortunately, substrate **2-6** underwent an elimination to form a conjugated diene (Figure 2.10).

Having examined the behaviour of the aforementioned acyclic allylic systems, we concluded that, if the desired reactivity was observed, low-yielding intractable mixtures of isomers that were extremely difficult to even characterize were obtained. Counterintuitively, the resolution to this problem involved employing a system that offers a greater range of potential reaction outcomes, enabling both allylic substitution and 1,4-addition. The 1,4-addition to α,β-unsaturated species, catalysed by rhodium, is widely recognised[83,84] and represents the primary pathway observed under specific conditions investigated in this study.

We also made an observation that all substrates that have undergone the desired Suzuki-Miyaura arylation under our conditions possessed a *Z*-double bond.[64,66,67,85]

Hence, we chose compound **2-9a** as our next model substrate (Table 2.1). **2-9a** is an acyclic internal allylic electrophile with two electronically different ends of the allylic

system and a *Z*-double bond. We chose a carbonate as our leaving group because of their stability and synthetic accessibility.

We attempted to couple (±)-**2-9a** with phenylboronic acid **2-7a** using methods similar to those previously reported for cyclic allylic halides and arylboronic acids.[64] No desired product was observed using privileged ligands such as BINAP **2-L1** and Xyl-P-Phos **2-L2** (Table 1, entries 1 and 2). Conjugated addition product **2-10a'** was obtained in reaction with SegPhos **2-L3** (entry 3). Garphos **2-L4** gave the desired chemoselectivity providing **2-10a** with 2.3:1 *Z*:*E* in 73% yield and 92% enantioselectivity (entry 4). Further ligand screening revealed **2-L7** gave highest enantioselectivity, yield and Z/E ratio. Generally, we observed high enantio- and regio- selectivity at lower temperatures, however the conversion was incomplete. In order to increase the conversion, we used a stronger base; however, aqueous caesium hydroxide proved to inhibit the reaction (entry 9). We managed to achieve good conversion at room temperature in toluene but this time the enantioselectivity was lowered (entry 10).

Table 2.1 Reaction optimisation.

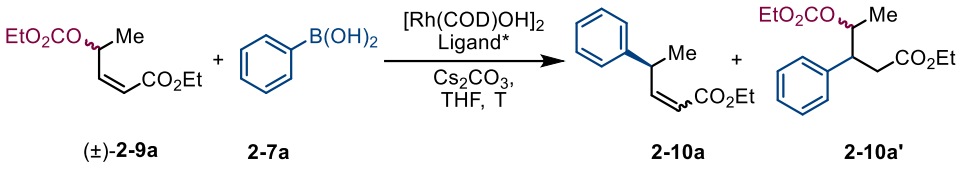

(±)-**2-9a** **2-7a** **2-10a** **2-10a'**

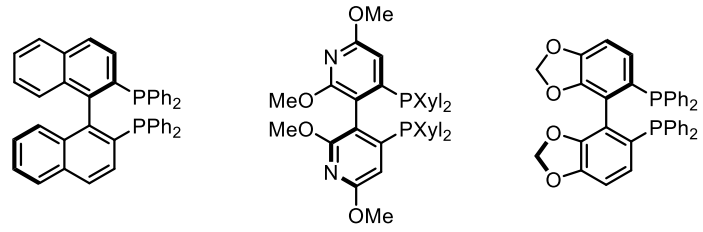

(*R*)-**2-L1** (*R*)-**2-L2** (*R*)-**2-L3**

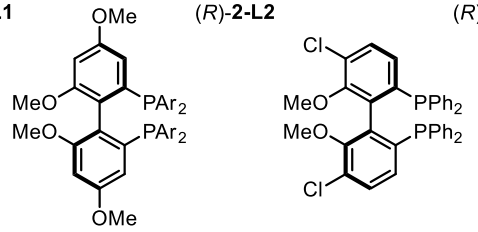

(*R*)-**2-L4** Ar = Ph
(*R*)-**2-L5** Ar = Tol
(*S*)-**2-L6** Ar = Xyl

(*R*)-**2-L7**

entry	ligand	T (°C)	yield of **2-10a** (%)	*ee* of **2-10a** (%)	*Z*:*E* of **2-10a**	yield of **2-10a'** (%)
1	**2-L1**	60	0	-	-	0
2	**2-L2**	60	0	-	-	0
3	**2-L3**	60	2	-	-	31
4	**2-L4**	60	73	92	2.3 : 1	0
5	**2-L5**	60	72	90	1.3 : 1	0
6	**2-L6**	60	55	84	1.2 : 1	0
7	**2-L7**	60	83	98	3.4 : 1	0
8	**2-L7**	r.t.	7	98	-	0
9[b]	**2-L7**	r.t.	5	97	-	0
10[c]	**2-L7**	r.t.	80	90	3.4 : 1	0

[a]Conditions: $[Rh(COD)OH]_2$ (2.5 mol %), ligand (6.0 mol %), Cs_2CO_3 (1.0 equiv.), phenylboronic acid (2.0 equiv.), 16 h. [b]50wt% aqueous CsOH used as a base. [c]Toluene used as a solvent. *Z*/*E* ratios were determined by ^1H NMR spectroscopy on crude reaction mixtures. Yields of **2-10a** determined by subsequent hydrogenation of the product mixture. Enantiomeric excesses were determined by hydrogenation of the product mixture and SFC analysis using a chiral non-racemic stationary phase.

In addition to the ligand, we explored the effect of the leaving group on the yield and *Z*/*E* ratio of these reactions (Figure 2.11). Using isopropyl carbonate as the leaving group in (±)-**2-9b** resulted in lower yield and *Z*/*E* ratio. Further increasing steric bulk of the leaving group by using a *tert*-butyl carbonate gave a higher *Z*/*E* ratio ((±)-**2-9c**). However,

we obtained low yield and unreacted starting material was present indicating that the reaction had not gone to completion and, that the Z/E ratio is inflated (see Mechanistic Studies section).

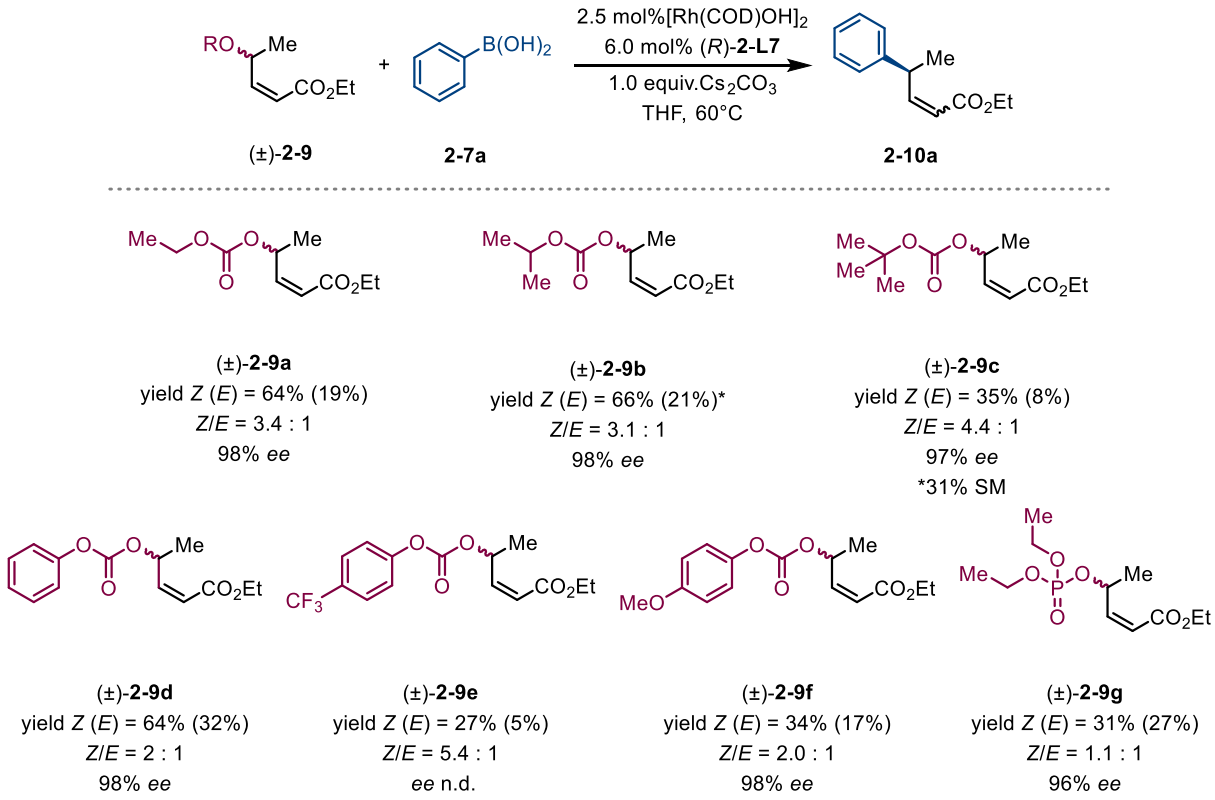

Figure 2.11 Effect of using different leaving groups in the asymmetric Suzuki-Miyaura coupling. (Z/E ratios were determined by ^{1}H NMR spectroscopy on crude reaction mixtures. Yields determined by subsequent hydrogenation of the product mixture. Enantiomeric excesses were determined by hydrogenation of the product mixture and SFC analysis using a chiral non-racemic stationary phase).

We also varied the electronic properties of the leaving group. Firstly, phenyl carbonate (±)-**2-9d**, where the electron density could be delocalised onto the aromatic ring such that it serves as a better leaving group, gave full conversion into the desired products in excellent *ee* albeit with a lower Z/E ratio (2 : 1). Both electron donating and withdrawing substituents in the 4-position of the phenyl ((±)-**2-9e** and (±)-**2-9f**) gave lower yields and no clear trend could be determined. We also attempted the reaction using a phosphate leaving group ((±)-**2-9g**). *Z* and *E* products were obtained in 1.1 : 1 ratio in moderate yield

and good *ee*, however unidentified byproducts suggest the phosphate substrate decomposes under the reaction conditions.

After a leaving group screening, ethyl carbonate remained the leaving group giving the most favourable combination of Z/E (3.4 : 1) selectivity and overall yield (83%).

We then checked whether any additive could be used to enhance the product Z/E ratio (Table 2.2). After an extensive additive screening, we found that most triflate salts gave high total yield of Z and E products with Z/E ratios varying between 2.5 : 1 for $Y(OTf)_3$ and 4.1 : 1 for AgOTf (entries 1-4). Surprisingly, addition of zinc chloride, bromide and iodide salts did not result in any formation of the product (entries 5-7). Silver containing salts tended to give lower yields (36-80%) with varying Z/E ratios (entry 9-14). Brønsted acid TfOH also worked relatively well furnishing the product in 73% yield and 3.1 : 1 Z/E ratio (entry 15). Finally, we identified that full conversion can be achieved using 20 mol% $Zn(OTf)_2$ at room temperature (entry 17). These conditions conserve high enantioselectivity and result in higher Z/E ratio than that observed at elevated temperatures.

Table 2.2 Additive screening.

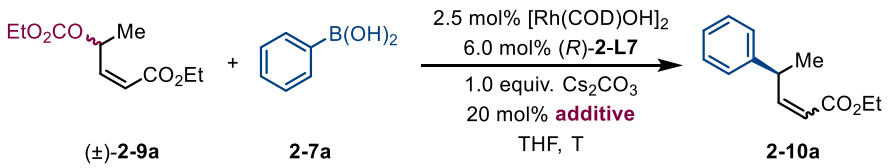

(±)-**2-9a** **2-7a** **2-10a**

Entry	Additive	T (°C)	*ee* of ***Z*-2-10a**/%	***Z*-2-10a** NMR yield /%	***E*-2-10a** NMR yield /%	Total yield of **2-10a**/%	***Z*:*E*** ratio	**2-9a** (SM) NMR yield /%
1	AgOTf	60	98	29	7	36	4.1 : 1	58
2	$Er(OTf)_3$	60	97	65	24	89	2.7 : 1	0
3	$Yt(OTf)_3$	60	97	62	25	87	2.5 : 1	0
4	$Zn(OTf)_2$	60	97	67	25	92	2.7 : 1	0
5	$ZnCl_2$	60	-	0	0	0	-	85
6	$ZnBr_2$	60	-	0	0	0	-	89
7	ZnI_2	60	-	0	0	0	-	100
8	$ZnCl_2$ (1.0M in Et_2O)	60	98	56	19	75	2.9 : 1	26
9	$AgNTf_2$	60	96	57	23	80	2.5 : 1	13
10	$AgSbF_6$	60	98	42	9	51	4.7 : 1	47
11	$AgBF_4$	60	98	50	14	64	3.6 : 1	36
12	$AgPF_6$	60	99	42	11	53	3.8 : 1	43
13	$AgIO_4$	60	-	0	0	0	-	0
14	$AgClO_4$	60	96	57	17	74	3.4 : 1	10
15	TfOH	60	97	55	18	73	3.1 : 1	0
16	$Cu(OTf)_2$	60	97	34	8	42	4.3 : 1	5
17	$Zn(OTf)_2$	r.t.	98	75	19	94	4.0 : 1	0
18	AgOTf	r.t.	98	28	7	36	4.1 : 1	54
19	TfOH	r.t.	97	55	18	73	3.1 : 1	20

Conditions: $[Rh(COD)OH]_2$ (2.5 mol %), (*R*)-**2-L7** (6.0 mol %), Cs_2CO_3 (1.0 equiv.), additive (0.2 equiv.), phenylboronic acid (2.0 equiv.), 16 h. *Z*/*E* ratios were determined by ^1H NMR spectroscopy on crude reaction mixtures. Enantiomeric excesses were determined by SFC analysis using a chiral non-racemic stationary phase.

We speculated that Lewis acid additives could activate the carbonate substrate by coordinating with the leaving group and hence enable the oxidative addition at a lower temperature. The utilization of $Zn(OTf)_2$ as an additive has been previously documented

to enhance both the substrate activation[86] and turnover frequency[87] in rhodium-catalysed reactions.

2.2.2 Scope of the enantioconvergent arylation with acyclic substrates

Table 2.3 Arylboronic acid scope.

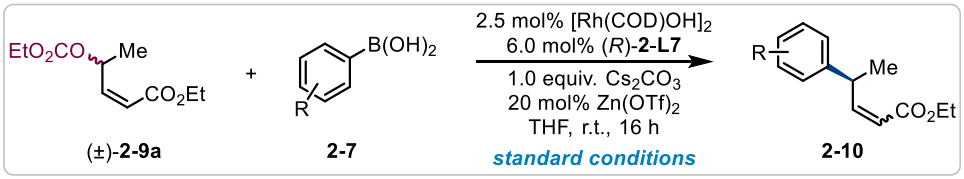

2-10a
94%, 98% *ee*
Z/*E* = 4.0 : 1

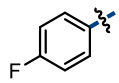

2-10b
90%, 98% *ee*
Z/*E* = 4.4 : 1

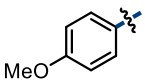

2-10c
93%, 97% *ee*
Z/*E* = 5.3 : 1

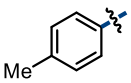

2-10d
98%, 96% *ee*
Z/*E* = 4.4 : 1

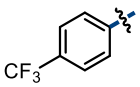

2-10e
78%, 98% *ee*
Z/*E* = 6.2 : 1

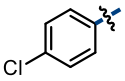

2-10f
60%, 98% *ee*
Z/*E* = 7.3 : 1

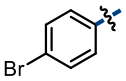

2-10g
74%, 97% *ee*
Z/*E* = 4.5 : 1

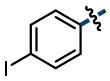

2-10h
57%, 98% *ee*
Z/*E* = 6.4 : 1

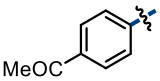

2-10i
82%, 98% *ee*
Z/*E* = 5.4 : 1

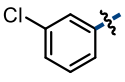

2-10j
88%, 95% *ee*
Z/*E* = 2.7 : 1

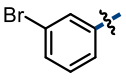

2-10k
98%, 96% *ee*
Z/*E* = 4.9 : 1

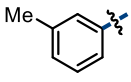

2-10l
94%, 96% *ee*
Z/*E* = 3.5 : 1

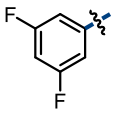

2-10m
83%, 97% *ee*
Z/*E* = 9.5 : 1

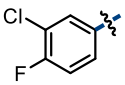

2-10n
85%, 95% *ee*
Z/*E* = 6.2 : 1

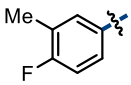

2-10o
92%, 94% *ee*
Z/*E* = 4.3 : 1

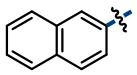

2-10p
97%, 90% *ee*
Z/*E* = 5.4 : 1

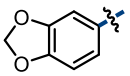

2-10q
83%, 92% *ee*
Z/*E* = 13 : 1

Reaction conditions: $[Rh(COD)OH]_2$ (2.5 mol%), (*R*)-**2-L7** (6.0 mol%), (±)-**2-9a** (0.4 mmol, 1.0 equiv), **2-7** (2.0 equiv), Cs_2CO_3 (1.0 equiv), $Zn(OTf)_2$ (20 mol%), THF (0.1 M), r.t., 16 h. All experiments were performed on 0.4 mmol scale. All compounds were isolated as single regioisomers (rr > 99:1). *Z*/*E* ratios were determined by ^{1}H NMR spectroscopy on crude reaction mixtures. Yields were determined by subsequent hydrogenation of the product mixture. Enantiomeric excesses were determined by hydrogenation of the product mixture and SFC analysis using a chiral non-racemic stationary phase. Absolute configurations were assigned by analogy to product **2-10d**, which was converted to (*S*)-curcumene as determined by comparing specific optical rotation values to those previously reported.

With optimised conditions established, we examined the boronic acid scope of the reaction (Table 2.3). The reported Z/E ratios are based on ^{1}H NMR spectroscopy of the crude reaction mixture. When desired, we found that would could (like in the case of **2-10d** below) separate the *Z* and *E* isomers by careful column chromatography, but for ease of characterization, the yield and *ee*'s of compounds reported in Tables 2 and 3 were determined on the product of hydrogenation of the alkenes obtained. Hydrogenation of the alkenes using Wilkinson's catalyst converted the Z/E mixture of compounds **2-10** and **2-12s** obtained in the arylation reaction to a common product. Pleasingly, a broad range of functionality was tolerated, including ether (**2-10c**) and halogen (**2-10f-h**, **2-10j**, **2-10k**) substituents. Disubstituted boronic acids furnished desired products in good yields and excellent enantioselectivities (**2-10m**-**2-10q**). In addition, electron-poor functionality was well tolerated with trifluoromethyl (**2-10e**) and acetyl (**2-10i**) substituted boronic acids providing desired product in good yield and excellent *ee*.

Table 2.4 Heteroarylboronic acid scope.

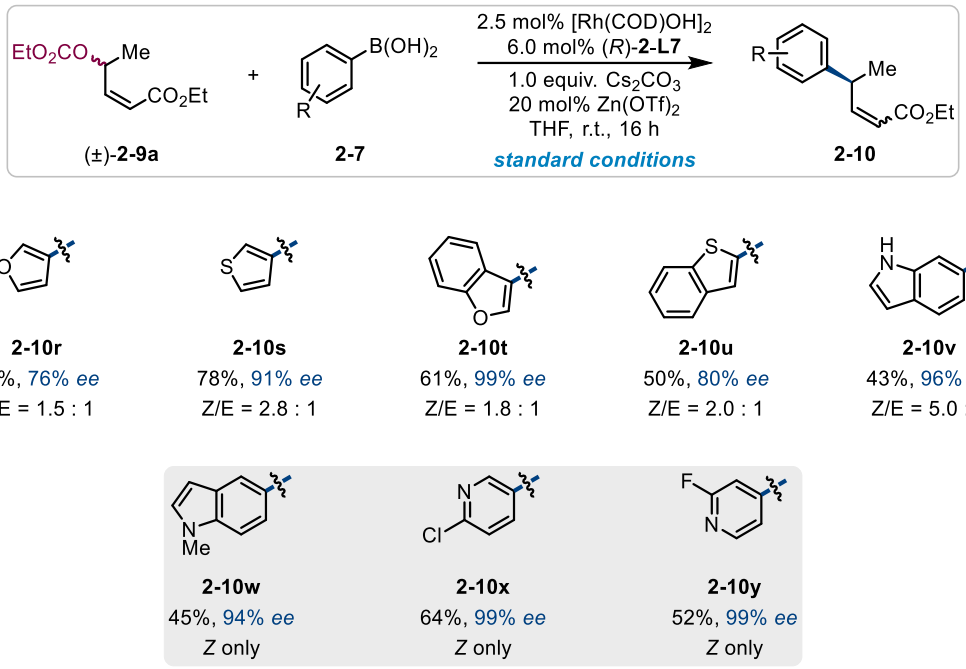

Reaction conditions: $[Rh(COD)OH]_2$ (2.5 mol %), (*R*)-**2-L7** (6.0 mol %), (±)-**2-9a** (0.4 mmol, 1.0 equiv), **2-7** (2.0 equiv), Cs_2CO_3 (1.0 equiv), $Zn(OTf)_2$ (20 mol %), THF (0.1 M), r.t., 16 h. All experiments were performed on 0.4 mmol scale. All compounds were isolated as single regioisomers (rr > 99:1). *Z*/*E* ratios were determined by ^{1}H NMR spectroscopy on crude reaction mixtures. Yields were determined by subsequent hydrogenation of the product mixture. Enantiomeric excesses were determined by hydrogenation of the product mixture and SFC analysis using a chiral non-racemic stationary phase.

Notably, the more challenging heteroaryl boronic acids,[88,89] displaying a variety of functional motifs and features common to pharmaceutical agents,[61,90-92] were suitable substrates for our methodology (Table 2.4). For example, indole-derived boronic acids produced the corresponding arylated unsaturated esters (**2-10v** and **2-10w**) in reasonable yields and excellent enantioselectivities. Furan and thiophene-derived coupling partners also performed well, although a reduction in enantioselectivity was observed when using furan-3-ylboronic acid (**2-10r**, **2-10s**). Pyridyl boronic acids can be employed too – products were obtained in moderate yield and excellent ee (**2-10x**, **2-10y**). The presence of 2-halide substituents on the pyridyl boronic acids is essential for their reactivity; however, these substituents possess the flexibility to be eliminated or utilised as sites for late-stage functionalisation.

The scope of allylic carbonate coupling partners was investigated too, as presented in Table 2.5. When employing a different primary alkyl-substituted substrate, chosen

arbitrarily, favorable outcomes were also achieved. For instance, utilizing *n*-propyl allylic carbonate (±)-**2-11a**, the formation of product **2-12a** was accomplished with a yield of 89%, exhibiting a *Z*:*E* ratio of 7:1 and an enantiomeric excess (*ee*) of 93%. Similar results were obtained with the bromine-substituted **2-12b** (98%, 3.6:1 *Z*/*E*, 93% ee). Examining the sterically demanding isopropyl-substituted (±)-**2-11**, the products **2-12c** and **2-12d** were obtained with >99% *ee*, albeit with slightly lower yields and *Z*/*E* ratios.

The introduction of a benzyl-protected alcohol on the aliphatic chain of an allylic carbonate led to the desired γ-arylation product, resulting in the formation of **2-12e** and **2-12f** with high yield and excellent enantioselectivity. Intriguingly, there was a slight reduction in regioselectivity compared to typical values (>99:1), as evidenced by ratios of 12:1 r.r. in **2-12e** and 16:1 r.r. in **2-12f**. This may be due to the competitive coordination of the benzyl ether with rhodium, which could direct arylation toward the α position of the ester.

Remarkably, the reaction exhibited tolerance towards C(sp^2)-hybridized phenyl substituents without requiring alterations to the ligand or any other reaction conditions. By employing phenyl-substituted (±)-**2-11g**, we successfully obtained the γ,γ-diarylsubstituted ester **2-12g** with a yield of 90% and an ee of 93%, albeit with a lower *Z*/*E* ratio of 1.7:1. Furthermore, the 3,4-chlorodisubstituted product **2-12h** was obtained with 86% yield, a *Z*/*E* ratio of 1.2:1, and excellent enantioselectivity (99% *ee*).

Crucially, allylic substrates containing *ortho*-substituted phenyl groups (**2-12k**, **2-12l**, and **2-12m**) were well-tolerated in the reaction, yielding products with >99% *ee*. As mentioned earlier, *ortho*-substituted boronic acid nucleophiles displayed unselective 1,4-addition. However, incorporating *ortho*-groups into the allyl unit facilitated the synthesis

of products with this substitution pattern. Product **2-12m** specifically features an *ortho*-Br group, providing further opportunities for product elaboration.

Moreover, a thiophene-substituted allylic carbonate yielded γ-arylation products **2-12n** and **2-12o** with isolated yields above 80% and excellent enantioselectivities (99% *ee*). However, exclusive formation of the branched products was not achieved, as evidenced by a ratio of 8:1 r.r. In the presence of highly electron-rich substituents on the allyl unit (**2-12i**, **2-12j**, **2-12n**, and **2-12o**), some α-products were observed too. Nonetheless, the isolated yields of the desired chiral products remained satisfactory.

The system also performs well when the ester moiety is varied, and excellent yields and enantioselectivities were obtained in products containing methyl (**2-12p** and **2-12q**) and bulky *tert*-butyl (**2-12r** and **2-12s**) esters.

Table 2.5 Scope of the allylic carbonate.

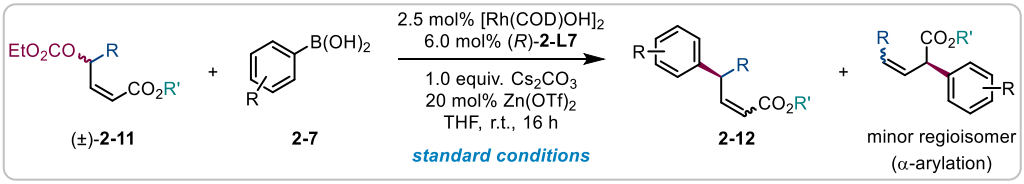

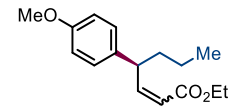

2-12a
89%, 93% *ee*
Z/*E* = 7.1 : 1

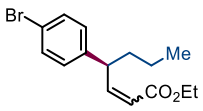

2-12b
98%, 93% *ee*
Z/*E* = 3.6 : 1

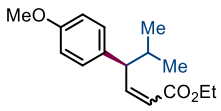

2-12c
57%, >99% *ee*
Z/*E* = 4.7 : 1

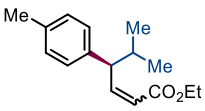

2-12d
81%, >99% *ee*
Z/*E* = 2.8 : 1

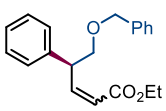

2-12e
79%, 96% *ee*
Z/*E* = 2.3 : 1
12 : 1 r.r.

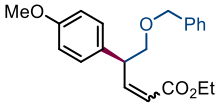

2-12f
77%, 99% *ee*
Z/*E* = 2.8 : 1
16 : 1 r.r

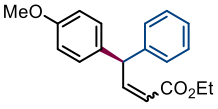

2-12g
90%, 93% *ee*
Z/*E* = 1.7 : 1

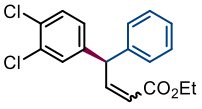

2-12h
86%, 99% *ee*
Z/*E* = 1.2 : 1

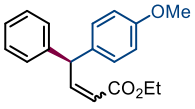

2-12i
78%, >99% *ee*
Z/*E* = 1.0 : 1
5.9 : 1 r.r.

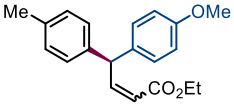

2-12j
76%, 99% *ee*
Z/*E* = 1.0 : 1
6.2 : 1 r.r.

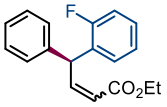

2-12k
81%, >99% *ee*
Z/*E* = 1.0 : 1

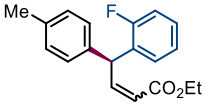

2-12l
63%, >99% *ee*
Z/*E* = 2.5 : 1

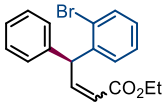

2-12m
51%, >99% *ee*
Z/*E* = 1.0 : 1

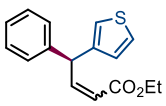

2-12n
80%, >99% *ee*
Z/*E* = 1.0 : 1
8 : 1 r.r.

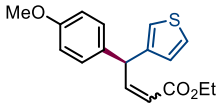

2-12o
83%, 99% *ee*
Z/*E* = 1.0 : 1
13 : 1 r.r.

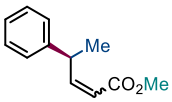

2-12p
89%, 96% *ee*
Z/*E* = 3.1 : 1

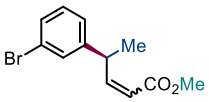

2-12q
94%, 94% *ee*
Z/*E* = 4.3 : 1

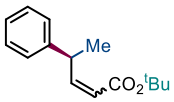

2-12r
87%, 97% *ee*
Z/*E* = 2.0 : 1

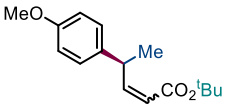

2-12s
70%, 96% *ee*
Z/*E* = 10 : 1

Reaction conditions: $[Rh(COD)OH]_2$ (2.5 mol %), (*R*)-**2-L7** (6.0 mol %), (±)-**2-11** (0.4 mmol, 1.0 equiv), **2-7** (2.0 equiv), Cs_2CO_3 (1.0 equiv), $Zn(OTf)_2$ (20 mol %), THF (0.1 M), r.t., 14 h, 0.4 mmol. Unless stated otherwise, all compounds were isolated as single regioisomers (r.r. > 99:1). *Z*/*E* and regioisomeric ratios were determined by ^1H NMR spectroscopy on crude reaction mixtures. Yields determined by subsequent hydrogenation of the product mixture. Enantiomeric excesses were determined by hydrogenation of the product mixture and SFC analysis using a chiral non-racemic stationary phase. Examples **2-12e**, **2-12f**, **2-12i**, **2-12j 2-12p** and **2-12q** (including the synthesis of the starting materials) we performed Ke Liu. Examples **2-12k**, **2-12l**, **2-12m**, **2-12n**, **2-12o, 2-12r** and **2-12s** (including the synthesis of the starting materials) were performed by Stephen J. Webster. Please see Experimental for more information.

It is worth to note that chiral nonracemic γ,γ-diarylsubstituted carbonyl scaffolds and their derivatives are present in a number of natural products, pharmaceuticals, and bioactive compounds.[93,94]

Enantioenriched γ,γ-diarylsubstituted carbonyl compounds are generally prepared through the transformation of optically pure precursors.[95-97] Alternative asymmetric catalysis methods are currently multi-step[97] and limited in scope.[98] Development of more convergent approaches is thus required. Our methodology overcomes this significant challenge and provides concise asymmetric access to γ,γ-diarylsubstituted carbonyl compounds.

2.2.3 Product derivatisation

The reaction product has useful functionality and can be further derivatized using well established reactions. Firstly, the major *Z*-product (***Z*-2-10d**, for example) can be isolated in good yields (Figure 2.12).

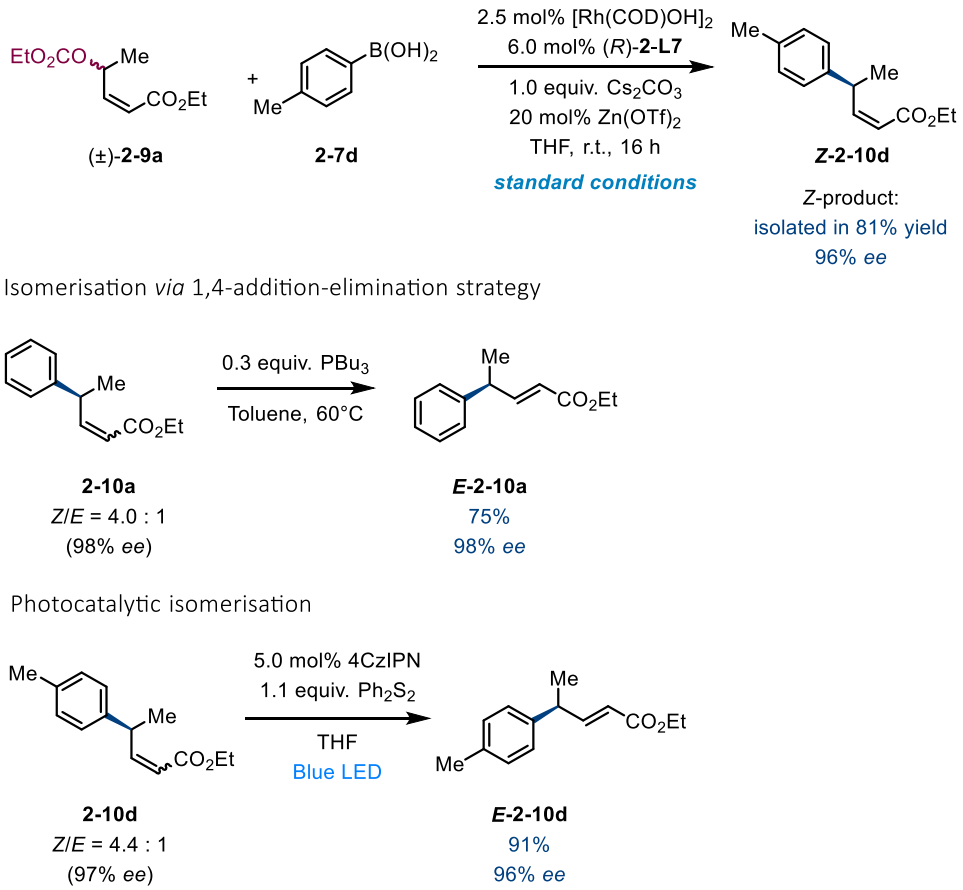

Figure 2.12 Isolation of the *Z*-product and isomerisation of the *Z*/*E* product mixture to *E*-isomer.

We also developed a procedure to convert the resulting mixture of *E* and *Z* products to the more thermodynamically stable *E*-isomer. Using tributylphosphine to facilitate a 1,4-addition-elimination sequence we manage to obtain the desired *E*-isomer of the product ***E*-2-10a** in good yield and conserve the enantiomeric ratio. Moreover, using an alternative photocatalytic isomerisation setup consisting of 4CzIPN and Ph_2S_2 under blue LED light, we achieve excellent yield of ***E*-2-10d** and the enantiomeric excess stays excellent (Figure 2.12).

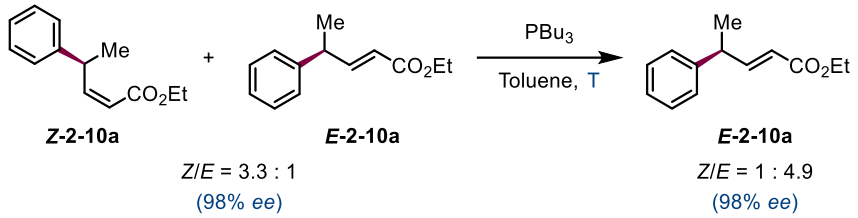

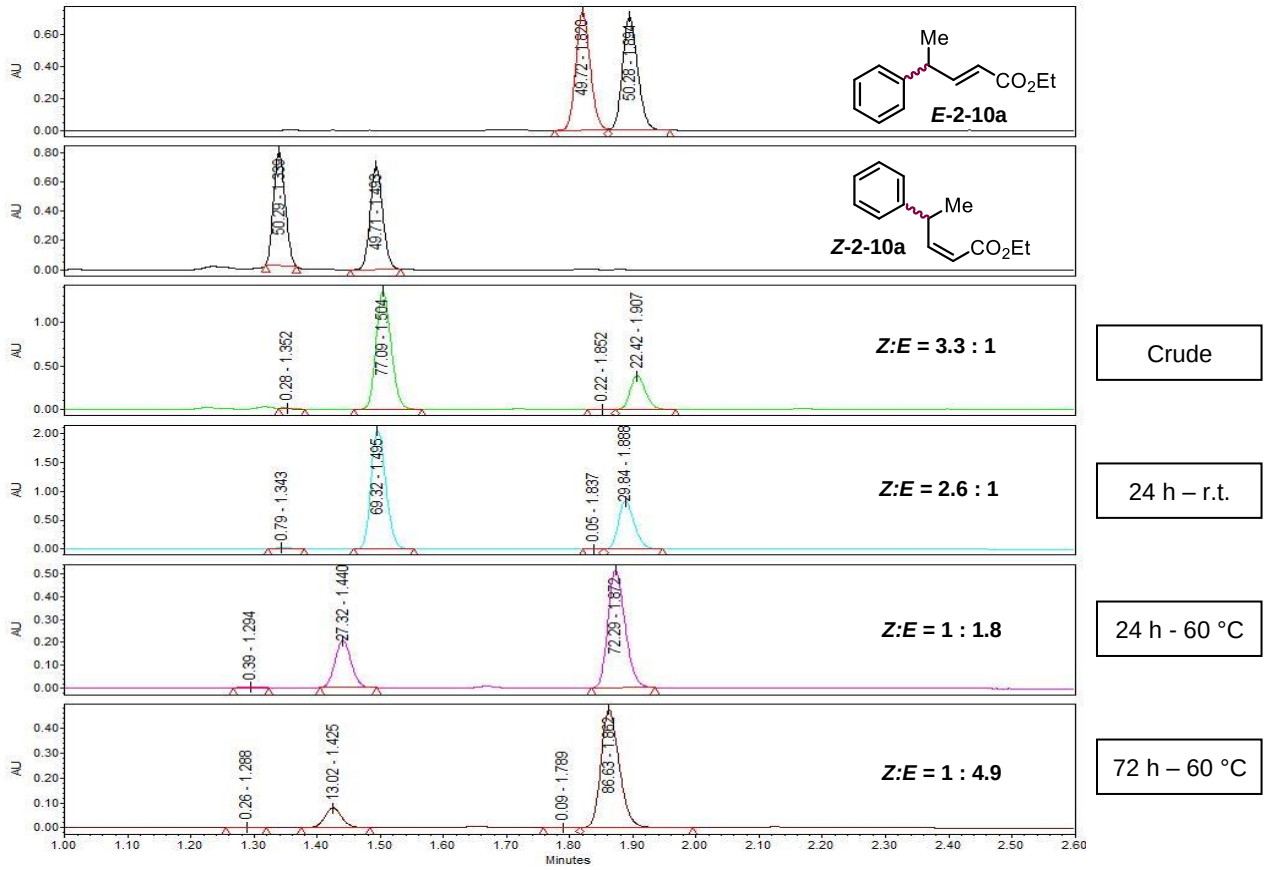

Figure 2.13 *Z* to *E* isomerisation monitoring over time by SFC. The two top traces are racemic *E* and *Z* products.

We sampled the isomerisation reaction (PBu_3 reaction conditions) and examined the SFC traces of the aliquots. As the isomerisation to more thermodynamically stable *E*-product proceeds, the *ee* of both *Z* and *E* products remains excellent (Figure 2.13). This data is consistent with the absolute stereochemistry of *Z* and *E* products at the newly formed stereogenic centre being identical.

One of the main challenges in asymmetric chemistry is the formation of contiguous stereocentres in acyclic molecules. It can be difficult to control the stereochemistry of each individual stereocenter, especially when the molecule becomes more complex. This can lead to a mixture of stereoisomers, which can be difficult to separate and can reduce the overall yield of the desired product.

Table 2.6 Optimization of 1,4-addition to obtain **2-13**.

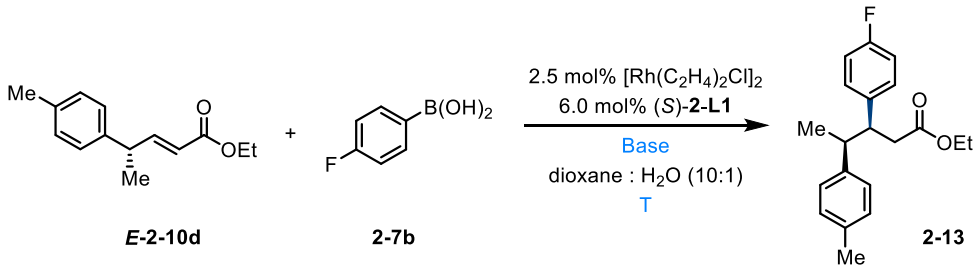

***E*-2-10d** **2-7b** **2-13**

Entry	Base	T / °C	Equiv. of **2-7b**	Conversion / %	d.r.
1	None	r.t.	3	-	-
2	None	60	3	-	-
3	KOH (0.5 eq.)	r.t.	3	-	-
4	KOH (0.5 eq.)	60	3	81 (78)	>20:1
5	KOH (0.5 eq.)	80	3	67	>20:1
6	KOH (1.0 eq.)	60	3	55	>20:1
7	KOH (0.5 eq.)	60	5	46	>20:1

Reaction conditions: $[Rh(C_2H_2)Cl]_2$ (2.5 mol %), (*R*)-**2-L1** (6.0 mol %), ***E*-2-10d** (0.2 mmol, 1.0 equiv), **2-7b**, base, dioxane : H_2O (10 : 1, 0.2 M), 14 h. Diastereomeric ratios were determined by ^{1}H NMR spectroscopy on crude reaction mixtures. Conversion reported by comparing ^{1}HNMR integrals to those of an external standard (dibromomethane). Isolated yield in parentheses.

The products of the developed allylic arylation reaction are α,β-unsaturated esters – this provides an opportunity to form two contiguous stereocenters *via* a sequential 1,4-addition. Rhodium-catalysed 1,4-additions of arylboronic acids to unsaturated carbonyls are useful for synthesizing a variety of complex, functionalized molecules.[84,99,100] Additionally, these reactions are typically performed under mild conditions, which makes them efficient and convenient to use.

Table 2.7 Optimization of 1,4-addition to obtain **2-14**.

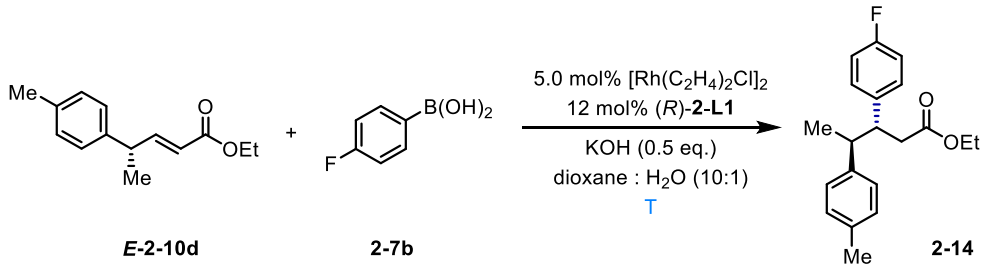

***E*-2-10d** **2-7b** **2-14**

Entry	Rh / %	T / °C	Equiv. of **2-7b**	Conversion / %	d.r.
1	2.5	60	3	12	>20:1
2	5.0	60	3	37	>20:1
3	5.0	80	3	72 (68)	>20:1
4	5.0	80	5	65	>20:1

Reaction conditions: $[Rh(C_2H_2)Cl]_2$ (5.0 mol %), (*R*)-**2-L1** (12.0 mol %), ***E*-2-10d** (0.2 mmol, 1.0 equiv.), **2-7b**, KOH (0.1 mmol, 0.5 equiv.), dioxane : H_2O (10 : 1, 0.2 M), 14 h. Diastereomeric ratios were determined by ^{1}H NMR spectroscopy on crude reaction mixtures. Conversion reported by comparing ^{1}HNMR integrals to those of an external standard (dibromomethane). Isolated yield in parentheses.

We attempted to perform 1,4-additions of 4-fluorophenylboronic **2-7b** acid with our allylic arylation product ***E*-2-10d**. After an extensive optimisation (Tables 2.6 and 2.7), both diastereomers of the product (**2-13** and **2-14**) could be accessed in reasonable yield and >20:1 d.r. using the two enantiomers of the chiral ligand. Any of the four diastereoisomers of the product can be synthesised using different combinations of ligands from a simple carbonate starting material (Figure 2.14).

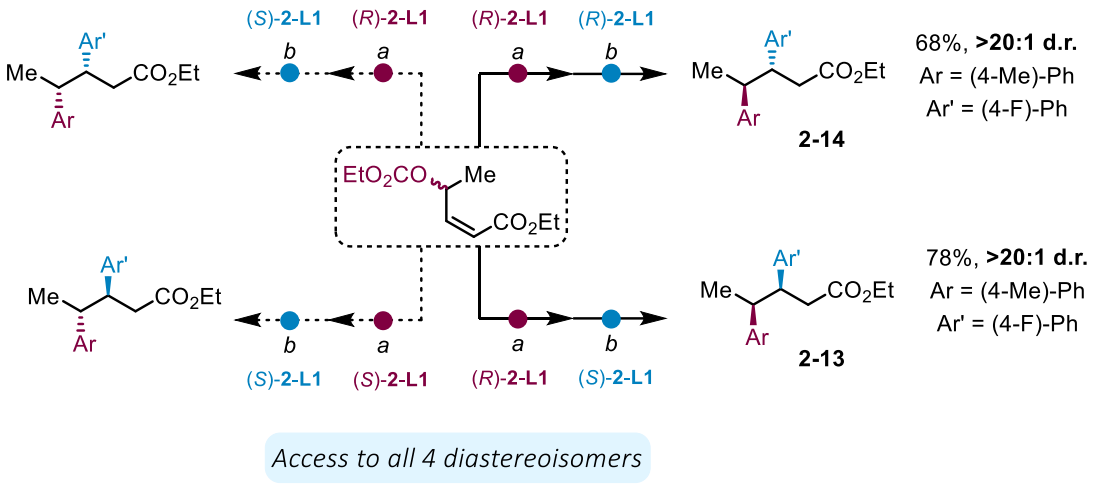

Figure 2.14 Strategy to access any of the four diastereomers of a molecule with two contiguous stereocenters. ([a][Rh(COD)OH]$_2$ (2.5 mol %), (*S*)- or (*R*)-Cl-MeO-BIPHEP (6.0 mol %), Cs_2CO_3 (1.0 equiv.), $Zn(OTf)_2$ (0.2 equiv.), (4-methyl)phenylboronic acid (2.0 equiv.), 16 h. [b][Rh(C_2H_4)$_2$Cl]$_2$, (*S*)- or (*R*)-BINAP, KOH, (4-fluoro)phenylboronic acid, dioxane : H_2O, 60 or 80 ºC).

Metathesis with ethylene affords a simple aliphatic fragment **2-15** in good yield while conserving the *ee* (Figure 2.15). This can be used in further metathesis reactions with a variety of different double bonds, including those found in alkenes, dienes, and other unsaturated compounds to introduce an aliphatic fragment with a chiral methyl group.

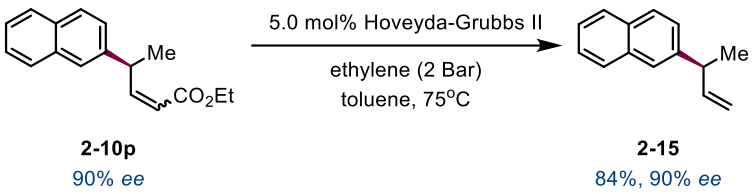

Figure 2.15 Grubbs metathesis to generate a chiral terminal alkene fragment from a Z/E mixture of Rh-reaction products.

To further demonstrate the synthetic value of this new versatile methodology, we synthesised natural products (*S*)-curcumene and (*S*)-4,7-dimethyl-1-tetralone which is a natural product precursor (Figure 2.16).

Reduction of the α,β-unsaturated ester **2-10d** with Wilkinson's catalyst leads to a γ-substituted ester ***red*-2-18**, a key intermediate in the synthesis of both natural products,

in good yield and excellent enantioselectivity (see SI for details). Further reduction with $LiAlH_4$ yields a remotely substituted alcohol **2-16**. Oxidation with Dess-Martin periodinane and Wittig reaction furnish (*S*)-curcumene **2-17** in good yield and excellent enantioselectivity. The γ-arylated acyclic ester ***red*-2-18** can also be hydrolysed and transformed into (*S*)-4,7-dimethyl-1-tetralone **2-19** by acid-promoted cyclisation.

The (*S*)-4,7-dimethyl-1-tetralone scaffold is known for its structural versatility and chemical reactivity, which makes it an attractive starting point for the synthesis of complex, functionalized molecules. In particular, (*S*)-4,7-dimethyl-1-tetralone **2-19** is a key intermediate in the total synthesis of several natural products, for example (–)-lacvigatin, (*S*)-*ar*-himachalene, and (+)-erogorgiaene.[101] Our method provides a conceptually new approach to these targets and a means to prepare analogues by starting with different boronic acids. It should allow access to a variety of terpene analogues and derivatives by starting with different allyl partners.

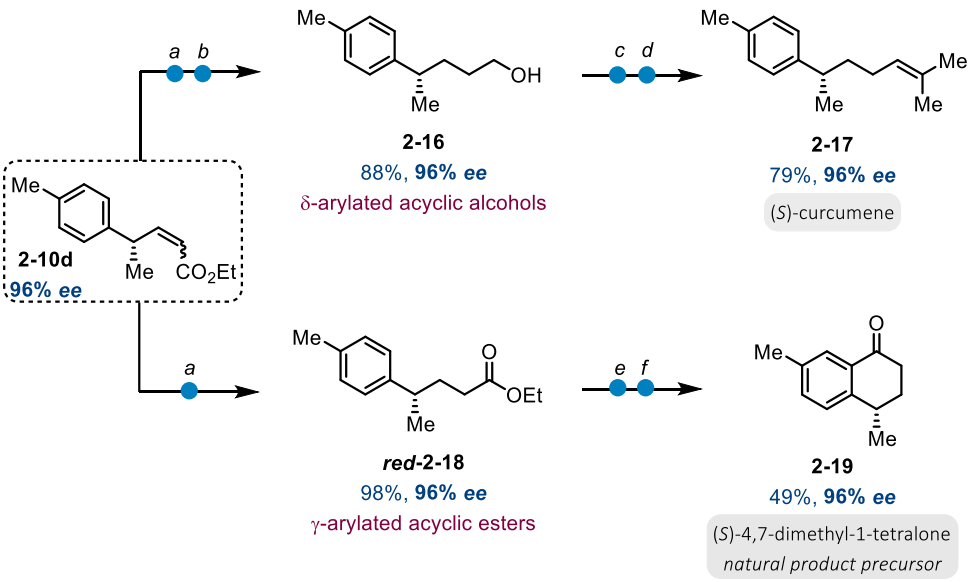

Figure 2.16 Application of methodology to natural product synthesis. ([a]H_2, $[Rh(PPh_3)_3Cl]$, THF. [b]$LiAlH_4$, THF. [c]DMP, THF, MeOH. [d]isopropyltriphenylphosphonium iodide, *n*BuLi. THF, -15 ºC. [e]LiOH, THF, MeOH. [f]TFA, TFAA, 0 ºC).

In addition, by hydrogenating **2-12d** and transforming its ester moiety into a methyl ketone we could obtain baccharisketone **2-20**, a natural product exhibiting cytotoxic activity against leukaemia cells (Figure 2.17).[102]

Cyclisation and reductive amination of ***red*-2-12f** (see above Table 2.3) is reported[103,104] to deliver sertraline (Zoloft®) (Figure 2.17). Sertraline **2-21** is a pharmaceutical drug that is used to treat a variety of conditions, including depression, anxiety, and obsessive-compulsive disorder.[105-109] It belongs to the class of selective serotonin reuptake inhibitors (SSRIs) and functions by inhibiting the reuptake of serotonin in the brain, thereby increasing the levels of this neurotransmitter. In addition to its established use as an antidepressant, sertraline and its derivatives have garnered recent attention for their potential as antiviral, antifungal, and anticancer agents.[110-113]

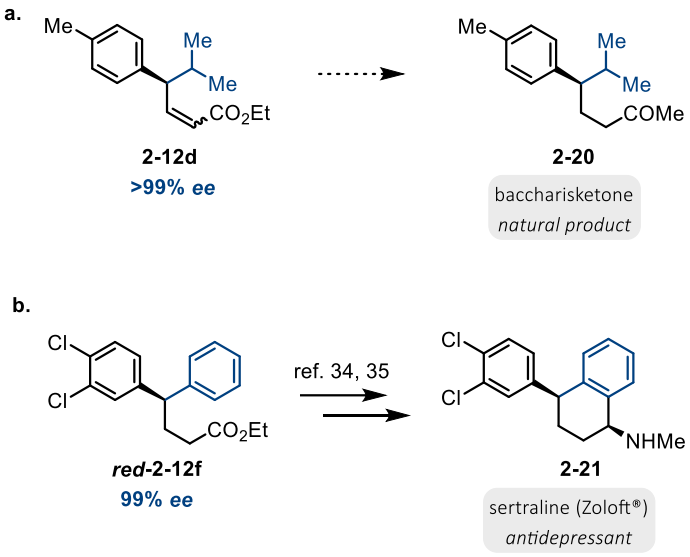

Figure 2.17 a. Our products are analogues of natural product baccharisketone. b. Formal total synthesis of antidepressant sertraline (Zoloft®).

In industry, Zoloft® is synthesized using a multistep process that involves several different chemical reactions, including aforementioned cyclization and reduction reactions.[114] Ultimately, enantiopure sertraline is obtained by resolution, making the process intrinsically inefficient. Our methodology constitutes a new way of preparing

sertraline asymmetrically. Libraries of enantioenriched sertraline derivatives expediently prepared using our methodology could lead to discovery of its more potent analogues.

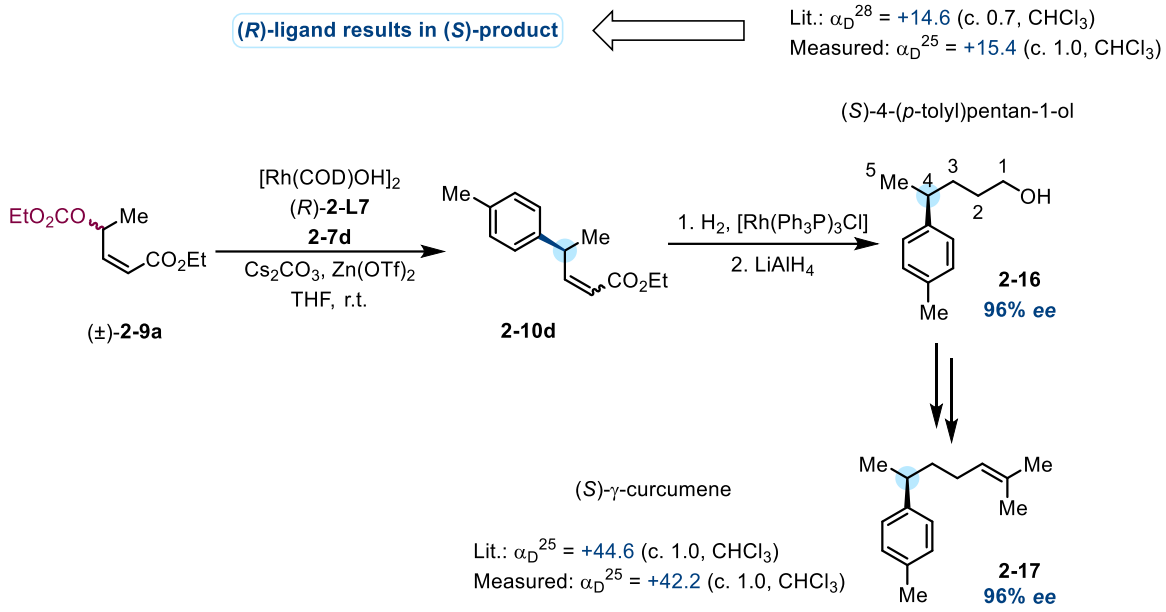

Figure 2.18 Determination of absolute stereochemistry by comparison of the specific optical rotation of 4-(*p*-tolyl)pentan-1-ol **2-16** with reported literature value.[115] Specific optical rotation value for curcumene **2-17** matches the literature reports too.[78]

While carrying out the synthesis of curcumene, we have measured the specific optical rotation value of the intermediates (for example, 4-(*p*-tolyl)pentan-1-ol **2-16**) and curcumene **2-17** itself (Figure 2.18). Comparison of the observed specific optical rotations with values reported in the literature revealed that the absolute stereochemistry at the newly formed chiral centre is (*S*).

2.2.4 Mechanistic studies

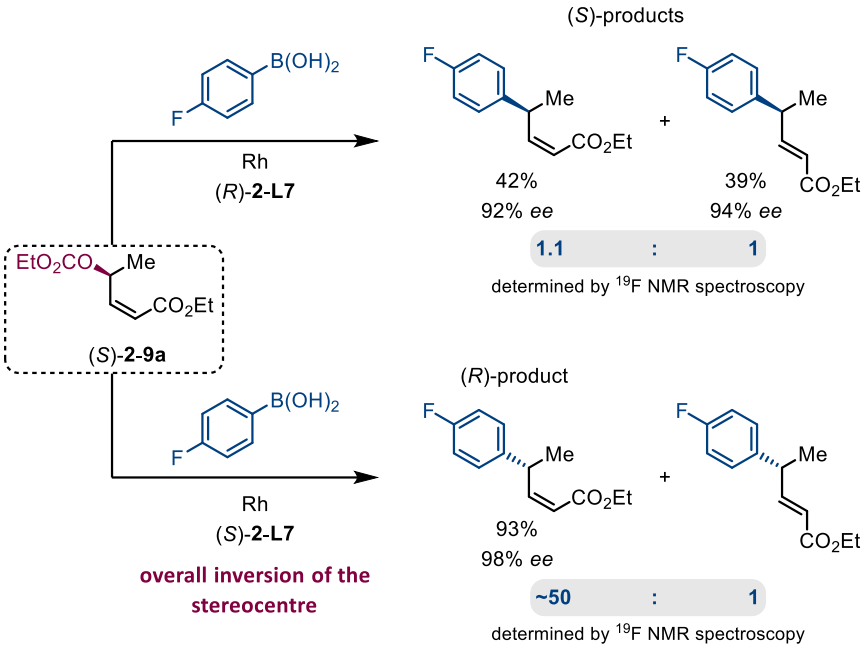

Figure 2.19 Using enantiopure (99% *ee*) (*S*)-**2-9a** starting material.

Next, we investigated the reaction mechanism. We prepared enantiopure starting material (*S*)-**2-9a** and subjected it to the standard reaction conditions using two different enantiomers of chiral ligand (Figure 2.19). Upon reaction with (*R*)-Cl-MeO-BIPHEP, (*S*)-**2-9a** was transformed into an around 1:1 mixture of *E* and *Z* products, both with good enantioselectivity. When using (*S*)-Cl-MeO-BIPHEP, *Z*-product was obtained exclusively with excellent enantioselectivity. This suggests that when a racemic substrate is used one enantiomer of the starting material favours forming the *Z*-product while another enantiomer forms both *Z* and *E* products. These results represent 'matched' and 'mismatched' cases of the steric configuration of substrate and chirality of the ligand used in the reaction. Final *Z*/*E* ratio is determined by the nature of boronic acid and its reaction pattern in the 'mismatched' case.

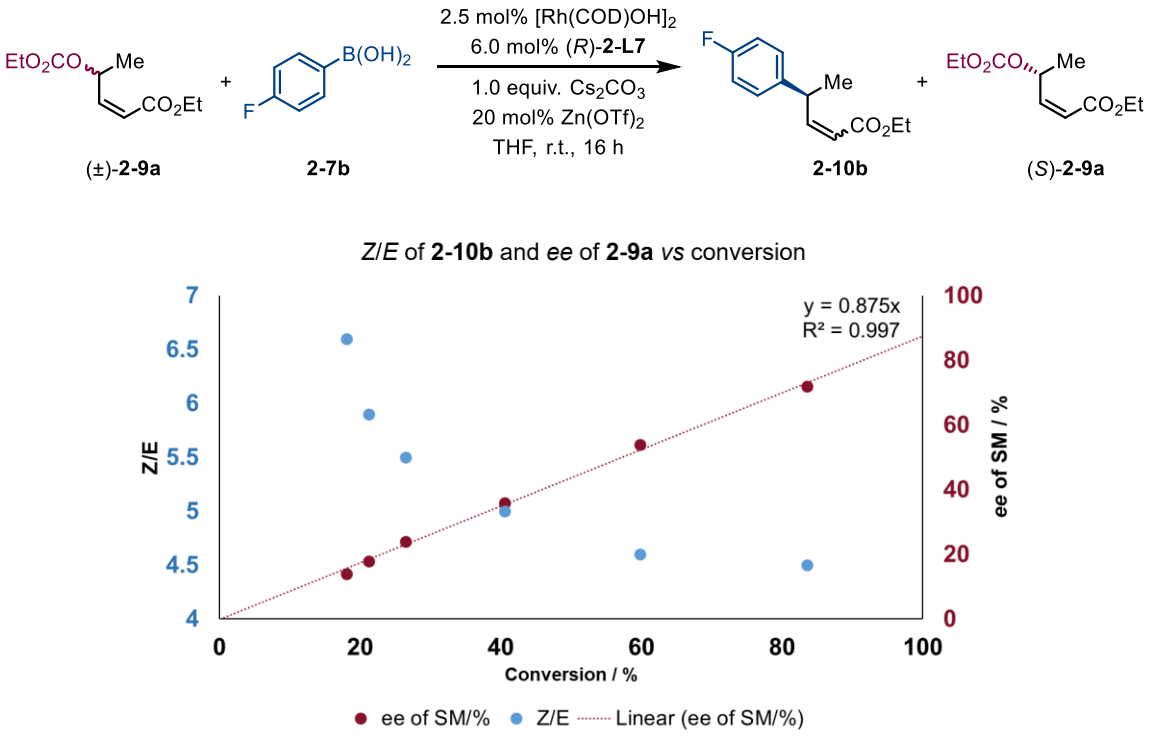

Figure 2.20 Changes of product Z/E ratio and *ee* of starting materials in time.

Further evidence for this process is obtained by monitoring Z/E ratio of **2-10b** as the reaction proceeds (Figure 2.20). At low conversion, Z/E ratio is high and it decreases over time until it plateaus as the full conversion is approached. Change in *ee* of the starting material **2-9a** over time also supports this hypothesis - it is directly proportional to the conversion.

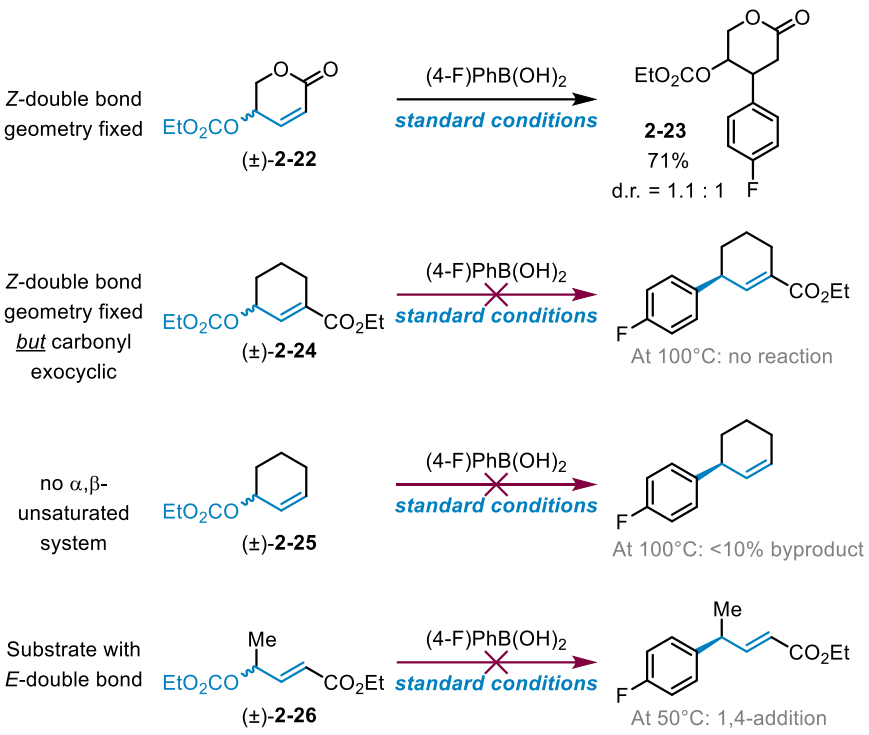

Figure 2.21 Control experiments with alternative allylic carbonates.

To establish what features of the starting material are required for these regioselective, enantioconvergent transformations we prepared a series of model substrates (Figure 2.21). Cyclic γ-carbonate unsaturated ester (±)-**2-22**, with a double bond fixed in the *Z*-configuration, underwent 1,4-addition to form **2-23**[116] instead of allylic arylation. Substrate (±)-**2-24** with an exocyclic carbonyl, on the other hand, is unreactive, even at 100 ºC. This could be due to a number of reasons, including having more substitution on the olefin or lack of Rh-carbonyl chelation. Further, 1,4-additions to such exocyclic electrophiles are rare. The simple allylic carbonate (±)-**2-25** also gave no arylation under our standard conditions, and <10% of an unknown product when the reaction was performed at a higher temperature (50 °C). In starting materials featuring an *E*-double bond (see (±)-**2-26**, Figure 2.21), the allylic system is again unreactive under standard reaction conditions. However, upon heating to 50 ºC, 1,4-addition is observed. Overall,

these experiments provide evidence supporting the regioselective γ-arylation being possible on allylic enones where the rhodium can chelate to the carbonyl.

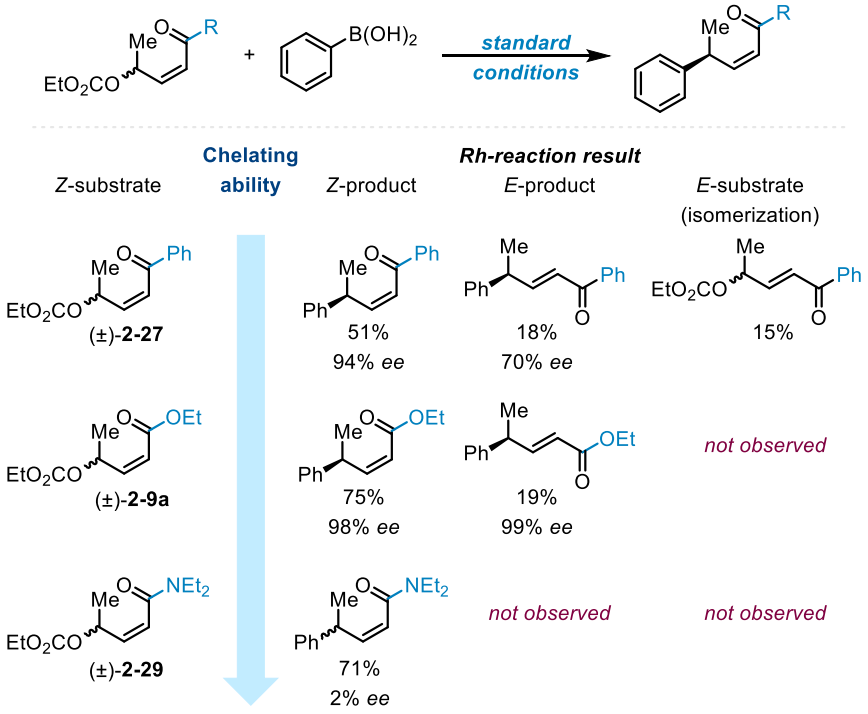

Figure 2.22 Control experiments using allylic carbonates with different chelating ability.

The reactivity profile observed when using substrates with different carbonyls (Figure 2.22) is consistent with chelating or directing ability of the carbonyl playing a key role in the reaction outcome. Amides are prominent directed metalation groups[117], and under the standard reaction conditions, amide (±)-**2-29** furnishes only the *Z*-product, albeit as an almost racemic mixture. Ketone (±)-**2-27**, on the other hand, furnishes *Z*-product in 51% yield and 94% *ee* but the *E*-product is formed in lower (70%) *ee*, and we also recovered some isomerised *E*-ketone while using (±)-**2-27**. Chelation-promoted reactivity is consistent with substrates (±)-**2-22**, (±)-**2-25** and (±)-**2-26** not undergoing arylation. We speculate that the Rh-carbonyl interaction facilitates oxidative addition and enables a pathway by which both enantiomers of the starting material may converge on

a single Rh-intermediate before reductive elimination to give a single enantiomer and regioisomer of product.

This evidence led us to conclude that the necessary components for the allylic arylation appear to be an allylic leaving group featuring a *Z*-olefin, conjugated to an ester.

2.2.5 Proposed mechanism

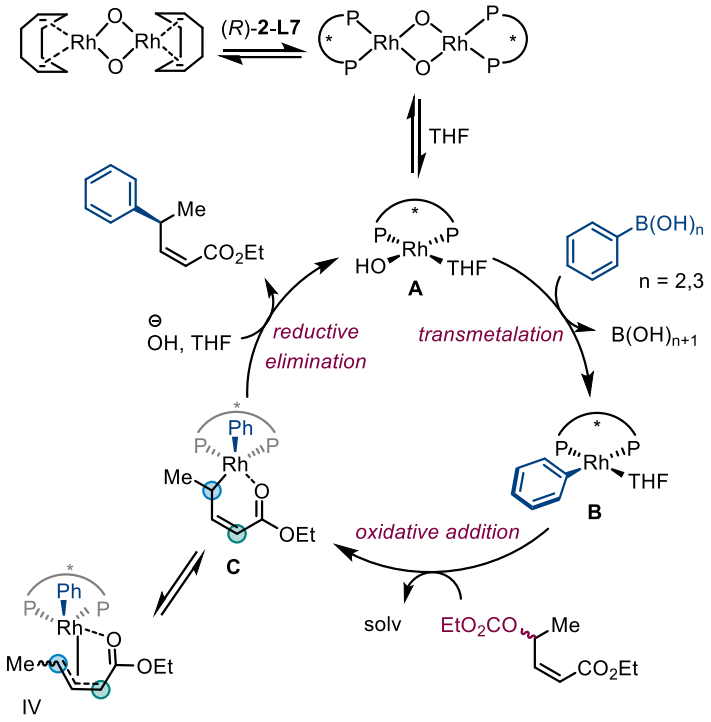

Figure 2.23 Proposed mechanism for the enantioconvergent arylation of allylic enoates (formation of major product).

Based on these experimental observations and previous mechanistic studies,[85] we propose a mechanism for Rh-catalyzed allylic arylation of acyclic substrates to form the major *Z*-product (Figure 2.23). First, an active catalytic complex **A** is formed by bisphospine ligand displacing COD on rhodium precatalyst. A rapid transmetallation of aryl boronic acid follows to furnish the intermediate complex **B**. This complex undergoes an oxidative addition with the substrate to form the intermediate **C**. Enantiodetermining irreversible reductive elimination leads to the observed *Z*-product. A combination of π-

σ-π interconversion and rotation of single bonds can lead to an *E* double bond in the intermediate **IV** and the minor *E*-product following a reductive elimination.

2.2.6 Synthesis of an anticancer agent Lasofoxifene

Selective estrogen receptor modulators (SERMs) are a group of compounds that bind to estrogen receptors and have agonist or antagonist effects in different tissues. SERMs have potential for use in the prevention or treatment of various diseases, particularly those related to aging, such as osteoporosis. Four chemical classes of SERMs have been approved for use in humans, including triphenylethylenes, benzothiophenes, indoles, and naphthalenes. Lasofoxifene (Fablyn),[118,119] a naphthalene-type derivative, has unique properties among SERMs, including a higher binding affinity to estrogen receptors and higher oral bioavailability than other SERMs. It has also shown potential for use in the prevention and treatment of breast cancer,[120] as well as positive effects on urogenital atrophy[121] and serum lipid levels.[122] The current synthetic routes for producing Lasofoxifene are limited and include the use of expensive or difficult-to-obtain precursors, and the need for chiral chromatography or enzymatic asymmetric deacylation to produce the enantiomerically pure compound.

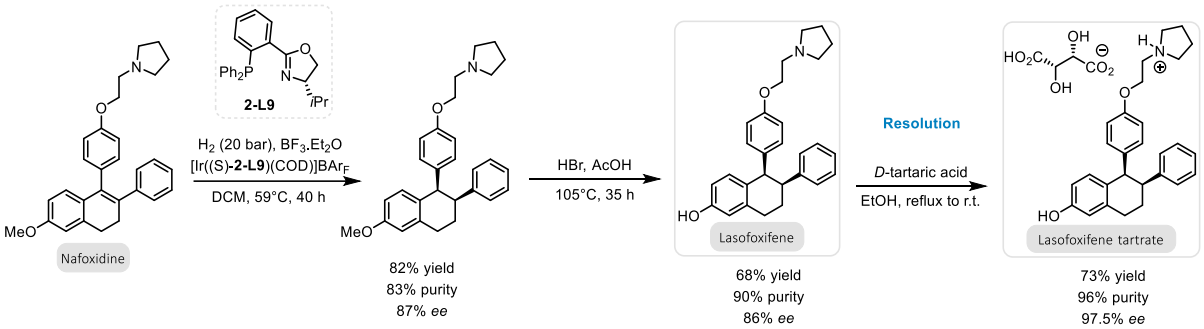

Figure 2.24 Example of a recently reported synthesis of Lasofoxifene.

A new approach featuring an asymmetric hydrogenation of Nafoxidine and similar compounds as a potential route to synthesizing Lasofoxifene tartrate has recently been

described (Figure 2.24).[123] However, stereoselective hydrogenation of tetrasubstituted olefins is particularly challenging.[124-126] The reported approach uses a complex system involving an iridium-based catalyst and the hydrogenation takes place in a biphasic system, with the catalyst and substrate dissolved in an aqueous phase and the hydrogen gas supplied in the organic phase. Another disadvantage of the transformation is the requirement for high H_2 gas pressure in order for it to occur. Importantly, when using this method, Lasofoxifene can be obtained in high purity and enantioselectivity only following a chiral resolution.

To the best of our knowledge, catalytic asymmetric synthesis of Lasofoxifene that provides high enantioselectivities has not been reported to date. Our methodology could enable the addition of both stereocenters prior to cyclisation, thereby circumventing the need for the sterically demanding hydrogenation and providing a general solution for this longstanding problem.

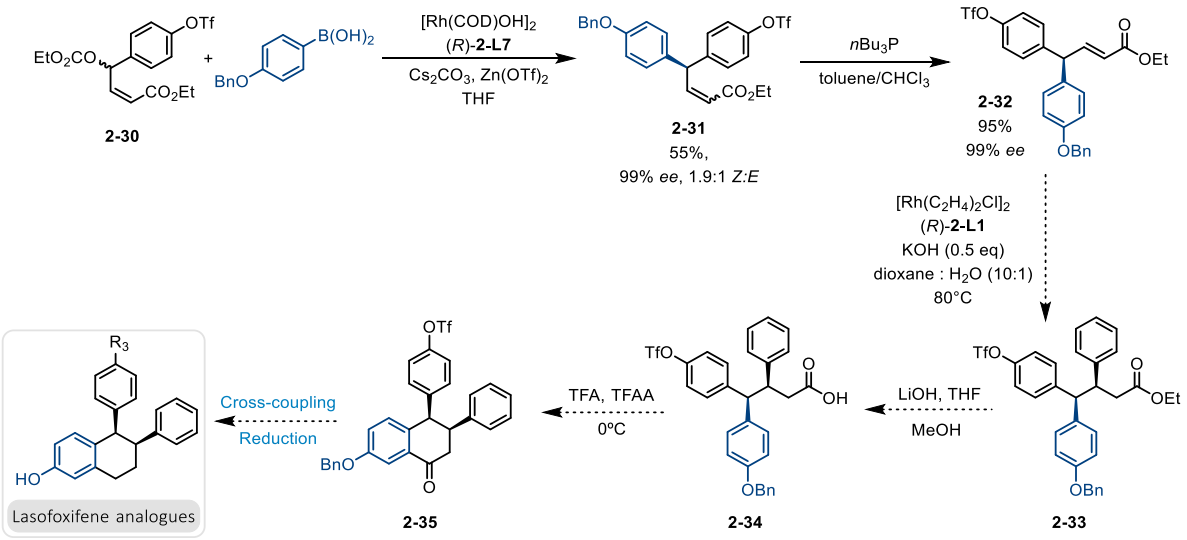

Figure 2.25 Structure of anticancer agent Lasofoxifene and an envisaged synthetic route to its analogues using our methodology.

We found that, using our rhodium-catalysed arylation methodology as a central step, Z/E mixture of arylated products **2-31** could be isomerised to yield the thermodynamically

more stable *E*-product **2-32** in yields exceeding 90% (Figure 2.25). An asymmetric 1,4-addition to the said *E*-α,β-unsaturated ester can be envisaged to give a γ,β-arylated ester **2-33** with both Lasofoxifene stereocenters established. Notably, since the absolute stereochemistry of the newly formed chiral centre can be controlled by choosing an appropriate ligand in each step, all 4 diastereomers of Lasofoxifene can be accessed. A Friedel-Crafts acylation followed by a cross-coupling and a global reduction to remove the benzylic ketone and the benzyl protecting group could complete the synthetic route. This approach to Lasofoxifene is modular – libraries of drug derivatives bearing different aryls could be efficiently synthesised. Such an approach is an asset in drug discovery campaigns where SAR studies necessarily require synthesis of multiple compound derivatives to identify the one with the highest affinity.

Currently we are in the process of Lasofoxifene synthesis using our developed asymmetric Suzuki-Miyaura coupling reaction, which would allow for the efficient and selective formation of the compound's complex molecular structure.

2.3 Conclusions

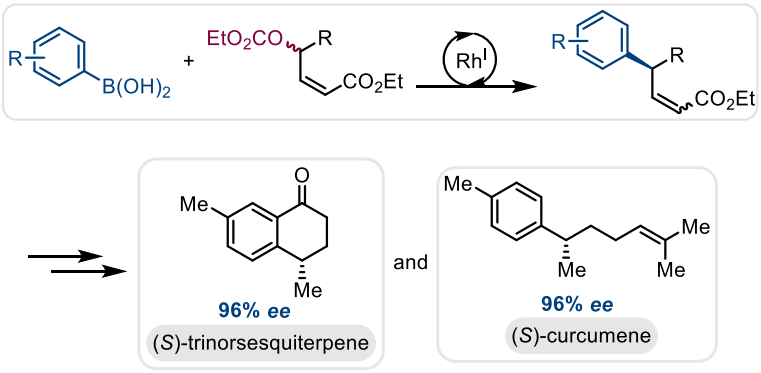

Figure 2.26 Summary of the developed asymmetric Suzuki-Miyaura coupling with acyclic allylic substrates.

To sum up, we have described an asymmetric arylation of acyclic internal allylic systems (Figure 2.26). Our procedure achieves a chemo-, regio-, *Z*/*E*- and enantioselective

arylation of γ-carbonate enoates. The mild and robust reaction conditions are compatible with a broad range of functionalities and substitution patterns on both boronic acids and allylic electrophiles. This cross coupling offers straightforward and modular asymmetric access to remotely substituted esters and alcohols – a privileged motif in many bioactive molecules. We exemplified the potential of this strategy with facile asymmetric total syntheses of natural products (*S*)-curcumene and (*S*)-4,7-dimethyl-1-tetralone. Moreover, a novel enantioselelctive route to sertraline (Zoloft®) and its derivatives was proposed. This method is anticipated to become a powerful tool in medicinal chemists' toolbox. Further research into this reaction and its applications has the potential to lead to important advances in the field of asymmetric catalysis.

2.4 Future directions

2.4.1 Asymmetric Suzuki-Miyaura coupling with vinylboronic acids

Our group has demonstrated that vinylboronic acids are viable coupling partners in Rh-catalysed asymmetric Suzuki-Miyaura reactions. For example, we coupled an array of vinylboronic acids with bicyclic allylic chlorides in good yields and enantioselectivities (Figure 2.27).[67]

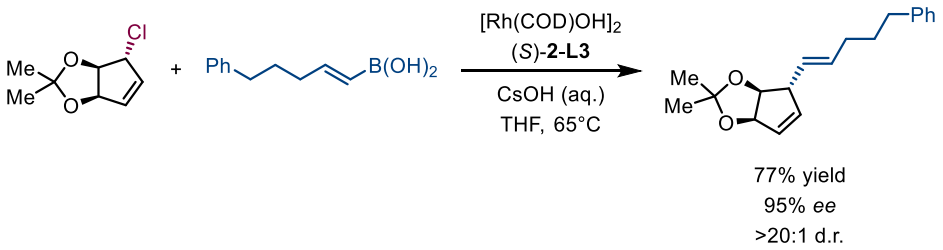

Figure 2.27 An example of Rh-catalysed diastereo- and enantioselective Suzuki-Miyaura cross-coupling of a bicyclic allylic halide with a vinylboronic acid.

Vinylboronic acids have not yet been explored for use in regioselective Suzuki couplings of acyclic substrates. We propose that vinylboronic acids could be equipped in

enantioconvergent allylic alkylations to generate a more complex acyclic molecule **2-37** with a remote stereocentre (Figure 2.28). The subsequent use of Wilkinson's catalyst for hydrogenation can selectively reduce the electron-poor double bond, leaving triply-substituted double bonds intact. Several other protocols for selective 1,4-hydrogenation of unsaturated carbonyls have also been reported.[127,128] This means it is possible to selectively reduce only the double bond conjugated to the carbonyl and access a remote allylic stereocenter in an acyclic molecule (**2-38**).

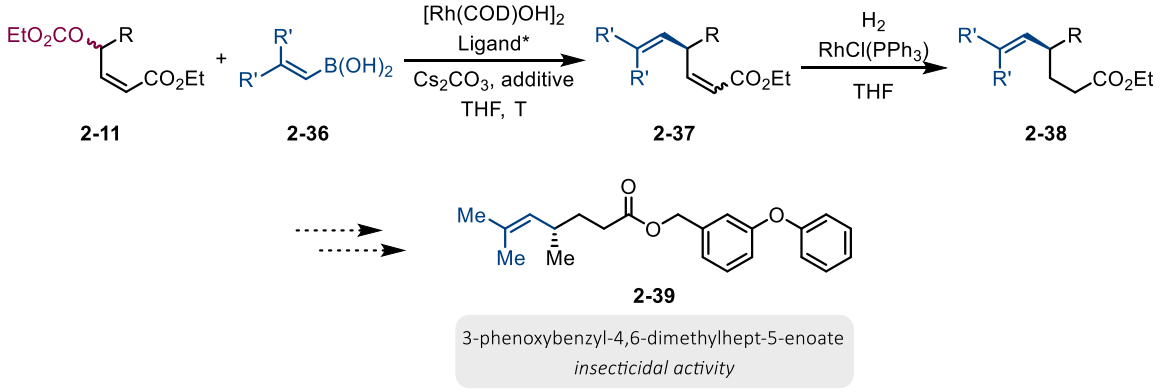

Figure 2.28 Employing vinylboronic acids in enantioconvergent Suzuki-Miyaura coupling with acyclic racemic allylic carbonates.

Currently there are no straightforward methods to generate these molecular motifs asymmetrically. For example, 3-phenoxybenzyl-4,6-dimethylhept-5-enoate **2-39** (Figure 2.28) has been synthesised from natural product (+)-citronellal already possessing the chiral centre. The resulting fragment is present in biologically active natural products and 3-phenoxybenzyl-4,6-dimethylhept-5-enoate **2-39** in particular has been shown to possess insecticidal activity.[129]

We believe that our approach using vinylboronic acids in enantioconvergent allylic arylations could be used to access a wide range of 3-phenoxybenzyl-4,6-dimethylhept-5-enoate derivatives in a rapid and efficient manner, potentially enabling the synthesis of libraries of biologically active compounds.

While further research is needed to fully assess the feasibility of this approach, the use of vinylboronic acids in enantioconvergent allylic arylations shows potential as a means of synthesizing complex acyclic molecules with controlled stereochemistry.

2.4.2 Synthesis of acyclic compounds with three contiguous stereocenters

One of the main challenges of enantioselectively forming multiple contiguous stereocenters in acyclic molecules is that it can be difficult to control the stereochemistry of each individual stereocenter, especially when the molecule becomes more complex. This can lead to a mixture of stereoisomers, which can be difficult to separate and can reduce the overall yield of the desired product.

Our methodology can be used to overcome these challenges. We have shown that two contiguous stereocenters can be formed employing Suzuki-Miyaura arylation/isomerisation/1,4-addition sequence. The third stereocenter can be introduced by α-functionalisation of the carbonyl moiety in ***E*-2-12**. For example, the ester could be converted[130] into an amide **2-41** that is reported to undergo nickel-catalysed enantioselective α-alkylation.[131]

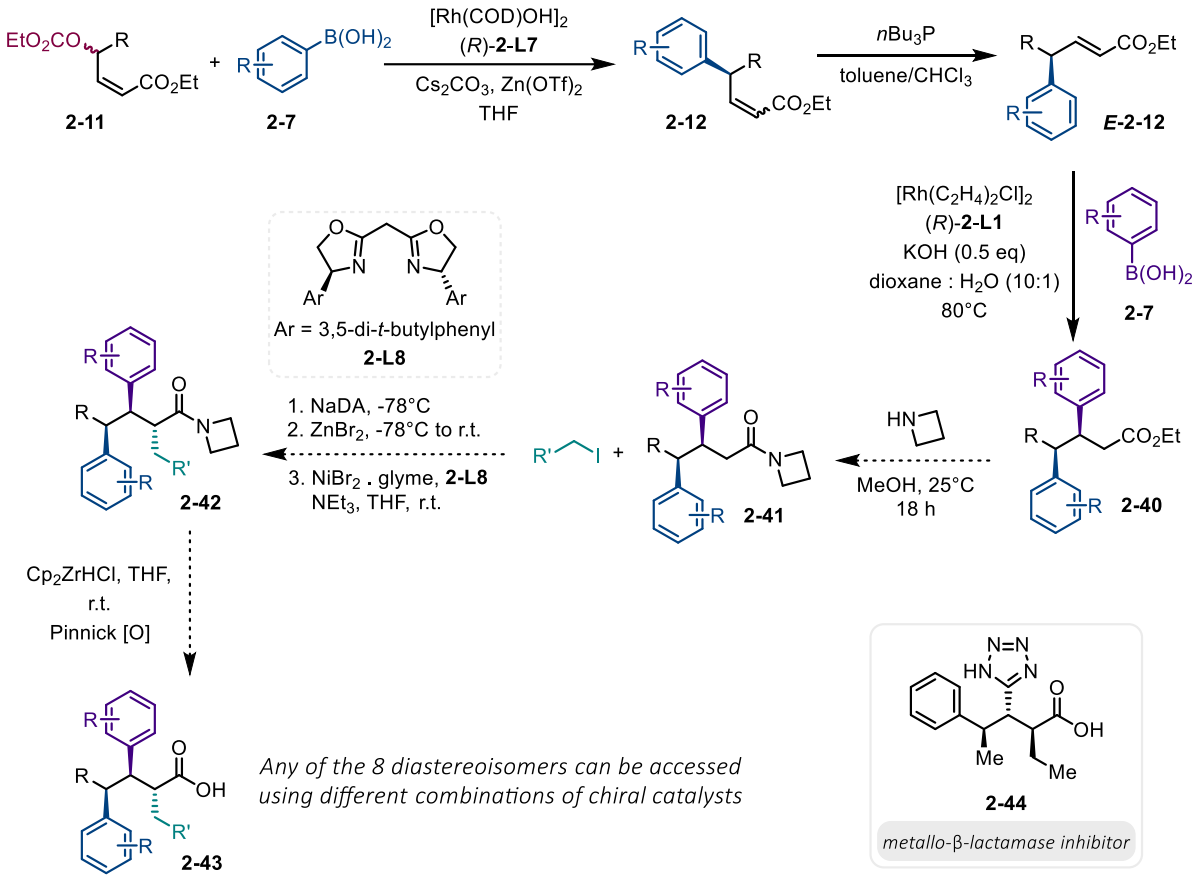

Figure 2.29 A strategy for asymmetric synthesis of acyclic molecules with multiple contiguous stereocenters.

The absolute stereochemistry of each new chiral centre formed is determined by the ligand used so all eight diastereomers can be accessed using an appropriate combination of ligands (Figure 2.29).

Another approach for enantioselective α-functionalisation of carbonyls involves introducing a chiral auxiliary group onto the carbonyl and then removing it after the desired stereocenters have been formed.[132,133] Other methods include the use of enzymatic catalysis[134] or Mukaiyama aldol reaction,[135,136] which utilises a chiral Lewis acid catalyst to promote the addition of an aldehyde or ketone to an enolate or imine intermediate.

Some acyclic compounds containing three adjacent stereocenters have been reported to have important biological activities. For example, β-tetrazolyl-propionic acids, exemplified by **2-44**, are a class of compounds that are known to have inhibitory activity against metallo-β-lactamases.[137] Metallo-β-lactamases are enzymes that are produced by bacteria and are responsible for hydrolysing β-lactam antibiotics, such as penicillins and cephalosporins. This makes the bacteria resistant to these antibiotics, which can be a major problem in the treatment of bacterial infections.

By using asymmetric Suzuki-Miyaura couplings to synthesize analogues of β-tetrazolyl-propionic acid **2-44** (Figure 2.29), it may be possible to develop compounds with improved potency and efficacy against metallo-β-lactamases.[137]

2.4.3 Synthesis of chiral indane derivatives

Our methodology offers the potential to synthesize substituted indane derivatives that feature contiguous stereogenic centers. To achieve this, we propose to employ a starting material of 2-bromophenyl substituted carbonate and implement our γ-arylation-isomerisation-1,4-addition strategy, to install the two chiral centers into the indane precursor. Subsequent hydrolysis of the ester moiety could yield the corresponding carboxylic acid (Figure 2.30).

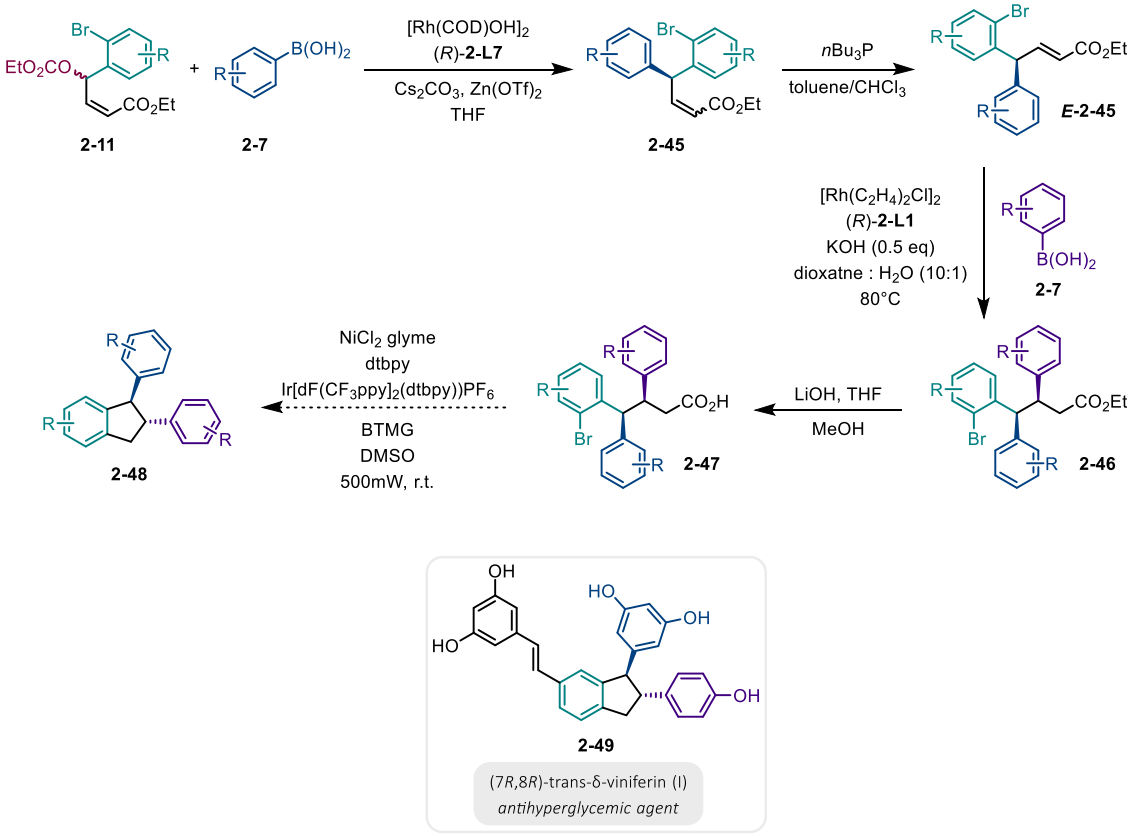

Figure 2.30 Employing our modular Rh-catalysed methodology to produce viniferin analogues enantioselectively.

Past studies have demonstrated the utilization of metallophotoredox catalysis for the coupling of unactivated carboxylic acids and aryl bromides.[138,139] In our particular investigation, we focus on the application of photochemical intramolecular decarboxylative coupling using the bromine handle, offering potential prospects for synthesizing diverse chiral indanes.

An exemplary compound within this scope, (7*R*,8*R*)-trans-δ-viniferin, has been patented as a promising therapeutic candidate for addressing hyperglycemia, a condition characterized by elevated blood sugar levels (Figure 2.30).[140]

Overall, the wide range of potential synthetic applications showcase that enantio- and regioselective Suzuki-Miyaura couplings with acyclic allylic electrophiles and boron

nucleophiles could be a valuable tool for synthesizing a wide range of compounds with complex structures and biological activity.

3 Studies towards asymmetric formation of all-carbon quaternary stereocenters *via* Suzuki-Miyaura cross-coupling of acyclic allylic systems

3.1 Introduction

3.1.1 All-carbon quaternary stereocenters in acyclic systems

Quaternary carbon stereocenters occur frequently in natural products, drugs and bioactive molecules (Figure 3.1).[6,141] For instance, out of the top 200 prescription drugs consumed in the US in 2011, 12% contain quaternary carbon stereocenters.[142] The high frequency of quaternary centers in both established and emerging drugs has generated a demand for efficient methodologies to introduce these centers. Although strategies for generating quaternary stereocenters through the addition of unstabilised nucleophiles have been evaluated in cyclic substrates,[143] the development of approaches to construct quaternary centers in acyclic molecules with greater conformational flexibility is limited.[144-146]

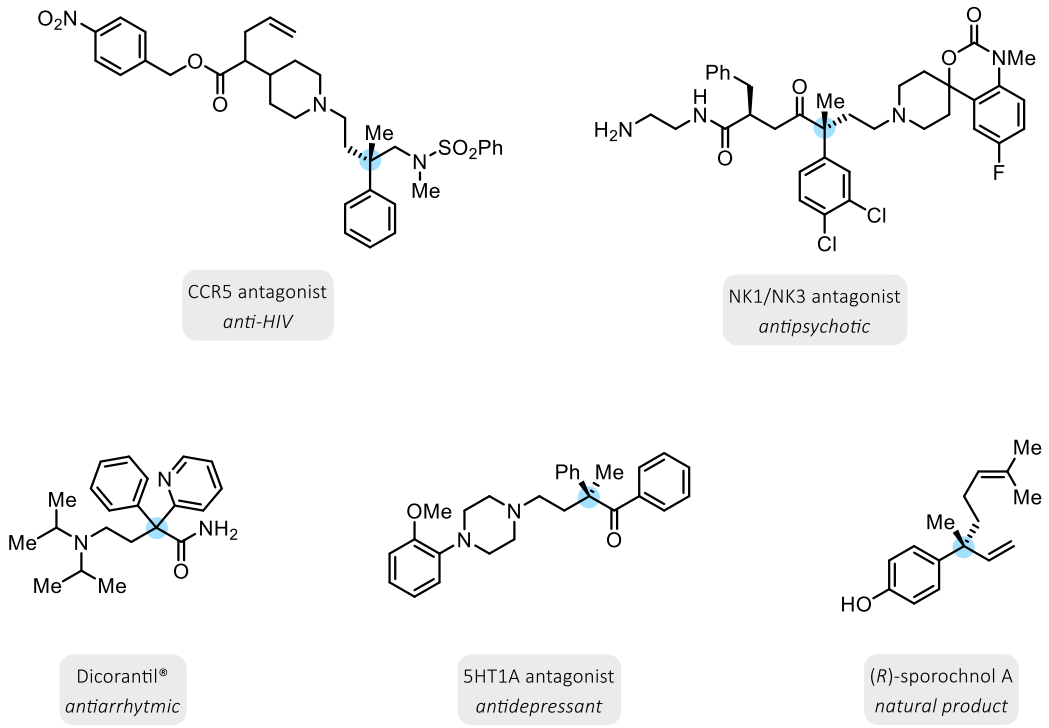

Figure 3.1 Biologically active compounds that feature acyclic quaternary stereocenters as part of their structure.

This gap is further exacerbated in the context of structurally complex and highly functionalized acyclic molecules. Thus, the synthetic and medicinal chemistry communities would benefit greatly from the development of novel methods to install quaternary centers in structurally complex acyclic molecules.

3.1.2 Project aims

Following the successful development of regio-and enantioselective allylic arylation of acyclic allylic carbonate (Figure 3.2, a), the objective of the project discussed in this chapter is to develop an asymmetric C(sp^2)-C(sp^3) cross-coupling reaction of racemic acyclic electrophiles with arylboronic acids to generate all-carbon quaternary stereocenters (Figure 3.2, b). During this process of discovery, we also intended to investigate the reactivity patterns and reaction outcomes of allylic substrates as the steric bulk surrounding the carbon carrying the leaving group is increased. We recognised that tertiary allylic carbonate would be a suitable substrate to achieve this aim. However, the use of unsymmetrically substituted allylic substrates with significant disparities in steric bulk and electronics at the two allylic termini could lead to significant challenges in achieving regiocontrol.

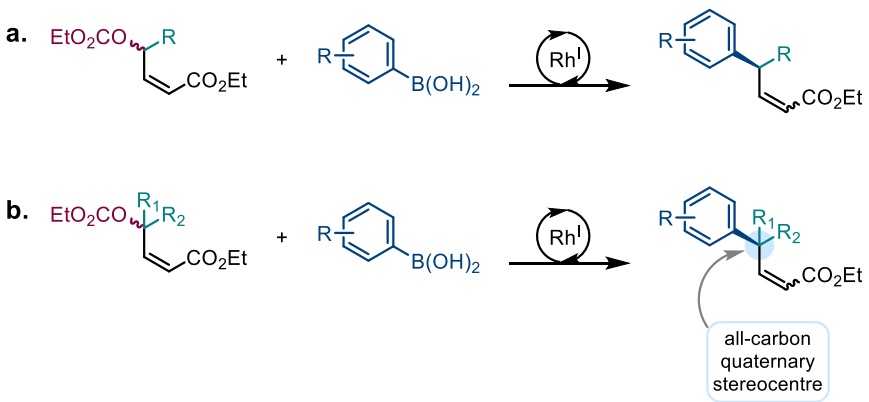

Figure 3.2 a, Asymmetric allylic arylation accomplished in the previous chapter. b, Goal of this chapter: generation of all-carbon quaternary strereocentres *via* rhodium-catalysed allylic arylation.

The allylic substitution reaction could yield two possible regioisomeric arylated products, each of which could have two possible *Z*- or *E*-stereoisomers, which in turn could produce two enantiomers each.

To summarise, our goal at the outset of this project was to design a reliable asymmetric rhodium-catalysed system that could regioselectively generate enantioenriched all-carbon quaternary stereocenters in acyclic structures, starting from a racemic mixture of the tertiary allylic substrate.

3.2 Results and Discussion

3.2.1 Synthesis of tertiary allylic substrates

We selected two substrates as the initial point of our study, namely a methyl-ethyl substituted allylic carbonate **3-3a** and a corresponding substrate featuring a phenyl substituent instead of an ethyl **3-3b** (for higher reactivity). The rationale for selecting these substrates was their potential to generate a new all-carbon quaternary stereocenter, provided that the regio- and enantioselective allylic arylation proceeded in a manner analogous to that observed with a secondary allylic carbonate, as detailed in Chapter 2.

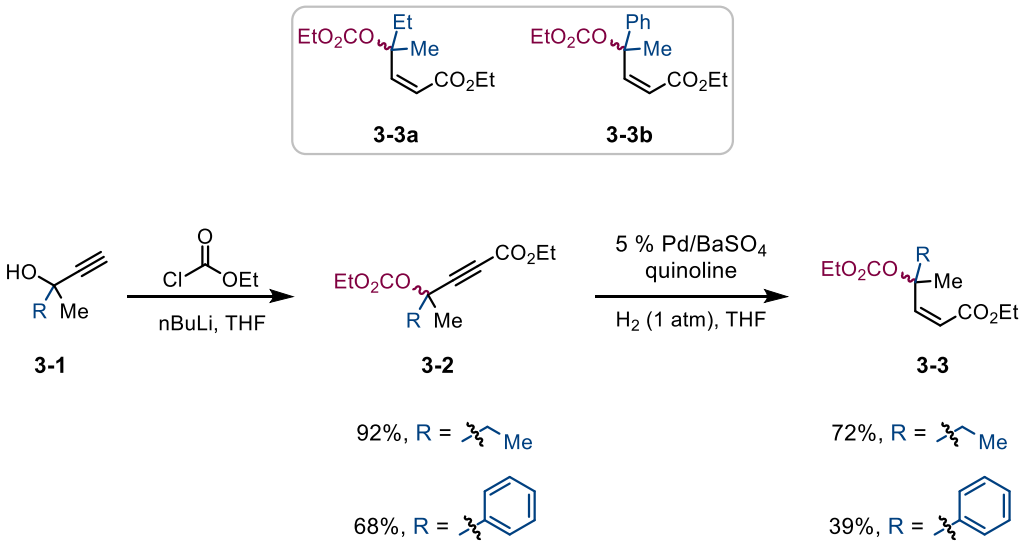

Figure 3.3 Synthesis of tertiary allylic carbonate substrates.

The synthesis of these substrates involved the use of corresponding propargylic alcohols **3-1**, wherein the first step included dual deprotonation and coupling with ethyl chloroformate, followed by partial reduction of the resulting ynoate **3-2a** or **3-2b** intermediates to *Z*-allylic carbonates using Rosenmund catalyst (Figure 3.3)[147]. Favourable yields were achieved for both **3-3a** and **3-3b** substrates in each of the two steps.

3.2.2 Preliminary results for Rh-catalysed arylation to form quaternary stereocentres

In our study, we investigated the reaction of the Me-Et starting material **3-3a** under standard conditions discovered in Chapter 2. However, the reaction generated a complex mixture and did not reach complete conversion at room temperature. Notably, both *Z*- and *E*-stereoisomers of the α-arylation product **3-5a** were produced in a 1:1 ratio, and these isomers could not be separated by column chromatography. To enhance the conversion of the starting material to the desired products, we conducted the reaction at various elevated temperatures. However, we did not observe an increase in the yield of the arylation product **3-5a** under any of the conditions as detailed in Table 3.1.

Table 3.1 Impact of reaction temperature on the yield **3-5a** (*Z* and *E* combined).

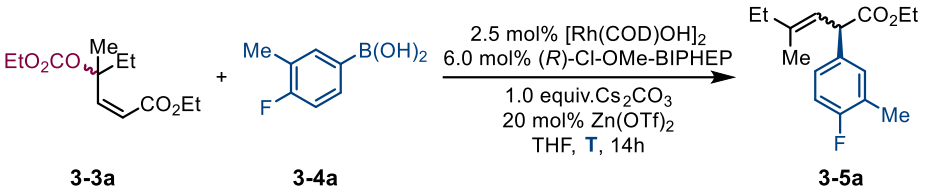

3-3a **3-4a** **3-5a**

Entry	T / °C	Yield of **3-5a** / %	Z/E ratio of **3-5a**
1	r.t.	42	1.1 : 1
2	50	32	1.0 : 1
3	60	20	1.1 : 1
5[a]	70	19	1.2 : 1
4[a]	80	14	1.2 : 1
6[a]	100	7	n.d.

NMR yields of **3-5a** are reported by comparing ^{1}HNMR integrals to those of an external standard (dibromomethane). [a]1,4-Dioxane used as a solvent.

Moreover, such conditions led to the formation of more complex crude reaction mixtures, possibly due to the decomposition of the starting material.

To enhance substrate reactivity, we hypothesized that replacing one of the aliphatic substituents with an aromatic group could improve the leaving group ability of the carbonate by stabilizing the developing positive charge *via* delocalization. We subsequently subjected the methyl-phenyl substituted allylic carbonate **3-3b** to standard reaction conditions identified during the investigations outlined in Chapter 2 (Figure 3.4).

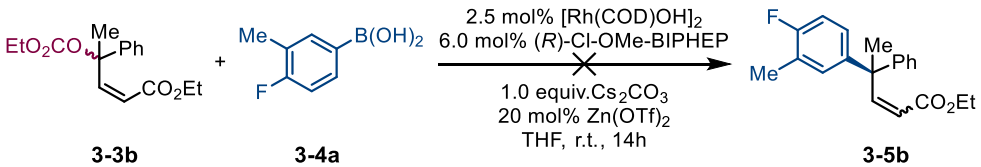

3-3b **3-4a** **3-5b**

Figure 3.4 Rh-catalysed arylation of the Me-Ph-substituted substrate **3-3b**.

However, we discovered that the Me-Ph starting material **3-3b** decomposed both during column chromatography purification and the reaction, leading to the formation of lactone **3-6** through cyclization (Figure 3.5).

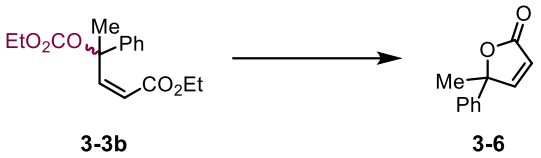

3-3b **3-6**

Figure 3.5 Lactonization side reaction.

This lactonization could explain the lack of reproducibility observed with the Me-Ph substrate **3-3b**, and thus prompted us to discontinue investigating its reactivity.

3.2.3 Synthesis of a simplified model substrate

In view of the challenges encountered while interpreting the experimental data resulting from the employment of substrates **3-3a** and **3-3b** in our rhodium-catalysed allylic arylation reaction, we opted to simplify the substrate structure to facilitate the acquisition of more comprehensible data through the examination of crude reaction mixtures. The adoption of substrate **3-3c** enabled us, in practice, to observe of a smaller number of products resulting from the arylation reaction, owing to the equivalence of *Z*- and *E*-α-arylation products.

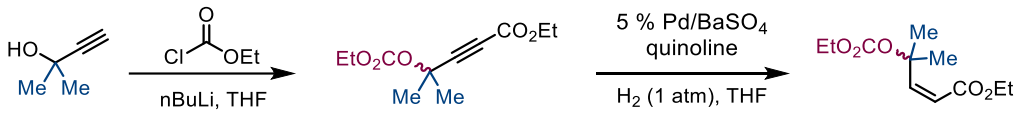

3-1c **3-2c** 87% **3-3c** 69%

Figure 3.6 The process of production of a model substrate with reduced complexity.

The synthesis of substrate **3-3c** involved a double addition of chloroformate to a tertiary propargylic alcohol, **3-1c**, followed by subsequent *cis*-reduction, as in our previous synthetic strategy (Figure 3.6).

3.2.4 Rh-catalysed arylation of a substrate with reduced complexity

Upon subjecting the reduced-complexity substrate to standard rhodium-catalyzed arylation reaction conditions, we were able to identify three species present in the crude reaction mixture, alongside the remaining starting material. The major product observed

with the most privileged ligands was the α-arylation product **3-5c**, although its yield never exceeded 50%. The best yield of the α-arylation product **3-5c** observed was 44% (Figure 3.7), using (*R*)-Cl-MeO-BIPHEP, which is the ligand that has been established as a part of standard conditions for the γ-arylation of secondary allylic carbonates.

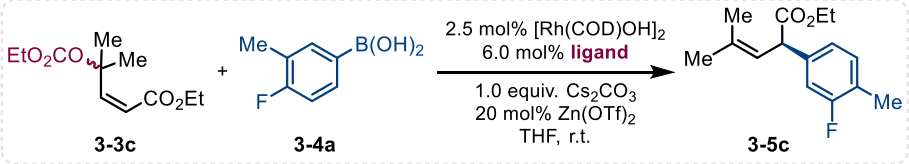

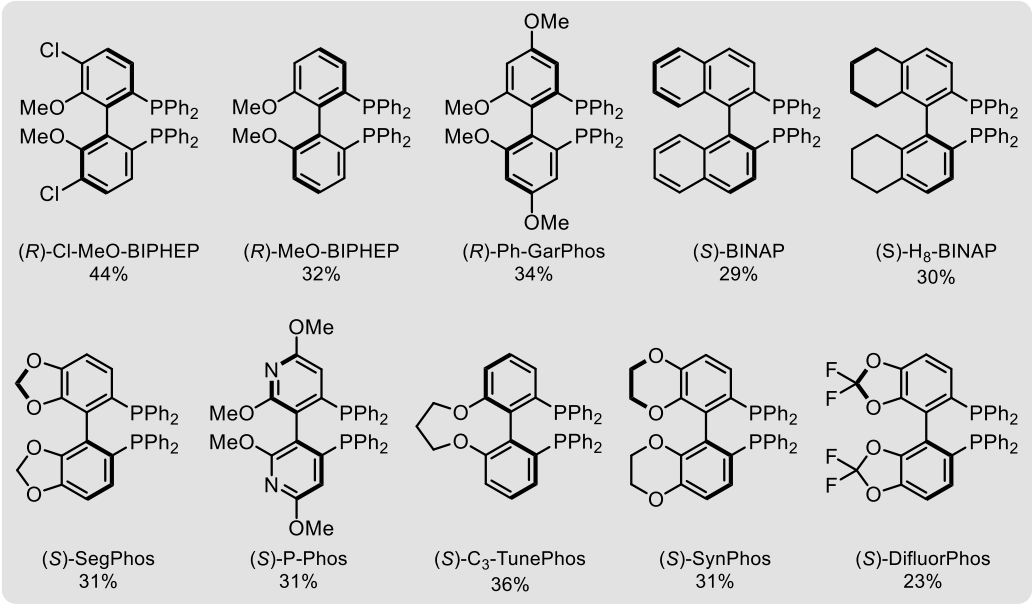

Figure 3.7 Preliminary ligand screen. NMR yields of **3-5c** are reported by comparing ^{1}HNMR integrals to those of an external standard (dibromomethane).

Further analysis of the reaction mixture components revealed the formation of two regioisomers, one of which possessed *Z*/*E*-isomers when a simplified tertiary allylic carbonate was used (Figure 3.8).

None of the single products could be obtained as a majority in the preliminary screen, and the α-arylation product could only be obtained in moderate yields. The overall α- to γ-product ratio varied between 1.3:1 and 1:1.5, and neither product was highly favored under any of the conditions tested. The privileged ligands, including the standard ligand

established in Chapter 2, did not provide significant differentiation between the transition states leading to all four stereoisomers that could be obtained during potential π-σ-π isomerisation and rotation about the double bond in the allylic system. This may be attributed to competing driving forces, where steric bulk drives the arylation to the α-position, while the ester promotes the formation of a hypothesized six-membered rhodocycle that facilitates arylation at the γ-position.

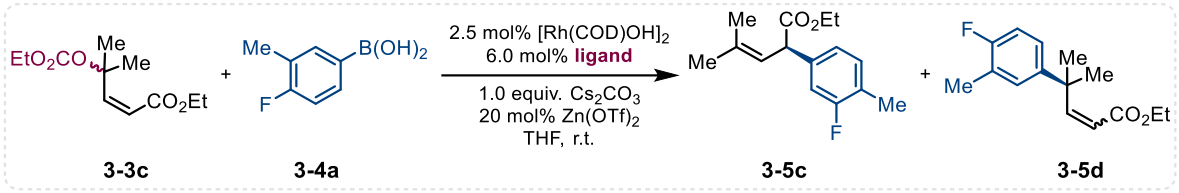

3-3c 3-4a 3-5c 3-5d

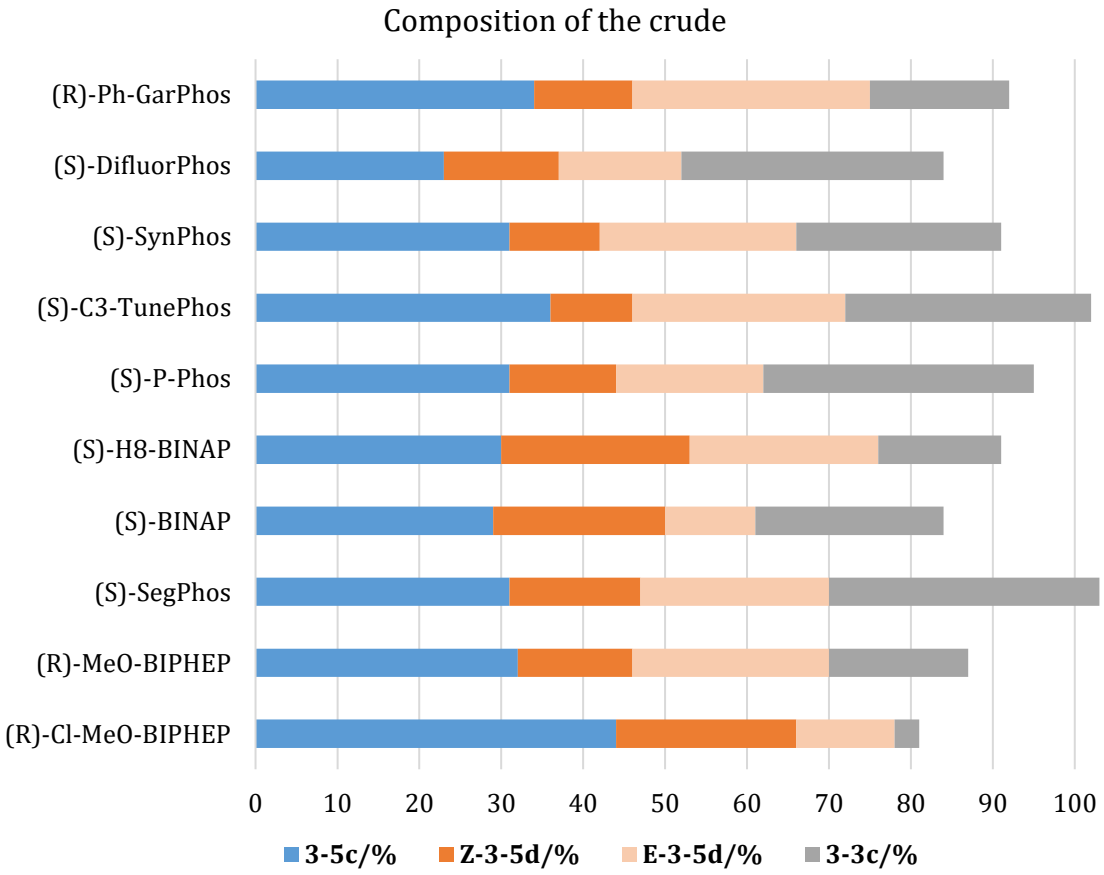

Figure 3.8 An in-depth analysis of the composition of the crude reaction mixture in the preliminary ligand screen. NMR yields of **3-5c** and **3-5d** are reported by comparing ^{1}HNMR integrals to those of an external standard (dibromomethane).

Subsequently, we attempted a selection of other ligands; however, ligands that were not based on a biphenylphosphine-like structure exhibited no reactivity with the tertiary allylic carbonate (Figure 3.9).

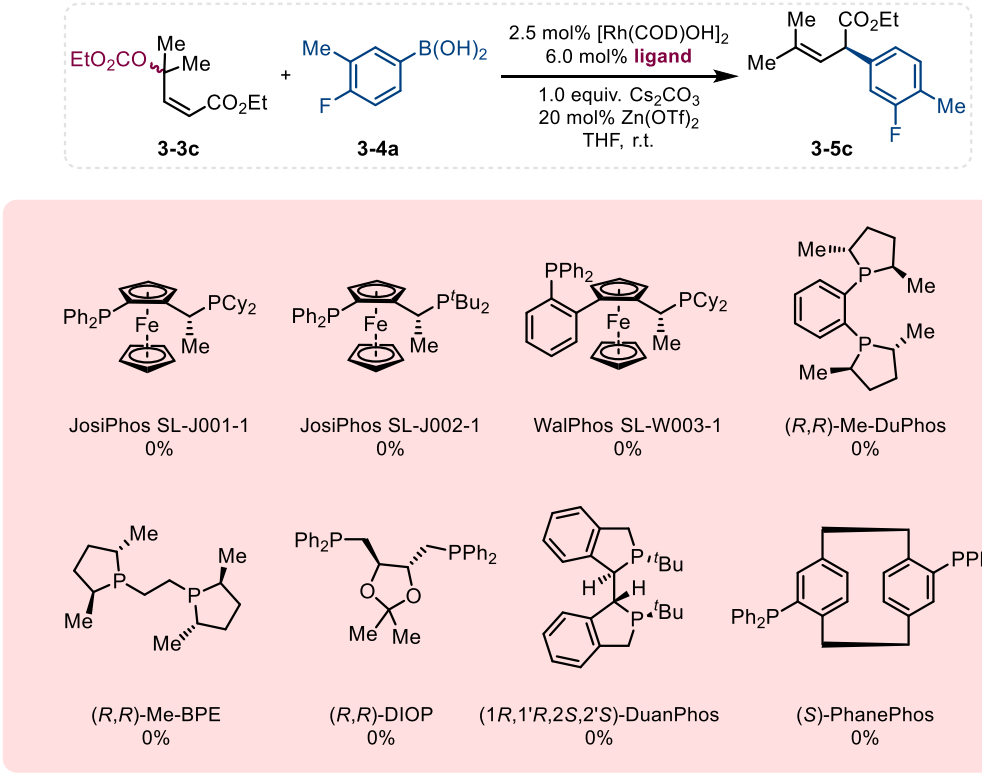

Figure 3.9 Results of a further ligand screen. NMR yields of **3-5c** are reported by comparing ^{1}HNMR integrals to those of an external standard (dibromomethane).

We then attempted variations of the MeO-BIPHEP ligand to investigate how the steric bulk of the aryl groups on the phosphorus of the ligand scaffold affects the formation of the α-arylation product **3-5c**. Unfortunately, none of the variations of MeO-BIPHEP provided a higher yield of the desired product than the original diphenyl-substituted MeO-BIPHEP (Figure 3.10). Interestigly, (*R*)-Xyl-MeO-BIPHEP gave the highest proportion of the γ-arylation products with γ to α ratio equalling 2.5 : 1, but this reaction did not reach full conversion either. Additionally, we discovered that the enantiomers of the only chiral product, the α-arylation product **3-5c**, could not be separated by any means, and as a result, enantioselectivity could not be determined.

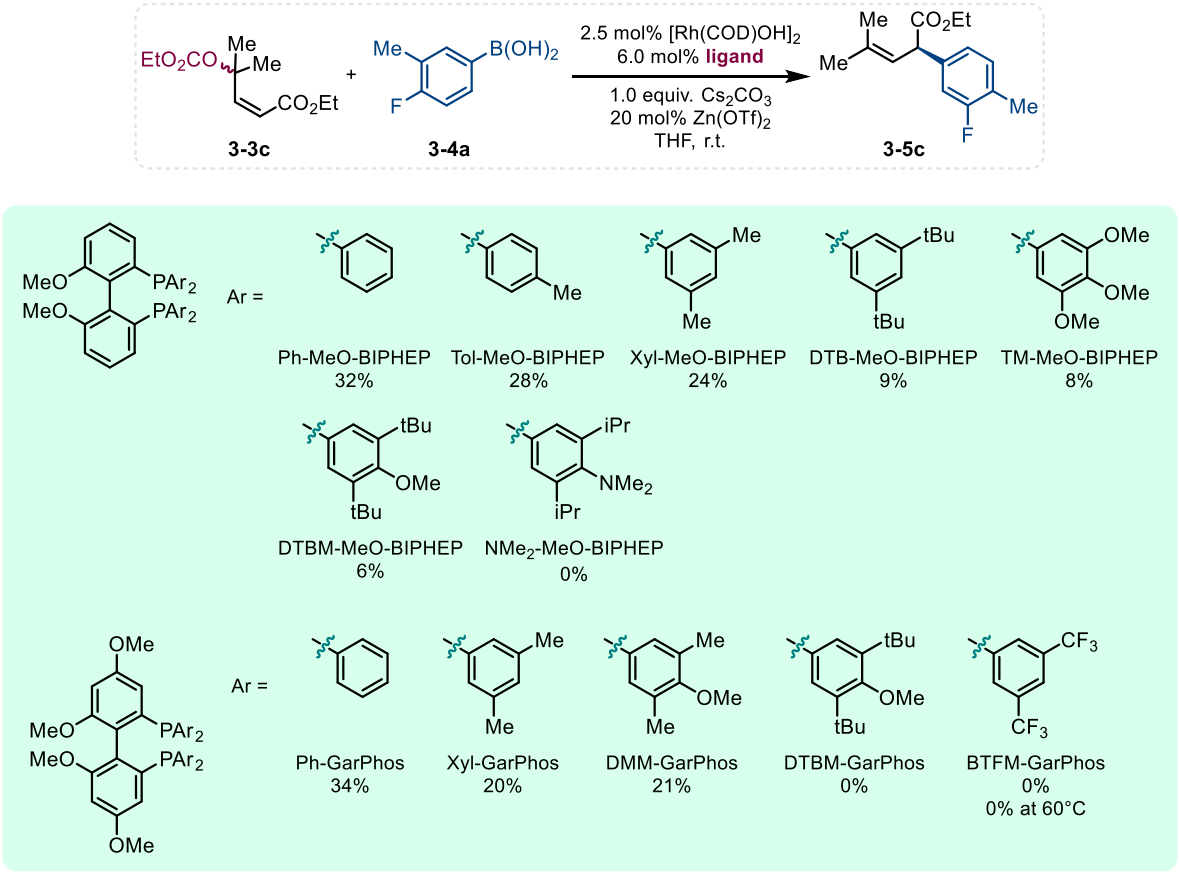

Figure 3.10 Results of the fine-tuning ligand screen. NMR yields of **3-5c** are reported by comparing ^{1}HNMR integrals to those of an external standard (dibromomethane).

At this point, knowing that the ligand usually has the greatest effect on the regio- and *Z*/*E*-selectivity, we concluded that we would not be able to achieve any of the products in significant excess.

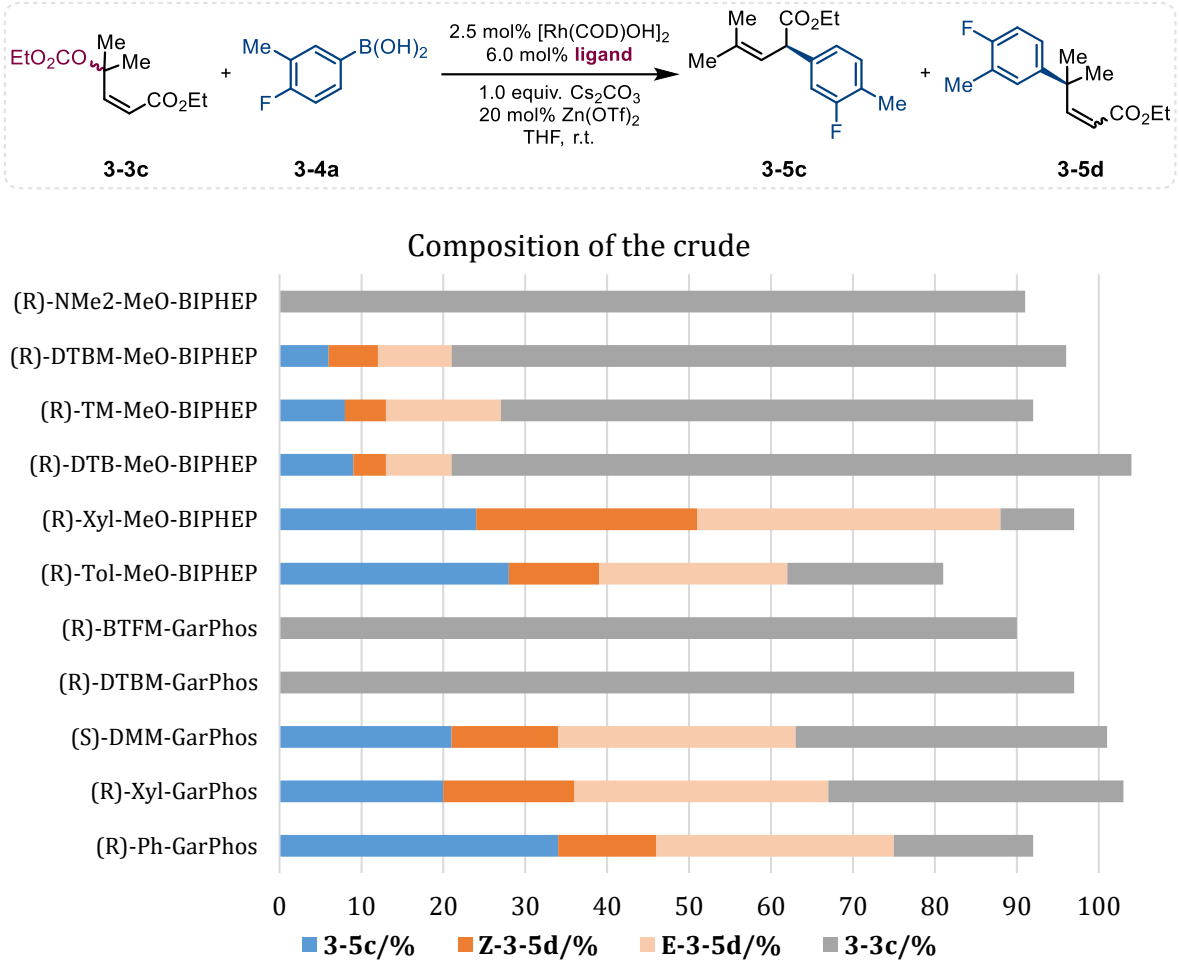

Figure 3.11 An in-depth analysis of the composition of the crude reaction mixture in the fine-tuning ligand screen. NMR yields of **3-5c** and **3-5d** are reported by comparing ^{1}HNMR integrals to those of an external standard (dibromomethane).

Consequently, we decided to discontinue our investigations into the reactivity of tertiary allyl carbonates **3-3c** carrying an ester group on one terminus.

3.3 Conclusions

This chapter aimed to investigate the reactivity trends and reaction outcomes of allylic substrates in response to increased steric bulk around the carbon carrying the leaving group. Our objective was to develop a new rhodium catalytic system to furnish remote quaternary stereocenters. Although certain ligands, such as Xyl-MeO-BIPHEP, were observed to produce the desired γ-arylation product, we encountered challenges in separating the product mixture into its individual components using column chromatography. Additionally, we faced challenges in reducing the double bonds in the acquired mixture of products in an attempt to converge *Z*- and *E*-products into the same compound.

These issues led us to conclude that an ester substrate is not an ideal candidate for achieving the desired γ-regioselectivity, possibly due to competing driving forces. Specifically, steric bulk drives arylation to the α-position, while the ester promotes the formation of a hypothesized six-membered rhodocycle that facilitates arylation at the γ-position.

The encouraging aspect is that using the model substrate with reduced complexity together with different ligands, we obtained both γ-arylation products and α-arylation products as the major products under different conditions. This observation is promising and suggests that by selecting a substrate carrying a group with a stronger directing ability and a suitable set of ligand, base, and additive, we have a potential opportunity produce a γ-arylation product bearing a remote all carbon quaternary stereocenter. Furthermore, we could adjust the reaction conditions to obtain an α-arylation product using an α,β-unsaturated carbonyl as the starting material. This result is noteworthy and

unusual, as boronic acids typically perform conjugate addition on α,β-unsaturated systems under rhodium catalysis.

3.4 Future directions

3.4.1 Employing amide as a directing group

Based on the mechanistic experiments described in Chapter 2 and the available literature,[117] it has been observed that the amide group exhibits a higher coordinating ability towards rhodium. Consequently, it can be inferred that amides serve as stronger directing groups in Rh-catalyzed arylation reactions.

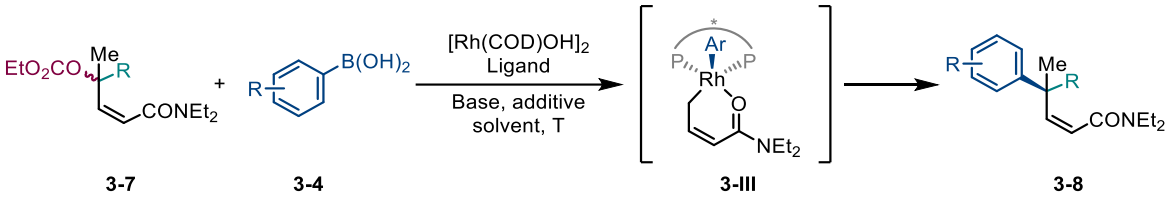

Figure 3.12 Potential to exploit stronger directing ability of an amide to exhibit control on regioselectivity.

Incorporating an amide substrate **3-7** into the reaction may result in the favourable formation of a six-membered rhodocycle, ultimately leading to an increased yield of the γ-arylation product **3-8** during the reductive elimination process (Figure 3.12).

A synthetic route for the reduced complexity amide substrate could be established by following the sequence of transformations outlined in Figure 3.13. Initially, hydroxy-ynamide **3-9** was obtained through a Sonogashira coupling reaction. Upon treatment with ethyl chloroformate under basic conditions, carbonate **3-10** was generated.

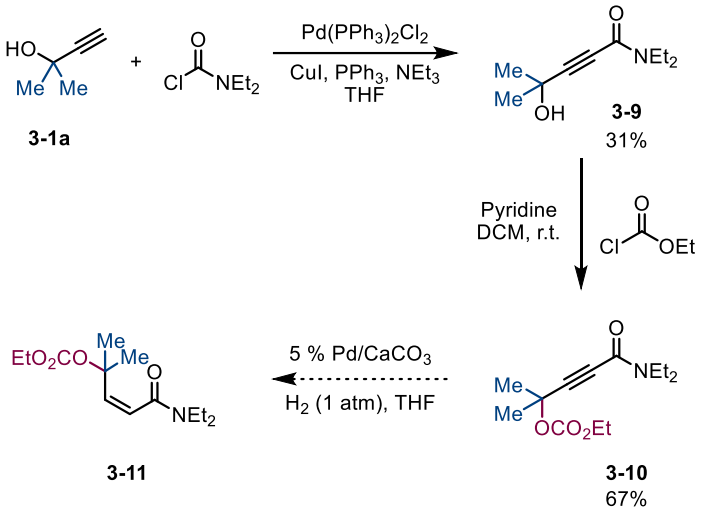

Figure 3.13 A proposed synthesis route for an alternative amide starting material.

Subsequently, partial reduction of the triple bond in **3-10** using a Lindlar catalyst is envisioned to furnish the desired (*Z*)-allylic carbonate **3-11**, which bears an amide functional group at one terminus (Figure 3.13).

3.4.2 Sythesis of bioactive substances containing remote quaternary stereocenters

Conditional upon identifying an efficient directing group for the installation of a quaternary stereocenter with satisfactory regio- and enantioselectivity, the presented methodology holds promise for the modular asymmetric synthesis of bioactive molecules (Figure 3.14).

For example, the natural product cucurbitacin B has garnered significant attention due to its numerous biological activities, particularly its potent antitumor effects. For example, in 2022, the Nan group developed a palladium-catalysed allylic coupling of cucurbitacin B with boronic acids. The methodology presented a one-step approach to increase the chemical diversity of the natural product and lead to discovery of potent bioactive substances, such as **3-12**.[148] Nonetheless, no attempts to establish an all-carbon stereocenter in an enantioselective manner were reported. Successful implementation of

our methodology would enable further exploration of the structure-activity relationships of cucurbitacin B derivatives and utilize stereochemical diversity as a means of discovering more potent analogues.

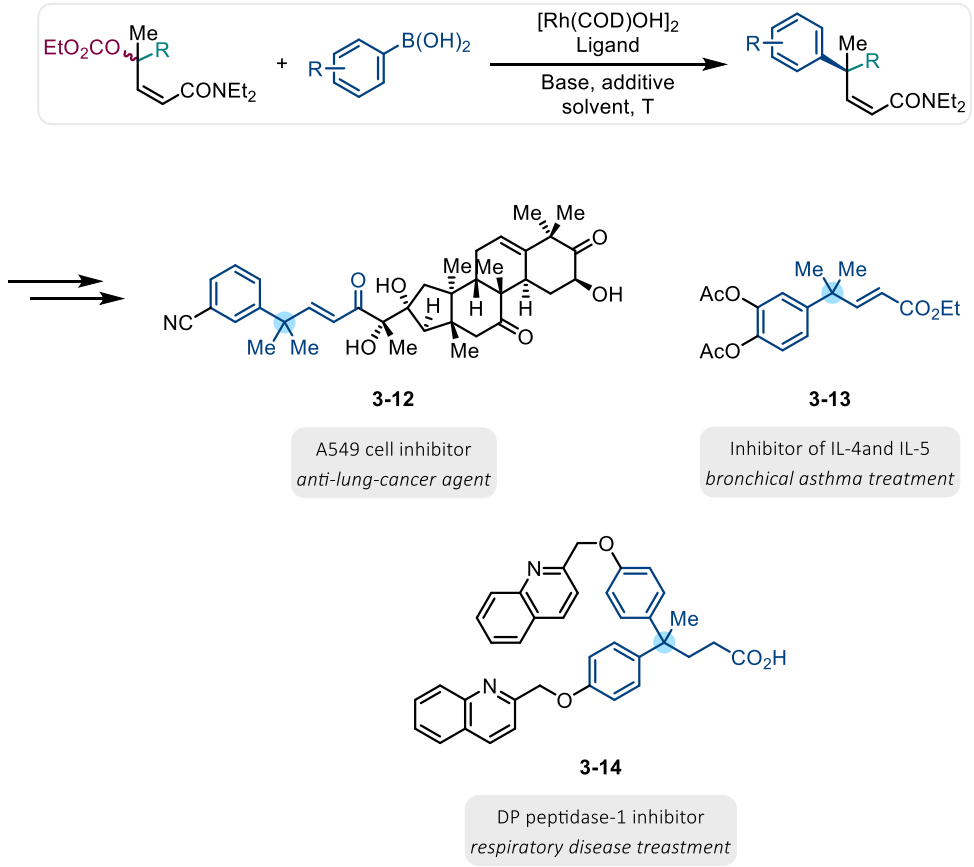

Figure 3.14 Examples of potential application of the methodology to produce bioactive molecules and their derivatives.

The pharmaceutical industry has directed substantial efforts towards investigating compounds that feature remote quaternary centers. To cite a few instances, compound **3-13**, which exhibits potential as a treatment for bronchial asthma, was patented in 2020.[149] It features an all-carbon quaternary center located in the γ-position of an α,β-unsaturated ester. Similarly, in 2023, DP peptidase-1 inhibitor **3-14** was patented as a prospective treatment for respiratory diseases.[150]

Once again, our rhodium-catalysed cross-couplings could potentially provide efficient access to these compounds and their numerous chiral analogues.

4 Modular asymmetric synthesis of 3-aryl-α-tetralones *via* sequential double arylation

4.1 Introduction

4.1.1 Initial project aims

In Chapter 2 we established a novel regio- and enantioselective arylation of conformationally flexible acyclic allylic carbonates. Chapter 3 investigated the impact of increasing steric bulk on one of the allylic termini by incorporating an additional substituent, revealing a loss of efficient control over regioselectivity. The primary objective of the present and final chapter was to elucidate the reactivity trends of the established allylic substrate as the steric bulk surrounding the carbon atom carrying the leaving group is varied in the opposite direction (i.e., decreased).

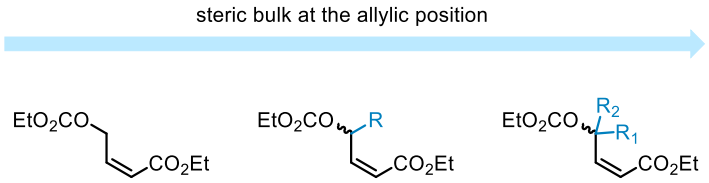

Figure 4.1 Aims of the project: exploration of how steric bulk of the allylic substrate affects its reactivity.

The introduction of a γ-aryl group in this particular system produces an achiral product, but altering the regioselectivity of the arylation process has the potential to furnish chiral α-arylation compounds. These α-arylated carbonyl compounds hold significant value as they are frequently encountered structural motifs in natural products and pharmaceutical agents.[151,152] Although some methods for arylating carbonyl compounds in the α-position are available,[153-156] the development of novel approaches for α-arylation of carbonyl compounds remains an active area of research, and the past year has witnessed the emergence of new methods, such as novel photocatalytic[157] and bismuth-catalysed[158] techniques. Nevertheless, even with these new protocols, achieving high enantioselectivity in the α-arylation of acyclic carbonyl compounds remains

challenging,[159] and the few systems that manage to attain high enantioselectivity exhibit low yields.[160]

The α-arylation of acyclic α,β-carbonyl compounds using arylboronic acids would represent a powerful method to synthesize these critical building blocks for diverse and useful bioactive compounds.

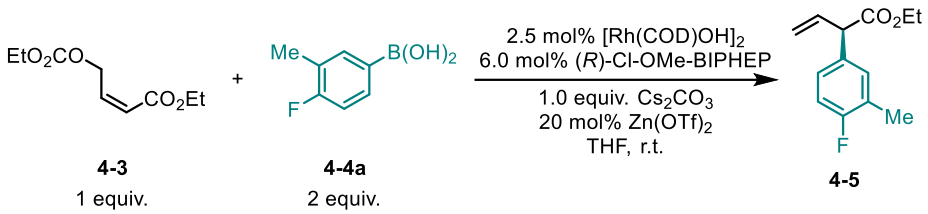

Figure 4.2 Initial desired outcome of the reaction.

Prior observations of the γ-directing contribution of the carbonyl group led us to anticipate challenges in reversing the regioselectivity of the aryl addition. However, we contemplated that it might be possible to overcome this effect by carefully selecting the appropriate combination of ligand, base, additive, and solvent.

4.1.1 Initial experiments

Initially, we subjected our terminal substrate to previously established standard conditions as described in Chapter 2. As expected, a gamma arylation product **4-6** was observed, but it did not constitute the major product. Interestingly, the majority of the crude reaction mixture was composed of a double arylation product **4-7a**. Based on our observations, we proposed that, after the initial ester-directed regioselective allylic γ-arylation, the intermediate **4-6** underwent a sequential rhodium-catalyzed 1,4-addition.

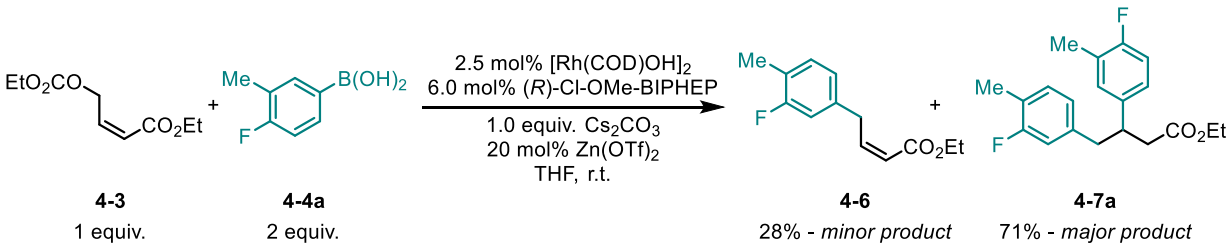

Figure 4.3 Outcome of the reaction of the substrate bearing a primary leaving group and an arylboronic acid under standard conditions.

The observed major double arylation product **4-7a** has been used as a precursor in synthesis of a set of 3-arylated α-tetralones, a group of compounds that are valuable due to their frequent occurrence in natural products and pharmaceutical agent scaffolds.[161-164] Presented with this unexpected result, we decided to look into and evaluate the current asymmetric syntheses of substituted α-tetralones.

4.1.2 The importance and current syntheses of α-tetralones

As mentioned above, the presence of chiral α-tetralones bearing functional groups at the 3-position is a common occurrence in natural products and pharmaceutical agents (Figure 4.4).[165-167] There are instances of 3-substituted α-tetralone compounds demonstrating considerable potency as estrogenic modulators[168] or fungicides.[169] Currently, α-tetralones and their derivatives are under investigation as possible therapeutic agents for a diverse range of diseases.[170] Asymmetric synthesis of such scaffolds is an area of active research in this field.

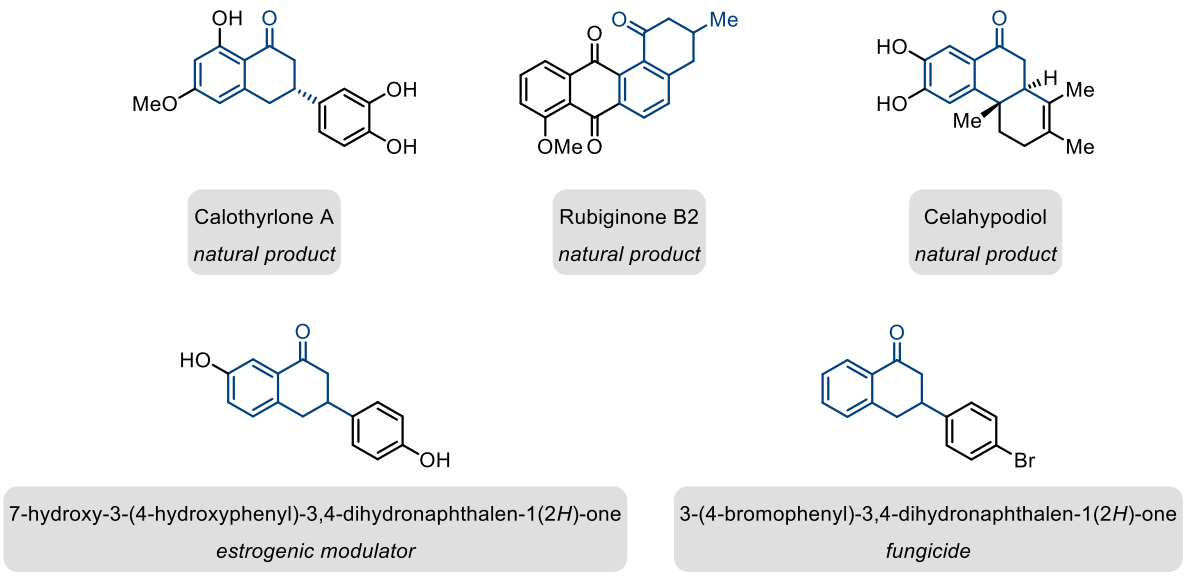

Figure 4.4 Examples of bioactive 3-substituted α-tetralones.

From an intuitive standpoint, it would seem plausible to functionalize an α,β-unsaturated tetralone through the implementation of a 1,4-addition reaction to the α,β-unsaturated ketone. However, the conjugate addition to dehydrotetralone for the purpose of accessing α-tetralones with a chiral carbon at the 3-position is unfeasible due to the inherent stability of 1-naphthol as the preferred tautomer of dehydrotetralone.[171,172] This leads to 1-naphthol being an unresponsive conjugate acceptor (Figure 4.5). Consequently, alternative and frequently lengthier and more intricate approaches are required to access the scaffold of 3-functionalized tetralones.

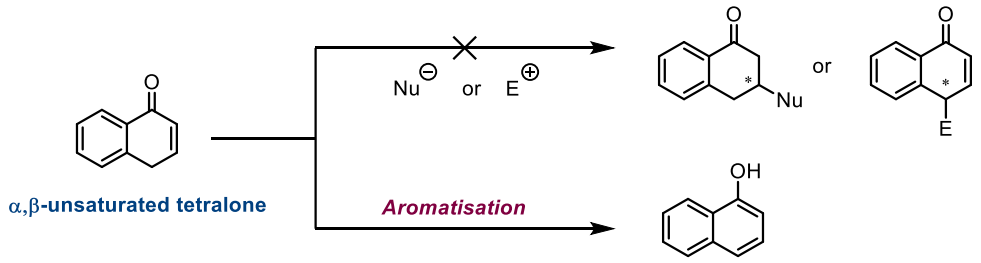

Figure 4.5 Difficulties in functionalisation of α,β-unsaturated tetralones due to tautomerisation.

Murakami and co-workers reported a novel rhodium-catalysed rearrangement reaction of 1-(2-haloaryl)cyclobutanols that leads to the formation of 3,3-disubstituted α-

tetralones.[173] Furthermore, the research group has developed an asymmetric variant of this reaction, whereby 3,3-disubstituted 1-(2-haloaryl)cyclobutanols serve as substrates to generate α-tetralones possessing a chiral quaternary carbon centre at the 3-position (Figure 4.6). The resulting products were obtained in good yield and exhibited acceptable levels of enantiomeric purity.

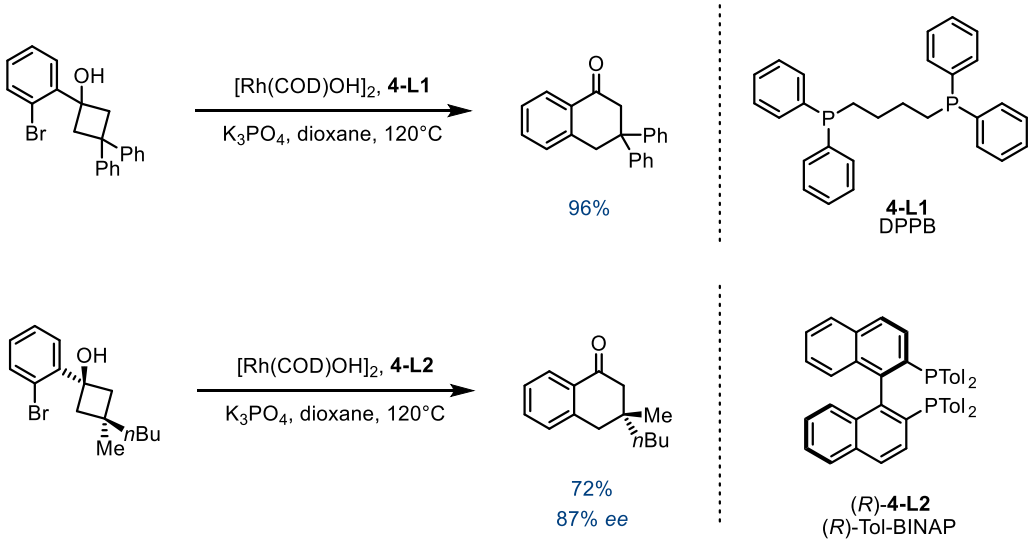

Figure 4.6 3,3-Disubstituted α-tetralone synthesis by Murakami.

During their investigation into the mechanism of asymmetric α-hydroxylation of tetralone-derived β-ketoesters using a guanidine-bisurea bifunctional organocatalyst in the presence of cumene hydroperoxide (CHP) to elucidate the origin of stereocontrol in the reaction, the Nagasawa group accomplished a kinetic resolution that generated 3-substituted α-tetralones.[174] The identified transition-state model was subsequently applied to design an enantioselective synthesis of 2- or 3-substituted tetralones through catalytic oxidative kinetic resolution reaction of tetralone-derived β-ketoesters (Figure 4.7). The kinetic resolution reaction of various tetralone derivatives proceeded with high yield and enantioselectivity. The potential utility of this oxidative kinetic resolution was exemplified by the synthesis of a natural product, namely (+)-linoxepin.

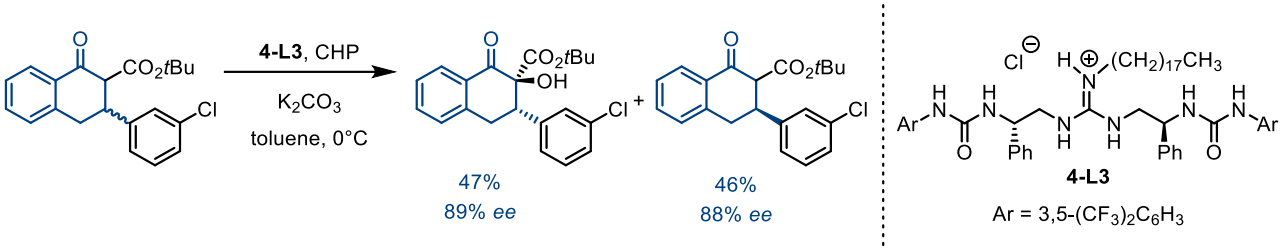

Figure 4.7 Asymmetric synthesis of 3-substituted α-tetralone derivatives through organocatalytic oxidative kinetic resolution.

The Stanley research group has developed a novel method for the synthesis of 3-substituted α-tetralones *via* rhodium-catalyzed hydroacylation of ortho-allylbenzaldehydes.[175] The desired hydroacylation reactions are facilitated by a catalyst produced *in situ* from [Rh(COD)Cl]$_2$, (*R*)-DTBM-SegPhos, and NaBARF. This catalyst has been shown to promote the desired reaction while simultaneously minimizing the formation of byproducts from competitive alkene isomerization and ene/dehydration pathways. Overall, the reaction affords 3-substituted α-tetralone products in moderate-to-high yields with exceptional enantioselectivities (Figure 4.8).

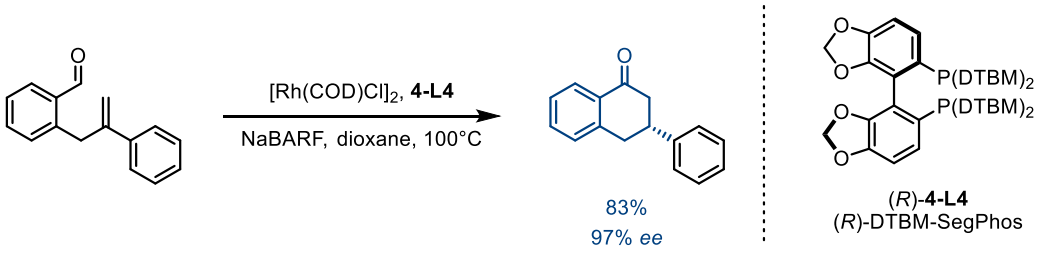

Figure 4.8 Enantioselective formation of 3-functionalised α-tetralones *via* hydroacylation.

Recently, in 2022, the Shenvi research team published a novel strategy for obtaining neuroactive alkaloids, namely GB22, GB13, and himgaline.[176] The group's methodology revolved around the production of 3-arylated α-tetralones through a photoinduced electron transfer ring-opening process of siloxycyclopropanes with bromoarenes (Figure 4.9). The products exhibited moderate to good yields; nevertheless, the procedure lacked

enantioselectivity. Additionally, the methodology exhibits drawbacks, such as the need for a high nickel precatalyst loading of 30%.

Figure 4.9 Shenvi's photochemical synthesis of 3-arylated α-tetralones.

Overall, several procedures for synthesis of 3-functionalised α-tetralones are present in the literature. However, often the compounds used as starting materials are more complex than the desired functionalised tetralone products which means the synthesis of these tetralone precursors is often inefficient and multi-step. Despite a few reports that have appeared recently, enantioselective synthesis of 3-arylated α-tetralones is still an underexplored area and new methods would contribute greatly to generation of libraries of potentially bioactive compounds and their precursors.

4.1.1 Revised project aims

After identifying the limitations and inconvenience of current approaches for accessing 3-arylated α-tetralones, we endeavoured to refine our reaction to generate exclusively ethyl 3,4-diarylbutanoates, which serve as precursors for 3-arylated α-tetralones, while ensuring good enantioselectivities (Figure 4.10).

Our hypothesis for the potential success of this transformation assumes that our designed starting material **4-3** undergoes allylic substitution faster than 1,4-addition when subjected to the same rhodium catalysed system (Figure 4.11).

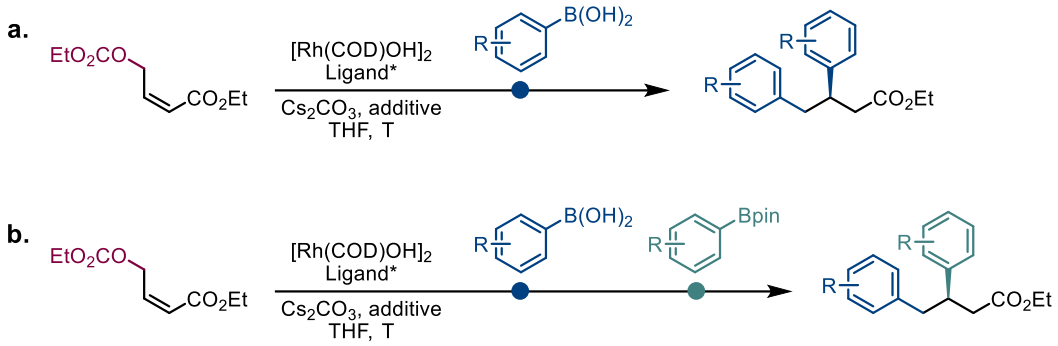

Figure 4.10 General scheme of revised project aims to make enantioenriched 3-arylated α-tetralones.

This, in turn, should enable systematically reacting our substrate **4-3** at two distinct coupling positions in a single step by using a variety of arylboronic acids and their derivatives, leading to the formation of more complex molecules where the two aryl groups added to the starting material are different.

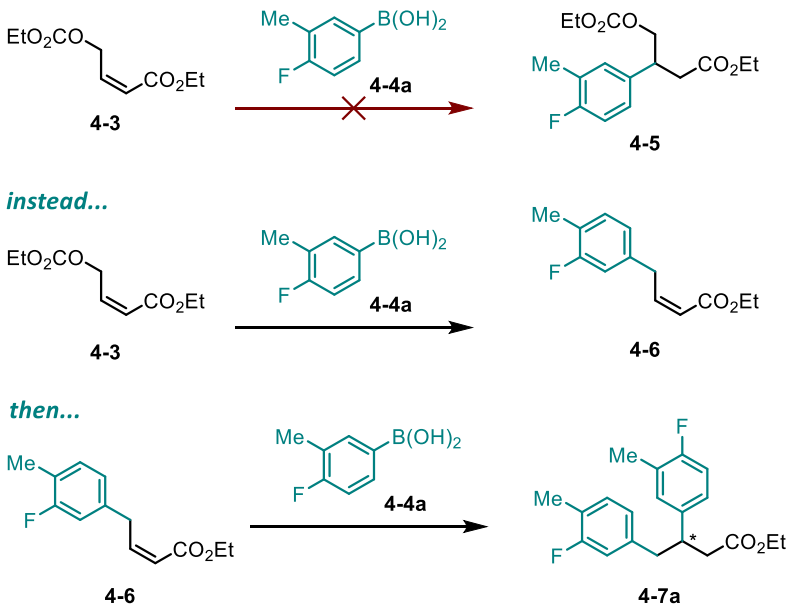

Figure 4.11 Hypothesised pathway for the sequential double arylation leading exclusively to one product.

4.2 Results and Discussion

4.2.1 Preparation of primary allylic substrate

The selection of gamma-carbonate enoate **4-3** as the model substrate was based on its structural similarity to the primary substrate utilized in Chapter 2. We accomplished the synthesis of this substrate through the dual deprotonation of propargylic alcohol **4-1**, followed by treatment with ethyl chloroformate, leading to intermediate **4-2** in high yield.[147]

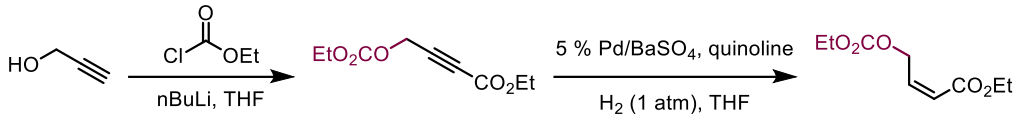

4-1 | **4-2** 71% | **4-3** 60%

Figure 4.12 Synthesis of the ester starting material.

Subsequently, the partial *cis*-reduction of the triple bond using Lindlar's catalyst resulted in the production of the model substrate **4-3** in good yield (Figure 4.12).

4.2.1 Rh-catalysed arylation of primary substrate

Despite the theoretical expectation that using a substrate-to-boronic acid ratio of 1:2 would only result in the formation of the double arylation product **4-7a**, practical observations show that the boronic acid **4-4a** undergoes side reactions, such as protodeboronation[177] and homocoupling,[178] thereby reducing the amount available for desired coupling reactions.

Consequently, to investigate how the distribution of single- and double-arylation product is affected by the proportion of boronic acid used, we conducted experiments varying the amount of boronic acid. Equimolar amounts of starting material and boronic acid predominantly yielded the single-arylation product **4-6** and a small amount of double arylation product **4-7a**, while 30% of the unreacted starting material **4-3** remained in the crude reaction mixture. We were delighted to find increasing the boronic acid loading to

three equivalents led to the desired product, ethyl (*R*)-3,4-bis(4-fluoro-3-methylphenyl)butanoate **4-7a**, in a high yield of 94% (Table 4.1).

Table 4.1 Reaction outcome changes depending on the proportion of boronic acid used.

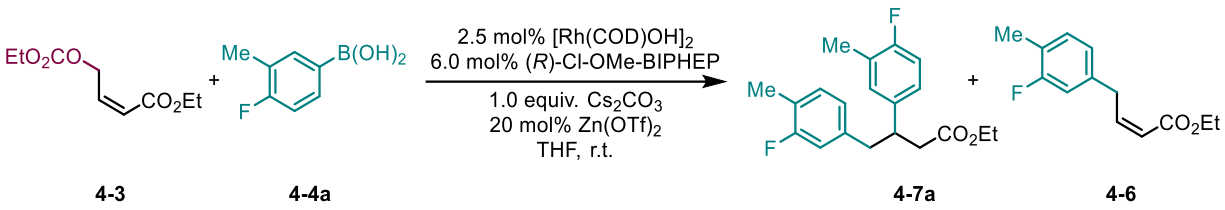

4-3 **4-4a** **4-7a** **4-6**

Entry	Equiv. of **4-4a**	NMR yield of **4-7a** / %	NMR yield of **4-6** / %
1	1	8	44
2	2	71	28
3	3	94	5

Reaction conditions: $[Rh(COD)OH]_2$ (2.5 mol %), (*R*)-Cl-MeO-BIPHEP (6.0 mol %), **4-3** (0.4 mmol, 1.0 equiv), **4-4a**, Cs_2CO_3 (1.0 equiv), $Zn(OTf)_2$ (20 mol %), THF (0.1 M), r.t., 16 h. All experiments were performed on 0.2 mmol scale. NMR yields of **4-7a** and **4-6** were determined by comparing ^1H NMR integrals to those of an external standard (dibromomethane).

To determine the enantioselectivity, we reduced the ester group of ethyl 3,4-diarylbutanoate **4-7a** to obtain the corresponding alcohol **4-9**, which displayed an enantioselectivity of 87% (Figure 4.13).

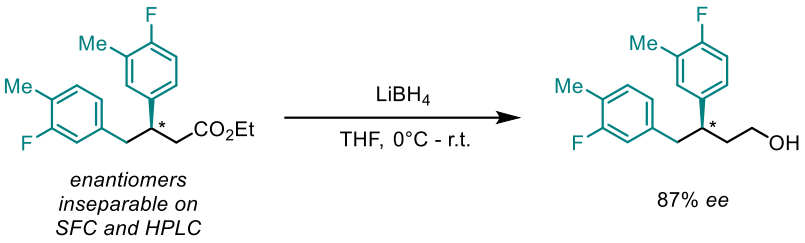

enantiomers inseparable on SFC and HPLC

87% *ee*

Figure 4.13 Determination of product enantioenrichment.

Similarly, employing our model substrate alongside (4-fluorophenyl)boronic **4-4b** acid resulted in ethyl (*R*)-3,4-bis(4-fluorophenyl)butanoate **4-7b** with an excellent yield of 98% and an enantioselectivity of 85% (Figure 4.14).

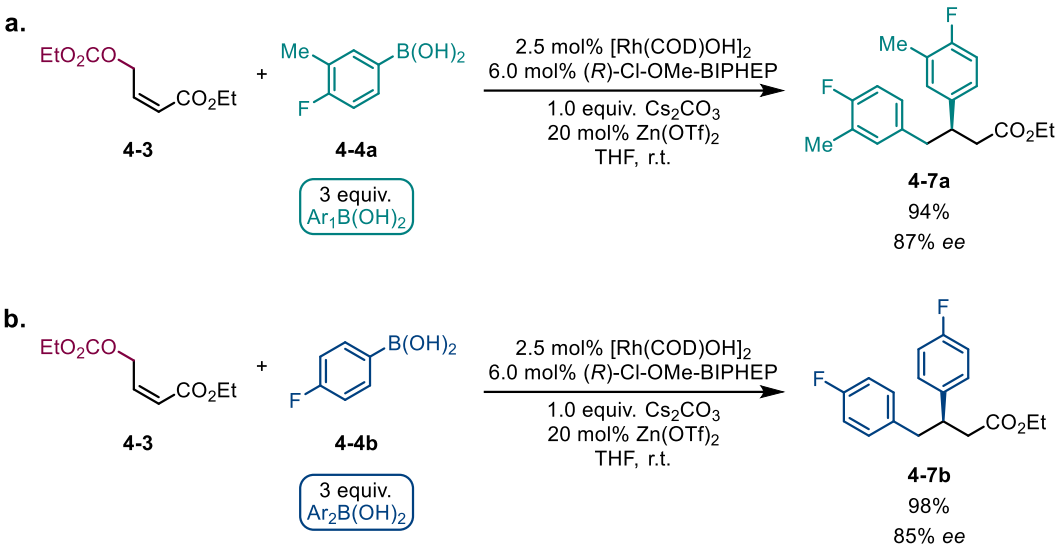

Figure 4.14 Experiments using one boronic acid species.

In general, employing this approach enables efficient arylation at two distinct positions on the primary allylic carbonate model substrate, ultimately affording a streamlined single-step synthesis of 3-arylated α-tetralone precursors in excellent yields and good enantioselectivities. However, bisphosphine ligands, such as BINAP, have been widely reported to exhibit remarkable enantioselectivities (typically exceeding 90%) in rhodium-catalysed 1,4-additions to unsaturated esters.[116] Our experimental findings do not align with these high levels of enantioselectivity. This discrepancy may be attributed to two plausible factors. Firstly, the BINAP ligand might be ineffective in inducing enantioselectivity during 1,4-addition on this specific substrate. Secondly, the initial allylic arylation reaction could generate two isomeric forms (*Z* and *E*) of the intermediate product, each of which yields opposite absolute stereochemistry following the subsequent 1,4-addition step.

4.2.1 Rh-catalysed arylation using two distinct boron nucleophiles

The initial step in both rhodium-catalysed allylic arylation and 1,4-addition involves transmetalation.[85,179] It is well-known that various boronic acid derivatives transmetalate to the rhodium catalyst at different rates.[180-182] We postulated that this

phenomenon could be exploited to achieve sequential arylations of our substrate at two different positions using two distinct boronic species.

We envisioned that the mechanistic pathway of this process could unfold as follows: initially, the boronic acid **4-4a** would transmetalate to the active rhodium-catalyst to form species II, which would then proceed through the sequence of oxidative addition and reductive elimination to generate intermediate **4-6**, as previously discussed in Chapter 2. Subsequently, once all the original substrate and boronic acid have been consumed, the boronic acid pinacol ester **4-10b** could initiate transmetalation of the active rhodium catalyst to form complex V. This transmetalated complex V could then react with compound **4-6** present in the reaction mixture to form intermediate complex VI. The Rh-O bond cleavage in complex VI could lead to the formation of the product **4-11** with two distinct aryl groups (Figure 4.15).

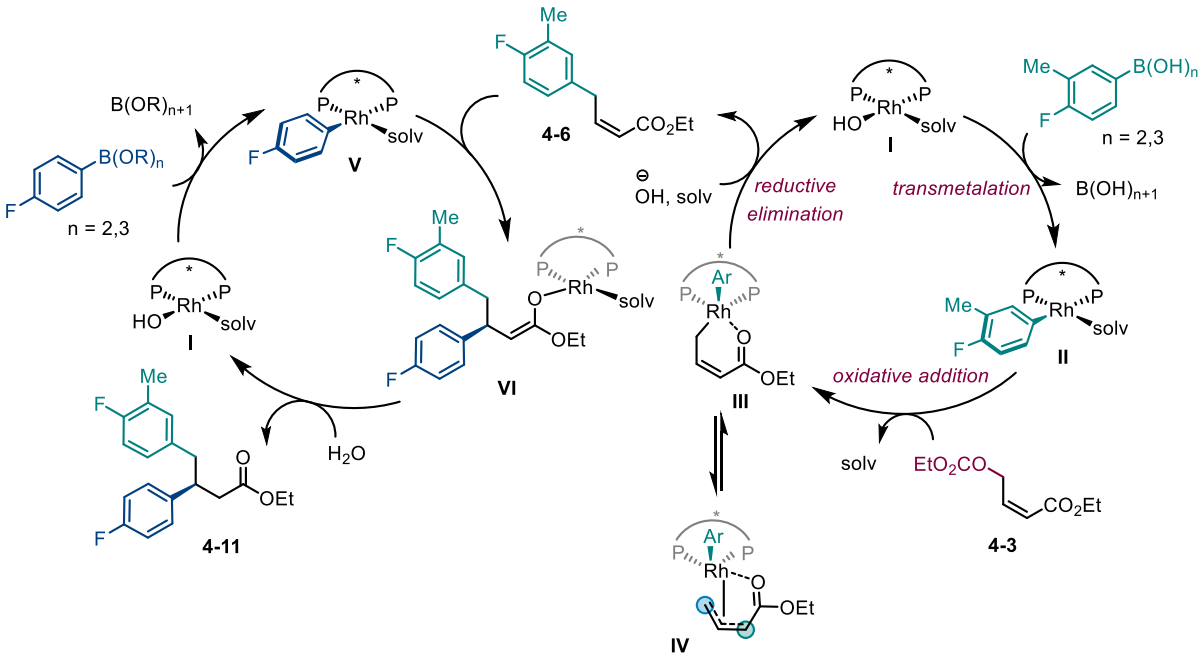

Figure 4.15 Proposed mechanism for the formation of the doubly arylated species.

To test our hypothesis, we subjected starting material **4-3** to our standard reaction conditions using boronic acid **4-4a** and boronic acid pinacol ester **4-10b** bearing two different aryl species.

During our investigations, we observed that the proposed second catalytic cycle did not occur in practice. Instead, a sole γ-arylation product **4-6** was obtained with a yield of 46% (Figure 4.16, a). Attempts to enhance the 1,4-addition process by increasing reaction temperatures and introducing water did not yield satisfactory results (Figure 4.16, b).

In view of this, we postulated that more vigorous conditions akin to those employed in 1,4-additions of boronic acid pinacol esters would be necessary to accomplish the second step of the dual arylation process. (*R*)- or (*S*)-BINAP, renowned for their efficacy as ligands in facilitating rhodium-catalysed asymmetric conjugate additions to α,β-unsaturated esters[183], were employed in our experiments.

In pursuit of this objective, we applied modified conditions to our substrate, which involved employing (*R*)-BINAP, KOH, and a higher reaction temperature of 90 °C. Importantly, we maintained the same quantities and ratios of the arylboronic acid and arylboronic acid pinacol ester as before (Figure 4.16, c). The primary product detected in the crude reaction mixture was the desired compound, **4-11**, which we isolated with a yield of 68% and an enantioselectivity of 81%. While a higher level of enantioselectivity would have been preferable, it is noteworthy that we achieved a satisfactory yield of 68% for the desired product. The arylboronic acid pinacol ester could be serving as a gradual release source for boronic acid, facilitating the stepwise incorporation of distinct aryl groups at two different positions in substrate **4-3**.

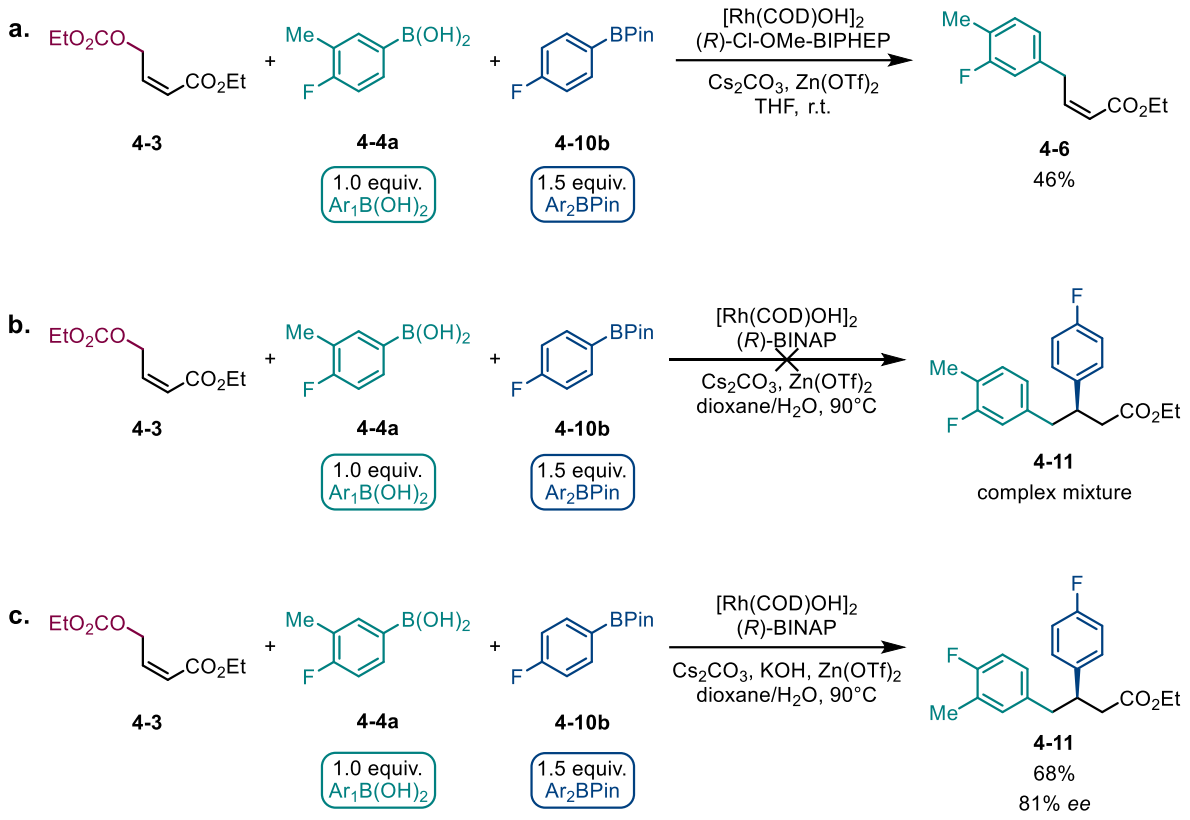

Figure 4.16 Experiments using two distinct boronic acid species.

Interestingly, upon examining the ^{19}F NMR spectrum of the crude reaction mixture, we observed the byproduct to be ethyl (*R*)-3,4-bis(4-fluoro-3-methylphenyl)butanoate **4-7a**. This indicates that some double addition of (4-fluoro-3-methylphenyl)boronic acid **4-4a** occurred prior to conjugate addition with (4-fluorophenyl)boronic acid pinacol ester **4-10b** (Figure 4.17).

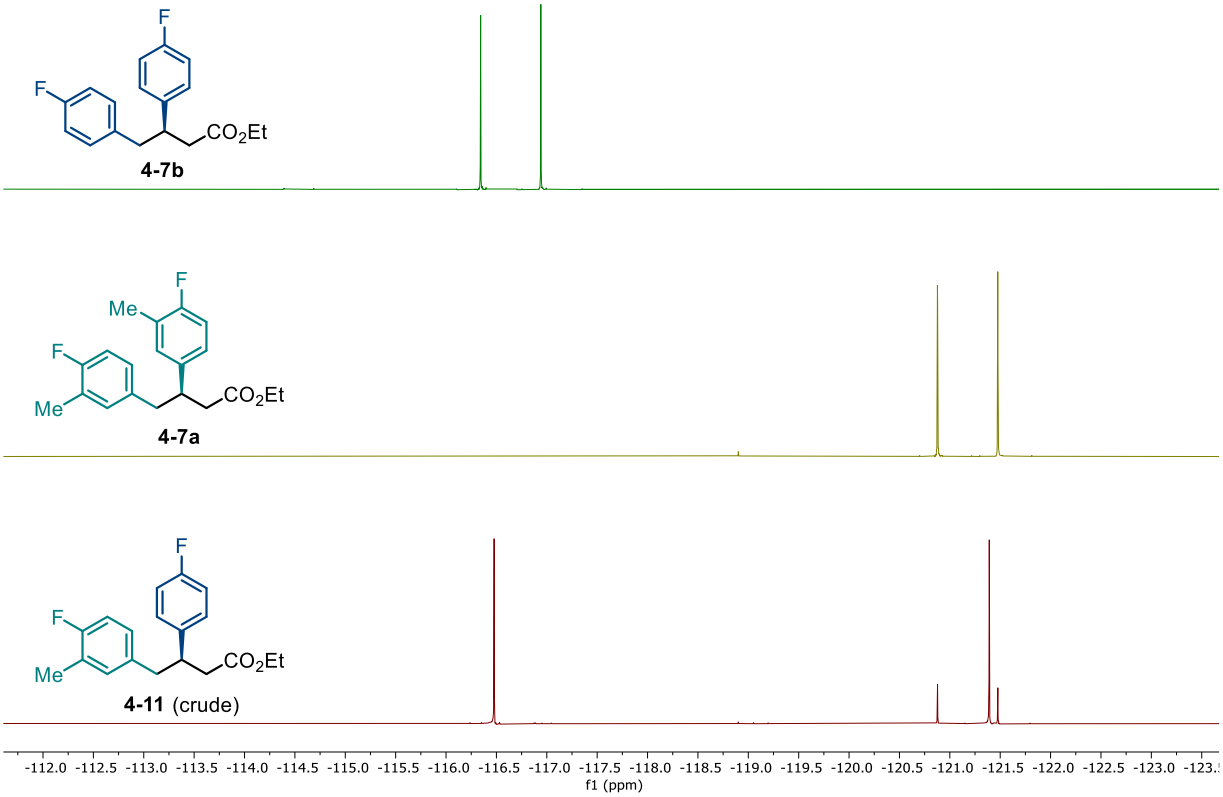

Figure 4.17 ^{19}F NMR spectra of double arylation products. The bottom spectrum is of the crude reaction mixture when two distinct arylborons were used.

This observation is consistent with our previous findings, where a small amount of double addition product was observed during the optimization of boronic acid equivalents despite incomplete consumption of the starting material (Table 4.1).

4.2.2 Application in synthesis of biologically active compounds

With the aid of our newly developed methodology, we have successfully synthesized **4-7c**, a precursor of 7-hydroxy-3-(4-hydroxyphenyl)-3,4-dihydronaphthalen-1(2H)-one, a potent estrogenic modulator (Figure 4.18).[168] This bioactive compound can be obtained through subsequent ester hydrolysis, Friedel-Crafts cyclization, and demethylation of the methoxy groups on the aromatic moieties.[168]

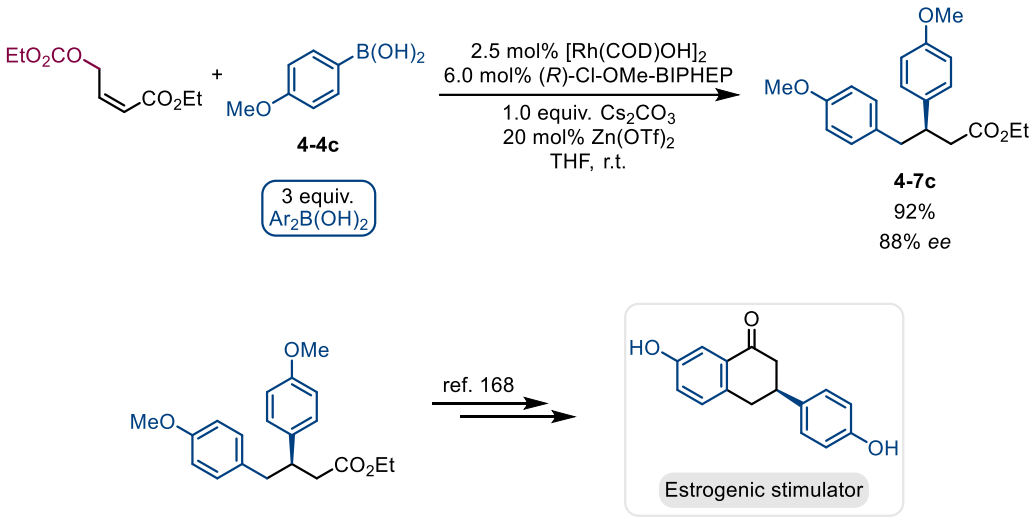

Figure 4.18 Asymmetric one-step synthesis of a precursor to an estrogenic modulating agent.

7-Hydroxy-3-(4-hydroxyphenyl)-3,4-dihydronaphthalen-1(2H)-one has been patented for its interaction with β-estrogen receptors and as a potential treatment for Alzheimer's disease, anxiety disorders and depressive disorders,[184] and expeditious modular asymmetric synthesis of its precursors may prove crucial in discovering more potent analogues.

4.3 Conclusions

In this chapter we investigated the patterns of reactivity and new reaction outcomes of the allylic substrate as the steric bulk surrounding the carbon carrying the leaving group was reduced.

Drawing on the results of prior optimisation studies and the findings presented in this chapter, our hypothesis asserts that chelation capacity of the ester group plays a critical role in enabling markedly accelerated allylic substitution reactions while remaining slow with respect to 1,4-addition. The use of *Z*-enoate in the allylic starting material is an additional influential factor promoting the formation of a 6-membered ring rhodocycle intermediate (proposed in Chapter 2) that ensures the preferential occurrence of allylic substitution. These factors ensure that the processes occurring during the reaction are stepwise and hence that one product is obtained in excess The reduction in steric hindrance near the carbon atom adjacent to the β-center of the 1,4-acceptor in the intermediate molecule **4-6** may explain why a subsequent conjugate addition of a boronic acid can occur under the same conditions that yield a sole γ-substituted product when using a secondary allylic carbonate **2-3**.

The investigated reaction has its relative merits – it is important to acknowledge that the precursors to 1,4-addition can be obtained through other approaches. For example, intermediate product can be acquired by employing olefin cross-metathesis[185] with acrylic esters or a Wittig reaction utilizing a stabilised phosphorus ylide[186]. Nevertheless, pursuing either of these methods would inevitably entail an extra step for isolation and purification.

Finally, we showcased the practicality of our methodology through the efficient one-step synthesis of a precursor to a β-estrogen receptor modulator, namely, 7-hydroxy-3-(4-hydroxyphenyl)-3,4-dihydronaphthalen-1(2H)-one **4-7c**. In doing so, we established that our approach facilitates the prompt synthesis of various derivatives of this bioactive compound using a single, structurally simple precursor. We hold a firm conviction that

with an increased enantioselectivity this elegant and straightforward methodology will be incorporated into multiple total syntheses of natural products in the future.

4.4 Future directions

4.4.1 Approaches to increasing enantioselectivity

To enhance the enantioselectivity, it is imperative to determine the underlying factors responsible for the observed enantioselectivities. This entails assessing whether the current enantioselectivities result from the choice of ligand or from the formation of Z/E mixtures of intermediate products. To assess this, we propose to subject the Z-intermediate product **4-6** to established reaction conditions (Figure 4.19). An increased enantioselectivity would ascertain that the formation of a Z/E product mixture after the initial step contribute to the diminished enantiomeric excess.

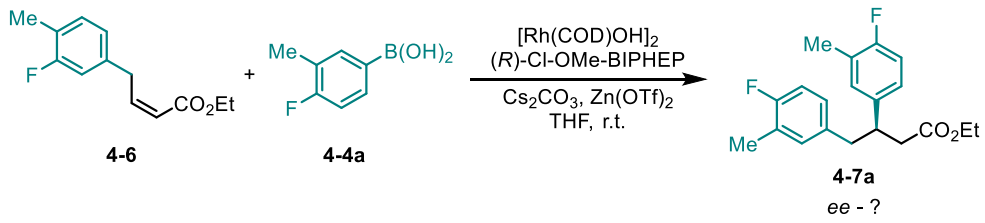

Figure 4.19 Proposed experiment to assess the cause of enantioselectivity erosion.

If this is indeed the case, the aforementioned issue can be overcome by employing an amide as the starting material. Previous investigations in Chapter 2 have demonstrated the exclusive formation of the Z-product using an amide substrate, albeit without enantioenrichment. When employing the primary amide starting material **4-14**, the lack of enantioselectivity becomes inconsequential, as the allylic arylation step does not generate a stereogenic center. Notably, this approach would exclusively generate Z-unsaturated amide as an intermediate product. Despite unsaturated amides being less favourable 1,4-acceptors due to heightened conjugation relative to esters, procedures

involving rhodium/bisphosphine catalysis have reported successful asymmetric arylation of α,β-unsaturated amides with boronic acids.[83,84]

Utilizing amide **4-14** as a starting material would also address the issue of double arylation with boronic acid, which leads to the formation of an undesired byproduct when employing the ester starting material **4-3**. The stronger chelation of the amide to rhodium is anticipated to accelerate the allylic arylation process, while the increased conjugation in amides should decelerate the 1,4-addition step. This difference in the relative reaction rates of the two consecutive steps could prevent the formation of the double arylation product, ultimately enhancing the yield of the desired product.

The amide substrate **4-14** was prepared by employing the transformations depicted in Figure 4.20. First, a Sonogashira coupling reaction involving propargylic alcohol **4-1** was utilised to synthesise the hydroxy-ynamide **4-12.**

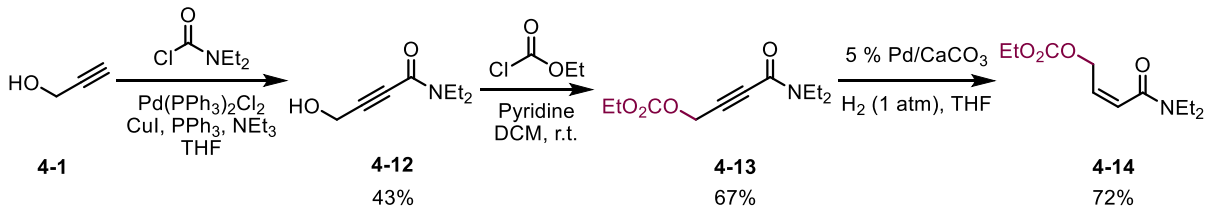

Figure 4.20 Synthesis route for an alternative amide starting material.

Subsequently, treatment of **4-12** with ethyl chloroformate under basic conditions led to the formation of primary carbonate **4-13**. Following this, a Lindlar catalyst was utilized to partially reduce the triple bond in **4-13**, resulting in the formation of the desired (*Z*)-allylic carbonate **4-14** (Figure 4.20).

4.4.2 Double functionalisation using vinylboronic acids

As previously noted in Chapter 2, our research group has established the viability of vinylboronic acids as coupling partners in Rh-catalysed asymmetric Suzuki-Miyaura

reactions. We propose that vinylboronic acids could be incorporated into an allylic alkylation-1,4-addition sequence to selectively generate complex acyclic molecules from our easily accessible precursor (Figure 4.21).

For instance, a GPR40 modulator[187] that has been patented as a potential diabetes II therapy could be produced using the sequential double functionalization approach.

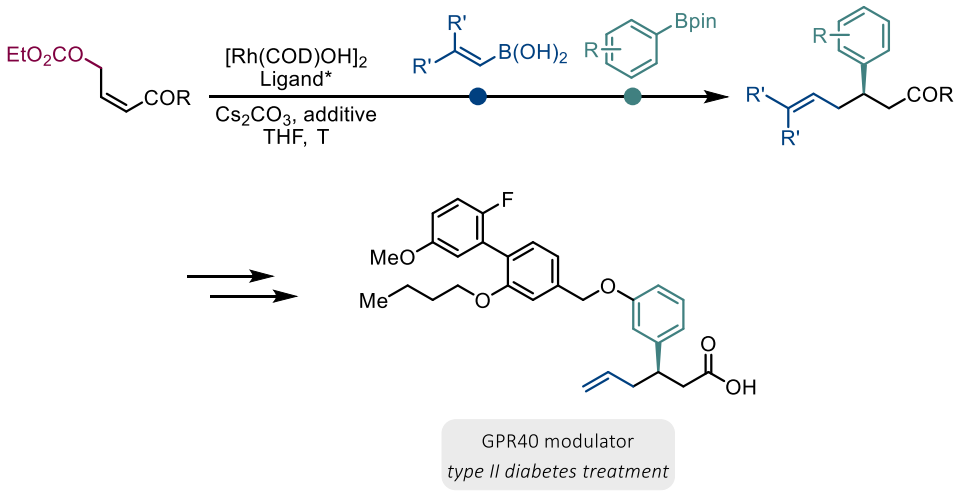

Figure 4.21 Double functionalisation using vinyl boronic acids and arylboronic acid pinacol esters.

While further research is required to fully evaluate the feasibility of this technique, the utilisation of vinylboronic acids in allylic arylation-1,4-addition reactions displays potential as a means of generating bioactive acyclic molecules and their derivatives with regulated stereochemistry.

Likewise, employing vinylboronic acid pinacol esters and aryl boronic acids (in the reverse order) could lead to the synthesis of a potent squalene epoxidase inhibitor (Figure 4.22).[188] This approach, which allows for diversification at two points within a single reaction, could facilitate the rapid production of several derivatives of the aforementioned inhibitor, potentially enhancing its efficacy.

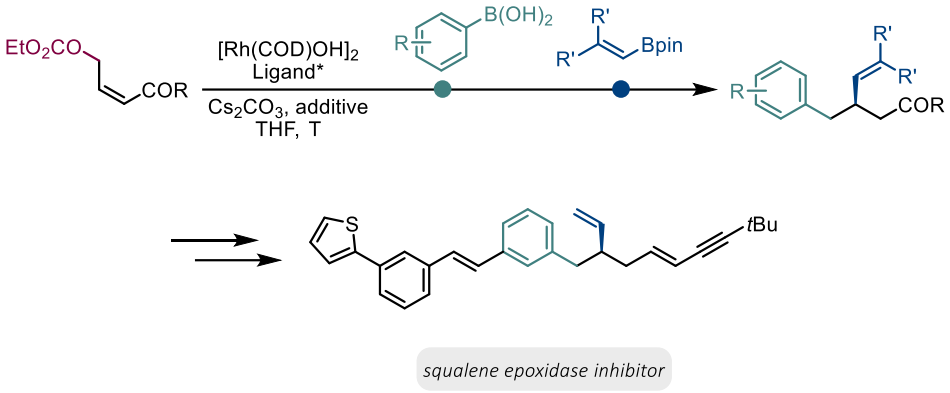

Figure 4.22 Double functionalisation using aryl boronic acids and vinylboronic acid pinacol esters.

In general, the sequential double alkylation with two distinct boronic acid species and acyclic allylic electrophiles has the potential to be a valuable approach for synthesizing a broad range of complex structured and biologically active compounds. We are confident in the capacity of the methodology we have developed to enable medicinal chemists to conduct controlled diversity-oriented synthesis in the future.

5 Experimental

5.1 General Methods

All reactions were carried out in flame-dried glassware, in anhydrous solvents with continuous magnetic stirring under an inert argon atmosphere. Heating was performed using DrySyn heating blocks.

Nuclear magnetic resonance (NMR) spectroscopy measurements were carried out at room temperature. ^{1}H NMR, ^{13}C NMR, ^{19}F NMR, COSY, HSQC, HMBC and NOESY experiments were carried out using Bruker AVN-400 (400/100 MHz), DQX-400 (400/100 MHz) or AVC-500 (500/125 MHz) spectrometers. Chemical shifts (δ) are reported in ppm relative to the residual solvent peak with corresponding coupling constants (*J*) in Hertz (Hz) and multiplicities (s: singlet, d: doublet, t: triplet, q: quartet, m: multiplet and combinations of these). Peak assignment follows HSQC, COSY, HMBC spectra, chemical shift and coupling constant analysis. Reported *Z*:*E* ratios were determined by ^{1}H NMR.

Specific optical rotations ($[\alpha]_D^{25}$) were recorded using a Perkin Elmer-241 Polarimeter. Concentrations (*c*) are reported in g/100 mL. Infrared (IR, neat, thin film) spectroscopy was carried out on a Bruker Tensor 27 FT–IR spectrometer with in internal calibration range of 4000 – 600 cm^{-1}. Only characteristic bands are reported.

Chiral SFC (supercritical fluid chromatography) separations were conducted on a Waters Acquity UPC2 system using Waters Empower software. Chiralpak® columns (150×3 mm, particle size 3 μm) were used as specified in the text. Solvents used were of HPLC grade (Fisher Scientific, Sigma Aldrich or Rathburn). Chiral GC (gas chromatography) separations were conducted on an Agilent Technologies 7820A system using Hydrodex β-3P (25 m, 0.25 mm ID) column.

Commercially available reagents were purchased from Sigma Aldrich, Alfa Aesar, Acros Organics, Flurochem and Strem Chemicals and unless otherwise stated were used without further purification. $[Rh(cod)OH]_2$ was bought from Sigma Aldrich and Strem Chemicals. All boronic acids were used without additional purification. Dry solvents were collected fresh from an mBraun SPS–800 solvent purification system after having passed through anhydrous alumina columns. Deuterated solvents were purchased from Sigma Aldrich.

Medium pressure chromatography was performed on a Combiflash Next Gen 100 system.

5.2 Experimental for Chapter 1

Figures 1.1 – 1.3 are reproduced and adapted from Figure 2 of Scott *et al.*[10] based on the supplementary material provided in the paper (Appendix A, Multimedia component 1 of Scott *et al.*), which consists of an XLSX format table of the molecular complexity, molecular weight, information density and SMILES descriptions of 1,112 drugs approved by the FDA between 1951 and 2021.
The authors describe that they obtained the number of stereocentres of each drug from its SMILES description, automatically where explicitly defined in the SMILES, and by manual counting for chiral drugs in which the stereocenters are not explicitly defined.

They then plotted a frequency bar plot of the overall number of centres, box plots of the distributions of molecular complexity and information density for different numbers of centres and a scatter plot of the information density of chiral and achiral drugs by their year of approval, with an overall line of best fit.
To reproduce this work, the XLSX file is first converted to CSV format, the caption removed, and the contents read. Rather than reproduce the authors' manual count of the chiral stereocenters of each drug where they are undefined (which they do not share), the RDKIT library (Landrum *et al.* https://buildmedia.readthedocs.org/media/pdf/rdkit/latest/rdkit.pdf) is used to automatically detect the number of undefined stereocenters of each drug based on its SMILES description. Plots similar to those of Scott *et al.*, adapted for clarity of presentation are then produced using Matplotlib.

The above is all implemented in Python 3.8.10 using the following code (assuming the CSV file is in location diversityfromstereochemistry.csv):

```
from count_centres import count_centres
from graphs import colours, labels, scatter_line, bar, box
import pandas as pd


# Load dataframe from CSV
d = pd.read_csv('diversityfromstereochemistry.csv')

# Detect and count chiral centres for each drug in the dataframe
d['centres'] = d['SMILES'].apply(lambda smiles: count_centres(smiles))

# Plot bar chart of frequency of different numbers of stereocentres
bar(d, 'centres', labels, colours['greenish'], 'num_centres_freq.png')

# Plot scatter graph of information density of each drug over time, split into chircal and
achiral
scatter_line(d, 'Approval Date', 'Information Density', labels,
        {
           'Achiral': d['centres'] == 0,
           'Chiral': d['centres'] > 0
        },
        {
           'Achiral': colours['burgundy'],
           'Chiral': colours['blue']
        }, colours['grey'], 'id_vs_year.png')


# Plot box plots of distributions of molecular complexity and information density for 4
categories of number of centres
centres_filters = {
```

```
  'Achiral': d['centres'] == 0,
  '1 centre': d['centres'] == 1,
  '2 centres': d['centres'] == 2,
  '>2 centres': d['centres'] > 2
}
box(d, 'centres', centres_filters, 'Cm', labels, 'cm_dist_vs_num_centres.png')
box(d, 'centres', centres_filters, 'Information Density', labels,
'id_dist_vs_num_centres.png')
```

The code is dependent on Pandas 0.25.3 and on two other Python scripts placed in the same folder. The first (count_centres.py), implements the counting of the number of chiral centres from the SMILES description of each drug, and is itself dependent on RDKIT 2022.09.3:

```
from rdkit import Chem


def count_centres(smiles):
  """
  Count the number of chiral stereocentres of a compound
  :param smiles: SMILES description of compound
  :return: Number of stereocentres
  """
  defined_centres = smiles.replace('@@', '@').count('@')

  if defined_centres > 0:
    return defined_centres
  else:
    try:
      undefined_centres =
len(Chem.FindMolChiralCenters(Chem.MolFromSmiles(smiles),
includeUnassigned=True))
    except Exception as e:
      print(e)
      undefined_centres = 0
    return undefined_centres
```

The second (graphs.py) contains functions for plotting the three types of graphs and is dependent on Matplotlib 3.1.2 and NumPy 1.17.4:

```
import matplotlib.pyplot as plt
import numpy as np

# Dictionary of colours to use in graphs for compatibility with thesis colour scheme
```

```
colours = {
  'dark_blue': (0, 0.25, 0.5),
  'blue': (0, 0.5, 0.75),
  'greenish': (0.25, 0.5, 0.5),
  'grey': (0.5, 0.5, 0.5),
  'sky_blue': (135 / 256, 206 / 256, 235 / 256),
  'burgundy': (0.5, 0, 0.25)
}

# Default axis labels for different columns
labels = {'Approval Date': 'Year of FDA approval',
      'Cm': 'Molecular complexity (mcbits)',
      'Information Density': 'Chemical information density (mcbits mol/g)',
      'centres': 'Number of stereocentres'}


def scatter_line(df, xcol, ycol, labels, filters, colour_dict, linecolour, fname, xmin=1950,
xmax=2025, xstep=5):
  """
  Creates and saves scatter plot of points, split into categories based on filters, with line of
best fit of all data
  :param df: Input Pandas dataframe
  :param xcol: Name of column of df to plot on x-axis
  :param ycol: Name of column of df to plot on y-axis
  :param labels: Dictionary where the name of each column points to the label to use for its
respective axis
  :param filters: Dictionary where the name of each category points to the filter used to
generate it from df
  :param colour_dict: Dictionary where the name of each category points to the colour to
display its points
  :param linecolour: Colour of line of best fit
  :param fname: Path to store output file
  :param xmin: Minimum value of the column to plot on the x-axis
  :param xmax: Maximum value of the column to plot on the y-axis
  :param xstep: Step between ticks to display on the x-axis
  :return:
  """
  x = np.array(list(df[xcol]))
  y = np.array(list(df[ycol]))
  m, c = np.linalg.lstsq(np.vstack([x, np.ones(len(x))]).T, y, rcond=None)[0]
  plt.figure(figsize=[15, 7.5])
  ax = plt.subplot(111)
  for j in filters:
    dfj = df if filters[j] is None else df[filters[j]]
    ax.scatter(dfj[xcol], dfj[ycol], c=colour_dict[j], marker='.', label=j)
```

```
    ax.plot([min(x), max(x)], [m * min(x) + c, m * max(x) + c], c=linecolour,
label='Regression line')
    ax.set_xticks(range(xmin, xmax, xstep))
    ax.legend()
    ax.set_xlabel(labels[xcol])
    ax.set_ylabel(labels[ycol])
    ax.spines['top'].set_visible(False)
    ax.spines['right'].set_visible(False)
    plt.savefig(fname)


def bar(df, col, labels, c, fname, ylabel='Number of drugs'):
    """
    Creates and saves a frequency bar chart of the different values of a column within a
dataframe
    :param df: Input Pandas dataframe
    :param col: Name of column in df
    :param labels: Dictionary where the name of each column points to the label to use for its
respective axis
    :param c: Colour of bars
    :param fname: Path to store output file
    :param ylabel: Label to display for y (frequency) axis
    :return:
    """
    nums = list(set(df[col]))
    freqs = [list(df[col]).count(x) for x in nums]
    plt.figure()
    ax = plt.subplot(111)
    ax.bar(nums, freqs, color=c)
    ax.set_xlabel(labels[col])
    ax.set_ylabel(ylabel)
    ax.spines['top'].set_visible(False)
    ax.spines['right'].set_visible(False)
    plt.savefig(fname)


def box(df, xcol, xfilters, ycol, labels, fname):
    """
    Box plot of the distribution of values of a column for different ranges of values of another
column
    :param df: Input Pandas dataframe
    :param xcol: Name of column in df for different ranges of which to plot values of ycol
    :param xfilters: Dictionary where labels to give each range of xcol point to filter defining
range
    :param ycol: Column in df the distribution of which to plot for each range of xcol defined
by xfilters
```

```
  :param labels: Dictionary where the name of each column points to the label to use for its
respective axis
  :param fname: Path to save output file
  :return:
  """
  plt.figure()
  ax = plt.subplot(111)
  bp = ax.boxplot([list(df[xfilters[key]][ycol]) for key in xfilters], patch_artist=True,
sym='.')
  plt.setp(bp['medians'], color=colours['dark_blue'])
  plt.setp(bp['fliers'], markeredgecolor=colours['dark_blue'])
  for patch in bp['boxes']:
    patch.set_facecolor(colours['sky_blue'])
  ax.spines['top'].set_visible(False)
  ax.spines['right'].set_visible(False)
  ax.set_xlabel(labels[xcol])
  ax.set_ylabel(labels[ycol])
  ax.set_xticklabels(xfilters.keys())
  plt.savefig(fname)
```

The above code outputs the following plots:

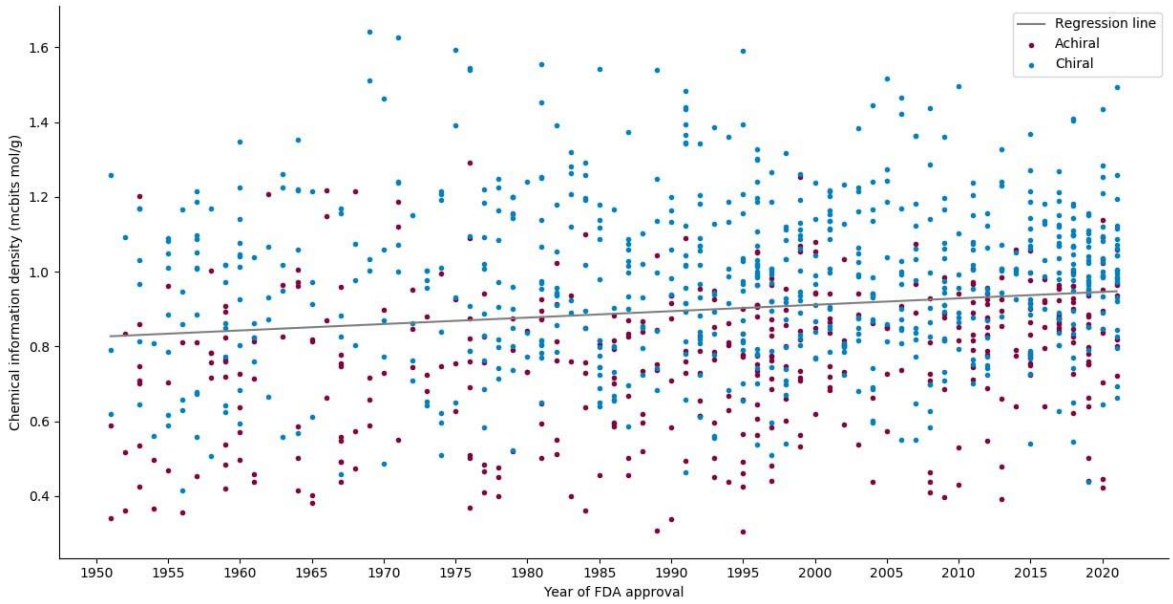

Figure 5.1 A scatter plot of chemical information density in FDA approved chiral and achiral pharmaceutical drugs over time (Figure 1.2 in Chapter 1).

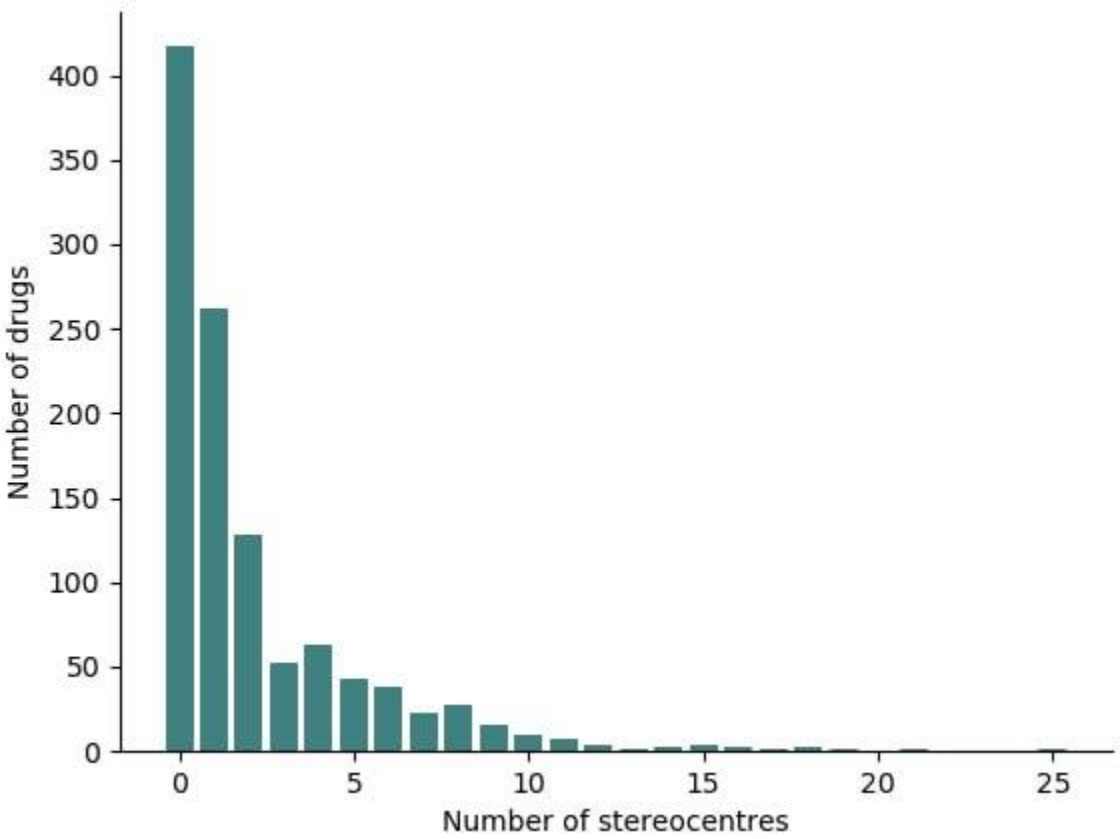

Figure 5.2 A frequency bar plot of the overall number of stereocentres in FDA approved pharmaceutical drugs (figure 1.1 in Chapter 1).

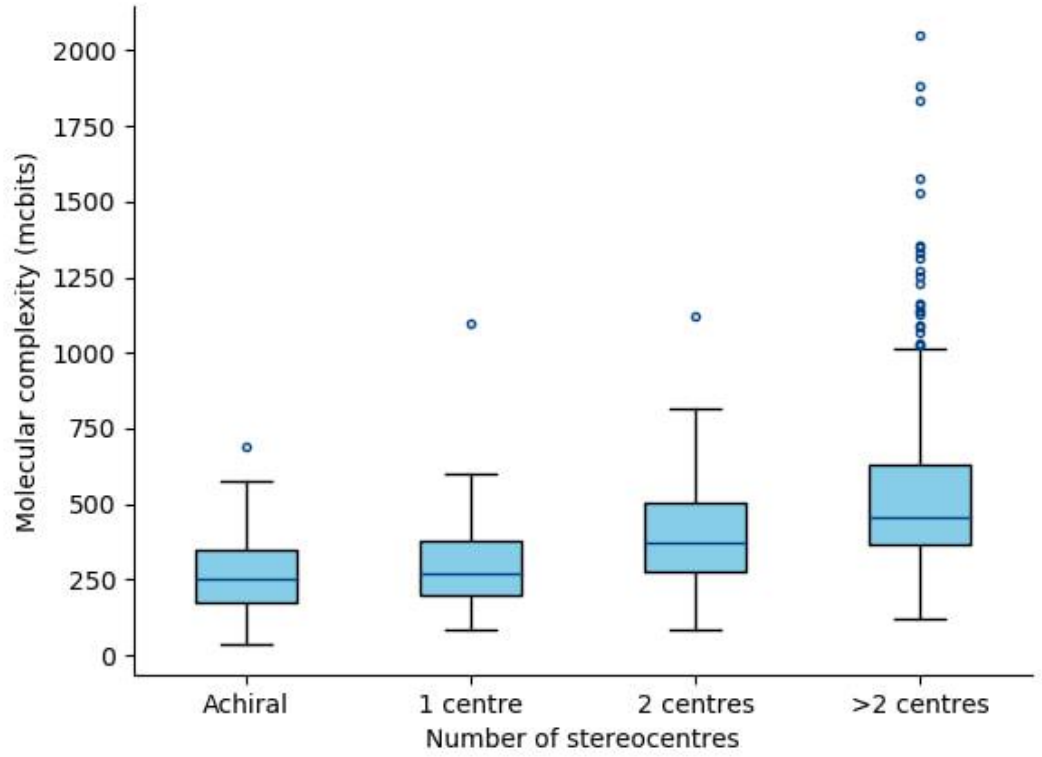

Figure 5.3 A box plot of the distribution of molecular complexity (in mcbits) for compounds with different numbers of stereogenic centres (Figure 1.3 in Chapter 1).

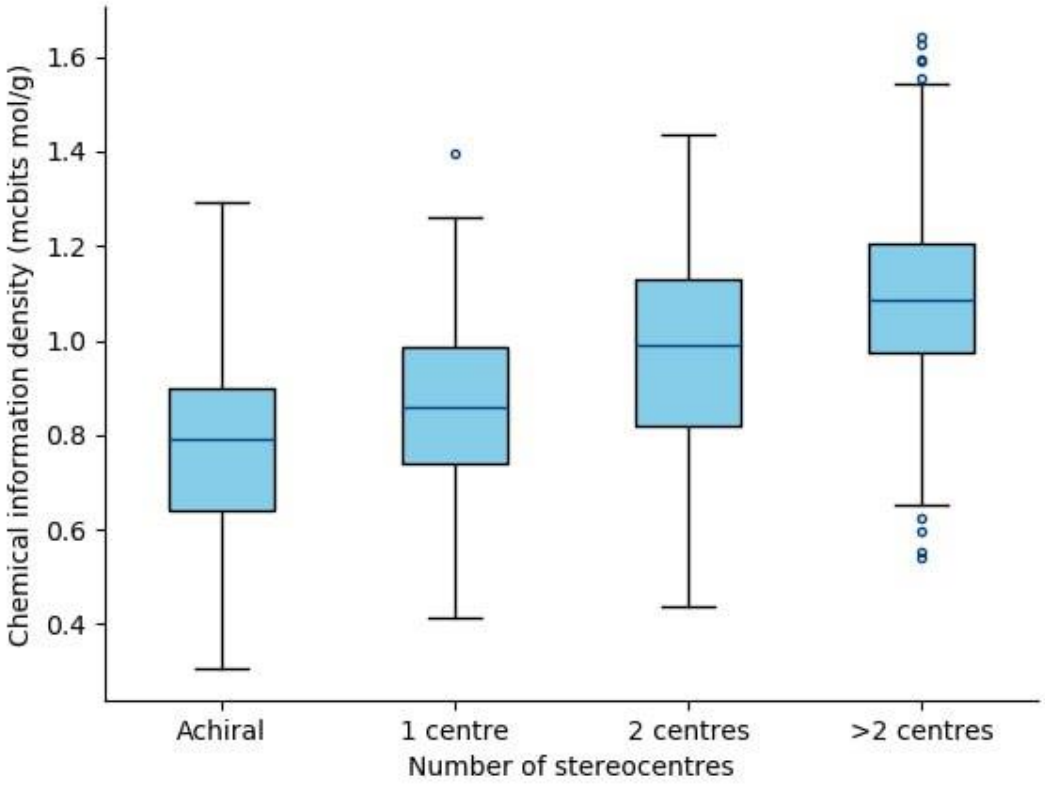

Figure 5.4 A box plot of the distribution of chemical information density (in mcbits mol/g) for compounds with different numbers of stereogenic centres (Figure 1.3 in Chapter 1).

5.3 Experimental for Chapter 2

5.3.1 Procedures for the synthesis of starting materials

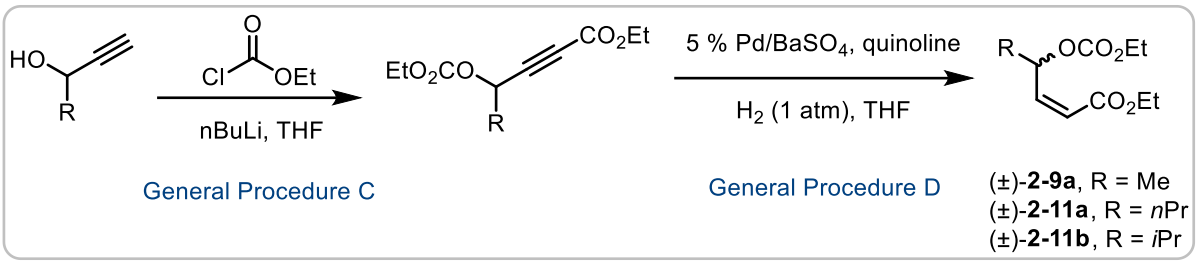

General procedure C:

*n*BuLi (2.5 M in hexane, 2.3 eq) was added to a solution of the propargylic alcohol (1.0 eq) in THF (0.4 M) at -78 °C. The mixture was stirred at -78 °C for 30 minutes and ethyl chloroformate (2.2 eq) was added dropwise. The reaction mixture was stirred at room temperature (23 °C) for 6 hours. A saturated solution of NH_4Cl was added at 0 °C and the aqueous layer was extracted with Et_2O (x3). Combined organic layers were washed with brine, dried over Na_2SO_4, filtered and concentrated *in vacuo*. Purification by automated medium-pressure flash chromatography (Et_2O/hexane) afforded the corresponding alkyne products **S1**, **S2** and **S3**.

General procedure D:

Rosenmund catalyst (Pd on $BaSO_4$, 0.15 equiv.) and quinoline (0.18 equiv.) were suspended in THF (0.37 M) and the suspension was purged with hydrogen gas (balloon) for 10 minutes. Then a solution of alkyne (1.0 equiv.) in THF (2 mL) was added and the reaction mixture was stirred under an atmosphere of H_2 (balloon) for 3 hours while being monitored. Upon consumption of starting material, the reaction was filtered through a plug of silica eluting with Et_2O and concentrated *in vacuo*. Purification by automated medium-pressure flash chromatography (Et_2O/hexane) afforded products (±)-**2-9a**, (±)-**2-11a** and (±)-**2-11b**.

Substrates (±)-**2-11c**, (±)-**2-11f**, (±)-**2-11g**, (±)-**2-11h** and (±)-**2-11j** we prepared by Stephen J. Webster. Substrates (±)-**2-11e** and (±)-**2-11i** were prepared by Ke Liu. Detailed procedures for preparation of these substrates and their full characterisation

data can be found in '**Chelation enables selectivity control in enantioconvergent Suzuki-Miyaura cross-couplings on acyclic allylic systems**', Violeta Stojalnikova, Stephen J. Webster, Ke Liu and Stephen P. Fletcher. 2023, *Nature Chemistry. Accepted.*

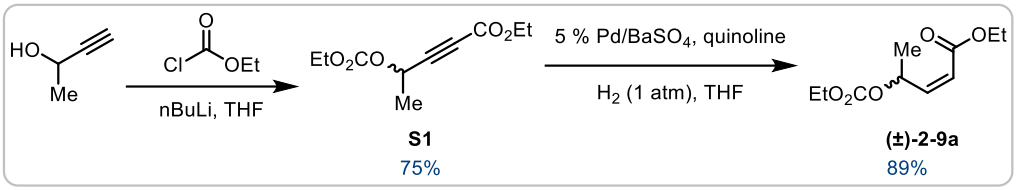

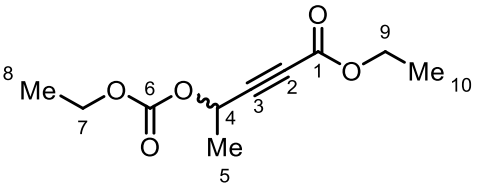

Ethyl 4-((ethoxycarbonyl)oxy)pent-2-ynoate S1

Ethyl 4-((ethoxycarbonyl)oxy)pent-2-ynoate **S1** was prepared from but-3-yn-2-ol (4.70 mL, 60.0 mmol, 1.0 eq) using General procedure C. Purification by automated medium-pressure flash chromatography (0 to 20% Et_2O/hexane) afforded ethyl 4-((ethoxycarbonyl)oxy)pent-2-ynoate **S1** (9.64 g, 45.0 mmol, 75%) as a colourless oil. Characterisation data match literature reports.[197]

^{1}H NMR (400 MHz, $CDCl_3$) δ 5.39 (q, *J* = 6.8 Hz, 1H, C(4)-H), 4.23 (q x2, *J* = 7.1 Hz, 4H, C(7)-H_2 and C(9)-H_2), 1.59 (d, *J* = 6.9 Hz, 3H, C(5)-H_3), 1.33 (t, *J* = 7.0 Hz, 3H, C(8)-H_3), 1.29 (t, *J* = 7.0 Hz, 3H, C(10)-H_3).

^{13}C NMR (101 MHz, $CDCl_3$) δ 153.9 (C(1)), 152.9 (C(6)), 83.9 (C(3)), 76.9 (C(2)), 64.6 (C(5)), 63.1 (C(7)), 62.2 (C(9)), 20.4 (C(5)), 14.2 (C(8)), 13.9 (C(10)).

HRMS (ESI): m/z calculated for $C_{10}H_{14}O_5Na^+$ $[M+Na]^+$ 237.0733 found 237.0728.

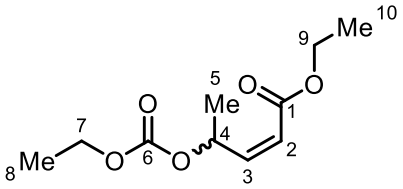

Ethyl (*Z*)-4-((ethoxycarbonyl)oxy)pent-2-enoate (±)-2-9a

Ethyl (I)-4-((ethoxycarbonyl)oxy)pent-2-enoate (±)-**2-9a** was prepared from ethyl 4-((ethoxycarbonyl)oxy)pent-2-ynoate **S1** (4.07 g, 19.0 mmol, 1.0 eq) using General procedure D. Purification by automated medium-pressure flash chromatography (gradient of 0 to 15% Et_2O/hexane in 10 minutes) afforded ethyl (Z)-4-((ethoxycarbonyl)oxy)pent-2-enoate (±)-**2-9a** (3.66 g, 16.9 mmol, 89%) as a colourless oil.

^{1}H NMR (400 MHz, $CDCl_3$) δ 6.15 (m, 2H, C(3)-H and C(4)-H), 5.77 (m, 1H, C(2)-H), 4.15 (q x2, *J* = 7.1 Hz, 4H, C(7)-H_2 and C(9)-H_2), 1.39 (d, *J* = 6.4 Hz, 3H, C(5)-H_3), 1.26 (t x2, *J* = 7.1 Hz, 6H, C(8)-H_3 and C(10)-H_3).

^{13}C NMR (101 MHz, $CDCl_3$) δ 165.2 (C(1)), 154.3 (C(6)), 147.7 (C(3)), 120.1 (C(2)), 72.0 (C(4)), 63.9 (C(7)), 60.4 (C(9)), 19.5 (C(5)), 14.2 (C(10)), 14.1 (C(8)).

HRMS (ESI): m/z calculated for $C_{10}H_{16}O_5Na^+$ $[M+Na]^+$ 239.0890 found 239.0890.

IR (CH_3Cl film): 2981 (m), 1746 (s), 1719 (s), 1654 (w), 1449 (w), 1371 (m), 1258 (s), 1195 (s), 1124 (m), 1042 (s), 1008 (m), 849 (m), 823 (m), 792 (m) cm^{-1}.

The enantiopure (*S*)-**2-9a** used in the mechanistic studies was prepared using the same set of procedures as (±)-**2-9a** but with (*S*)-but-3-yn-2-ol as a starting material. The resulting ethyl (*S*)-(ethyl (Z)-4-((ethoxycarbonyl)oxy)pent-2-enoate (*S*)-**2-9a** was obtained with 99% *ee* (as shown by SFC analysis, SI Figure 6.131).

SFC: Chiralpak® IG, 1500 psi, 30 °C; flow: 1.0 mL/min; 1% to 30% MeOH over 5 min, 99.5:0.5 e.r. (minor enantiomer t_R = 1.27 min, major enantiomer t_R = 1.20 min).

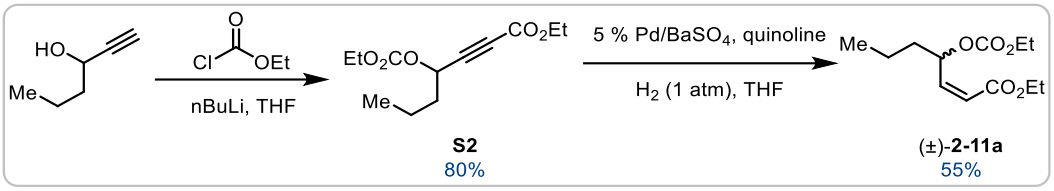

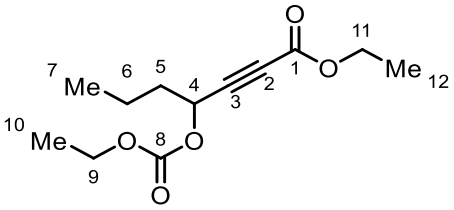

Ethyl 4-((ethoxycarbonyl)oxy)hept-2-ynoate S2

Ethyl 4-((ethoxycarbonyl)oxy)hept-2-ynoate **S2** was prepared from hex-1-yn-3-ol (2.19 mL, 20.0 mmol, 1.0 equiv.) using General procedure C. Purification by automated medium-pressure flash chromatography (0 to 20% Et_2O/hexane) afforded ethyl 4-((ethoxycarbonyl)oxy)hept-2-ynoate **S2** (3.88 g, 16.0 mmol, 80%) as a yellow oil.

^{1}H NMR (400 MHz, $CDCl_3$) δ 5.30 (t, *J* = 6.7 Hz, 1H, C(4)-H), 4.21 (q x2, *J* = 7.1 Hz, 4H, C(9)-H_2 and C(11)-H_2), 1.83 (m, 2H, C(5)-H_2), 1.49 (h, *J* = 7.5 Hz, 2H, C(6)-H_2), 1.30 (q, *J* = 7.1 Hz, 6H, C(10)-H_3 and C(12)-H_3), 0.94 (t, *J* = 7.4 Hz, 3H, C(7)-H_3).

^{13}C NMR (101 MHz, $CDCl_3$) δ 154.1 (C(1)), 153.0 (C(8)), 83.4 (C(3)), 77.5 (C(2)), 66.7 (C(4)), 64.6 (C(9)), 62.2 (C(11)), 36.0 (C(5)), 18.1 (C(6)), 14.2 (C(10)), 13.9 (C(12)), 13.4 (C(7)).

HRMS (ESI): m/z calculated for $C_{12}H_{18}O_5Na^+$ $[M+Na]^+$ 265.1046 found 265.1040.

IR (CH_3Cl film): 2965 (w), 1751 (m), 1717 (m), 1467 (w), 1372 (w), 1242 (s), 1074 (w), 1008 (m), 951 (w), 913 (w), 878 (w), 790 (w), 733 (m) cm^{-1}.

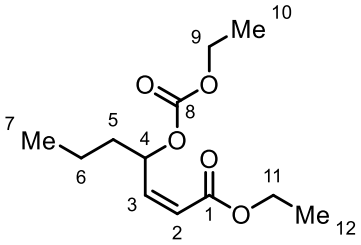

Ethyl (*Z*)-4-((ethoxycarbonyl)oxy)hept-2-enoate (±)-2-11a

Ethyl (*Z*)-4-((ethoxycarbonyl)oxy)hept-2-enoate (±)-**2-11a** was prepared from ethyl 4-((ethoxycarbonyl)oxy)hept-2-ynoate **S2** (3.88 g, 16.0 mmol, 1.0 equiv.) using General procedure D. Purification by automated medium-pressure flash chromatography (gradient of 0 to 20% Et_2O/hexane in 10 minutes) afforded ethyl (*Z*)-4-((ethoxycarbonyl)oxy)hept-2-enoate (±)-**2-11a** (2.15 g, 8.80 mmol, 55%) as a colourless oil.

^{1}H NMR (400 MHz, $CDCl_3$) δ 6.12 (m, 2H, C(3)-H and C(4)-H), 5.83 (m, 1H, C(2)-H), 4.18 (p, *J* = 7.1 Hz, 4H, C(9)-H_2 and C(11)-H_2), 1.75 (m, 1H, C(5)-H), 1.63 (m, 1H, C(5)-H), 1.44 (m, 2H, C(6)-H_2), 1.29 (td, *J* = 7.1, 1.3 Hz, 6H, C(10)-H_3 and C(12)-H_3), 0.93 (t, *J* = 7.3 Hz, 3H, C(7)-H_3).

^{13}C NMR (101 MHz, $CDCl_3$) δ 165.3 (C(1)), 154.7 (C(8)), 146.9 (C(3)), 120.7 (C(2)), 75.1 (C(4)), 63.9 (C(9)), 60.4 (C(11)), 36.0 (C(5)), 18.3 (C(6)), 14.2 (C(10) and C(12)), 13.8 (C(7)).

HRMS (ESI): m/z calculated for $C_{12}H_{20}O_5Na^+$ $[M+Na]^+$ 267.1203 found 267.1202.

IR (CH_3Cl film): 2964 (w), 1746 (m), 1719 (m), 1372 (w), 1257 (s), 1192 (m), 1010 (w), 954 (w), 910 (m), 825 (w), 750 (s), 649 (w) cm^{-1}.

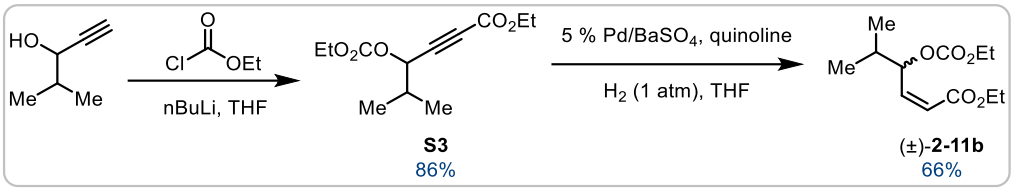

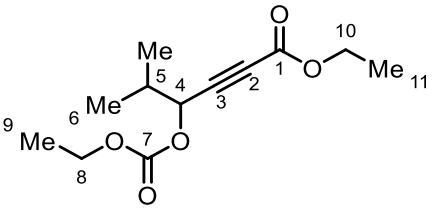

Ethyl 4-((ethoxycarbonyl)oxy)-5-methylhex-2-ynoate S3

Ethyl 4-((ethoxycarbonyl)oxy)-5-methylhex-2-ynoate **S3** was prepared from 4-methylpent-1-yn-3-ol (1.00 g, 10.0 mmol, 1.0 equiv.) using General procedure C. Purification by automated medium-pressure flash chromatography (0 to 20% Et_2O/hexane) afforded ethyl 4-((ethoxycarbonyl)oxy)-5-methylhex-2-ynoate **S3** (2.09 g, 8.62 mmol, 86%) as a colourless oil.

^{1}H NMR (400 MHz, $CDCl_3$) δ 5.14 (d, *J* = 6.3 Hz, 1H, C(4)-H), 4.22 (q, *J* = 7.2 Hz, 4H, C(8)-H_2 and C(10)-H_2), 2.11 (dh, *J* = 7.0, 6.5 Hz, 1H, C(5)-H), 1.30 (q, *J* = 7.6, Hz, 6H, C(9)-H_3 and C(11)-H_3), 1.05 (m, 6H, C(6)-H_3 x2).

^{13}C NMR (101 MHz, $CDCl_3$) δ 154.3 (C(1)), 153.0 (C(7)), 82.4 (C(3)), 78.2 (C(2)), 71.9 (C(4)), 64.6 (C(8)), 62.2 (C(10)), 32.4 (C(5)), 18.0 (C(6)), 17.6 (C(6)), 14.2 (C(9)), 14.0 (C(11)).

HRMS (ESI): m/z calculated for $C_{12}H_{18}O_5Na^+$ $[M+Na]^+$ 265.1046 found 265.1048.

IR (CH_3Cl film): 2979 (w), 1751 (m), 1716 (m), 1468 (w), 1372 (w), 1241 (s), 1007 (m), 910 (m), 880 (w), 789 (w), 732 (m) cm^{-1}.

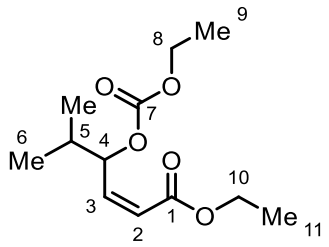

Ethyl (*Z*)-4-((ethoxycarbonyl)oxy)-5-methylhex-2-enoate (±)-2-11b

Ethyl (*Z*)-4-((ethoxycarbonyl)oxy)-5-methylhex-2-enoate (±)-**2-11b** was prepared from ethyl 4-((ethoxycarbonyl)oxy)-5-methylhex-2-ynoate **S3** (1.05 g, 4.32 mmol, 1.0 equiv.) using General procedure D. Purification by automated medium-pressure flash chromatography (gradient of 0 to 20% Et_2O/hexane in 10 minutes) afforded ethyl (*Z*)-4-((ethoxycarbonyl)oxy)-5-methylhex-2-enoate (±)-**2-11b** (0.795 g, 2.9 mmol, 66%) as a colourless oil.

^{1}H NMR (400 MHz, $CDCl_3$) δ 6.09 (dd, *J* = 11.6, 8.4 Hz, 1H, C(3)-H), 6.02 (ddd, *J* = 8.4, 5.3, 1.0 Hz, 1H, C(4)-H), 5.91 (dd, *J* = 11.6, 1.0 Hz, 1H, C(2)-H), 4.18 (m, 4H, C(8)-H_2 and C(10)-H_2), 2.04 (heptd, *J* = 6.9, 5.2 Hz, 1H, C(5)-H), 1.29 (t x2, *J* = 7.2 Hz, 6H, C(9)-H_3 and C(11)-H_3), 0.98 (d, *J* = 6.9 Hz, 6H, C(6)-H_3 x2).

^{13}C NMR (101 MHz, $CDCl_3$) δ 165.3 (C(1)), 154.8 (C(7)), 145.3 (C(3)), 122.0 (C(2)), 78.6 (C(4)), 63.9 (C(8)), 60.4 (C(10)), 32.4 (C(5)), 18.3 (C(9)), 17.2 (C(11)), 14.2 (C(6)), 14.1 (C(6)).

HRMS (ESI): m/z calculated for $C_{12}H_{20}O_5Na^+$ $[M+Na]^+$ 267.1203 found 267.1206.

IR (CH_3Cl film): 2981 (w), 1745 (w), 1372 (w), 1258 (m), 1196 (m), 1008 (w), 945 (w), 908 (s), 650 (w) cm^{-1}.

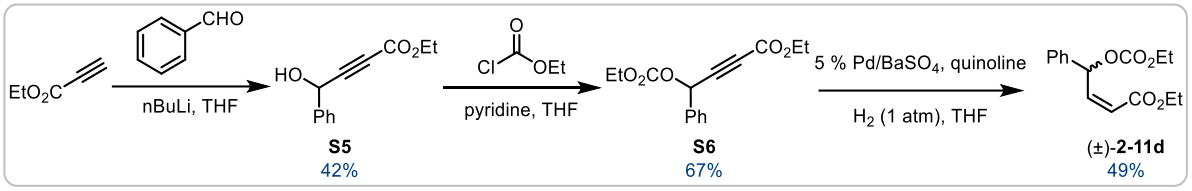

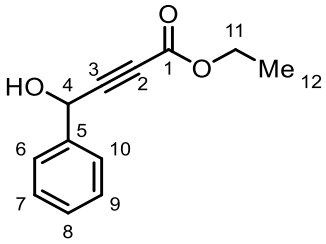

Ethyl 4-hydroxy-4-phenylbut-2-ynoate S4

Ethyl propiolate (3.04 mL, 30.0 mmol, 1.0 equiv.) was dissolved in THF (75 mL, 0.40 M). *n*BuLi (2.5 M in hexane, 13.20 mL, 33.0 mmol, 1.1 equiv.) was added dropwise at -78 °C and the reaction mixture was stirred at -78 °C for 30 minutes. Then, benzaldehyde (3.35 mL, 33.0 mmol, 1.1 equiv.) was added dropwise, the reaction mixture was warmed to room temperature and stirred for 6 hours. A saturated solution of NH_4Cl was added at 0 °C and the aqueous layer was extracted with EtOAc (x3). Combined organic layers were washed with brine, dried over Na_2SO_4, filtered and concentrated *in vacuo*. Purification by flash chromatography (EtOAc/hexane) afforded ethyl 4-hydroxy-4-phenylbut-2-ynoate **S4** (2.55 g, 12.5 mmol, 42%) as a yellow oil. Characterisation data match literature reports.[198]

^{1}H NMR (400 MHz, $CDCl_3$) δ 7.51 (m, 2H, C(7)-H and C(9)-H), 7.38 (m, 3H, C(6)-H, , C(8)-H and , C(10)-H), 5.55 (d, *J* = 5.5 Hz, 1H, C(4)-H), 4.24 (q, *J* = 7.1 Hz, 2H, C(11)-H_2), 2.92 (d, *J* = 6.0 Hz, 1H, -OH), 1.30 (t, *J* = 7.1 Hz, 3H, C(12)-H_3).

^{13}C NMR (101 MHz, $CDCl_3$) δ 153.4 (C(1)), 138.6 (C(5)), 128.9 (C(8)), 128.8 (C(7) and C(9)), 126.7 (C(6) and C(10)), 86.2 (C(3)), 77.9 (C(2)), 64.3 (C(4)), 62.3 (C(11)), 14.0 (C(12)).

HRMS (ESI): m/z calculated for $C_{12}H_{12}O_3Na^+$ $[M+Na]^+$ 227.0679 found 227.0678.

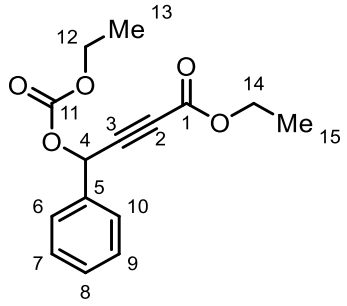

Ethyl 4-((ethoxycarbonyl)oxy)-4-phenylbut-2-ynoate S5

Following a modified procedure by Lindner[147], ethyl 4-hydroxy-4-phenylbut-2-ynoate **S4** (2.55 g, 12.5 mmol, 1.0 equiv.) and ethyl chloroformate (1.31 mL, 13.7 mmol, 1.1 equiv.) were dissolved in DCM (62 mL, 0.20 M). To this mixture, pyridine (1.21 mL, 15.0 mmol, 1.2 equiv.) was added at 0 °C. The reaction mixture was allowed to warm to room temperature and stirred for 3 hours. A 1 M aqueous $KHSO_4$ solution was added and the aqueous layer was extracted with DCM (x3). Combined organic layers were washed with saturated aqueous $NaHCO_3$ solution, brine, dried over Na_2SO_4, filtered and concentrated *in vacuo*. Purification by flash chromatography (Et_2O/hexane) afforded ethyl 4-((ethoxycarbonyl)oxy)-4-phenylbut-2-ynoate **S5** (2.00g, 8.3 mmol, 67%) as a colourless oil.

^{1}H NMR (400 MHz, $CDCl_3$) δ 7.52 (m, 2H, C(7)-H and C(9)-H), 7.39 (m, 3H, C(6)-H, C(8)-H and C(10)-H), 6.37 (s, 1H, C(4)-H), 4.23 (m, 4H, C(12)-H_2 and C(14)-H_2), 1.30 (t x2, *J* = 7.1 Hz, 6H, C(13)-H_3 and C(15)-H_3).

^{13}C NMR (101 MHz, $CDCl_3$) δ 153.9 (C(1)), 152.9 (C(11)), 134.6 (C(5)), 129.7 (C(8)), 128.9 (C(7) and C(9)), 127.8 (C(6) and C(10)), 82.1 (C(3)), 79.0 (C(2)), 68.5 (C(4)), 64.9 (C(12) or C(14)), 62.3 (C(12) or C(14)), 14.2 (C(13) or C(15)), 14.0 (C(13) or C(15)).

HRMS (ESI): m/z calculated for $C_{15}H_{16}O_5Na^+$ $[M+Na]^+$ 299.0890 found 299.0891.

IR (CH_3Cl film): 1750 (m), 1713 (m), 1371 (w), 1239 (m), 1006 (w), 908 (s), 730 (s), 697 (w), 650 (w) cm^{-1}.

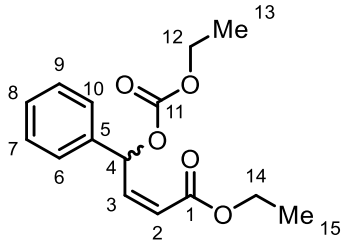

Ethyl (*Z*)-4-((ethoxycarbonyl)oxy)-4-phenylbut-2-enoate (±)-2-11d

Rosenmund catalyst (Pd on $BaSO_4$, 132.4 mg, 1.2 mmol, 0.15 equiv.) and quinoline (0.17 mL, 1.4 mmol, 0.18 equiv.) were suspended in THF (22 mL, 0.37 M) and the suspension was purged with hydrogen gas (balloon) for 10 minutes. Then a solution of ethyl 4-((ethoxycarbonyl)oxy)-4-phenylbut-2-ynoate **S5** (2.29 g, 8.3 mmol, 1.0 equiv.) in THF (2 mL) was added and the reaction mixture was stirred under an atmosphere of H_2 (balloon) for 3 hours while being monitored. Upon consumption of starting material, the reaction was filtered through a plug of silica eluting with Et_2O and concentrated *in vacuo*. Purification by automated medium-pressure flash chromatography (gradient of 0 to 15% Et_2O/hexane in 10 minutes) afforded ethyl (*Z*)-4-((ethoxycarbonyl)oxy)-4-phenylbut-2-enoate (±)-**2-11d** (1.12g, 4.0mmol, 49%) as a colourless oil.

^{1}H NMR (400 MHz, $CDCl_3$) δ 7.51 (m, 2H, C(7)-H and C(9)-H), 7.33 (m, 4H, C(4)-H, C(6)-H, C(8)-H and C(10)-H), 6.39 (dd, *J* = 11.5, 8.7 Hz, 1H, C(3)-H), 5.90 (dd, *J* = 11.6, 1.2 Hz, 1H, C(2)-H), 4.20 (m, 4H, C(12)-H_2 and C(14)-H_2), 1.29 (t x2, *J* = 7.1 Hz, 6H, C(13)-H_3 and C(15)-H_3).

^{13}C NMR (101 MHz, $CDCl_3$) δ 165.3 (C(1)), 154.1 (C(11)), 144.4 (C(3)), 138.2 (C(5)), 128.7 (C(Ar) x2), 128.5 (C(8)), 127.1 (C(Ar) x2), 120.9 (C(3)), 75.2 (C(4)), 64.2 (C(12) or C(14)), 60.6 (C(12) or C(14)), 14.2 (C(13) or C(15)), 14.2 (C(13) or C(15)).

HRMS (ESI): m/z calculated for $C_{15}H_{18}O_5Na^+$ $[M+Na]^+$ 301.1046 found 301.1047.

IR (CH_3Cl film): 1748 (m), 1718 (m), 1653 (w), 1455 (w), 1371 (w), 1254 (s), 1199 (m), 1005 (w), 909 (s), 790 (w), 731 (s), 701 (m), 650 (w) cm^{-1}.

5.3.2 Procedures for the rhodium-catalysed reactions

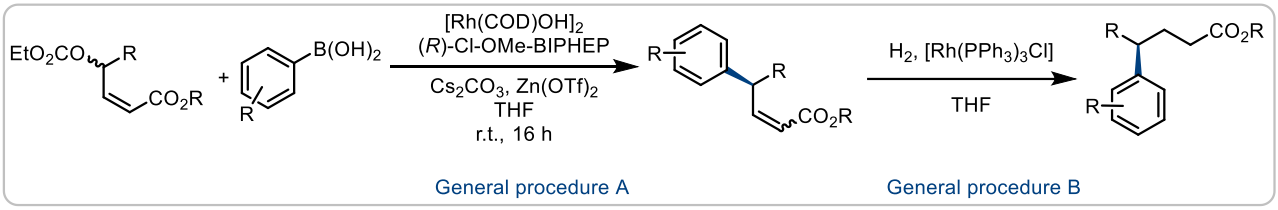

General procedure A (Rhodium-catalysed arylation)

All reactions were carried out under an inert argon atmosphere using standard Schlenk techniques with all reagents weighed open to air.

$[Rh(cod)OH]_2$ (20.5 mg, 0.045 mmol, 2.5 mol%) and (*R*)-Cl-MeO-BIPHEP (70.4 mg, 0.108 mmol, 6.0 mol%) were added to 25 mL flask containing a stirring bar, and dissolved in dry THF (18.0 mL) under an argon atmosphere at ambient temperature (23 °C). This solution was stirred for 5 minutes and used for four asymmetric reactions on a 0.4 mmol scale).

Boronic acid (0.80 mmol, 2.0 equiv.), Cs_2CO_3 (130.3 mg, 0.40 mmol, 1.0 equiv.) and $Zn(OTf)_2$ (29.1 mg, 0.08 mmol, 0.2 equiv.) were added to a 7 mL vial containing a stirring bar. To this vial a stock solution of the rhodium hydroxy complex (4.0 mL) was added *via* syringe under an argon atmosphere. The allylic carbonate (0.40 mmol, 1.0 equiv.) was added *via* microsyringe and the reaction mixture was stirred at ambient temperature (23 °C).

The mixture was diluted with hexane (4.0 mL) and filtered through a plug of silica. The crude was loaded onto Chem Tube-Hydromatrix and flash column chromatography was performed to afford the desired products.

General procedure B (Hydrogenation)

Hydrogen (~1 atm, from a balloon) was bubbled through a solution of $[RhCl(PPh_3)_3]$ (37.1 mg, 0.040 mmol, 0.10 equiv.) in THF (0.70 mL) for 5 minutes. A mixture of *Z*- and *E*-products obtained from the rhodium arylation reaction (General procedure A) dissolved in THF (0.30 mL) was then added *via* syringe to the catalyst solution. Hydrogen (~1 atm, from a balloon) was bubbled through the reaction mixture for a further 5 minutes. The

reaction mixture was equipped with a hydrogen balloon and stirred at ambient temperature (23 °C) for 16 h.

Then, the mixture was diluted with hexane (4.0 mL) and filtered through a plug of silica. The crude was loaded onto Chem Tube-Hydromatrix and flash column chromatography was performed to afford the desired product.

Racemates

Racemic samples were prepared using (±)-Cl-MeO-BIPHEP instead of (*R*)-Cl-MeO-BIPHEP on a 0.2 mmol scale.

Rh-catalysed reactions of (±)-**2-9a**

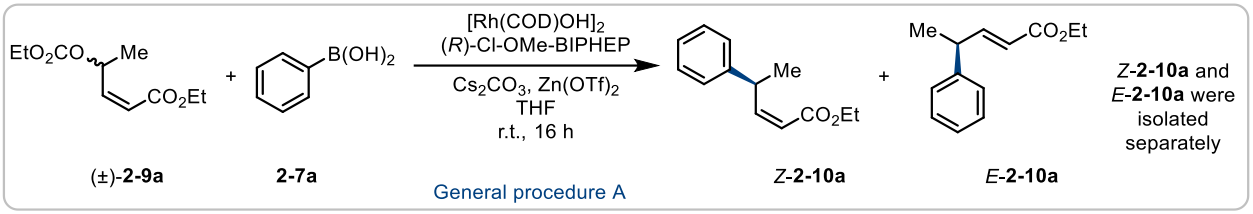

Z-**2-10a** and *E*-**2-10a** were prepared using General procedure A with phenylboronic acid. Crude mixture (*Z:E*=4.0:1) was purified by automated medium-pressure chromatography (E_2tO/hexane = 0/100 to 15/85) to afford (+)-ethyl (*S,Z*)-4-phenylpent-2-enoate *Z*-**2-10a** (61.3 mg, 0.30 mmol, 75%) as a colourless oil and (–)-ethyl (*S,E*)-4-phenylpent-2-enoate *E*-**2-10a** (15.5 mg, 0.08 mmol, 19%) as a colourless oil. SFC analysis showed an enantiomeric excess of 98% of *Z*-**2-10a** and 99% of *E*-**2-10a**.

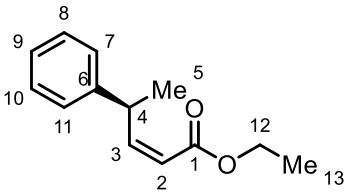

(+)-Ethyl (*S,Z*)-4-phenylpent-2-enoate *Z*-2-10a

^{1}H NMR (400 MHz, $CDCl_3$) δ 7.22 (m, 4H, C(Ar)-H x4), 7.13 (m, 1H, C(9)-H), 6.17 (dd, *J* = 11.4, 10.3 Hz, 1H, C(3)-H), 5.65 (dd, *J* = 11.5, 1.0 Hz, 1H, C(2)-H), 4.83 (dq, *J* = 10.4, 6.9 Hz, 1H, C(4)-H), 4.12 (q, *J* = 7.0 Hz, 2H, C(12)-H_2), 1.32 (d, *J* = 6.9 Hz, 3H, C(5)-H_3), 1.22 (t, *J* = 7.1 Hz, 3H, C(13)-H_3).

^{13}C NMR (101 MHz, $CDCl_3$) δ 166.3 (C(1)), 153.7 (C(3)), 144.6 (C(6)), 128.6 (C(Ar) x2), 127.1 (C(Ar) x2), 126.4 (C(2)), 117.9 (C(9)), 60.0 (C(12)), 37.7 (C(4)), 20.9 (C(5)), 14.3 (C(13)).

IR (CH_3Cl film): 3027 (w), 2980 (w), 1716 (m), 1614 (w), 1414 (w), 1184 (s), 1030 (w), 830 (w), 754 (s), 700 (m), 668 (w) cm^{-1}.

HRMS (ESI): m/z calculated for $C_{13}H_{16}O_2Na^+$ $[M+Na]^+$ 227.1043 found 227.1044.

SFC: Chiralpak® IG, 1500 psi, 30 °C; flow: 1.0 mL/min; 1% to 30% MeOH over 5 min, 98.8:1.2 e.r. (minor enantiomer t_R = 1.46 min, major enantiomer t_R = 1.30 min).

$[\alpha]_D^{25}$ = +326.2 (c = 1.0, $CHCl_3$).

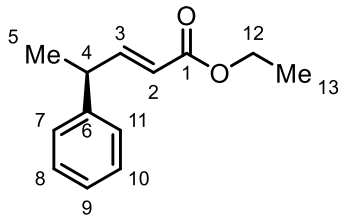

(–)-Ethyl (*S,E*)-4-phenylpent-2-enoate *E*-2-10a

^{1}H NMR (400 MHz, $CDCl_3$) δ 7.32 (m, 2H, C(Ar)-H x2), 7.22 (m, 3H, C(Ar)-H, x3), 7.12 (dd, *J* = 15.7, 6.7 Hz, 1H, C(3)-H), 5.81 (dd, *J* = 15.7, 1.5Hz, 1H, C(2)-H), 4.18 (q, *J* = 7.1 Hz, 2H, C(12)-H_2), 3.62 (pd, *J* = 7.0, 1.6 Hz, 1H, C(4)-H), 1.44 (d, *J* = 7.0 Hz, 3H, C(5)-H_3), 1.28 (t, *J* = 7.1 Hz, 3H, C(13)-H_3).

^{13}C NMR (101 MHz, $CDCl_3$) δ 166.8 (C(1)), 152.6 (C(3)), 143.4 (C(6)), 128.7 (C(Ar) x2), 127.4 (C(Ar) x2), 126.7 (C(9)), 120.2 (C(2)), 60.3 (C(12)), 42.1 (C(4)), 20.2 (C(5)), 14.3 (C(13)).

IR (CH_3Cl film): 2952 (w), 1722 (m), 1653 (m), 1437 (m), 1281 (m), 1173 (m), 1018 (m), 909 (m), 762 (m), 729 (m), 699 (s) cm^{-1}.

HRMS (ESI): m/z calculated for $C_{13}H_{17}O_2^+$ $[M+H]^+$ 205.1223 found 205.1225.

SFC: Chiralpak® IG, 1500 psi, 30 °C; flow: 1.0 mL/min; 1% to 30% MeOH over 5 min, 99.5:0.5 e.r. (minor enantiomer t_R = 1.85 min, major enantiomer t_R = 1.68 min).

$[\alpha]_D^{25}$ = –14.8 (c = 1.0, $CHCl_3$).

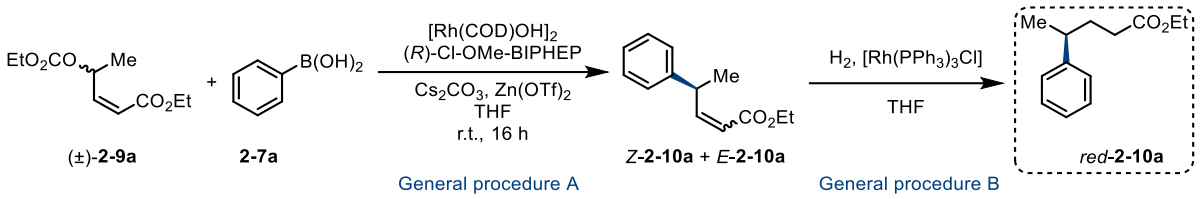

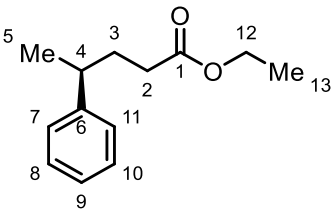

(+)-Ethyl (*S*)-4-phenylpentanoate *red*-**2-10a**

(+)-Ethyl (*S*)-4-phenylpentanoate *red*-**2-10a** was prepared using General procedure A with phenylboronic acid **2-7a**, followed by reduction of the resulting crude mixture of products (*Z*:*E*=4.0:1) using General procedure B. Purification by automated medium-pressure chromatography (E_2tO/hexane = 0/100 to 15/85) afforded (+)-ethyl (*S*)-4-phenylpentanoate *red*-**2-10a** (77.6 mg, 0.38 mmol, 94%) as a colourless oil. SFC analysis showed an enantiomeric excess of 98%.

^{1}H NMR (400 MHz, $CDCl_3$) δ 7.30 (td, *J* = 7.0, 1.3 Hz, 2H, C(Ar)-H x2), 7.19 (td, *J* = 7.0, 1.5 Hz, 3H, C(Ar)-H x3), 4.09 (q, *J* = 7.1 Hz, 2H, C(12)-H_2), 2.72 (h, *J* = 7.0 Hz, 1H. C(4)-H), 2.18 (m, 2H, C(2)-H_2), 1.92 (m, 2H, C(3)-H_2), 1.28 (d, *J* = 7.0 Hz, 3H, C(5)-H_3), 1.23 (t, *J* = 7.1 Hz, 3H, C(13)-H_3).

^{13}C NMR (101 MHz, $CDCl_3$) δ 173.7 (C(1)), 146.3 (C(6)), 128.5 (C(Ar) x2), 127.0 (C(Ar) x2), 126.2 (C(Ar)), 60.2 (C(12)), 39.5 (C(4)), 33.3 (C(2)), 32.6 (C(3)), 22.2 (C(5)), 14.2 (C(13)).

IR (CH_3Cl film): 2963 (w), 1733 (s), 1453 (w), 1375 (w), 1216 (m), 1163 (m), 1027 (w), 754 (s), 701 (s), 668 (w) cm^{-1}.

HRMS (ESI): m/z calculated for $C_{13}H_{18}O_2Na^+$ $[M+Na]^+$ 229.1199 found 229.1200.

SFC: Chiralpak® IG, 1500 psi, 30 °C; flow: 1.0 mL/min; 1% to 30% MeOH over 5 min, 99:1 e.r. (minor enantiomer t_R = 1.64 min, major enantiomer t_R = 1.52 min

$[\alpha]_D^{25}$ = +19.4 (c = 1.0, $CHCl_3$).

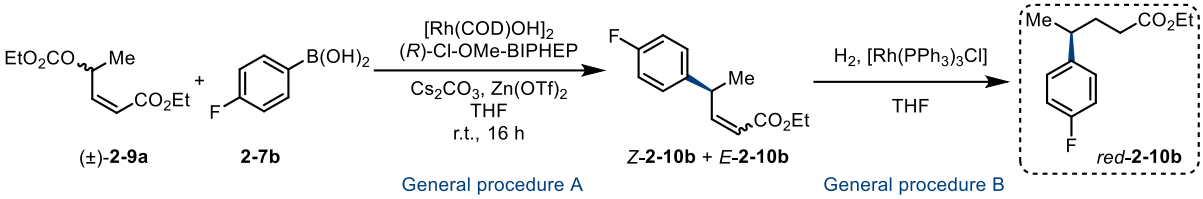

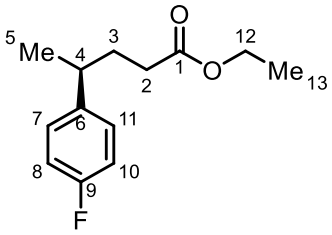

(+)-Ethyl (*S*)-4-(4-fluorophenyl)pentanoate *red*-**2-10b**

(+)-Ethyl (*S*)-4-(4-fluorophenyl)pentanoate *red*-**2-10b** was prepared using General procedure A with 4-fluorophenyl boronic acid **2-7b**, followed by reduction of the resulting crude mixture of products (*Z*:*E*=4.4:1) using General procedure B. Purification by automated medium-pressure chromatography (E_2tO/hexane = 0/100 to 20/80) afforded (+)-ethyl (*S*)-4-(4-fluorophenyl)pentanoate *red*-**2-10b** (80.7 mg, 0.36 mmol, 90%) as a colourless oil. SFC analysis showed an enantiomeric excess of 98%.

^{1}H NMR (400 MHz, $CDzCl_3$) δ 7.12 (m, 2H, C(Ar)-H x2), 6.97 (m, 2H, C(Ar)-H x2), 4.08 (q, *J* = 7.1 Hz, 2H, C(12)-H_2), 2.71 (dp, *J* = 8.9, 6.8 Hz, 1H, C(4)-H), 2.16 (m, 2H, C(2)-H_2), 1.88 (m, 2H, C(3)-H_2), 1.23 (m, 6H, C(5)-H_3 and C(13)-H_3).

^{13}C NMR (101 MHz, $CDCl_3$) δ 173.5 (C(1)), 161.4 (d, *J* = 243.6 Hz, C(9)), 141.9 (d, *J* = 3.1 Hz, C(6)), 128.3 (d, *J* = 7.8 Hz, C(7) and C(11)), 115.2 (d, *J* = 21.0 Hz, C(8) and C(10)), 60.3 (C(12)), 38.7 (C(4)), 33.3 (C(3)), 32.5 (C(2)), 22.3 (C(5)), 14.2 (C(13)).

^{19}F (13C)NMR (376 MHz, $CDCl_3$) δ −117.3.

IR (CH_3Cl film): 2980 (w), 1733 (m), 1510 (s), 1377 (m), 1223 (s), 1159 (s), 1033 (w), 835 (m), 757 (s), 668 (w) cm^{-1}.

HRMS (ESI): m/z calculated for $C_{13}H_{18}O_2F^+$ $[M+H]^+$ 225.1285 found 225.1286.

SFC: Chiralpak® IG, 1500 psi, 30 °C; flow: 1.0 mL/min; 1% to 30% MeOH over 5 min, 99:1 e.r. (minor enantiomer t_R = 1.54 min, major enantiomer t_R = 1.31 min).

$[\alpha]_D^{25}$ = +19.9 (c = 1.0, $CHCl_3$).

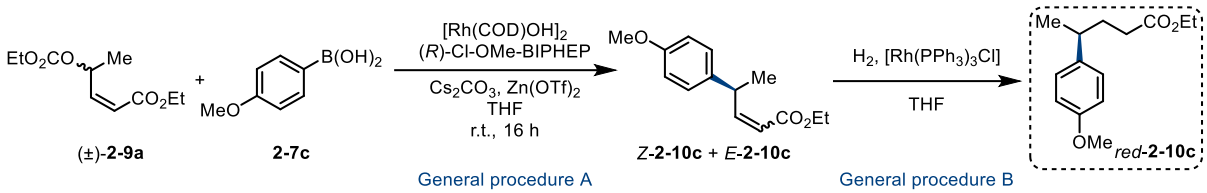

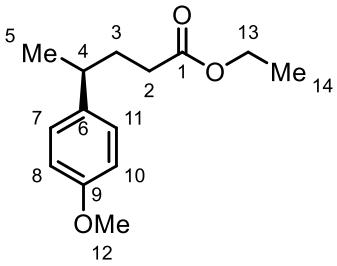

(+)-Ethyl (*S*)-4-(4-methoxyphenyl)pentanoate *red*-**2-10c**

(+)-Ethyl (*S*)-4-(4-methoxyphenyl)pentanoate *red*-**2-10c** was prepared using General procedure A with 4-methoxyphenylboronic acid **2-7c**, followed by reduction of the resulting crude mixture of products (*Z:E*=5.3:1) using General procedure B. Purification by automated medium-pressure chromatography (E_2tO/hexane = 0/100 to 15/85) afforded (+)-ethyl (*S*)-4-(4-methoxyphenyl)pentanoate *red*-**2-10c** (87.9 mg, 0.37 mmol, 93%) as a colourless oil. SFC analysis showed an enantiomeric excess of 97%.

^{1}H NMR (400 MHz, $CDCl_3$) δ 7.09 (d, *J* = 8.6 Hz, 2H, C(Ar)-H x2), 6.84 (d, *J* = 8.6 Hz, 2H, C(Ar)-H x2), 4.08 (q, *J* = 7.1 Hz, 2H, C(13)-H_2), 3.79 (s, 3H, C(12)-H_3), 2.67 (h, *J* = 6.8 Hz, 1H, C(4)-H), 2.18 (m, 2H, C(2)-H_2), 1.87 (m, 2H, C(3)-H_2), 1.23 (m, 6H, C(5)-H_3 and C(14)-H_3).

^{13}C NMR (101 MHz, $CDCl_3$) δ 173.7 (C(1)), 158.0 (C(9)), 138.4 (C(6)), 127.9 (C(7) and C(11)), 113.8 (C(8) and C(10)), 60.2 (C(13)), 55.2 (C(12)), 38.6 (C(4)), 33.4 (C(2)), 32.6 (C(3)), 22.3 (C(5)), 14.2 (C(14)).

IR (CH_3Cl film): 2981 (w), 1733 (s), 1513 (s), 1377 (m), 1247 (s), 1178 (m), 1035 (m), 831 (m), 755 (m), 668 (w) cm^{-1}.

HRMS (ESI): m/z calculated for $C_{14}H_{20}O_3Na^+$ $[M+Na]^+$ 259.1305 found 259.1304.

SFC: Chiralpak® IG, 1500 psi, 30 °C; flow: 1.0 mL/min; 1% to 30% MeOH over 5 min, 98.6:1.4 e.r. (minor enantiomer t_R = 2.42 min, major enantiomer t_R = 2.01 min).

$[\alpha]_D^{25}$ = +21.6 (c = 1.0, $CHCl_3$).

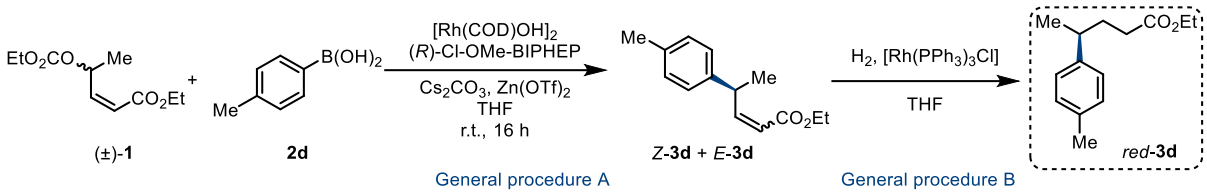

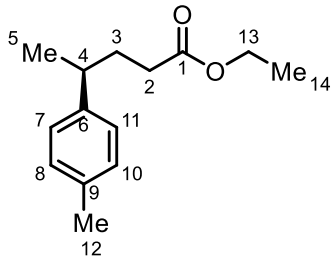

(+)-Ethyl (S)-4-(*p*-tolyl)pentanoate *red*-**2-10d**

(+)-Ethyl (S)-4-(*p*-tolyl)pentanoate *red*-**2-10d** was prepared using General procedure A with *p*-tolylboronic acid **2-7d**, followed by reduction of the resulting crude mixture of products (*Z:E*=4.4:1) using General procedure B. Purification by automated medium-pressure chromatography (E_2tO/hexane = 0/100 to 15/85) afforded (+)-ethyl (*S*)-4-(*p*-tolyl)pentanoate *red*-**2-10d** (85.9 mg, 0.39 mmol, 98%) as a colourless oil. SFC analysis showed an enantiomeric excess of 96%. Characterisation data match literature reports.[189]

^{1}H NMR (400 MHz, $CDCl_3$) δ 7.12 (dd, *J* = 8.0, 2.3 Hz, 2H, C(Ar)-H x2), 7.08 (d, *J* = 8.1 Hz, 2H, C(Ar)-H x2), 4.10 (q, *J* = 7.1 Hz, 2H, C(13)-H_2), 2.69 (dp, *J* = 8.7, 6.8 Hz, 1H, C(4)-H), 2.33 (s, 3H, C(12)-H_3), 2.19 (m, 2H, C(2)-H_2), 1.90 (m, 2H, C(3)-H_2), 1.27 (d, *J* = 7.0 Hz, 3H, C(5)-H_3), 1.23 (t, *J* = 7.1 Hz, 3H, C(14)-H_3).

^{13}C NMR (101 MHz, $CDCl_3$) δ 173.7 (C(1)), 143.3 (C(6)), 135.6 (C(9)), 129.1 (C(Ar) x2), 126.9 (C(Ar) x2), 60.2 (C(13)), 39.0 (C(4)), 33.3 (C(2)), 32.6 (C(3)), 22.3 (C(12)), 21.0 (C(5)), 14.2 (C(14)).

IR (CH_3Cl film): 3021 (w), 1728 (m), 1515 (w), 1217 (m), 1033 (w), 819 (w), 755 (s), 668 (w) cm^{-1}.

HRMS (ESI): m/z calculated for $C_{14}H_{20}O_2Na^+$ $[M+Na]^+$ 243.1356 found 243.1357.

SFC: Chiralpak® IG, 1500 psi, 30 °C; flow: 1.0 mL/min; 1% to 30% MeOH over 5 min, 98.6:1.4 e.r. (minor enantiomer t_R = 1.83 min, major enantiomer t_R = 1.64 min).

$[\alpha]_D^{25}$ = +18.4 (c = 1.0, $CHCl_3$) (Lit[189].: $[\alpha]_D^{25}$ = +13.9 (c = 4.9, $CHCl_3$)).

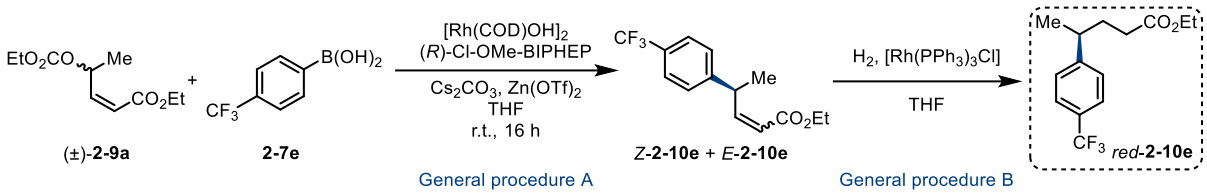

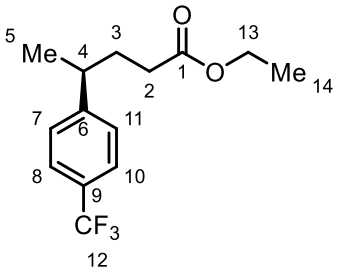

(+)-Ethyl (*S*)-4-(4-(trifluoromethyl)phenyl)pentanoate *red*-**2-10e**

(+)-Ethyl (*S*)-4-(4-(trifluoromethyl)phenyl)pentanoate *red*-**2-10e** was prepared using General procedure A with 4-(trifluoromethyl boronic acid **2-7e**, followed by reduction of the resulting crude mixture of products (*Z:E*=6.2:1) using General procedure B. Purification by automated medium-pressure chromatography (E_2tO/hexane = 0/100 to 20/80) afforded (+)-ethyl (*S*)-4-(4-(trifluoromethyl)pentanoate *red*-**3e** (85.6 mg, 0.31 mmol, 78%) as a colourless oil. SFC analysis showed an enantiomeric excess of 98%.

^{1}H NMR (400 MHz, $CDCl_3$) δ 7.55 (d, *J* = 8.0 Hz, 2H, C(8)-H and C(10)-H), 7.29 (d, *J* = 8.0 Hz, 2H, C(7)-H and C(11)-H), 4.08 (q, *J* = 7.1 Hz, 2H, C(13)-H_2), 2.80 (dp, *J* = 8.7, 6.9 Hz, 1H, C(4)-H), 2.17 (m, 2H, C(2)-H_2), 1.93 (m, 2H, C(3)-H_2), 1.28 (d, *J* = 7.0 Hz, 3H, C(5)-H_3), 1.22 (t, *J* = 7.1 Hz, 3H, C(14)-H_3).

^{13}C NMR (101 MHz, $CDCl_3$) δ 173.3 (C(1)), 150.5 (C(6)), 128.6 (q, *J* = 32.2 Hz, C(9)), 127.4 (C(7) and C(11)), 125.4 (q, *J* = 3.8 Hz, C(8) and C(10)), 124.3 (q, *J* = 271.8 Hz, C(12)), 60.3 (C(13)), 39.3 (C(4)), 33.0 (C(2)), 32.4 (C(3)), 21.9 (C(5)), 14.2 (C(14)).

^{19}F (13C)NMR (376 MHz, $CDCl_3$) δ −62.4.

IR (CH_3Cl film): 2980 (w), 1735 (s), 1619 (w), 1327 (s), 1164 (s), 1122 (s), 1069 (m), 1017 (w), 841 (m) cm^{-1}.

HRMS (ESI): m/z calculated for $C_{14}H_{18}O_2F_3^+$ $[M+H]^+$ 275.1253 found 275.1254.

SFC: Chiralpak® IG, 1500 psi, 30 °C; flow: 1.0 mL/min; 1% to 30% MeOH over 5 min, 98.8:1.2 e.r. (minor enantiomer t_R = 1.30 min, major enantiomer t_R = 1.08 min).

$[\alpha]_D^{25}$ = +18.6 (c = 1.0, $CHCl_3$).

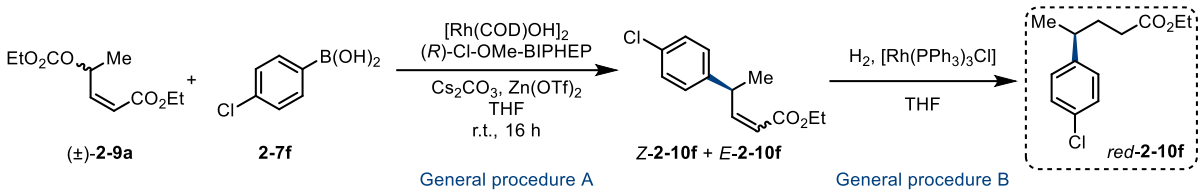

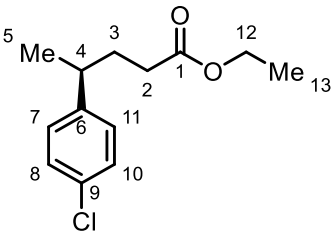

(+)-Ethyl (*S*)-4-(4-chlorophenyl)pentanoate *red*-**2-10f**

(+)-Ethyl (*S*)-4-(4-chlorophenyl)pentanoate *red*-**2-10f** was prepared using General procedure A with (4-chlorophenyl)boronic acid **2-7f**, followed by reduction of the resulting crude mixture of products (*Z:E*=7.3:1) using General procedure B. Purification by automated medium-pressure chromatography (E_2tO/hexane = 0/100 to 15/85) afforded (+)-ethyl (*S*)-4-(4-chlorophenyl)pentanoate *red*-**2-10f** (57.8 mg, 0.24 mmol, 60%) as a colourless oil. SFC analysis showed an enantiomeric excess of 98%.

^{1}H NMR (400 MHz, $CDCl_3$) δ 7.26 (d, *J* = 8.5 Hz, 2H, C(Ar)-H x2), 7.11 (d, *J* = 8.4 Hz, 2H, C(Ar)-H x2), 4.08 (q, *J* = 7.2 Hz, 2H, C(12)-H_2), 2.70 (dp, *J* = 8.9, 6.8 Hz, 1H, C(4)-H), 2.16 (m, 2H, C(2)-H_2), 1.88 (m, 2H, C(3)-H_2), 1.23 (m, 6H, C(5)-H_3 and C(13)-H_3).

^{13}C NMR (101 MHz, $CDCl_3$) δ 173.5 (C(1)), 144.8 (C(6)), 131.8 (C(9)), 128.6 (C(Ar) x2), 128.4 (C(Ar) x2), 60.3 (C(12)), 38.9 (C(4)), 33.1 (C(2)), 32.5 (C(3)), 22.1 (C(5)), 14.2 (C(13)).

IR (CH_3Cl film): 2970 (w), 1733 (s), 1459 (w), 1375 (w), 1215 (m), 1063 (m), 1033 (w), 754 (s), 698 (m), 668 (w) cm^{-1}.

HRMS (ESI): m/z calculated for $C_{13}H_{18}O_2Cl^+$ $[M+H]^+$ 241.0990 found 241.0991.

SFC: Chiralpak® IG, 1500 psi, 30 °C; flow: 1.0 mL/min; 1% to 30% MeOH over 5 min, 98.9:1.1 e.r. (minor enantiomer t_R = 2.17 min, major enantiomer t_R = 1.75 min).

$[\alpha]_D^{25}$ = +24.1 (c = 1.0, $CHCl_3$).

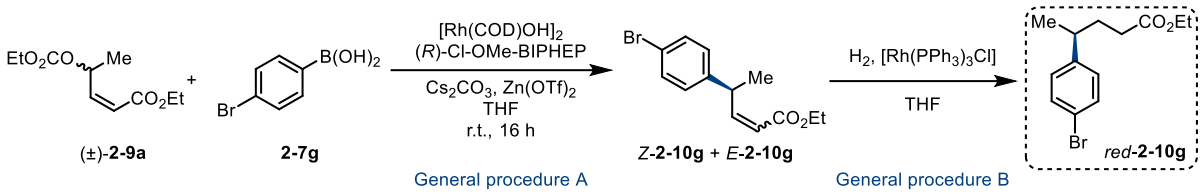

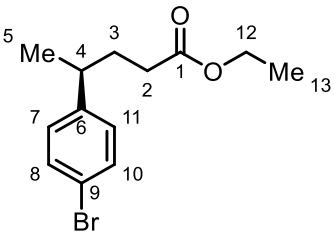

(+)-Ethyl (*S*)-4-(4-bromophenyl)pentanoate *red*-**2-10g**

(+)-Ethyl (*S*)-4-(4-bromophenyl)pentanoate *red*-**2-10g** was prepared using General procedure A with (4-bromophenyl)boronic acid **2-7g**, followed by reduction of the resulting crude mixture of products (*Z:E*=4.5:1) using General procedure B. Purification by automated medium-pressure chromatography (Et_2O/hexane = 0/100 to 15/85) afforded (+)-ethyl (*S*)-4-(4-bromophenyl)pentanoate *red*-**2-10g** (84.4 mg, 0.30 mmol, 74%) as a colourless oil. SFC analysis showed an enantiomeric excess of 97%.

^{1}H NMR (400 MHz, $CDCl_3$) δ 7.41 (d, *J* = 8.4 Hz, 1H, C(8)-H and C(10)-H), 7.05 (d, *J* = 8.4 Hz, 1H, C(7)-H and C(11)-H), 4.08 (q, *J* = 7.2 Hz, 2H, C(12)-H_2), 2.69 (dp, *J* = 8.9, 6.9 Hz, 1H, C(4)-H), 2.16 (m, 2H, C(2)-H_2), 1.88 (m, 2H, C(3)-H_2), 1.23 (m, 6H, C(5)-H_3 and C(13)-H_3).

^{13}C NMR (101 MHz, $CDCl_3$) δ 173.4 (C(1)), 145.3 (C(6)), 131.5 (C(7) and C(11)), 128.8 (C(8) and C(10)), 119.8 (C(9)), 60.3 (C(12)), 38.9 (C(4)), 33.1 (C(2)), 32.4 (C(3)), 22.0 (C(5)), 14.2 (C(13)).

IR (CH_3Cl film): 2963 (w), 1732 (s), 1490 (w), 1215 (m), 1010 (w), 824 (w), 755 (s), 668 (w) cm^{-1}.

HRMS (ESI): m/z calculated for $C_{13}H_{18}O_2Br^+$ $[M+H]^+$ 285.0485 found 285.0485.

SFC: Chiralpak® IG, 1500 psi, 30 °C; flow: 1.0 mL/min; 1% to 30% MeOH over 5 min, 98.4:1.6 e.r. (minor enantiomer t_R = 2.62 min, major enantiomer t_R = 2.04 min).

$[\alpha]_D^{25}$ = +23.0 (c = 1.0, $CHCl_3$).

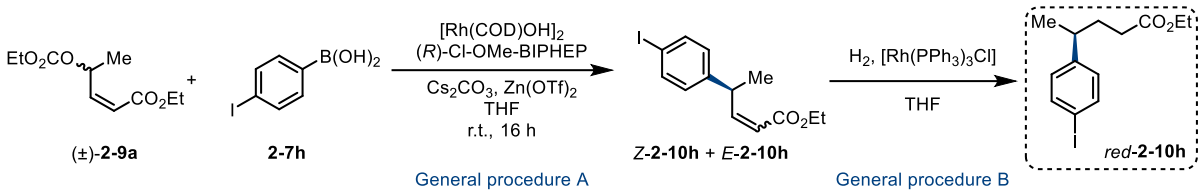

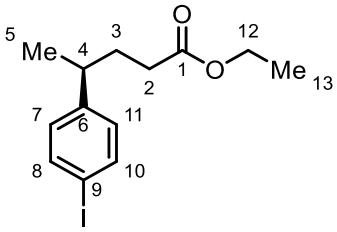

(+)-Ethyl (*S*)-4-(4-iodophenyl)pentanoate *red*-**2-10h**

(+)-Ethyl (*S*)-4-(4-iodophenyl)pentanoate *red*-**2-10h** was prepared using General procedure A with (4-iodophenyl)boronic acid **2-7h**, followed by reduction of the resulting crude mixture of products (*Z*:*E*=6.4:1) using General procedure B. Purification by automated medium-pressure chromatography (E_2tO/hexane = 0/100 to 15/85) afforded (+)-ethyl (*S*)-4-(4-iodophenyl)pentanoate *red*-**2-10h** (75.7 mg, 0.23 mmol, 57%) as a colourless oil. SFC analysis showed an enantiomeric excess of 98%.

^{1}H NMR (400 MHz, $CDCl_3$) δ 7.61 (d, *J* = 8.3 Hz, 2H, C(8)-H and C(10)-H), 6.93 (d, *J* = 8.3 Hz, 2H, C(7)-H and C(11)-H), 4.08 (q, *J* = 7.1 Hz, 2H, C(12)-H_2), 2.67 (dp, *J* = 9.0, 6.8 Hz, 1H, C(4)-H), 2.17 (m, 2H, C(2)-H_2), 1.88 (m, 2H, C(3)-H_2), 1.23 (m, 6H, C(5)-H_3 and C(13)-H_3).

^{13}C NMR (101 MHz, $CDCl_3$) δ 173.5 (C(1)), 146.0 (C(6)), 137.5 (C(8) and C(10)), 129.2 (C(7) and C(11)), 91.2 (C(9)), 60.3 (C(12)), 39.0 (C(4)), 33.0 (C(2)), 32.4 (C(3)), 22.0 (C(5)), 14.2 (C(13)).

IR (CH_3Cl film): 2962 (w), 1732 (s), 1486 (w), 1375 (m), 1162 (m), 1031 (m), 1006 (m), 821 (m), 756 (s), 668 (w) cm^{-1}.

HRMS (ESI): m/z calculated for $C_{13}H_{18}O_2I^+$ $[M+H]^+$ 333.0346 found 333.0346.

SFC: Chiralpak® IF, 1500 psi, 30 °C; flow: 1.0 mL/min; 1% to 30% MeOH over 5 min, 98.8:1.2 e.r. (minor enantiomer t_R = 2.66 min, major enantiomer t_R = 2.21 min).

$[\alpha]_D^{25}$ = +22.8 (c = 1.0, $CHCl_3$).

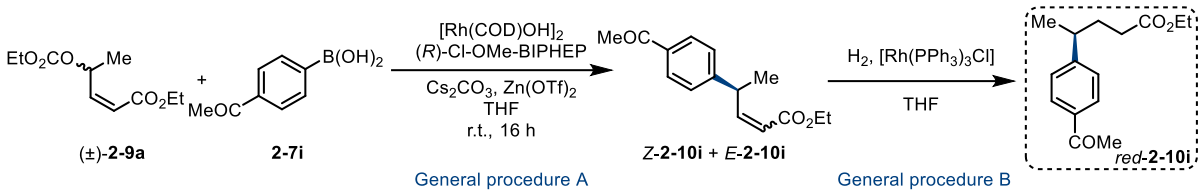

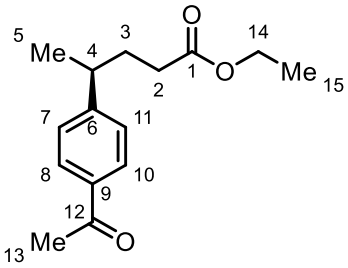

(+)-Ethyl (*S*)-4-(4-acetylphenyl)pentanoate *red*-**2-10i**

(+)-Ethyl (*S*)-4-(4-acetylphenyl)pentanoate *red*-**2-10i** was prepared using General procedure A with (4-acetylphenyl)boronic acid **2-7i**, followed by reduction of the resulting crude mixture of products (*Z*:*E*=5.4:1) using General procedure B. Purification by automated medium-pressure chromatography (E_2tO/hexane = 0/100 to 40/60) afforded (+)-ethyl (*S*)-4-(4-acetylphenyl)pentanoate *red*-**2-10i** (81.4 mg, 0.33 mmol, 82%) as a colourless oil. SFC analysis showed an enantiomeric excess of 98%.

^{1}H NMR (400 MHz, $CDCl_3$) δ 7.90 (d, *J* = 8.2 Hz, 1H, C(7)-H and C(11)-H), 7.27 (d, *J* = 8.1 Hz, 1H, 1H, C(8)-H and C(10)-H), 4.09 (q, *J* = 7.2 Hz, 2H, C(14)-H_2), 2.80 (dp, *J* = 8.7, 6.8 Hz, 1H, C(4)-H), 2.58 (s, 3H, C(13)-H_3), 2.17 (m, 2H, C(2)-H_2), 1.94 (m, 2H, C(3)-H_2), 1.29 (d, *J* = 6.9 Hz, 3H, C(5)-H_3), 1.22 (t, *J* = 7.1 Hz, 3H, C(15)-H_3).

^{13}C NMR (101 MHz, $CDCl_3$) δ 197.8 (C(12)), 173.4 (C(1)), 152.1 (C(6)), 135.5 (C(9)), 128.7 (C(8) and C(10)), 127.3 (C(7) and C(11)), 60.3 (C(14)), 39.5 (C(4)), 32.9 (C(2)), 32.4 (C(3)), 26.5 (C(13)), 21.8 (C(5)), 14.2 (C(15)).

IR (CH_3Cl film): 2965 (w), 1733 (s), 1683 (s), 1607 (m), 1458 (w), 1360 (m), 1267 (s), 1183 (m), 1032 (w), 957 (m), 835 (m) cm^{-1}.

HRMS (ESI): m/z calculated for $C_{15}H_{21}O_3^+$ $[M+H]^+$ 249.1485 found 249.1486.

SFC: Chiralpak® IG, 1500 psi, 30 °C; flow: 1.0 mL/min; 1% to 30% MeOH over 5 min, 98.8:1.2 e.r. (minor enantiomer t_R = 3.87 min, major enantiomer t_R = 3.31 min).

$[\alpha]_D^{25}$ = +27.6 (c = 1.0, $CHCl_3$).

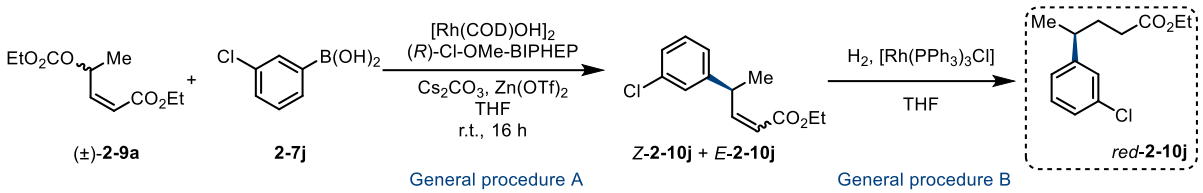

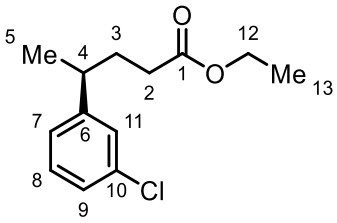

(+)-Ethyl (*S*)-4-(3-chlorophenyl)pentanoate *red*-**2-10j**

(+)-Ethyl (*S*)-4-(3-chlorophenyl)pentanoate *red*-**2-10j** was prepared using General procedure A with 3-chlorophenyl boronic acid **2-7j**, followed by reduction of the resulting crude mixture of products (*Z*:*E*=2.7:1) using General procedure B. Purification by automated medium-pressure chromatography (E_2tO/hexane = 0/100 to 15/85) afforded (+)-ethyl (*S*)-4-(3-chlorophenyl)pentanoate *red*-**2-10j** (84.7 mg, 0.35 mmol, 88%) as a colourless oil. SFC analysis showed an enantiomeric excess of 95%.

^{1}H NMR (400 MHz, $CDCl_3$) δ 7.22 (dd, *J* = 8.6, 7.4 Hz, 1H, C(8)-H), 7.17 (m, 2H, C(Ar)-H x2), 7.05 (dt, *J* = 7.5, 1.5 Hz, 1H, C(7)-H), 4.09 (q, *J* = 7.2 Hz, 2H, C(12)-H_2), 2.70 (dp, *J* = 8.8, 6.8 Hz, 1H, C(4)-H), 2.17 (m, 2H, C(2)-H_2), 1.90 (m, 2H, C(3)-H_2), 1.24 (m, 6H, C(5)-H_3 and C(13)-H_3).

^{13}C NMR (101 MHz, $CDCl_3$) δ 173.4 (C(1)), 148.5 (C(6)), 134.3 (C(10)), 129.7 (C(Ar)), 127.2 (C(Ar)), 126.4 (C(Ar)), 125.3 (C(Ar)), 60.3 (C(12)), 39.2 (C(4)), 33.0 (C(2)), 32.4 (C(3)), 21.9 (C(5)), 14.2 (C(13)).

IR (CH_3Cl film): 2970 (w), 1733 (s), 1459 (m), 1375 (m), 1215 (m), 1163 (m), 1033 (w), 754 (s), 698 (m), 668 (w) cm^{-1}.

HRMS (ESI): m/z calculated for $C_{13}H_{18}O_2Cl^+$ $[M+H]^+$ 241.0990 found 241.0991.

SFC: Chiralpak® ID, 1500 psi, 30 °C; flow: 1.0 mL/min; 1% to 30% MeOH over 5 min, 97.6:2.4 e.r. (minor enantiomer t_R = 1.29 min, major enantiomer t_R = 1.36 min).

$[\alpha]_D^{25}$ = +21.1 (c = 1.0, $CHCl_3$)

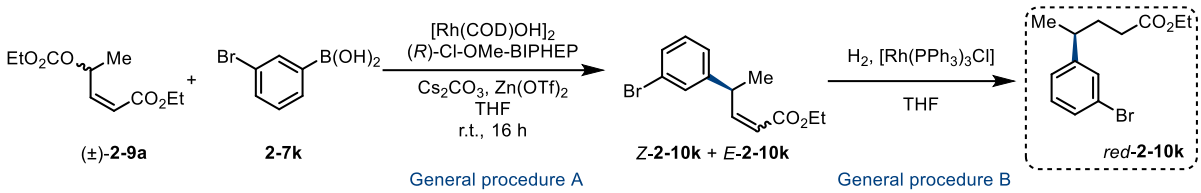

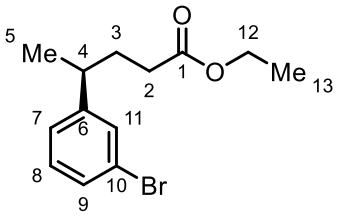

(+)-Ethyl (*S*)-4-(3-bromophenyl)pentanoate *red*-**2-10k**

(+)-Ethyl (*S*)-4-(3-bromophenyl)pentanoate *red*-**2-10k** was prepared using General procedure A with 3-bromophenyl boronic acid **2-7k**, followed by reduction of the resulting crude mixture of products (*Z:E*=4.9:1) using General procedure B. Purification by automated medium-pressure chromatography (E_2tO/hexane = 0/100 to 15/85) afforded (+)-ethyl (*S*)-4-(3-bromophenyl)pentanoate *red*-**2-10k** (111.4 mg, 0.39 mmol, 98%) as a colourless oil. SFC analysis showed an enantiomeric excess of 96%.

^{1}H NMR (400 MHz, $CDCl_3$) δ 7.32 (m, 2H, C(Ar)-H x2), 7.16 (t, *J* = 8.0 Hz, 1H, C(8)-H), 7.10 (dt, *J* = 7.7, 1.5 Hz, 1H, C(7)-H), 4.09 (q, *J* = 7.2 Hz, 2H, C(12)-H_2), 2.69 (dp, *J* = 8.7, 6.8 Hz, 1H, C(4)-H), 2.17 (m, 2H, C(2)-H_2), 1.89 (m, 2H, C(3)-H_2), 1.24 (m, 6H, C(5)-H_3 and C(13)-H_3).

^{13}C NMR (101 MHz, $CDCl_3$) δ 173.4 (C(1)), 148.8 (C(6)), 130.2 (C(Ar)), 130.1 (C(Ar)), 129.3 (C(Ar)), 125.8 (C(Ar)), 122.6 (C(10)), 60.3 (C(12)), 39.2 (C(4)), 33.0 (C(2)), 32.4 (C(3)), 22.0 (C(5)), 14.2 (C(13)).

IR (CH_3Cl film): 2969 (w), 1734 (s), 1491 (w), 1235 (m), 1215 (m), 1017 (w), 823 (w), 756 (s), 668 (w) cm^{-1}.

HRMS (ESI): m/z calculated for $C_{13}H_{18}O_2Br^+$ $[M+H]^+$ 287.0465 found 287.0464.

SFC: Chiralpak® IF, 1500 psi, 30 °C; flow: 1.0 mL/min; 1% to 30% MeOH over 5 min, 98.2:1.8 e.r. (minor enantiomer t_R = 1.64 min, major enantiomer t_R = 1.69 min).

$[\alpha]_D^{25}$ = +20.8 (c = 1.0, $CHCl_3$)

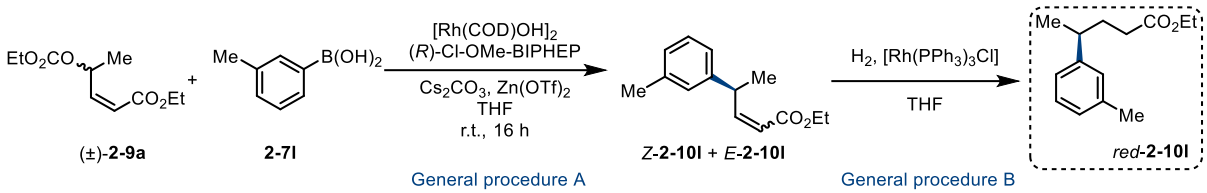

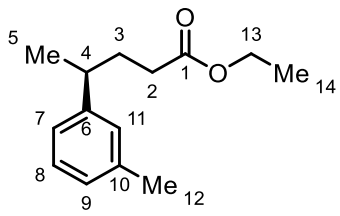

(+)-Ethyl (*S*)-4-(*m*-tolyl)pentanoate *red*-**2-10l**

(+)-Ethyl (*S*)-4-(*m*-tolyl)pentanoate *red*-**2-10l** was prepared using General procedure A with *m*-tolyl boronic acid **2-7l**, followed by reduction of the resulting crude mixture of products (*Z*:*E*=3.5:1) using General procedure B. Purification by automated medium-pressure chromatography (E_2tO/hexane = 0/100 to 15/85) afforded (+)-ethyl (*S*)-4-(*m*-tolyl)pentanoate *red*-**2-10l** (82.8 mg, 0.38 mmol, 94%) as a colourless oil. SFC analysis showed an enantiomeric excess of 96%.

^{1}H NMR (400 MHz, $CDCl_3$) δ 7.19 (td, *J* = 7.3, 1.1 Hz, 1H, C(Ar)-H), 7.00 (m, 3H, C(Ar)-H x3), 4.10 (q, *J* = 7.1 Hz, 2H, C(13)-H_2), 2.69 (dp, *J* = 8.5, 6.8 Hz, 1H, C(4)-H), 2.34 (s, 3H, C(12)-H_3), 2.20 (m, 2H, C(2)-H_2), 1.91 (m, 2H, C(3)-H_2), 1.27 (d, *J* = 6.9 Hz, 3H, C(5)-H_3), 1.24 (t, *J* = 7.1 Hz, 3H, C(14)-H_3).

^{13}C NMR (101 MHz, $CDCl_3$) δ 173.7 (C(1)), 146.3 (C(6)), 137.9 (C(10)), 128.3 (C(Ar)), 127.8 (C(Ar)), 126.9 (C(Ar)), 124.0 (C(Ar)), 60.2 (C(13)), 39.4 (C(4)), 33.2 (C(2)), 32.7 (C(3)), 22.2 (C(12)), 21.5 (C(5)), 14.2 (C(14)).

IR (CH_3Cl film): 2960 (w), 2928 (w), 1725 (s), 1458 (m), 1376 (m), 1181 (m), 1035 (w), 751 (s), 668 (m) cm^{-1}.

HRMS (ESI): m/z calculated for $C_{14}H_{21}O_2^+$ $[M+H]^+$ 221.1536 found 221.1538.

SFC: Chiralpak® IG, 1500 psi, 30 °C; flow: 1.0 mL/min; 1% to 30% MeOH over 5 min, 97.8:2.2 e.r. (minor enantiomer t_R = 1.42 min, major enantiomer t_R = 1.35 min).

$[\alpha]_D^{25}$ = +19.8 (c = 1.0, $CHCl_3$)

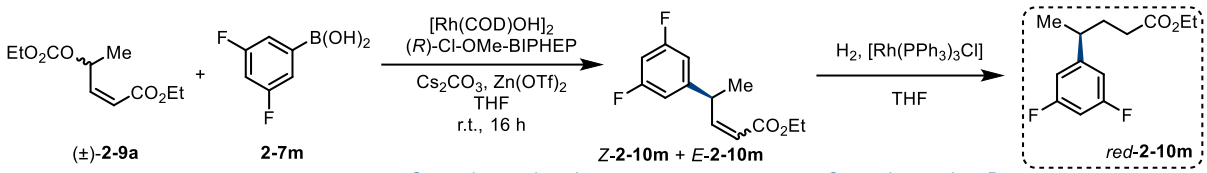

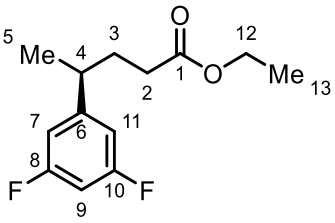

(+)-Ethyl (*S*)-4-(3,5-difluorophenyl)pentanoate *red*-**2-10m**

(+)-Ethyl (*S*)-4-(3,5-difluorophenyl)pentanoate *red*-**2-10m** was prepared using General procedure A with 3,5-difluorophenyl boronic acid **2-7m**, followed by reduction of the resulting crude mixture of products (*Z*:*E*=9.5:1) using General procedure B. Purification by automated medium-pressure chromatography (Et_2O/hexane = 0/100 to 20/80) afforded (+)-ethyl (*S*)-4-(3,5-difluorophenyl)pentanoate *red*-**2-10m** (80.4 mg, 0.33 mmol, 83%) as a colourless oil. SFC analysis showed an enantiomeric excess of 97%.

^{1}H NMR (400 MHz, $CDCl_3$) δ 6.69 (m, 2H, C(7)-H and C(11)-H), 6.62 (tt, *J* = 8.9, 2.3 Hz, 1H, C(9)-H), 4.09 (q, *J* = 7.1 Hz, 2H, C(12)-H_2), 2.72 (dp, *J* = 8.5, 6.7 Hz, 1H, C(4)-H), 2.19 (m, 2H, C(2)-H_2), 1.88 (m, 2H, C(3)-H_2), 1.23 (m, 6H, C(5)-H_3 and C(13)-H_3).

^{13}C NMR (101 MHz, $CDCl_3$) δ 173.2 (C(1)), 163.13 (dd, *J* = 248.0, 12.9 Hz, C(8) and C(10)), 150.5 (t, *J* = 8.4 Hz, C(6)), 109.8 (d, *J* = 24.6Hz, C(7) and C(11)), 101.6 (t, *J* = 25.3 Hz, C(9)), 60.3 (C(12)), 39.3 (t, *J* = 2.0 Hz, C(4)), 32.8 (C(2)), 32.3 (C(3)), 21.7 (C(5)), 14.2 (C(13)).

^{19}F (13C)NMR (376 MHz, $CDCl_3$) δ −110.2.

IR (CH_3Cl film): 2936 (w), 2360 (w), 1725 (s), 1624 (s), 1597 (s), 1461 (s), 1375 (m), 1307 (w), 1263 (w), 1182 (m), 1138 (s), 1035 (w), 944 (s), 849 (s), 750 (s), 693 (m) cm^{-1}.

HRMS (GC EI MS): m/z calculated for $C_{13}H_{16}F_2O_2^+$ $[M]^+$ 242.11129 found 242.11268.

SFC: Chiralpak® IG, 1500 psi, 30 °C; flow: 1.0 mL/min; isocratic: 100% CO_2 for 3 min then gradient: 0% to 10% MeOH/CO_2 over 5 min, 98.6:1.4 e.r. (minor enantiomer t_R = 3.75 min, major enantiomer t_R = 4.20 min).

$[\alpha]_D^{25}$ = +25.0 (c = 1.0, $CHCl_3$)

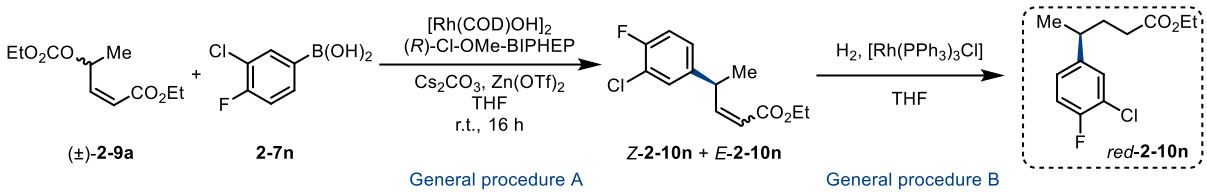

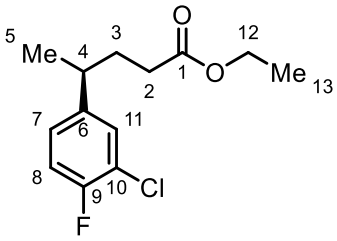

(+)-Ethyl (*S*)-4-(3-chloro-4-fluorophenyl)pentanoate *red*-**2-10n**

(+)-Ethyl (*S*)-4-(3-chloro-4-fluorophenyl)pentanoate *red*-**2-10n** was prepared using General procedure A with 3-chloro-4-fluorophenyl boronic acid **2-7n**, followed by reduction of the resulting crude mixture of products (*Z:E*=6.2:1) using General procedure B. Purification by automated medium-pressure chromatography (E_2tO/hexane = 0/100 to 20/80) afforded (+)-ethyl (*S*)-4-(3-chloro-4-fluorophenyl)pentanoate *red*-**2-10n** (88.0 mg, 0.34 mmol, 85%) as a colourless oil. SFC analysis showed an enantiomeric excess of 95%.

^{1}H NMR (400 MHz, $CDCl_3$) δ 7.20 (dd, *J* = 7.1, 2.0 Hz, 1H, C(8)-H), 7.05 (m, 2H, C(Ar)-H x2), 4.09 (q, *J* = 7.2 Hz, 2H, C(12)-H_2), 2.70 (dp, *J* = 8.8, 6.9 Hz, 1H, C(4)-H), 2.17 (m, 2H, C(2)-H_2), 1.87 (m, 2H, C(3)-H_2), 1.23 (t, *J* = 7.1 Hz, 6H, C(5)-H_3 and C(13)-H_3).

^{13}C NMR (101 MHz, $CDCl_3$) δ 173.3 (C(1)), 156.6 (d, *J* = 246.8 Hz, C(9)), 143.4 (d, *J* = 3.9 Hz, C(6)), 129.0 (C(11)), 126.6 (d, *J* = 6.8 Hz, C(7)), 120.7 (d, *J* = 17.7 Hz, C(10)), 116.4 (d, *J* = 20.7 Hz, C(8)), 60.3 (C(12)), 38.6 (C(4)), 33.1 (C(2)), 32.4 (C(3)), 22.0 (C(5)), 14.2 (C(13)).

^{19}F (13C)NMR (376 MHz, $CDCl_3$) δ −119.4.

IR (CH_3Cl film): 2962 (w), 2361 (w), 1732 (s), 1507 (s), 1460 (w), 1374 (w), 1249 (s), 1205 (m), 1165 (m), 1099 (w), 1061 (m), 1034 (m), 823 (w), 754 (w) cm^{-1}.

HRMS (ESI): m/z calculated for $C_{13}H_{17}ClFO_2^+$ $[M+H]^+$ 259.0896 found 259.0897.

SFC: Chiralpak® IG, 1500 psi, 30 °C; flow: 1.0 mL/min; 1% to 30% MeOH over 5 min, 97.6:2.4 e.r. (minor enantiomer t_R = 1.48 min, major enantiomer t_R = 1.43 min).

$[\alpha]_D^{25}$ = +24.7 (c = 1.0, $CHCl_3$)

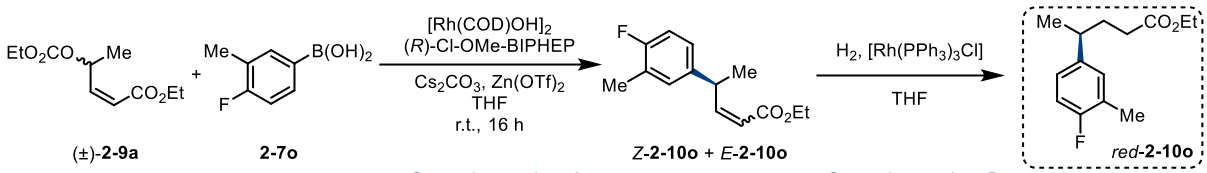

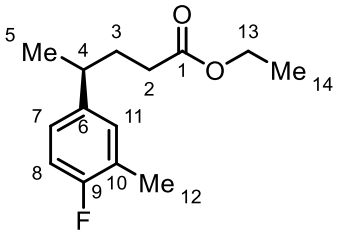

(+)-Ethyl (*S*)-4-(4-fluoro-3-methylphenyl)pentanoate *red*-**2-10o**

(+)-Ethyl (*S*)-4-(4-fluoro-3-methylphenyl)pentanoate *red*-**2-10o** was prepared using General procedure A with 4-fluoro-3-methylphenyl boronic acid **2-7o**, followed by reduction of the resulting crude mixture of products (*Z:E*=4.3:1) using General procedure B. Purification by automated medium-pressure chromatography (E_2tO/hexane = 0/100 to 20/80) afforded (+)-ethyl (*S*)-4-(4-fluoro-3-methylphenyl)pentanoate *red*-**2-10o** (87.7mg, 0.37 mmol, 92%) as a colourless oil. SFC analysis showed an enantiomeric excess of 94%.

^{1}H NMR (400 MHz, $CDCl_3$) δ 6.97 (dt, *J* = 8.3, 1.4 Hz, 1H, C(7)-H), 6.92 (m, 2H, C(Ar)-H), 4.09 (q, *J* = 7.1 Hz, 2H, C(13)-H_2), 2.66 (dp, *J* = 9.0, 6.8 Hz, 1H, C(4)-H), 2.25 (d, *J* = 2.0 Hz, 3H, C(12)-H_3), 2.17 (m, 2H, C(2)-H_2), 1.87 (m, 2H, C(3)-H_2), 1.24 (m, 6H, C(5)-H_3 and C(14)-H_3).

^{13}C NMR (101 MHz, $CDCl_3$) δ 173.6 (C(1)), 159.9 (d, *J* = 242.4 Hz, C(9)), 141.7 (d, *J* = 3.6 Hz, C(6)), 129.9 (d, *J* = 5.0 Hz, C(11)), 125.5 (d, *J* = 7.8 Hz, C(7)), 124.5 (d, *J* = 17.1 Hz, C(10)), 114.8 (d, *J* = 22.1 Hz, C(8)), 60.2 (C(13)), 38.7 (C(4)), 33.3 (C(2)), 32.5 (C(3)), 22.3 (C(5)), 14.6 (d, *J* = 3.6 Hz, C(12)), 14.2 (C(14)).

^{19}F (13C)NMR (376 MHz, $CDCl_3$) δ −121.63.

IR (CH_3Cl film): 2961 (w), 2361 (w), 1725 (w), 1504 (s), 1453 (w), 1375 (w), 1247 (m), 1213 (s), 1177 (m), 1121 (m), 1035 (m), 885 (w), 821 (m), 762 (s) cm^{-1}.

HRMS (ESI): m/z calculated for $C_{14}H_{20}O_2F^+$ $[M+H]^+$ 239.1442 found 239.1444.

SFC: Chiralpak® IG, 1500 psi, 30 °C; flow: 1.0 mL/min; isocratic: 100% CO_2 for 3 min then gradient: 0% to 10% MeOH/CO_2 over 5 min, 96.8:3.2 e.r. (minor enantiomer t_R = 4.62 min, major enantiomer t_R = 3.75 min).

$[\alpha]_D^{25}$ = +22.0 (c = 1.0, $CHCl_3$).

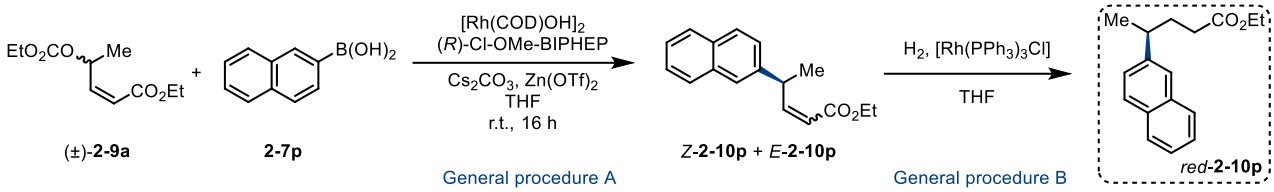

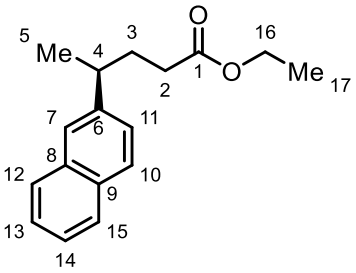

(+)-Ethyl (*S*)-4-(naphthalen-2-yl)pentanoate *red*-**2-10p**

(+)-Ethyl (*S*)-4-(naphthalen-2-yl)pentanoate *red*-**2-10p** was prepared using General procedure A with naphthalen-2-ylboronic acid **2-7p**, followed by reduction of the resulting crude mixture of products (*Z:E*=5.4:1) using General procedure B. Purification by automated medium-pressure chromatography (E_2tO/hexane = 0/100 to 15/85) afforded (+)-ethyl (*S*)-4-(naphthalen-2-yl)pentanoate *red*-**2-10p** (99.5 mg, 0.39 mmol, 97%) as a colourless oil. SFC analysis showed an enantiomeric excess of 90%.

^{1}H NMR (400 MHz, $CDCl_3$) δ 7.81 (m, 3H, C(Ar)-H x3), 7.62 (d, *J* = 2.0 Hz, 1H, C(7)-H), 7.47 (t, *J* = 7.1 Hz, 1H, C(Ar)-H), 7.44 (t, *J* = 6.6 Hz, 1H, C(Ar)-H), 7.36 (dd, *J* = 8.5, 1.8 Hz, 1H, C(Ar)-H), 4.08 (q, *J* = 7.2 Hz, 2H, C(16)-H_2), 2.92 (h, *J* = 7.1 Hz, 1H, C(4)-H), 2.23 (m, 2H, C(2)-H_2), 2.03 (m, 2H, C(3)-H_2), 1.38 (d, *J* = 6.9 Hz, 3H, C(5)-H_3), 1.22 (t, *J* = 7.4 Hz, 3H, C(17)-H_3).

^{13}C NMR (101 MHz, $CDCl_3$) δ 173.7 (C(1)), 143.7 (C(6)), 133.6 (C(8)), 132.3 (C(9)), 128.2 (C(Ar)), 127.62 (C(Ar)), 127.59 (C(Ar)), 126.0 (C(Ar)), 125.6 (C(Ar)), 125.4 (C(Ar)), 125.3 (C(Ar)), 60.2 (C(16)), 39.6 (C(4)), 33.1 (C(2)), 32.6 (C(3)), 22.2 (C(5)), 14.2 (C(17)).

IR (CH_3Cl film): 2965 (w), 1729 (w), 1507 (w), 1457 (w), 1374 (w), 1216 (m), 1032 (m), 885 (w), 856 (w), 820 (w), 753 (s), 668 (w) cm^{-1}.

HRMS (ESI): m/z calculated for $C_{17}H_{20}O_2Na^+$ $[M+Na]^+$ 279.1356 found 279.1355.

SFC: Chiralpak® IG, 1500 psi, 30 °C; flow: 1.0 mL/min; 1% to 30% MeOH over 5 min, 95.1:4.9 e.r. (minor enantiomer t_R = 2.79 min, major enantiomer t_R = 2.51 min).

$[\alpha]_D^{25}$ = +22.3 (c = 1.0, $CHCl_3$).

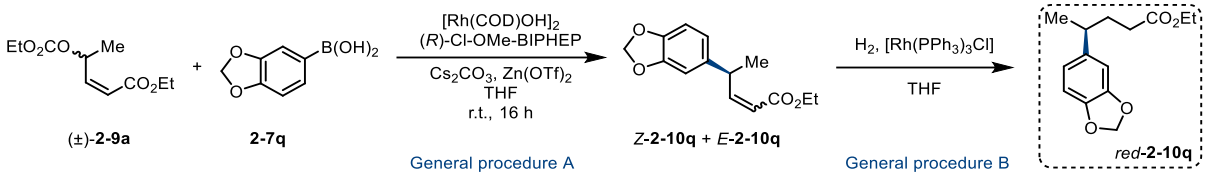

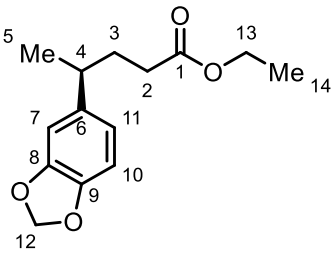

(+)-Ethyl (*S*)-4-(benzo[d][1,3]dioxol-5-yl)pentanoate *red*-**2-10q**

(+)-Ethyl (*S*)-4-(benzo[d][1,3]dioxol-5-yl)pentanoate *red*-**2-10q** was prepared using General procedure A with benzo[d][1,3]dioxol-5-ylboronic acid **2-7q**, followed by reduction of the resulting crude mixture of products (*Z:E*=13:1) using General procedure B. Purification by automated medium-pressure chromatography (E_2tO/hexane = 0/100 to 20/80) afforded (+)-ethyl (*S*)-4-(benzo[d][1,3]dioxol-5-yl)pentanoate *red*-**2-10q** (83.1 mg, 0.33 mmol, 83%) as a colourless oil. SFC analysis showed an enantiomeric excess of 92%.

^{1}H NMR (400 MHz, $CDCl_3$) δ 6.72 (d, *J* = 7.9 Hz, 1H, C(10)-H), 6.67 (d, *J* = 1.7 Hz, 1H, C(7)-H), 6.61 (dd, *J* = 7.9, 1.8 Hz, 1H, C(11)-H), 5.91 (s, 2H, C(12)-H_2), 4.09 (q, *J* = 7.3 Hz, 2H, C(13)-H_2), 2.64 (h, *J* = 6.8 Hz, 1H, C(4)-H), 2.17 (m, 2H, C(2)-H_2), 1.86 (m, 2H, C(3)-H_2), 1.23 (m, 6H, C(5)-H_3 and C(14)-H_3).

^{13}C NMR (101 MHz, $CDCl_3$) δ 173.6 (C(1)), 147.7 (C(6)), 145.8 (C(8)), 140.3 (C(9)), 120.0 (C(7)), 108.1 (C(11)), 107.2 (C(10)), 100.8 (C(12)), 60.2 (C(13)), 39.2 (C(4)), 33.4 (C(2)), 32.5 (C(3)), 22.4 (C(5)), 14.2 (C(14)).

IR (CH_3Cl film): 2962 (m), 1732 (s), 1505 (m), 1487 (s), 1440 (m), 1374 (m), 1214 (s), 1039 (s), 938 (m), 859 (w), 812 (m), 755 (s), 639 (w) cm^{-1}.

HRMS (ESI): m/z calculated for $C_{14}H_{18}O_4Na^+$ $[M+Na]^+$ 273.1097 found 273.1096.

SFC: Chiralpak® IG, 1500 psi, 30 °C; flow: 1.0 mL/min; 1% to 30% MeOH over 5 min, 96.0:4.0 e.r. (minor enantiomer t_R = 2.53 min, major enantiomer t_R = 2.79 min).

$[\alpha]_D^{25}$ = +26.5 (c = 1.0, $CHCl_3$).

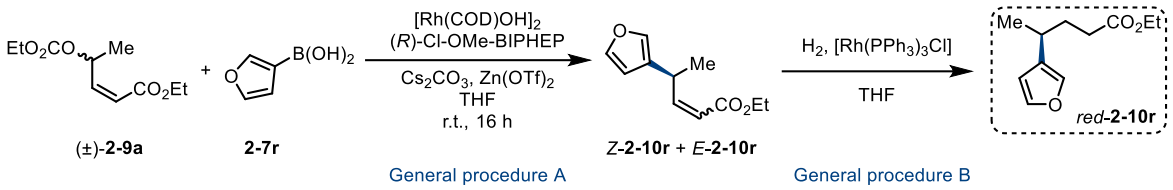

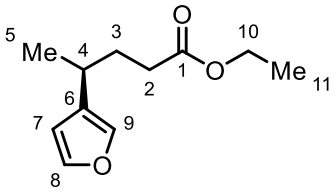

(+)-Ethyl (*S*)-4-(furan-3-yl)pentanoate *red*-**2-10r**

(+)-Ethyl (*S*)-4-(furan-3-yl)pentanoate *red*-**2-10r** was prepared using General procedure A with furan-3-ylboronic acid **2-7r**, followed by reduction of the resulting crude mixture of products (*Z*:*E*=1.5:1) using General procedure B. Purification by automated medium-pressure chromatography (Et_2O/hexane = 0/100 to 35/65) afforded (+)-ethyl (*S*)-4-(furan-3-yl)pentanoate *red*-**2-10r** (66.7 mg, 0.34 mmol, 85%) as a colourless oil. SFC analysis showed an enantiomeric excess of 76%.

^{1}H NMR (400 MHz, $CDCl_3$) δ 7.35 (t, *J* = 1.7 Hz, 1H, C(Ar)-H), 7.21 (dt, *J* = 1.6, 0.8 Hz, 1H, C(Ar)-H), 6.28 (dd, *J* = 2.0, 0.9 Hz, 1H, C(Ar)-H), 4.11 (q, *J* = 7.2 Hz, 2H, C(10)-H_2), 2.68 (h, *J* = 6.9 Hz, 1H, C(4)-H), 2.25 (t, *J* = 8.0 Hz, 2H, C(2)-H_2), 1.83 (m, 2H, C(3)-H_2), 1.24 (t, *J* = 7.1 Hz, 3H, C(11)-H_3), 1.21 (d, *J* = 6.9 Hz, 3H, C(5)-H_3).

^{13}C NMR (101 MHz, $CDCl_3$) δ 173.7 (C(1)), 142.9 (C(Ar)), 138.3 (C(Ar)), 129.7 (C(6)), 109.3 (C(7)), 60.3 (C(10)), 32.5 (C(4)), 32.2 (C(2)), 29.7 (C(3)), 21.1 (C(5)), 14.2 (C(11)).

IR (CH_3Cl film): 2962 (w), 1733 (s), 1456 (w), 1375 (w), 1164 (s), 1027 (m), 874 (m), 755 (s), 668 (w) cm^{-1}.

HRMS (ESI): m/z calculated for $C_{11}H_{17}O_3^+$ $[M+H]^+$ 197.1172 found 197.1174.

SFC: Chiralpak® IG, 1500 psi, 30 °C; flow: 1.0 mL/min; 1% to 30% MeOH over 5 min, 87.8:12.2 e.r. (minor enantiomer t_R = 1.53 min, major enantiomer t_R = 1.36 min).

$[\alpha]_D^{25}$ = +12.9 (c = 1.0, $CHCl_3$).

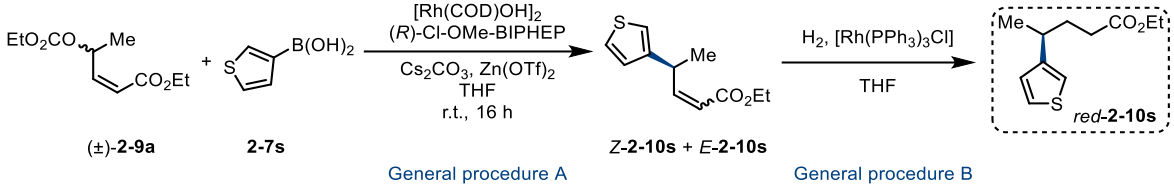

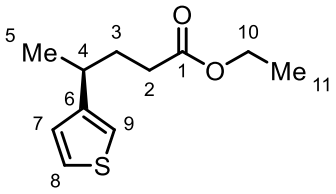

(+)-Ethyl (*S*)-4-(thiophen-3-yl)pentanoate *red*-**2-10s**

(+)-Ethyl (*S*)-4-(thiophen-3-yl)pentanoate *red*-**2-10s** was prepared using General procedure A with thiophen-3-ylboronic acid **2-7s**, followed by reduction of the resulting crude mixture of products (*Z*:*E*=2.8:1) using General procedure B. Purification by automated medium-pressure chromatography (Et_2O/hexane = 0/100 to 30/70) afforded (+)-ethyl (*S*)-4-(thiophen-3-yl)pentanoate *red*-**2-10s** (66.2 mg, 0.31 mmol, 78%) as a colourless oil. SFC analysis showed an enantiomeric excess of 91%.

^{1}H NMR (400 MHz, $CDCl_3$) δ 7.17 (dd, *J* = 4.9, 2.9 Hz, 1H, C(Ar)-H), 6.88 (dd, *J* = 5.0, 1.3 Hz, 1H, C(Ar)-H), 6.86 (dd, *J* = 3.0, 1.4 Hz, 1H, C(Ar)-H), 4.02 (q, *J* = 7.2 Hz, 2H, C(10)-H_2), 2.80 (h, *J* = 7.0 Hz, 1H, C(4)-H), 2.14 (m, 2H, C(2)-H_2), 1.82 (m, 2H, C(3)-H_2), 1.19 (d, *J* = 7.0 Hz, 3H, C(5)-H_3), 1.15 (t, *J* = 7.1 Hz, 3H, C(11)-H_3).

^{13}C NMR (101 MHz, $CDCl_3$) δ 173.7 (C(1)), 147.3 (C(4)), 126.6 (C(Ar)), 125.5 (C(Ar)), 119.4 (C(Ar)), 60.2 (C(10)), 34.7 (C(4)), 33.1 (C(2)), 32.4 (C(3)), 21.7 (C(5)), 14.2 (C(11)).

IR (CH_3Cl film): 2966 (w), 2361 (w), 1727 (w), 1457 (w), 1376 (w), 1322 (w), 1216 (m), 1035 (m), 1033 (w), 931 (w), 852 (w), 753 (s), 668 (w) cm^{-1}.

HRMS (GC EI MS): m/z calculated for $C_{11}H_{16}O_2S^+$ $[M]^+$ 212.08655 found 212.09113.

SFC: Chiralpak® IG, 1500 psi, 30 °C; flow: 1.0 mL/min; 1% to 30% MeOH over 5 min, 95.5:4.5 e.r. (minor enantiomer t_R = 2.03 min, major enantiomer t_R = 1.79 min).

$[\alpha]_D^{25}$ = +24.8 (c = 1.0, $CHCl_3$).

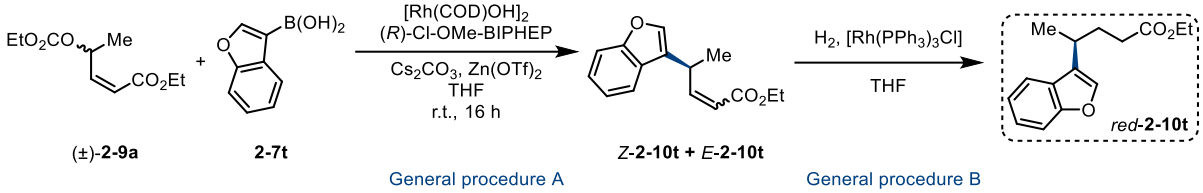

(±)-**2-9a** **2-7t** *Z*-**2-10t** + *E*-**2-10t**

General procedure A General procedure B

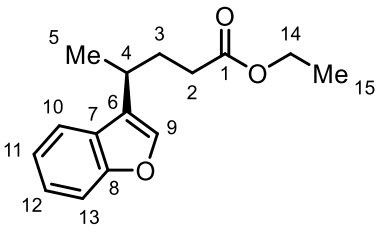

(+)-Ethyl (*S*)-4-(benzofuran-3-yl)pentanoate *red*-**2-10t**

(+)-Ethyl (*S*)-4-(benzofuran-3-yl)pentanoate *red*-**2-10t** was prepared using General procedure A with benzofuran-3-ylboronic acid **2-7t**, followed by reduction of the resulting crude mixture of products (*Z*:*E*=1.8:1) using General procedure B. Purification by automated medium-pressure chromatography (Et_2O/hexane = 0/100 to 25/75) afforded (+)-ethyl (*S*)-4-(benzofuran-3-yl)pentanoate *red*-**2-10t** (60.1 mg, 0.24 mmol, 61%) as a colourless oil. SFC analysis showed an enantiomeric excess of 99%.

^{1}H NMR (400 MHz, $CDCl_3$) δ 7.61 (ddd, *J* = 7.6, 1.5, 0.8 Hz, 1H, C(Ar)-H), 7.47 (dt, *J* = 8.3, 0.9 Hz, 1H, C(Ar)-H), 7.40 (d, *J* = 0.8 Hz, 1H, C(9)-H), 7.27 (m, 1H, C(Ar)-H), 7.22 (td, *J* = 7.4, 1.1 Hz, 1H, C(Ar)-H), 4.09 (q, *J* = 7.1 Hz, 2H, C(14)-H_2), 3.00 (h, *J* = 7.0 Hz, 1H, C(4)-H), 2.32 (t, *J* = 7.9 Hz, 2H, C(2)-H_2), 2.12 (dq, *J* = 13.6, 7.6 Hz, 1H, C(3)-H), 1.98 (ddt, *J* = 13.8, 8.1, 7.2 Hz, 1H, C(3)-H), 1.38 (d, *J* = 7.0 Hz, 3H, C(5)-H_3), 1.22 (t, *J* = 7.1 Hz, 3H, C(15)-H_3).

^{13}C NMR (101 MHz, $CDCl_3$) δ 173.6 (C(1)), 155.6 (C(8)), 140.6 (hC(9)), 127.3 (C(Ar)), 124.8 (C(Ar)), 124.1 (C(Ar)), 122.2 (C(Ar)), 120.2 (C(Ar)), 111.6 (C(13)), 60.3 (C(14)), 32.3 (C(4)), 31.5 (C(2)), 29.4 (C(3)), 20.3 (C(5)), 14.2 (C(15)).

IR (CH_3Cl film): 2960 (w), 1728 (w), 1512 (m), 1453 (w), 1243 (m), 1211 (s), (m), 1103 (w), 1034 (m), 885 (w), 762 (s), 668 (w) cm^{-1}.

HRMS (ESI): m/z calculated for $C_{15}H_{18}O_3Na^+$ $[M+Na]^+$ 269.1148 found 269.1148.

SFC: Chiralpak® IG, 1500 psi, 30 °C; flow: 1.0 mL/min; 1% to 30% MeOH over 5 min, 99.7:0.3 e.r. (minor enantiomer t_R = 2.67 min, major enantiomer t_R = 2.26 min).

$[\alpha]_D^{25}$ = +20.9 (c = 1.0, $CHCl_3$).

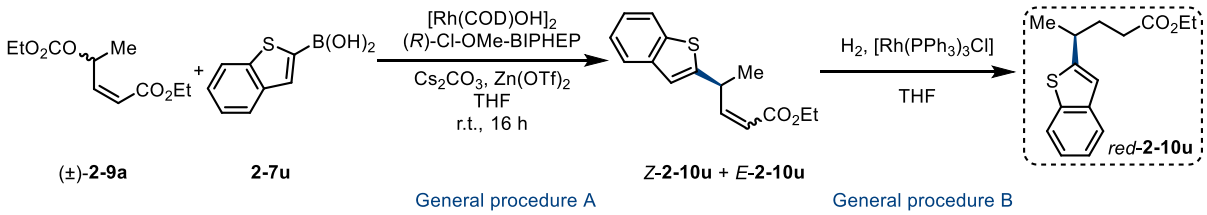

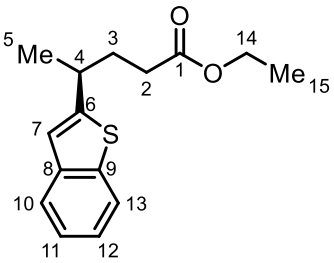

(+)-Ethyl (*S*)-4-(benzo[b]thiophen-2-yl)pentanoate *red*-**2-10u**

(+)-Ethyl (*S*)-4-(benzo[b]thiophen-2-yl)pentanoate *red*-**2-10u** was prepared using General procedure A with benzo[b]thiophen-3-yl boronic acid **2-7u**, followed by reduction of the resulting crude mixture of products (*Z*:*E*=2.0:1) using General procedure B. Purification by automated medium-pressure chromatography (Et_2O/hexane = 0/100 to 20/80) afforded (+)-ethyl (*S*)-4-(benzo[b]thiophen-3-yl)pentanoate *red*-**2-10u** (52.5 mg, 0.20 mmol, 50%) as a colourless oil. SFC analysis showed an enantiomeric excess of 80%.

^{1}H NMR (400 MHz, $CDCl_3$) δ 7.78 (ddt, *J* = 7.8, 1.4, 0.8 Hz, 1H, C(Ar)-H), 7.68 (ddd, *J* = 7.8, 1.4, 0.7 Hz, 1H, C(Ar)-H), 7.29 (m, 2H, C(Ar)-H x2), 7.03 (d, *J* = 0.8 Hz, 1H, C(7)-H), 4.11 (q, *J* = 7.2 Hz, 2H, C(14)-H_2), 3.15 (m, 1H, C(4)-H), 2.32 (m, 2H, C(2)-H_2), 2.02 (m, 2H, C(3)-H_2), 1.41 (d, *J* = 6.9 Hz, 3H, C(5)-H_3), 1.24 (t, *J* = 7.1 Hz, 3H, C(15)-H_3).

^{13}C NMR (101 MHz, $CDCl_3$) δ 173.4 (C(1)), 151.3 (C(6)), 139.9 (C(Ar)), 138.9 (C(Ar)), 124.1 (C(Ar)), 123.6 (C(Ar)), 122.9 (C(Ar)), 122.3 (C(Ar)), 119.7 (C(7)), 60.3 (C(14)), 35.6 (C(4)), 33.6 (C(2)), 32.2 (C(3)), 22.7 (C(5)), 14.2 (C(15)).

IR (CH_3Cl film): 2968 (w), 1732 (s), 1457 (w), 1437 (w), 1376 (w), 1316 (m), 1216 (m), 1184 (m), 1097 (w), 1024 (m), 857 (w), 827 (m), 750 (s), 727 (m), 668 (w) cm^{-1}.

HRMS (ESI): m/z calculated for $C_{15}H_{18}O_2NaS^+$ $[M+Na]^+$ 285.0920 found 285.0920.

SFC: Chiralpak® IG, 1500 psi, 30 °C; flow: 1.0 mL/min; 1% to 30% MeOH over 5 min, 89.9:10.1 e.r. (minor enantiomer t_R = 3.40 min, major enantiomer t_R = 2.95 min).

$[\alpha]_D^{25}$ = +33.2 (c = 1.0, $CHCl_3$).

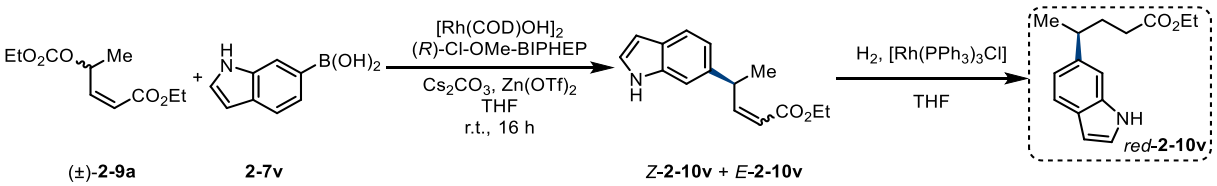

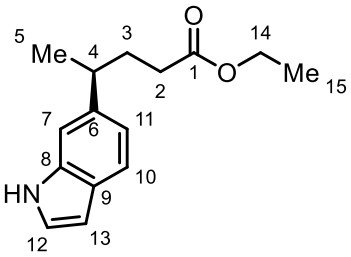

(+)-Ethyl (*S*)-4-(1H-indol-6-yl)pentanoate *red*-**2-10v**

(+)-Ethyl (*S*)-4-(1H-indol-6-yl)pentanoate *red*-**2-10v** was prepared using General procedure A with (1H-indol-6-yl)boronic acid **2-7v**, followed by reduction of the resulting crude mixture of products (*Z*:*E*=5.0:1) using General procedure B. Purification by automated medium-pressure chromatography (EtOAc/hexane = 0/100 to 30/70) afforded (+)-ethyl (*S*)-4-(1H-indol-6-yl)pentanoate *red*-**2-10v** (98.1 mg, 0.17 mmol, 43%) as a colourless oil. SFC analysis showed an enantiomeric excess of 96%.

^{1}H NMR (400 MHz, $CDCl_3$) δ 8.10 (s, 1H, -NH), 7.57 (dt, *J* = 8.2, 0.8 Hz, 1H, C(Ar)-H), 7.19 (dt, *J* = 1.4, 0.7 Hz, 1H, C(Ar)-H), 7.16 (dd, *J* = 3.2, 2.4 Hz, 1H, C(Ar)-H), 6.97 (dd, *J* = 8.2, 1.5 Hz, 1H, C(Ar)-H), 6.51 (ddd, *J* = 3.1, 2.0, 1.0 Hz, 1H, C(Ar)-H), 4.08 (q, *J* = 7.2 Hz, 2H, C(14)-H_2), 2.82 (dp, *J* = 8.8, 6.9 Hz, 1H, C(4)-H), 2.21 (m, 2H, C(2)-H_2), 1.97 (m, 2H, C(3)-H_2), 1.33 (d, *J* = 7.0 Hz, 3H, C(5)-H_3), 1.22 (t, *J* = 7.1 Hz, 3H, C(15)-H_3).

^{13}C NMR (101 MHz, $CDCl_3$) δ 174.0 (C(1)), 140.5 (C(6)), 136.2 (C(8)), 126.4 (C(9)), 123.8 (C(Ar)), 120.6 (C(Ar)), 119.5 (C(Ar)), 109.1 (C(Ar)), 102.4 (C(Ar)), 60.2 (C(14)), 39.7 (C(4)), 33.7 (C(2)), 32.8 (C(3)), 22.8 (C(5)), 14.2 (C(15)).

IR (CH_3Cl film): 2962 (w), 1731 (m), 1455 (w), 1376 (w), 1298 (m), 1243 (m), 1150 (m), 1065 (m), 921 (m), 743(s) cm^{-1}.

HRMS (ESI): m/z calculated for $C_{15}H_{19}O_2NNa^+$ $[M+Na]^+$ 268.1308 found 268.1307.

SFC: Chiralpak® IG, 1500 psi, 30 °C; flow: 1.0 mL/min; 1% to 30% MeOH over 5 min, 97.8:2.2 e.r. (minor enantiomer t_R = 3.95 min, major enantiomer t_R = 3.42 min).

$[\alpha]_D^{25}$ = +34.1 (c = 1.0, $CHCl_3$).

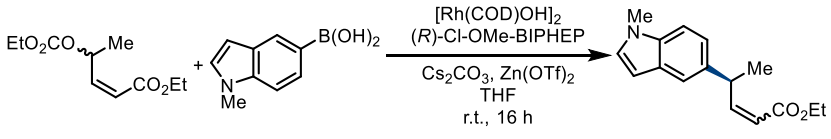

(±)-**2-9a** **2-7w** *Z*-**2-10w** (*Z* only)

General procedure A

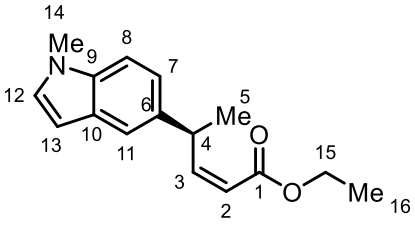

(+)-Ethyl (*S,Z*)-4-(1-methyl-1H-indol-5-yl)pent-2-enoate *Z*-2-10w

(+)-Ethyl (*S,Z*)-4-(1-methyl-1H-indol-5-yl)pent-2-enoate *Z*-**2-10w** was prepared using General procedure A with (1-methyl-1H-indol-5-yl)boronic acid **2-7w**. Only Z product was observed in the crude mixture. Purification by automated medium-pressure chromatography (Et_2O/hexane = 0/100 to 25/75) afforded (+)-ethyl (*S,Z*)-4-(1-methyl-1H-indol-5-yl)pent-2-enoate *Z*-**2-10w** (46.32 mg, 0.18 mmol, 45%) as a colourless oil. SFC analysis showed an enantiomeric excess of 94%.

^{1}H NMR (400 MHz, $CDCl_3$) δ 7.47 (dd, *J* = 1.8, 0.8 Hz, 1H, C(11)-H), 7.18 (dd, *J* = 8.9, 1.0 Hz, 1H, C(Ar)-H), 7.10 (dd, *J* = 8.5, 1.7 Hz, 1H, C(Ar)-H), 6.94 (d, *J* = 3.1 Hz, 1H, (12)-H), 6.36 (dd, *J* = 3.1, 0.8 Hz, 1H, C(13)-H), 6.25 (dd, *J* = 11.4, 10.5 Hz, 1H, C(3)-H), 5.61 (dd, *J* = 11.4, 1.0 Hz, 1H, C(2)-H), 4.92 (dq, *J* = 10.5, 6.9 Hz, 1H, C(4)-H), 4.14 (q, *J* = 7.2 Hz, 2H, C(15)-H_3), 3.68 (s, 3H, C(14)-H_3), 1.38 (d, *J* = 7.0 Hz, 3H, C(5)-H_3), 1.24 (t, *J* = 7.1 Hz, 3H, C(16)-H_3).

^{13}C NMR (101 MHz, $CDCl_3$) δ 166.5 (C(1)), 155.0 (C(3)), 135.6 (C(Ar)), 129.1 (C(Ar)), 128.7 (C(Ar)), 121.3 (C(2)), 118.7 (C(Ar)), 116.9 (C(Ar)), 109.3 (C(Ar)), 100.8 (C(Ar)), 59.9 (C(15)), 37.7 (C(6)), 32.8 (C(14)), 21.3 (C(5)), 14.3 (C(16)).

IR (CH_3Cl film): 2961 (w), 1716 (s), 1608 (s), 1504 (s), 1453 (w), 1375 (w), 1169 (m), 1123 (m), 1033 (m), 825 (m), 755 (m), 668 (w) cm^{-1}.

HRMS (ESI): m/z calculated for $C_{16}H_{20}O_2N^+$ $[M+H]^+$ 258.1489 found 258.1489.

SFC: Chiralpak® ID, 1500 psi, 30 °C; flow: 1.0 mL/min; 1% to 30% MeOH over 5 min, 96.8:3.2 e.r. (minor enantiomer t_R = 2.23 min, major enantiomer t_R = 2.15 min).

[α]$_D^{25}$ = +332.0 (c = 1.0, $CHCl_3$).

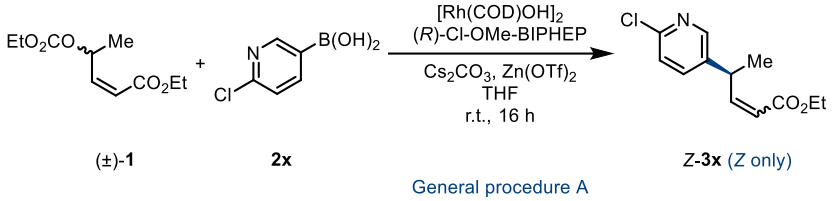

(±)-**1** **2x** *Z*-**3x** (*Z* only)

General procedure A

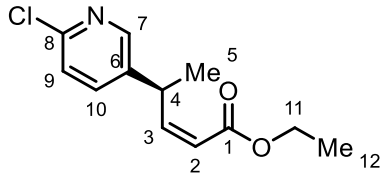

(+)-Ethyl (*S,Z*)-4-(6-chloropyridin-3-yl)pent-2-enoate *Z*-2-10x

(+)-Ethyl (*S,Z*)-4-(6-chloropyridin-3-yl)pent-2-enoate ***Z*-2-10x** was prepared using General procedure A with 6-chloropyridin-3-ylboronic acid **2-7x**. Only *Z* product was observed in the crude mixture. Purification by automated medium-pressure chromatography (Et_2O/hexane = 0/100 to 45/55) afforded (+)-ethyl (*S,Z*)-4-(6-chloropyridin-3-yl)pent-2-enoate ***Z*-2-10x** (61.4 mg, 0.26 mmol, 64%) as a colourless oil. SFC analysis showed an enantiomeric excess of 99%.

^{1}H NMR (400 MHz, $CDCl_3$) δ 8.31 (dd, *J* = 2.6, 0.7 Hz, 1H, C(7)-H), 7.57 (ddd, *J* = 8.3, 2.6 Hz, 1H, C(10)-H), 7.24 (dd, *J* = 8.2, 0.7 Hz, 1H, C(9)-H), 6.16 (dd, *J* = 11.3, 10.1 Hz, 1H, C(3)-H), 5.78 (dd, *J* = 11.4, 1.0 Hz, 1H, C(2)-H), 4.91 (dq, *J* = 10.2, 7.4 Hz, 1H, C(4)-H), 4.17 (q, *J* = 7.1 Hz, 2H, C(11)-H_2), 1.39 (d, *J* = 7.0 Hz, 3H, C(5)-H_3), 1.28 (t, *J* = 7.1 Hz, 3H, C(12)-H_3).

^{13}C NMR (101 MHz, $CDCl_3$) δ 165.9 (C(1)), 151.4 (C(3)), 149.5 (C(8)), 148.6 (C(7)), 138.9 (C(6)), 137.6 (C(10)), 124.1 (C(2)), 119.3 (C(9)), 60.2 (C(11)), 34.7 (C(4)), 20.6 (C(5)), 14.2 (C(12)).

IR (CH_3Cl film): 1715 (s), 1614 (w), 1457 (s), 1386 (m), 1107 (s), 1111 (m), 1029 (m), 829 (m), 753 (m), 633 (w) cm^{-1}.

HRMS (ESI): m/z calculated for $C_{12}H_{15}O_2NCl^+$ $[M+H]^+$ 240.0786 found 240.0786.

SFC: Chiralpak® IG, 1500 psi, 30 °C; flow: 1.0 mL/min; 1% to 30% MeOH over 5 min, 99.5:0.5 e.r. (minor enantiomer t_R = 2.03 min, major enantiomer t_R = 1.96 min).

$[\alpha]_D^{25}$ = +321.6 (c = 1.0, $CHCl_3$).

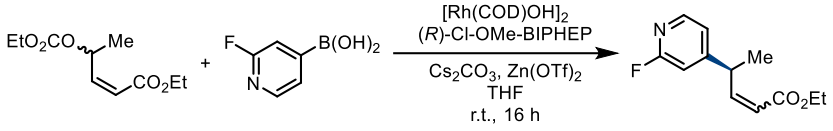

(±)-**2-9a** **2-7y** *Z*-**10-2y** (*Z* only)

General procedure A

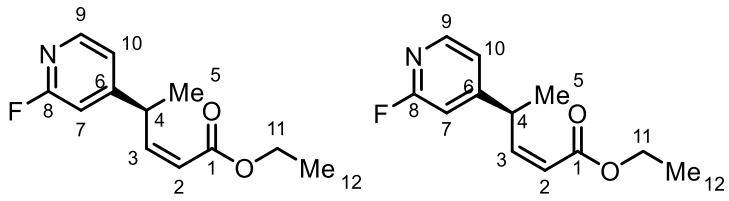

(+)-Ethyl (*S,Z*)-4-(2-fluoropyridin-4-yl)pent-2-enoate *Z*-2-10y

(+)-Ethyl (*S,Z*)-4-(2-fluoropyridin-4-yl)pent-2-enoate *Z*-**2-10y** was prepared using General procedure A with 2-fluoropyridin-4-yl boronic acid **2-7y**. Only Z product was observed in the crude mixture. Purification by automated medium-pressure chromatography (Et_2O/hexane = 0/100 to 40/60) afforded (+)-ethyl (*S,Z*)-4-(2-fluoropyridin-4-yl)pent-2-enoate *Z*-**2-10y** (46.4 mg, 0.21 mmol, 52%) as a colourless oil. SFC analysis showed an enantiomeric excess of 99%.

^{1}H NMR (400 MHz, $CDCl_3$) δ 8.13 (d, *J* = 2.0 Hz, 1H, C(Ar)-H), 7.71 (tdd, *J* = 7.8, 2.6, 0.5 Hz, 1H, C(Ar)-H), 6.86 (dd, *J* = 8.5, 3.0 Hz, 1H, C(Ar)-H), 6.18 (dd, *J* = 11.3, 10.2 Hz, 1H, C(3)-H), 5.78 (dd, *J* = 11.4, 1.0 Hz, 1H, C(2)-H), 4.94 (dq, *J* = 10.2, 7.0 Hz, 1H, C(4)-H), 4.19 (q, *J* = 7.1 Hz, 2H, C(11)-H_2), 1.41 (d, *J* = 7.0 Hz, 3H, C(5)-H_3), 1.29 (t, *J* = 7.1 Hz, 3H, C(12)-H_3).

^{13}C NMR (101 MHz, $CDCl_3$) δ 166.0 (C(1)), 162.5 (d, *J* = 237.6 Hz, C(8)-H), 151.8 (C(3)), 146.1 (d, *J* = 14.7 Hz, C(6)), 139.9 (d, *J* = 7.8 Hz, C(Ar)), 137.6 (d, *J* = 4.5 Hz, C(Ar)), 119.1 (C(2)), 109.3 (d, *J* = 37.4 Hz, C(7)), 60.2 (C(11)), 34.5 (C(4)), 20.7 (C(5)), 14.2 (C(12)).

^{19}F (13C)NMR (376 MHz, $CDCl_3$) δ −119.4.

IR (CH_3Cl film): 1719 (s), 1621 (w), 1458 (m), 1109(s), 1113 (m), 1033 (m), 829 (m), 755 (s), 638 (w) cm^{-1}.

HRMS (ESI): m/z calculated for $C_{12}H_{15}FNO_2^+$ $[M+H]^+$ 224.1081 found 224.1082.

SFC: Chiralpak® IG, 1500 psi, 30 °C; flow: 1.0 mL/min; 1% to 30% MeOH over 5 min, 99.6:0.4 e.r. (minor enantiomer t_R = 1.94 min, major enantiomer t_R = 1.76 min).

$[\alpha]_D^{25}$ = +323.8 (c = 1.0, $CHCl_3$).

5.3.2.1 1,4-Addition of ortho-boronic acid to (±)-**2-9a**

The use of *ortho*-boronic acids gave rise to 1,4-addition to (±)-**2-9a** instead of the γ-selective Suzuki-Miyarua reaction. In the case of the reaction between *ortho*-methylphenyl boronic acid and (±)-**2-9a** under the standard reaction conditions, the 1,4-addition product was obtained in 30% yield, as a 1.4:1 ratio of diastereomers with 80% *ee* in the major diastereomer. Asymmetric 1,4-addition is well described, so we did not pursue these results any further. (*Experiment performed by Stephen J. Webster*).

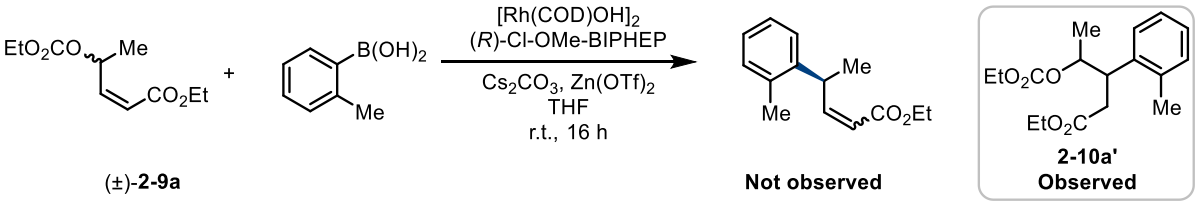

(±)-**2-9a**

Not observed

General procedure A

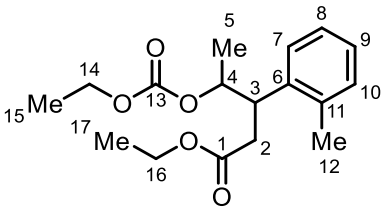

Major diastereomer of ethyl 4-((ethoxycarbonyl)oxy)-3-(*o*-tolyl)pentanoate **2-10a'**:

^{1}H NMR (400 MHz, $CDCl_3$) δ 7.23 (dd, *J* = 7.4, 1.6 Hz, 1H, C(Ar)-H), 7.14 (m, 3H, C(Ar)-H x3), 4.99 (qd, *J* = 6.4, 4.9 Hz, 1H, C(4)-H), 4.17 (q, *J* = 7.1 Hz, 2H, C(14)-H_2 or C(16)-H_2), 4.01 (q, *J* = 7.1 Hz, 2H, C(14)-H_2 or C(16)-H_2), 3.82 (ddd, *J* = 9.2, 6.2, 4.9 Hz, 1H, C(3)-H), 2.81 (m, 2H, C(2)-H_2), 2.44 (s, 3H, C(12)-H_3), 1.28 (t, *J* = 7.1 Hz, 3H, C(15)-H_3 or C(17)-H_3), 1.18 (d, *J* = 6.4 Hz, 3H, C(5)-H_3), 1.10 (t, *J* = 7.1 Hz, 3H, C(15)-H_3 or C(17)-H_3).

^{13}C NMR (101 MHz, $CDCl_3$) δ 172.1 (C(1)), 154.8 (C(13)), 137.7 (C(Ar)), 137.3 (C(Ar)), 130.6 (C(Ar)), 127.2 (C(Ar)), 126.9 (C(Ar)), 126.2 (C(Ar)), 76.2 (C(4)), 64.0 (C(14) or C(16)), 60.6 (C(14) or C(16)), 40.9 (C(3)), 35.6 (C(2)), 20.0 (C(12)), 16.4 (C(5)), 14.4 (C(15) or C(17)), 14.1 (C(15) or C(17)).

IR (CH_3Cl film): 2987, 2362, 2339, 1744, 1466, 1374, 1270, 1178, 1036 cm^{-1}.

HRMS (ESI): m/z calculated for $C_{17}H_{24}O_5Na^+$ $[M+Na]^+$ 331.1516 found 331.1512.

SFC: Chiralpak® IG, 1500 psi, 30 °C; flow: 1.0 mL/min; 1% to 30% MeOH over 5 min, 89.9:10.1 e.r. (minor enantiomer t_R = 2.40 min, major enantiomer t_R = 2.04 min).

5.3.2.2 *Rh-catalysed reactions of (±)-**2-11a-j***

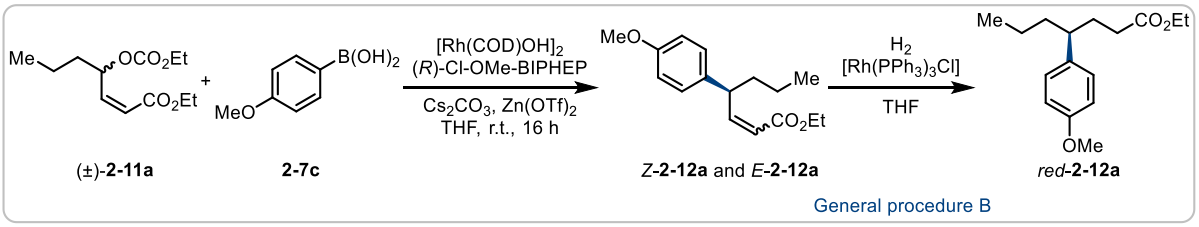

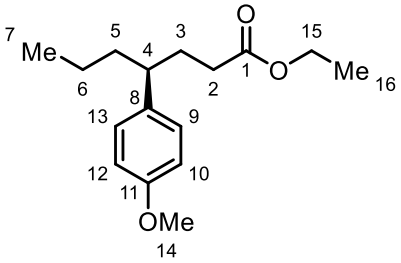

(+)-Ethyl (*S*)-4-(4-methoxyphenyl)heptanoate *red*-2-12a

(+)-Ethyl (*S*)-4-(4-methoxyphenyl)heptanoate *red*-**2-12a** was prepared using General procedure A with 4-methoxyphenyl boronic acid **2-7c**, followed by reduction of the resulting crude mixture of products (*Z:E* = 7.1:1) using General procedure B. Purification by automated medium-pressure chromatography (Et_2O/hexane = 0/100 to 15/85) was performed to afford (+)-ethyl (*S*)-4-(4-methoxyphenyl)heptanoate *red*-**2-12a** (94.1 mg, 0.36 mmol, 89%) as a colourless oil. SFC analysis showed an enantiomeric excess of 93%.

^{1}H NMR (400 MHz, $CDCl_3$) δ 7.04 (d, *J* = 8.7 Hz, 2H, C(9)-H and C(13)-H), 6.83 (d, *J* = 8.6 Hz, 2H, C(10)-H and C(12)-H), 4.07 (q, *J* = 7.2 Hz, 1H, C(15)-H_2), 3.79 (s, 3H, C(14)-H_3), 2.47 (tt, *J* = 9.9, 5.2 Hz, 1H, C(4)-H), 2.11 (m, 2H, C(2)-H_2), 1.98 (m, 1H, C(3)-H), 1.77 (m, 1H, C(3)-H), 1.56 (m, 2H, C(5)-H_2), 1.20 (m, 5H, C(6)-H_2 and C(16)-H_3), 0.83 (t, *J* = 7.3 Hz, 3H, C(7)-H_3).

^{13}C NMR (101 MHz, $CDCl_3$) δ 173.8 (C(1)), 157.9 (C(11)), 136.8 (C(8)), 128.5 (C(9) and C(13)), 113.8 (C(10) and C(12)), 60.2 (C(15)), 55.2 (C(14)), 44.3 (C(4)), 39.2 (C(5)), 32.5 (C(2)), 32.0 (C(3)), 20.6 (C(6)), 14.2 (C(16)), 14.1 (C(7)).

HRMS (ESI): m/z calculated for $C_{16}H_{25}O_3^+$ $[M+H]^+$ 265.1798 found 265.1798.

IR (CH_3Cl film): 2956 (w), 2932 (w), 2871 (w), 1734 (s), 1612 (w), 1584 (w), 1513 (s), 1464 (w), 1375 (w), 1302 (w), 1248 (s), 1178 (m), 1116 (w), 1037 (m), 810 (m), 762 (w) cm^{-1}.

SFC: Chiralpak® IF, 1500 psi, 30 °C; flow: 0.6 mL/min; 1% to 5% MeOH over 11 min, 96.5:3.5 e.r. (minor enantiomer t_R = 6.19 min, major enantiomer t_R = 6.34 min).

$[\alpha]_D^{25}$ = +12.3 (c = 1.0, $CHCl_3$).

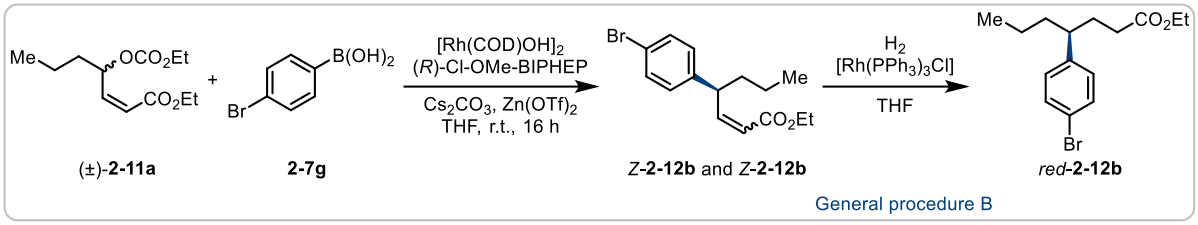

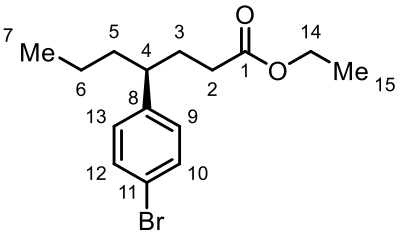

(+)-Ethyl (*S*)-4-(4-bromophenyl)heptanoate *red*-2-12b

(+)-Ethyl (*S*)-4-(4-bromophenyl)heptanoate *red*-**2-12b** was prepared using General procedure A with 4-bromophenyl boronic acid **2-7g**, followed by reduction of the resulting crude mixture of products (*Z:E* = 3.6:1) using General procedure B. Purification by automated medium-pressure chromatography (Et_2O/hexane = 0/100 to 20/80) was performed to afford (+)-ethyl (*S*)-4-(4-bromophenyl)heptanoate *red*-**2-12b** (122.8 mg, 0.39 mmol, 98%) as a colourless oil. SFC analysis showed an enantiomeric excess of 93%.

^{1}H NMR (400 MHz, $CDCl_3$) δ 7.40 (d, *J* = 8.4 Hz, 2H, C(9)-H and C(13)-H), 7.01 (d, *J* = 8.4 Hz, 2H, C(10)-H and C(12)-H), 4.07 (q, *J* = 7.1 Hz, 2H, C(14)-H_2), 2.50 (tt, *J* = 9.9, 5.1 Hz, 1H, C(4)-H), 2.10 (dd, *J* = 9.1, 7.2 Hz, 2H, C(2)-H_2), 2.00 (m, 1H, C(3)-H), 1.78 (m, 1H, C(3)-H), 1.55 (m, 2H, C(5)-H_2), 1.21 (t, *J* = 7.1 Hz, 3H, C(15)-H_3), 1.15 (m, 2H, C(6)-H_2), 0.83 (t, *J* = 7.3 Hz, 3H, C(7)-H_3).

^{13}C NMR (101 MHz, $CDCl_3$) δ 173.5 (C(1)), 143.8 (C(4)), 131.5 (C(Ar) x2), 129.5 (C(Ar) x2), 119.8 (C(11)), 60.3 (C(14)), 44.7 (C(4)), 38.9 (C(5)), 32.4 (C(3)), 31.7 (C(2)), 20.5 (C(6)), 14.2 (C(15)), 14.0 (C(7)).

HRMS (ESI): m/z calculated for $C_{15}H_{22}O_2Br^+$ $[M+H]^+$ 315.0777 found 315.0777.

IR (CH_3Cl film): 2958 (w), 1732 (m), 1486 (w), 1376 (w), 1217 (w), 1160 (w), 1074 (w), 1035 (w), 1010 (w), 823 (w), 758 (s), 668 (w) cm^{-1}.

SFC: Chiralpak® IG, 1500 psi, 30 °C; flow: 1.0 mL/min; 1% to 30% MeOH over 5 min, 96.5:3.5 e.r. (minor enantiomer t_R = 2.01 min, major enantiomer t_R = 1.90 min).

$[\alpha]_D^{25}$ = +15.1 (c = 1.0, $CHCl_3$).

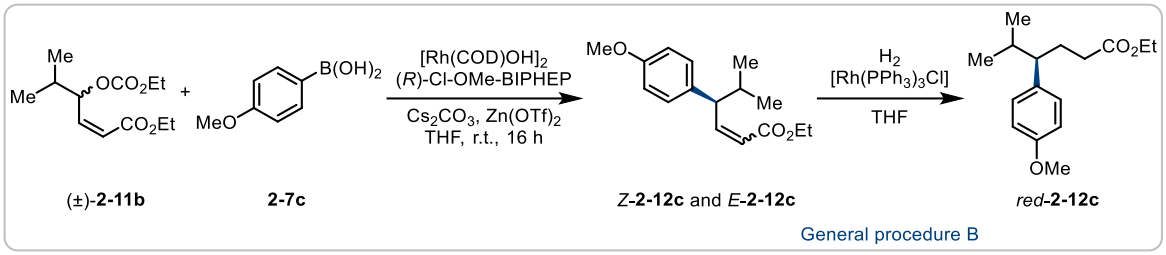

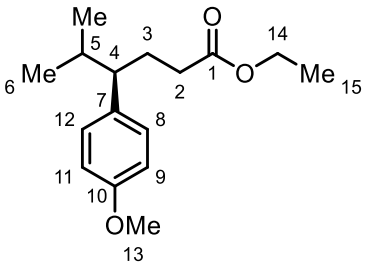

(+)-Ethyl (*R*)-4-(4-methoxyphenyl)-5-methylhexanoate *red*-2-12c

(+)-Ethyl (*R*)-4-(4-methoxyphenyl)-5-methylhexanoate *red*-**2-12c** was prepared using General procedure A with 4-methoxyphenyl boronic acid **2-7c**, followed by reduction of the resulting crude mixture of products (*Z:E* = 4.7:1) using General procedure B. Purification by automated medium-pressure chromatography (E_2tO/hexane = 0/100 to 15/85) was performed to afford (+)-ethyl (*R*)-4-(4-methoxyphenyl)-5-methylhexanoate *red*-**2-12c** (60.3 mg, 0.23 mmol, 57%) as a colourless oil. SFC analysis showed an enantiomeric excess of >99%.

^{1}H NMR (400 MHz, $CDCl_3$) δ 7.01 (d, *J* = 8.7 Hz, 2H, C(8)-H and C(12)-H), 6.82 (d, *J* = 8.7 Hz, 1H, C(9)-H and C(11)-H), 4.06 (q, *J* = 7.2 Hz, 2H, C(14)-H_2), 3.79 (s, 3H, C(13)-H_3), 2.16 (m, 1H, C(4)-H and C(5)-H), 2.04 (m, 1H, C(2)-H_2), 1.80 (m, 1H, C(3)-H_2), 1.21 (t, *J* = 7.1 Hz, 3H, C(15)-H_3), 0.96 (d, *J* = 6.6 Hz, 3H, C(6)-H_3), 0.71 (d, *J* = 6.7 Hz, 3H, C(6)-H_3).

^{13}C NMR (101 MHz, $CDCl_3$) δ 173.9 (C(1)), 157.9 (C(11)), 135.4 (C(7)), 129.3 (C(8) and C(12)), 113.5 (C(9) and C(11)), 60.1 (C(14)), 55.2 (C(13)), 51.8 (C(4)), 33.6 (C(2)), 32.9 (C(3)), 28.3 (C(5)), 20.9 (C(6)), 20.7 (C(6)), 14.2 (C(15)).

HRMS (ESI): m/z calculated for $C_{16}H_{25}O_3^+$ $[M+H]^+$ 265.1798 found 265.1798.

IR (CH_3Cl film): 2958 (w), 2874 (w), 1733 (s), 1611 (w), 1512 (s), 1466 (w), 1369 (w), 1303 (w), 1248 (s), 1216 (m), 1179 (m), 1038 (m), 828 (w), 757 (s), 668 (w) cm^{-1}.

SFC: Chiralpak® IG, 1500 psi, 30 °C; flow: 1.0 mL/min; 1% to 30% MeOH over 5 min, 99.8:0.2 e.r. (minor enantiomer t_R = 1.97 min, major enantiomer t_R = 1.82 min).

$[\alpha]_D^{25}$ = +9.0 (c = 1.0, $CHCl_3$).

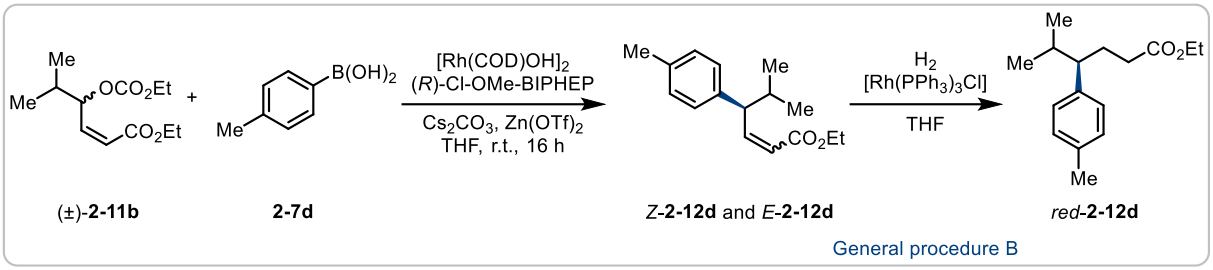

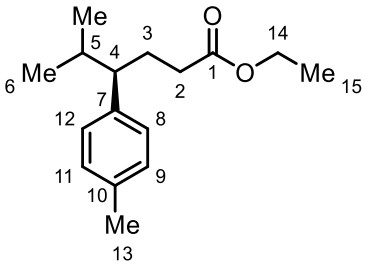

(+)-Ethyl (*R*)-5-methyl-4-(*p*-tolyl)hexanoate *red*-2-12d

(+)-Ethyl (*R*)-5-methyl-4-(*p*-tolyl)hexanoate *red*-**2-12d** was prepared using General procedure A with *p*-tolyl boronic acid **2-7d**, followed by reduction of the resulting crude mixture of products (*Z:E* = 2.8:1) using General procedure B. Purification by automated medium-pressure chromatography (E_2tO/hexane = 0/100 to 15/85) was performed to afford (+)-ethyl (*R*)-5-methyl-4-(*p*-tolyl)hexanoate *red*-**2-12d** (80.5 mg, 0.32 mmol, 81%) as a colourless oil. SFC analysis showed an enantiomeric excess of >99%.

^{1}H NMR (400 MHz, $CDCl_3$) δ 7.08 (d, *J* = 8.0 Hz, 2H, C(Ar)-H x2), 6.98 (d, *J* = 7.9 Hz, 2H, C(Ar)-H x2), 4.06 (q, *J* = 7.1 Hz, 2H, C(14)-H_2), 2.32 (s, 3H, C(13)-H_3), 2.20 (m, 1H, C(4)-H), 2.12 (m, 1H, C(5)-H), 2.05 (m, 2H, C(2)-H_2), 1.82 (m, 2H, C(3)-H_2), 1.20 (t, *J* = 7.1 Hz, 3H, C(15)-H_3), 0.96 (d, *J* = 6.7 Hz, 3H, C(6)-H_3), 0.72 (d, *J* = 6.7 Hz, 3H, C(6)-H_3).

^{13}C NMR (101 MHz, $CDCl_3$) δ 173.9 (C(1)), 140.3 (C(7)), 135.5 (C(10)), 128.8 (C(Ar) x2), 128.3 (C(Ar) x2), 60.1 (C(14)), 52.2 (C(4)), 33.5 (C(5)), 32.9 (C(2)), 28.2 (C(3)), 21.0 (C(13)), 20.9 (C(6)), 20.8 (C(6)), 14.2 (C(15)).

HRMS (ESI): m/z calculated for $C_{16}H_{25}O_2^+$ $[M+H]^+$ 249.1849 found 249.1849.

IR (CH_3Cl film): 2958 (w), 2873 (w), 1736 (s), 1514 (w), 1452 (w), 1370 (w), 1305 (w), 1246 (m), 1217 (m), 1162 (m), 1038 (w), 812 (w), 764 (s), 669 (s), 641 (w), 618 (w) cm^{-1}.

SFC: Chiralpak® IC, 1500 psi, 30 °C; flow: 0.6 mL/min; 1% to 5% MeOH over 8 min, >99.9:0.1 e.r. (minor enantiomer t_R = 3.80 min, major enantiomer t_R = 3.64 min).

$[\alpha]_D^{25}$ = +11.1 (c = 1.0, $CHCl_3$).

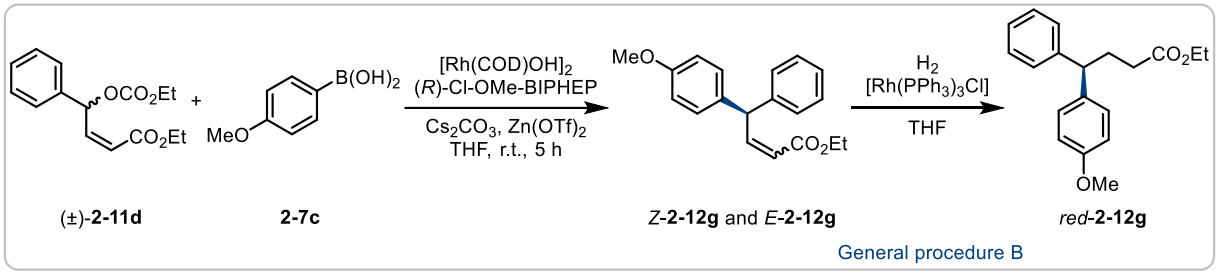

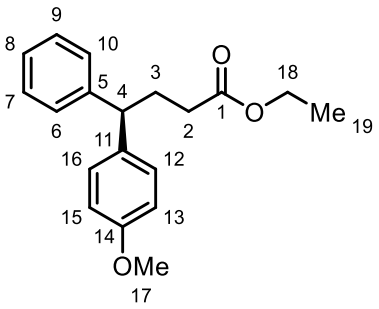

(-)-Ethyl (*R*)-4-(4-methoxyphenyl)-4-phenylbutanoate *red*-2-12g

Ethyl (*R*)-4-(4-methoxyphenyl)-4-phenylbutanoate *red*-**2-12g** was prepared using General procedure A with 4-methoxyphenyl boronic acid **2-7c**, followed by reduction of the resulting crude mixture of products (*Z:E* = 1.7:1) using General procedure B. Purification by automated medium-pressure chromatography (E_2tO/hexane = 0/100 to 25/75) was performed to afford ethyl (*R*)-4-(4-methoxyphenyl)-4-phenylbutanoate *red*-**2-12g** (107.4 mg, 0.36 mmol, 90%) as a colourless oil. SFC analysis showed an enantiomeric excess of 93%. Characterisation data match literature reports.[190]

^{1}H NMR (400 MHz, $CDCl_3$) δ 7.17 (m, 4H, C(Ar)-H x4), 7.08 (m, 3H, C(Ar)-H x3), 6.75 (d, *J* = 8.7 Hz, 2H, C(13)-H and C(15)-H), 4.02 (q, *J* = 7.1 Hz, 2H, C(18)-H_2), 3.80 (t, *J* = 7.8 Hz, 1H, C(4)-H), 3.69 (s, 3H, C(17)-H_3), 2.27 (m, 2H, C(2)-H_2), 2.18 (m, 2H, C(3)-H_2), 1.15 (t, *J* = 7.1 Hz, 3H, C(19)-H_3).

^{13}C NMR (101 MHz, $CDCl_3$) δ 173.5 (C(1)), 158.1 (C(14)), 144.6 (C(11)), 136.3 (C(5)), 128.8 (C(Ar) x2), 128.5 (C(Ar) x2), 127.8 (C(Ar) x2), 126.3 (C(8)), 113.9 (C(13) and C(15)), 60.3 (C(18)), 55.2 (C(17)), 49.7 (C(4)), 32.9 (C(2)), 30.8 (C(3)), 14.3 (C(19)).

HRMS (ESI): m/z calculated for $C_{19}H_{22}O_3Na_2^+$ $[M+Na]^+$ 321.1461 found 321.1461.

IR (CH_3Cl film): 2952 (w), 1732 (s), 1611 (w), 1512 (s), 1453 (w), 1376 (w), 1303 (m), 1250 (s), 1178 (m), 1036 (m), 830 (w), 763 (s), 701 (m), 668 (m), 655 (w) cm^{-1}.

SFC: Chiralpak® IE, 1500 psi, 30 °C; flow: 1.0 mL/min; 1% to 10% MeOH over 5 min, 96.3:3.7 e.r. (minor enantiomer t_R = 5.06 min, major enantiomer t_R = 5.19 min).

$[\alpha]_D^{25}$ = −3.0 (c = 1.0, $CHCl_3$).

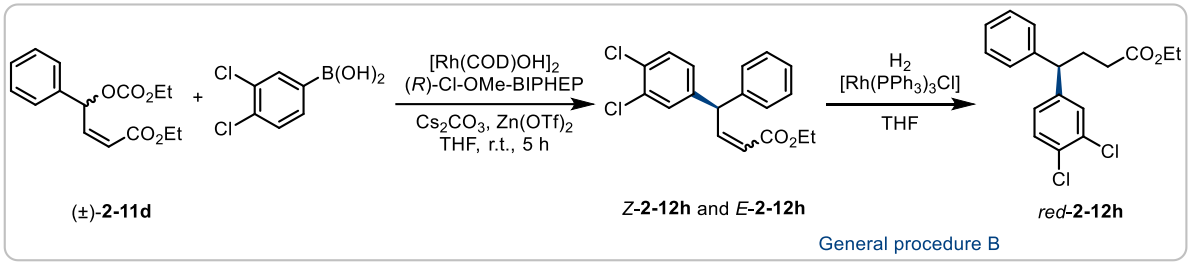

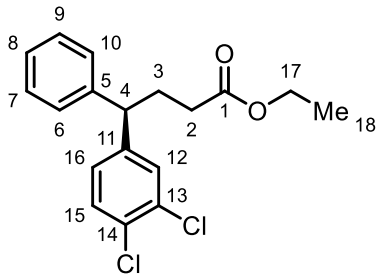

Ethyl (*R*)-4-(3,4-dichlorophenyl)-4-phenylbutanoate *red*-2-12h

Ethyl (*R*)-4-(3,4-dichlorophenyl)-4-phenylbutanoate *red*-**2-12h** was prepared using General procedure A with 3,4-dichlorophenyl boronic acid, followed by reduction of the resulting crude mixture of products (*Z:E* = 1.2:1) using General procedure B. Purification by automated medium-pressure chromatography (E_2tO/hexane = 0/100 to 25/75) was performed to afford ethyl (*R*)-4-(3,4-dichlorophenyl)-4-phenylbutanoate ***red*-2-12h** (116.0 mg, 0.34 mmol, 86%) as a colourless oil. SFC analysis showed an enantiomeric excess of 99%. Characterisation data match literature reports.[191]

^{1}H NMR (400 MHz, $CDCl_3$) δ 7.35 (d, *J* = 8.3 Hz, 1H, C(Ar)-H), 7.31 (m, 3H, C(Ar)-H x3), 7.20 (m, 3H, C(Ar)-H x3), 7.07 (ddd, *J* = 8.3, 2.2, 0.5 Hz, 1H, C(Ar)-H), 4.11 (q, *J* = 7.1 Hz, 2H, C(17)-H_2), 3.90 (t, *J* = 7.8 Hz, 1H, C(4)-H), 2.34 (m, 2H, C(2)-H_2), 2.26 (m, 2H, C(3)-H_2), 1.24 (t, *J* = 7.1 Hz, 3H, C(18)-H_3).

^{13}C NMR (101 MHz, $CDCl_3$) δ 173.1 (C(1)), 144.6 (C(Ar)), 142.8 (C(Ar)), 132.5 (C(Ar)), 130.5 (C(Ar)), 130.4 (C(Ar)), 129.8 (C(Ar)), 128.8 (C(Ar) x2), 127.8 (C(Ar) x2), 127.3 (C(Ar)), 126.9 (C(Ar)), 60.5 (C(17)), 49.7 (C(4)), 32.5 (C(2)), 30.3 (C(3)), 14.2 (C(18)).

HRMS (ESI): m/z calculated for $C_{18}H_{19}O_2Cl_2^+$ $[M+H]^+$ 337.0757 found 337.0756.

IR (CH_3Cl film): 3028 (w), 2885 (w), 1732 (s), 1472 (m), 1376 (w), 1239 (m), 1180 (m), 1156 (m), 1030 (m), 886 (m), 763 (s), 700 (m), 678 (w), 654 (w), 642 (w), 618 (w) cm^{-1}.

SFC: Chiralpak® IA, 1500 psi, 30 °C; flow: 1.0 mL/min; 1% to 30% MeOH over 5 min, 99.5:0.5 e.r. (minor enantiomer t_R = 2.52 min, major enantiomer t_R = 2.66 min).

$[\alpha]_D^{25}$ = −4.5 (c = 1.0, $CHCl_3$).

Absolute configuration was determined by comparing specific optical rotation of *red*-**2-12h** to that of (*R*)-methyl 4-(3,4-dichlorophenyl)-4-phenylbutanoate.[192]

Products (*S*)-**2-12e**, (*S*)-**2-12f**, (*S*)-**2-12i**, (*S*)-**2-12j**, (*S*)-**2-12p** and (*S*)-**2-12q** were prepared by Ke Liu. Products (*S*)-**2-12k**, (*S*)-**2-12l**, (*S*)-**2-12m**, (*S*)-**2-12n**, (*S*)-**2-12o**, (*S*)-**2-12r** and (*S*)-**2-12s** we prepared by Stephen J. Webster. Detailed procedures for preparation of these compounds and their full characterisation data can be found in '**Chelation enables selectivity control in enantioconvergent Suzuki-Miyaura cross-couplings on acyclic allylic systems**', Violeta Stojalnikova, Stephen J. Webster, Ke Liu and Stephen P. Fletcher. 2023, *Nature Chemistry. Accepted.*

5.3.3 Procedures for the product derivatization

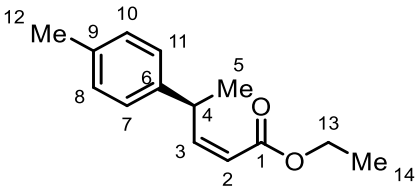

(+)-Ethyl (*S,Z*)-4-(*p*-tolyl)pent-2-enoate *Z*-2-10d

General Procedure A was carried out using (4-methyl)phenylboronic acid **2-7d** (108.8 mg, 0.80 mmol, 2.0 equiv.) and only Z-product was isolated by medium-pressure automated flash chromatography to afford (+)-ethyl (*S,Z*)-4-(*p*-tolyl)pent-2-enoate *Z*-**2-10d** (70.7 mg, 32.4 mmol, 81%) as a colourless oil. SFC analysis showed an enantiomeric excess of 96%.

^{1}H NMR (400 MHz, $CDCl_3$) δ 7.20 (d, *J* = 8.1 Hz, 2H, C(7)-H and C(11)-H), 7.13 (d, *J* = 7.9 Hz, 2H, C(8)-H and C(10)-H), 6.25 (dd, *J* = 11.4, 10.4 Hz, 1H, C(3)-H), 5.72 (dd, *J* = 11.4, 1.0 Hz, 1H, C(2)-H), 4.87 (dq, *J* = 10.4, 7.0 Hz, 1H, C(4)-H), 4.20 (q, *J* = 7.2 Hz, 2H, C(13)-H_2), 2.32 (s, 3H, C(12)-H_3), 1.39 (d, *J* = 6.9 Hz, 3H, C(5)-H_3), 1.31 (t, *J* = 7.1 Hz, 3H, C(14)-H_3).

^{13}C NMR (101 MHz, $CDCl_3$) δ 166.3 (C(1)), 154.0 (C(3)), 141.7 (C(6)), 136.0 (C(9)), 129.3 (C(8) and C(10)), 126.9 (C(7) and C(11)), 117.6 (C(2)), 59.9 (C(13)), 37.3 (C(4)), 21.0 (C(12)), 20.9 (C(5)), 14.3 (C(14)).

IR (CH_3Cl film): 2978 (w), 1718 (s), 1642 (m), 1513 (m), 1455(w), 1441 (w), 1100 (s), 1098 (w), 1033 (m), 815 (m), 755 (s) cm^{-1}.

HRMS (ESI): m/z calculated for $C_{14}H_{19}O_2^+$ $[M+H]^+$ 219.1380 found 219.1382.

SFC: Chiralpak® IG, 1500 psi, 30 °C; flow: 1.0 mL/min; 1% to 30% MeOH over 5 min, 97.8:2.2 e.r. (minor enantiomer t_R = 1.72 min, major enantiomer t_R = 1.52 min).

$[\alpha]_D^{25}$ = +337.5 (c = 1.0, $CHCl_3$)

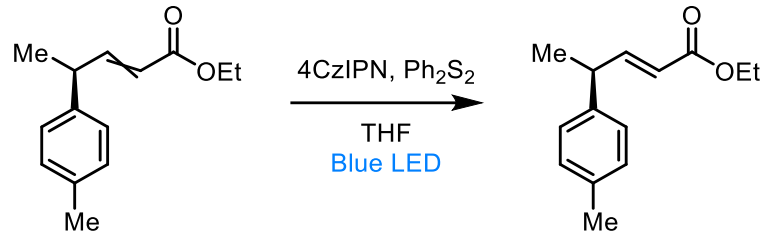

Z-**2-10d** and *E*-**2-10d**

E-**2-10d**
91% (over 2 steps)
96% *ee*

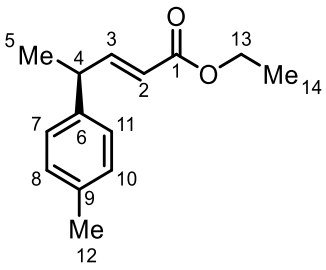

(−)-Ethyl (*S,E*)-4-(*p*-tolyl)pent-2-enoate *E*-2-10d

General Procedure A was carried out using (*p*-tolyl)phenylboronic acid **2-7d** (108.8 mg, 0.80 mmol, 2.0 equiv.) and crude product (containing *Z*-**2-10d** and *E*-**2-10d** with *Z:E* ratio of 4.4:1) was used in the next step.

4CzIPN (15.8 mg, 0.020 mmol, 0.05 equiv.), diphenyl disulphide (96.1 mg, 0.44 mmol, 1.1 equiv.) and THF (4.0 mL) were added to the crude product (containing *Z*-**2-10d** and *E*-**2-10d**) and the reaction mixture was irradiated with blue light (Evoluchem 450PF 450 nm CREE XPE (part number HCK1012-01-002), 18 W power consumption and 34 mW/cm^2 output relative irradiance) for 2 h. The mixture was filtered through a plug of silica with Et_2O and the solvent was removed in vacuo. Purification by flash chromatography afforded (−)-ethyl (*S,E*)-4-(*p*-tolyl)pent-2-enoate *E*-**2-10d** (79.5 mg, 0.36 mmol, 91%) as a colourless oil. SFC analysis showed an enantiomeric excess of 96%. Characterisation data match literature reports.[199]

^{1}H NMR (400 MHz, $CDCl_3$) δ 7.10 (m, 5H, C(3)-H, C(7)-H, C(8)-H, C(10)-H and C(11)-H), 5.79 (dd, *J* = 15.7, 1.6 Hz, 1H, C(2)-H), 4.17 (q, *J* = 7.1 Hz, 2H, C(13)-H_2), 3.58 (m, 1H, C(4)-H), 2.33 (s, 3H, C(12)-H_3), 1.41 (d, *J* = 7.0 Hz, 3H, C(5)-H_3), 1.27 (t, *J* = 7.1 Hz, 3H, C(14)-H_3).

^{13}C NMR (101 MHz, $CDCl_3$) δ 166.8 (C(1)), 152.8 (C(3)), 140.3 (C(6)), 136.3 (C(9)), 129.4 (C(8) and C(10)), 127.2 (C(7) and C(11)), 120.0 (C(2)), 60.3 (C(13)), 41.7 (C(4)), 21.0 (C(12)), 20.3 (C(5)), 14.3 (C(14)).

IR (CH_3Cl film): 2971 (w), 1716 (m), 1651 (w), 1514 (w), 1455(w), 1368 (w), 1268 (m), 1216 (m), 1174 (m), 1131 (w), 1036 (m), 1016 (w), 981 (w), 866 (w), 818 (m), 754 (s), 668 (m), cm^{-1}.

HRMS (ESI): m/z calculated for $C_{14}H_{19}O_2^+$ $[M+H]^+$ 219.1380 found 219.1379.

SFC: Chiralpak® IG, 1500 psi, 30 °C; flow: 1.0 mL/min; 1% to 30% MeOH over 5 min, 97.9:2.1 e.r. (minor enantiomer t_R = 2.27 min, major enantiomer t_R = 1.86 min).

$[\alpha]_D^{25}$ = −11.2 (c = 1.0, $CHCl_3$) (Lit[115].: $[\alpha]_D^{30}$ = −13.6 (c = 1.3, $CHCl_3$)).

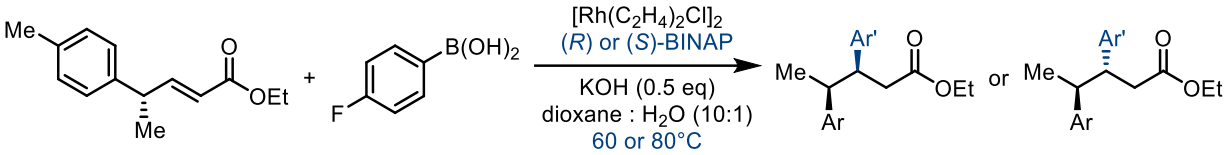

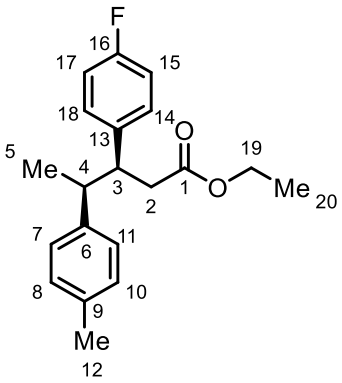

(+)-Ethyl (3*S*,4*S*)-3-(4-fluorophenyl)-4-(*p*-tolyl)pentanoate 2-13

$[Rh(C_2H_4)_2Cl]_2$ (1.9 mg, 0.005 mmol, 0.025 equiv.) and (*S*)-BINAP (7.5 mg, 0.012 mmol, 0.06 equiv.) were dissolved in dioxane (1.0 mL, 0.2 M) and stirred for 10 minutes. KOH (1 M/H_2O, 0.10 mL, 0.10 mmol, 0.5 equiv.) was added; the mixture was stirred for further 5 minutes and transferred into a flask containing (4-fluoro)phenylboronic acid **2-7b** (84.0 mg, 0.60 mmol, 3.0 equiv.). (−)-Ethyl (*S,E*)-4-(*p*-tolyl)pent-2-enoate *E*-**2-10d** (43.7 mg, 0.20 mmol, 1.0 equiv.) was added and the reaction mixture was stirred at 60 °C for 14 h. The reaction was quenched with hexane (5 mL) and filtered through a plug of silica. The solvent was evaporated in vacuo and the residue was purified by column chromatography to give (+)-ethyl (3*S*,4*S*)-3-(4-fluorophenyl)-4-(*p*-tolyl)pentanoate **2-13** (49.0 mg, 0.16 mmol, 78%) as a colourless oil.

^{1}H NMR (400 MHz, $CDCl_3$) δ 6.98 (dd, *J* = 7.5, 0.8 Hz, 2H, C(Ar)-H x2), 6.86 (m, 6H, C(Ar)-H x6), 3.97 (m, 2H, C(19)-H_2), 3.34 (ddd, *J* = 10.0, 7.2, 5.7 Hz, 1H, C(3)-H), 2.97 (p, *J* = 7.1 Hz, 1H, C(4)-H), 2.76 (dd, *J* = 15.3, 5.7 Hz, 1H, C(2)-H), 2.57 (dd, *J* = 15.3, 10.0 Hz, 1H, C(2)-H), 2.27 (s, 3H, C(12)-H_3), 1.27 (d, *J* = 7.1 Hz, 3H, C(5)-H_3), 1.07 (t, *J* = 7.1 Hz, 3H, C(20)-H_3).

^{13}C NMR (126 MHz, $CDCl_3$) δ 172.4 ((C(1)), 161.4 (d, *J* = 243.9 Hz, C(16)), 140.7 (C(Ar)), 137.4 (d, *J* = 3.2 Hz, C(13)), 135.7 (C(Ar)), 129.9 (d, *J* = 7.8 Hz, C(14) and C(18)), 128.6

(C(Ar) x2), 128.0 (C(Ar) x2), 114.5 (d, *J* = 21.2 Hz, C(15) and C(17)), 60.3 (C(19)), 47.8 (C(3)), 44.5 (C(4)), 38.2 (C(2)), 21.0 (C(12)), 18.8 (C(5)), 14.1 (C(20)).

^{19}F (13C)NMR (470 MHz, $CDCl_3$) δ −116.6.

IR (CH_3Cl film): 3968 (br), 1732 (s), 1605 (m), 1511 (s), 1375 (m), 1219 (s), 1159 (s), 1103 (w), 1017 (w), 834 (m), 756 (s), 668 (w), 629 (w) cm^{-1}.

HRMS (ESI): m/z calculated for $C_{20}H_{23}O_2FNa^+$ $[M+Na]^+$ 337.1574 found 337.1574.

$[\alpha]_D^{25}$ = +25.3 (c = 1.0, $CHCl_3$)

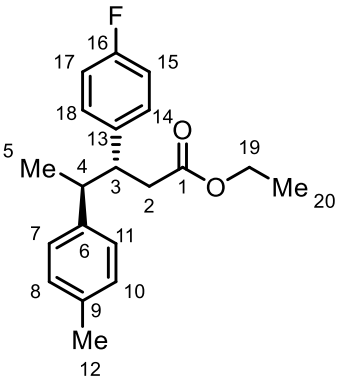

(+)-Ethyl (3*R*,4*S*)-3-(4-fluorophenyl)-4-(*p*-tolyl)pentanoate 2-14

$[Rh(C_2H_4)_2Cl]_2$ (3.9 mg, 0.010 mmol, 0.05 equiv.) and (*R*)-BINAP (14.9 mg, 0.024 mmol, 0.12 equiv.) were dissolved in dioxane (1.0 mL, 0.2 M) and stirred for 10 minutes. KOH (1 M/H_2O, 0.10 mL, 0.10 mmol, 0.5 equiv.) was added; the mixture was stirred for further 5 minutes and transferred into a flask containing (4-fluoro)phenylboronic acid **2-7b** (84.0 mg, 0.60 mmol, 3.0 equiv.). (−)-Ethyl (*S,E*)-4-(*p*-tolyl)pent-2-enoate *E*-**2-10d** (43.7 mg, 0.20 mmol, 1.0 equiv.) was added and the reaction mixture was stirred at 80 °C for 14 h. The reaction was quenched with hexane (5 mL) and filtered through a plug of silica. The solvent was evaporated in vacuo and the residue was purified by column chromatography to give (+)-ethyl (3*R*,4*S*)-3-(4-fluorophenyl)-4-(*p*-tolyl)pentanoate **2-14** (42.8 mg, 0.14 mmol, 68%) as a colourless oil.

^{1}H NMR (400 MHz, $CDCl_3$) δ 7.19 (m, 2H), 7.12 (m, 4H), 7.00 (m, 2H), 3.84 (q, *J* = 7.2 Hz, 2H), 3.20 (td, *J* = 10.0, 5.6 Hz, 1H), 2.80 (dq, *J* = 10.4, 6.9 Hz, 1H), 2.40 (d, *J* = 2.2 Hz, 1H), 2.38 (d, *J* = 6.4 Hz, 1H), 2.34 (s, 3H), 1.00 (m, 6H).

^{13}C NMR (126 MHz, $CDCl_3$) δ 172.3, 161.6 (d, *J* = 244.1 Hz), 142.1, 138.4 (d, *J* = 3.5 Hz), 136.1, 129.6 (d, *J* = 7.7 Hz), 129.3, 127.4, 115.1 (d, *J* = 21.0 Hz), 60.1, 48.6, 45.5, 40.2, 21.0, 20.6, 14.0.

^{19}F (13C)NMR (470 MHz, $CDCl_3$) δ −116.6.

IR (CH_3Cl film): 2974 (m), 2361 (w), 1733 (s), 1605 (m), 1510 (s), 1455 (m), 1374 (m), 1224 (s), 1159 (s), 1103 (m) cm^{-1}.

HRMS (ESI): m/z calculated for $C_{20}H_{24}O_2F^+$ $[M+H]^+$ 315.1755 found 315.1755.

$[\alpha]_D^{25}$ = +4.5 (c = 1.0, $CHCl_3$)

Absolute stereochemistry was assigned by comparing ^{1}H NMR and $[\alpha]_D$ of **2-14** to those of ethyl (3S,4R)-3,4-diphenylpentanoate.[201]

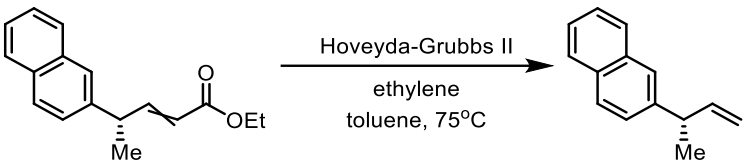

Z-**2-10p** and *E*-**2-10p**
90% *ee*

2-15
84%, 90% *ee*

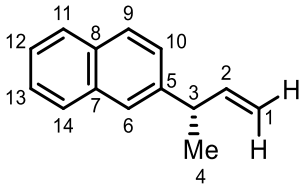

(+)-(*S*)-2-(but-3-en-2-yl)naphthalene 2-15

A mixture of (*S*,*Z*)-and (*S*,*E*)-4-(naphthalen-2-yl)pent-2-enoate *Z*-**2-10p** and *E*-**2-10p** resulting from the Rh-catalysed coupling reaction (0.4 mmol, 1.0 equiv.) was dissolved in toluene (2.0 mL) in a 10 mL ampoule fitted with a Young's valve and Hoveyda-Grubbs II catalyst (12.5 mg, 0.02 mmol, 5 mol%) was added. The ampoule was cycled onto a Schlenk line, carefully evacuated, and then pressurised to 2 Bar with ethylene. The reaction mixture was stirred at 75 °C for 24 h, after which the ampoule was vented carefully. The reaction mixture was diluted with hexane, filtered through a short plug of silica eluting with hexane and concentrated *in vacuo.* Purification by flash column chromatography (hexane, 100%) afforded (+)-(*S*)-2-(but-3-en-2-yl)naphthalene **2-15** (61.2 mg, 0.34 mmol, 84%) as a colourless oil. SFC analysis showed an enantiomeric excess of 90%. Characterisation data match literature reports.[200]

^{1}H NMR (400 MHz, $CDCl_3$) δ 7.80 (ddd, *J* = 8.3, 4.7, 1.9 Hz, 3H, C(Ar)-H x3), 7.65 (dd, *J* = 1.7, 0.9 Hz, 1H, C(Ar)-H), 7.44 (m, 2H, C(Ar)-H x2), 7.37 (dd, *J* = 8.5, 1.8 Hz, 1H, C(Ar)-H), 6.09 (ddd, *J* = 17.2, 10.3, 6.4 Hz, 1H, C(2)-H), 5.10 (m, 2H, C(1)-H x2), 3.64 (p, *J* = 7.0 Hz, 1H, C(3)-H), 1.46 (d, *J* = 7.0 Hz, 3H, C(4)-H_3).

^{13}C NMR (126 MHz, $CDCl_3$) δ 143.1 C(2), 143.0 C(Ar), 133.6 C(Ar), 132.2 C(Ar), 128.0 C(Ar), 127.6 C(Ar), 127.6 C(Ar), 126.3 C(Ar), 125.9 C(Ar), 125.3 C(Ar), 125.2 C(Ar), 113.4 C(1), 43.3 C(3), 20.7 C(4).

IR (CH_3Cl film): 3056 (w), 2928 (w), 1632 (m), 1600 (w), 1506 (m), 1453 (m), 1412 (w), 1373 (w), 1271 (w) cm^{-1}.

HRMS (GC EI MS): m/z calculated for $C_{14}H_{14}^{+}$ $[M]^{+}$ 182.10900 found 182.11142.

SFC: Chiralpak® IG, 1500 psi, 30 °C; flow: 1.0 mL/min; 0% MeOH for 3min; 0% to 10% MeOH over 5 min, 94.8:5.2 e.r. (minor enantiomer t_R = 4.72 min, major enantiomer t_R = 4.38 min).

$[\alpha]_D^{25}$ = +10.6 (c = 1.0, $CHCl_3$) (Lit[56].: $[\alpha]_D^{28}$ = +12.6 (*ee* = 96%, c = 1.0, $CHCl_3$)).

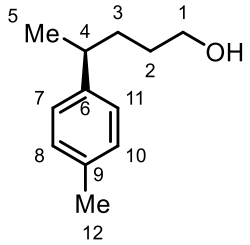

(+)-(*S*)-4-(*p*-tolyl)pentan-1-ol 2-16

$LiAlH_4$ (0.44 mL, 0.88 mmol, 2.2 eq, 2.0 M solution in THF) was added to a solution of ethyl (+)-(*S*)-4-(*p*-tolyl)pentanoate *red*-**2-10d** (81.7 mg, 0.40 mmol, 1.0 equiv.) in THF (1.10 mL) at 0 °C and the mixture was refluxed for 5 hours. Reaction mixture was cooled to 0 °C and diluted with EtOAc. The reaction was quenched by slow addition of water and 10% NaOH. Organic and aqueous layers were separated and aqueous layer was extracted with Et_2O (x3). Combined organic phases were washed with brine and dried over Na_2SO_4. The solvent was evaporated in vacuo and the residue was purified by column chromatography to give (+)-(*S*)-4-(*p*-tolyl)pentan-1-ol **2-16** (62.4 mg, 0.35 mmol, 88%) as a colourless liquid. SFC analysis showed an enantiomeric excess of 96%. Characterisation data match literature reports.[202]

^{1}H NMR (400 MHz, $CDCl_3$) δ 7.11 (m, 4H, C(Ar)-H x4), 3.59 (t, *J* = 6.5 Hz, 2H, C(1)-H_2), 2.68 (h, *J* = 7.0 Hz, 1H, C(4)-H), 2.33 (s, 3H, C(12)-H_3), 1.63 (m, 2H, C(2)-H_2), 1.48 (m, 2H, C(3)-H_2), 1.26 (dd, *J* = 6.9, 1.1 Hz, 3H, C(5)-H_3).

^{13}C NMR (101 MHz, $CDCl_3$) δ 144.3 (C(6)), 135.4 (C(9)), 129.1 (C(Ar) x2), 126.9 (C(Ar) x2), 63.1 (C(1)), 39.4 (C(4)), 34.4 (C(2)), 31.0 (C(3)), 22.5 (C(5)), 21.0 (C(12)).

IR (CH_3Cl film): 3334 (br), 2955 (s), 2930 (s), 2870 (s), 1515 (s), 1455 (m), 1059 (s), 1023 (m), 816 (s), 757 (s) cm^{-1}.

HRMS (ESI): m/z calculated for $C_{12}H_{18}ONa^+$ $[M+Na]^+$ 201.1250 found 201.1250.

SFC: Chiralpak® IG, 1500 psi, 30 °C; flow: 1.0 mL/min; 1% to 30% MeOH over 5 min, 97.8:2.2 e.r. (minor enantiomer t_R = 3.69 min, major enantiomer t_R = 3.59 min).

$[\alpha]_D^{25}$ = +15.4 (c = 1.0, $CHCl_3$) (Lit[115].: $[\alpha]_D^{28}$ = +14.6 (c = 0.7, $CHCl_3$)).

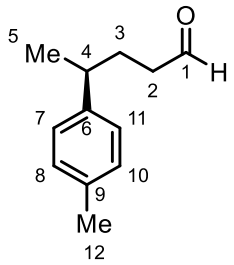

(+)-(*S*)-4-(*p*-tolyl)pentanal S6

(+)-(*S*)-4-(*p*-tolyl)pentan-1-ol **2-16** (28.7 mg, 0.16 mmol, 1.0 equiv.) in CH_2Cl_2 (0.6 mL) was added to a solution of Dess-Martin periodinane (81.8 mg, 0.19 mmol, 1.2 equiv.) in CH_2Cl_2 (1.0 mL) at 0 °C. The reaction mixture was stirred at ambient temperature (23 °C) for 1 h, then diluted with Et_2O and poured into a solution of sodium thiosulfate in saturated aqueous $NaHCO_3$. The aqueous layer was extracted with Et_2O (x2). Combined organic phases were washed with brine and dried over Na_2SO_4. The solvent was evaporated in vacuo and the residue was purified by column chromatography to (+)-give (*S*)-4-(*p*-tolyl)pentanal **S6** (23.7 mg, 0.13 mmol, 84%) as a colourless oil. Characterisation data match literature reports.[203]

^{1}H NMR (400 MHz, $CDCl_3$) δ 9.68 (t, *J* = 1.6 Hz, 1H, -COH), 7.12 (m, 2H, C(Ar)-H x2), 7.06 (m, 2H C(Ar)-H x2), 2.68 (m, 1H, C(4)-H), 2.32 (m, 5H, C(2)-H and C(12)-H_3), 1.89 (m, 2H, C(3)-H), 1.27 (d, *J* = 6.9 Hz, 3H, C(5)-H_3).

^{13}C NMR (101 MHz, $CDCl_3$) δ 202.5 (C(1)), 143.0 (C(6)), 135.8 (C(9)), 129.2 (C(Ar) x2), 126.9 (C(Ar) x2), 42.2 (C(2)), 38.9 (C(4)), 30.4 (C(3)), 22.4 (C(5)), 21.0 (C(12)).

IR (CH_3Cl film): 3020 (w), 2960 (w), 2926 (w), 2720 (w), 1724 (s), 1515 (w), 1456 (w), 1377 (w), 1217 (w), 1019 (w), 817 (m), 756 (s), 668 (w) cm^{-1}.

HRMS (GC/EI-MS): m/z calculated for $C_{12}H_{16}O^+$ $[M]^+$ 176.11957 found 176.11867.

$[\alpha]_D^{25}$ = +17.4 (c = 1.0, $CHCl_3$) (Lit[203].: $[\alpha]_D^{20}$ = +17.9 (c = 1.4, $CHCl_3$)).

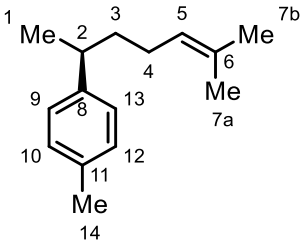

(+)-(*S*)-curcumene 2-17

*n*BuLi (2.5 M in hexane, 0.13 mL, 0.33 mmol, 3.0 equiv.) was added dropwise to a stirred suspension of isopropyltriphenylphosphonium iodide (141.4 mg, 0.33 mmol, 3.0 equiv.) in THF (1.0 mL) at -10 °C. The mixture was stirred at -10 °C for 30 min. (+)-(*S*)-4-(*p*-tolyl)pentanal **S6** (19.2 mg, 0.11 mmol, 1.0 equiv.) in THF (0.5 mL) was added slowly at 0 °C and the resulting mixture was stirred at ambient temperature (23 °C) for 1 h. The reaction was quenched by slow addition of saturated aqueous NH_4Cl. The aqueous layer was extracted with Et_2O (x3). Combined organic phases were washed with brine and dried over Na_2SO_4. The solvent was evaporated in vacuo and the residue was purified by column chromatography to give (+)-(*S*)-curcumene **2-17** (17.4 mg, 0.086 mmol, 79%) as a colourless oil. SFC analysis showed an enantiomeric excess of 96%. Characterisation data match literature reports.[204]

^{1}H NMR (500 MHz, $CDCl_3$) δ 7.09 (m, 4H, C(Ar)-H x4), 5.10 (tt, *J* = 7.2, 1.5 Hz, 1H, C(5)-H), 2.66 (h, *J* = 7.0 Hz, 1H, C(2)-H), 2.32 (s, 3H, C(14)-H_3), 1.88 (m, *J* = 7.4 Hz, 2H, C(4)-H_2), 1.68 (s, 3H, C(7b)-H_3), 1.59 (m, 2H), 1.53 (s, 3H, C(7a)-H_3), 1.22 (d, *J* = 6.9 Hz, 3H, C(1)-H_3).

^{13}C NMR (126 MHz, $CDCl_3$) δ 144.7 (C(8)), 135.2 (C(11)), 131.4 (C(6)), 129.0 (C(Ar)-H x2), 126.9 (C(Ar)-H x2), 124.6 (C(5)), 39.0 (C(2)), 38.5 (C(3)), 26.2 (C(4)), 25.7 (C(7b)), 22.5 (C(14)), 21.0 (C(1)), 17.7 (C(7a)).

IR (CH_3Cl film): 3657 (w), 2981 (s), 2926 (m), 2888 (m), 1733 (w), 1514 (w), 1455 (w), 1380 (m), 1252 (w), 1217 (w), 1152 (w), 1073 (w), 955 (w), 816 (w), 757 (s), 668 (w) cm^{-1}.

HRMS (GC/EI-MS): m/z calculated for $C_{15}H_{22}^+$ $[M]^+$ 202.17160 found 202.17255.

SFC: Chiralpak® ID, 1500 psi, 30 °C; flow: 1.0 mL/min; 0% MeOH for 3 min, 0% to 10% MeOH over 5 min, 97.9:2.1 e.r. (minor enantiomer t_R = 2.08 min, major enantiomer t_R = 2.19 min).

$[\alpha]_D^{25}$ = +42.2 (c = 1.0, $CHCl_3$) (Lit[78].: $[\alpha]_D^{25}$ = +44.6 (c = 1.0, $CHCl_3$)).

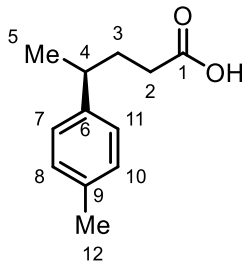

(+)-(*S*)-4-(*p*-tolyl)pentanoic acid S7

A solution LiOH (38.3 mg, 1.60 mmol, 4 equiv.) in water (0.10 mL) was added to of ethyl (+)-(*S*)-4-(*p*-tolyl)pentanoate *red*-**2-10d** (81.7 mg, 0.40 mmol, 1.0 equiv.) in THF (0.20 mL) and MeOH (0.10 mL) at 0 °C. The reaction mixture was stirred at 50 °C for 3h. The reaction was quenched by slow addition of 1 M HCl solution at 0 °C. The aqueous layer was extracted with Et_2O (x3). Combined organic phases were washed with brine and dried over Na_2SO_4. The solvent was evaporated in vacuo and the residue was purified by column chromatography to give (+)-(*S*)-4-(*p*-tolyl)pentanoic acid **S7** (59.0 mg, 0.31 mmol, 77%) as a pale-yellow oil. Characterisation data match literature reports.[205]

^{1}H NMR (400 MHz, $CDCl_3$) δ 7.13 (d, *J* = 8.1 Hz, 2H, C(Ar)-H x2), 7.09 (d, *J* = 8.2 Hz, 2H, C(Ar)-H x2), 2.71 (m, 1H, C(4)-H), 2.34 (s, 3H, C(12)-H_3), 2.25 (m, 2H, C(2)-H_2), 1.91 (m, 2H, C(3)-H_2), 1.28 (d, *J* = 6.9 Hz, 3H, C(5)-H_3).

^{13}C NMR (101 MHz, $CDCl_3$) δ 180.3 (C(1)), 143.0 (C(6)), 135.8 (C(9)), 129.2 (C(Ar) x2), 126.9 (C(Ar) x2), 38.9 (C(4)), 33.0 (C(2)), 32.4 (C(3)), 22.3 (C(12)), 21.0 (C(5)).

IR (CH_3Cl film): 2960 (w), 2926 (w), 1707 (s), 1515 (w), 1455 (w), 1414 (w), 1285 (w), 940 (w), 818 (m), 757 (m) cm^{-1}.

HRMS (ESI): m/z calculated for $C_{12}H_{15}O_2^-$ $[M-H]^-$ 191.1078 found 191.1071.

$[\alpha]_D^{25}$ = +15.6 (c = 1.0, $CHCl_3$) (Lit[205].: $[\alpha]_D^{25}$ = +14.2 (c = 1.0, $CHCl_3$)).

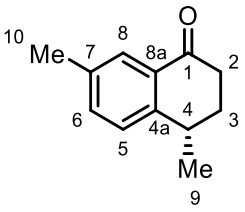

(−)-(*S*)-4,7-dimethyl-1-tetralone 2-19

A solution of trifluoroacetic anhydride (0.17 mL, 1.23 mmol, 4.0 equiv.) and trifluoroacetic acid (0.17 mL, 2.15 mmol, 7.0 equiv.) was added to (+)-(*S*)-4-(*p*-tolyl)pentanoic acid **S7** (59.0 mg, 0.31 mmol, 1.0 equiv.) at 0 °C. The reaction mixture was stirred at ambient temperature (23 °C) for 10 h, then saturated aqueous $NaHCO_3$ was added to the reaction mixture at 0 °C. The aqueous layer was extracted with Et_2O (x3). Combined organic phases were washed with brine and dried over Na_2SO_4. The solvent was evaporated in vacuo and the residue was purified by column chromatography to give (−)-(*S*)-4,7-dimethyl-1-tetralone **2-19** (35.6 mg, 0.20 mmol, 66%) as a colourless oil. SFC analysis showed an enantiomeric excess of 96%. Characterisation data match literature reports.[206]

^{1}H NMR (400 MHz, $CDCl_3$) δ 7.84 (d, *J* = 1.3 Hz, 1H, C(8)-H), 7.33 (ddd, *J* = 7.9, 2.0, 0.7 Hz, 1H, C(6)-H), 7.23 (d, *J* = 7.9 Hz, 1H, C(5)-H), 3.06 (pd, *J* = 7.1, 4.2 Hz, 1H, C(4)-H), 2.78 (ddd, *J* = 17.4, 8.5, 4.5 Hz, 1H, C(2)-H), 2.58 (ddd, *J* = 17.3, 8.8, 4.8 Hz, 1H, C(2)-H), 2.36 (s, 3H, C(10)-H_3), 2.23 (ddt, *J* = 13.2, 8.5, 4.6 Hz, 1H, C(3)-H), 1.88 (dddd, *J* = 13.4, 8.9, 7.4, 4.6 Hz, 1H, C(3)-H), 1.38 (d, *J* = 7.0 Hz, 3H, C(9)-H_3).

^{13}C NMR (126 MHz, $CDCl_3$) δ 198.7 (C(1)), 146.1 (C(8a)), 136.2 (C(4a)), 134.6 (C(Ar)), 131.6 (C(7)), 127.4 (C(Ar) x2), 36.5 (C(2)), 32.5 (C(4)), 30.7 (C(3)), 20.9 (C(10)), 20.7 (C(9)).

HRMS (ESI): m/z calculated for $C_{12}H_{15}O^+$ $[M+H]^+$ 175.1117 found 175.1117.

IR (CH_3Cl film): 3023 (w), 2927 (w), 1684 (s), 1612 (w), 1495 (w), 1458 (w), 1409 (w), 1304 (m), 1181 (m), 943 (w), 817 (w), 754 (w) cm^{-1}.

SFC: Chiralpak® IG, 1500 psi, 30 °C; flow: 1.0 mL/min; 0% MeOH for 3 min, 0% to 6% MeOH over 3 min, 6% to 9% MeOH over 10 min, 98:2 e.r. (minor enantiomer t_R = 7.66 min, major enantiomer t_R = 7.72 min).

$[\alpha]_D^{25}$ = −9.3 (c = 1.0, $CHCl_3$) (Lit[205].: $[\alpha]_D^{25}$ = −10.0 (c = 1.0, $CHCl_3$)).

5.3.4 Reaction optimisation

5.3.4.1 Screening of reaction additives

Table 5.1 Additive screening.

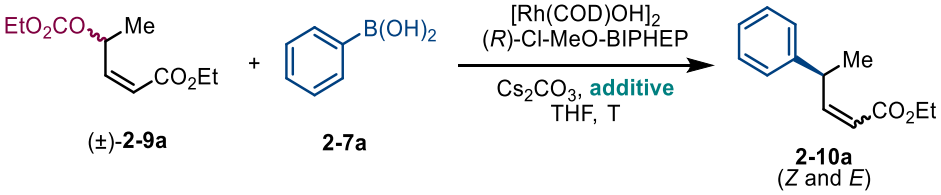

Entry	Additive	T (°C)	*ee* of ***Z*** / %	NMR yield of ***Z*** / %	NMR yield of ***E*** / %	Total yield /%	Ratio (***Z*:*E***)	SM / %
1	AgOTf	60	98	29	7	36	4.1 : 1	58
2	$Er(OTf)_3$	60	97	65	24	89	2.7 : 1	0
3	$Yt(OTf)_3$	60	97	62	25	87	2.5 : 1	0
4	$Zn(OTf)_2$	60	97	67	25	92	2.7 : 1	0
5	$ZnCl_2$	60	-	0	0	0	-	85
6	$ZnBr_2$	60	-	0	0	0	-	89
7	ZnI_2	60	-	0	0	0	-	100
8	$ZnCl_2$ (in Et_2O)	60	98	56	19	75	2.9 : 1	26
9	$AgNTf_2$	60	96	57	23	80	2.5 : 1	13
10	$AgSbF_6$	60	98	42	9	51	4.7 : 1	47
11	$AgBF_4$	60	98	50	14	64	3.6 : 1	36
12	$AgPF_6$	60	99	42	11	53	3.8 : 1	43
13	$AgIO_4$	60	-	0	0	0	-	0
14	$AgClO_4$	60	96	57	17	74	3.4 : 1	10
15	TfOH	60	97	55	18	73	3.1 : 1	0
16	$Cu(OTf)_2$	60	97	34	8	42	4.3 : 1	5
17	$Zn(OTf)_2$	r.t.	98	75	19	94	4.0 : 1	0
18	AgOTf	r.t.	98	28	7	36	4.1 : 1	54
19	TfOH	r.t.	97	55	18	73	3.1 : 1	20

Conditions: $[Rh(COD)OH]_2$ (2.5 mol %), (*R*)-Cl-MeO-BIPHEP (6.0 mol %), Cs_2CO_3 (1.0 equiv.), additive (0.2 equiv.), phenylboronic acid (2.0 equiv.), 16 h.

5.3.4.2 *Variation of additive equivalents*

Table 5.2 Effect of $Zn(OTf)_2$ equivalents on the reaction outcome.

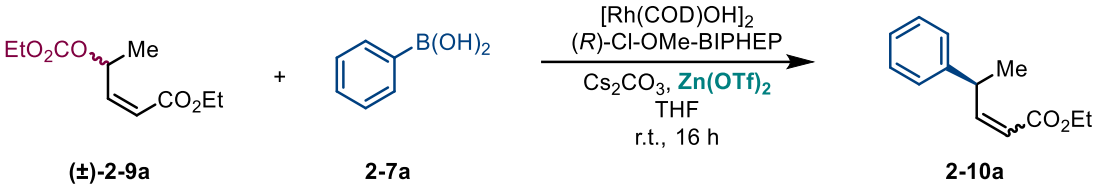

(±)-2-9a **2-7a** **2-10a**

Entry	$Zn(OTf)_2$ equiv.	yield of **2-10a** / %	*ee* of **2-10a** / %	*Z*/*E* of **2-10a**
1	0.1 equiv.	89	97	3.9 : 1
2	0.2 equiv.	94	98	4.0 : 1
3	0.5 equiv.	91	98	3.4 : 1
4	1 equiv.	56	85	2.6 : 1

Reaction conditions: $[Rh(cod)OH]_2$ (2.5 mol %), (*R*)-Cl-MeO-BIPHEP (6.0 mol %), (±)-**2-9a** (0.4 mmol, 1.0 equiv.), **2-7a** (2.0 equiv.), Cs_2CO_3 (1.0 equiv.), $Zn(OTf)_2$, THF (0.1 M), r.t., 16 h. All experiments were performed on 0.20 mmol scale. All compounds were isolated as single regioisomers (rr > 99:1). Enantiomeric ratios were determined by subsequent hydrogenation of the product mixture and SFC analysis on a chiral non-racemic stationary phase.

5.3.4.3 *Variation of base*

Table 5.3 Effect varying base on the reaction outcome.

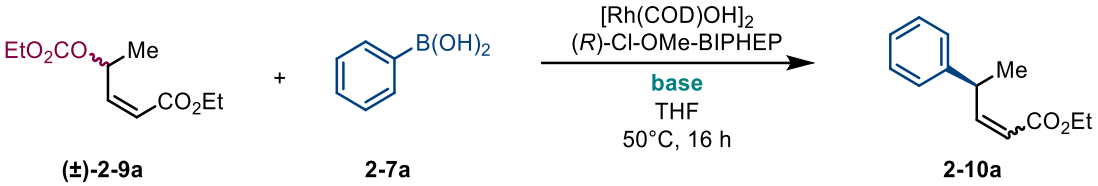

(±)-2-9a **2-7a** **2-10a**

Entry	Base	yield of **2-10a** / %	*ee* of **2-10a** / %	*Z*/*E* of **2-10a**
1	Cs_2CO_3	82	98	3.4 : 1
2	CsOH (50wt% aq.)	5	97	N/A
3	K_3PO_4	63	97	3.2 : 1
4	KOAc	35	96	3.8 : 1
5	NaOMe	25	96	3.2 : 1
6	KO^{t}Bu	18	95	2.5 : 1
7	KOH	19	95	3.7 : 1
8	NEt_3	0	N/A	N/A

Reaction conditions: $[Rh(cod)OH]_2$ (2.5 mol %), (*R*)-Cl-MeO-BIPHEP (6.0 mol %), (±)-**2-9a** (0.4 mmol, 1.0 equiv.), **2-7a** (2.0 equiv.), base (1.0 equiv.), THF (0.1 M), 50 °C, 16 h. All experiments were performed on 0.20 mmol scale. All compounds were isolated as single regioisomers (rr > 99:1). Enantiomeric ratios were determined by subsequent hydrogenation of the product mixture and SFC analysis on a chiral non-racemic stationary phase.

5.3.5 Procedures for the synthesis of substrates for mechanistic studies

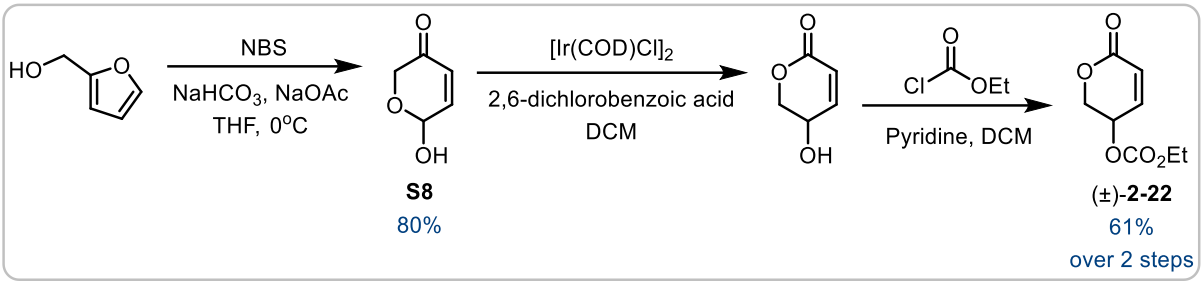

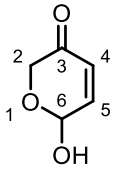

6-hydroxy-2*H*-pyran-3(6*H*)-one S8

Following a procedure by Waldmann[207], NBS (4.58 g, 25.7 mmol, 1.05 equiv.) was added to a solution of furfuryl alcohol (2.13 mL, 24.5 mmol, 1.0 equiv.), $NaHCO_3$ (4.12 g, 49.0 mmol, 2.0 equiv.) and NaOAc (2.01 g, 24.5 mmol, 1.0 equiv.) in THF/H_2O (4/1, 40 mL) at 0 °C. After 10 min, the reaction mixture was extracted with EtOAc (x3). The combined organic phases were dried over Na_2SO_4, filtered and concentrated *in vacuo*. Purification by automated medium-pressure chromatography (EtOAc/hexane = 10/90 to 60/40) afforded 6-hydroxy-2*H*-pyran-3(6*H*)-one **S8** (2.24 g, 19.6 mmol, 80%) as a white solid. Characterisation data match literature reports.[208]

^{1}H NMR (400 MHz, $CDCl_3$) δ 6.95 (dd, *J* = 10.4, 3.0 Hz, 1H, C(5)-H), 6.16 (dd, *J* = 10.4, 1.1 Hz, 1H, C(4)-H), 5.63 (m, 1H, C(6)-H), 4.56 (dd, *J* = 16.9, 1.1 Hz, 1H, C(2)-H), 4.13 (dd, *J* = 16.5, 0.8 Hz, 1H, C(2)-H), 3.53 (br s, 1H, -OH).

^{13}C NMR (101 MHz, $CDCl_3$) δ 195.2 (C(3)), 146.4 (C(5)), 127.7 (C(4)), 88.2 (C(6)), 66.6 (C(2)).

HRMS (ESI): m/z calculated for $C_5H_5O_3^-$ $[M-H]^-$ 113.0244 found 113.0244.

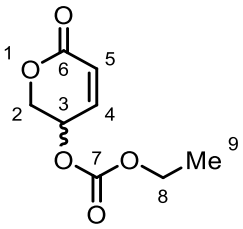

ethyl (6-oxo-3,6-dihydro-2*H*-pyran-3-yl) carbonate (±)-2-22

Following a procedure by Tang[209], 6-hydroxy-2*H*-pyran-3(6*H*)-one **S8** (2.24 g, 19.6 mmol, 1.0 equiv.), [Ir(COD)Cl_2] (329.7 mg, 0.50 mmol, 0.025 equiv.) and 2,6-dichlorobenzoic acid (1.88 mg, 9.8 mmol, 0.5 equiv.) were dissolved in anhydrous $CHCl_3$ (196 mL) under argon. The reaction mixture was stirred at room temperature (23 °C) for 3 hours and the solvent was removed under reduced pressure. Purification by automated medium-pressure chromatography (EtOAc/hexane = 20/80 to 80/20) afforded 5-hydroxy-5,6-dihydro-2*H*-pyran-2-one (1.95 g, 17.1 mmol, 87%) as a yellow oil.

5-hydroxy-5,6-dihydro-2*H*-pyran-2-one (1.95 mg, 17.1 mmol, 1.0 equiv.) and ethyl chloroformate (1.79 mL, 18.8 mmol, 1.1 equiv.) were dissolved in dry CH_2Cl_2 (85 mL). Pyridine (1.65 mL, 20.5 mmol, 1.2 equiv.) was added dropwise at 0 °C. The reaction mixture was stirred at room temperature (23 °C) for 4 hours and then quenched with 1M $KHSO_4$ solution. The aqueous layer was extracted with DCM (x3). Combined organic layers were washed with saturated aqueous $NaHCO_3$ and brine, dried over Na_2SO_4, filtered and concentrated *in vacuo*. Purification by medium-pressure automated flash chromatography (EtOAc/hexane = 10/90 to 60/40) afforded ethyl ethyl (6-oxo-3,6-dihydro-2*H*-pyran-3-yl) carbonate (±)-**2-22** (2.08 g, 11.2 mmol, 70%) as a yellow oil.

^{1}H NMR (400 MHz, $CDCl_3$) δ 6.95 (ddt, *J* = 9.9, 4.8, 0.8 Hz, 1H, C(4)-H), 6.20 (ddt, *J* = 9.8, 1.7, 0.7 Hz, 1H, C(5)-H), 5.22 (dtt, *J* = 4.6, 3.8, 0.8 Hz, 1H, C(3)-H), 4.55 (dt, *J* = 3.8, 0.8 Hz, 2H, C(2)-H_2), 4.23 (qt, *J* = 7.1, 1.1 Hz, 2H, C(8)-H_2), 1.32 (tt, *J* = 7.1, 1.1 Hz, 3H, C(9)-H_3).

^{13}C NMR (101 MHz, $CDCl_3$) δ 161.6 (C(6)), 154.1 (C(7)), 140.4 (C(4)), 124.9 (C(5)), 68.8 (C(3)), 64.9 (C(2) and C(8)), 14.1 (C(9)).

IR (CH_3Cl film): 2982 (w), 1734 (s), 1372 (m), 1250 (s), 1103 (m), 1061 (m), 1006 (m), 841 (m), 788 (m) cm^{-1}.

HRMS (ESI): m/z calculated for $C_8H_{10}O_5Na^+$ $[M+Na]^+$ 209.0420 found 209.0421.

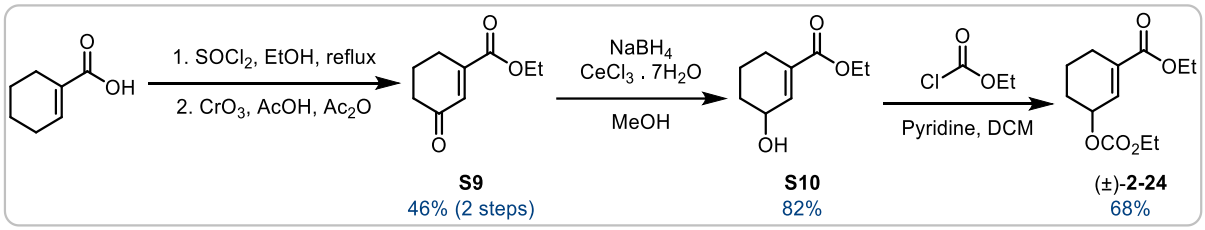

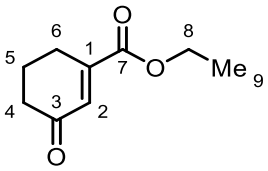

ethyl 3-oxocyclohex-1-ene-1-carboxylate S9

Thionyl chloride (0.18 mL, 2.5 mmol, 0.5 equiv.) was added to a solution of cyclohex-1-ene-1-carboxylic acid (0.57 mL, 5.0 mmol, 1.0 equiv.) in anhydrous EtOH (10 mL). The reaction mixture was refluxed for 5 hours and concentrated *in vacuo*. Filtration through a plug of silica afforded ethyl cyclohex-1-ene-1-carboxylate (740.2 mg, 4.8 mmol, 96%) as a colourless oil, and it was used in the next step without further purification.

A solution of CrO_3 (1.32 g, 13.2 mmol, 2.8 equiv.) in acetic acid (2.75 mL) and acetic anhydride (1.25 mL) was added to a solution of ethyl ethyl cyclohex-1-ene-1-carboxylate (740.2 mg, 4.8 mmol, 1.0 equiv.) in DCM (9.6 mL) dropwise at 0 °C. The reaction mixture was stirred at room temperature (23 °C) for 2 hours and then quenched with 1M KOH solution at 0 °C. The aqueous layer was extracted with DCM (x3). Combined organic layers were washed with water and brine, dried over Na_2SO_4, filtered and concentrated *in vacuo*. Purification by medium-pressure automated flash chromatography (Et_2O/hexane = 10/90 to 50/50) afforded ethyl 3-oxocyclohex-1-ene-1-carboxylate **S9** (384.4 mg, 2.3 mmol, 48%) as a colourless oil. Characterisation data match literature reports.[210]

^{1}H NMR (400 MHz, $CDCl_3$) δ 6.74 (t, *J* = 1.9 Hz, 1H, C(2)-H), 4.27 (q, *J* = 7.1 Hz, 2H, C(8)-H_2), 2.58 (td, *J* = 6.0, 1.9 Hz, 2H, C(4)-H_2), 2.45 (m, 2H, C(6)-H_2), 2.06 (m, 2H, C(5)-H_2), 1.32 (t, *J* = 7.1 Hz, 3H, C(9)-H_3).

^{13}C NMR (101 MHz, $CDCl_3$) δ 200.2 (C(3)), 166.5 (C(7)), 149.2 (C(1)), 132.9 (C(2)), 61.7 (C(8)), 37.7 (C(4)), 24.8 (C(6)), 22.2 (C(5)), 14.1 (C(9)).

HRMS (ESI): m/z calculated for $C_9H_{13}O_3^+$ $[M+H]^+$ 169.0859 found 169.0860.

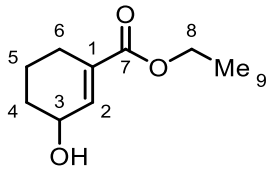

ethyl 3-hydroxycyclohex-1-ene-1-carboxylate S10

A solution of $NaBH_4$ (86.5 g, 2.3 mmol, 1.0 equiv.) in MeOH (5 mL) was added to a solution of ethyl 3-oxocyclohex-1-ene-1-carboxylate **S9** (384.4 mg, 2.3 mmol, 1.0 equiv.) and $CeCl_3 \cdot 7H_2O$ (600.0 mg, 2.3 mmol, 1.0 equiv.) in MeOH (10 mL) dropwise at 0 °C. The reaction mixture was stirred at room temperature (23 °C) for 2 hours and then quenched with 1M HCl solution at 0 °C. The aqueous layer was extracted with Et_2O (x3). Combined organic layers were washed with brine, dried over Na_2SO_4, filtered and concentrated *in vacuo*. Purification by medium-pressure automated flash chromatography (EtOAc/hexane = 0/100 to 40/60) afforded ethyl 3-hydroxycyclohex-1-ene-1-carboxylate **S10** (321.0 mg, 1.9 mmol, 82%) as a colourless oil. Characterisation data match literature reports.[211]

^{1}H NMR (400 MHz, $CDCl_3$) δ 6.86 (dtd, *J* = 2.7, 1.9, 0.7 Hz, 1H, C(2)-H), 4.35 (d, *J* = 8.4 Hz, 1H, C(3)-H), 4.19 (q, *J* = 7.1 Hz, 2H, C(8)-H_2), 2.25 (m, 2H, C(6)-H_2), 1.86 (m, 3H, C(4)-H_3 and -OH), 1.58 (m, 2H, C(5)-H_2), 1.28 (t, *J* = 7.1 Hz, 3H, C(9)-H_3).

^{13}C NMR (101 MHz, $CDCl_3$) δ 167.3 (C(7)), 139.5 (C(2)), 132.7 (C(1)), 66.0 (C(3)), 60.6 (C(8)), 31.2 (C(6)), 24.2 (C(4)), 19.1 (C(5)), 14.2 (C(9)).

HRMS (ESI): m/z calculated for $C_9H_{15}O_3^+$ $[M+H]^+$ 171.1016 found 171.1016.

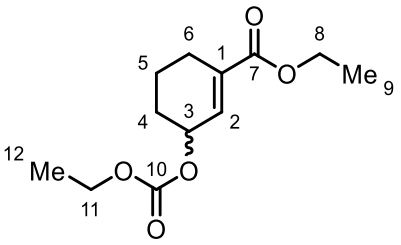

ethyl 3-((ethoxycarbonyl)oxy)cyclohex-1-ene-1-carboxylate (±)-2-24

Ethyl 3-hydroxycyclohex-1-ene-1-carboxylate **S10** (321.0 mg, 1.9 mmol, 1.0 equiv.) and ethyl chlorofomate (0.20 mL, 2.1 mmol, 1.1 equiv.) were dissolved in DCM (15 mL). Pyridine (0.18 mL, 2.3 mmol, 1.2 equiv.) was added dropwise at 0 °C. The mixture was stirred at room temperature (23 °C) for 3 hours and then quenched with 1M $KHSO_4$ solution. The aqueous layer was extracted with DCM (x3). Combined organic layers were washed with saturated aqueous $NaHCO_3$ and brine, dried over Na_2SO_4, filtered and concentrated *in vacuo* at 0 °C. Purification by medium-pressure automated flash chromatography (EtOAc/hexane = 0/100 to 55/45) afforded ethyl 3-((ethoxycarbonyl)oxy)cyclohex-1-ene-1-carboxylate (±)-**2-24** (313.0 mg, 1.3 mmol, 68%) as a colourless oil.

^{1}H NMR (400 MHz, $CDCl_3$) δ 6.85 (dt, *J* = 3.7, 2.0 Hz, 1H, C(2)-H), 5.25 (dt, *J* = 8.5, 3.2 Hz, 1H, C(3)-H), 4.20 (d x2, *J* = 7.1 Hz, 4H, C(8)-H_2 and C(11)-H_2), 2.33 (m, 1H, C(6)-H), 2.23 (m, 1H, C(6)-H), 1.93 (m, 1H, C(4)-H), 1.74 (m, 3H, C(4)-H and C(5)-H_2), 1.29 (t x2, *J* = 7.1 Hz, 6H, C(9)-H_3 and C(12)-H_3).

^{13}C NMR (101 MHz, $CDCl_3$) δ 166.7 (C(7)), 154.7 (C(10)), 135.1 (C(1)), 134.4 (C(2)), 71.5 (C(3)), 64.1 (C(11)), 60.7 (C(8)), 27.5 (C(6)), 24.1 (C(4)), 18.8 (C(5)), 14.3 (C(9)), 14.2 (C(12)).

IR (CH_3Cl film): 2982 (w), 1742 (s), 1716 (s), 1373 (w), 1235 (s), 1084 (m), 1013 (m), 941 (w), 874 (w), 791 (m), 749 (m) cm^{-1}.

HRMS (ESI): m/z calculated for $C_{12}H_{18}O_5Na^+$ $[M+Na]^+$ 265.1046 found 265.1045.

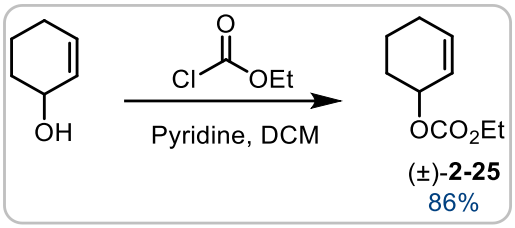

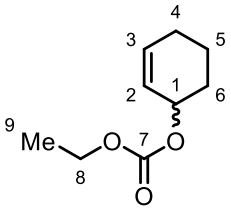

cyclohex-2-en-1-yl ethyl carbonate (±)-2-25

Cyclohex-2-en-1-ol (294.4 mg, 3.0 mmol, 1.0 equiv.) and ethyl chlorofomate (0.31 mL, 3.3 mmol, 1.1 equiv.) were dissolved in DCM (15 mL). Pyridine (0.29 mL, 3.6 mmol, 1.2 equiv.) was added dropwise at 0 °C. The mixture was stirred at room temperature (23 °C) for 2 hours and then quenched with 1M $KHSO_4$ solution. The aqueous layer was extracted with DCM (x3). Combined organic layers were washed with saturated aqueous $NaHCO_3$ and brine, dried over Na_2SO_4, filtered and concentrated *in vacuo* at 0 °C. Purification by medium-pressure automated flash chromatography (EtOAc/hexane = 10/90 to 60/40) afforded cyclohex-2-en-1-yl ethyl carbonate (±)-**2-25** (439.1 mg, 2.58 mmol, 86%) as a colourless oil. Characterisation data match literature reports.[212]

^{1}H NMR (500 MHz, $CDCl_3$) δ 5.96 (dddd, *J* = 10.1, 4.3, 3.4, 1.2 Hz, 1H, C(2)-H), 5.77 (ddt, *J* = 10.1, 4.1, 2.2 Hz, 1H, C(3)-H), 5.11 (tdq, *J* = 5.2, 3.3, 1.7 Hz, 1H, C(1)-H), 4.18 (q, *J* = 7.1 Hz, 2H, C(8)-H_2), 2.08 (m, 1H), 1.98 (m, 1H), 1.82 (m, 3H), 1.63 (m, 1H), 1.30 (t, *J* = 7.1 Hz, 3H, C(9)-H_3).

^{13}C NMR (126 MHz, $CDCl_3$) δ 154.9 (C(7)), 133.3 (C(2)), 125.0 (C(3)), 71.6 (C(1)), 63.7 (C(8)), 28.2 (C(6)), 24.8 (C(4)), 18.6 (C(5)), 14.3 (C(9)).

HRMS (ESI): m/z calculated for $C_9H_{14}O_3Na^+$ $[M+Na]^+$ 193.0835 found 193.0836.

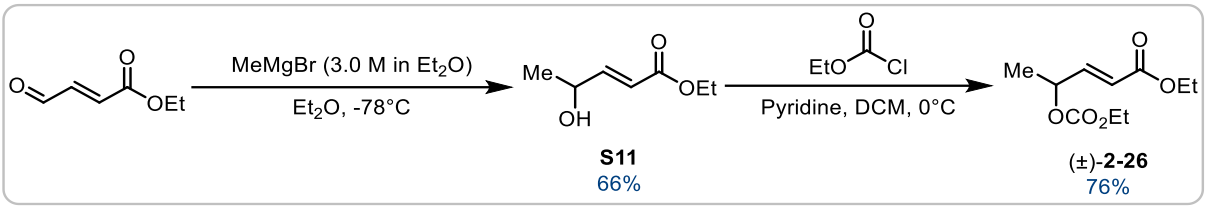

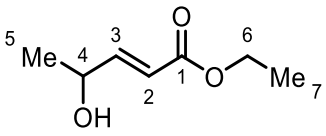

ethyl (E)-4-hydroxypent-2-enoate S11

Following a modified procedure by Fu[213], MeMgBr (3.0 M in Et2O, 13.3 mL, 44.0 mmol, 1.1 equiv.) was added dropwise to a solution of ethyl (E)-4-oxo-2-butenoate (5.13 g, 40.0 mmol, 1.0 equiv.) in Et_2O (100 mL) at –78 °C. The reaction mixture was stirred at –78 °C for 3 hours. A saturated solution of NH_4Cl was added at 0 °C, and the aqueous layer was extracted with Et_2O (x3). Combined organic layers were washed with brine, dried over Na_2SO_4, filtered and concentrated *in vacuo*. Purification by medium-pressure automated flash chromatography (Et_2O/hexane = 0/100 to 30/70) afforded ethyl (E)-4-hydroxypent-2-enoate **S11** (951.5 mg, 6.6 mmol, 66%) as a colourless oil. Characterisation data match literature reports.[214]

^{1}H NMR (400 MHz, $CDCl_3$) δ 6.96 (dd, *J* = 15.7, 4.7 Hz, 1H, C(3)-H), 6.02 (dd, *J* = 15.7, 1.7 Hz, 1H, C(2)-H), 4.49 (qtd, *J* = 6.6, 4.7, 1.7 Hz, 1H, C(4)-H), 4.20 (q, *J* = 7.1 Hz, 2H, C(6)-H_2), 1.67 (d, *J* = 4.8 Hz, 1H, -OH), 1.34 (d, *J* = 6.6 Hz, 3H, C(5)-H_3), 1.29 (t, *J* = 7.1 Hz, 3H, C(7)-H_3).

^{13}C NMR (126 MHz, $CDCl_3$) δ 166.7 (C(1)), 151.0 (C(2)), 119.6 (C(3)), 67.1 (C(4)), 60.5 (C(6)), 22.7 (C(5)), 14.2 (C(7)).

HRMS (ESI): m/z calculated for $C_7H_{13}O_3^+$ $[M+H]^+$ 145.0859 found 145.0859.

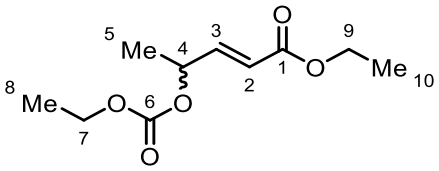

ethyl (*E*)-4-((ethoxycarbonyl)oxy)pent-2-enoate (±)-2-26

Ethyl (*E*)-4-hydroxypent-2-enoate **S11** (778.5 mg, 5.4 mmol, 1.0 equiv.) and ethyl chloroformate (0.57 mL, 5.9 mmol, 1.1 equiv.) were dissolved in DCM (25 mL). Pyridine (0.52 mL, 6.5 mmol, 1.2 equiv.) was added dropwise at 0 °C. The mixture was stirred at room temperature (23 °C) for 5 hours and then quenched with 1M $KHSO_4$ aqueous solution. The aqueous layer was extracted with DCM (x3). Combined organic layers were washed with saturated aqueous $NaHCO_3$ and brine, dried over Na_2SO_4, filtered and concentrated *in vacuo*. Purification by medium-pressure automated flash chromatography (Et_2O/hexane = 0/100 to 20/80) afforded ethyl (*E*)-4-((ethoxycarbonyl)oxy)pent-2-enoate (±)-**2-26** (887.4 mg, 4.10 mmol, 76%) as a colourless oil. Characterisation data match literature reports.[215]

^{1}H NMR (400 MHz, $CDCl_3$) δ 6.85 (dd, *J* = 15.8, 5.1 Hz, 1H, C(3)-H), 5.98 (dd, *J* = 15.8, 1.5 Hz, 1H, C(2)-H), 5.31 (qdd, *J* = 6.7, 5.1, 1.6 Hz, 1H, C(4)-H), 4.17 (q, *J* = 7.1 Hz, 4H, C(7)-H_2 and C(9)-H_2), 1.39 (d, *J* = 6.7 Hz, 3H, C(5)-H_3), 1.28 (t x2, *J* = 7.1 Hz, 6H, C(8)-H_3 and C(10)-H_3).

^{13}C NMR (101 MHz, $CDCl_3$) δ 165.9 (C(1)), 154.2 (C(6)), 145.5 (C(3)), 121.4 (C(2)), 72.5 (C(4)), 64.1 (C(7)), 60.5 (C(9)), 19.7 (C(5)), 14.2 (C(8)), 14.1 (C(10)).

HRMS (ESI): m/z calculated for $C_{10}H_{16}O_5Na^+$ $[M+Na]^+$ 239.0890 found 239.0889.

5.3.6 Mechanistic studies

*5.3.6.1 Reactions of enantiopure substrate (S)-**2-9a***

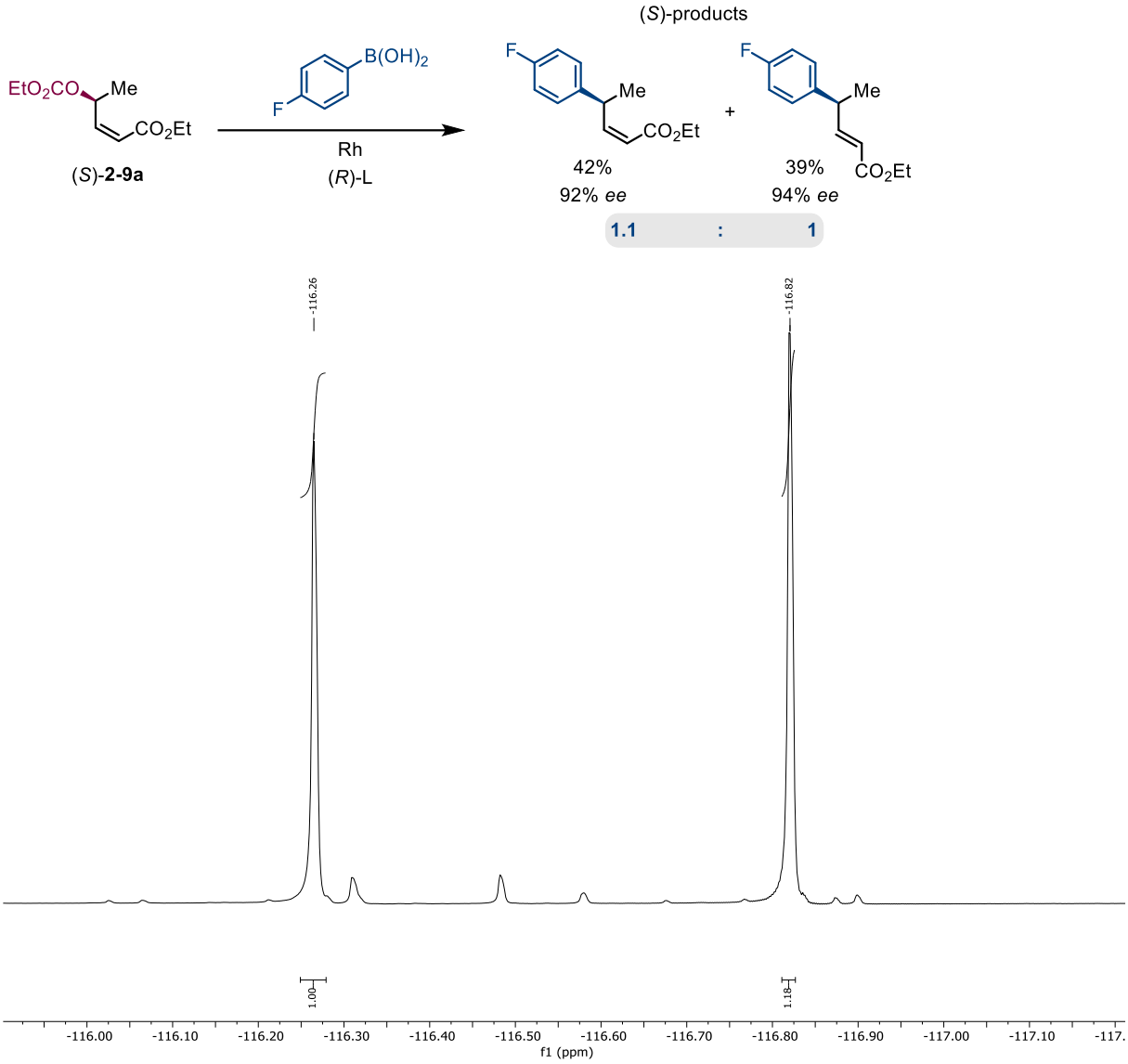

Figure 5.5 ^{19}F (13C)NMR (376 MHz) spectrum of a crude reaction mixture obtained using (*S*)-**2-9a** and (*R*)-Cl-MeO-BIPHEP.

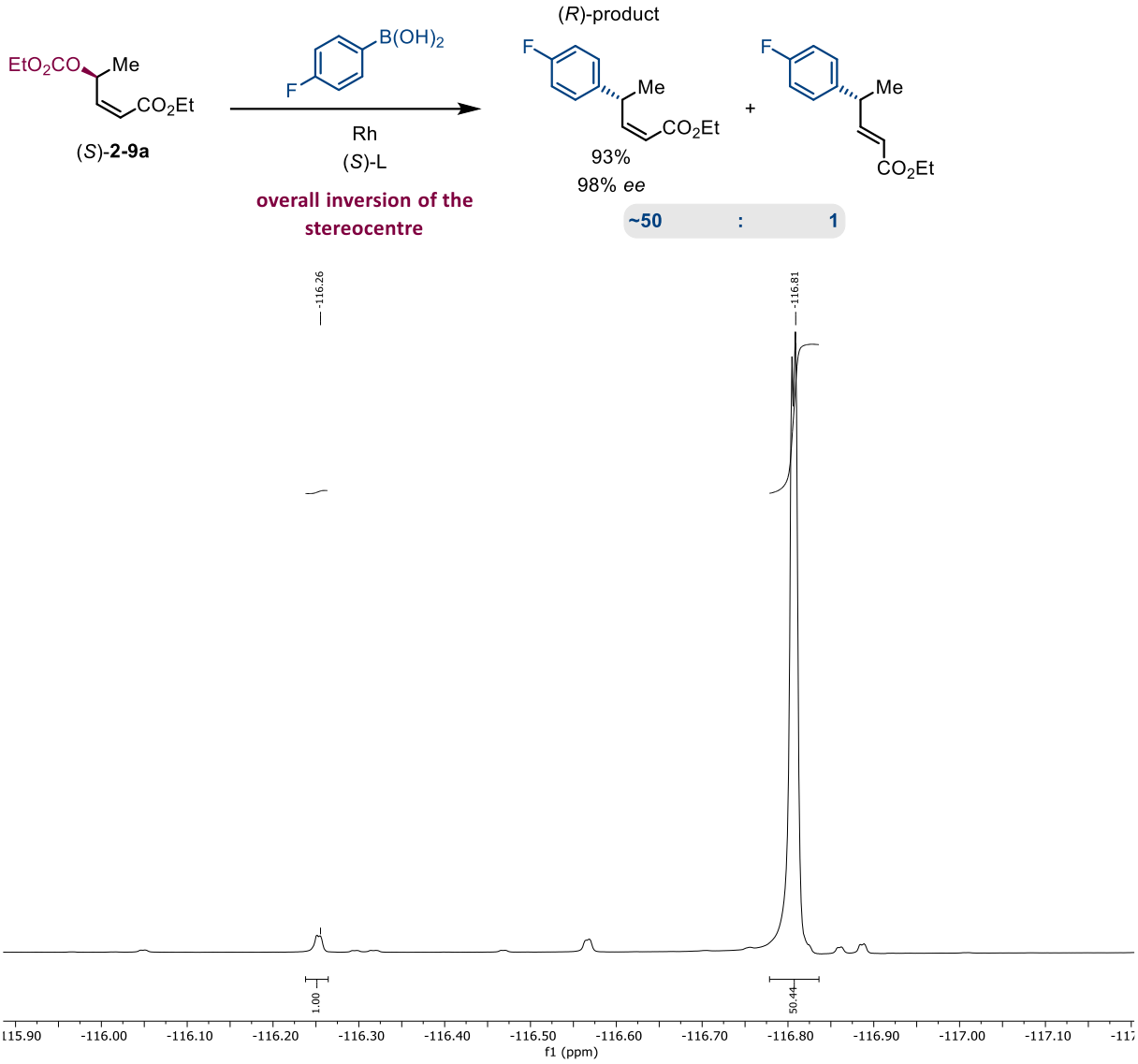

Figure 5.6 ^{19}F (13C)NMR (376 MHz) spectrum of a crude reaction mixture obtained using (*S*)-**2-9a** and (*S*)-Cl-MeO-BIPHEP.

5.3.6.2 (S)- and (R)-ligands result in opposite absolute stereochemistry

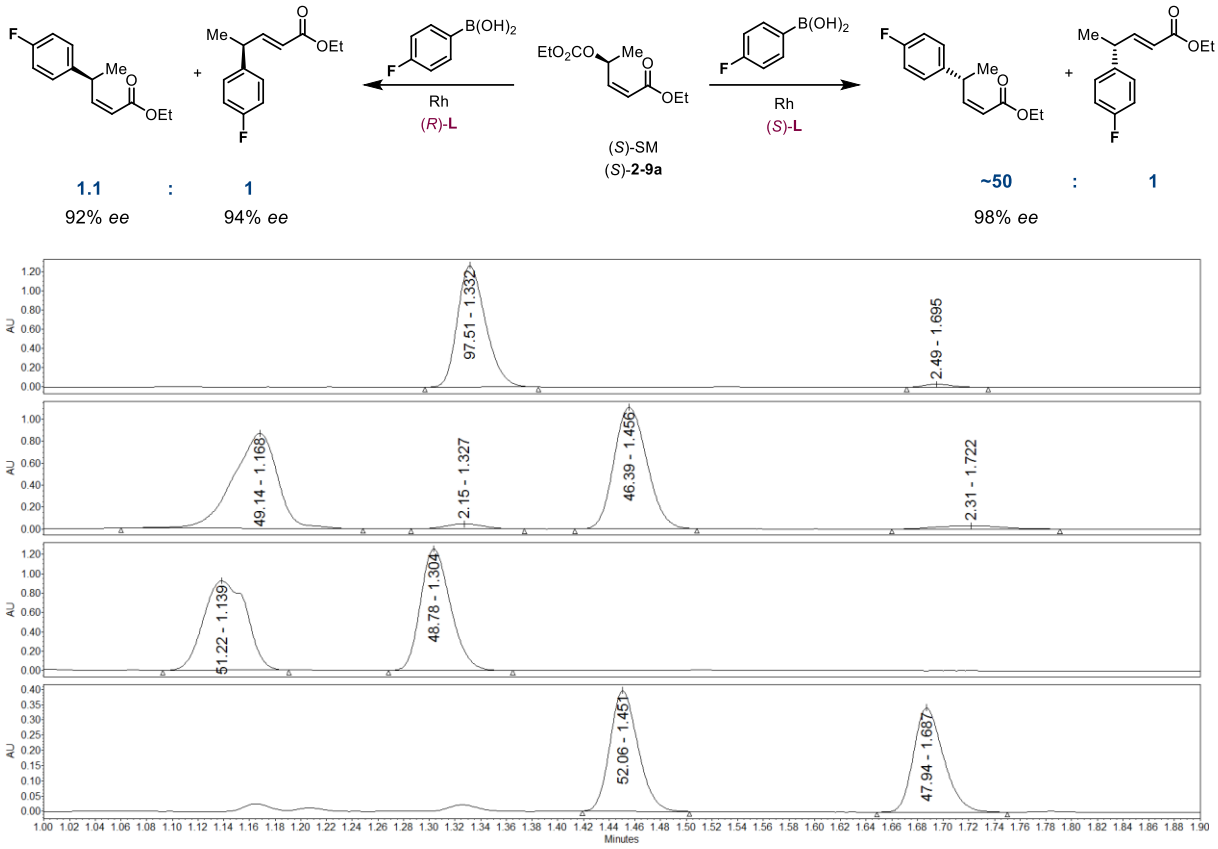

Figure 5.7 SFC traces comparing outcomes of reaction using enantiopure starting material (*S*)-**2-9a** and ligands with opposite absolute stereochemistry. Reaction conditions: $[Rh(cod)OH]_2$ (2.5 mol%), Cl-MeO-BIPHEP (6.0 mol%), (*S*)-**2-9a** (0.4 mmol, 1.0 equiv), **2-7b** (2.0 equiv), Cs_2CO_3 (1.0 equiv), $Zn(OTf)_2$ (20 mol%), THF (0.1 M), r.t., 14 h.

5.3.6.3 Reaction monitoring

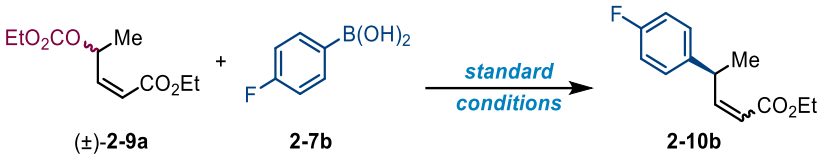

Time / min	Z/E of **3b**	**1**/*Z*-**2-10b**	*ee* of SM / %	Conversion / %
0	N/A	N/A	N/A	N/A
2	6.6	5.2	14	18.1
5	5.9	4.3	18	21.2
15	5.5	3.3	24	26.5
60	5	1.8	36	40.5
180	4.6	0.8	54	59.8
360	4.5	0.2	72	83.6

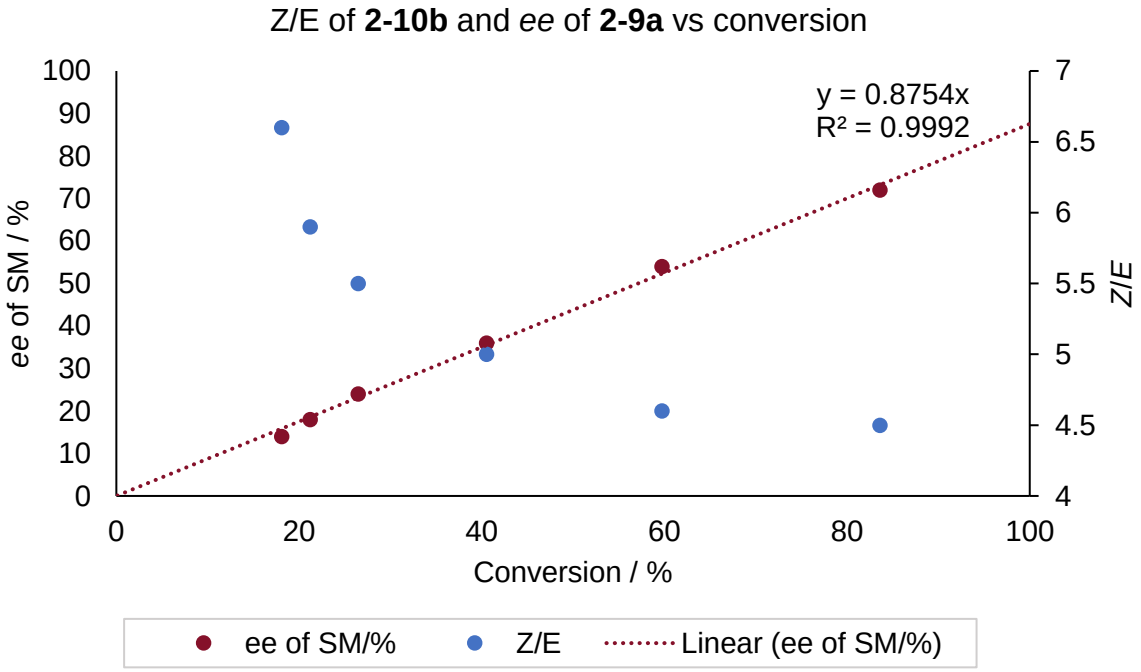

Figure 5.8 Changes of product *Z*/*E* ratio and *ee* of starting material in time. Reaction conditions: $[Rh(cod)OH]_2$ (2.5 mol%), (*R*)-Cl-MeO-BIPHEP (6.0 mol%), (*S*)-**2-9a** (0.4 mmol, 1.0 equiv), **2-7b** (2.0 equiv), Cs_2CO_3 (1.0 equiv), $Zn(OTf)_2$ (20 mol%), THF (0.1 M), r.t.

5.4 Experimental for Chapter 3

5.4.1 Procedures for the synthesis of the starting materials

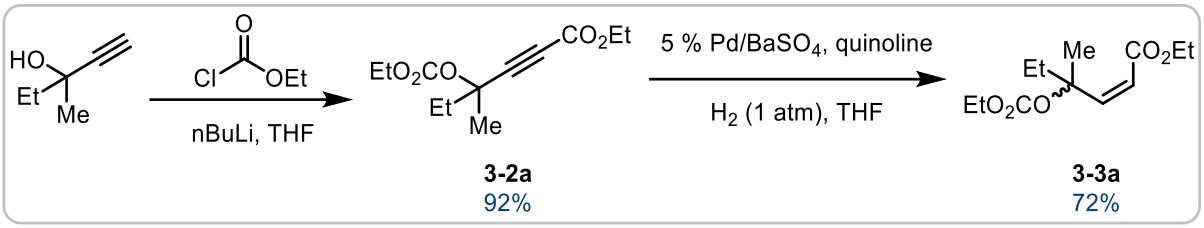

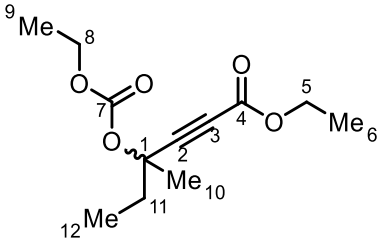

ethyl 4-((ethoxycarbonyl)oxy)-4-methylhex-2-ynoate 3-2a

*n*BuLi (2.5 M in hexane, 18.4 mL, 46.0 mmol, 2.3 eq) was added to a solution of 3-methylpent-1-yn-3-ol (1.96 g, 20.0 mmol, 1.0 eq) in THF (50 mL) at -78 °C. The mixture was stirred at -78 °C for 30 minutes and ethyl chloroformate (4.2 mL, 44.0 mmol, 2.2 eq) was added dropwise. The reaction mixture was stirred at room temperature (23 °C) for 7 hours. A saturated solution of NH_4Cl was added at 0 °C and the aqueous layer was extracted with Et_2O (x3). Combined organic layers were washed with brine, dried over Na_2SO_4, filtered and concentrated *in vacuo*. Purification by automated medium-pressure flash chromatography (gradient of 0 to 20% Et_2O/hexane in 10 minutes) afforded ethyl 4-((ethoxycarbonyl)oxy)-4-methylhex-2-ynoate (4.48 g, 18.5 mmol, 92%) as a yellow oil.

^{1}H NMR (400 MHz, $CDCl_3$) δ 4.18 (q x2, *J* = 7.1 Hz, 4H, C(5)-H_2 and C(8)-H_2), 1.94 (m, 2H, C(11)-H_2), 1.69 (s, 3H, C(10)-H_3), 1.28 (t x2, *J* = 7.1 Hz, 6H, C(6)-H_3 and C(9)-H_3), 1.03 (t, *J* = 7.4 Hz, 3H, C(12)-H_3).

^{13}C NMR (101 MHz, $CDCl_3$) δ 153.2 (C(4) or C(7)), 152.8 (C(4) or C(7)), 85.9 (C(2)), 77.4 (C(3)), 76.4 (C(1)), 63.9 (C(5) or C(8)), 62.1 (C(5) or C(8)), 34.0 (C(11)), 25.1 (C(10)), 14.1 (C(6) or C(9)), 14.0 (C(6) or C(9)), 8.3 (C(12)).

HRMS (ESI): m/z calculated for $C_{12}H_{18}O_5Na^+$ $[M+Na]^+$ 265.1046 found 265.1046.

IR (CH_3Cl film): 2984 (w), 1753 (m), 1714 (m), 1465 (w), 1370 (w), 1304 (w), 1243 (s), 1210 (w), 1160 (w), 1100 (w), 1032 (m), 909 (m), 862 (w), 790 (w), 731 (s), 649 (w) cm^{-1}.

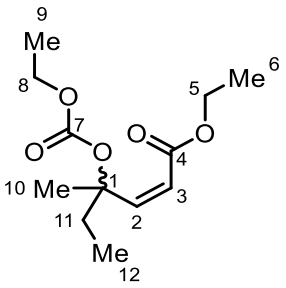

ethyl (*Z*)-4-((ethoxycarbonyl)oxy)-4-methylhex-2-enoate 3-3a

Rosenmund catalyst (Pd on $BaSO_4$, 295.1 mg, 2.8 mmol, 0.15 eq) and quinoline (0.39 mL, 3.3 mmol, 0.18 eq) were suspended in THF (50 mL) and the suspension was purged with hydrogen gas (balloon) for 10 minutes. Then a solution of ethyl 4-((ethoxycarbonyl)oxy)-4-methylhex-2-ynoate (4.48 g, 18.5 mmol, 1.0 eq) was added and the reaction mixture was stirred under an atmosphere of H_2 (balloon) for 4 hours while being monitored. Upon consumption of starting material, the reaction was filtered through a plug of silica eluting with E_2O and concentrated *in vacuo*. Purification by automated medium-pressure flash chromatography (gradient of 0 to 20% Et_2O/hexane in 12 minutes) afforded ethyl (*Z*)-4-((ethoxycarbonyl)oxy)-4-methylhex-2-enoate (3.25 g, 13.2 mmol, 72%) as a colourless oil.

^{1}H NMR (400 MHz, $CDCl_3$) δ 6.19 (d, *J* = 13.2 Hz, 1H, C(2)-H), 5.76 (d, *J* = 13.2 Hz, 1H, C(3)-H), 4.13 (m, 4H, C(5)-H_2 and C(8)-H_2), 2.10 (dq, *J* = 9.4, 7.3 Hz, 2H, C(11)-H_2), 1.71 (s, 3H, C(10)-H_3), 1.28 (t, *J* = 7.1, 3H, C(6)-H_3 or C(9)-H_3), 1.26 (t, *J* = 7.1, 3H, C(6)-H_3 or C(9)-H_3), 0.91 (t, *J* = 7.5 Hz, 3H, C(12)-H_3).

^{13}C NMR (101 MHz, $CDCl_3$) δ 165.7 (C(4)), 153.6 (C(7)), 148.5 (C(2)), 119.1 (C(3)), 85.5 (C(1)), 63.4 (C(5) or C(8)), 60.4 (C(5) or C(8)), 31.6 (C(11)), 22.9 (C(10)), 14.2 (C(6) or C(9)), 14.1 (C(6) or C(9)), 8.1 (C(12)).

HRMS (ESI): m/z calculated for $C_{12}H_{20}O_5Na^+$ $[M+Na]^+$ 267.1203 found 267.1203.

IR (CH_3Cl film): 2983 (w), 1741 (s), 1646 (w), 1463 (w), 1371 (w), 1261 (s), 1185 (s), 1128 (w), 1102 (m), 1031 (m), 913 (m), 856 (w), 794 (w), 732 (s), 649 (w) cm^{-1}.

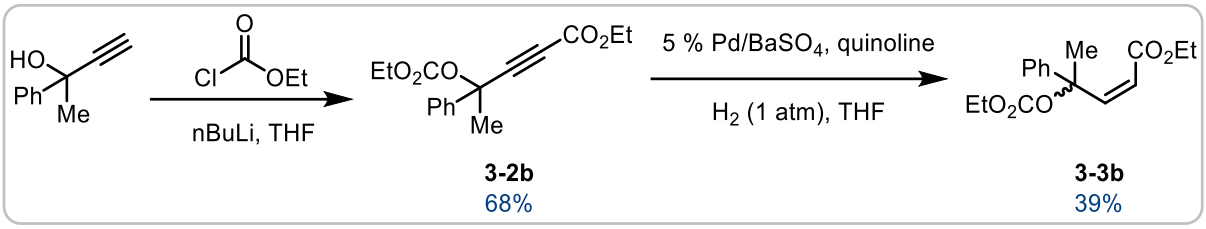

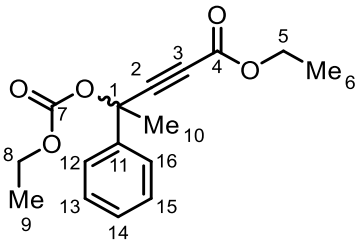

ethyl 4-((ethoxycarbonyl)oxy)-4-phenylpent-2-ynoate 3-2b

*n*BuLi (2.5 M in hexane, 18.4 mL, 46.0 mmol, 2.3 eq) was added to a solution of 2-phenylbut-3-yn-2-ol (2.92 g, 20.0 mmol, 1.0 eq) in THF (50 mL) at -78 °C. The mixture was stirred at -78 °C for 30 minutes and ethyl chloroformate (4.2 mL, 44.0 mmol, 2.2 eq) was added dropwise. The reaction mixture was stirred at room temperature (23 °C) for 6 hours. A saturated solution of NH_4Cl was added at 0 °C and the aqueous layer was extracted with Et_2O (x3). Combined organic layers were washed with brine, dried over Na_2SO_4, filtered and concentrated *in vacuo*. Purification by flash chromatography (Et_2O/hexane) afforded ethyl 4-((ethoxycarbonyl)oxy)-4-phenylpent-2-ynoate (3.95 g, 13.6 mmol, 68%) as an amber oil.

^{1}H NMR (400 MHz, $CDCl_3$) δ 7.58 (m, 2H, C(Ar)-H x2), 7.37 (m, 3H, C(Ar)-H x3), 4.28 (q, *J* = 7.1 Hz, 2H, C(8)-H_2 or C(5)-H_2), 4.14 (m, 2H, C(8)-H_2 or C(5)-H_2), 1.96 (s, 3H, C(10)-H_3), 1.34 (t, *J* = 7.1 Hz, 3H, C(6)-H_3 or C(9)-H_3), 1.27 (t, *J* = 7.1 Hz, 3H, C(6)-H_3 or C(9)-H_3).

^{13}C NMR (101 MHz, $CDCl_3$) δ 153.2 (C(4) or C(7)), 152.4 (C(4) or C(7)), 140.5 (C(Ar)), 128.6 (C(Ar)), 128.6 (C(Ar)), 124.8 (C(Ar)), 85.0 (C(2)), 79.4 (C(3)), 76.9 (C(1)), 64.2 (C(5) or C(8)), 62.3 (C(5) or C(8)), 31.3 (C(10)), 14.1 (C(6) or C(9)), 14.0 (C(6) or C(9)).

HRMS (ESI): m/z calculated for $C_{16}H_{18}O_5Na^+$ $[M+Na]^+$ 313.1046 found 313.1049.

IR (CH_3Cl film): 2988 (w), 1758 (m), 1714 (m), 1448 (m), 1253 (s), 1052 (m), 1029 (m), 1002 (m), 909 (s), 731 (s), 699 (m) cm^{-1}.

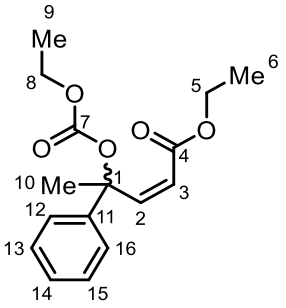

ethyl (*Z*)-4-((ethoxycarbonyl)oxy)-4-phenylpent-2-enoate 3-3b

Rosenmund catalyst (Pd on $BaSO_4$, 217.1 mg, 2.0 mmol, 0.15 eq) and quinoline (0.29 mL, 2.4 mmol, 0.18 eq) were suspended in THF (37 mL) and the suspension was purged with hydrogen gas (balloon) for 10 minutes. Then a solution of ethyl 4-((ethoxycarbonyl)oxy)-4-phenylpent-2-ynoate (3.95 g, 13.6 mmol, 1.0 eq) was added and the reaction mixture was stirred under an atmosphere of H_2 (balloon) for 12 hours while being monitored. Upon consumption of starting material, the reaction was filtered through a plug of silica eluting with E_2O and concentrated *in vacuo*. Purification by automated medium-pressure flash chromatography (gradient of 0 to 20% Et_2O/hexane in 10 minutes) afforded ethyl (*Z*)-4-((ethoxycarbonyl)oxy)-4-phenylpent-2-enoate (1.39 g, 4.8 mmol, 39%) as a colourless oil.

^{1}H NMR (400 MHz, $CDCl_3$) δ 7.51 (m, 2H, C(Ar)-H x2), 7.31 (m, 4H, C(Ar)-H x4), 6.36 (d, *J* = 12.9 Hz, 1H, C(2)-H), 5.86 (d, *J* = 12.9 Hz, 1H, C(3)-H), 4.07 (q, *J* = 7.2 Hz, 2H, C(5)-H_2 or C(8)-H_2), 4.00 (q, *J* = 7.2 Hz, 1H, C(5)-H_2 or C(8)-H_2), 2.12 (s, 3H, C(10)-H_3), 1.24 (t, *J* = 7.1 Hz, 3H, C(6)-H_3 or C(9)-H_3), 1.16 (t, *J* = 7.1 Hz, 3H, C(6)-H_3 or C(9)-H_3).

^{13}C NMR (101 MHz, $CDCl_3$) δ 165.9 (C(4) or C(7)), 152.8 (C(4) or C(7)), 145.0 (C(2)), 141.5 (C(11), 128.0 (C(Ar) x2), 127.9 (C(14)), 126.3 (C(Ar) x2), 120.1 (C(3)), 84.5 (C(1)), 63.5 (C(5) or C(8)), 60.5 (C(5) or C(8)), 24.5 (C(10)), 14.2 (C(6) or C(9)), 13.9 (C(6) or C(9)).

HRMS (ESI): m/z calculated for $C_{16}H_{20}O_5Na^+$ $[M+Na]^+$ 315.1203 found 315.1206.

IR (CH_3Cl film): 1745 (m), 1371 (m), 1264 (w), 1056 (w), 908 (s), 730 (s), 699 (w), 649 (w) cm^{-1}.

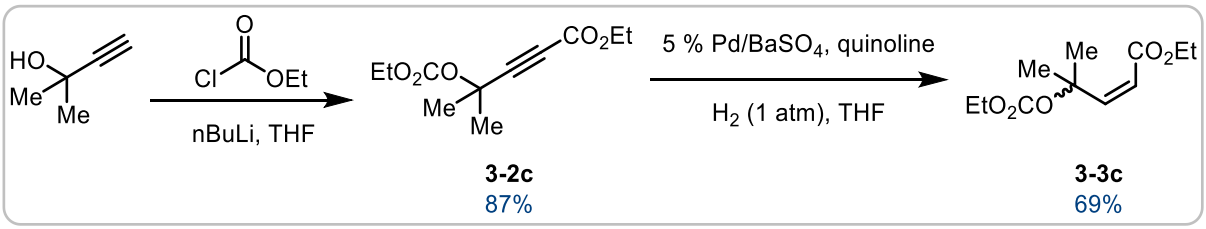

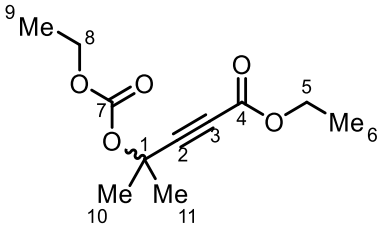

ethyl 4-((ethoxycarbonyl)oxy)-4-methylpent-2-ynoate 3-2c

*n*BuLi (2.5 M in hexane, 18.4 mL, 46.0 mmol, 2.3 eq) was added to a solution of 2-methyl-3-butyn-2-ol (1.94 mL, 1.68 g, 20.0 mmol, 1.0 eq) in THF (50 mL) at -78 °C. The mixture was stirred at -78 °C for 30 minutes and ethyl chloroformate (4.2 mL, 44.0 mmol, 2.2 eq) was added dropwise. The reaction mixture was stirred at room temperature (23 °C) for 9 hours. A saturated solution of NH_4Cl was added at 0 °C and the aqueous layer was extracted with Et_2O (x3). Combined organic layers were washed with brine, dried over Na_2SO_4, filtered and concentrated *in vacuo*. Purification by automated medium-pressure flash chromatography (gradient of 0 to 10% Et_2O/hexane in 10 minutes) afforded ethyl 4-((ethoxycarbonyl)oxy)-4-methylpent-2-ynoate (3.97 g, 17.4 mmol, 87%) as a light-yellow oil.

^{1}H NMR (400 MHz, $CDCl_3$) δ 4.20 (q, *J* = 7.2 Hz, 2H, C(5)-H_2 or C(8)-H_2), 4.18 (q, *J* = 7.2 Hz, 2H, C(5)-H_2 or C(8)-H_2), 1.71 (s, 6H, C(10)-H_3 and C(11)-H_3), 1.30 (t, *J* = 7.1, 2H, C(6)-H_3 or C(9)-H_3), 1.28 (t, *J* = 7.1, 2H, C(6)-H_3 or C(9)-H_3)).

^{13}C NMR (101 MHz, $CDCl_3$) δ 153.3 (C(4) or C(7)), 152.7 (C(4) or C(7)), 86.6 (C(2)), 76.4 (C(3)), 72.8 (C(1)), 64.0 (C(5) or C(8)), 62.1 (C(5) or C(8)), 28.1 (C(10) and C(11)), 14.2 (C(6) or C(9))., 14.0 (C(6) or C(9)).

HRMS (ESI): m/z calculated for $C_{11}H_{16}NaO_5^+$ $[M+Na]^+$ 251.0890 found 251.0897.

IR (CH_3Cl film): 2990 (w), 1754 (s), 1715 (s), 1469 (w), 1369 (w), 1254 (s), 1224 (m), 1194 (w), 1141 (m), 1100 (w), 1033 (w), 1002 (w), 847 (w), 790 (w), 752 (w) cm^{-1}.

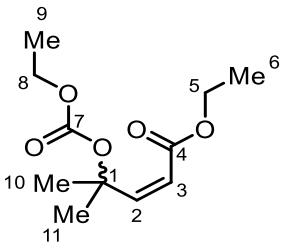

ethyl (*Z*)-4-((ethoxycarbonyl)oxy)-4-methylpent-2-enoate 3-3c

Rosenmund catalyst (Pd on $BaSO_4$, 277.8 mg, 2.6 mmol, 0.15 eq) and quinoline (0.37 mL, 3.1 mmol, 0.18 eq) were suspended in THF (47 mL) and the suspension was purged with hydrogen gas (balloon) for 10 minutes. Then a solution of ethyl 4-((ethoxycarbonyl)oxy)-4-methylpent-2-ynoate **3-00** (3.97 g, 17.4 mmol, 1.0 eq) was added and the reaction mixture was stirred under an atmosphere of H_2 (balloon) for 2 hours while being monitored. Upon consumption of starting material, the reaction was filtered through a plug of silica eluting with E_2O and concentrated *in vacuo*. Purification by automated medium-pressure flash chromatography (gradient of 0 to 20% Et_2O/hexane in 12 minutes) afforded ethyl (*Z*)-4-((ethoxycarbonyl)oxy)-4-methylpent-2-enoate **3-00** (2.76 g, 12.0 mmol, 69%) as a colourless oil.

^{1}H NMR (400 MHz, $CDCl_3$) δ 6.29 (d, *J* = 13.1 Hz, 1H, C(2)-H), 5.72 (d, *J* = 13.1 Hz, 1H, C(3)-H), 4.14 (q x2, *J* = 7.1 Hz, 4H, C(5)-H_2 and C(8)-H_2), 1.72 (s, 6H, C(10)-H_3 and C(11)-H_3), 1.27 (t x2, *J* = 7.1 Hz, 6H, C(6)-H_3 and C(9)-H_3).

^{13}C NMR (101 MHz, $CDCl_3$) δ 165.6 (C(4)), 153.5 (C(7)), 149.4 (C(2)), 118.6 (C(3)), 82.9 (C(1)), 63.4 (C(5) or C(8)), 60.4 C(5) or C(8)), 25.7 (C(10) and C(11)), 14.2 (C(6) or C(9)), 14.1 (C(6) or C(9)).

HRMS (ESI): m/z calculated for $C_{11}H_{19}O_5^+$ $[M+H]^+$ 231.1227 found 231.1231.

IR (CH_3Cl film): 2984 (w), 1742 (s), 1725 (s), 1649 (w), 1467 (w), 1414 (w), 1370 (w), 1266 (s), 1225 (w), 1181 (s), 1130 (m), 1100 (m), 1029 (w), 1002 (w), 845 (w), 794 (w) cm^{-1}.

5.4.2 Procedures for the rhodium-catalysed reactions

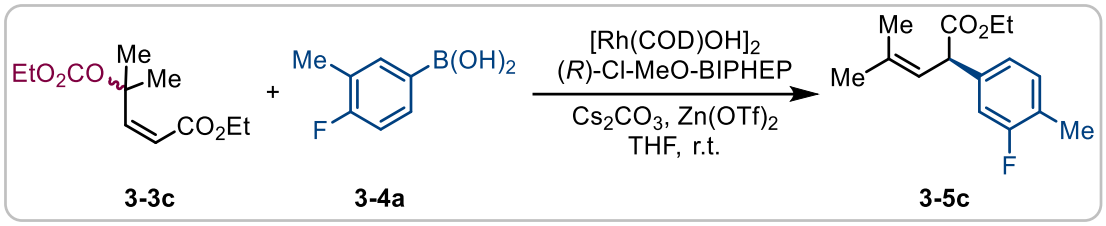

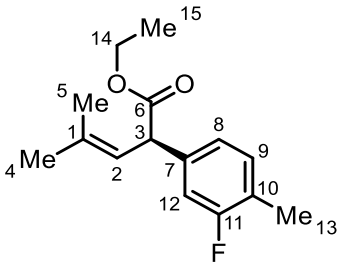

Ethyl (*R*)-2-(3-fluoro-4-methylphenyl)-4-methylpent-3-enoate 3-5c

[Rh(cod)OH]$_2$ (4.6 mg, 0.010 mmol, 2.5 mol%) and (*R*)-Cl-MeO-BIPHEP (15.6 mg, 0.024 mmol, 6.0 mol%) were added to 7 mL vial containing a stirring bar and dissolved in dry THF (4.0 mL) under an argon atmosphere at ambient temperature (23 °C). This solution was stirred for 5 minutes.

(4-fluoro-3-methylphenyl)boronic acid (61.6 mg, 0.40 mmol, 1.0 equiv.), Cs_2CO_3 (130.3 mg, 0.40 mmol, 1.0 equiv.) and Zn(OTf)$_2$ (29.1 mg, 0.08 mmol, 0.2 equiv.) were added to a 7 mL vial containing a stirring bar. To this vial a stock solution of the rhodium hydroxy complex (4.0 mL) was added *via* syringe under an argon atmosphere. Ethyl (*Z*)-4-((ethoxycarbonyl)oxy)-4-methylpent-2-enoate **3-3c** (92.1 mg, 0.40 mmol, 1.0 equiv.) was added *via* microsyringe and the reaction mixture was stirred at ambient temperature (23 °C) for 14 hours.

The mixture was diluted with hexane (4.0 mL) and filtered through a plug of silica. The crude was loaded onto Chem Tube-Hydromatrix and automated medium-pressure chromatography (Et$_2$O/hexane = 0/100 to 20/80) was performed to afford ethyl (*R*)-2-(3-fluoro-4-methylphenyl)-4-methylpent-3-enoate **3-5c** (44.1 mg, 0.18 mmol, 44%) as a colourless oil.

^{1}H NMR (400 MHz, $CDCl_3$) δ 7.10 (m, 2H, C(Ar)-H x2), 6.93 (dd, *J* = 9.5, 8.4 Hz, 1H), 5.60 (dp, *J* = 9.4, 1.4 Hz, 1H), 4.41 (d, *J* = 9.4 Hz, 1H), 4.13 (m, 2H), 2.25 (d, *J* = 2.1 Hz, 3H), 1.76 (d, *J* = 1.4 Hz, 3H), 1.67 (d, *J* = 1.4 Hz, 3H), 1.23 (t, *J* = 7.1 Hz, 3H).

^{13}C NMR (126 MHz, $CDCl_3$) δ 173.2 (C(00)), 160.4, 135.0, 130.7, 126.5, 124.9, 122.1, 115.0, 60.9, 49.8, 25.9, 18.1, 14.6, 14.1.

^{19}F NMR (471 MHz, $CDCl_3$) δ -120.3.

IR (CH_3Cl film): 2972 (w), 1735 (m), 1509 (w), 1460 (w), 1367 (w), 1270 (m), 1213 (m), 1176 (m), 1127 (w), 1033 (m), 1015 (w), 977 (w), 870 (w), 820 (w), 753 (m), 663 (w) cm^{-1}.

HRMS (ESI): m/z calculated for $C_{15}H_{20}FO_2^+$ $[M+H]^+$ 251.1442 found 251.1441.

5.5 Experimental for Chapter 4

5.5.1 Procedures for the synthesis of starting materials

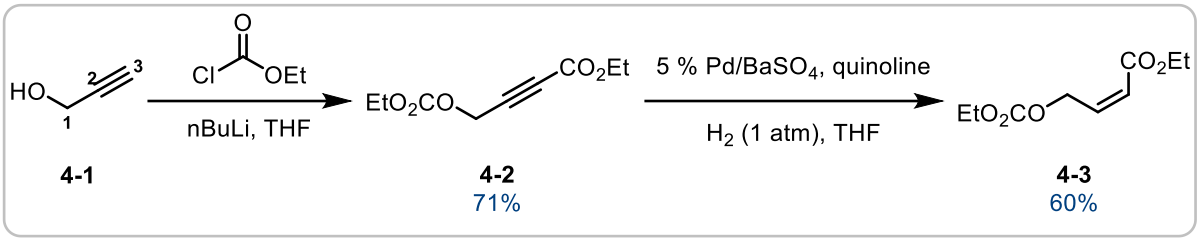

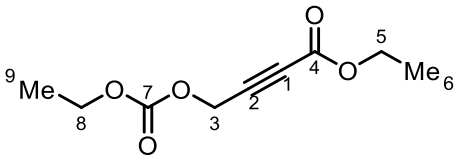

ethyl 4-((ethoxycarbonyl)oxy)but-2-ynoate 4-2

*n*BuLi (2.5 M in hexane, 27.6 mL, 69.0 mmol, 2.3 eq) was added to a solution of prop-2-yn-1-ol (1.73 mL, 30.0 mmol, 1.0 eq) in THF (75 mL) at -78 °C. The mixture was stirred at -78 °C for 30 minutes and ethyl chloroformate (6.3 mL, 66.0 mmol, 2.2 eq) was added dropwise. The reaction mixture was stirred at room temperature (23 °C) for 5 hours. A saturated solution of NH_4Cl was added at 0 °C and the aqueous layer was extracted with Et_2O (x3). Combined organic layers were washed with brine, dried over Na_2SO_4, filtered and concentrated *in vacuo*. Purification by flash chromatography (Et_2O/hexane) afforded ethyl 4-((ethoxycarbonyl)oxy)but-2-ynoate **4-2** (4.26 g, 21.3 mmol, 71%) as a colourless oil. Characterisation data match literature reports.[216]

^{1}H NMR (400 MHz, $CDCl_3$) δ 4.84 (s, 2H, C(3)-H_2), 4.24 (q x2, *J* = 7.1 Hz, 4H, C(5)-H_2 and C(8)-H_2), 1.32 (q, *J* = 7.2 Hz, 6H, C(6)-H_3 and C(9)-H_3).

^{13}C NMR (101 MHz, $CDCl_3$) δ 154.3 (C(4)), 152.8 (C(7)), 80.1 (C(2)), 78.6 (C(1)), 65.0 (C(3)), 62.3 (C(8)), 54.4 (C(5)), 14.2 (C(9)), 14.0 (C(6)).

HRMS (ESI): m/z calculated for $C_9H_{13}O_5^+$ $[M+H]^+$ 201.0758 found 201.0758.

IR (CH_3Cl film: 2939 (w), 1755 (w), 1716 (w), 1380 (w), 1245 (s), 1015 (w), 909 (s), 731 (s), 649 (w) cm^{-1}.

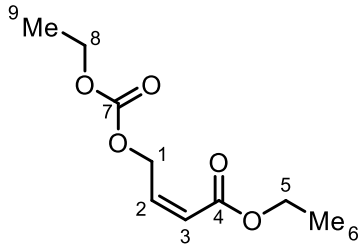

ethyl (*Z*)-4-((ethoxycarbonyl)oxy)but-2-enoate 4-3

Lindlar catalyst (Pd on $CaCO_3$, 340.0 mg, 3.2 mmol, 0.15 eq) and quinoline (0.45 mL, 3.8 mmol, 0.18 eq) were suspended in THF (58 mL, 0.37 M) and the suspension was purged with hydrogen gas (balloon) for 10 minutes. Then a solution of ethyl 4-((ethoxycarbonyl)oxy)but-2-ynoate **4-2** (4.26 g, 21.3 mmol, 1.0 eq) was added and the reaction mixture was stirred under an atmosphere of H_2 (balloon) for 1 hour while being monitored. Upon consumption of starting material, the reaction was filtered through a plug of silica eluting with Et_2O and concentrated *in vacuo*. Purification by automated medium-pressure flash chromatography (gradient of 0 to 15% Et_2O/hexane in 10 minutes) afforded ethyl (*Z*)-4-((ethoxycarbonyl)oxy)but-2-enoate **4-3** (2.58 g, 12.8 mmol, 60%) as a pale-yellow oil. Characterisation data match literature reports.[216]

^{1}H NMR (400 MHz, $CDCl_3$) δ 6.28 (dt, *J* = 11.7, 4.9 Hz, 1H, C(2)-H), 5.85 (dt, *J* = 11.7, 2.4 Hz, 1H, C(3)-H), 5.23 (dd, *J* = 4.9, 2.4 Hz, 2H, C(1)-H_2), 4.19 (q x2, *J* = 7.1 Hz, 4H, C(5)-H_2 and C(8)-H_2), 1.29 (t x2, *J* = 7.1 Hz, 6H, C(6)-H_3 and C(9)-H_3).

^{13}C NMR (101 MHz, $CDCl_3$) δ 165.6 (C(4)), 154.9 (C(7)), 144.1 (C(2)), 120.8 (C(3)), 65.8 (C(1)), 64.2 (C(8)), 60.5 (C(5)), 14.2 (C(9)), 14.2 (C(6)).

HRMS (ESI): m/z calculated for $C_9H_{15}O_5^+$ $[M+H]^+$ 203.0914 found 203.0908.

IR (CH_3Cl film): 2984 (w), 1748 (w), 1718 (w), 1374 (w), 1343 (w), 1269 (m), 1194 (m), 1008 (w), 911 (s), 792 (w), 734 (s), 650 (w) cm^{-1}.

5.5.2 Procedures for the rhodium-catalysed reactions

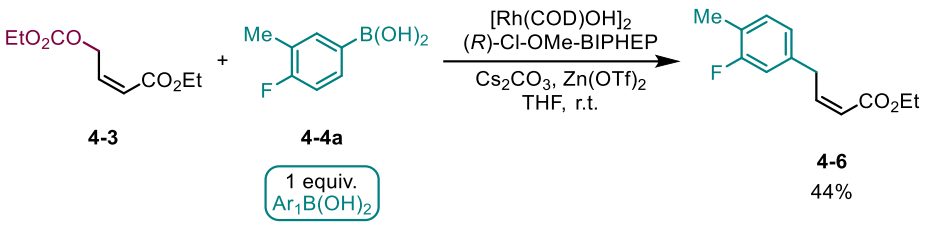

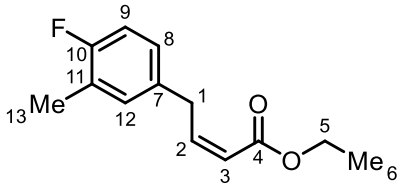

ethyl (*Z*)-4-(4-fluoro-3-methylphenyl)but-2-enoate 4-6

[Rh(cod)OH]$_2$ (4.6 mg, 0.010 mmol, 2.5 mol%) and (*R*)-Cl-MeO-BIPHEP (15.6 mg, 0.024 mmol, 6.0 mol%) were added to 7 mL vial containing a stirring bar and dissolved in dry THF (4.0 mL) under an argon atmosphere at ambient temperature (23 °C). This solution was stirred for 5 minutes.

Cs_2CO_3 (130.3 mg, 0.40 mmol, 1.0 equiv.), (4-fluoro-3-methylphenyl)boronic acid (61.6 mg, 0.40 mmol, 1.0 equiv.) and Zn(OTf)$_2$ (29.1 mg, 0.08 mmol, 0.2 equiv.) were added to a 7 mL vial containing a stirring bar. To this vial a stock solution of the rhodium hydroxy complex (4.0 mL) was added *via* syringe under an argon atmosphere. Ethyl (*Z*)-4-((ethoxycarbonyl)oxy)but-2-enoate **4-3** (80.9 mg, 0.40 mmol, 1.0 equiv.) was added *via* microsyringe and the reaction mixture was stirred at ambient temperature (23 °C) for 14 hours.

The mixture was diluted with hexane (4.0 mL) and filtered through a plug of silica. The crude was loaded onto Chem Tube-Hydromatrix and automated medium-pressure chromatography (Et_2O/hexane = 0/100 to 20/80) was performed to afford ethyl (Z)-4-(4-fluoro-3-methylphenyl)but-2-enoate **4-6** (39.1 mg, 0.18 mmol, 44%) as a colourless oil.

^{1}H NMR (400 MHz, $CDCl_3$) δ 7.01 (m, 2H, C(8)-H and C(12)-H), 6.92 (dd, *J* = 9.5, 8.3 Hz, 1H, C(9)-H), 6.30 (dt, *J* = 11.4, 7.6 Hz, 1H, C(2)-H), 5.84 (dt, *J* = 11.4, 1.8 Hz, 1H, C(3)-H),

4.22 (q, *J* = 7.1 Hz, 2H, C(5)-H_2), 3.95 (ddd, *J* = 7.6, 1.6, 0.8 Hz, 2H, C(1)-H_2), 2.25 (d, *J* = 2.0 Hz, 3H, C(13)-H_3), 1.32 (t, *J* = 7.1 Hz, 3H, C(6)-H_3).

^{13}C NMR (101 MHz, $CDCl_3$) δ 166.4 (C(4)), 160.1 (d, *J* = 242.9 Hz, C(10)), 147.9 (C(2)), 134.8 (d, *J* = 3.6 Hz, C(7)), 131.6 (d, *J* = 5.1 Hz, C(12)), 127.2 (d, *J* = 7.9 Hz, C(8)), 124.8 (d, *J* = 17.3 Hz, C(11)), 119.9 (C(3)), 115.0 (d, *J* = 22.2 Hz, C(9)), 60.0 (C(5)), 34.3 (C(1)), 14.5 (d, *J* = 3.6 Hz, C(13)), 14.3 (C(6)).

^{19}F NMR (376 MHz, $CDCl_3$) δ -121.4.

HRMS (ESI): m/z calculated for $C_{13}H_{16}FO_2^+$ $[M+H]^+$ 223.1129 found 223.1134.

IR (CH_3Cl film): 2984 (w), 1714 (m), 1645 (w), 1503 (m), 1362 (w), 1202 (m), 1166 (m), 1120 (w), 1041 (w), 909 (s), 820 (w), 733 (s) cm^{-1}.

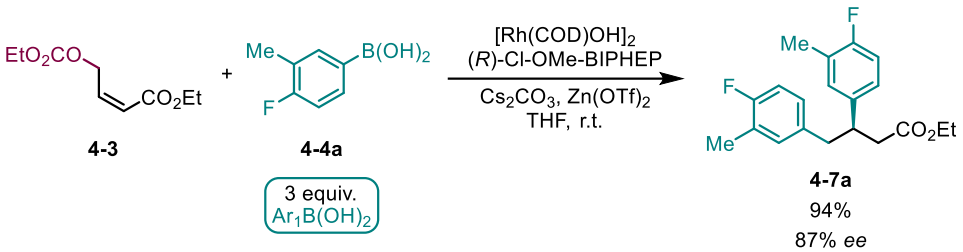

General procedure E (Rhodium-catalysed double arylation):

$[Rh(cod)OH]_2$ (4.6 mg, 0.010 mmol, 2.5 mol%) and (*R*)-Cl-MeO-BIPHEP (15.6 mg, 0.024 mmol, 6.0 mol%) were added to 7 mL vial containing a stirring bar and dissolved in dry THF (4.0 mL) under an argon atmosphere at ambient temperature (23 °C). This solution was stirred for 5 minutes.

Cs_2CO_3 (130.3 mg, 0.40 mmol, 1.0 equiv.), boronic acid (1.20 mmol, 3.0 equiv.) and $Zn(OTf)_2$ (29.1 mg, 0.08 mmol, 0.2 equiv.) were added to a 7 mL vial containing a stirring bar. To this vial a stock solution of the rhodium hydroxy complex (4.0 mL) was added *via* syringe under an argon atmosphere. Ethyl (*Z*)-4-((ethoxycarbonyl)oxy)but-2-enoate **4-3** (80.9 mg, 0.40 mmol, 1.0 equiv.) was added *via* microsyringe and the reaction mixture was stirred at ambient temperature (23 °C) for 14 hours.

The mixture was diluted with hexane (4.0 mL) and filtered through a plug of silica. The crude was loaded onto Chem Tube-Hydromatrix and automated medium-pressure chromatography (Et_2O/hexane = 0/100 to 20/80) was performed to afford products **4-7a**, **4-7b** and **4-7c**.

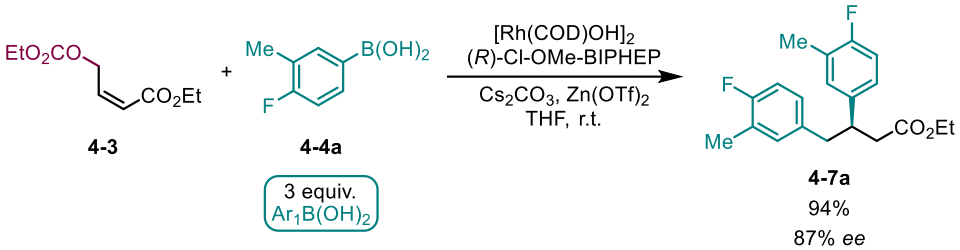

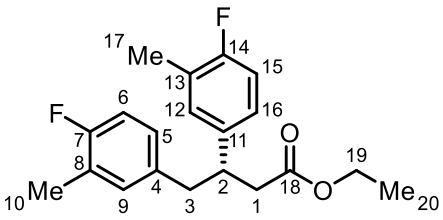

(+)-Ethyl (*S*)-3,4-bis(4-fluoro-3-methylphenyl)butanoate 4-7a

(+)-Ethyl (*S*)-3,4-bis(4-fluoro-3-methylphenyl)butanoate **4-7a** was prepared using General procedure E with 4-fluoro-3-methylphenylboronic acid **4-4a**. Purification by automated medium-pressure chromatography (Et_2O/hexane = 0/100 to 20/80) afforded (+)-ethyl (*S*)-3,4-bis(4-fluoro-3-methylphenyl)butanoate **4-7a** (125.0 mg, 0.38 mmol, 94%) as a colourless oil.

^{1}H NMR (500 MHz, $CDCl_3$) δ 6.87 (m, 5H, C(Ar)-H x5), 6.77 (m, 1H, C(Ar)-H), 4.00 (q, *J* = 7.1 Hz, 2H, C(19)-H_2), 3.29 (m, 1H, C(2)-H), 2.79 (d, *J* = 7.5 Hz, 2H, C(3)-H_2), 2.61 (dd, *J* = 15.4, 6.5 Hz, 1H, C(1)-H), 2.53 (dd, *J* = 15.4, 8.7 Hz, 1H, C(1)-H), 2.22 (d, *J* = 1.9 Hz, 3H, C(10)-H_3 or C(17)-H_3), 2.20 (d, *J* = 1.9 Hz, 3H, C(10)-H_3 or C(17)-H_3), 1.12 (t, *J* = 7.1 Hz, 3H, C(20)-H_3).

^{13}C NMR (126 MHz, $CDCl_3$) δ 172.2, (C(18)), 160.1 (d, *J* = 243.3 Hz, (C(7) or C(14)), 160.0 (d, *J* = 242.8 Hz, C(7) or C(14)), 138.6 (d, *J* = 3.6 Hz, C(4) or C(11)), 134.8 (d, *J* = 3.7 Hz, C(4) or C(11)), 132.1 (d, *J* = 5.0 Hz, C(9) or C(12)), 130.5 (d, *J* = 5.0 Hz, C(9) or C(12)), 127.8 (d, *J* = 7.8 Hz, C(5) or C(16)), 126.1 (d, *J* = 7.8 Hz, C(5) or C(16)), 124.5 (d, *J* = 13.3 Hz, C(8) or C(13)), 124.4 (d, *J* = 13.5 Hz, C(8) or C(13)), 114.7 (d, *J* = 18.7 Hz, C(6) or C(15)), 114.6 (d, *J* = 18.7 Hz, C(6) or C(15)), 60.3 (C(19)), 43.3 (C(2)), 42.2 (C(3)), 40.3 (C(1)), 14.6 (d, *J* = 3.6 Hz, C(10) or C(17)), 14.5 (d, *J* = 3.6 Hz, C(10) or C(17)), 14.1 (C(20)).

^{19}F NMR (470 MHz, $CDCl_3$) δ -120.9, -121.5.

HRMS (ESI): m/z calculated for $C_{20}H_{23}F_2O_2^+$ $[M+H]^+$ 333.1661 found 333.1658.

IR (CH_3Cl film): 2982 (w), 1730 (m), 1605 (w), 1511 (m), 1374 (w), 1250 (m), 1216 (w), 1120 (w), 1038 (w), 910 (s), 834 (m), 735 (s) cm^{-1}.

$\mathbf{[\alpha]_D^{25}}$ = +50.3 (c = 1.0, $CHCl_3$).

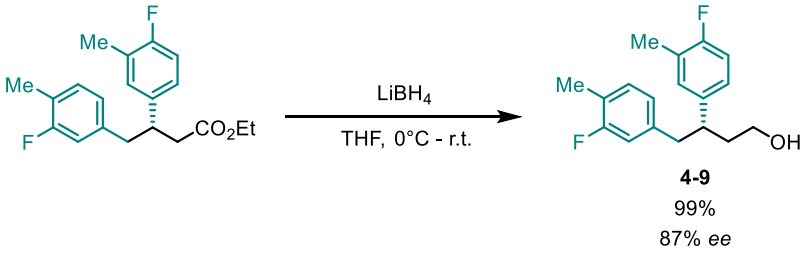

4-9
99%
87% *ee*

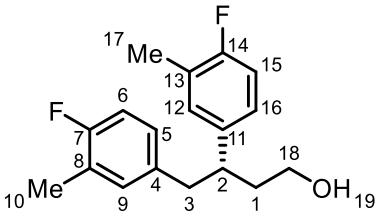

(−)-(*S*)-3,4-bis(4-fluoro-3-methylphenyl)butan-1-ol 4-9

$LiBH_4$ (0.42 mL, 0.84 mmol, 2.2 eq, 2.0 M solution in THF) was added to a solution of ethyl (+)-(*S*)-3,4-bis(4-fluoro-3-methylphenyl)butanoate **4-7a** (125.0 mg, 0.38 mmol, 1.0 equiv.) in THF (1.00 mL) at 0 °C and the mixture was refluxed for 5 hours. Reaction mixture was cooled to 0 °C and diluted with EtOAc. The reaction was quenched by slow addition of water and 10% NaOH. Organic and aqueous layers were separated and aqueous layer was extracted with Et_2O (x3). Combined organic phases were washed with brine and dried over Na_2SO_4. The solvent was evaporated in vacuo and the residue was purified by column chromatography to give (−)-(*S*)-3,4-bis(4-fluoro-3-methylphenyl)butan-1-ol **4-9** (109.2 mg, 0.38 mmol, 99%) as a colourless liquid. SFC analysis showed an enantiomeric excess of 87%.

^{1}H NMR (400 MHz, $CDCl_3$) δ 6.91 (m, 3H, C(Ar)-H x3), 6.85 (m, 2H, C(Ar)-H x2), 6.78 (ddd, *J* = 8.0, 5.0, 2.2 Hz, 1H, C(Ar)-H), 3.54 (m, 1H, C(18)-H), 3.43 (m, 1H, C(18)-H), 2.92 (m, 1H, C(2)-H), 2.80 (d, *J* = 7.4 Hz, 2H, C(3)-H_2), 2.26 (d, *J* = 1.6 Hz, 3H, C(10)-H_3 or C(17)-H_3), 2.22 (d, *J* = 2.0 Hz, 3H, C(10)-H_3 or C(17)-H_3), 1.96 (dddd, *J* = 13.7, 7.8, 7.0, 4.4 Hz, 1H, C(1)-H), 1.81 (dddd, *J* = 13.7, 10.4, 6.4, 5.1 Hz, 1H, C(1)-H), 1.15 (br s, 1H, -OH).

^{13}C NMR (101 MHz, $CDCl_3$) δ 160.0 (d, *J* = 243.0 Hz, C(7) or C(14)), 159.9 (d, *J* = 242.4 Hz, C(7) or C(14)), 139.5 (d, *J* = 3.5 Hz, C(4) or C(11)), 135.5 (d, *J* = 3.7 Hz, C(4) or C(11)), 132.1 (d, *J* = 4.9 Hz, C(9) or C(12)), 130.5 (d, *J* = 5.0 Hz, C(9) or C(12)), 127.7 (d, *J* = 7.7 Hz, C(5) or C(16)), 126.2 (d, *J* = 7.9 Hz, C(5) or C(16)), 124.6 (d, *J* = 17.1 Hz, C(8) or C(13)), 124.2 (d, *J* = 17.2 Hz, C(8) or C(13)), 114.8 (d, *J* = 21.9 Hz, C(6) or C(15)), 114.5 (d, *J* = 22.0

Hz, C(6) or C(15)), 61.0 (C(18)), 43.8 (C(2)), 43.1 (C(3)), 38.1 (C(1)), 14.7 (d, *J* = 3.5 Hz, C(10) or C(17)), 14.5 (d, *J* = 3.6 Hz, C(10) or C(17)).

^{19}F NMR (376 MHz, $CDCl_3$) δ -121.1, -121.9.

HRMS (ESI): m/z calculated for $C_{18}H_{21}F_2O^+$ $[M+H]^+$ 291.1555 found 291.1559.

IR (CH_3Cl film): 3421 (br), 2978 (w), 1604 (w), 1505 (w), 1372 (w), 1255 (m), 1222 (m), 1118 (w), 1042 (w), 914 (s), 830 (w), 731 (s) cm^{-1}.

SFC: Chiralpak® IG, 1500 psi, 30 °C; flow: 1.0 mL/min; 1% to 10% MeOH over 5 min, 93.3:6.7 e.r. (minor enantiomer t_R = 4.89 min, major enantiomer t_R = 4.97 min).

$[\alpha]_D^{25}$ = –63.2 (c = 1.0, $CHCl_3$).

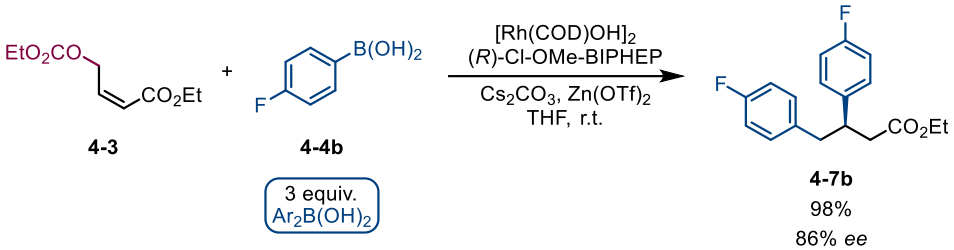

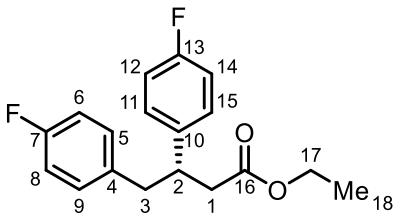

(+)-Ethyl (*S*)-3,4-bis(4-fluorophenyl)butanoate 4-7b

(+)-Ethyl (*S*)-3,4-bis(4-fluorophenyl)butanoate **4-7b** was prepared using General procedure E with 4-fluoro-3-methylphenylboronic acid **4-4b**. Purification by automated medium-pressure chromatography (Et_2O/hexane = 0/100 to 20/80) afforded (+)-ethyl (*S*)-3,4-bis(4-fluorophenyl)butanoate **4-7b** (125.0 mg, 0.39 mmol, 98%) as a colourless oil. SFC analysis showed an enantiomeric excess of 86%.

^{1}H NMR (400 MHz, $CDCl_3$) δ 7.05 (m, 2H, C(Ar)-H x2), 6.92 (m, 6H, C(Ar)-H x6), 4.01 (q, *J* = 7.1 Hz, 2H, C(17)-H_2), 3.35 (tt, *J* = 8.4, 6.7 Hz, 1H, C(2)-H), 2.90 (dd, *J* = 13.6, 6.8 Hz, 1H, C(3)-H), 2.81 (dd, *J* = 13.6, 8.2 Hz, 1H, C(3)-H), 2.65 (dd, *J* = 15.4, 6.7 Hz, 1H, C(1)-H), 2.58 (dd, *J* = 15.4, 8.5 Hz, 1H, C(1)-H), 1.13 (t, *J* = 7.1 Hz, 3H, C(18)-H_3).

^{13}C NMR (101 MHz, $CDCl_3$) δ 172.0 (C(16)), 161.6 (d, *J* = 244.6 Hz, C(7) or C(13)), 161.5 (d, *J* = 244.2 Hz, C(7) or C(13)), 138.6 (d, *J* = 3.2 Hz, C(4) or C(10)), 134.9 (d, *J* = 3.3 Hz, C(4) or C(10)), 130.6 (d, *J* = 7.9 Hz, C(5,9) or C(11,15)), 129.0 (d, *J* = 7.9 Hz, C(5,9) or C(11,15)), 115.2 (d, *J* = 16.5 Hz, C(6,8) or C(12,14)), 115.0 (d, *J* = 16.5 Hz, C(6,8) or C(12,14)), 60.4 (C(17)), 43.5 (C(2)), 42.2 (C(3)), 40.4 (C(1)), 14.1 (C(18)).

^{19}F NMR (376 MHz, $CDCl_3$) δ -116.3, -116.9.

HRMS (ESI): m/z calculated for $C_{18}H_{19}F_2O_2^+$ $[M+H]^+$ 305.1348 found 305.1346.

IR (CH_3Cl film): 2985 (w), 2256 (w), 1730 (m), 1604 (w), 1510 (w), 1446 (w), 1374 (w), 1224 (s), 1182 (m), 1158 (w), 1095 (w), 1036 (w), 909 (s), 834 (m), 732 (s) cm^{-1}.

SFC: Chiralpak® IA, 1500 psi, 30 °C; flow: 1.0 mL/min; 1% to 30% MeOH over 5 min, 92.9:7.1 e.r. (minor enantiomer t_R = 1.71 min, major enantiomer t_R = 1.55 min).

$\mathbf{[\alpha]_D^{25}}$ = +47.2 (c = 1.0, $CHCl_3$).

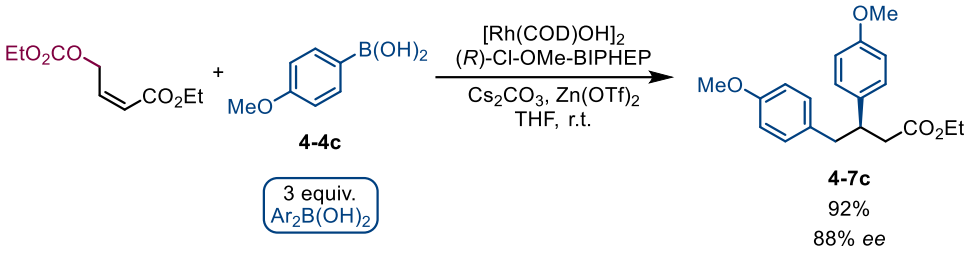

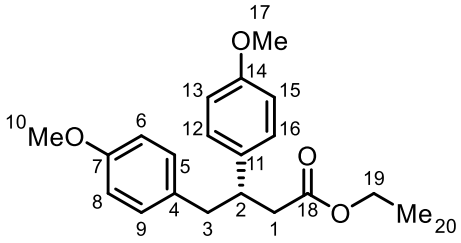

(+)-Ethyl (*S*)-3,4-bis(4-methoxyphenyl)butanoate 4-7c

(+)-Ethyl (*S*)-3,4-bis(4-methoxyphenyl)butanoate **4-7c** was prepared using General procedure E with 4-fluoro-3-methylphenylboronic acid **4-4c**. Purification by automated medium-pressure chromatography (Et_2O/hexane = 0/100 to 20/80) afforded (+)-ethyl (*S*)-3,4-bis(4-methoxyphenyl)butanoate **4-7c** (121.5 mg, 0.37 mmol, 93%) as a colourless oil. SFC analysis showed an enantiomeric excess of 89%. Characterisation data match literature reports.[217]

^{1}H NMR (400 MHz, $CDCl_3$) δ 7.06 (d, *J* = 8.7 Hz, 2H H, C(Ar)-H x2), 6.95 (d, *J* = 8.6 Hz, 2H H, C(Ar)-H x2), 6.80 (d, *J* = 8.7 Hz, 2H H, C(Ar)-H x2), 6.76 (d, *J* = 8.6 Hz, 2H H, C(Ar)-H x2), 4.00 (q, *J* = 7.1 Hz, 2H H, C(19)-H_2), 3.77 (s, 3H, C(17)-H_3 or C(10)-H_3), 3.76 (s, 3H, C(17)-H_3 or C(10)-H_3), 3.33 (dq, *J* = 8.8, 7.3 Hz, 1H, C(2)-H), 2.83 (d, *J* = 7.4 Hz, 2H, C(3)-H), 2.64 (dd, *J* = 15.2, 6.6 Hz, 1H, C(1)-H), 2.55 (dd, *J* = 15.2, 8.7 Hz, 1H, C(1)-H), 1.13 (t, *J* = 7.1 Hz, 3H, C(20)-H_3).

^{13}C NMR (101 MHz, $CDCl_3$) δ 172.4 (C(18)), 158.1 (C(7) or C(14)), 158.0 (C(7) or C(14)), 135.6 (C(4) or C(11)), 131.7 (C(4) or C(11)), 130.2 (C(Ar) x2), 128.5 (C(Ar) x2), 113.7 (C(6,8) or C(13,15)), 113.6 (C(6,8) or C(13,15)), 60.2 (C(19)), 55.2 (C(10) and C(17)), 43.4 (C(2)), 42.3 (C(3)), 40.5 (C(1)), 14.1 (C(20)).

HRMS (ESI): m/z calculated for $C_{20}H_{25}O_4^+$ $[M+H]^+$ 329.1747 found 329.1752.

IR (CH_3Cl film): 2935 (w), 2254 (w), 1729 (m), 1612 (w), 1513 (m), 1465 (w), 1373 (w), 1300 (w), 1247 (m), 1178 (m), 1147 (w), 1037 (m), 909 (s), 830 (m), 731 (s) cm^{-1}.

SFC: Chiralpak® ID, 1500 psi, 30 °C; flow: 1.0 mL/min; 1% to 30% MeOH over 5 min, 94.3:5.7 e.r. (minor enantiomer t_R = 2.79 min, major enantiomer t_R = 2.58 min).

$[\alpha]_D^{25}$ = +52.9 (c = 1.0, $CHCl_3$).

Absolute stereochemistry was determined by comparing $[\alpha]_D$ of **4-7c** to that of (*R*)-2,3,5,6-tetrafluoro-4-methylbenzyl 3-(4-methoxyphenyl)-4-(*p*-tolyl)butanoate.[218]

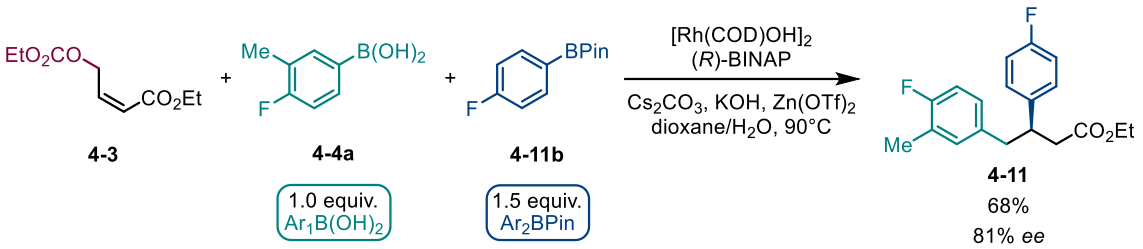

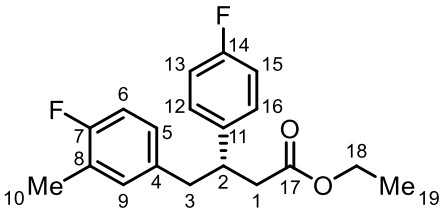

(+)-Ethyl (*S*)-4-(4-fluoro-3-methylphenyl)-3-(4-fluorophenyl)butanoate 4-11

$[Rh(cod)OH]_2$ (4.6 mg, 0.010 mmol, 2.5 mol%) and (*R*)-BINAP (14.9 mg, 0.024 mmol, 6.0 mol%) were added to 7 mL vial containing a stirring bar and dissolved in dry THF (4.0 mL) under an argon atmosphere at ambient temperature (23 °C). This solution was stirred for 5 minutes.

Cs_2CO_3 (130.3 mg, 0.40 mmol, 1.0 equiv.), (4-fluoro-3-methylphenyl)boronic acid (61.6 mg, 0.40 mmol, 1.0 equiv.), (4-fluorophenyl)boronic acid pinacol ester (133.2 mg, 0.60 mmol, 1.5 equiv.) and $Zn(OTf)_2$ (29.1 mg, 0.08 mmol, 0.2 equiv.) were added to a 7 mL vial containing a stirring bar. To this vial a stock solution of the rhodium hydroxy complex (4.0 mL) was added *via* syringe under an argon atmosphere. Ethyl (*Z*)-4-((ethoxycarbonyl)oxy)but-2-enoate **4-3** (80.9 mg, 0.40 mmol, 1.0 equiv.) was added *via* microsyringe and the reaction mixture was stirred at ambient temperature (23 °C) for 14 hours.

The mixture was diluted with hexane (4.0 mL) and filtered through a plug of silica. The crude was loaded onto Chem Tube-Hydromatrix and automated medium-pressure chromatography (Et_2O/hexane = 0/100 to 20/80) was performed to afford (+)-ethyl (*S*)-4-(4-fluoro-3-methylphenyl)-3-(4-fluorophenyl)butanoate **4-11** (86.6 mg, 0.27 mmol, 68%) as a colourless oil. SFC analysis showed an enantiomeric excess of 81%.

^{1}H NMR (400 MHz, $CDCl_3$) δ 7.07 (m, 2H, C(Ar)-H x2), 6.94 (m, 2H, C(Ar)-H x2), 6.82 (m, 2H, C(Ar)-H x2), 6.75 (m, 1H, C(Ar)-H), 4.00 (q, *J* = 7.2 Hz, 2H, C(18)-H_2), 3.34 (p, *J* = 7.5 Hz, 1H, C(2)-H), 2.83 (dd, *J* = 13.6, 7.1 Hz, 1H, C(3)-H), 2.77 (dd, *J* = 13.6, 7.9 Hz, 1H, C(3)-

H), 2.64 (dd, *J* = 15.4, 6.6 Hz, 1H, C(1)-H), 2.55 (dd, *J* = 15.4, 8.7 Hz, 1H, C(1)-H), 2.19 (d, *J* = 2.0 Hz, 3H, C(10)-H_3), 1.12 (t, *J* = 7.2 Hz, 3H, C(19)-H_3).

^{13}C NMR (126 MHz, $CDCl_3$) δ 172.1 (C(17)), 161.6 (C(7) or C(14)), 160.0 (C(7) or C(14)), 138.8 (C(4) or C(11)), 134.6 (C(4) or C(11)), 132.1 (C(9)), 129.0 (C(12) and C(16)), 127.8 (C(5)), 124.4 (C(8)), 115.1 (C(13) and C(15)), 114.6 (C(6)), 60.4 (C(18)), 43.4 (C(2)), 42.2 (C(3)), 40.3 (C(1)), 14.5 (C(10)), 14.1 (C(19)).

^{19}F NMR (376 MHz, $CDCl_3$) δ -116.5, -121.4.

IR (CH_3Cl film): 2971 (w), 1729w (m), 1651 (w), 1514 (w), 1455(w), 1368 (w), 1268 (m), 1216 (m), 1174 (m), 1131 (w), 1036 (m), 1016 (w), 981 (w), 866 (w), 818 (m), 754 (s), 668 (m) cm^{-1}.

HRMS (ESI): m/z calculated for $C_{19}H_{20}F_2NaO_2^+$ $[M+Na]^+$ 341.1324 found 341.1320.

SFC: Chiralpak® IG, 1500 psi, 30 °C; flow: 1.0 mL/min; 1% to 30% MeOH over 5 min, 90.6:9.4 e.r. (minor enantiomer t_R = 1.98 min, major enantiomer t_R = 1.83 min).

$[\alpha]_D^{25}$ = +49.0 (c = 1.0, $CHCl_3$).

6 Supplementary Information

6.1 NMR spectra

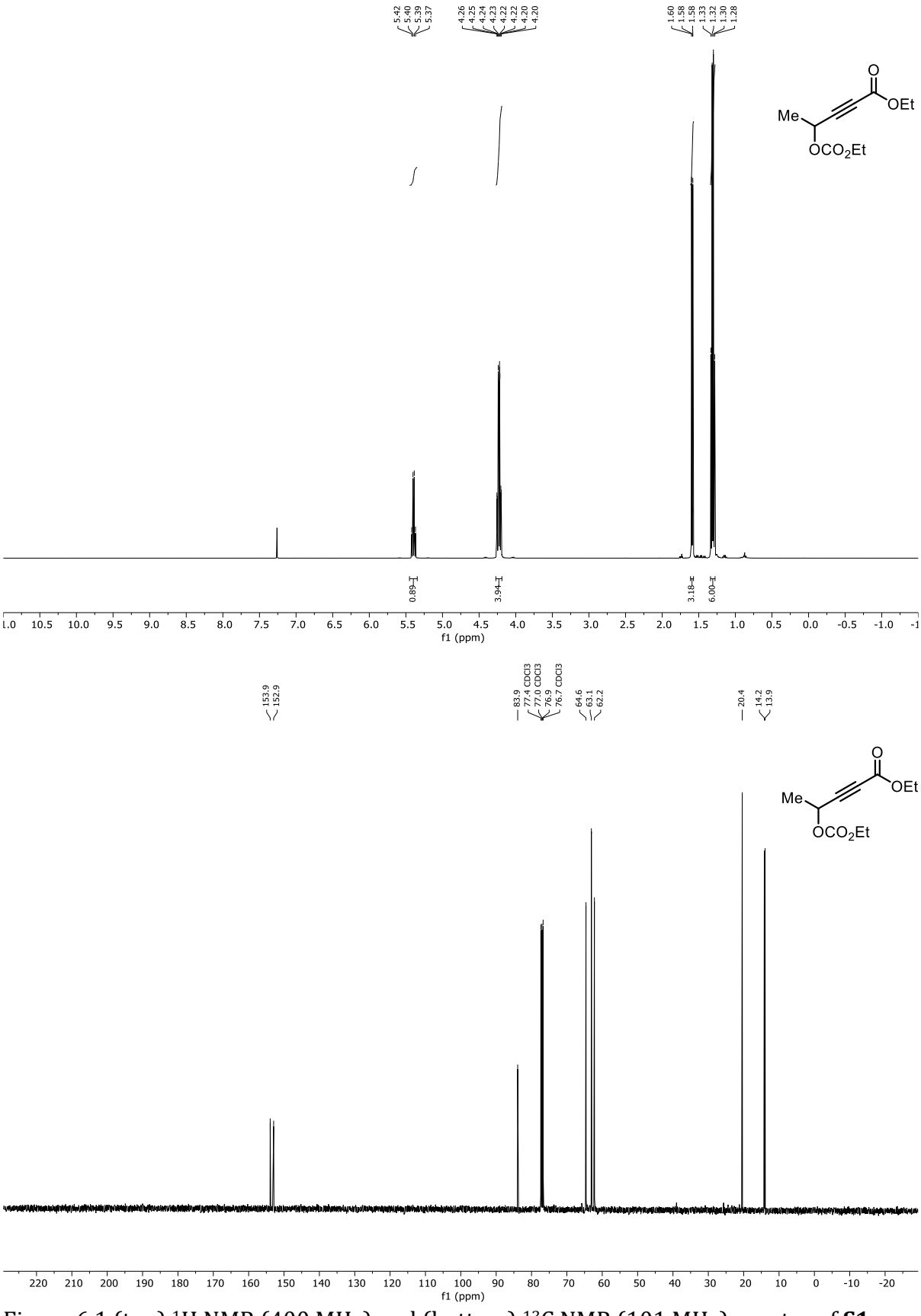

Figure 6.1 (top) ^{1}H NMR (400 MHz) and (bottom) ^{13}C NMR (101 MHz) spectra of **S1**.

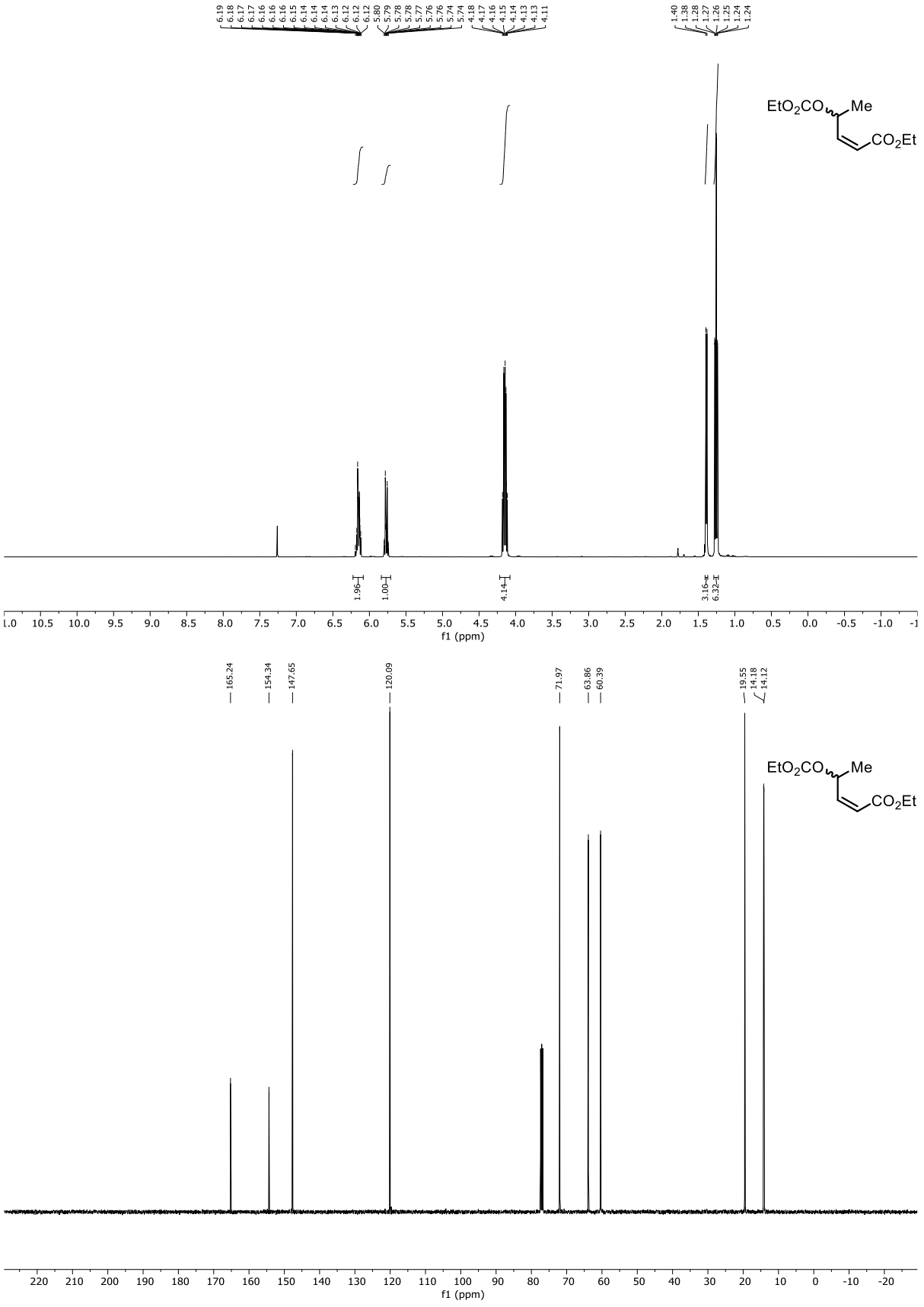

Figure 6.2 (top) ^{1}H NMR (400 MHz) and (bottom) ^{13}C NMR (101 MHz) spectra of (±)-**2-9a**.

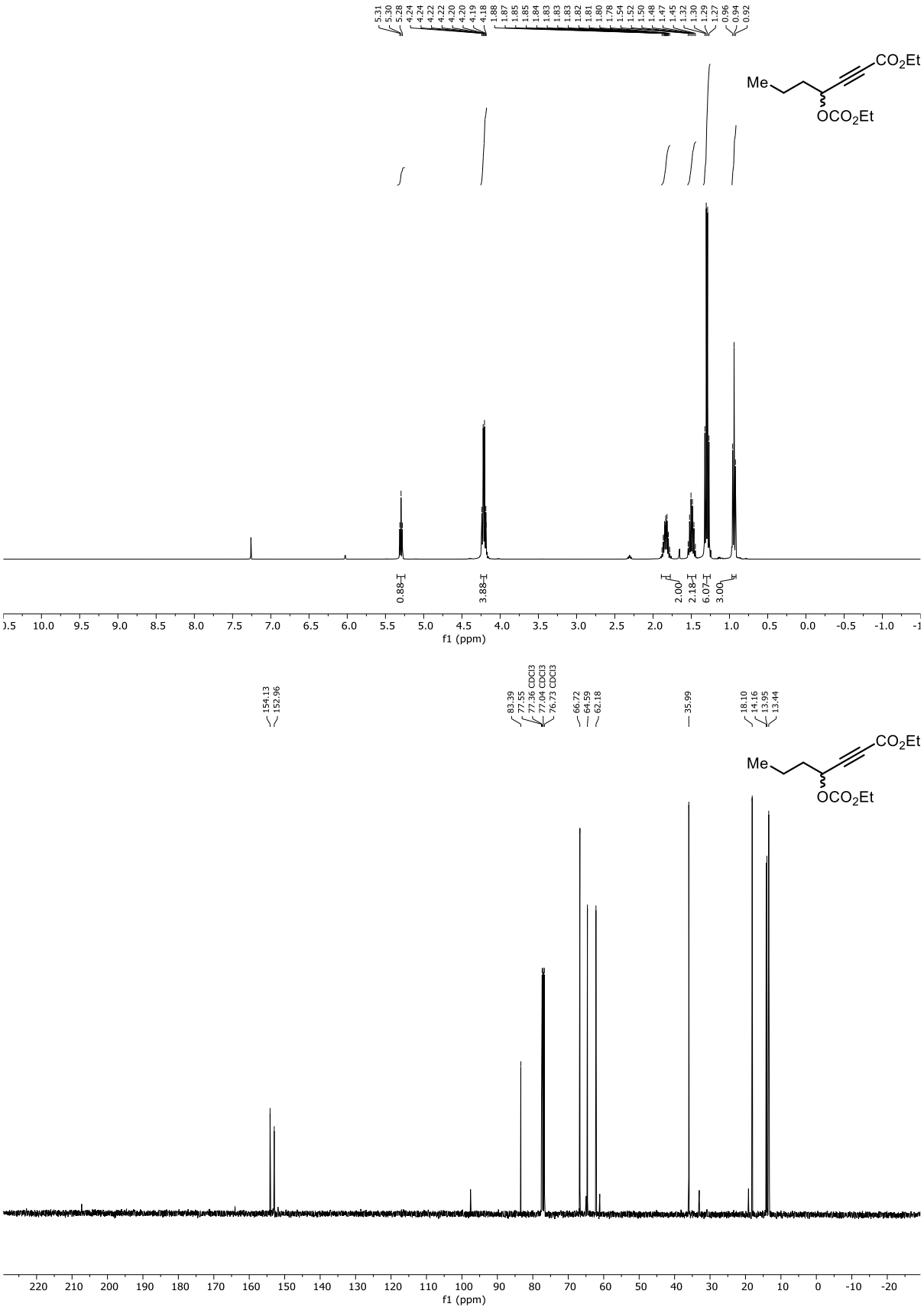

Figure 6.3 (top) ^{1}H NMR (400 MHz) and (bottom) ^{13}C NMR (101 MHz) spectra of **S2**.

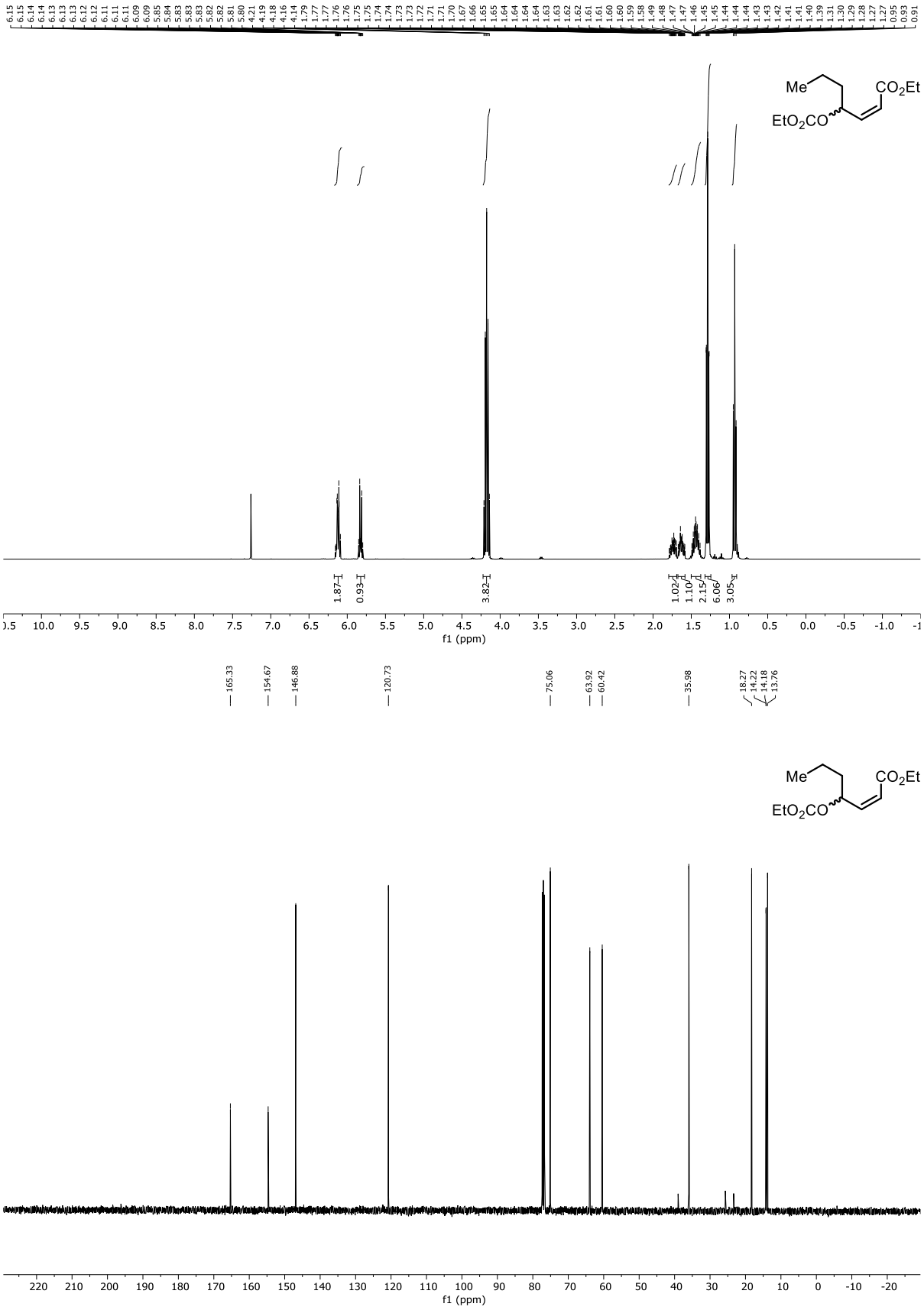

Figure 6.4 (top) ^{1}H NMR (400 MHz) and (bottom) ^{13}C NMR (101 MHz) spectra of (±)-**2-11a**.

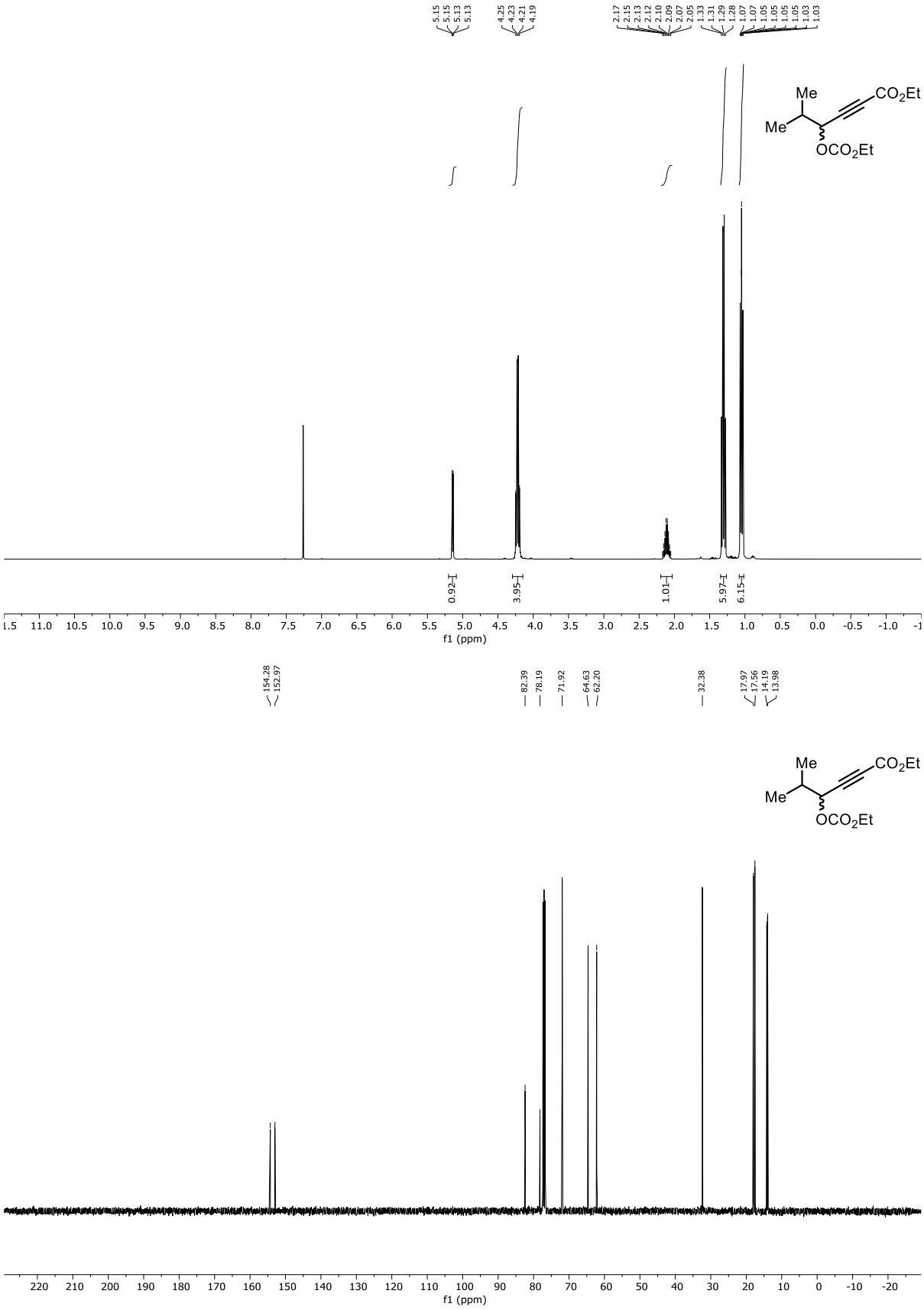

Figure 6.5 (top) ^{1}H NMR (400 MHz) and (bottom) ^{13}C NMR (101 MHz) spectra of **S3**.

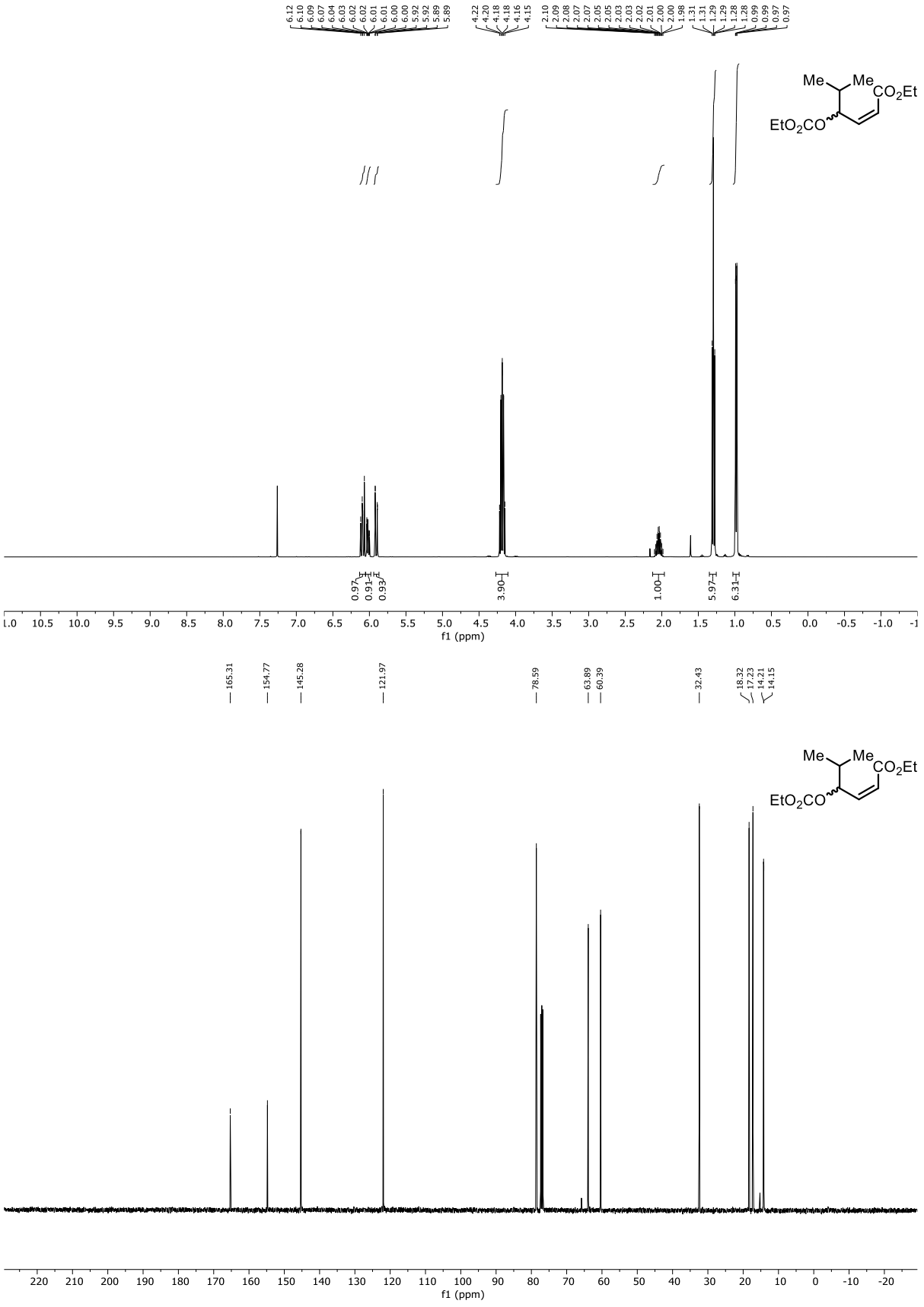

Figure 6.6 (top) ^{1}H NMR (400 MHz) and (bottom) ^{13}C NMR (101 MHz) spectra of (±)-**2-11b**.

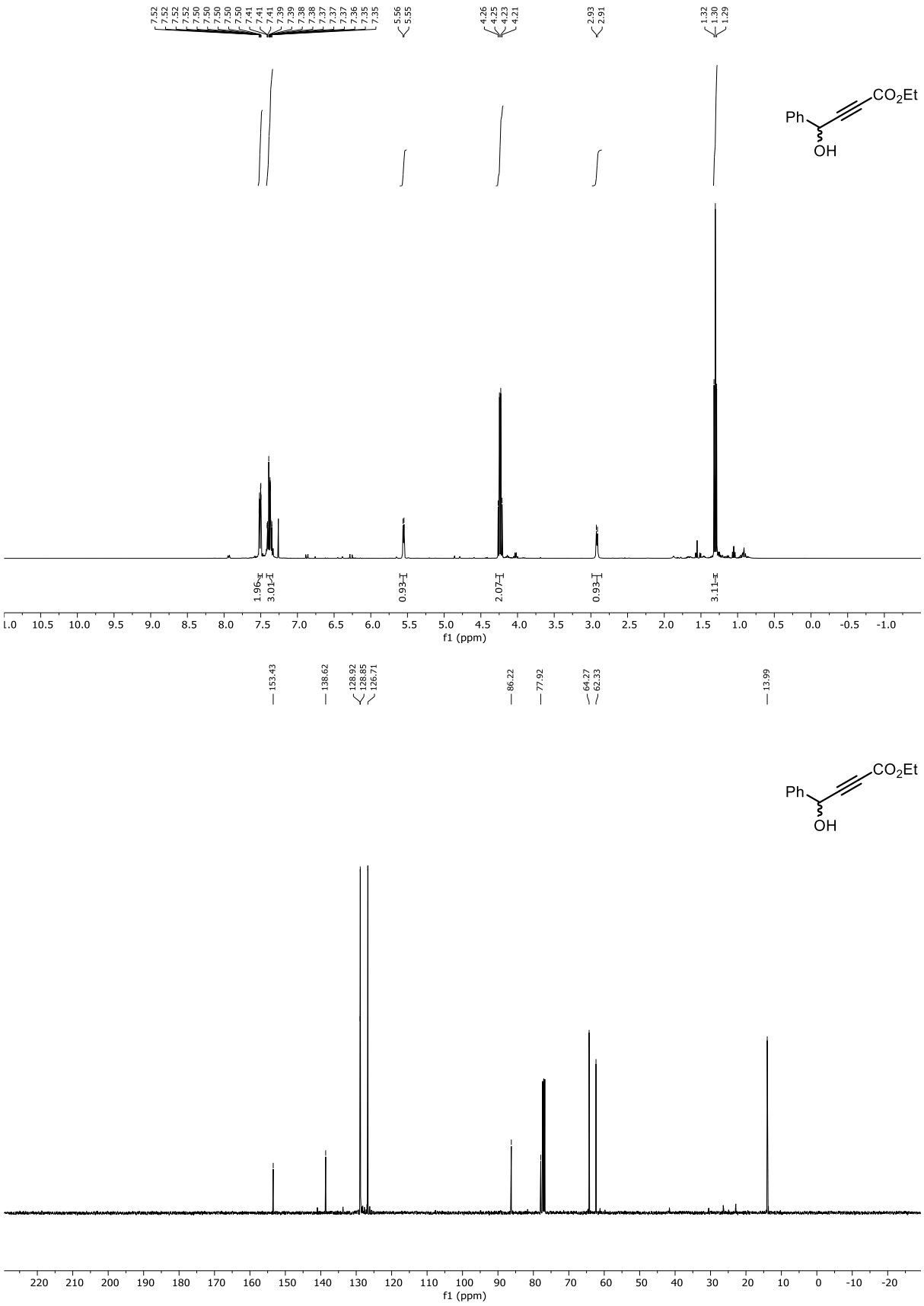

Figure 6.7 (top) ^{1}H NMR (400 MHz) and (bottom) ^{13}C NMR (101 MHz) spectra of **S4**.

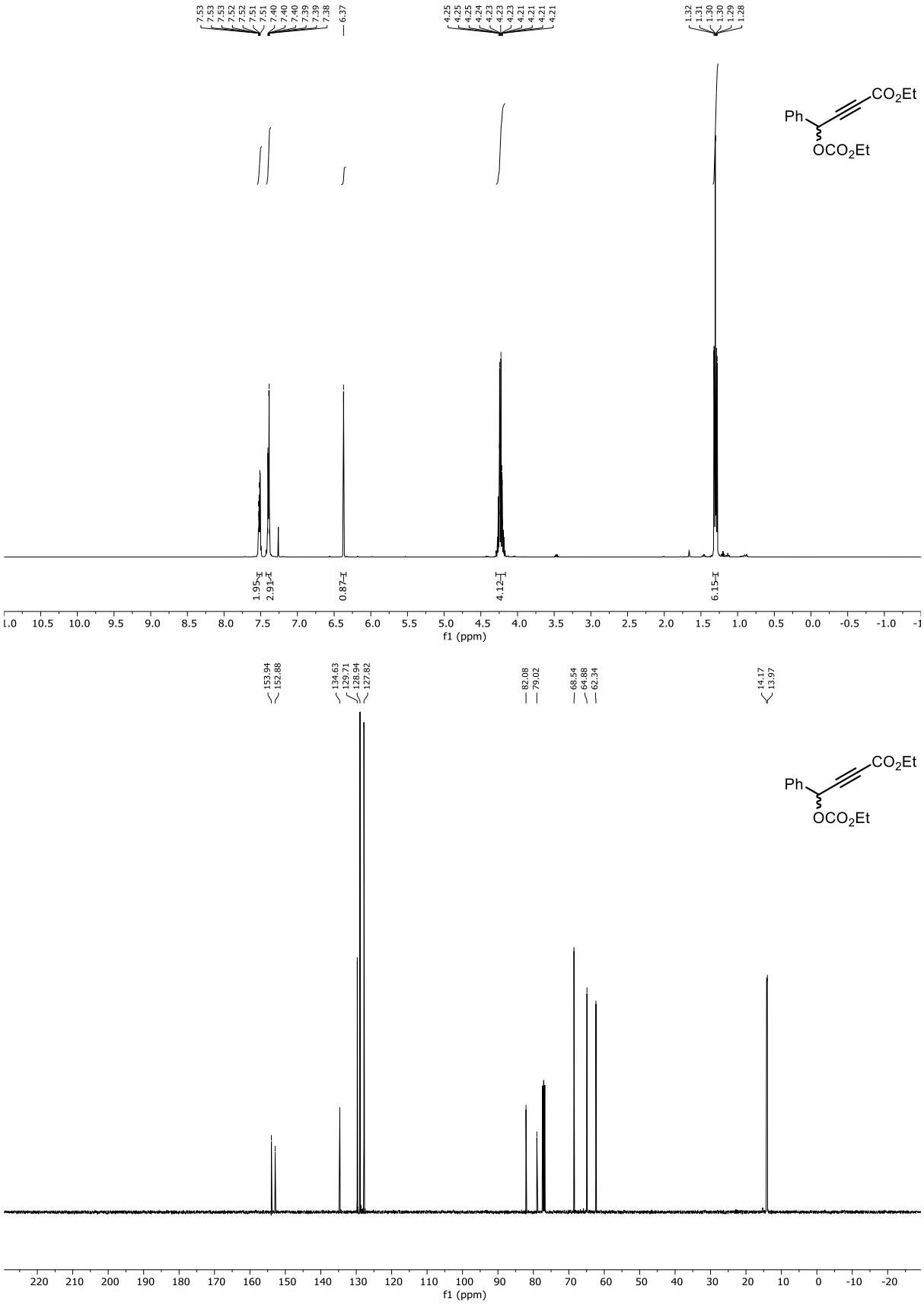

Figure 6.8 (top) ^{1}H NMR (400 MHz) and (bottom) ^{13}C NMR (101 MHz) spectra of **S5**.

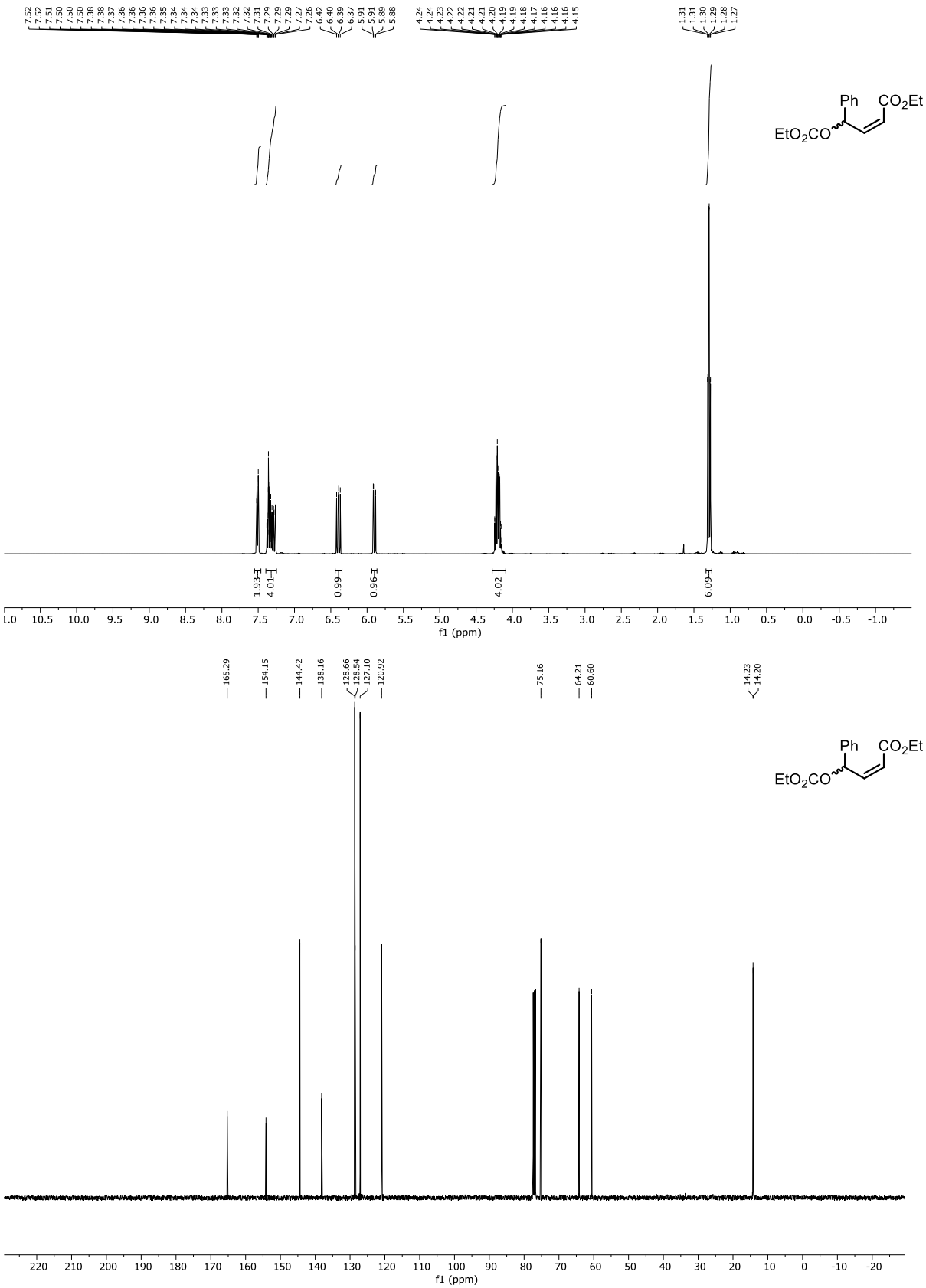

Figure 6.9 (top) ^{1}H NMR (400 MHz) and (bottom) ^{13}C NMR (101 MHz) spectra of (±)-**2-11d**.

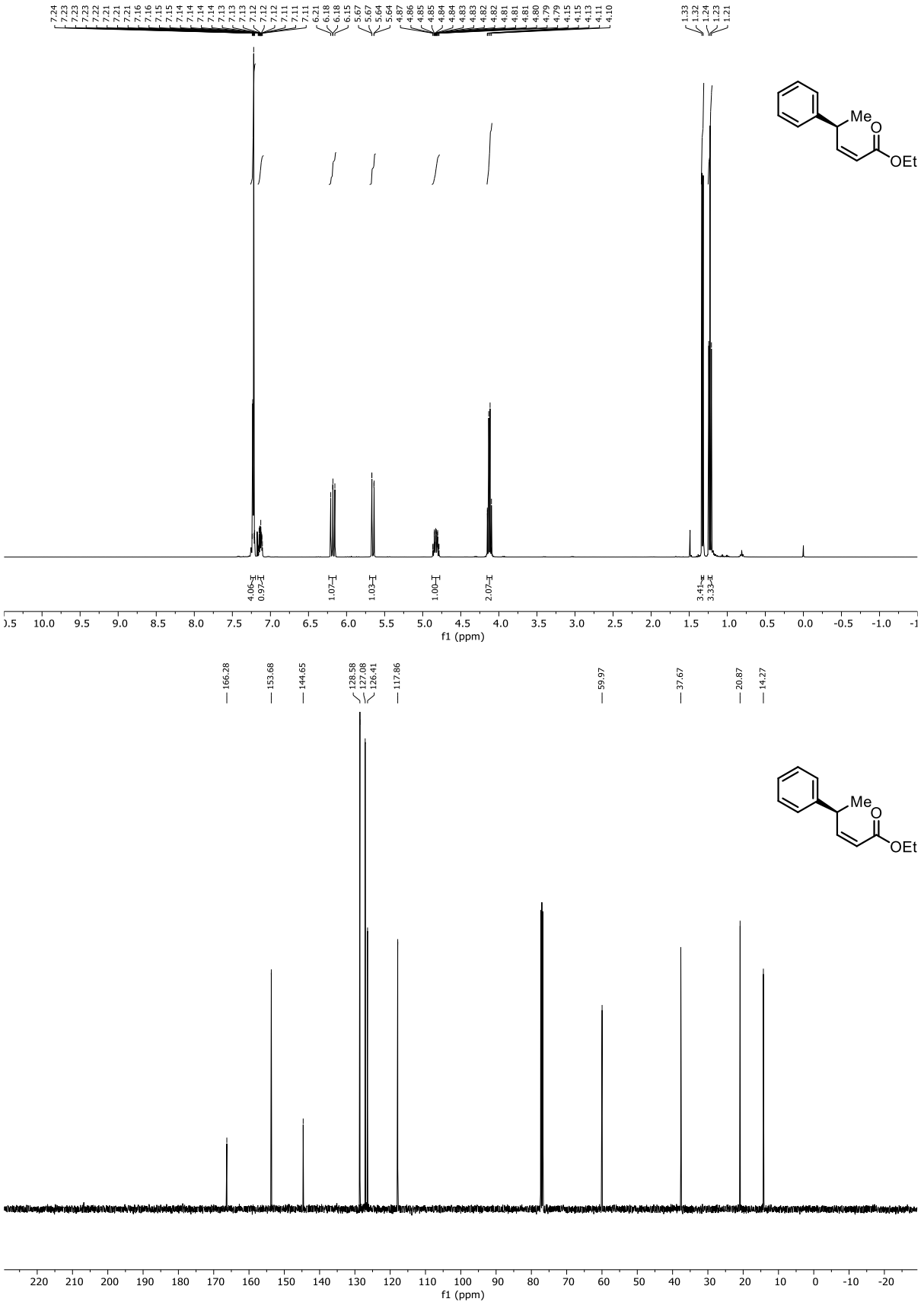

Figure 6.10 (top) ^{1}H NMR (400 MHz) and (bottom) ^{13}C NMR (101 MHz) spectra of *Z*-**2-10a**.

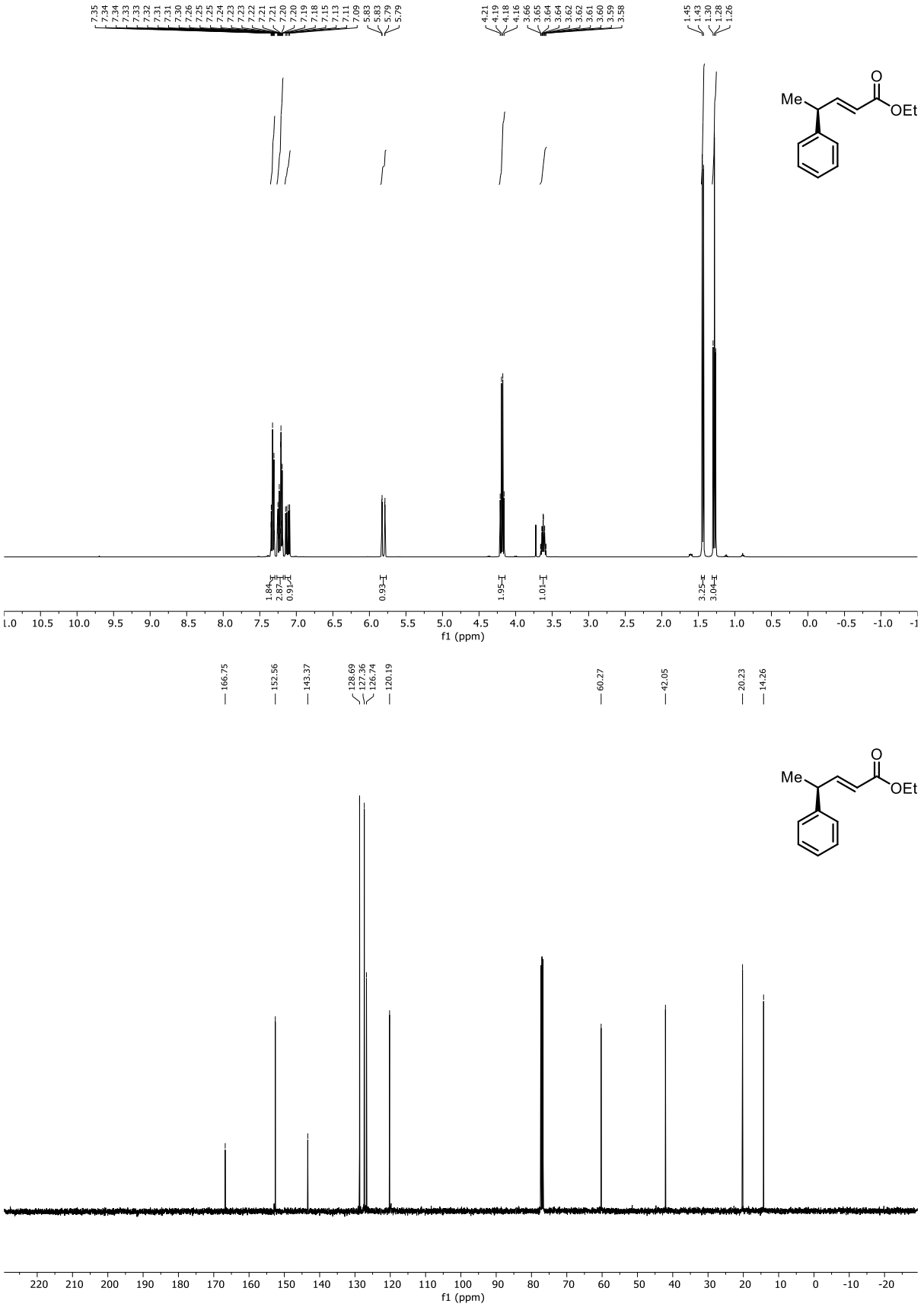

Figure 6.11 (top) ^{1}H NMR (400 MHz) and (bottom) ^{13}C NMR (101 MHz) spectra of *E*-**2-10a**.

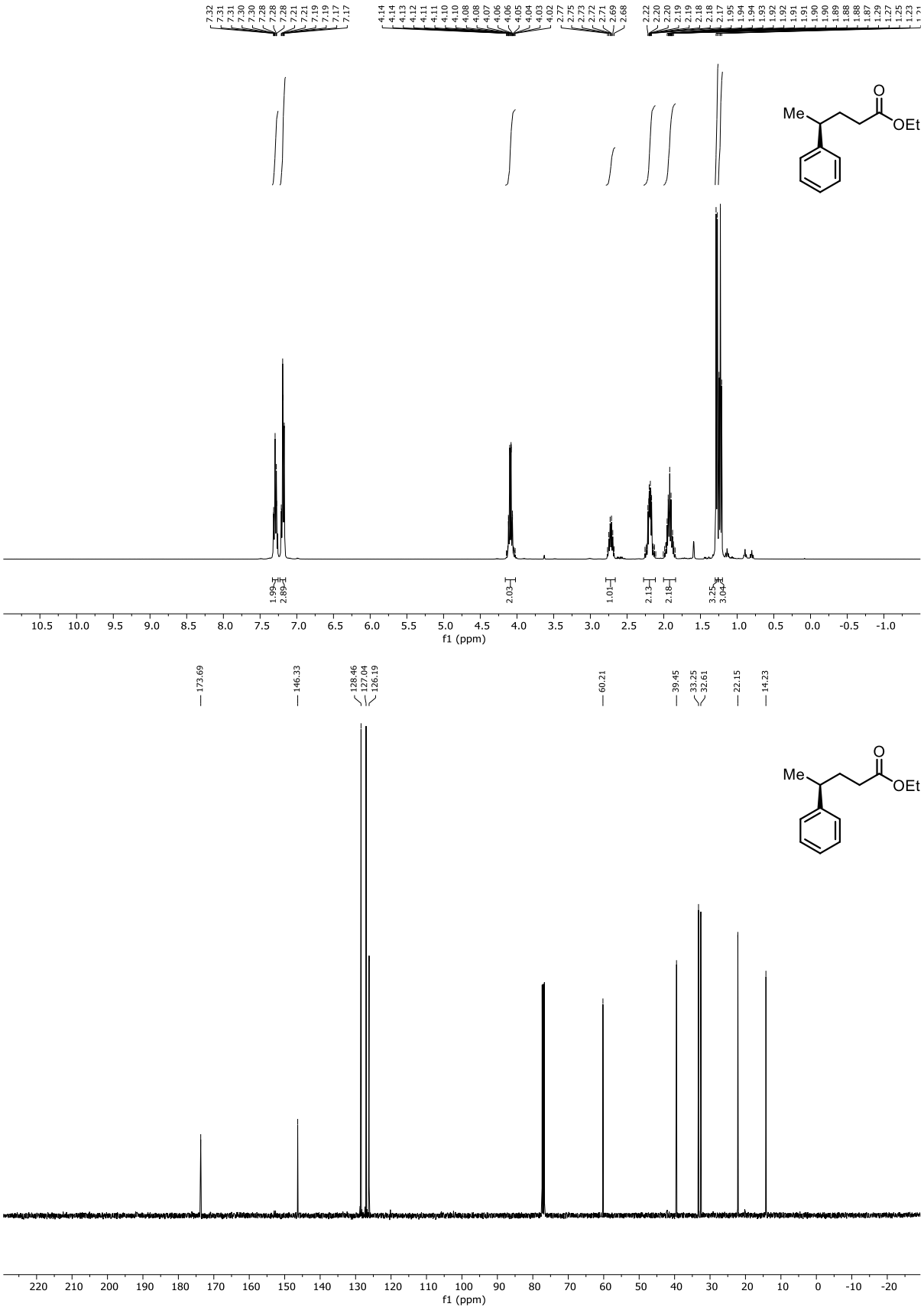

Figure 6.12 (top) ^{1}H NMR (400 MHz) and (bottom) ^{13}C NMR (101 MHz) spectra of *red*-**2-10a**.

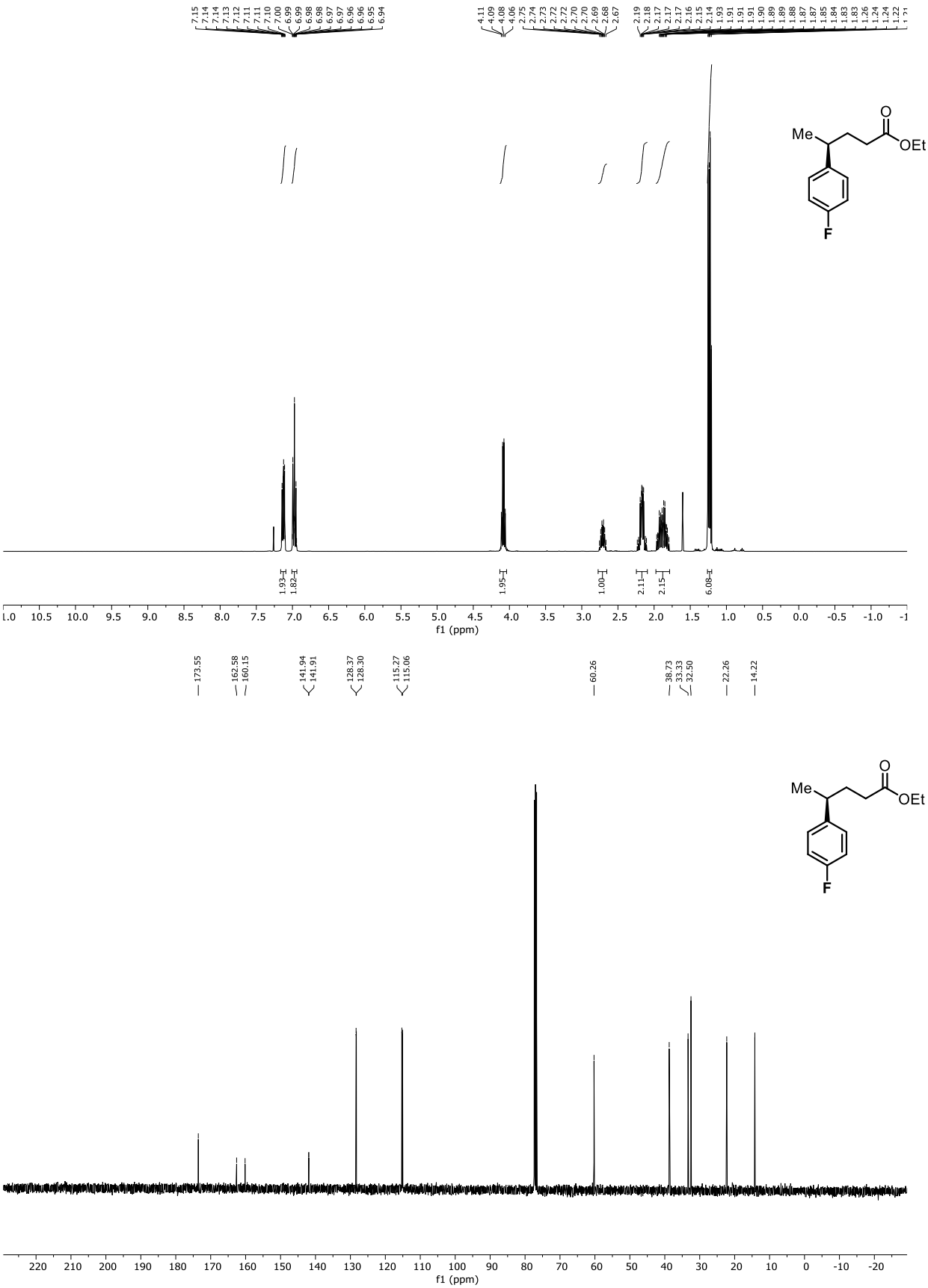

Figure 6.13 (top) ^{1}H NMR (400 MHz) and (bottom) ^{13}C NMR (101 MHz) spectra of *red*-**2-10b**.

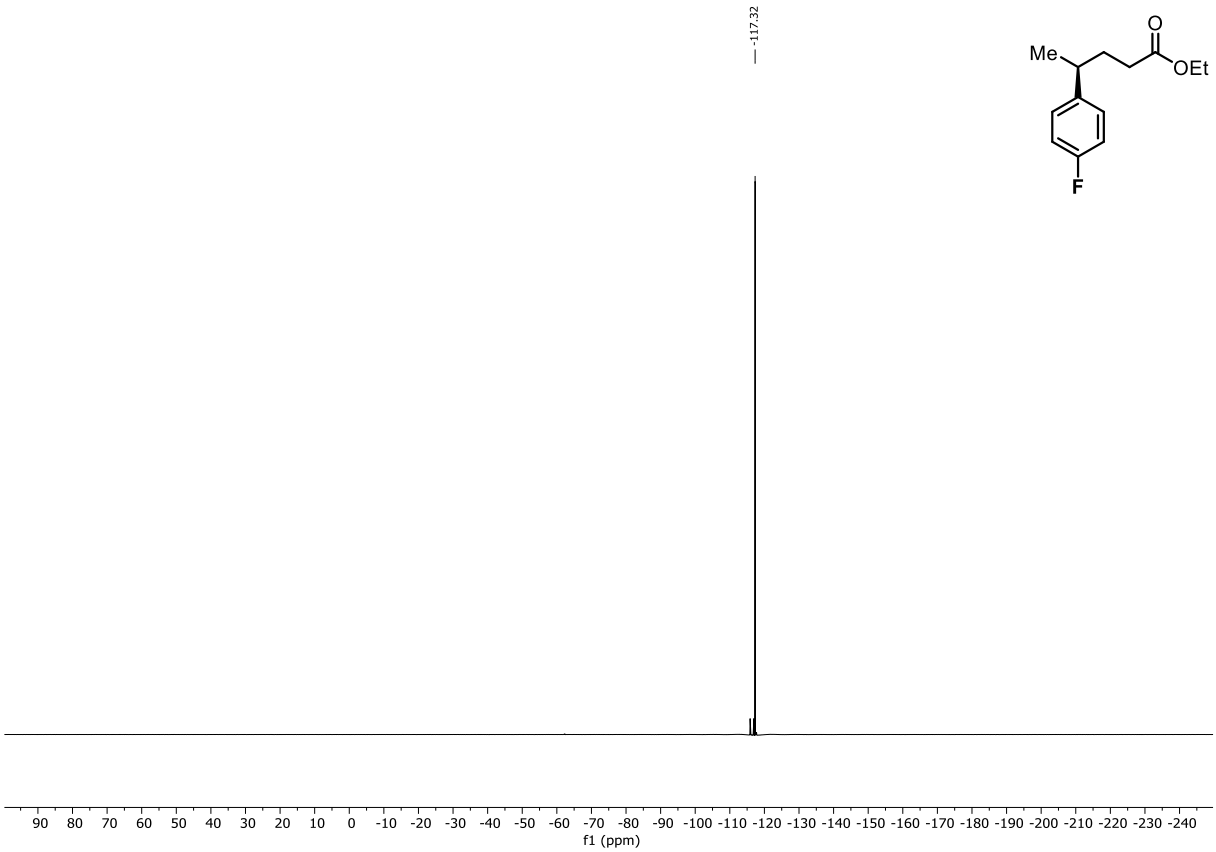

Figure 6.14 ^{19}F (13C)NMR (376 MHz) spectrum of *red*-**2-10b**.

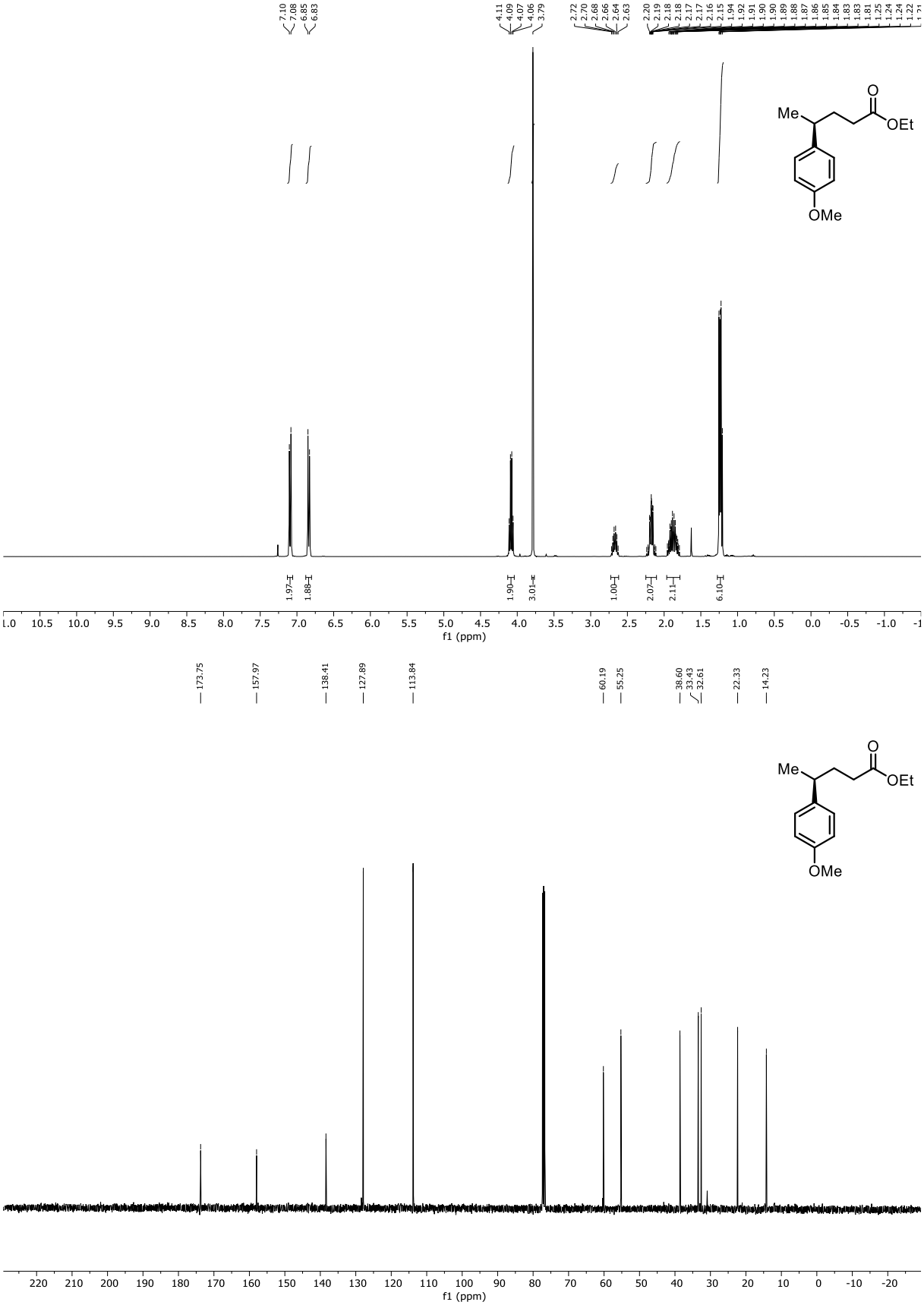

Figure 6.15 (top) ^{1}H NMR (400 MHz) and (bottom) ^{13}C NMR (101 MHz) spectra of *red*-**2-10c**.

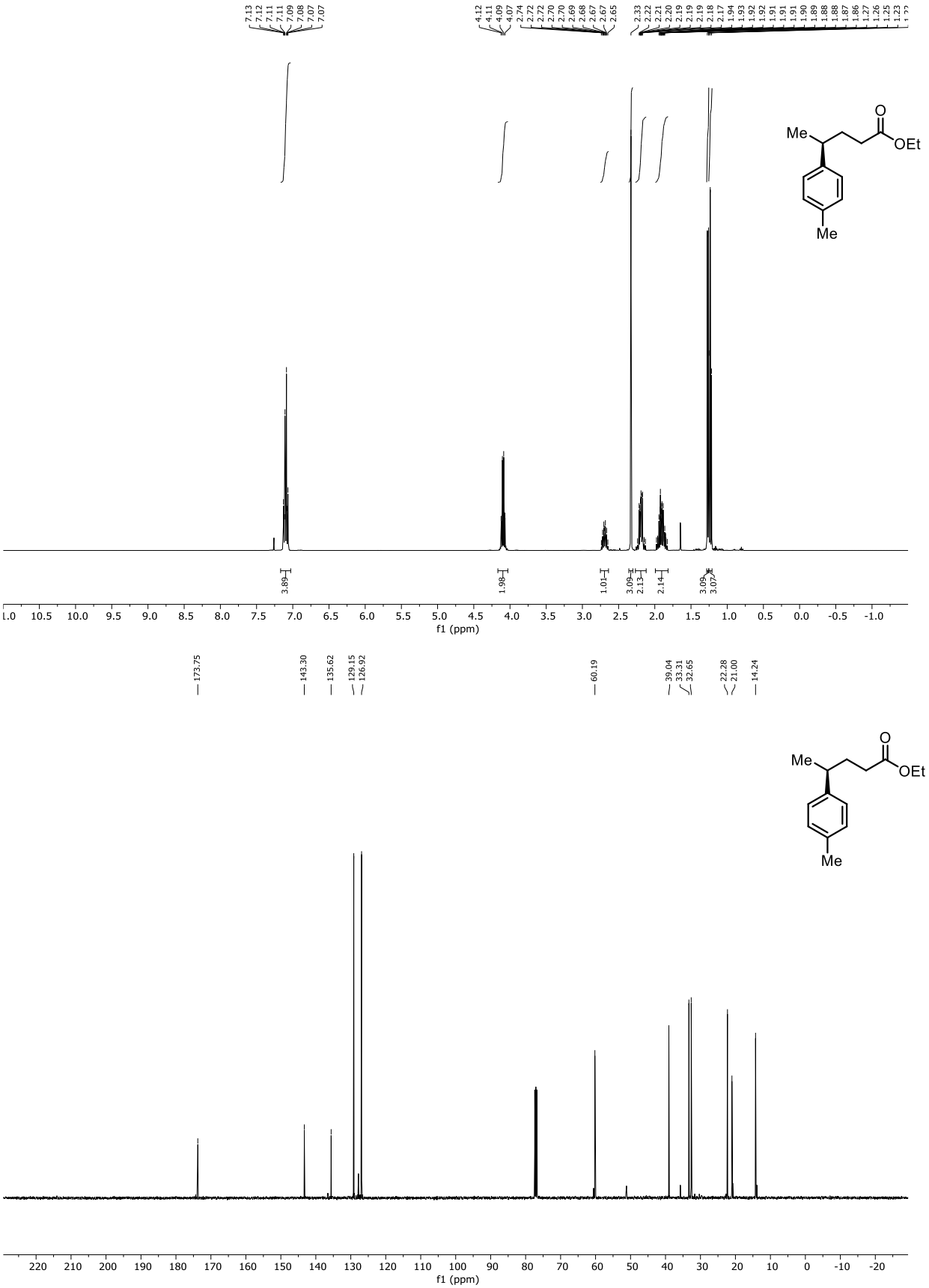

Figure 6.16 (top) ^{1}H NMR (400 MHz) and (bottom) ^{13}C NMR (101 MHz) spectra of *red*-**2-10d**.

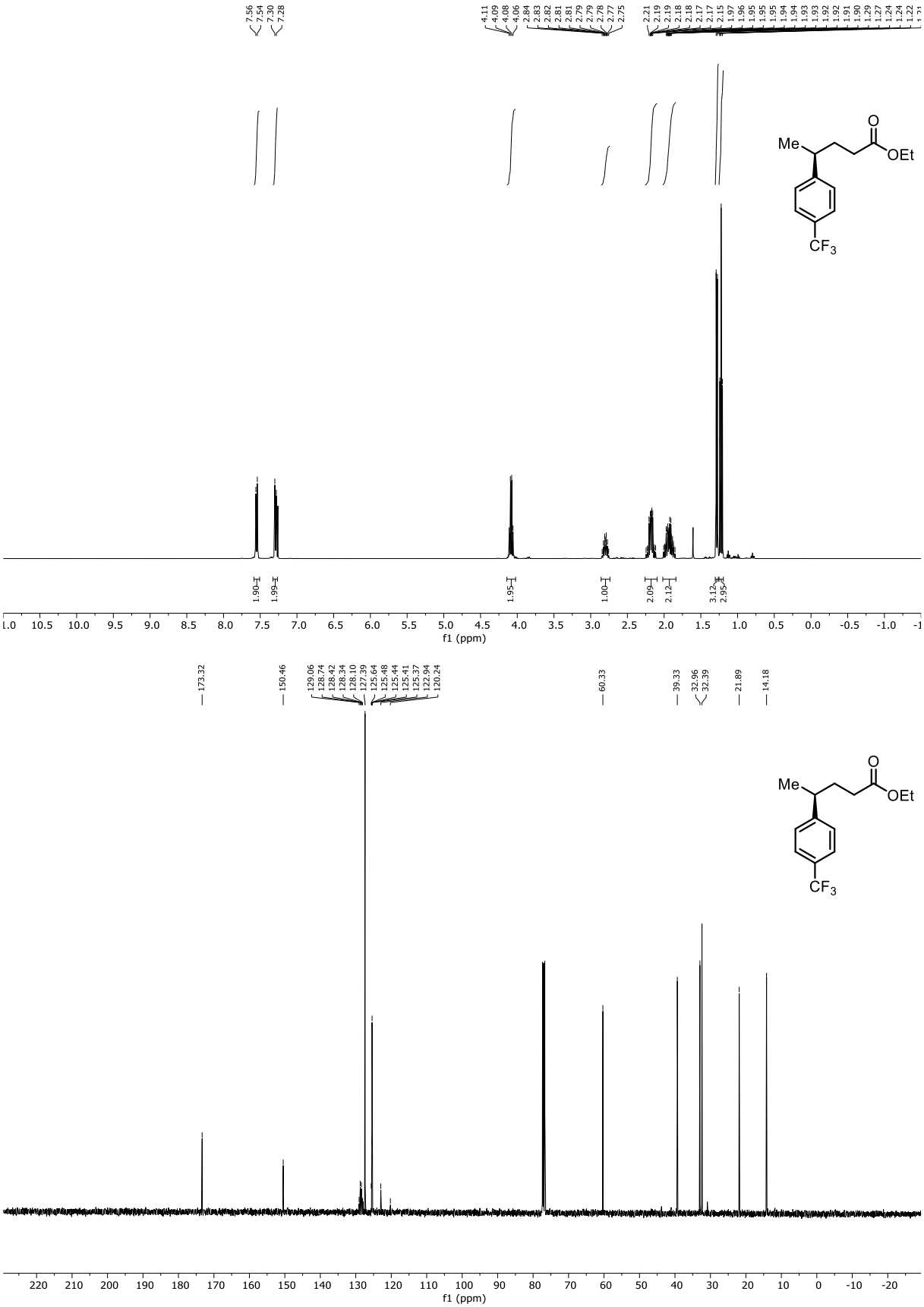

Figure 6.17 (top) ^{1}H NMR (400 MHz) and (bottom) ^{13}C NMR (126 MHz) spectra of *red*-**2-10**.

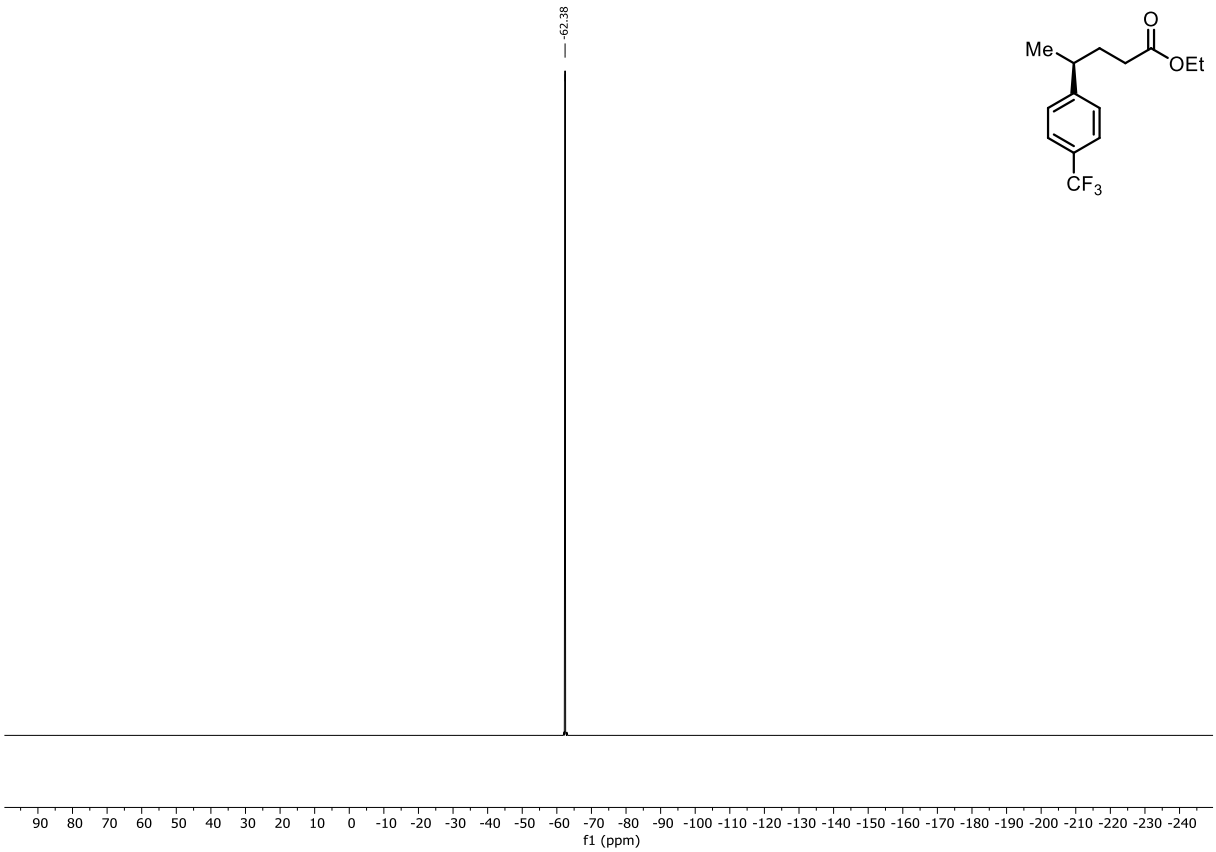

Figure 6.18 ^{19}F (13C)NMR (376 MHz) spectrum of *red*-**2-10e**.

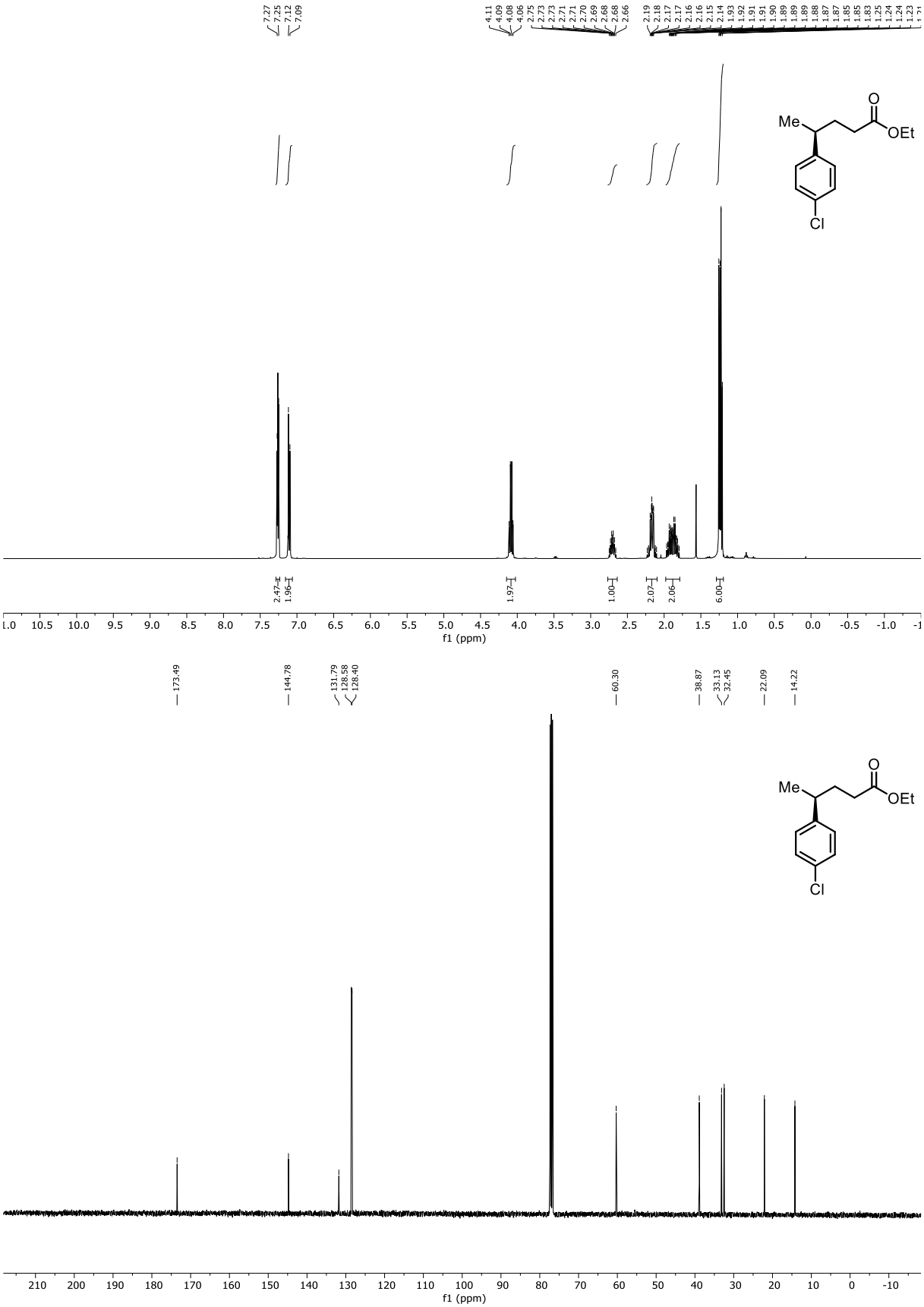

Figure 6.19 (top) ^{1}H NMR (400 MHz) and (bottom) ^{13}C NMR (126 MHz) spectra of *red*-**2-10f**.

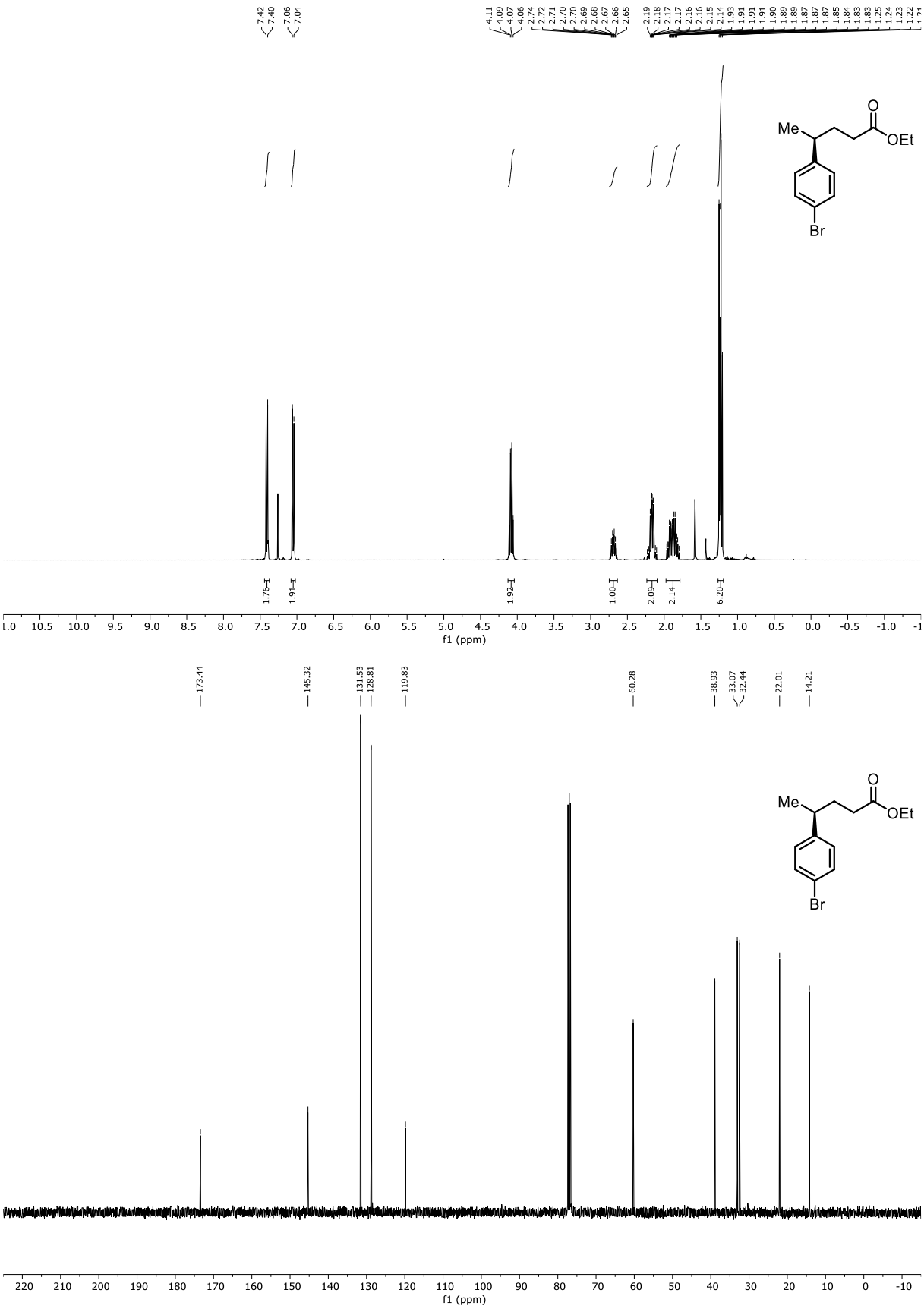

Figure 6.20 (top) ^{1}H NMR (400 MHz) and (bottom) ^{13}C NMR (101 MHz) spectra of *red*-**2-10g**.

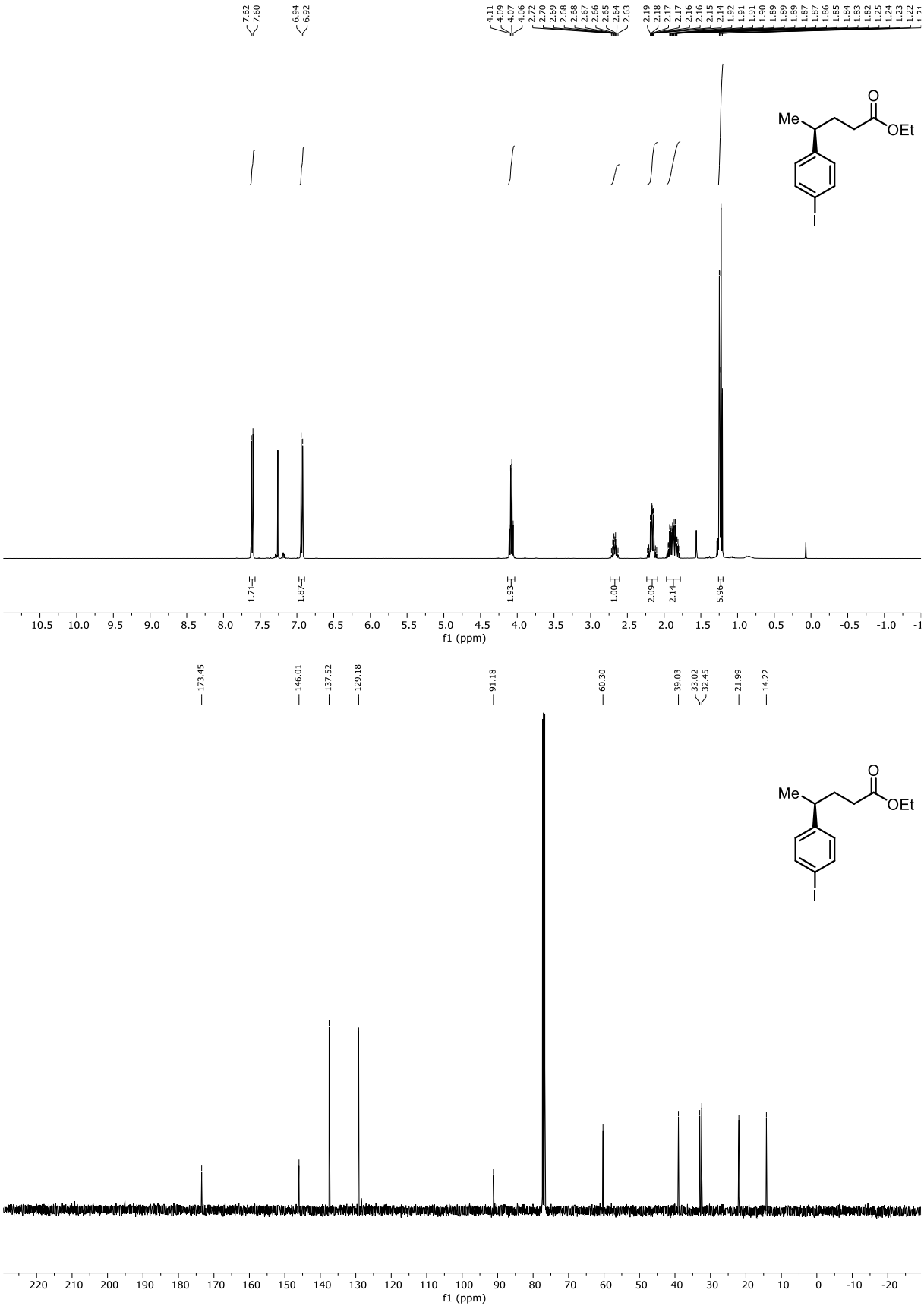

Figure 6.21 (top) ^{1}H NMR (400 MHz) and (bottom) ^{13}C NMR (101 MHz) spectra of *red*-**2-10h**.

Figure 6.22 (top) ^{1}H NMR (400 MHz) and (bottom) ^{13}C NMR (101 MHz) spectra of *red*-**2-10i**.

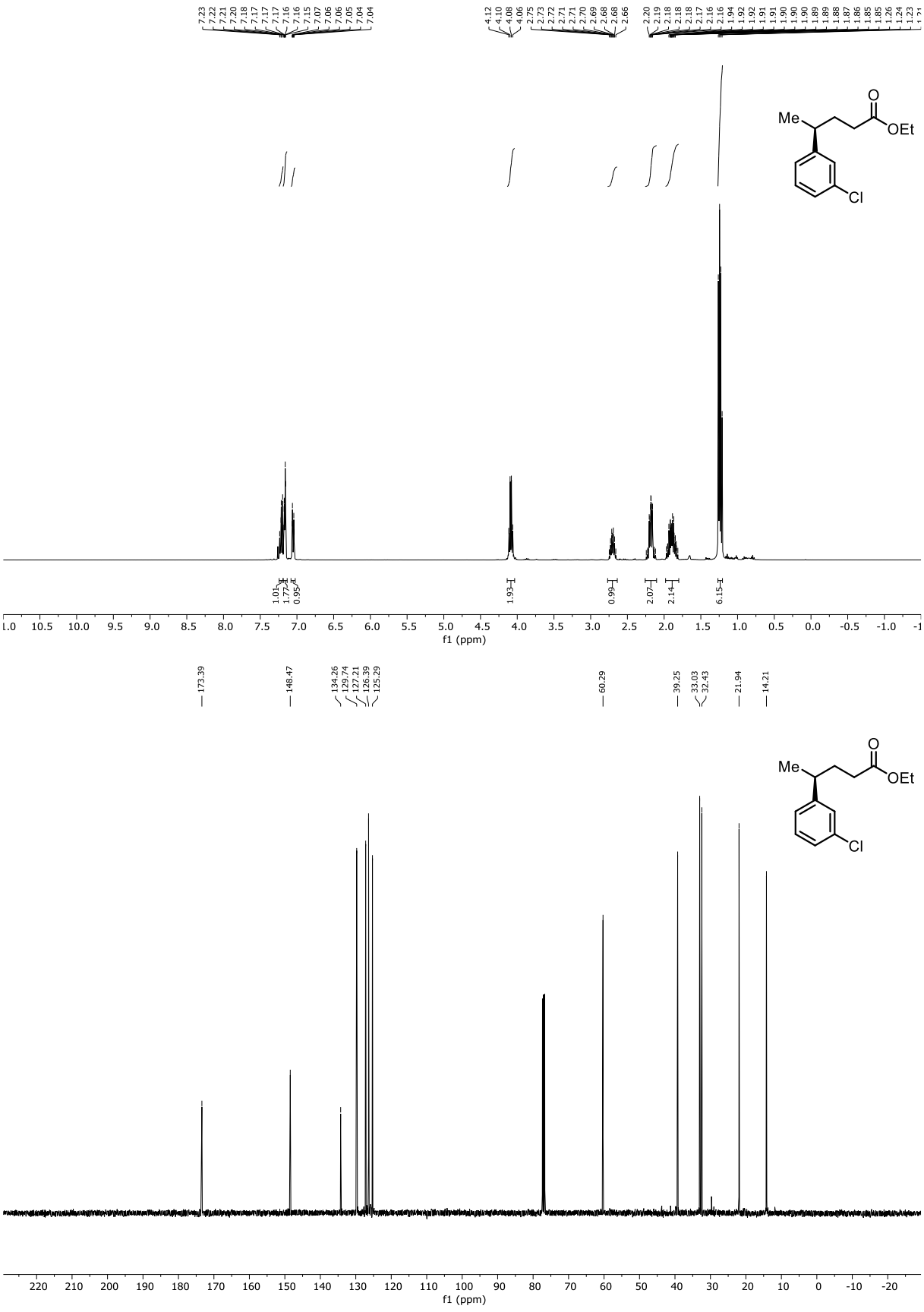

Figure 6.23 (top) ^{1}H NMR (400 MHz) and (bottom) ^{13}C NMR (101 MHz) spectra of *red*-**2-10j**.

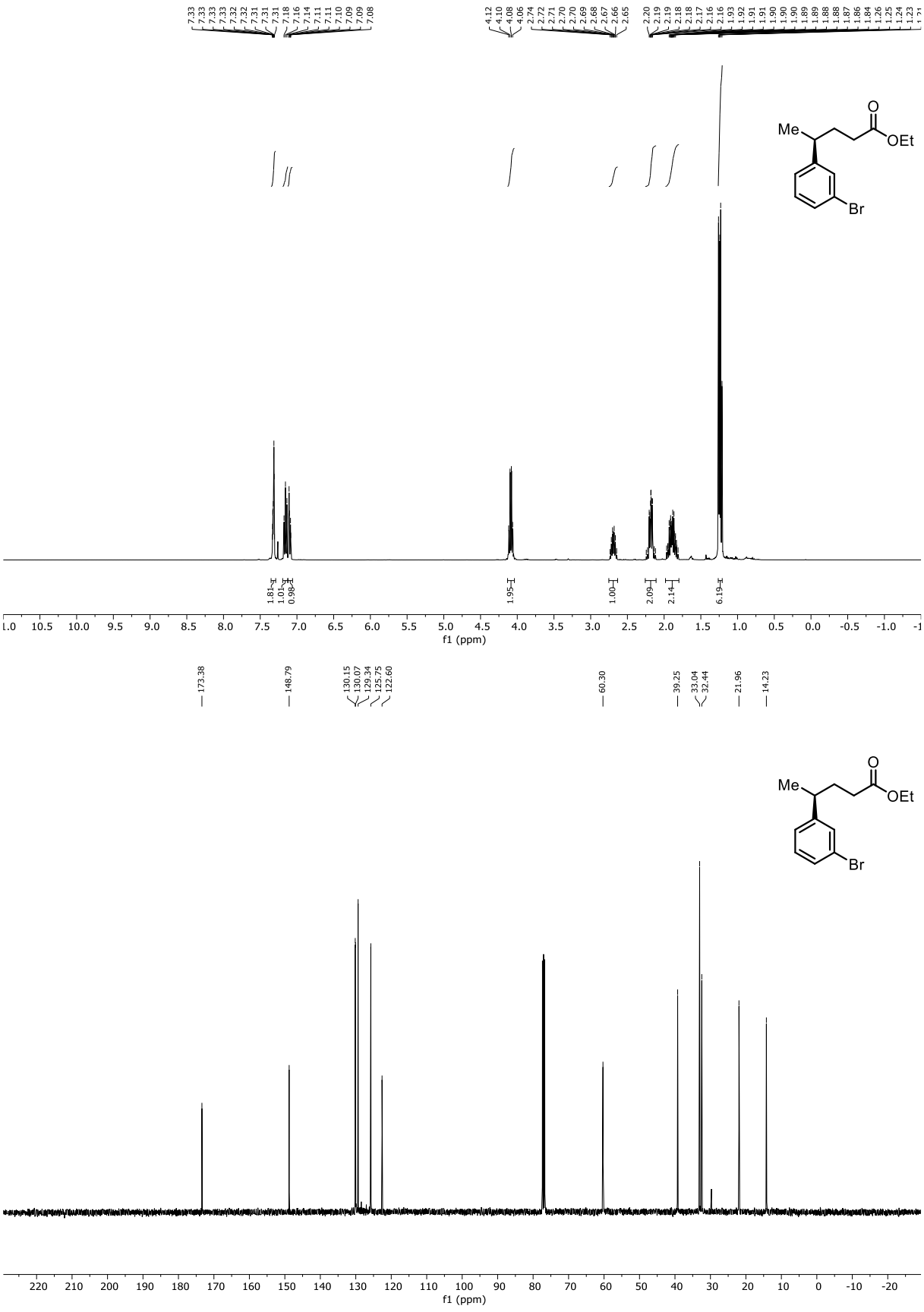

Figure 6.24 (top) ^{1}H NMR (400 MHz) and (bottom) ^{13}C NMR (101 MHz) spectra of *red*-**2-10k**.

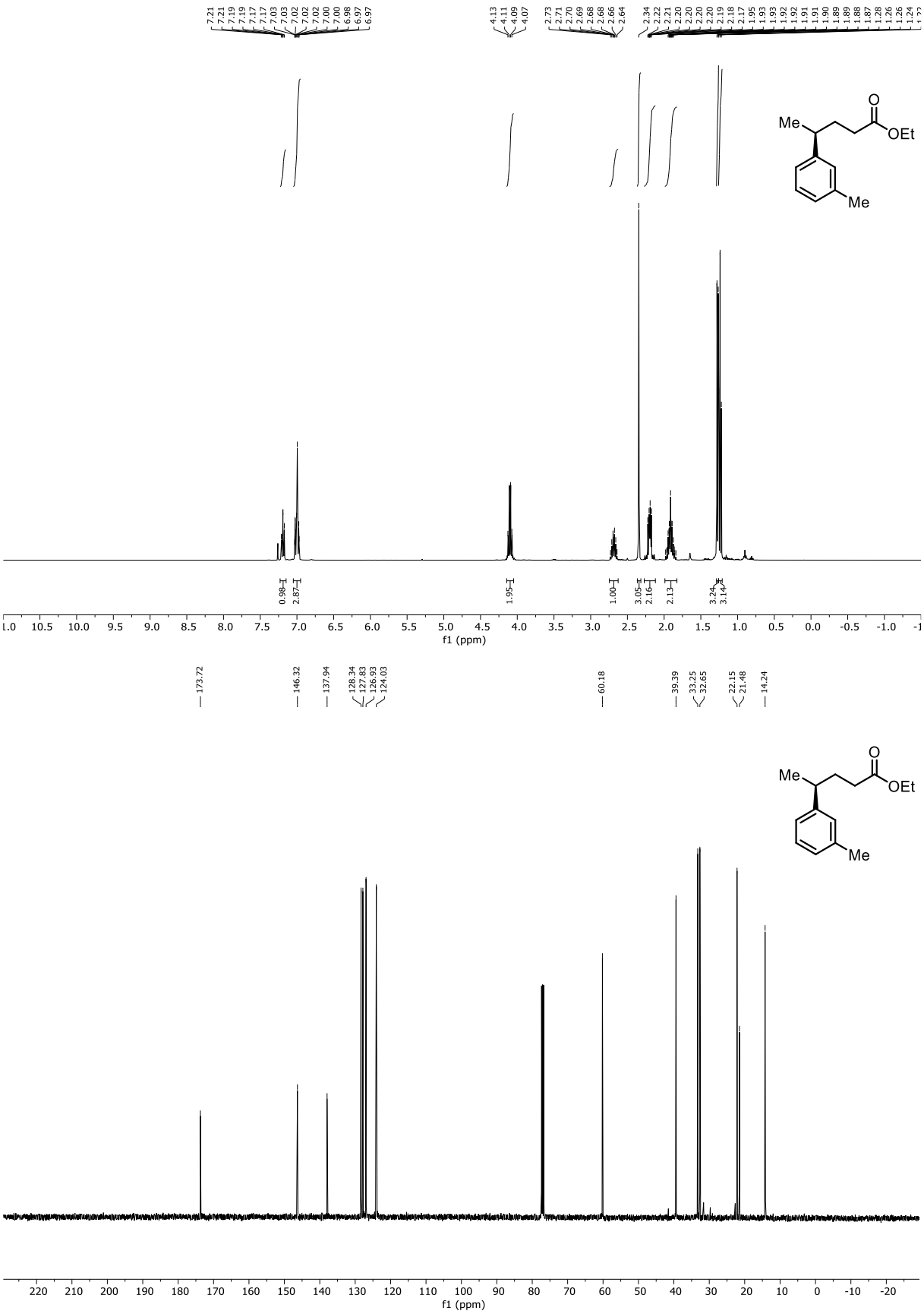

Figure 6.25 (top) ^{1}H NMR (400 MHz) and (bottom) ^{13}C NMR (101 MHz) spectra of *red*-**2-10l**.

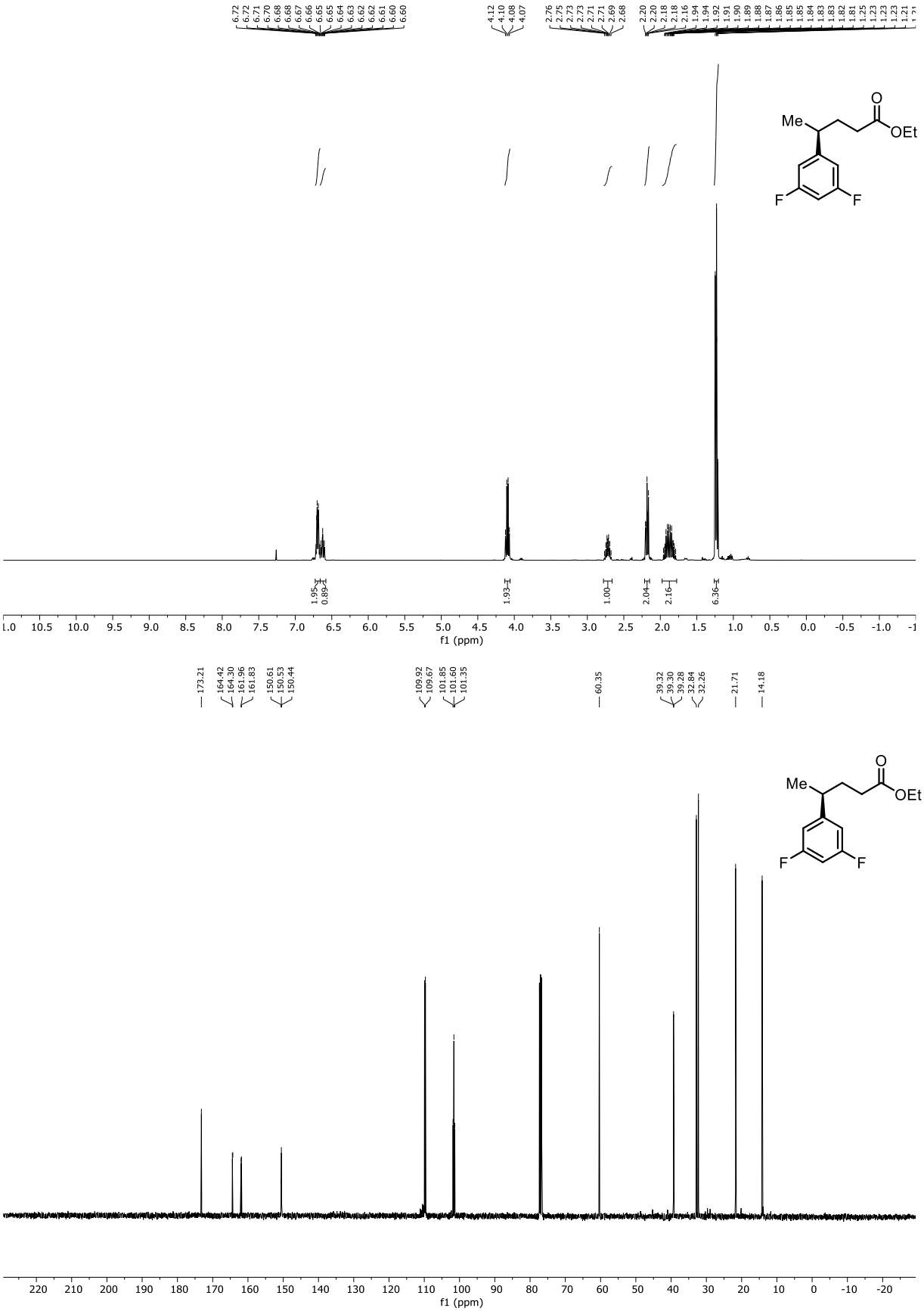

Figure 6.26 (top) ^{1}H NMR (400 MHz) and (bottom) ^{13}C NMR (101 MHz) spectra of *red*-**2-10m**.

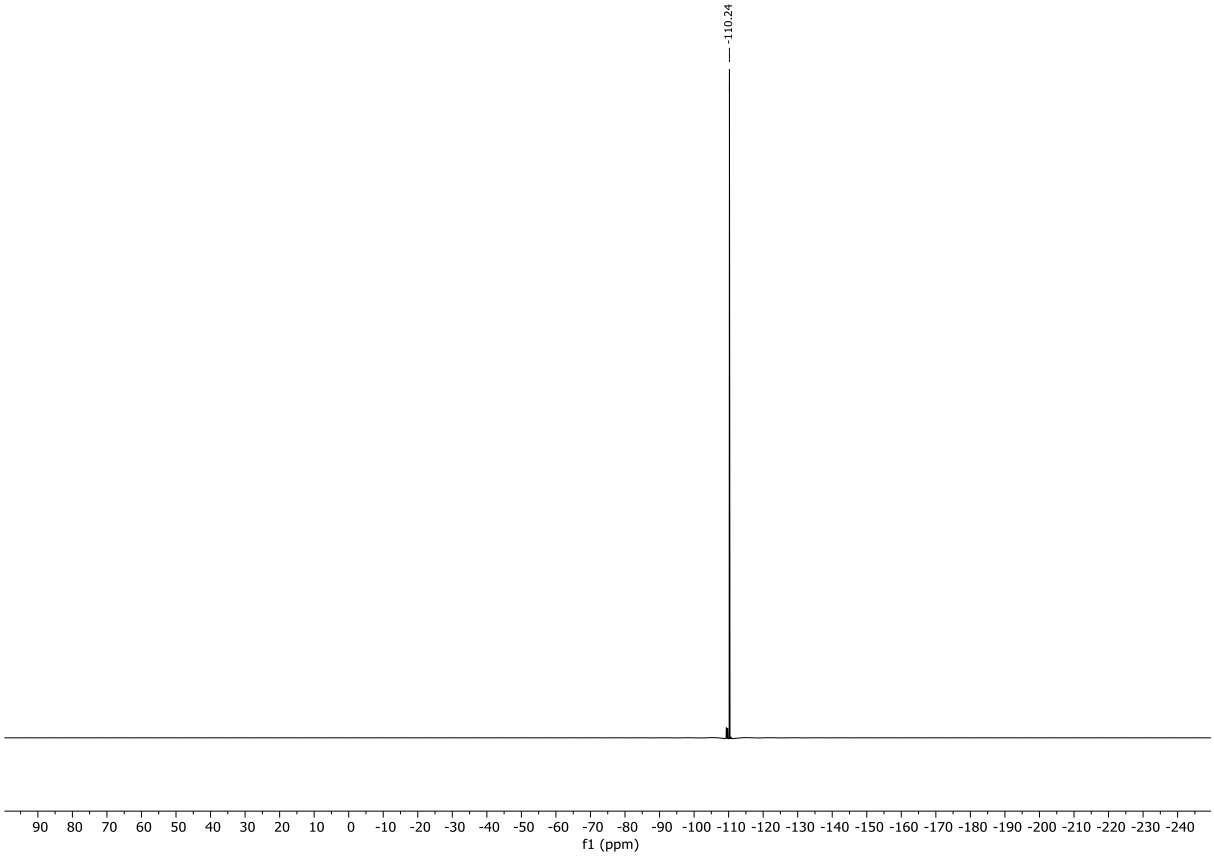

Figure 6.27 ^{19}F (13C)NMR (376 MHz) spectrum of *red*-**2-10m**.

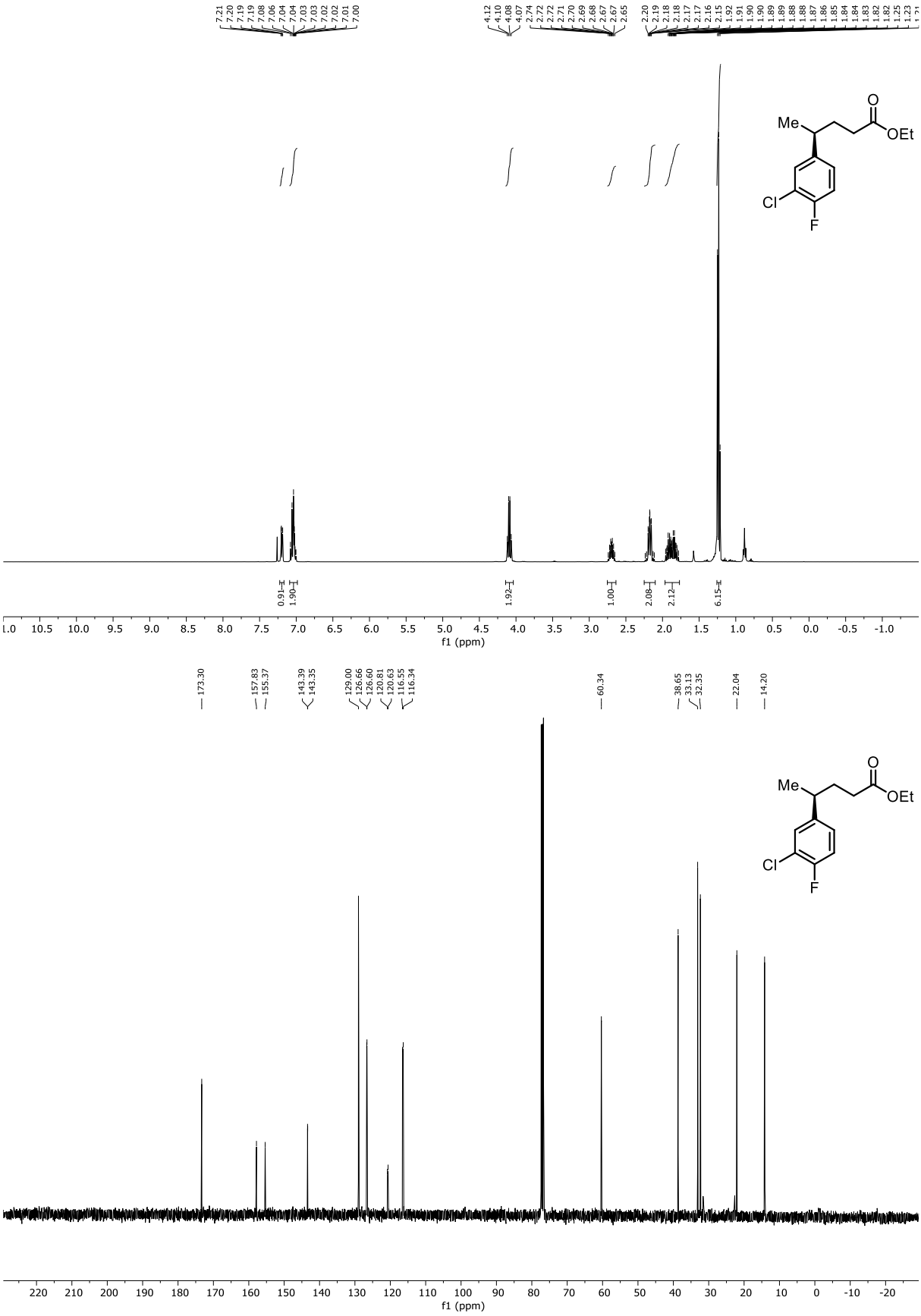

Figure 6.28 (top) ^{1}H NMR (400 MHz) and (bottom) ^{13}C NMR (101 MHz) spectra of *red*-**2-10n**.

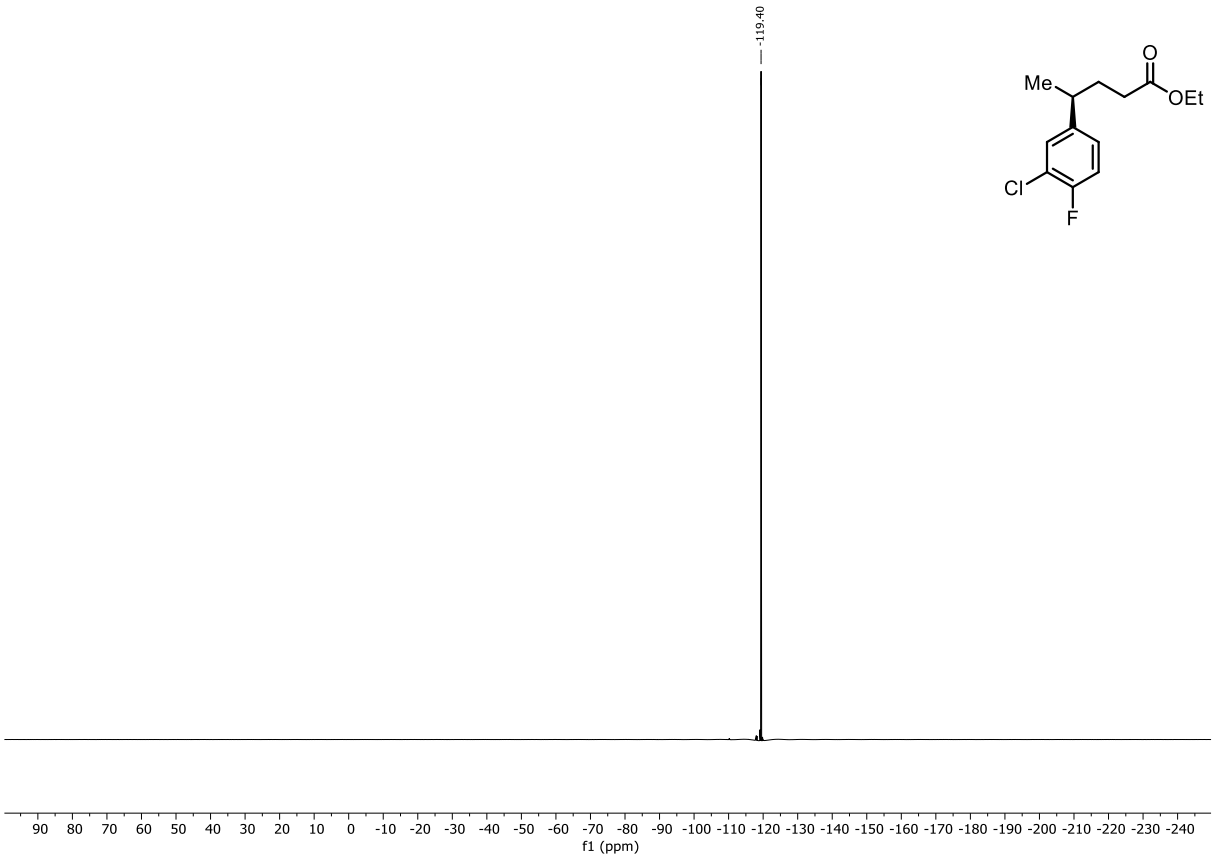

Figure 6.29 ^{19}F (13C)NMR (376 MHz) spectrum of *red*-**2-10n**.

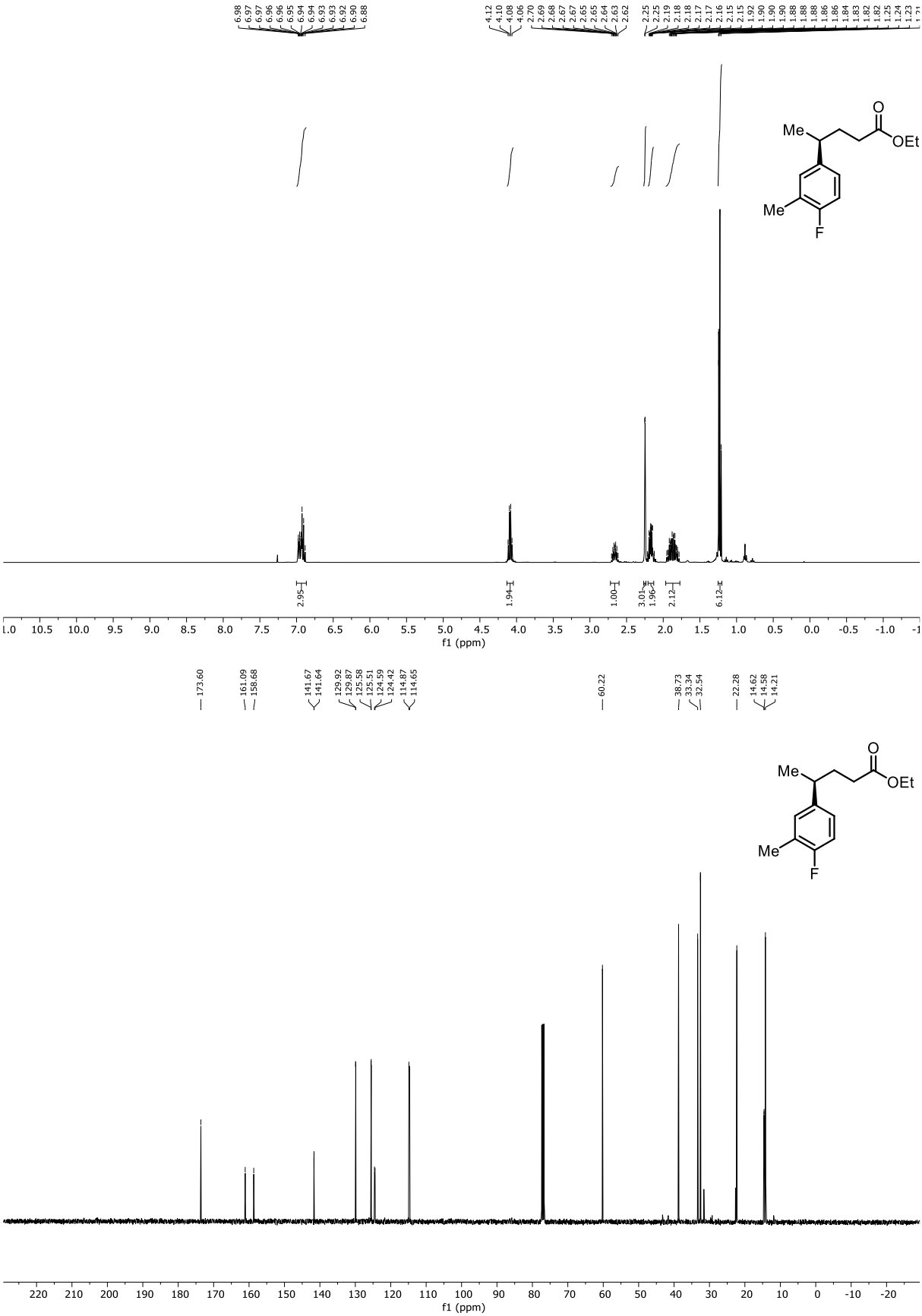

Figure 6.30 (top) ^{1}H NMR (400 MHz) and (bottom) ^{13}C NMR (101 MHz) spectra of *red*-**2-10o**.

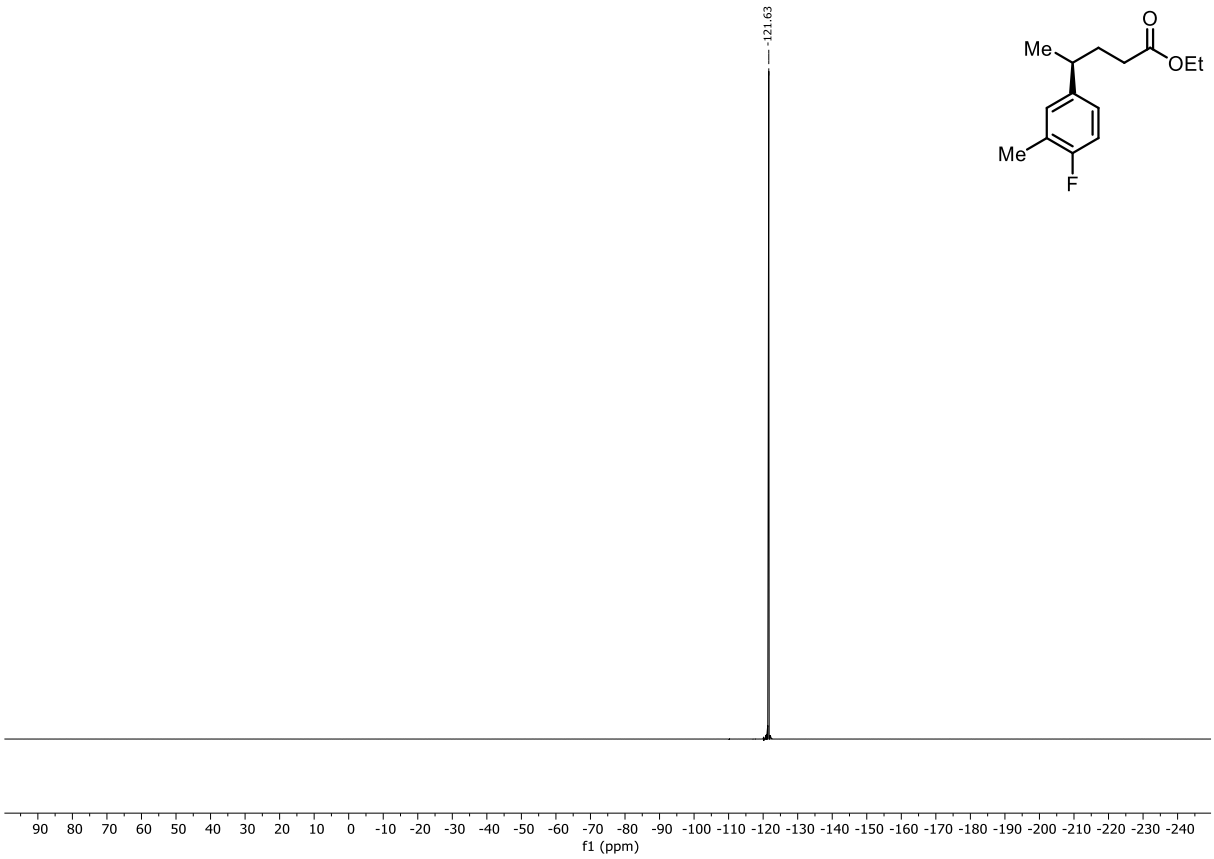

Figure 6.31 ^{19}F (13C)NMR (376 MHz) spectrum of *red*-**2-10o**.

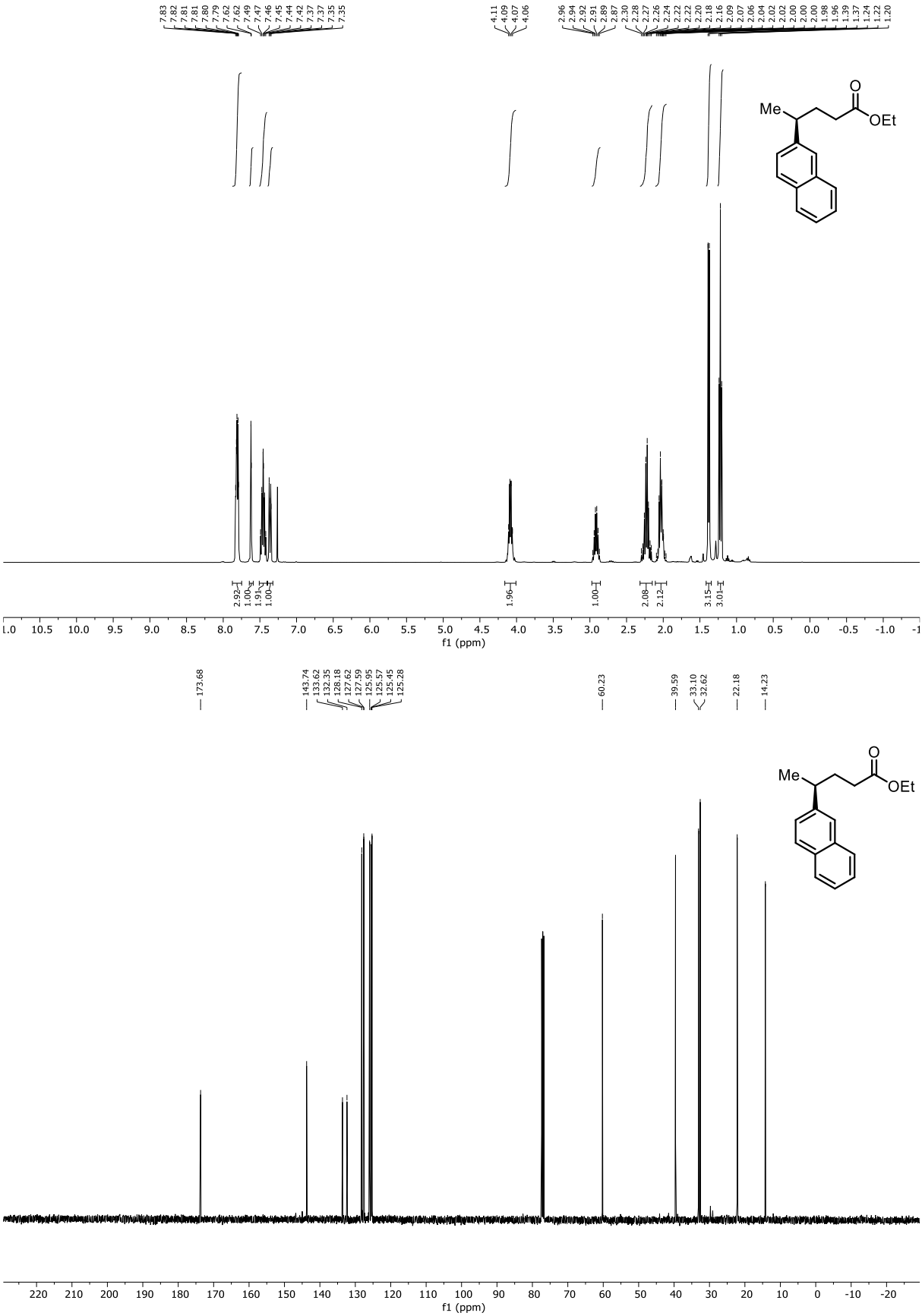

Figure 6.32 (top) ^{1}H NMR (400 MHz) and (bottom) ^{13}C NMR (101 MHz) spectra of *red*-**2-10p**.

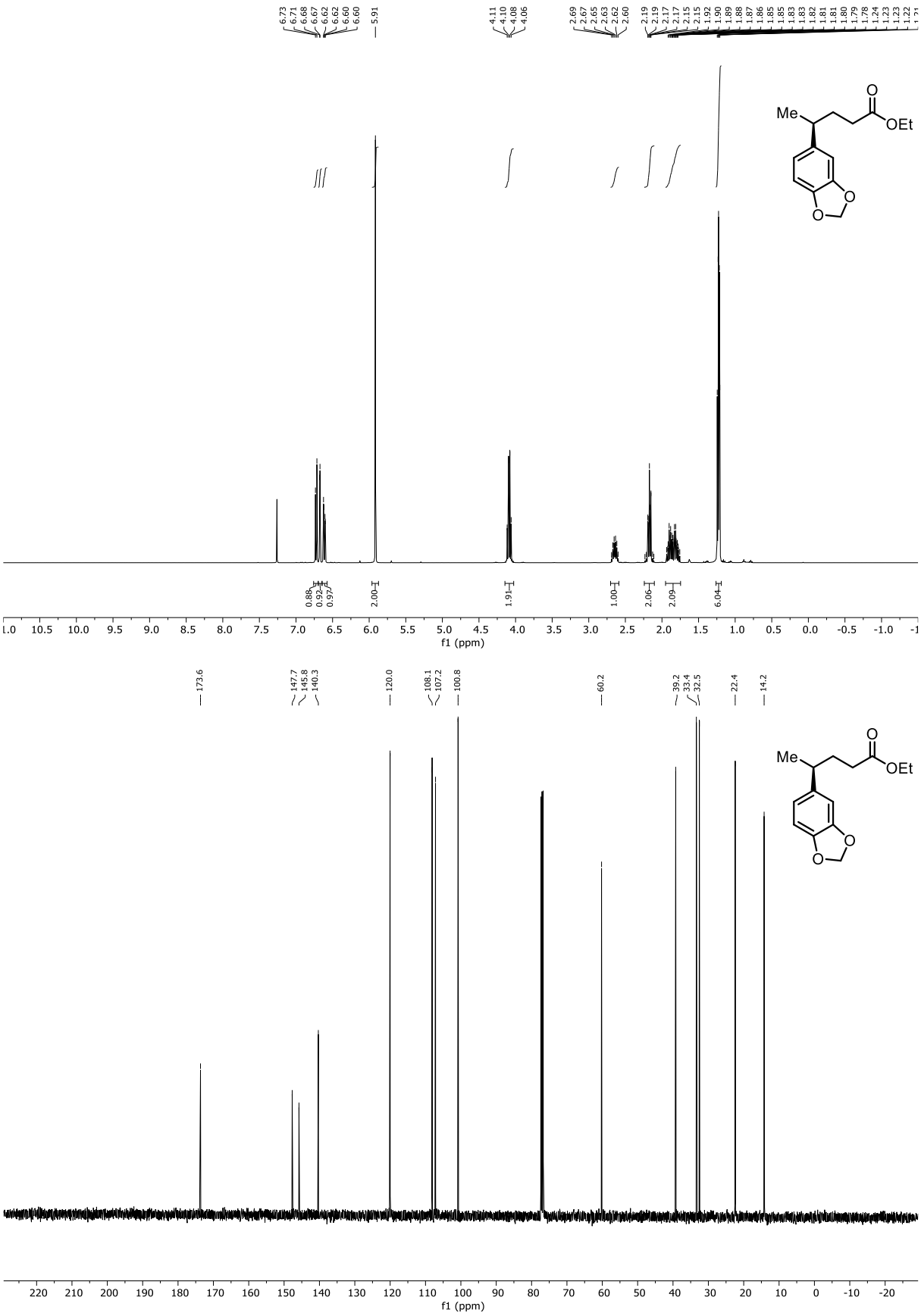

Figure 6.33 (top) ^{1}H NMR (400 MHz) and (bottom) ^{13}C NMR (101 MHz) spectra of *red*-**2-10q**.

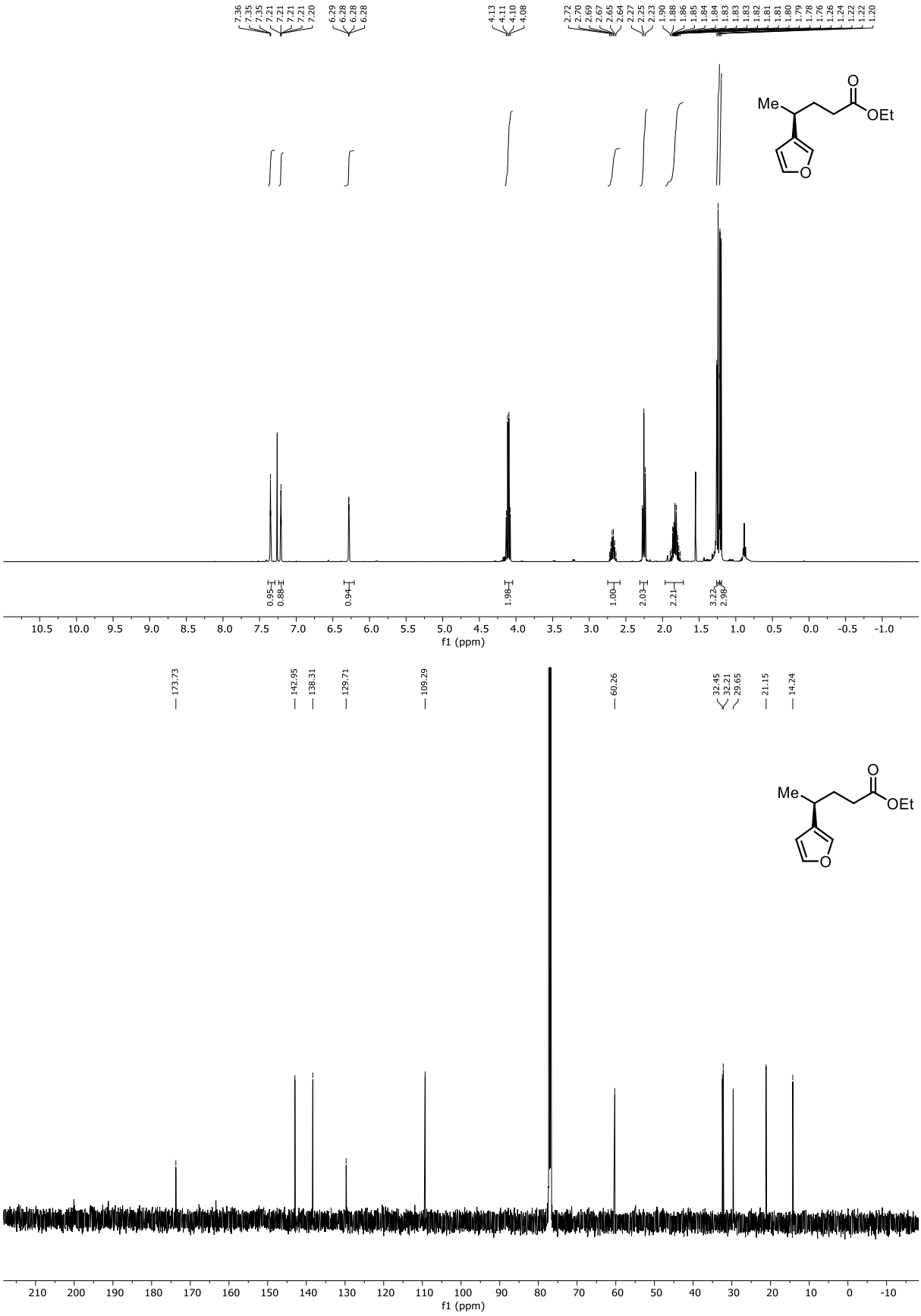

Figure 6.34 (top) ^{1}H NMR (400 MHz) and (bottom) ^{13}C NMR (101 MHz) spectra of *red*-**2-10r**.

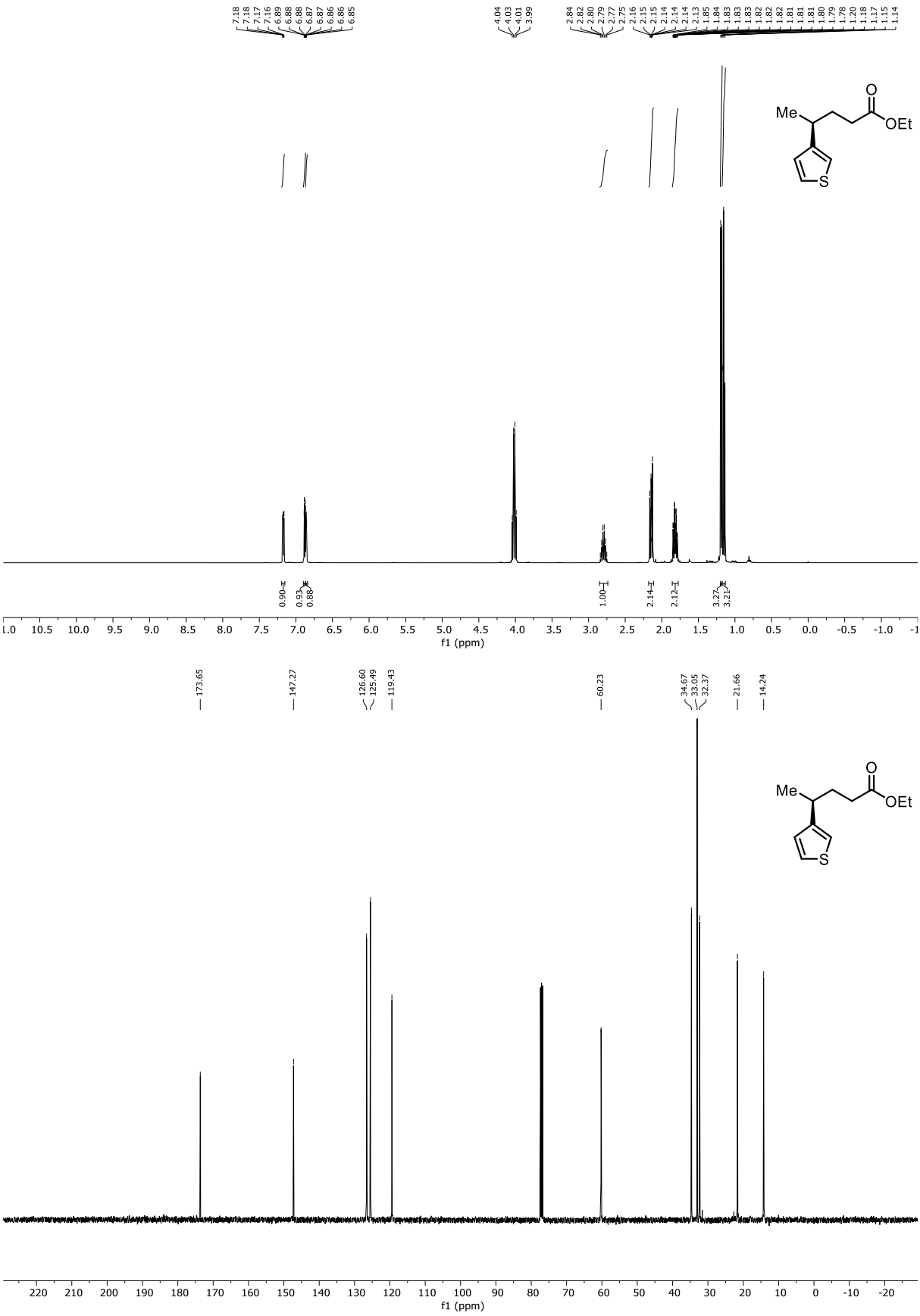

Figure 6.35 (top) ^{1}H NMR (400 MHz) and (bottom) ^{13}C NMR (101 MHz) spectra of *red*-**2-10s**.

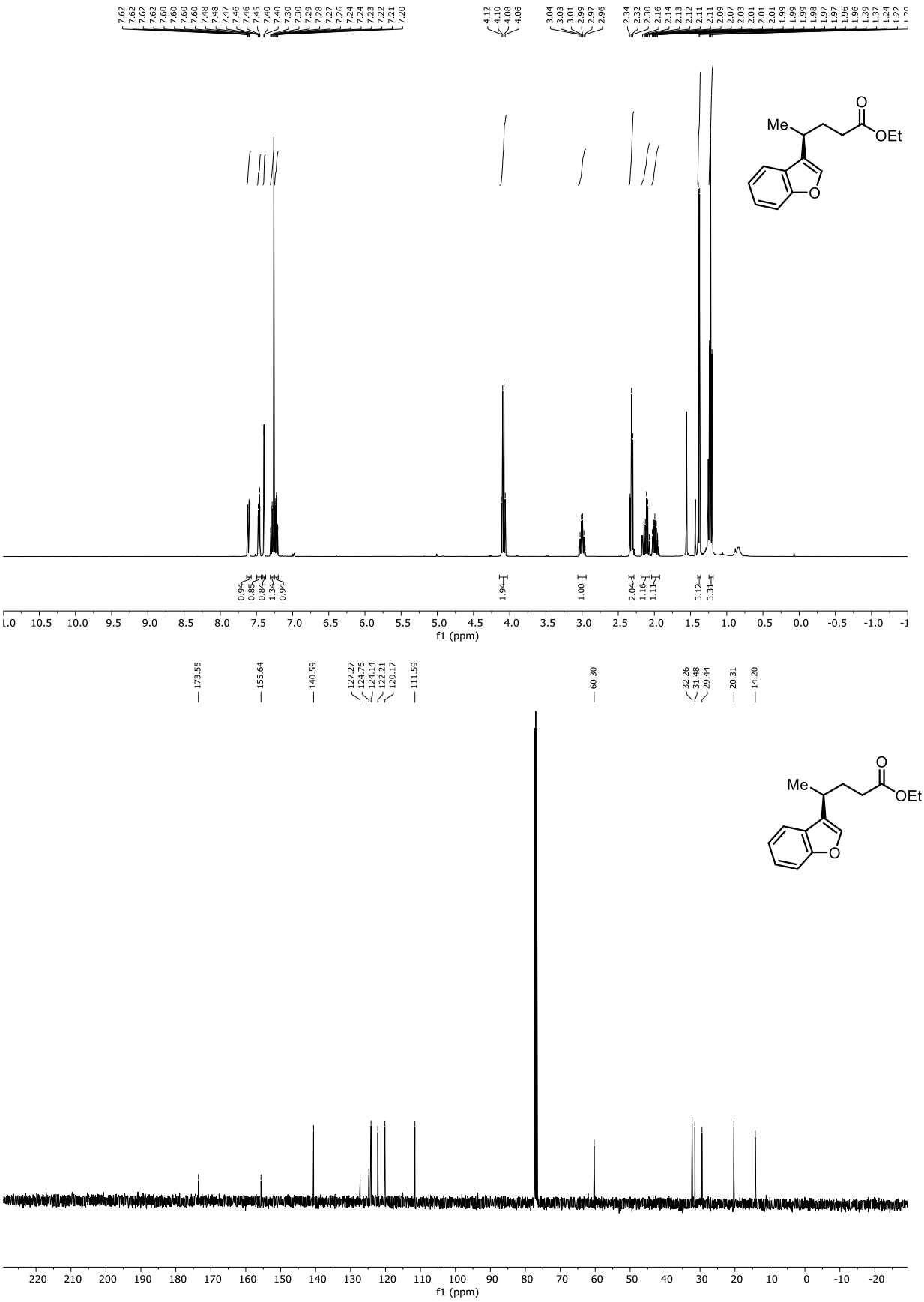

Figure 6.36 (top) ^{1}H NMR (400 MHz) and (bottom) ^{13}C NMR (101 MHz) spectra of *red*-**2-10t**.

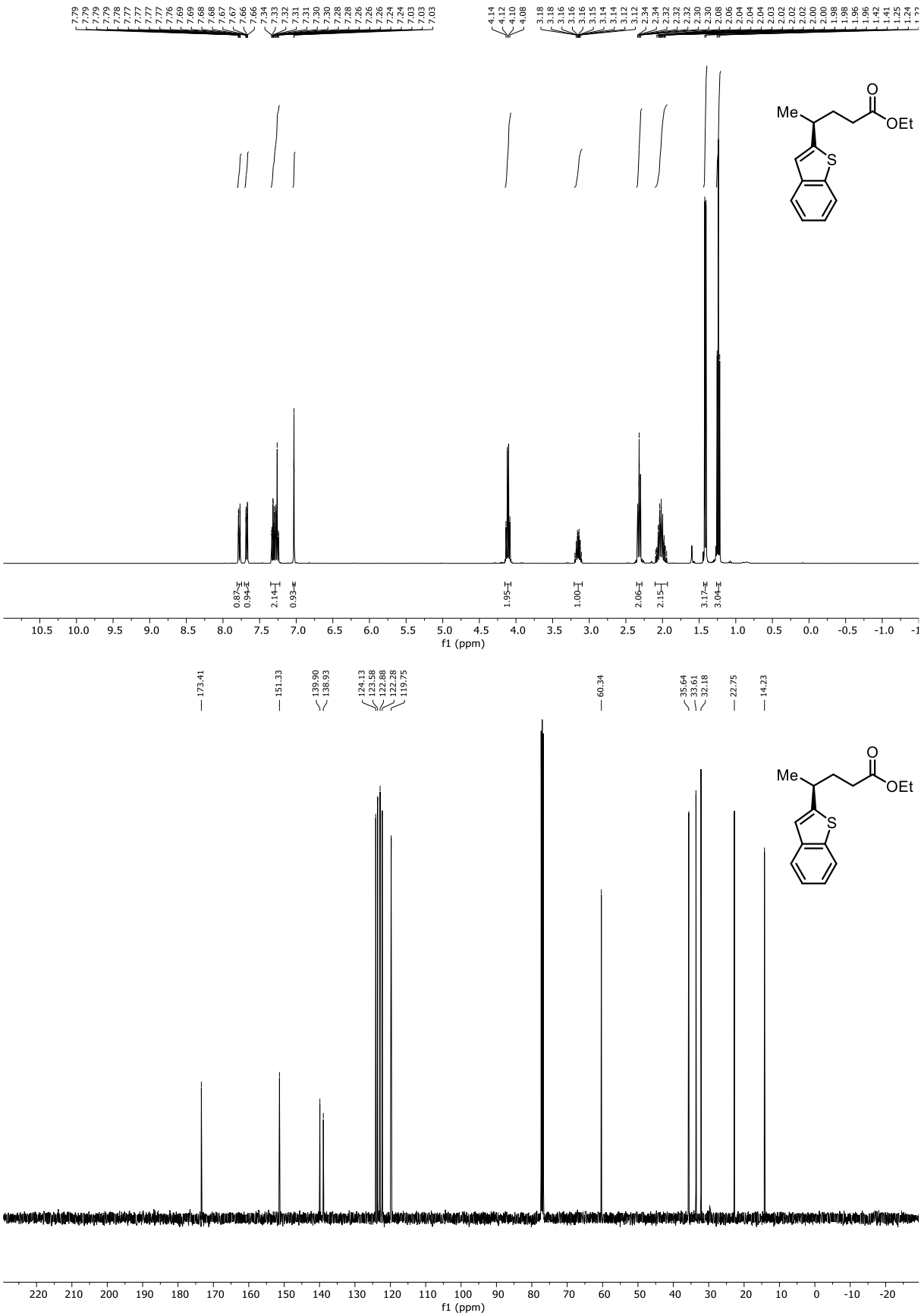

Figure 6.37 (top) ^{1}H NMR (400 MHz) and (bottom) ^{13}C NMR (101 MHz) spectra of *red*-**2-10u**.

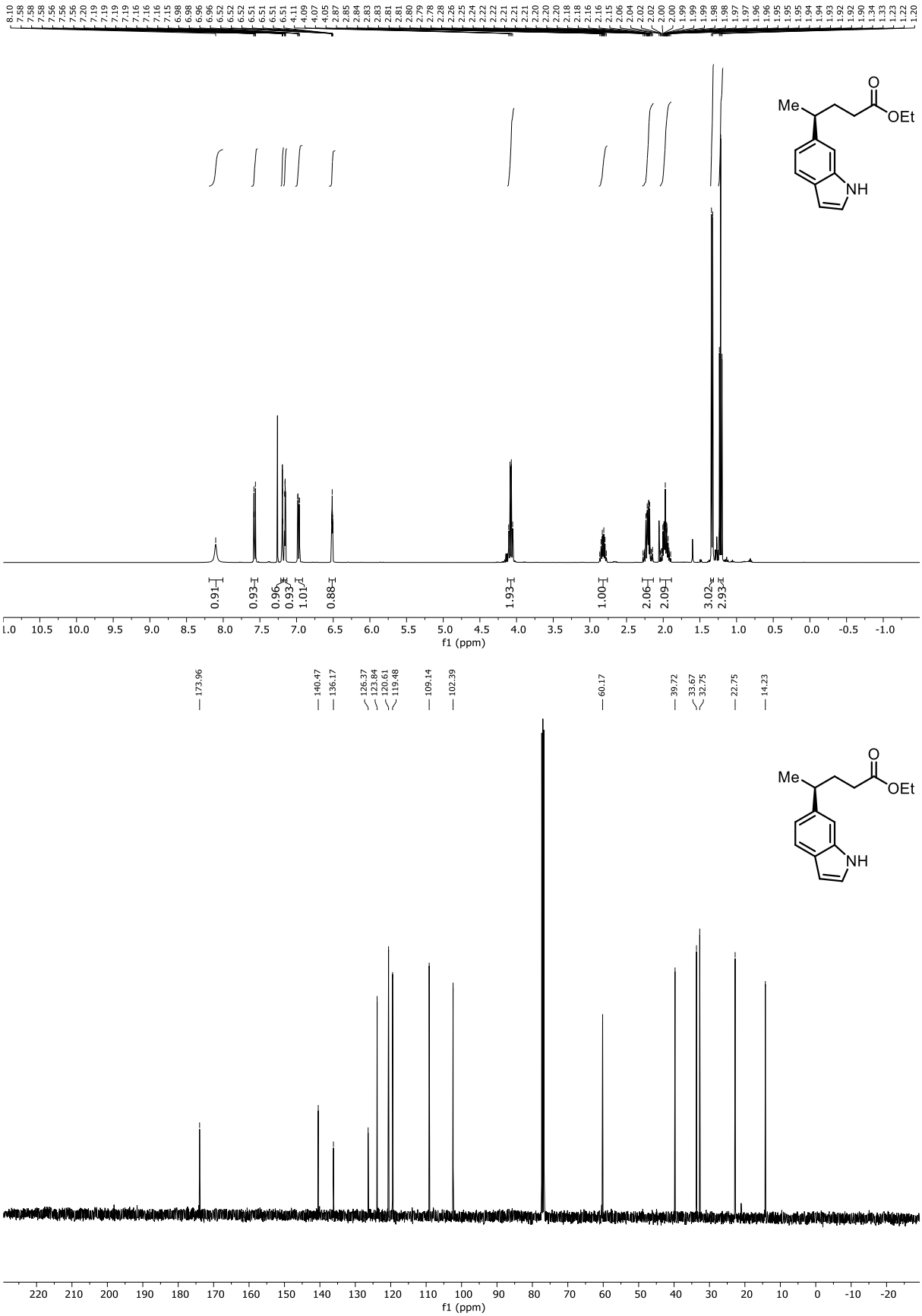

Figure 6.38 (top) ^{1}H NMR (400 MHz) and (bottom) ^{13}C NMR (101 MHz) spectra of *red*-**2-10v**.

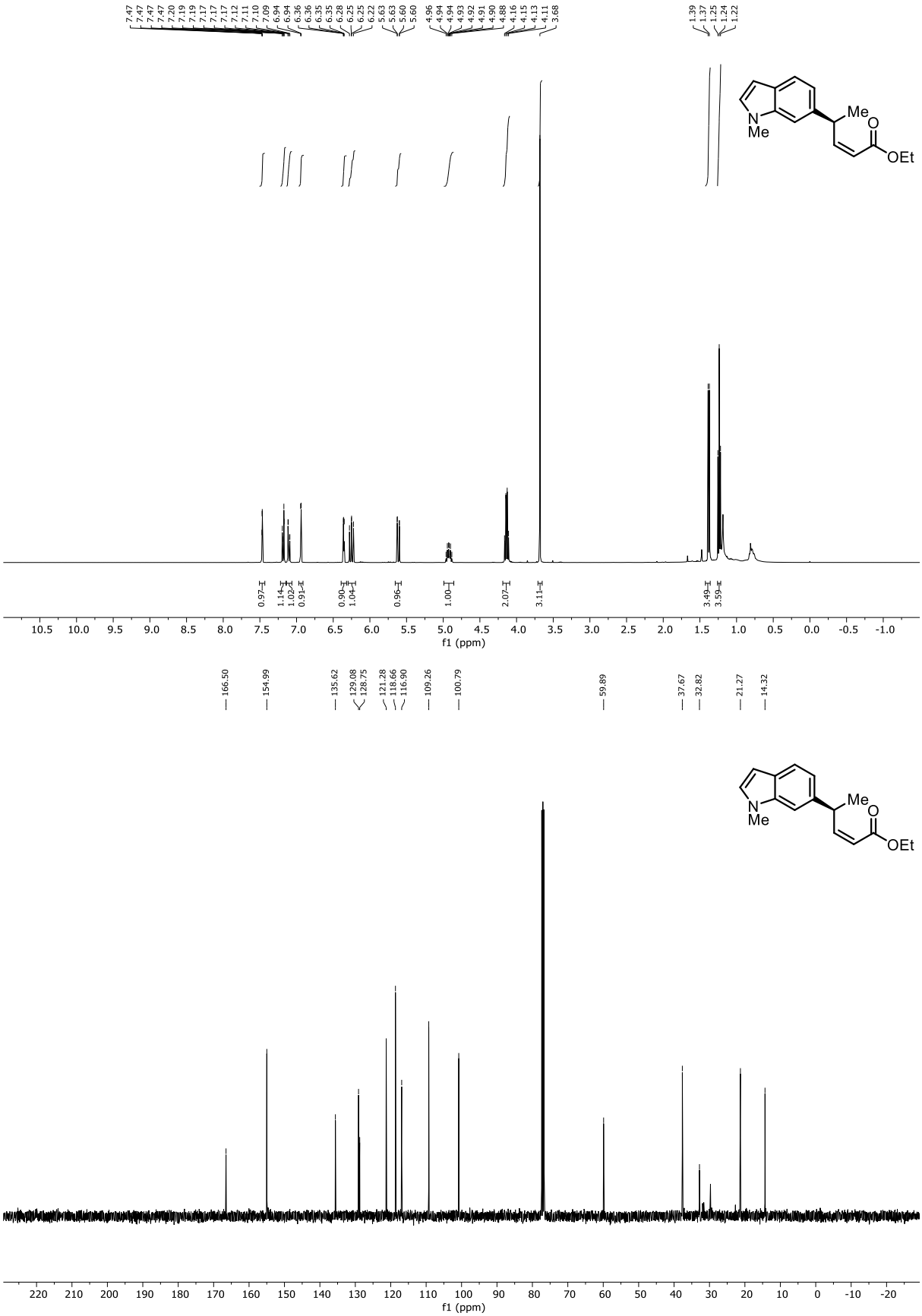

Figure 6.39 (top) ^{1}H NMR (400 MHz) and (bottom) ^{13}C NMR (101 MHz) spectra of *Z*-**2-10w**.

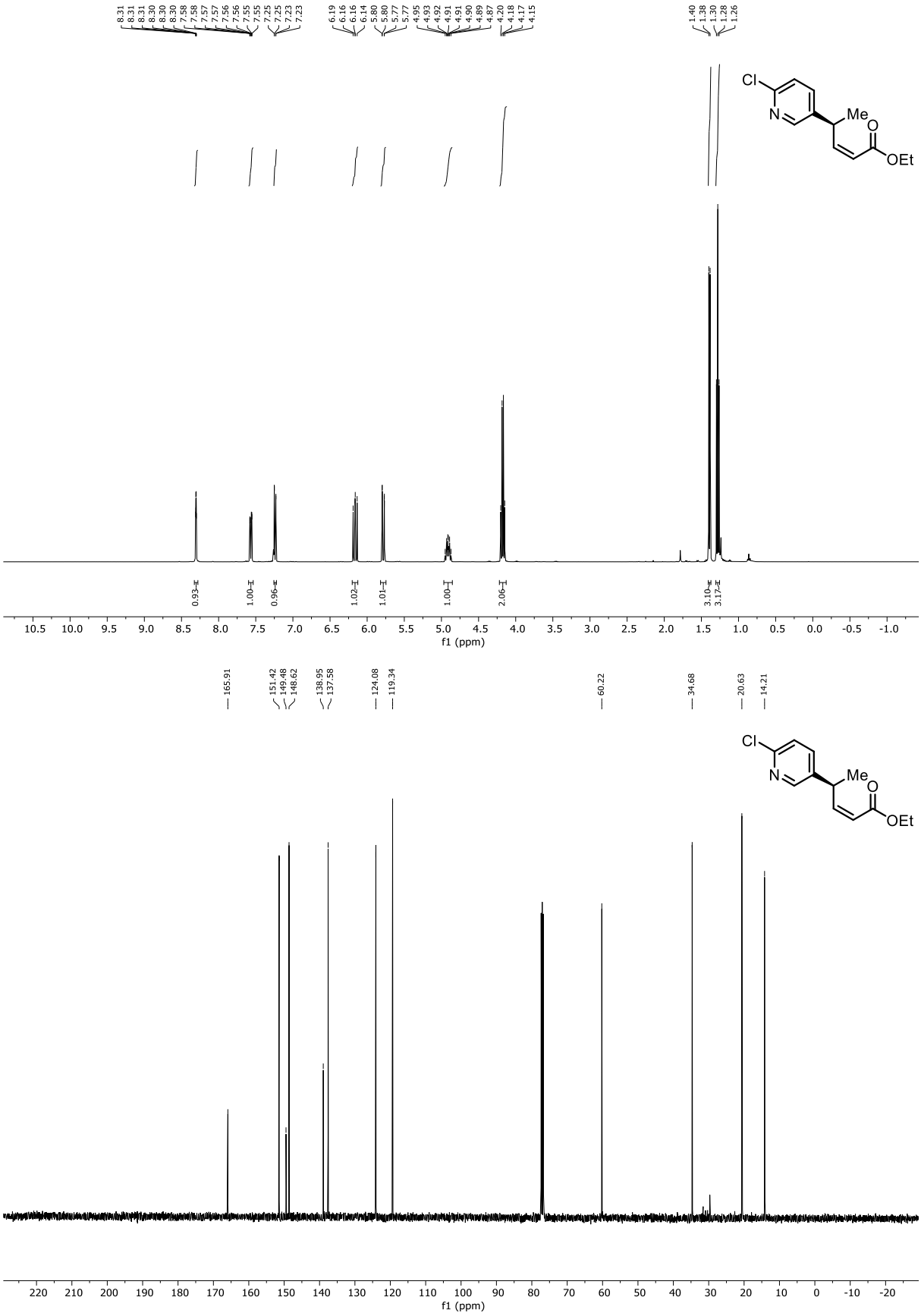

Figure 6.40 (top) ^{1}H NMR (400 MHz) and (bottom) ^{13}C NMR (101 MHz) spectra of *Z*-**2-10x**.

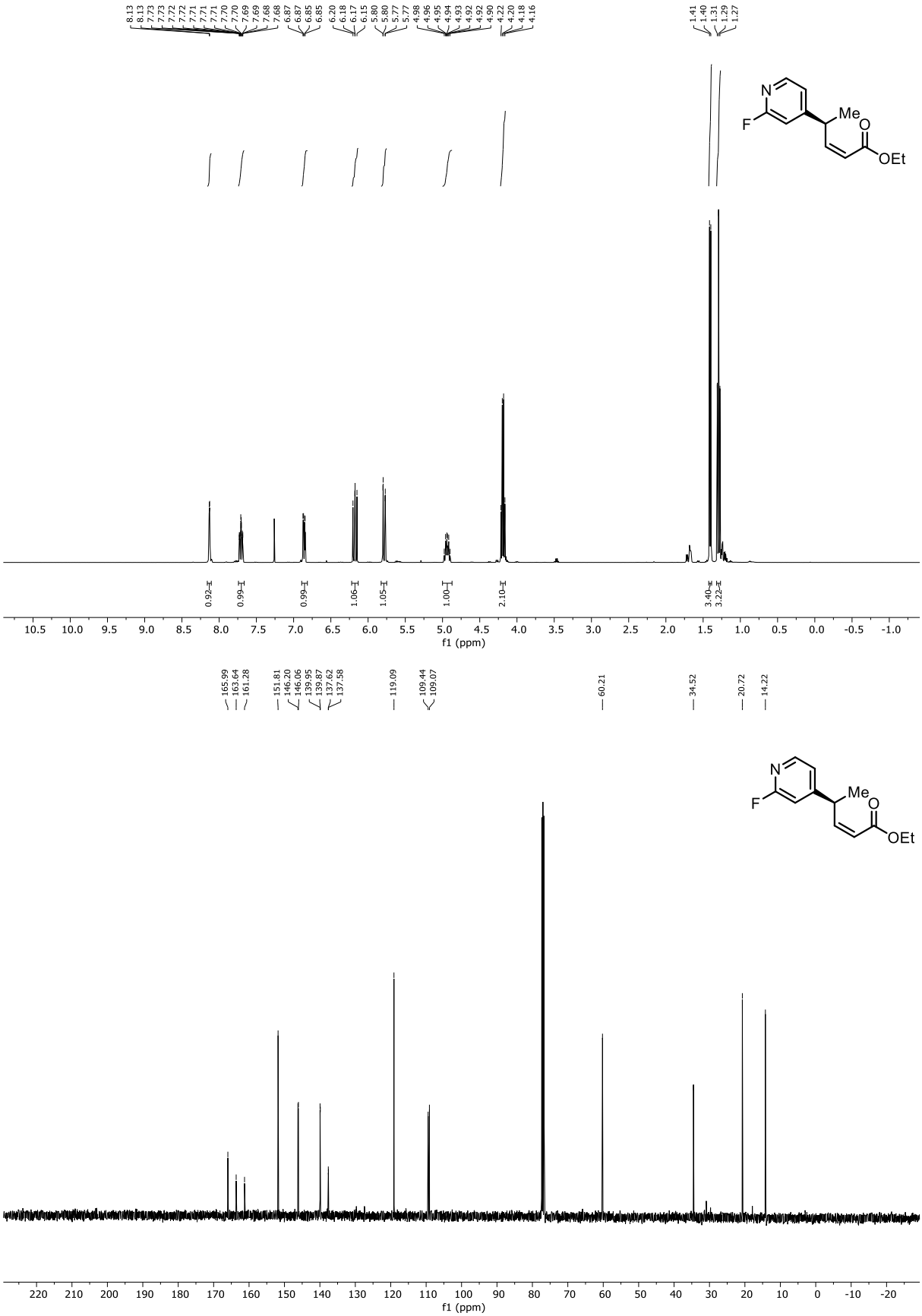

Figure 6.41 (top) ^{1}H NMR (400 MHz) and (bottom) ^{13}C NMR (101 MHz) spectra of *Z*-**2-10y**.

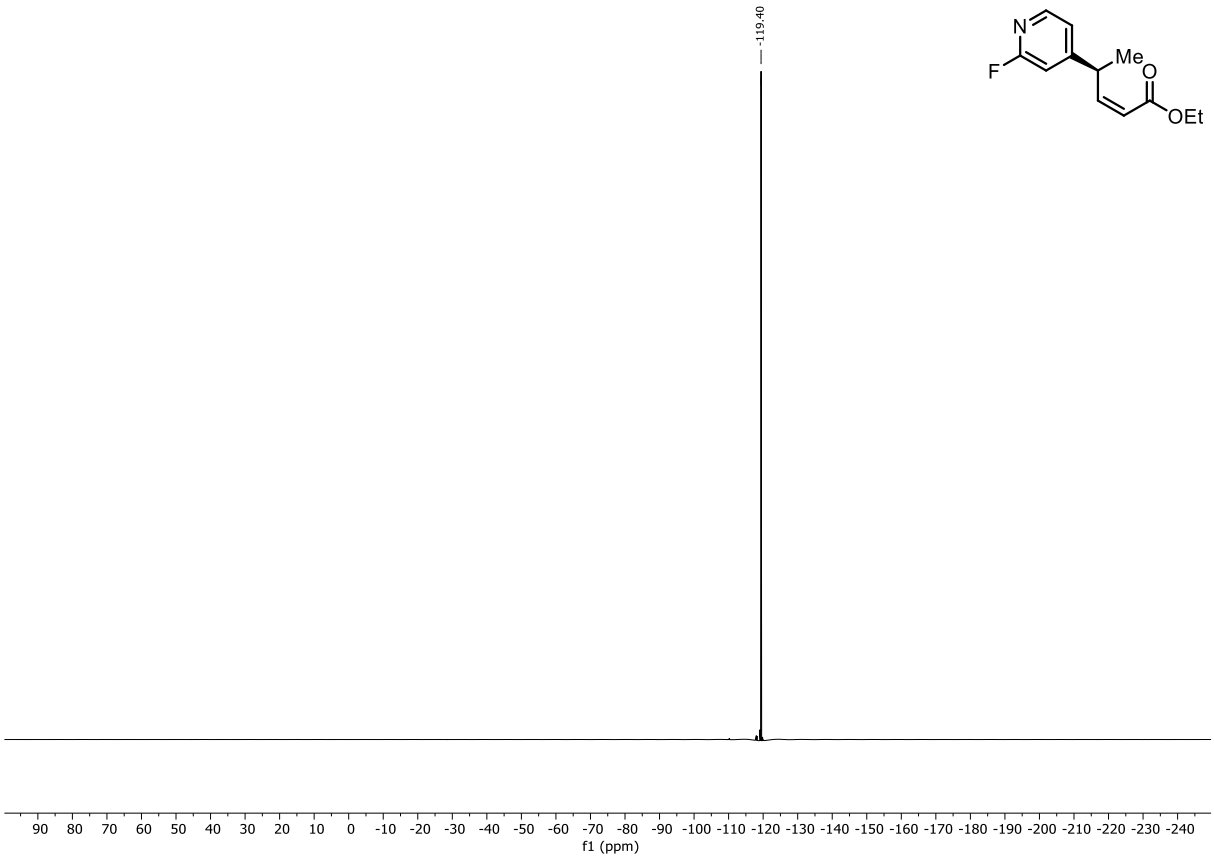

Figure 6.42 ^{19}F (13C)NMR (376 MHz) spectrum of *Z*-**2-10y**.

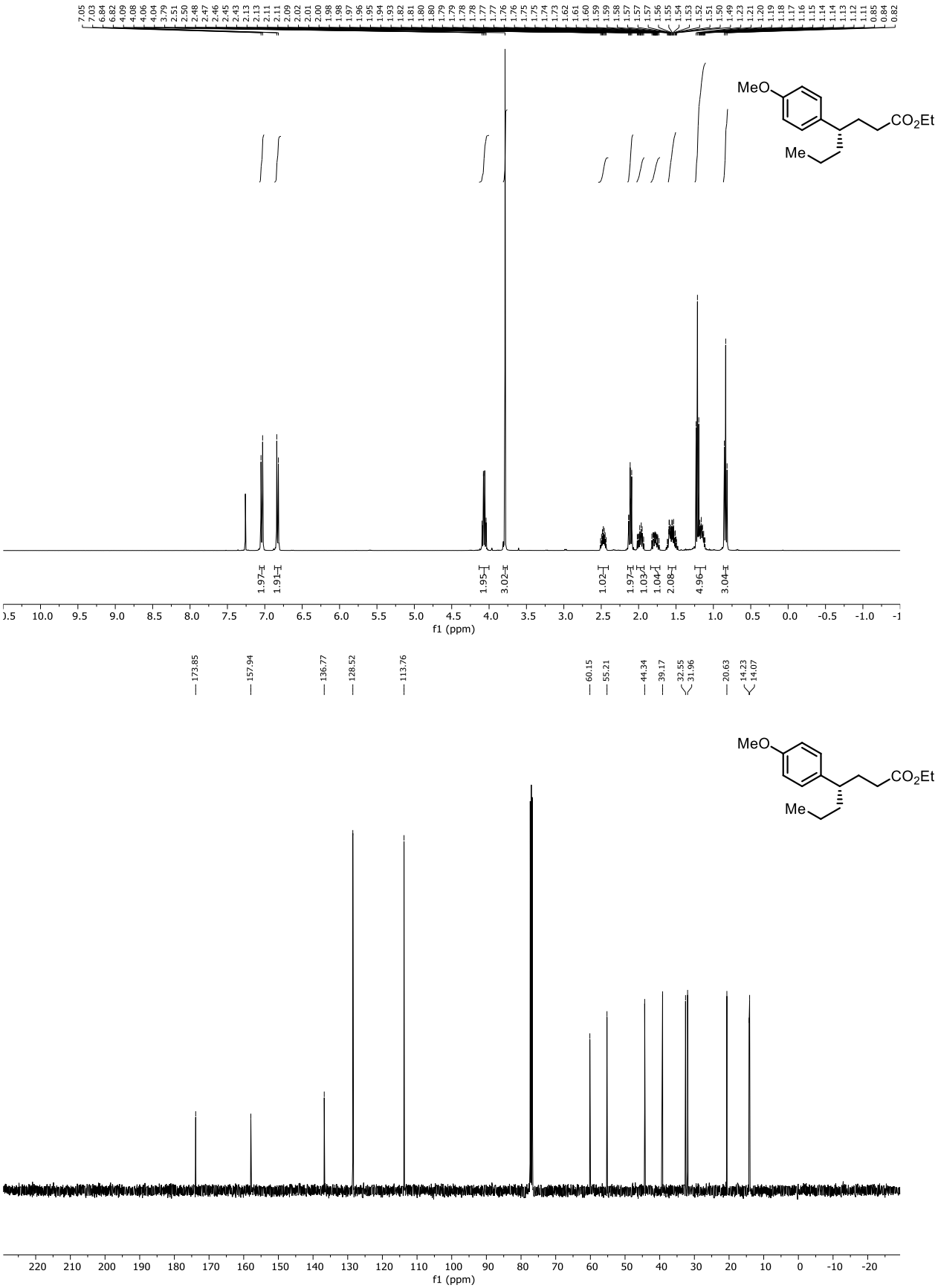

Figure 6.43 (top) ^{1}H NMR (400 MHz) and (bottom) ^{13}C NMR (101 MHz) spectra of *red*-**2-12a**.

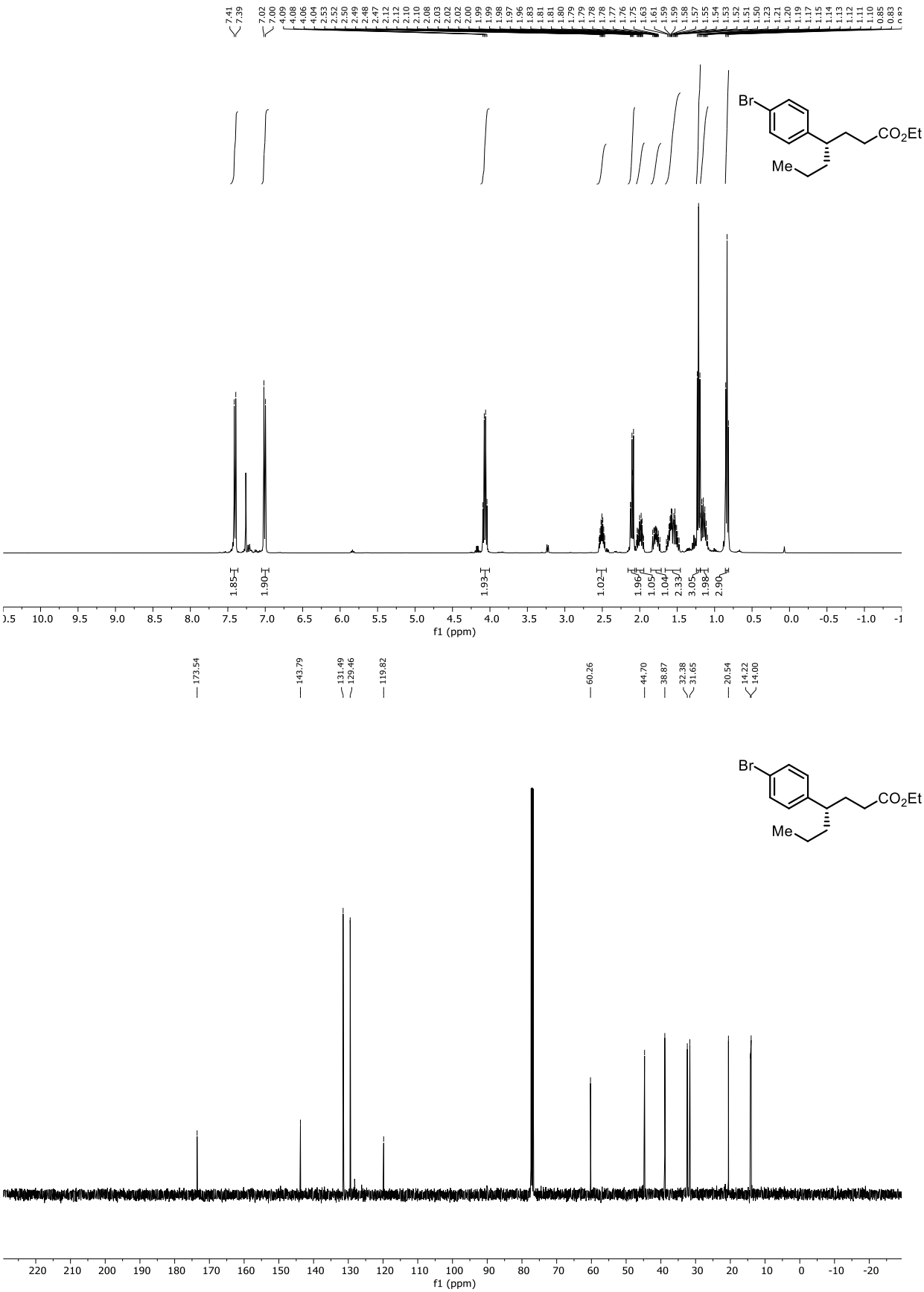

Figure 6.44 (top) ^{1}H NMR (400 MHz) and (bottom) ^{13}C NMR (101 MHz) spectra of *red*-**2-12b**.

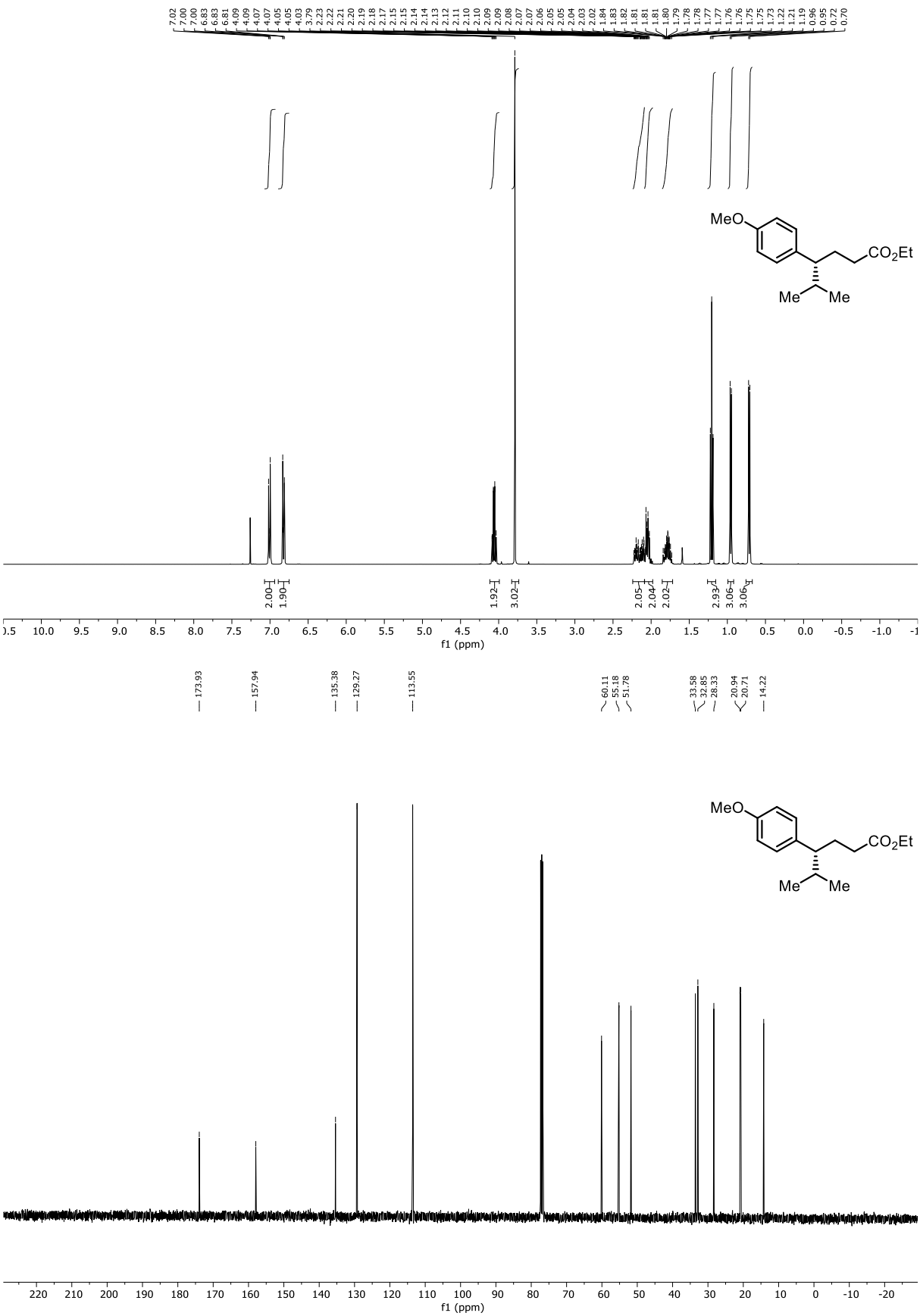

Figure 6.45 (top) ^{1}H NMR (400 MHz) and (bottom) ^{13}C NMR (101 MHz) spectra of *red*-**2-12c**.

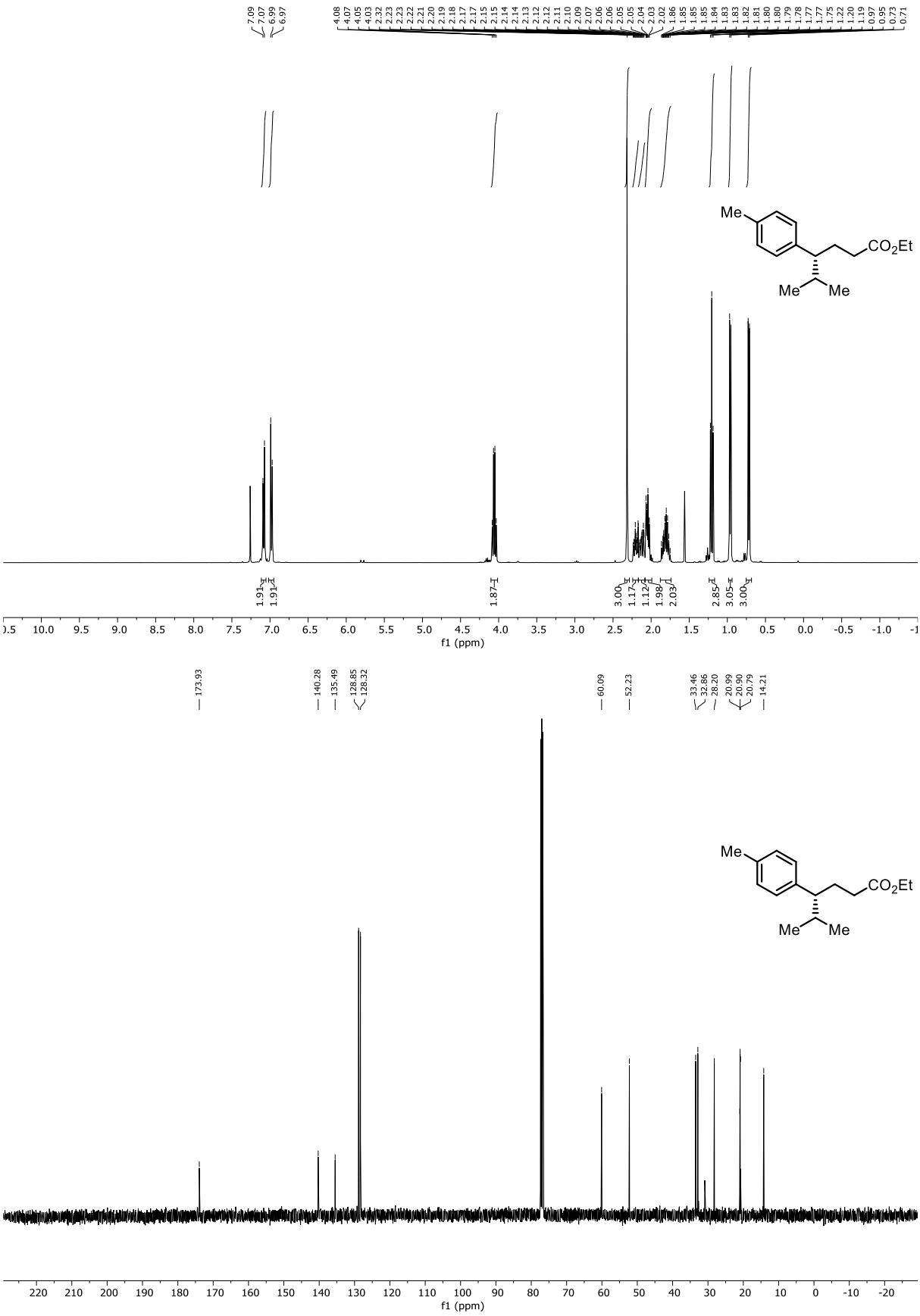

Figure 6.46 (top) ^{1}H NMR (400 MHz) and (bottom) ^{13}C NMR (101 MHz) spectra of *red*-**2-12d**.

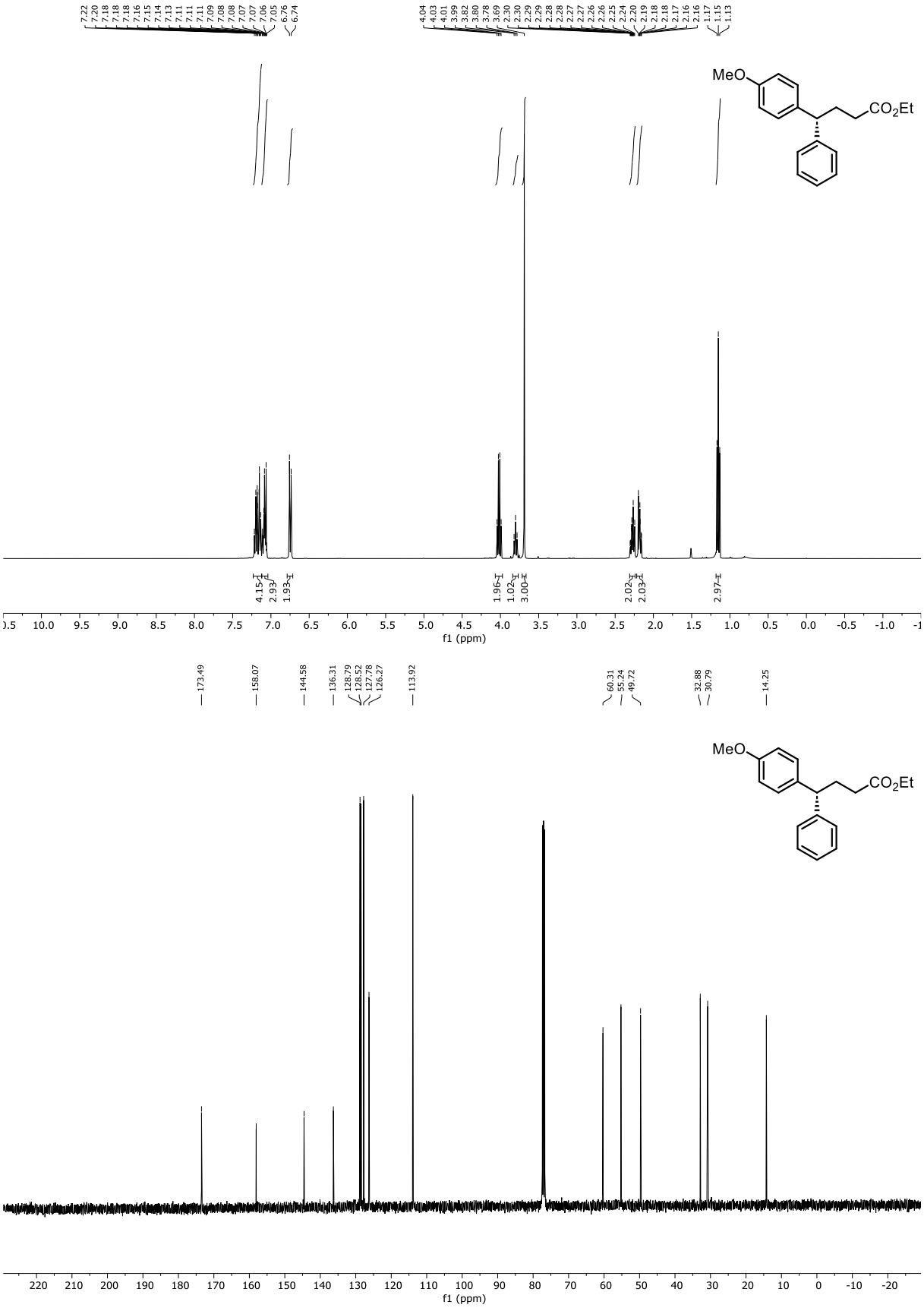

Figure 6.47 (top) ^{1}H NMR (400 MHz) and (bottom) ^{13}C NMR (101 MHz) spectra of *red*-**2-12g**.

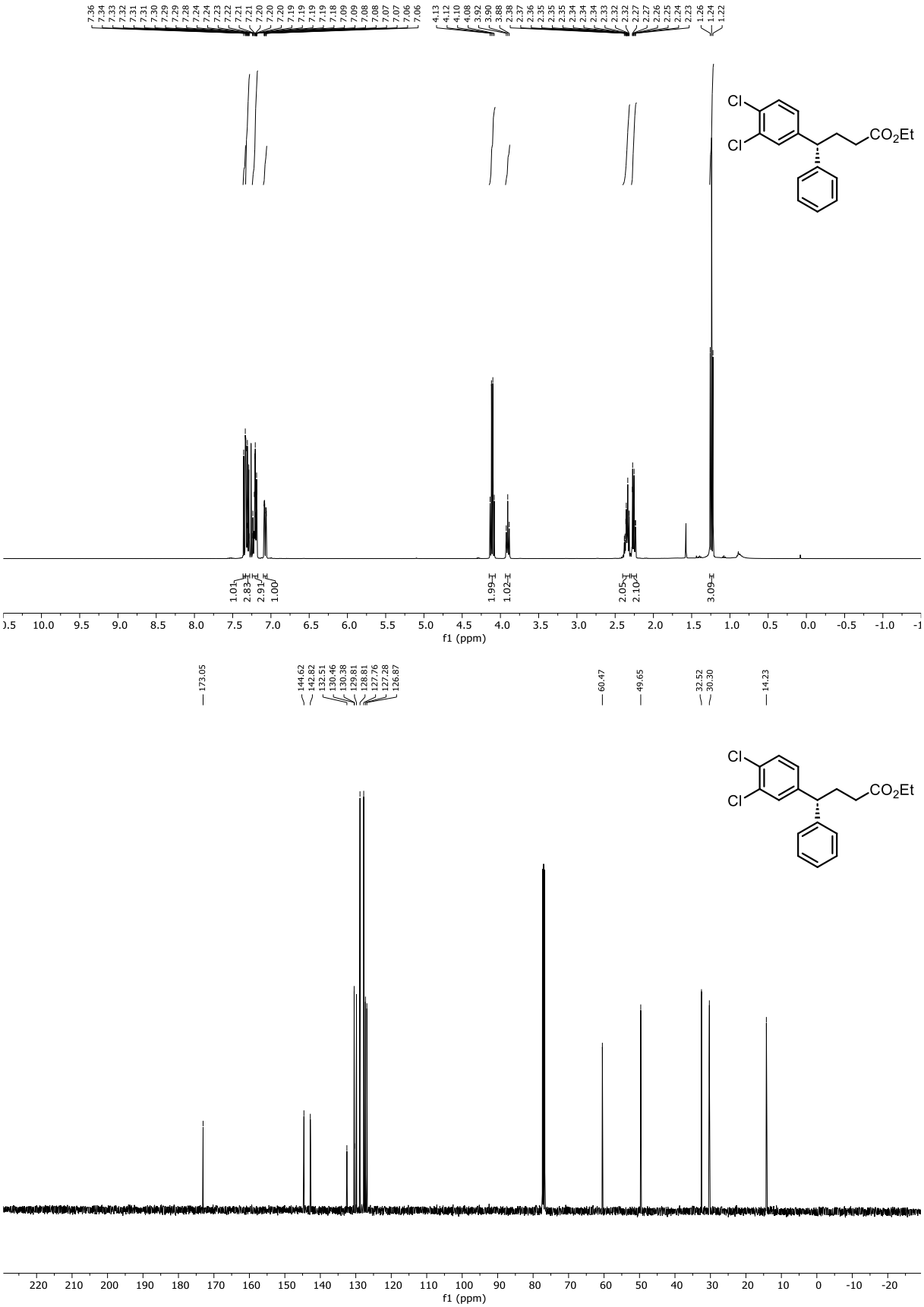

Figure 6.48 (top) ^{1}H NMR (400 MHz) and (bottom) ^{13}C NMR (101 MHz) spectra of *red*-**2-12h**.

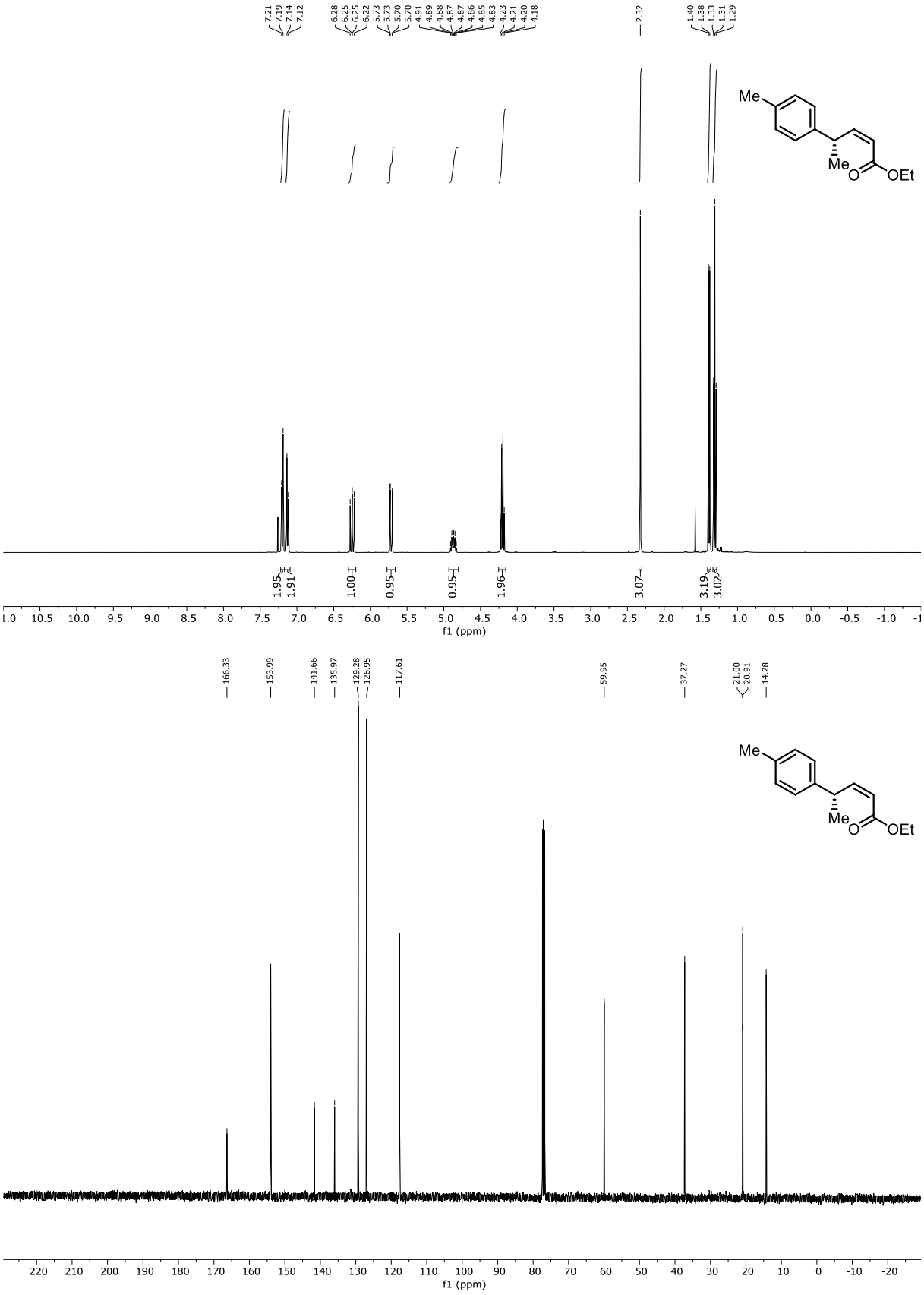

Figure 6.49 (top) ^{1}H NMR (400 MHz) and (bottom) ^{13}C NMR (101 MHz) spectra of *Z*-**2-10d**.

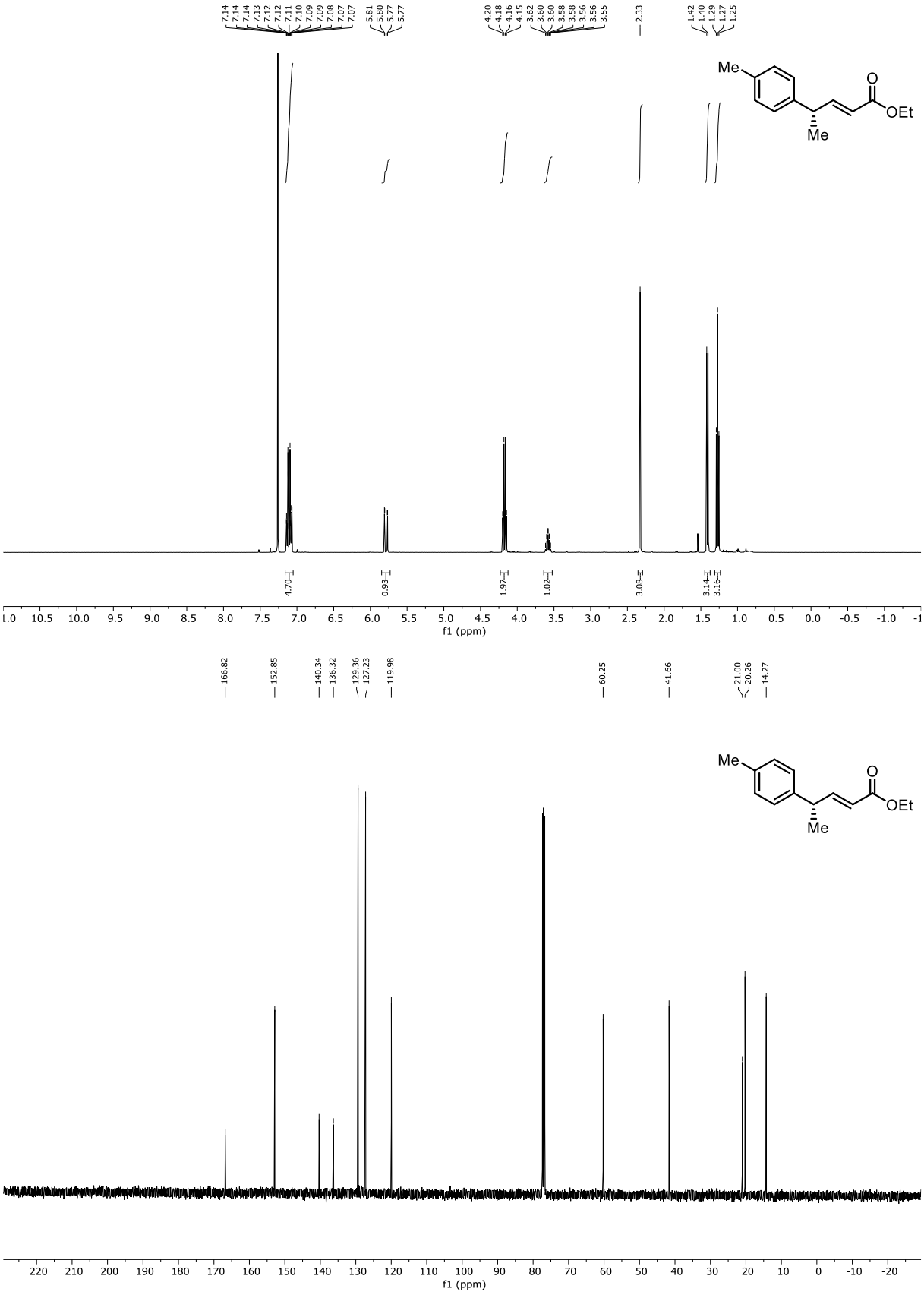

Figure 6.50 (top) ^{1}H NMR (400 MHz) and (bottom) ^{13}C NMR (101 MHz) spectra of *E*-**2-10d**.

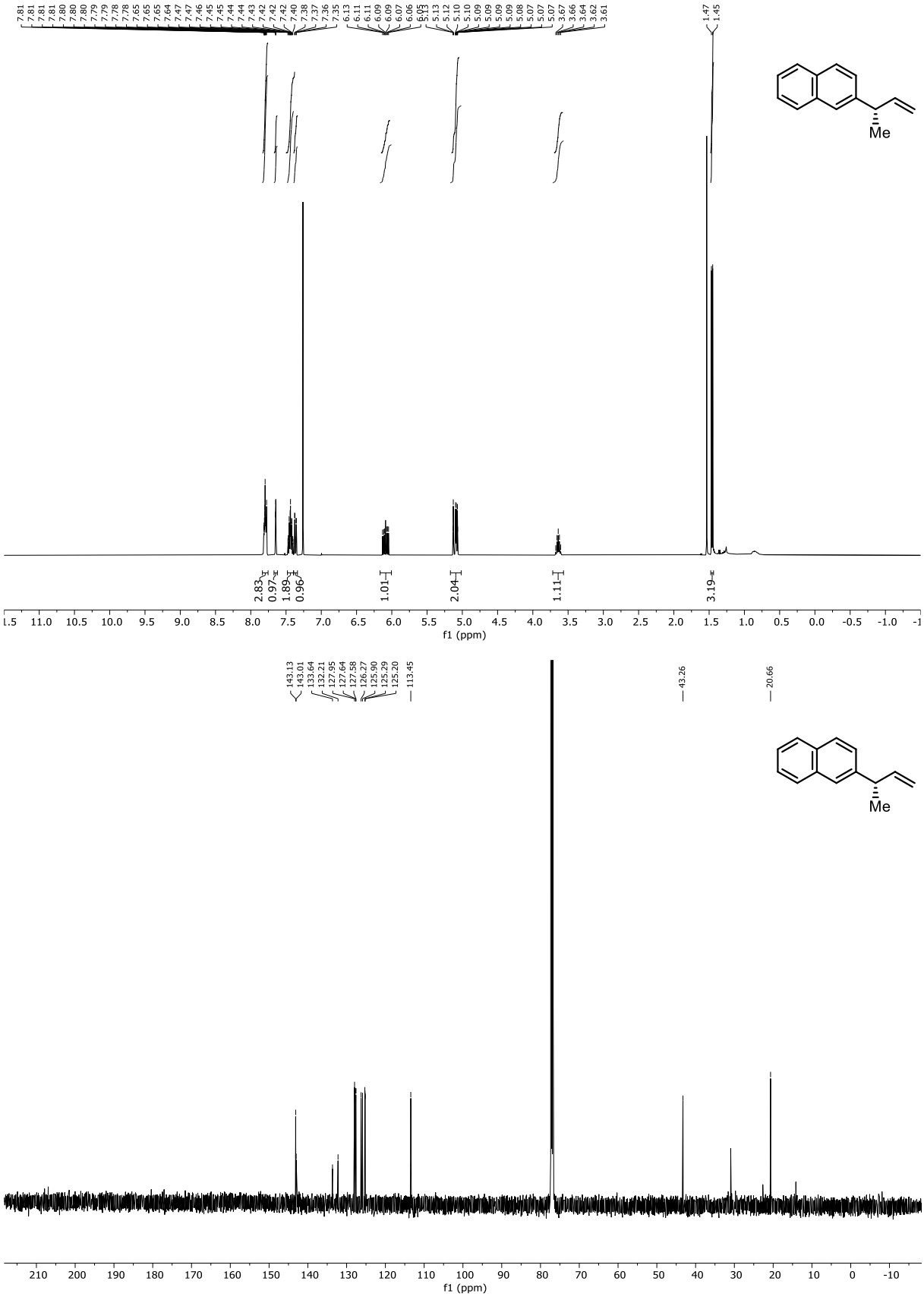

Figure 6.51 (top) ^{1}H NMR (400 MHz) and (bottom) ^{13}C NMR (101 MHz) spectra of **2-15**.

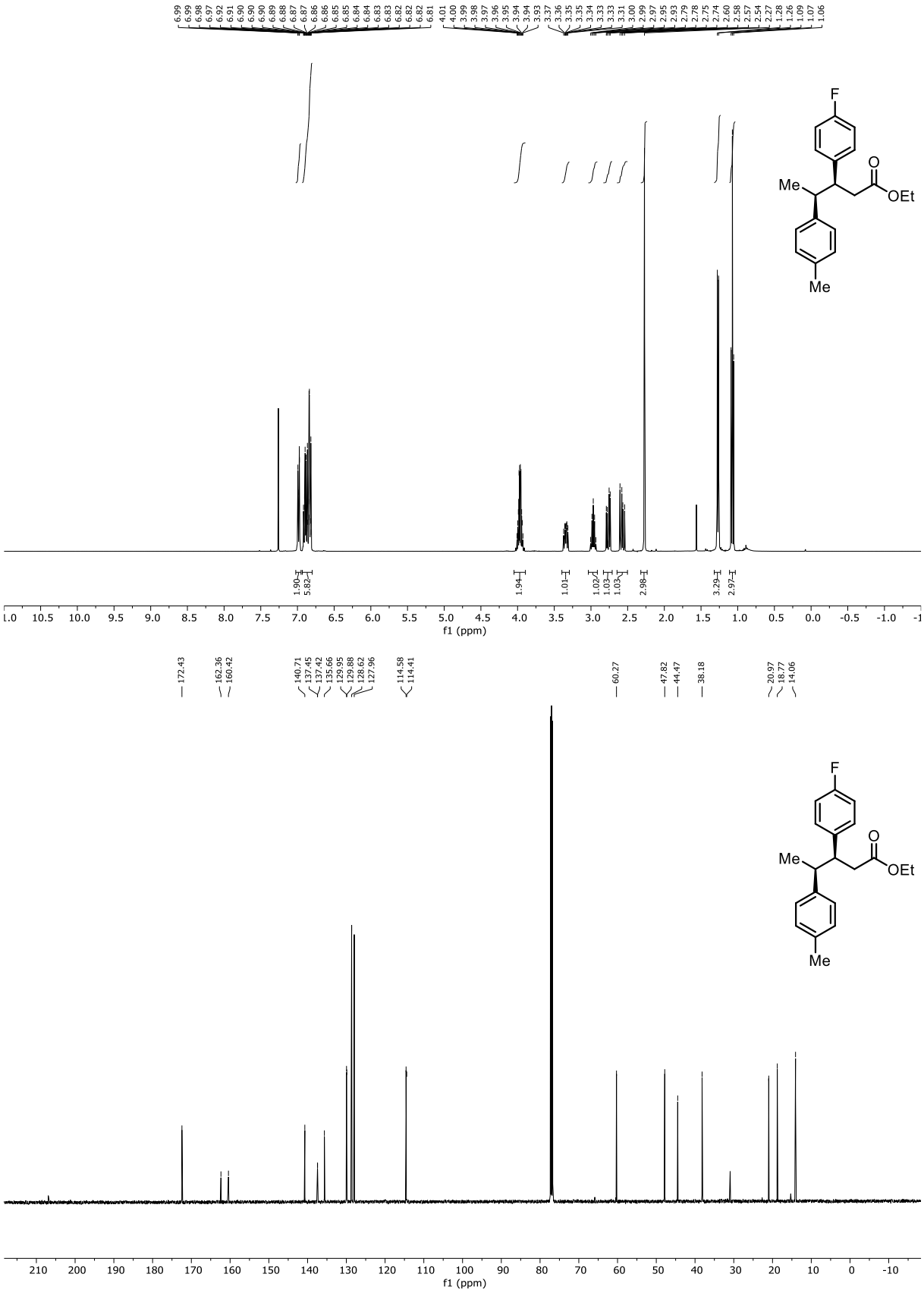

Figure 6.52 (top) ^{1}H NMR (400 MHz) and (bottom) ^{13}C NMR (101 MHz) spectra of **2-13**.

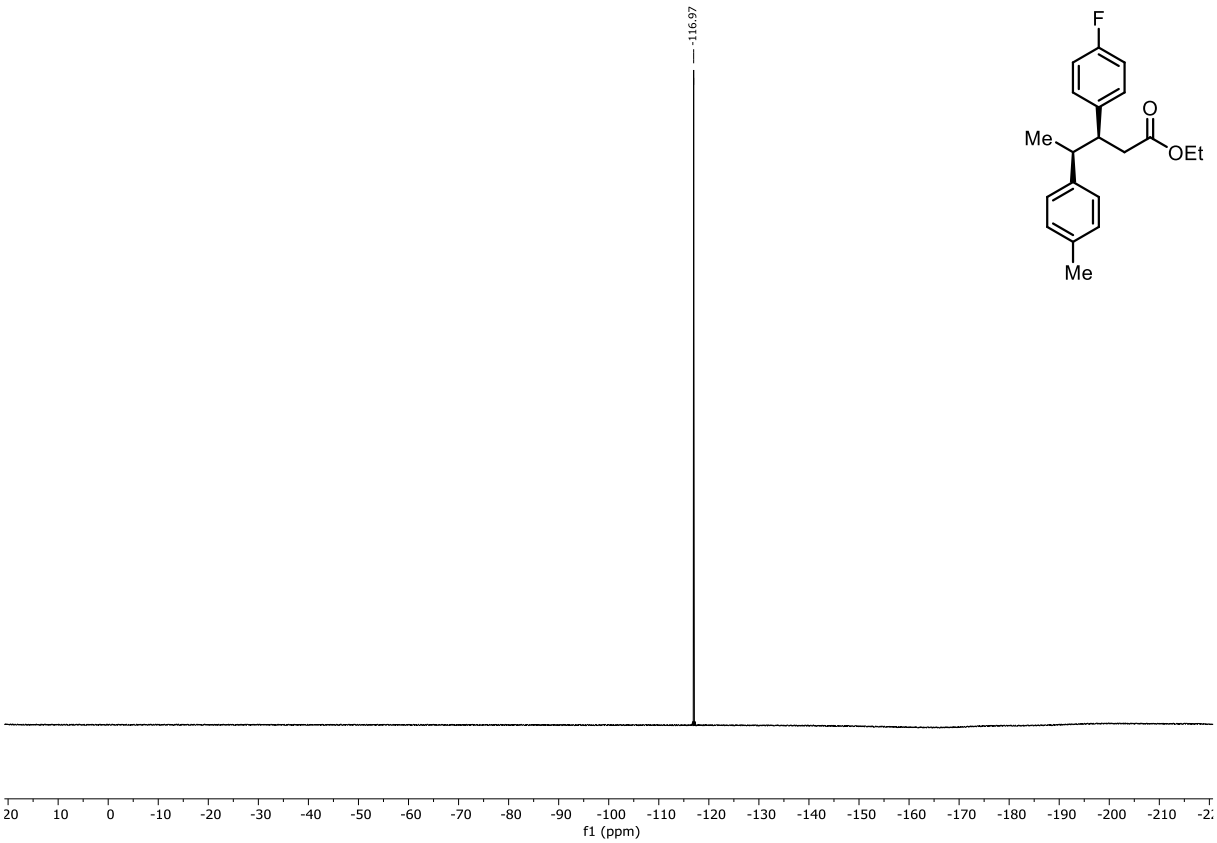

Figure 6.53 ^{19}F (13C)NMR (470 MHz) spectrum of **2-13**.

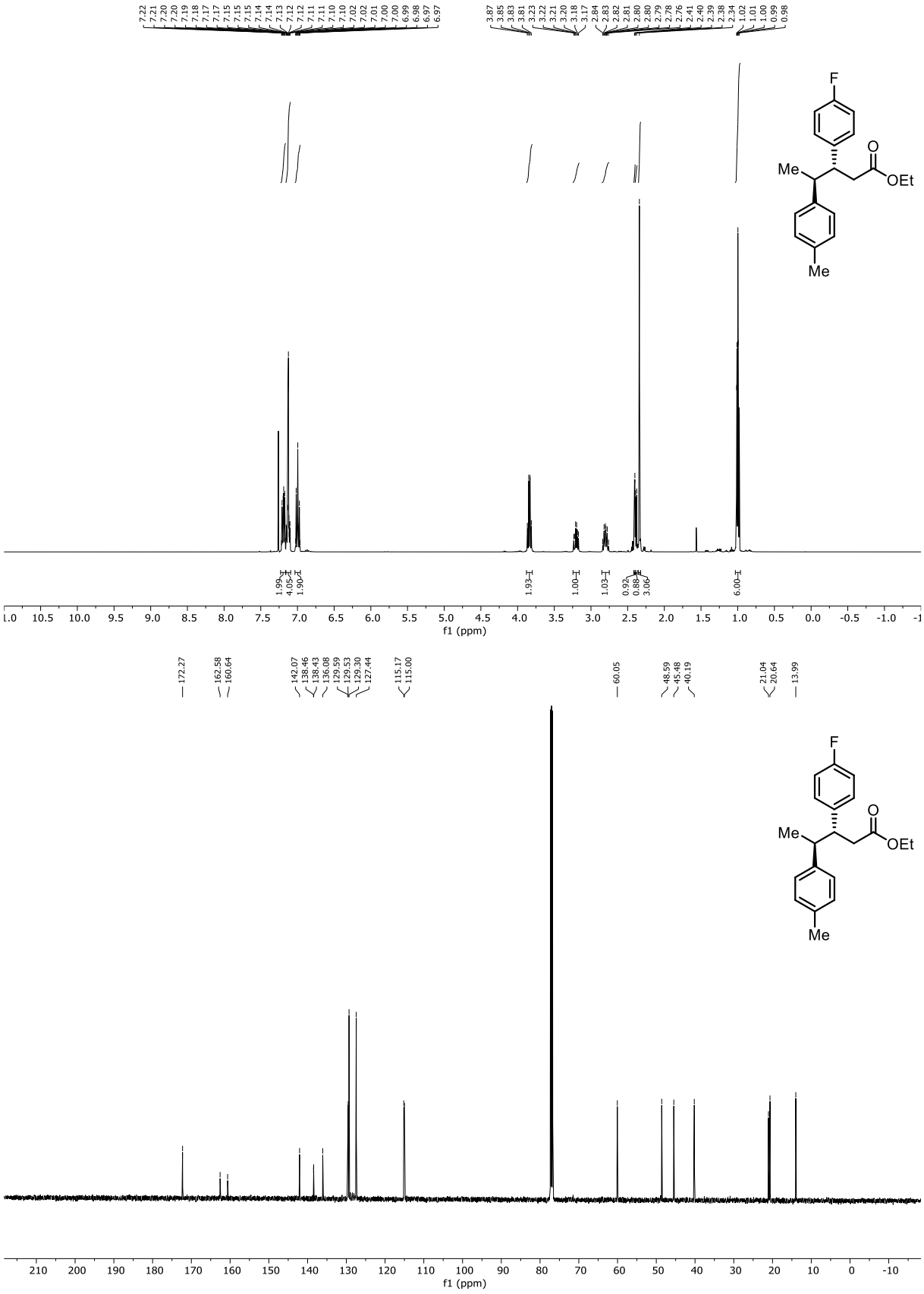

Figure 6.54 (top) ^{1}H NMR (400 MHz) and (bottom) ^{13}C NMR (101 MHz) spectra of **2-14**.

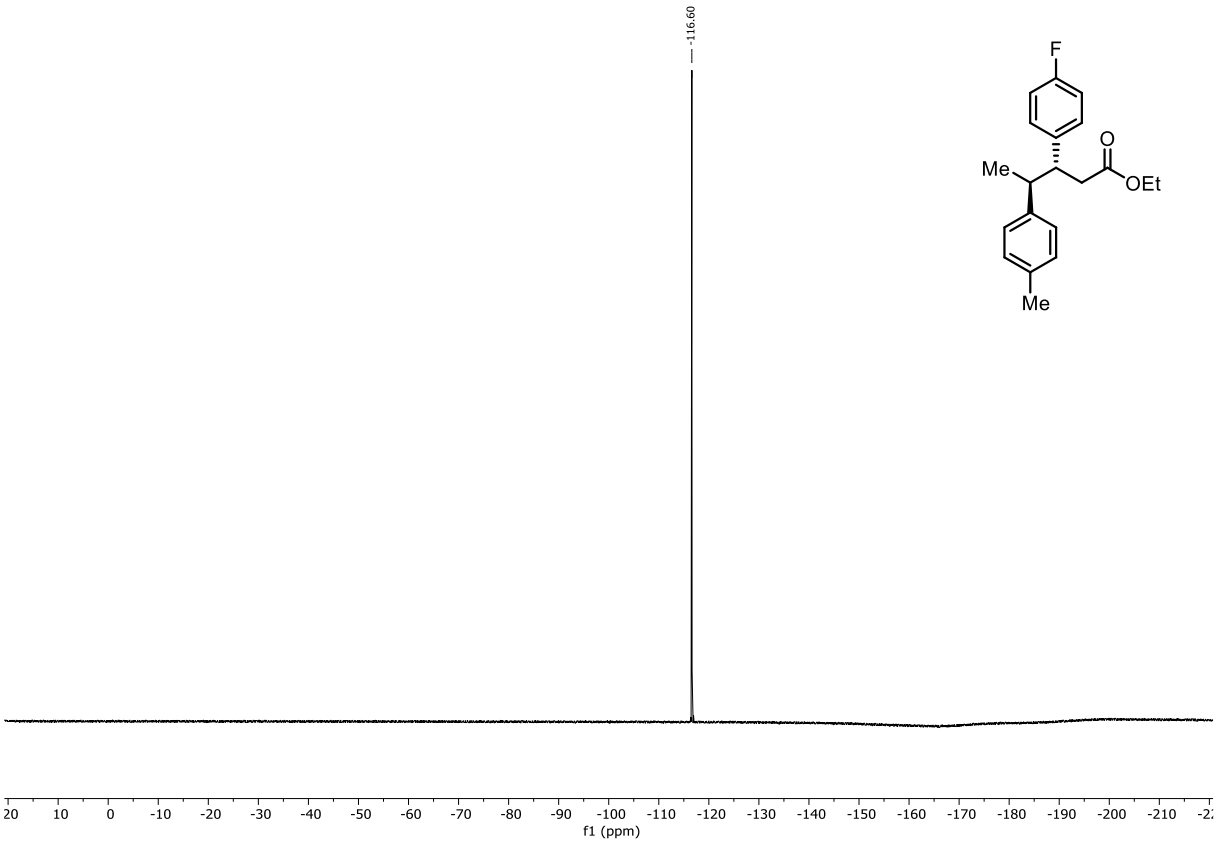

Figure 6.55 ^{19}F (13C)NMR (470 MHz) spectrum of **2-14**.

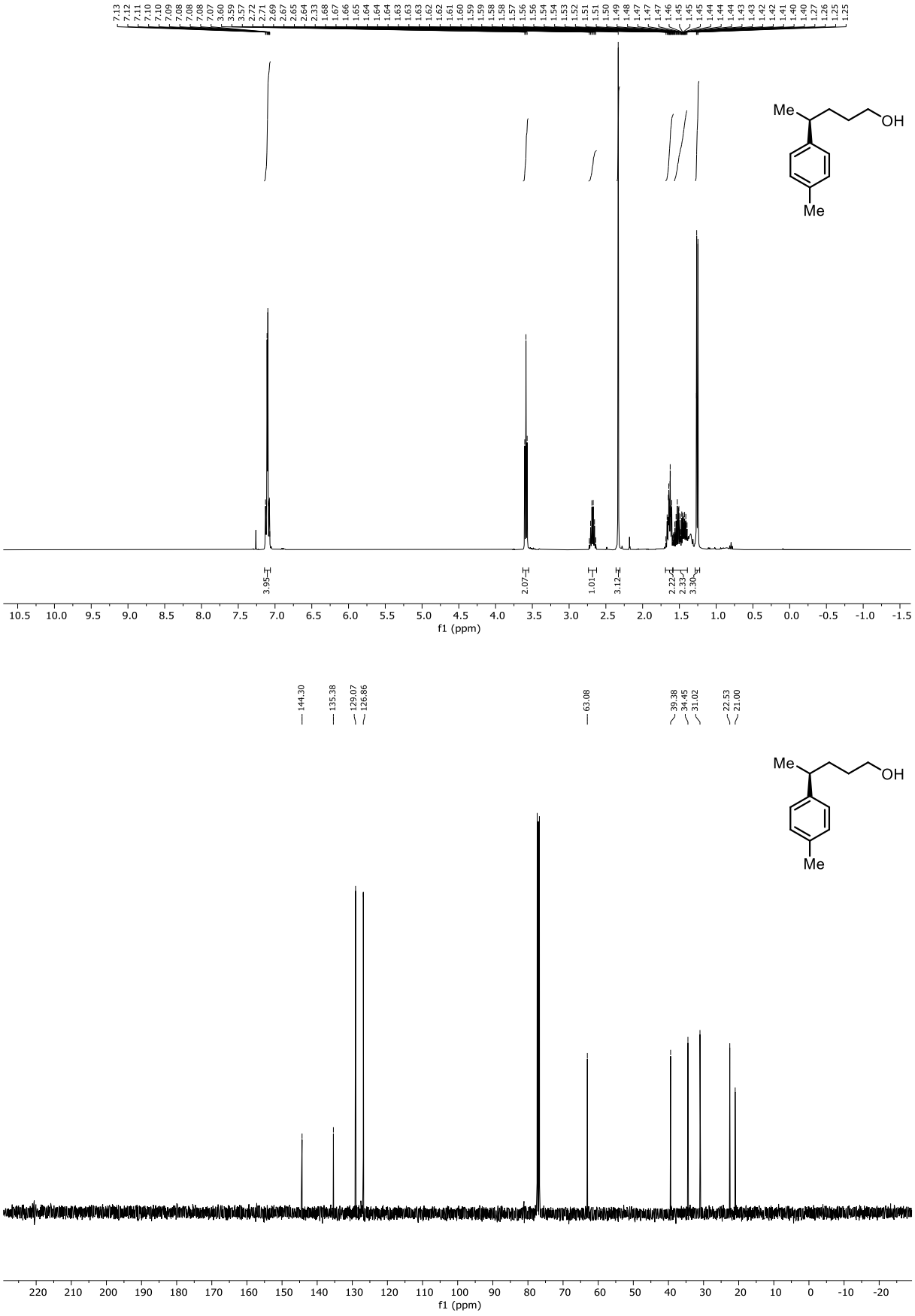

Figure 6.56 (top) ^{1}H NMR (400 MHz) and (bottom) ^{13}C NMR (101 MHz) spectra of **2-16**.

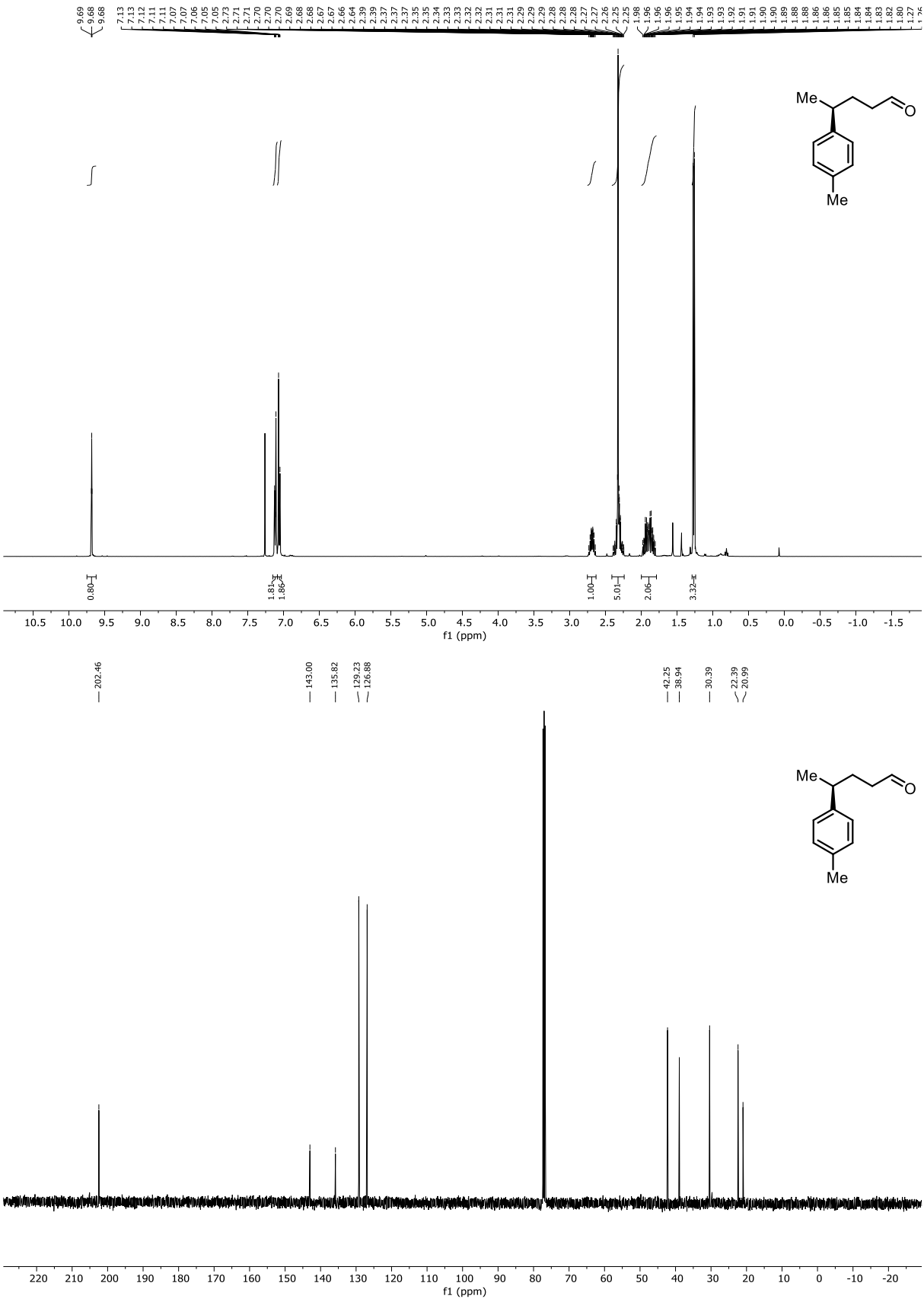

Figure 6.57 (top) ^{1}H NMR (400 MHz) and (bottom) ^{13}C NMR (101 MHz) spectra of **S6**.

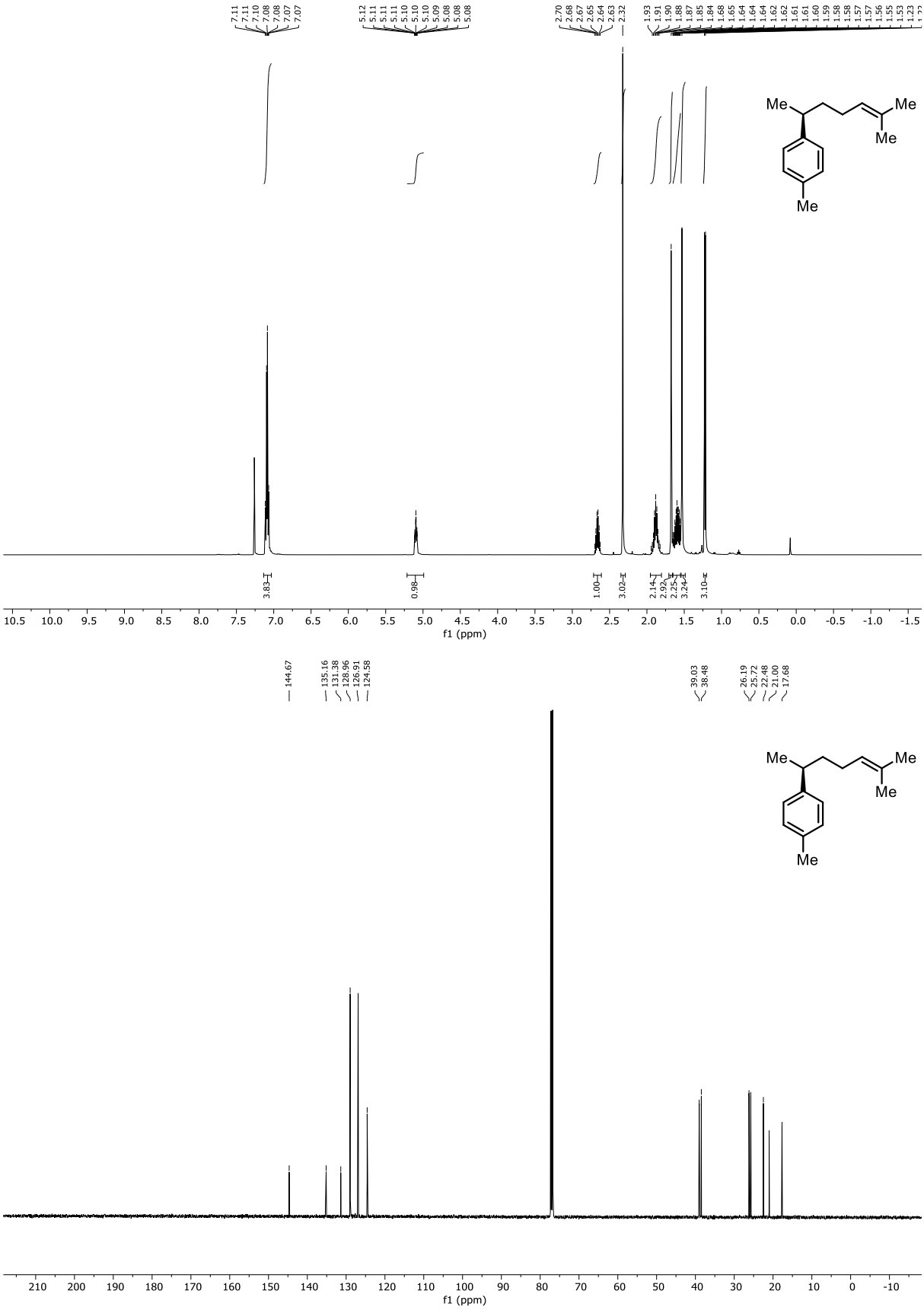

Figure 6.58 (top) ^{1}H NMR (400 MHz) and (bottom) ^{13}C NMR (101 MHz) spectra of **2-17**.

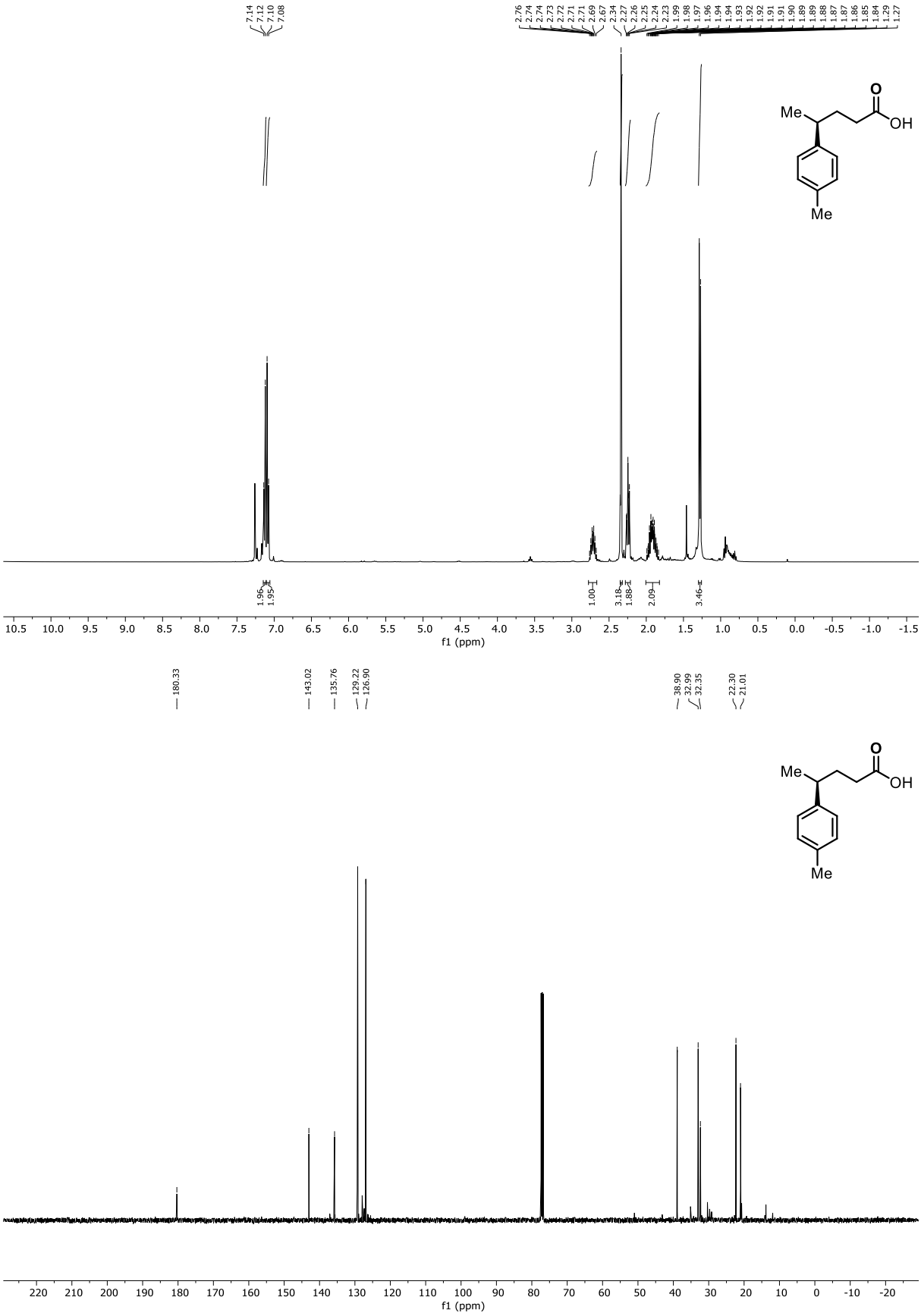

Figure 6.59 (top) ^{1}H NMR (400 MHz) and (bottom) ^{13}C NMR (101 MHz) spectra of **S7**.

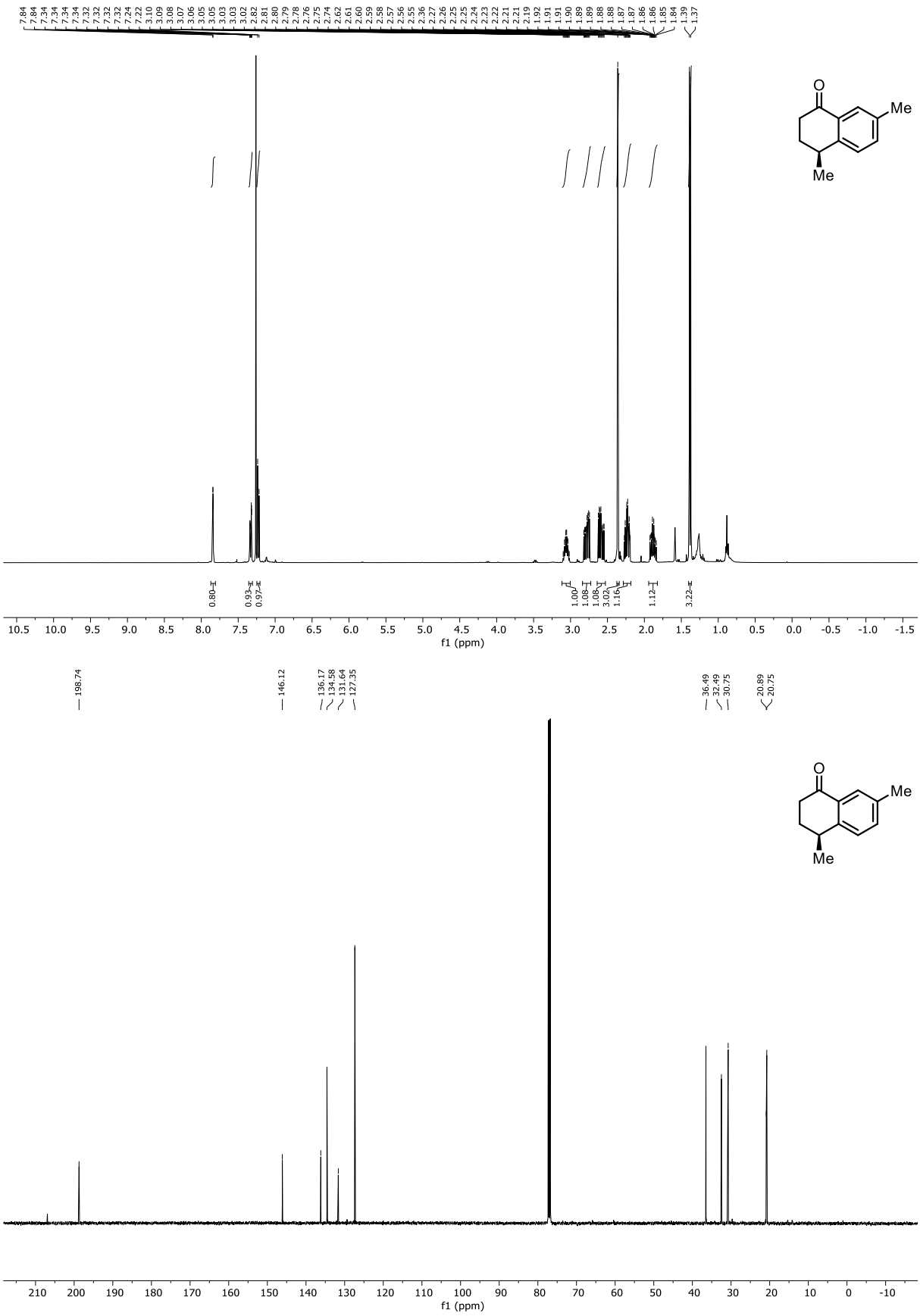

Figure 6.60 (top) ^{1}H NMR (400 MHz) and (bottom) ^{13}C NMR (101 MHz) spectra of **2-19**.

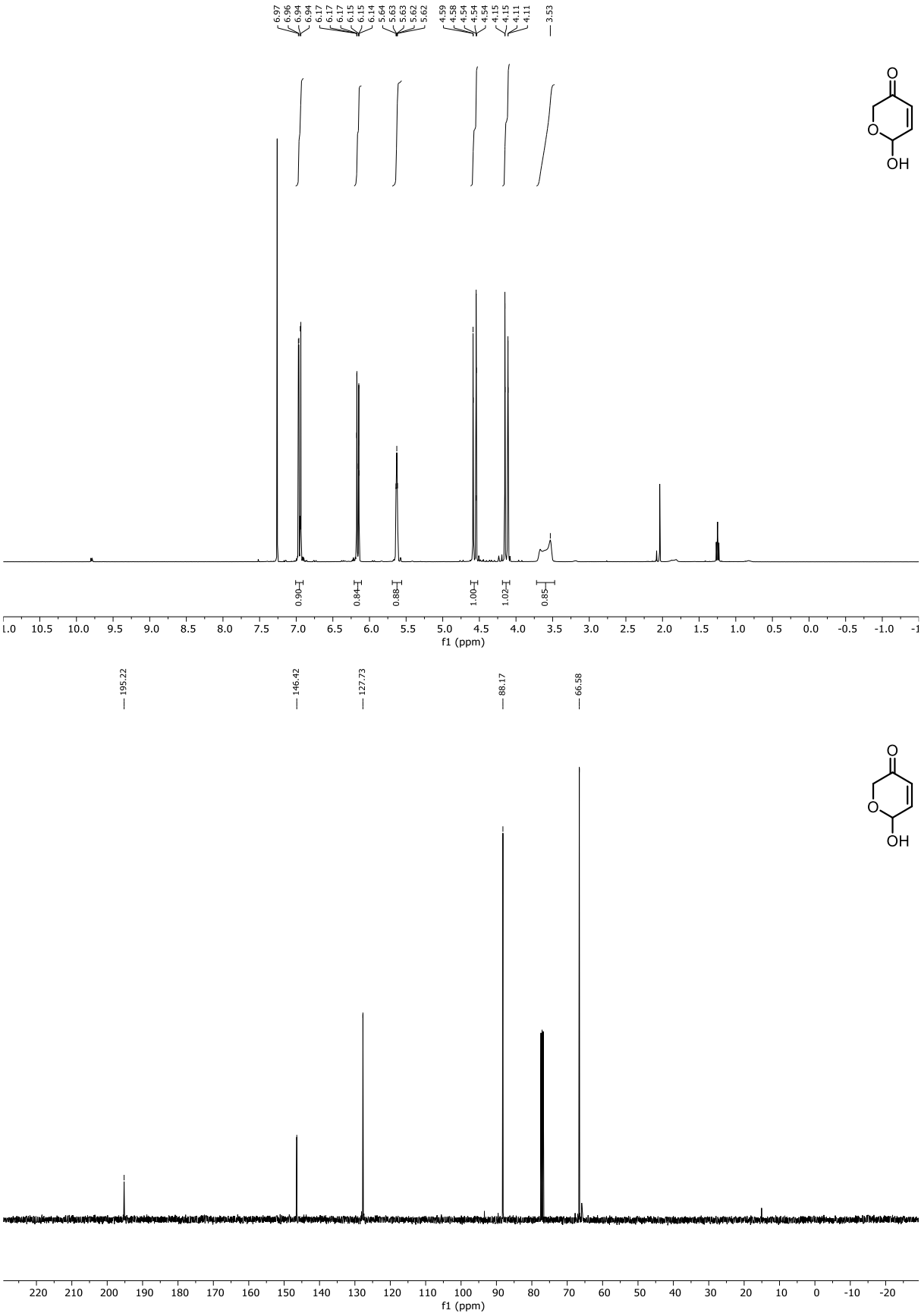

Figure 6.61 (top) ^{1}H NMR (400 MHz) and (bottom) ^{13}C NMR (101 MHz) spectra of **S8**.

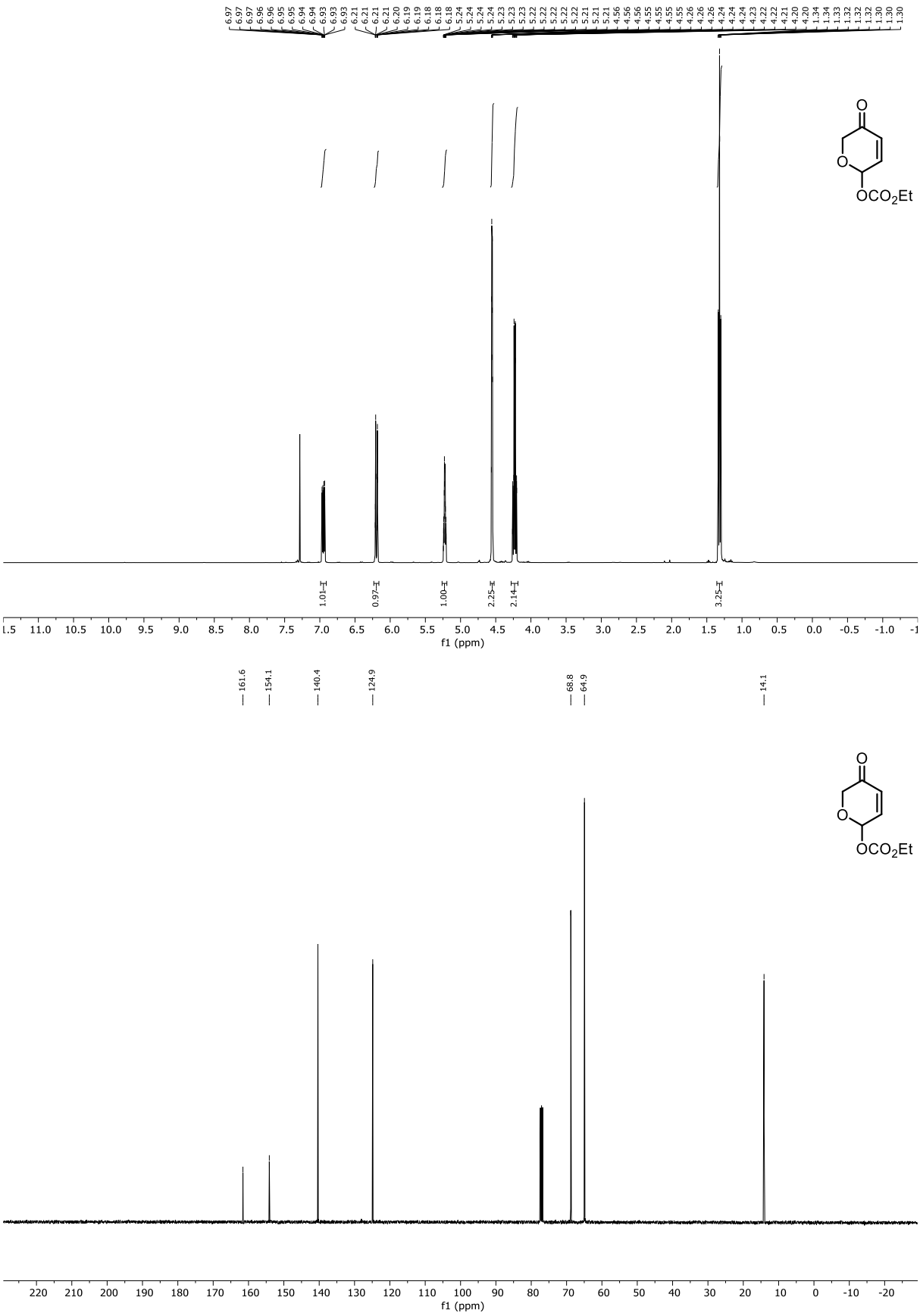

Figure 6.62 (top) ^{1}H NMR (400 MHz) and (bottom) ^{13}C NMR (101 MHz) spectra of (±)-**2-22**.

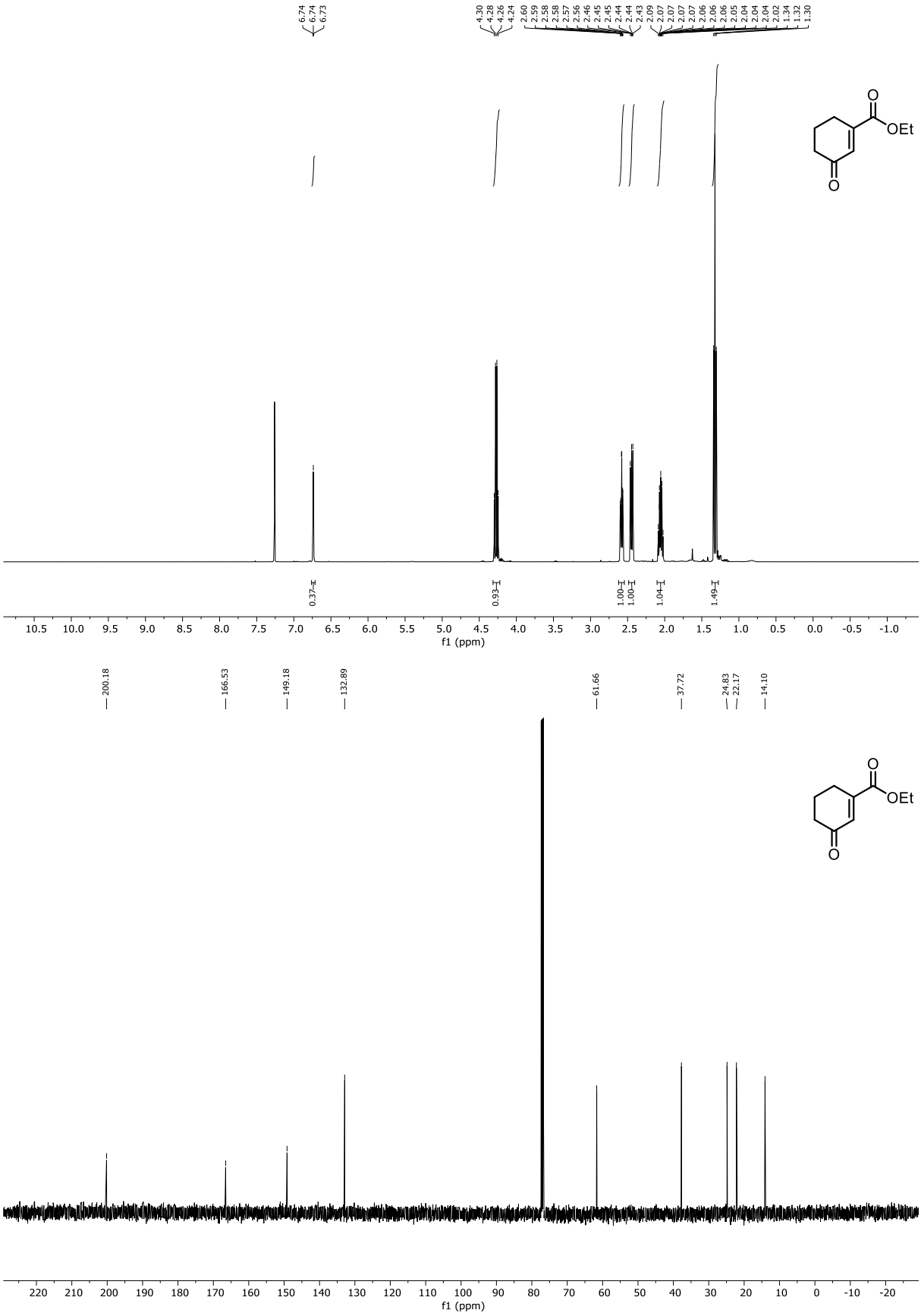

Figure 6.63 (top) ^{1}H NMR (400 MHz) and (bottom) ^{13}C NMR (101 MHz) spectra of **S9**.

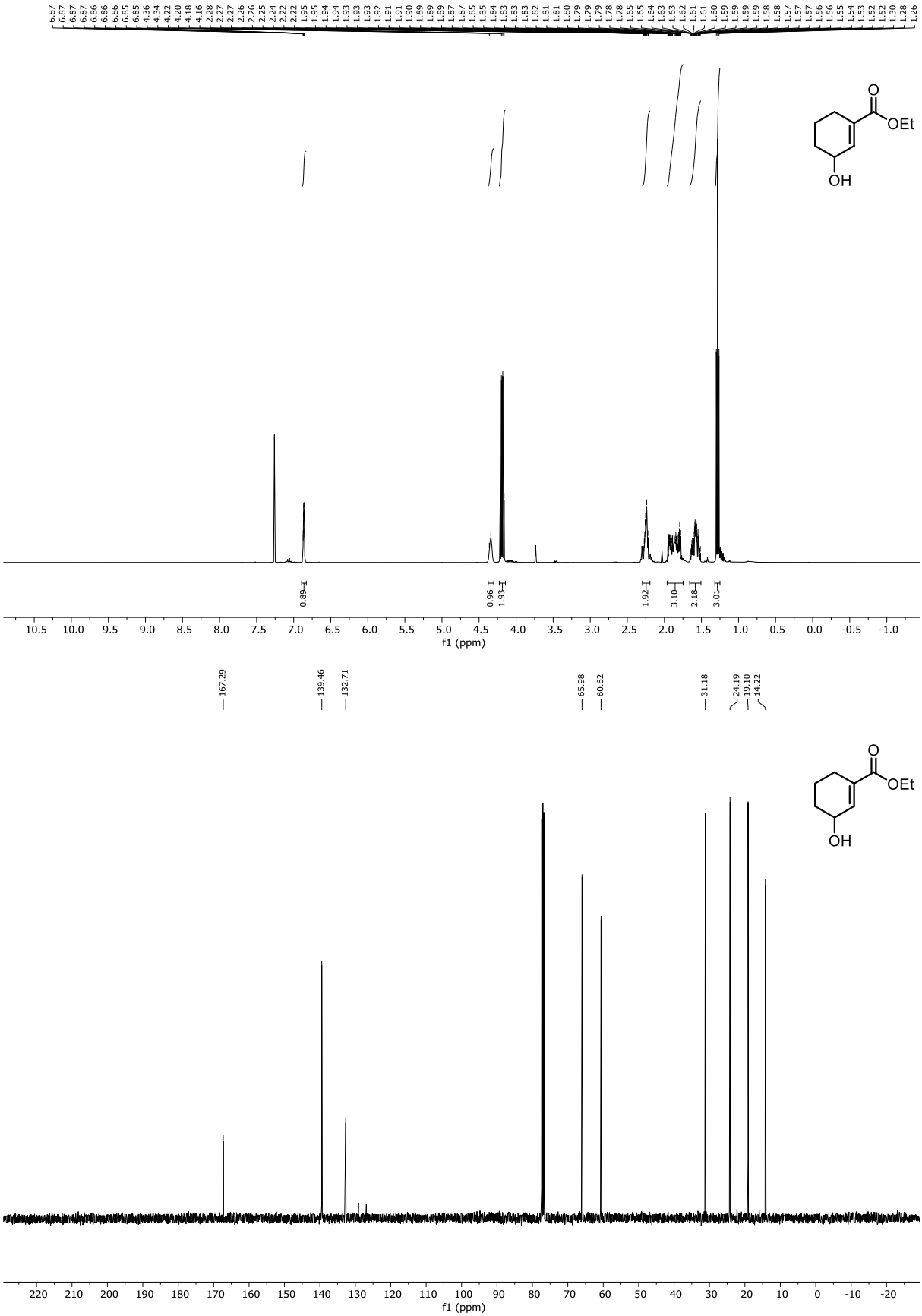

Figure 6.64 (top) ^{1}H NMR (400 MHz) and (bottom) ^{13}C NMR (101 MHz) spectra of **S10**.

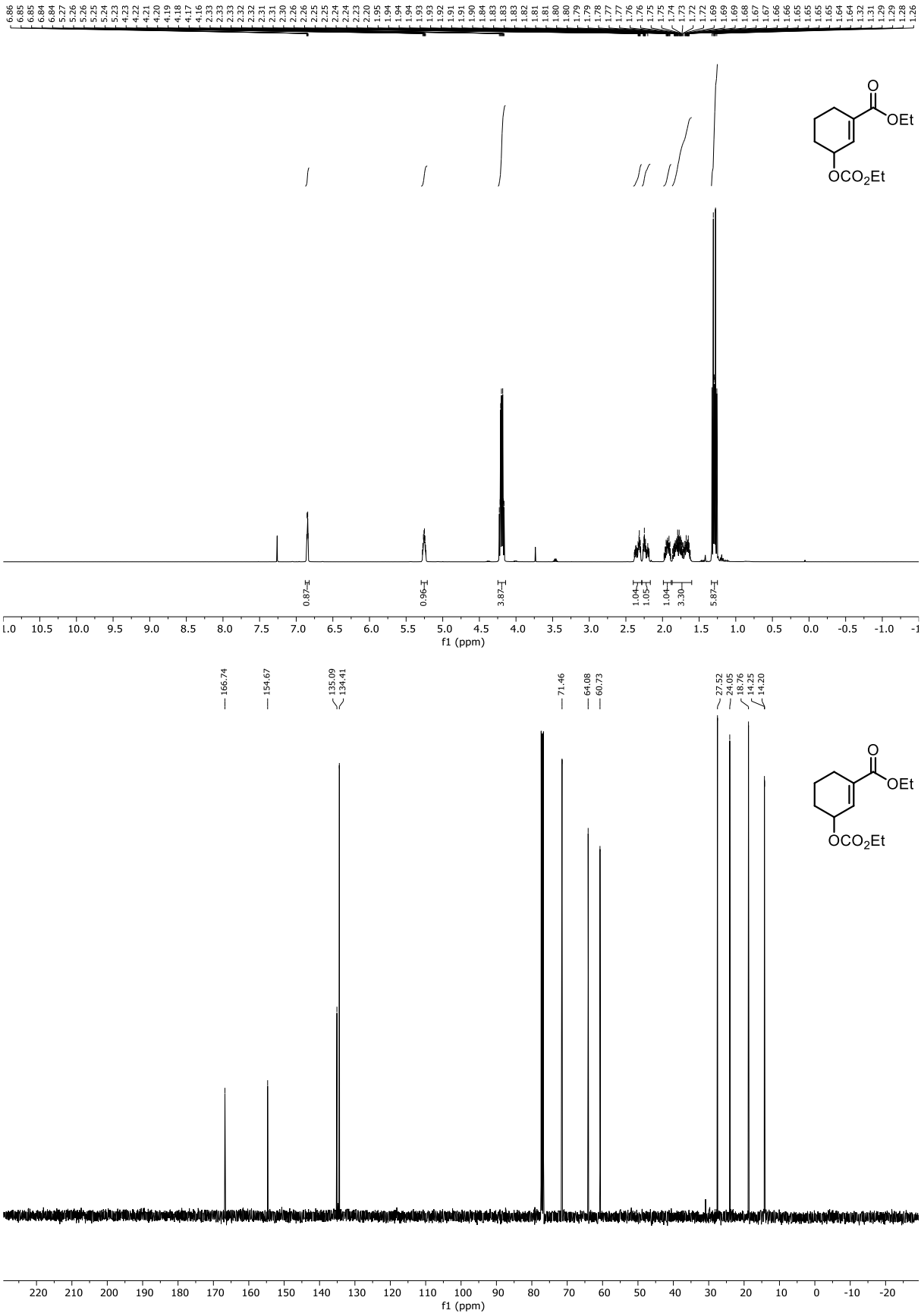

Figure 6.65 (top) ^{1}H NMR (400 MHz) and (bottom) ^{13}C NMR (101 MHz) spectra of (±)-**2-24**.

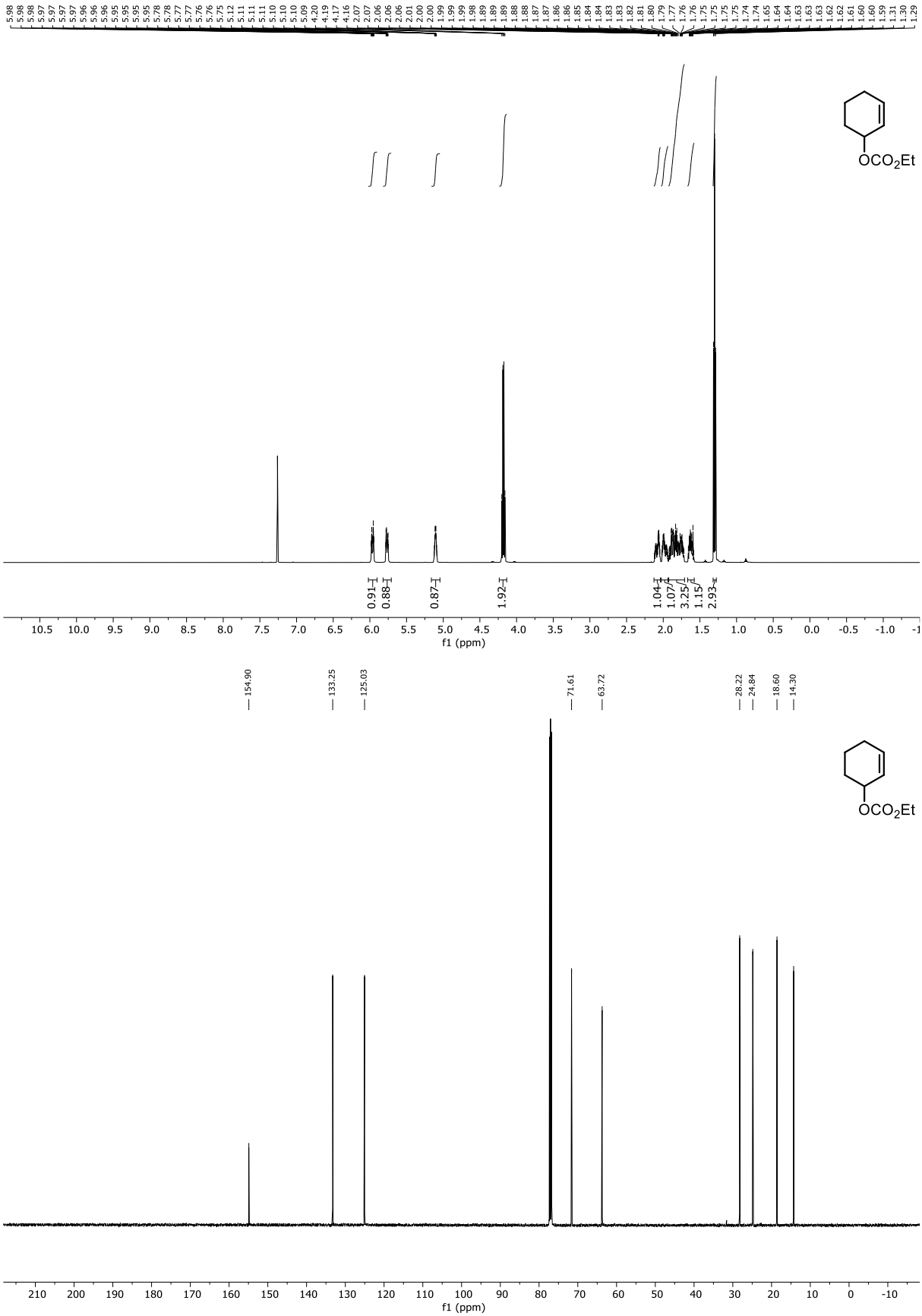

Figure 6.66 (top) ^{1}H NMR (400 MHz) and (bottom) ^{13}C NMR (101 MHz) spectra of (±)-**2-25**.

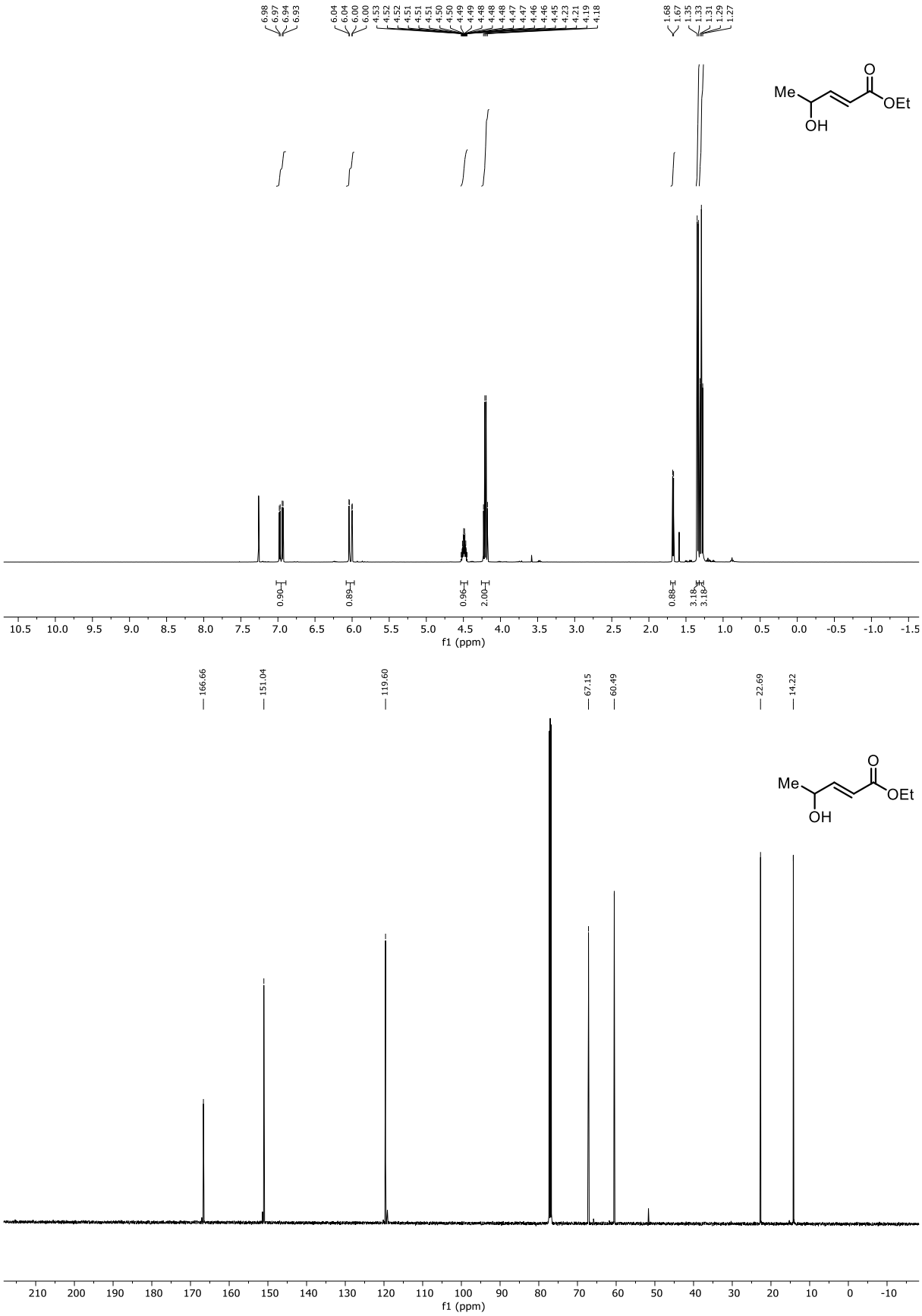

Figure 6.67 (top) ^{1}H NMR (400 MHz) and (bottom) ^{13}C NMR (101 MHz) spectra of **S11**.

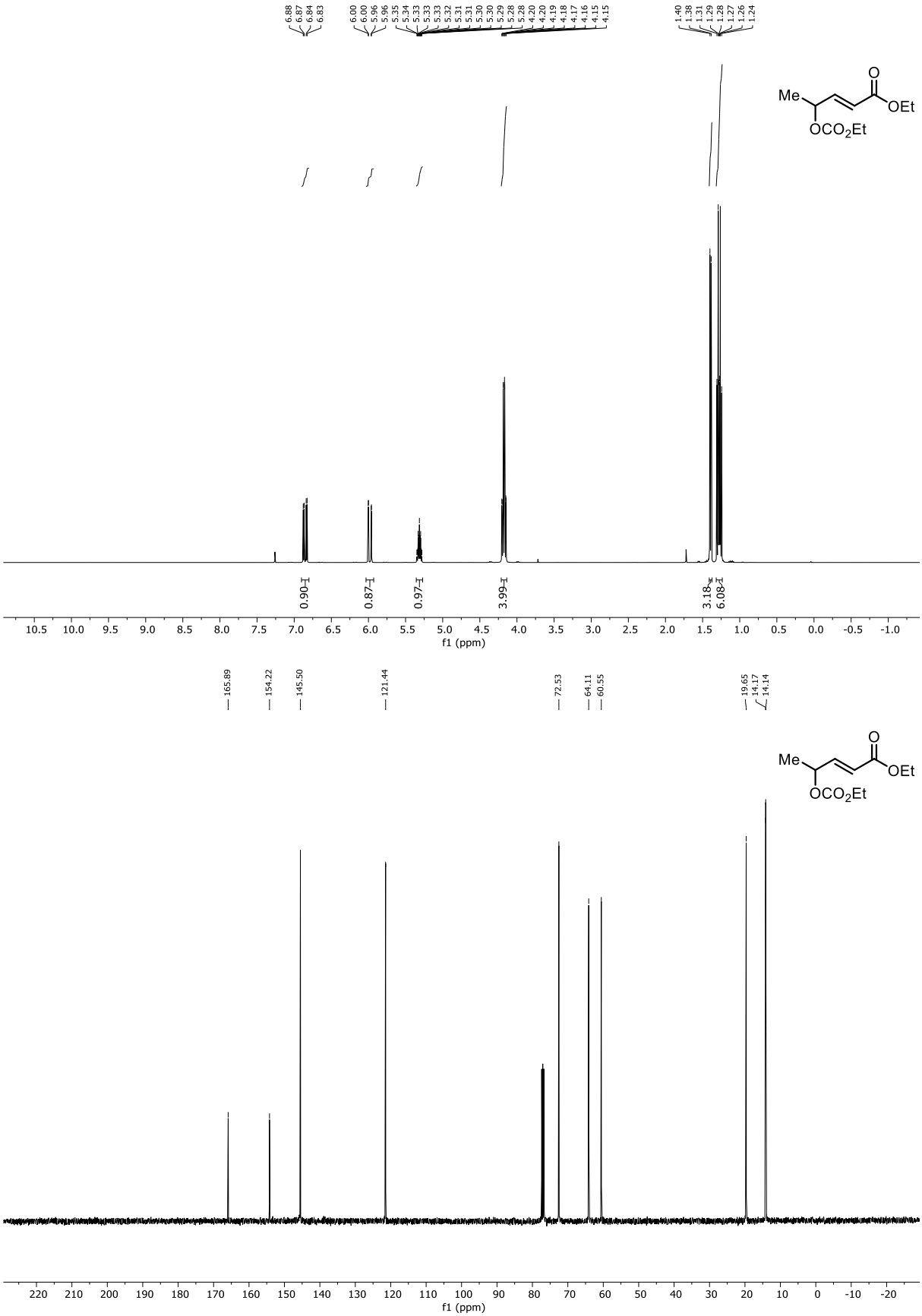

Figure 6.68 (top) ^{1}H NMR (400 MHz) and (bottom) ^{13}C NMR (101 MHz) spectra of (±)-**2-26**.

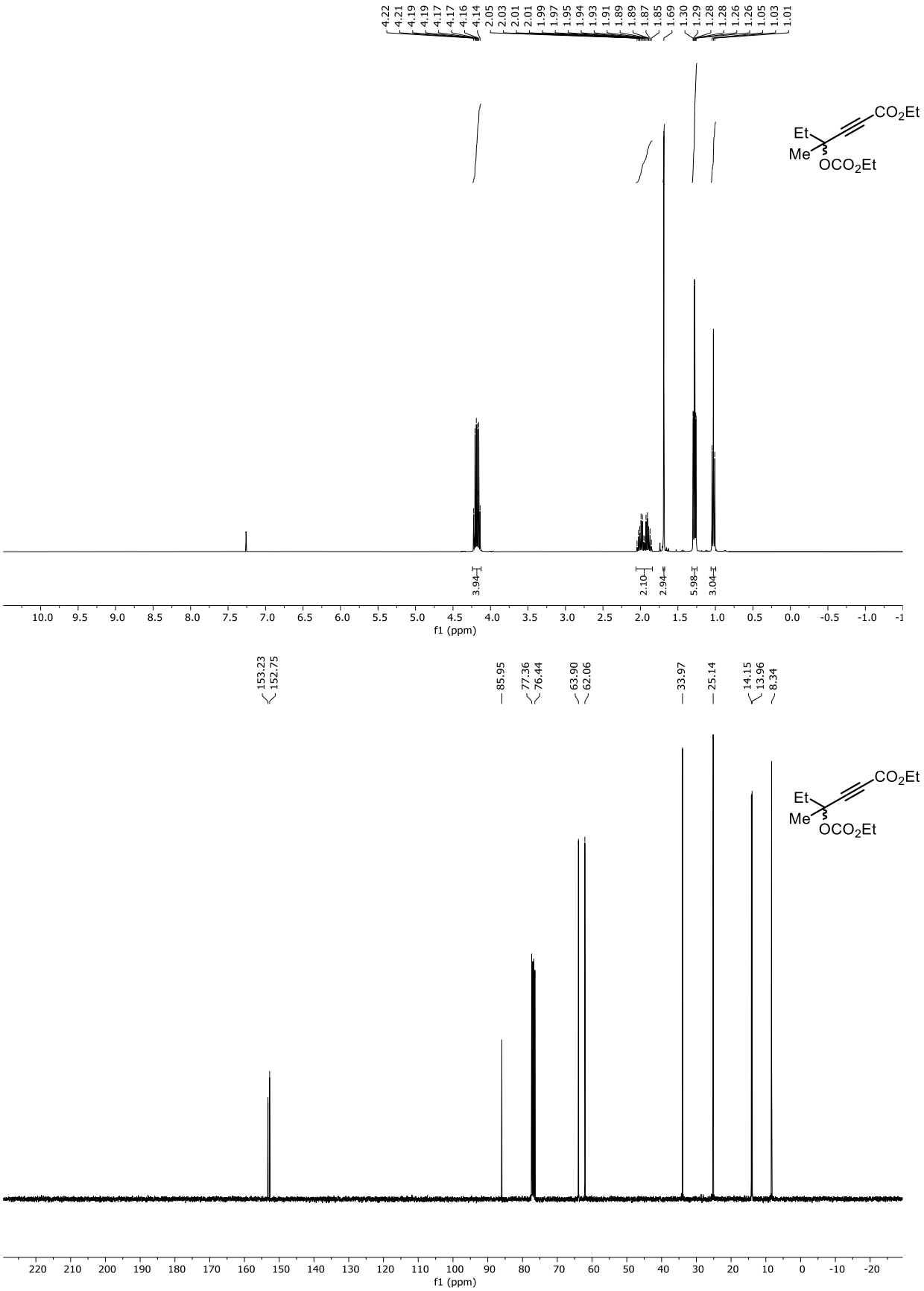

Figure 6.69 (top) ^{1}H NMR (400 MHz) and (bottom) ^{13}C NMR (101 MHz) spectra of **3-2a**.

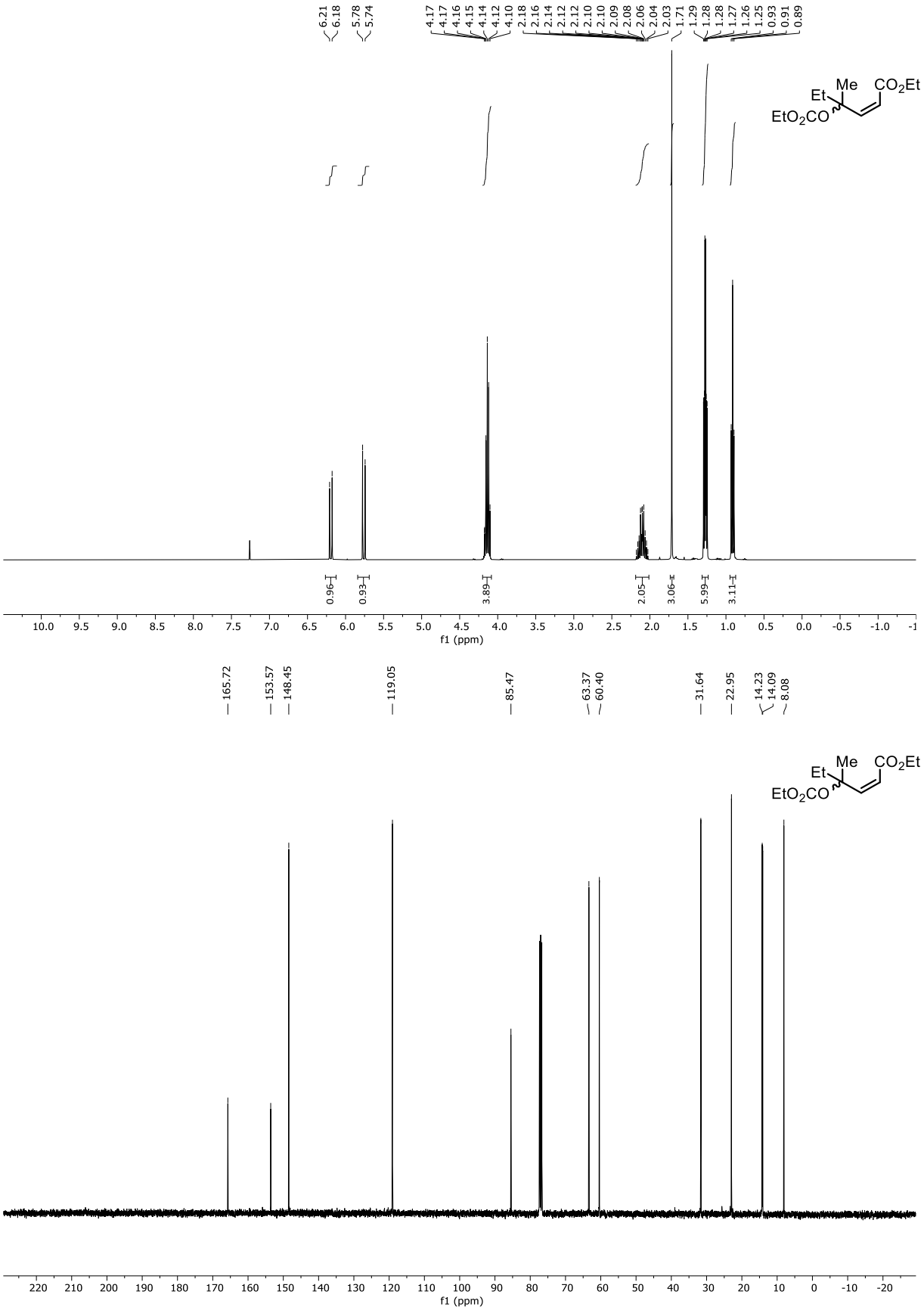

Figure 6.70 (top) ^{1}H NMR (400 MHz) and (bottom) ^{13}C NMR (101 MHz) spectra of **3-3a**.

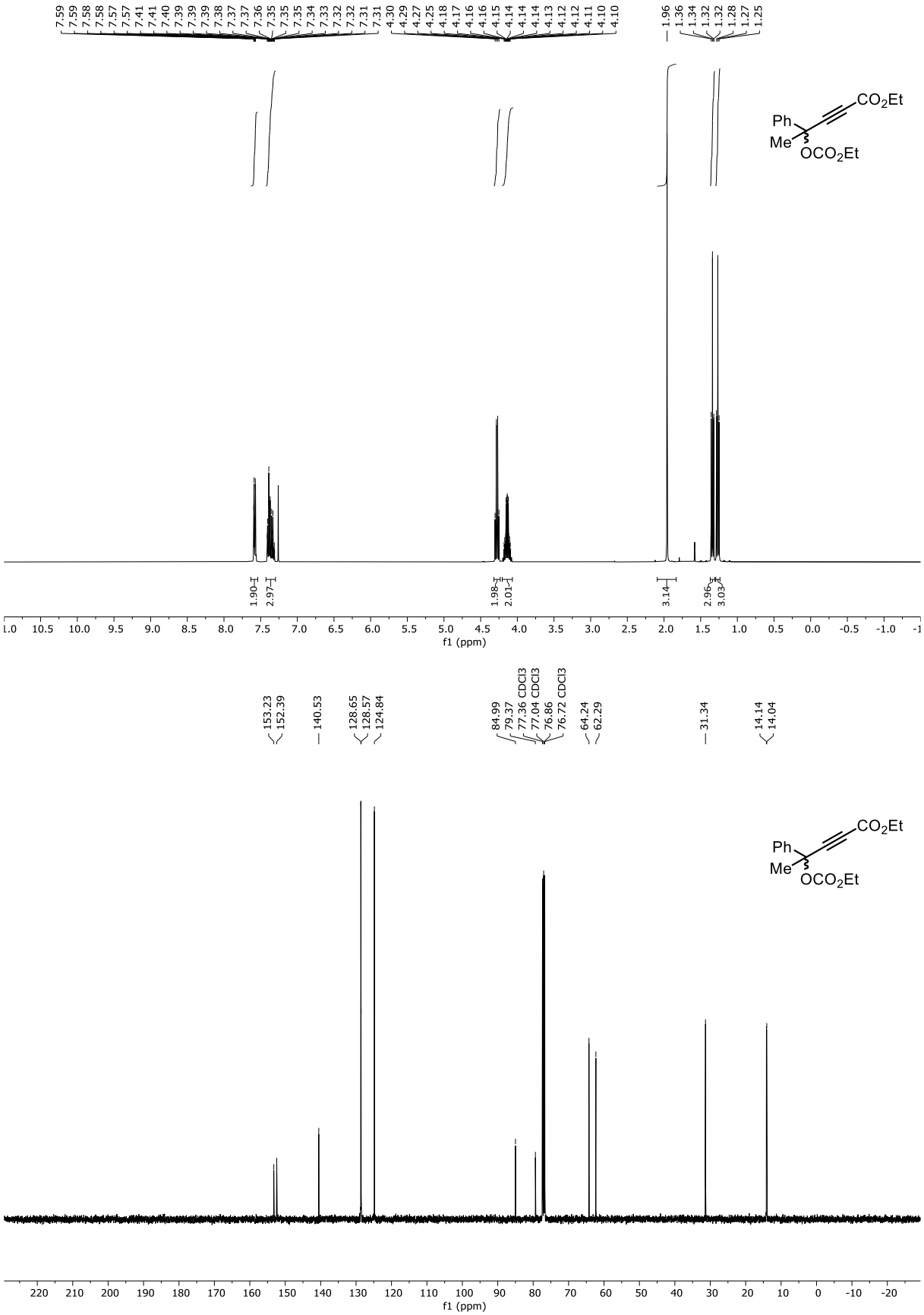

Figure 6.71 (top) ^{1}H NMR (400 MHz) and (bottom) ^{13}C NMR (101 MHz) spectra of **3-2b**.

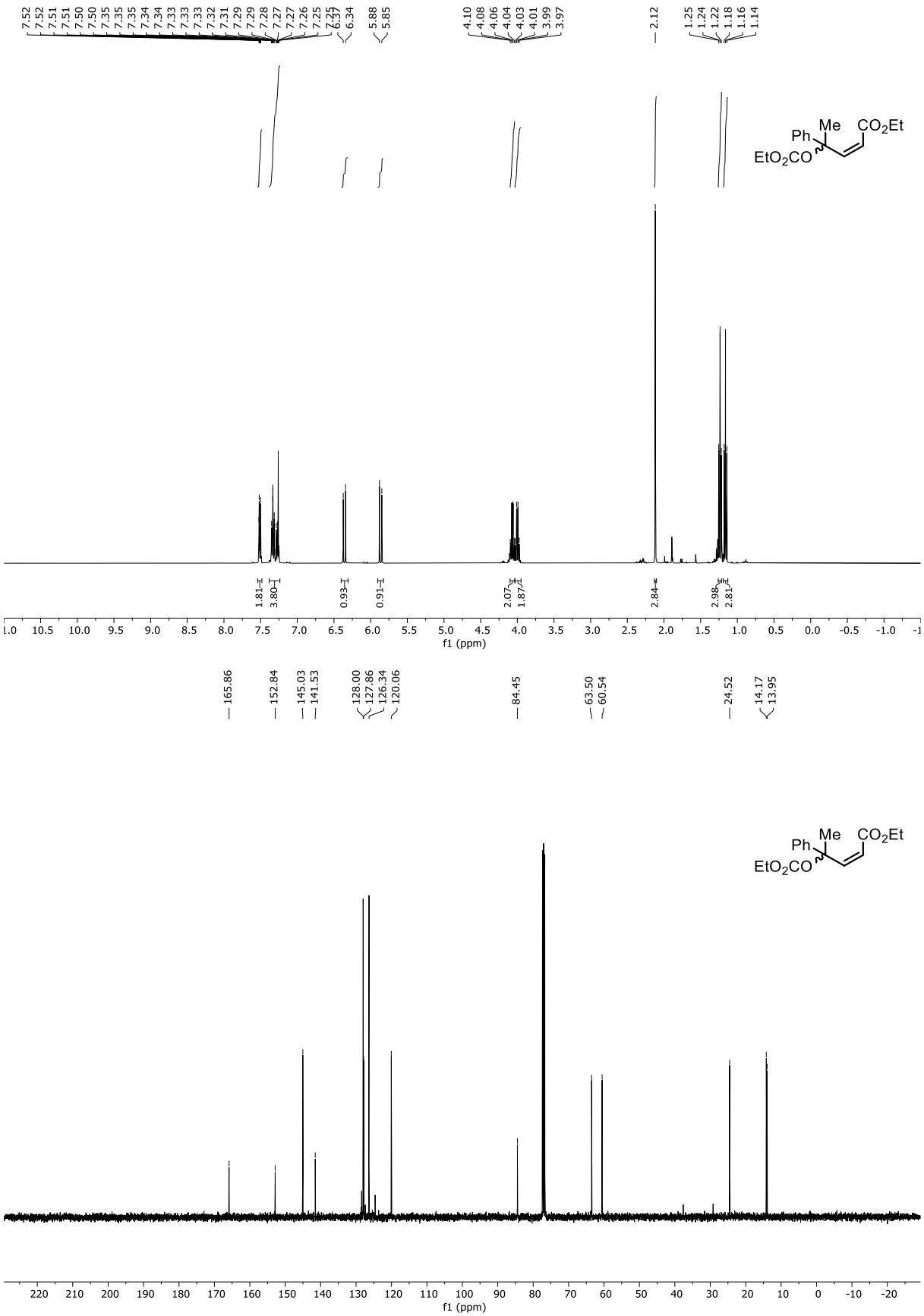

Figure 6.72 (top) ^{1}H NMR (400 MHz) and (bottom) ^{13}C NMR (101 MHz) spectra of **3-3b**.

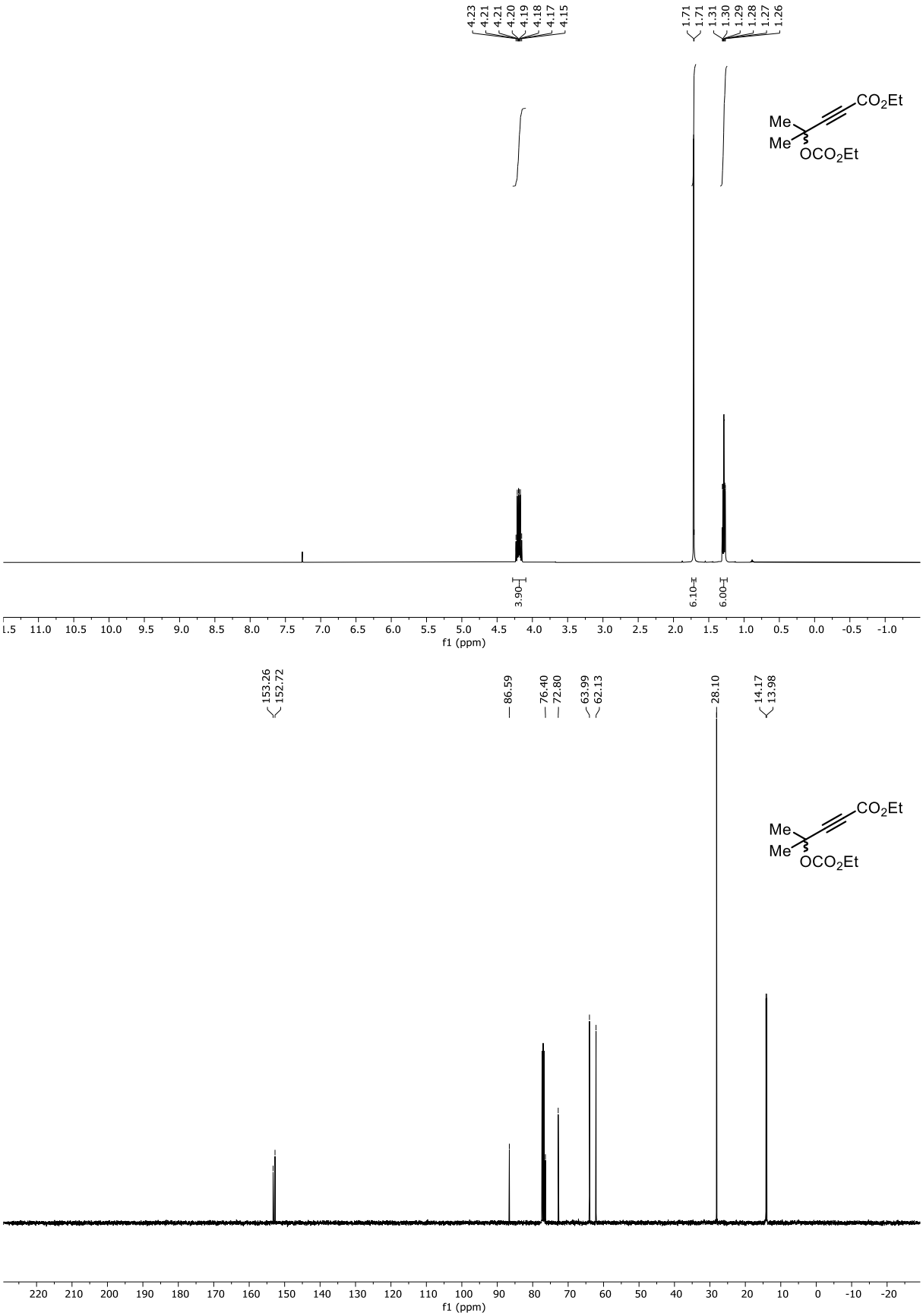

Figure 6.73 (top) ^{1}H NMR (400 MHz) and (bottom) ^{13}C NMR (101 MHz) spectra of **3-2c**.

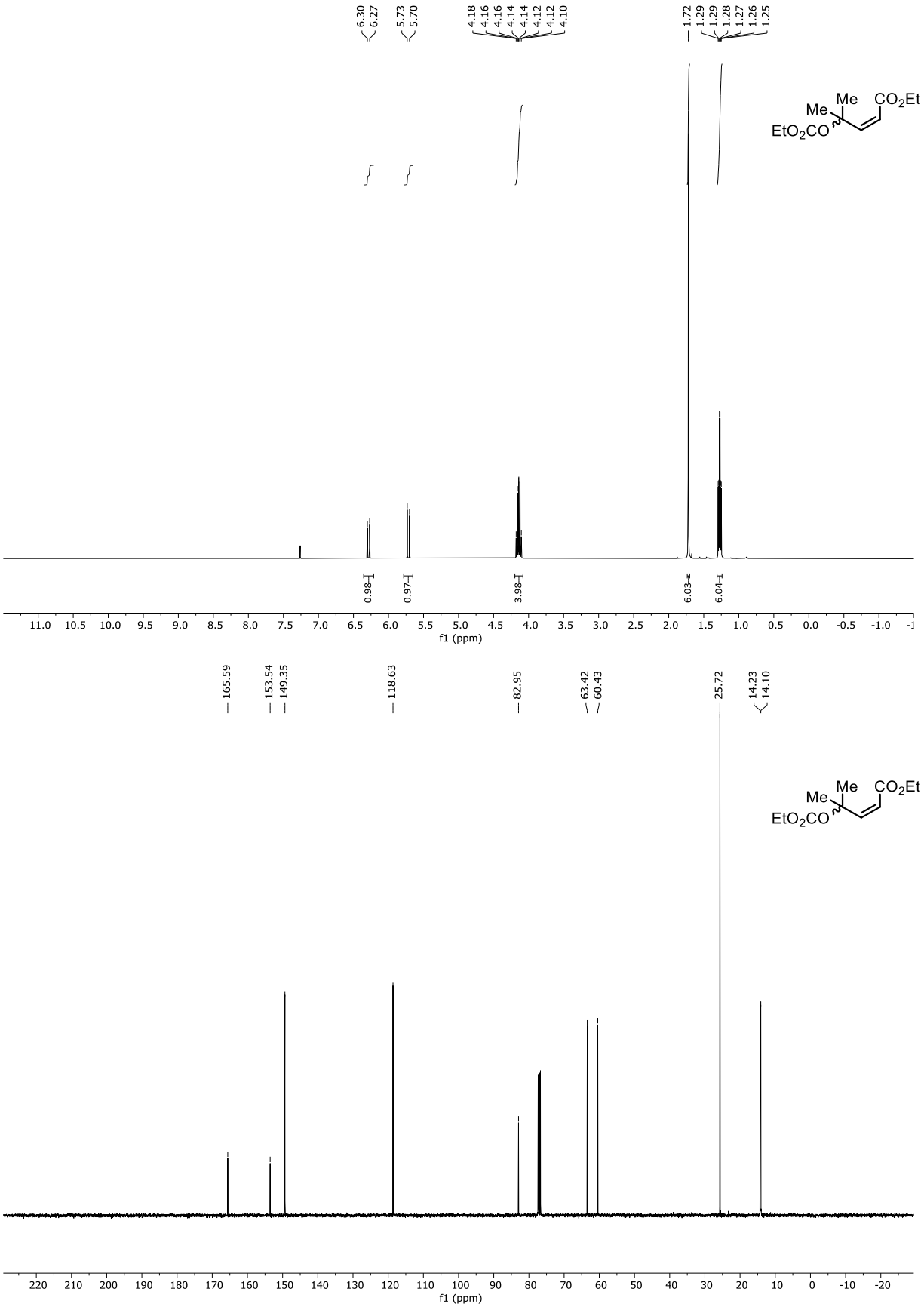

Figure 6.74 (top) ^{1}H NMR (400 MHz) and (bottom) ^{13}C NMR (101 MHz) spectra of **3-3c**.

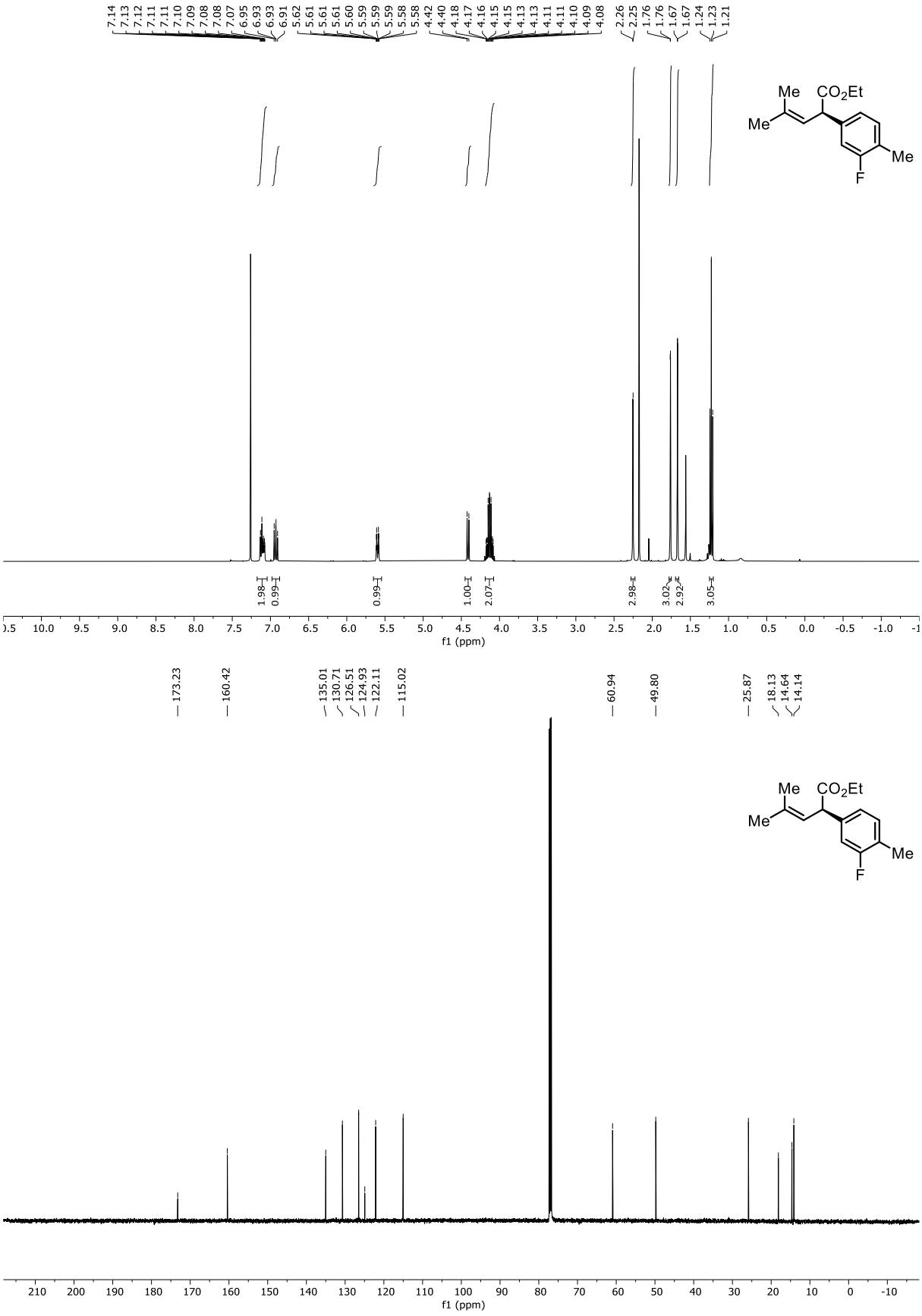

Figure 6.75 (top) ^{1}H NMR (400 MHz) and (bottom) ^{13}C NMR (101 MHz) spectra of **3-5c**.

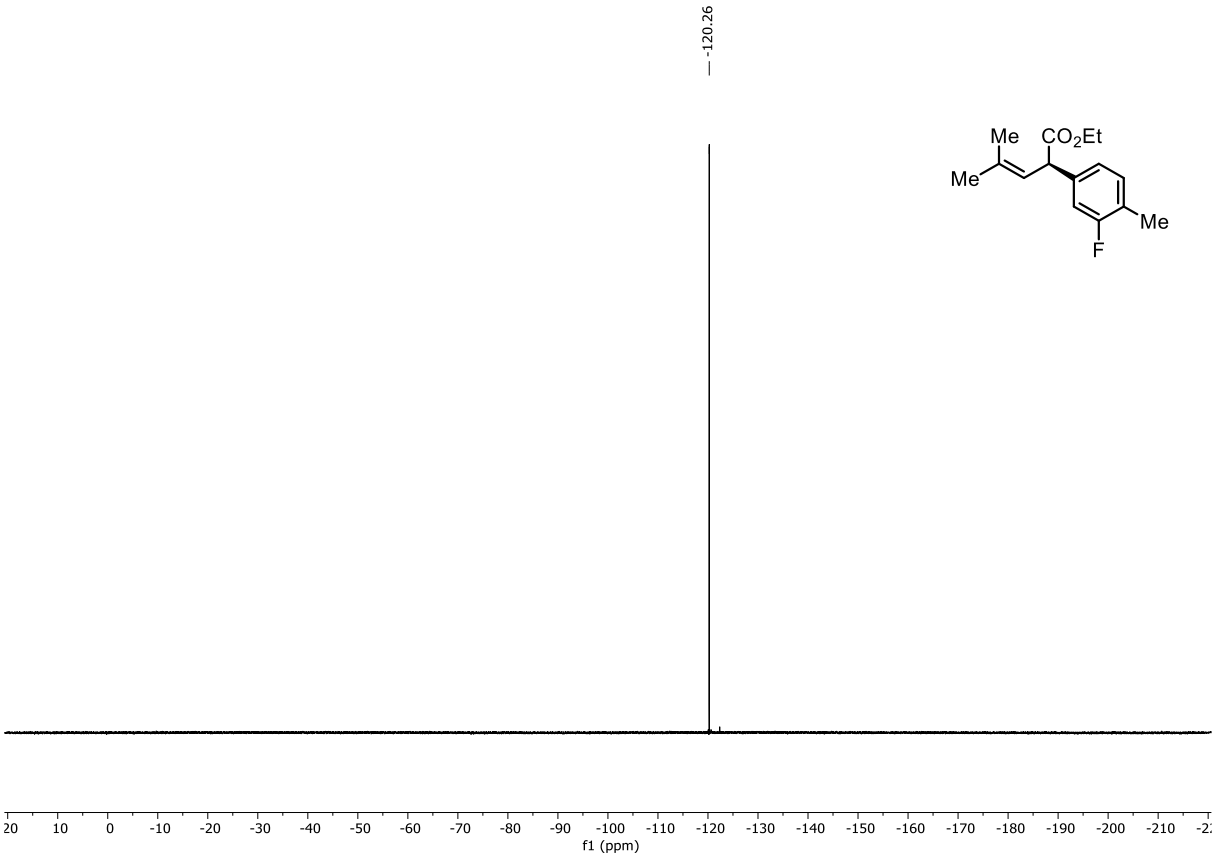

Figure 6.76 ^{19}F (13C)NMR (376 MHz) spectrum of **3-5c**.

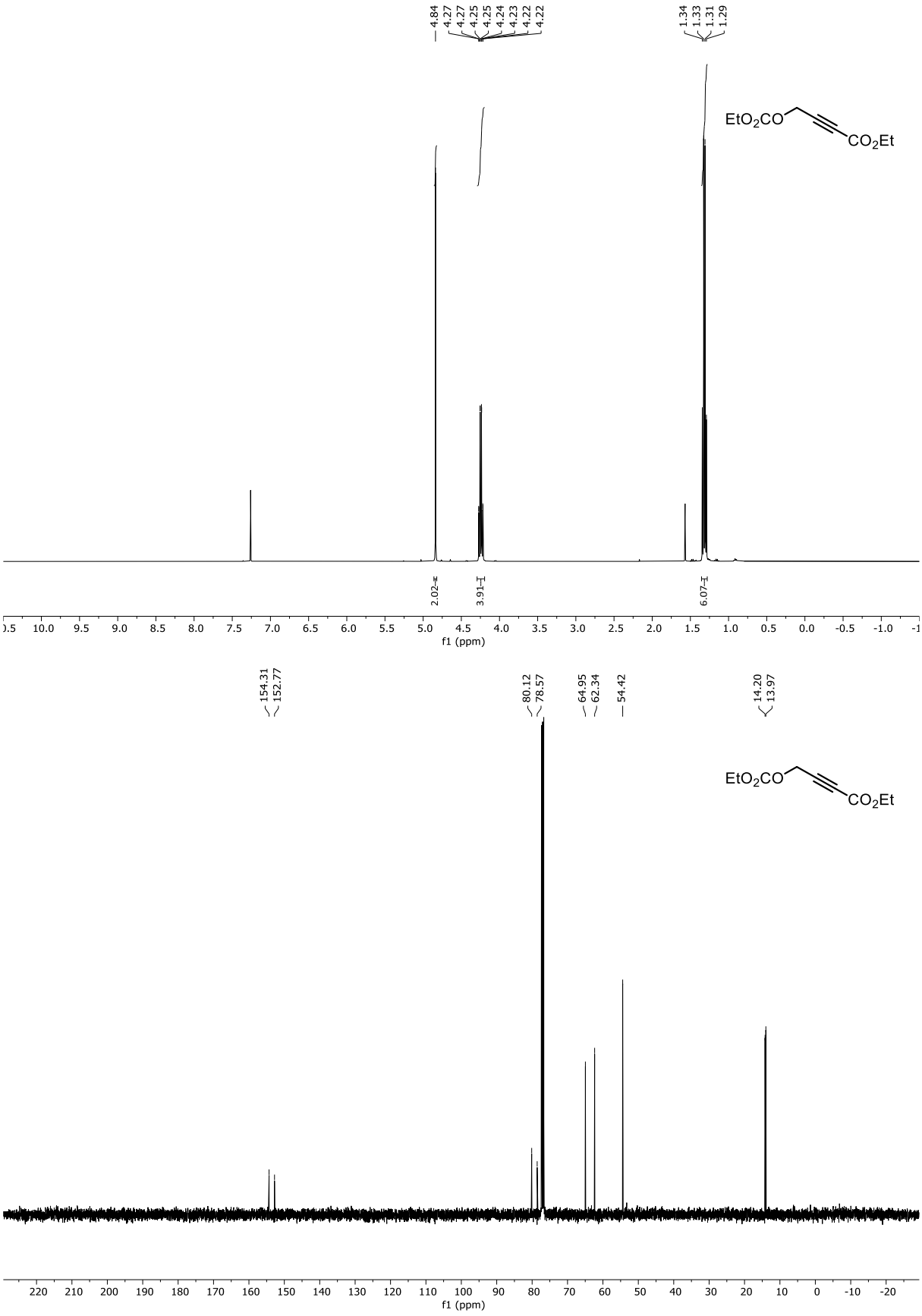

Figure 6.77 (top) ^{1}H NMR (400 MHz) and (bottom) ^{13}C NMR (101 MHz) spectra of **4-2**.

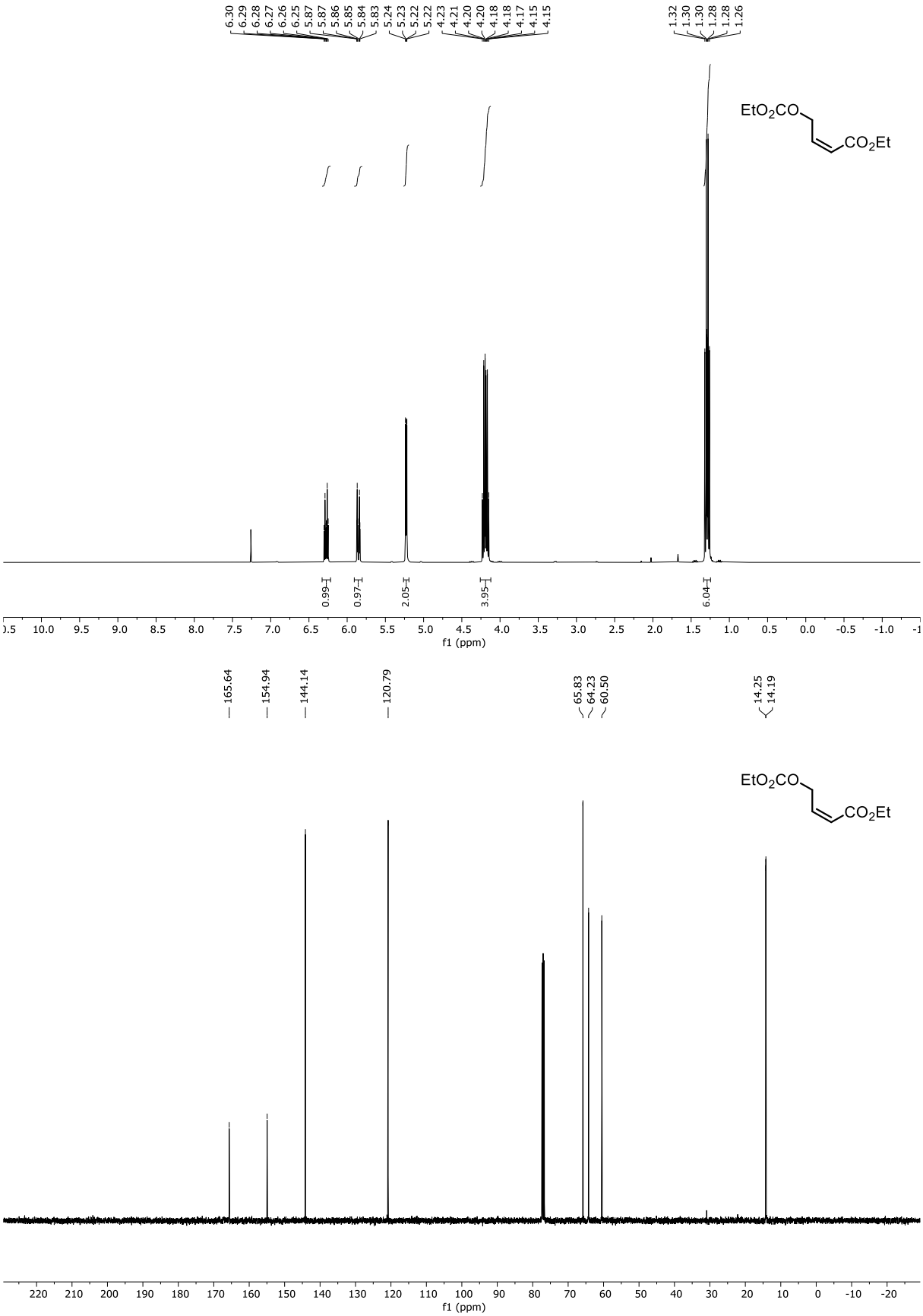

Figure 6.78 (top) ^{1}H NMR (400 MHz) and (bottom) ^{13}C NMR (101 MHz) spectra of **4-3**.

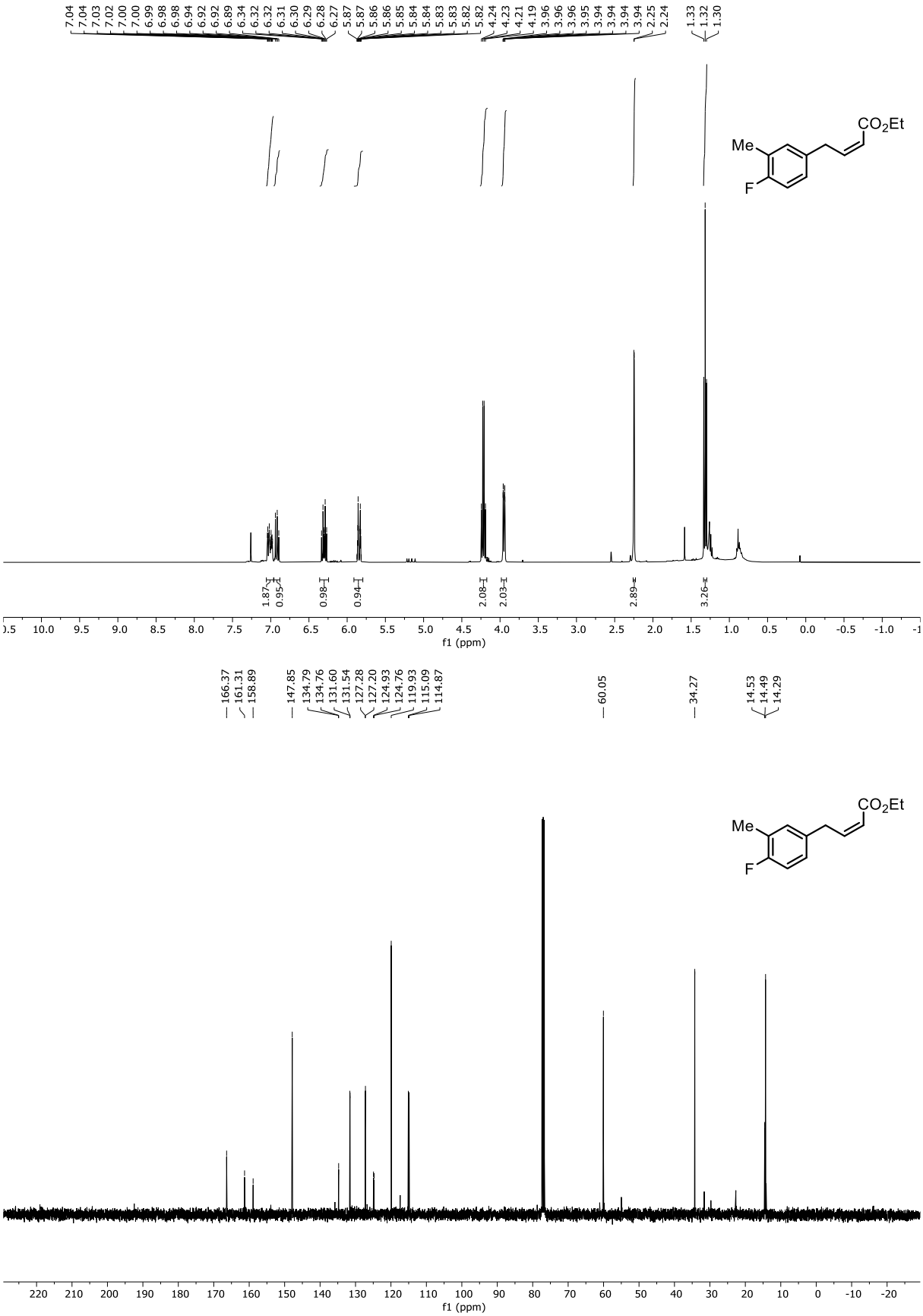

Figure 6.79 (top) ^{1}H NMR (400 MHz) and (bottom) ^{13}C NMR (101 MHz) spectra of **4-6**.

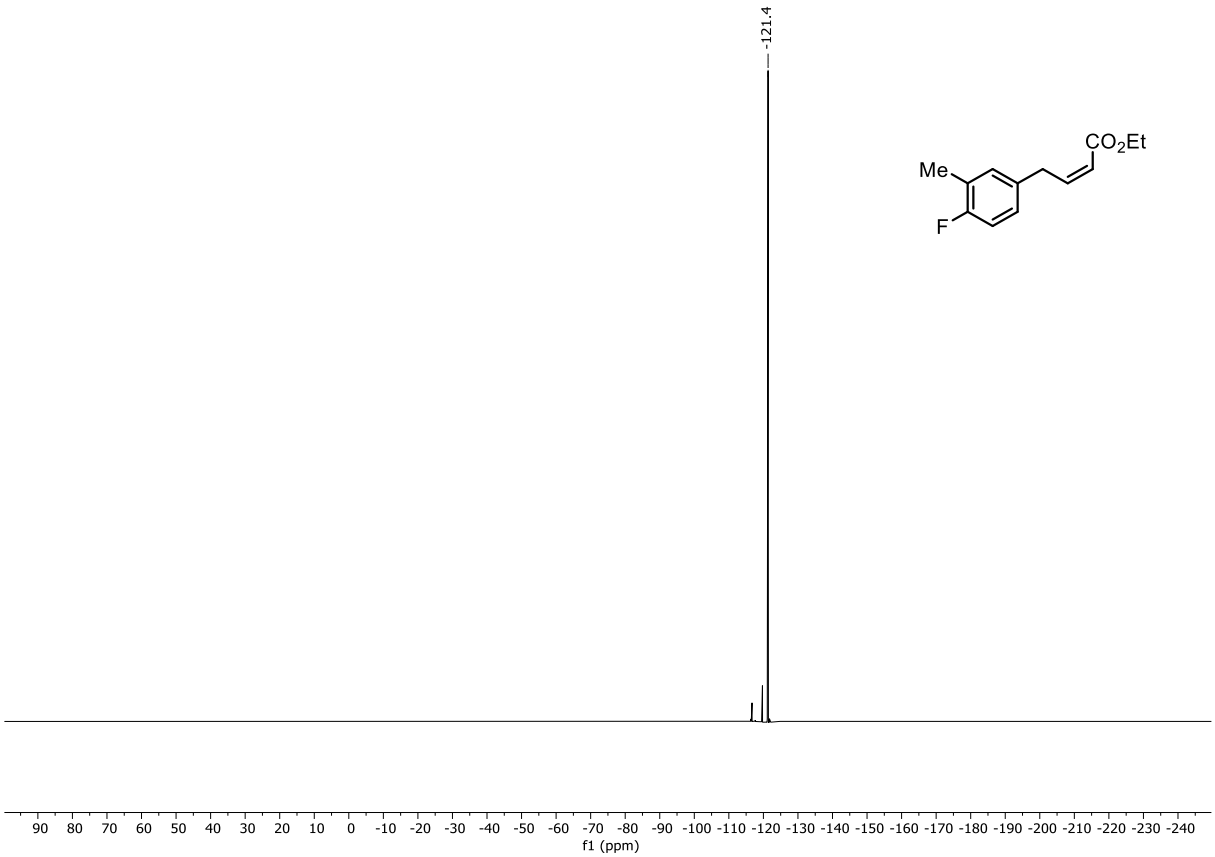

Figure 6.80 ^{19}F (13C)NMR (376 MHz) spectrum of **4-6**.

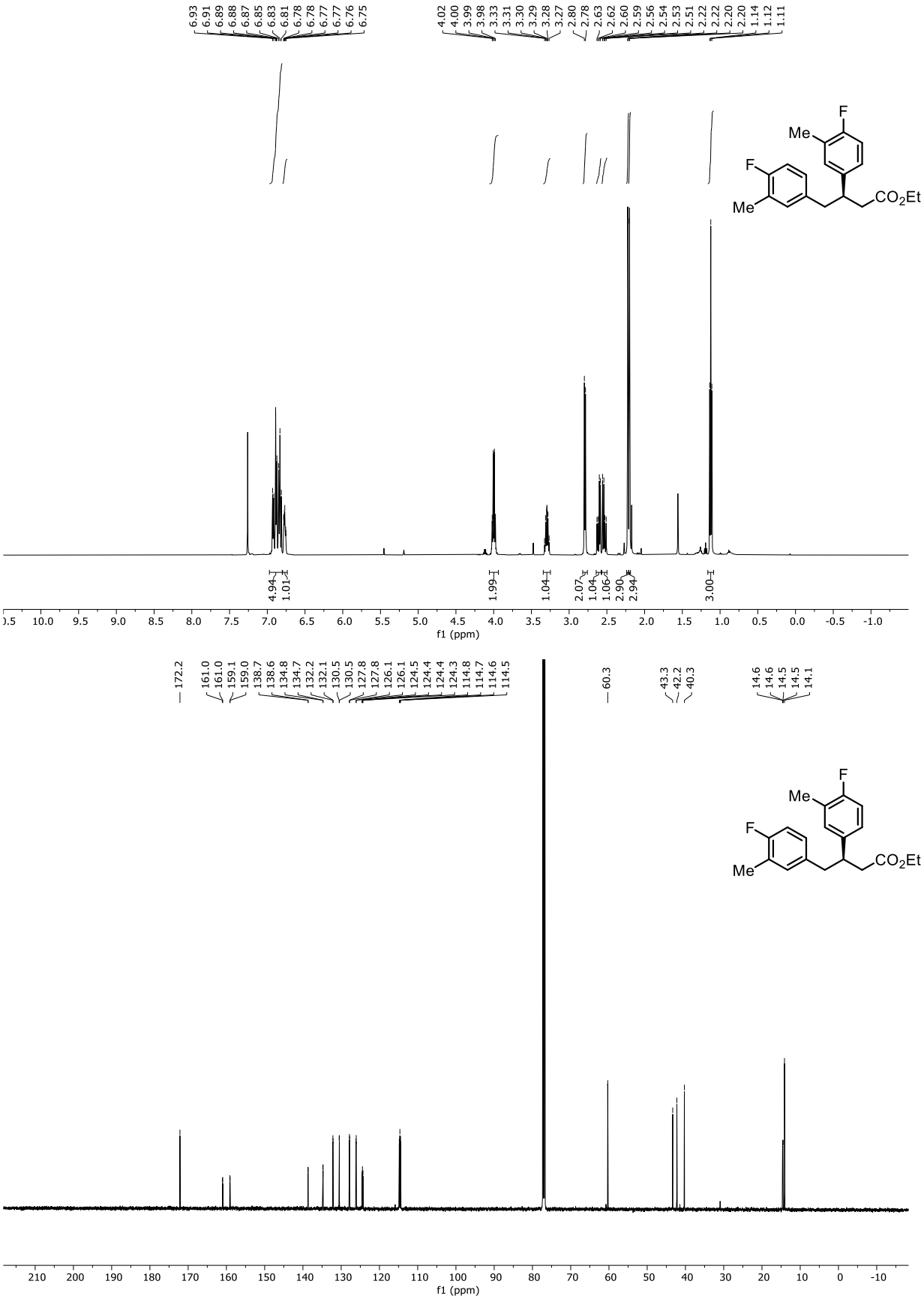

Figure 6.81 (top) ^{1}H NMR (400 MHz) and (bottom) ^{13}C NMR (101 MHz) spectra of **4-7a**.

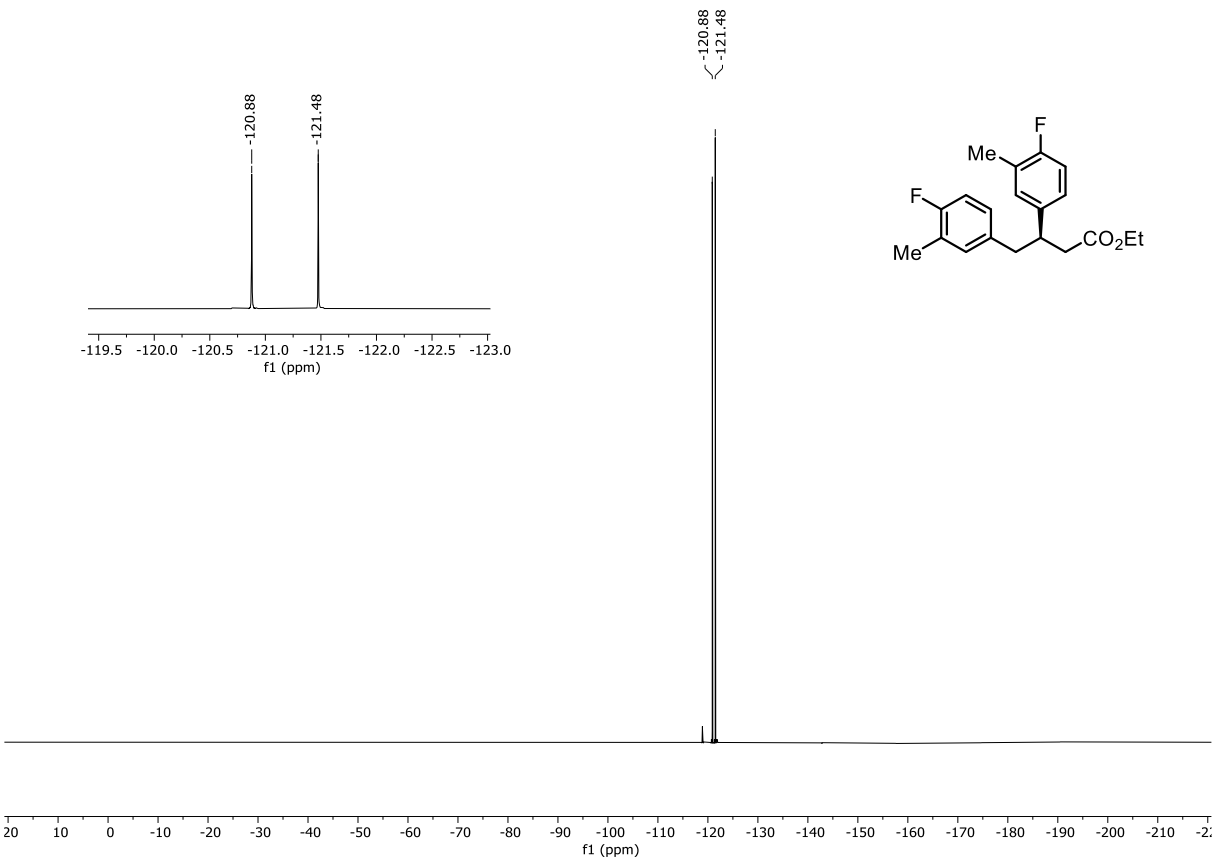

Figure 6.82 ^{19}F (13C)NMR (376 MHz) spectrum of **4-7a**.

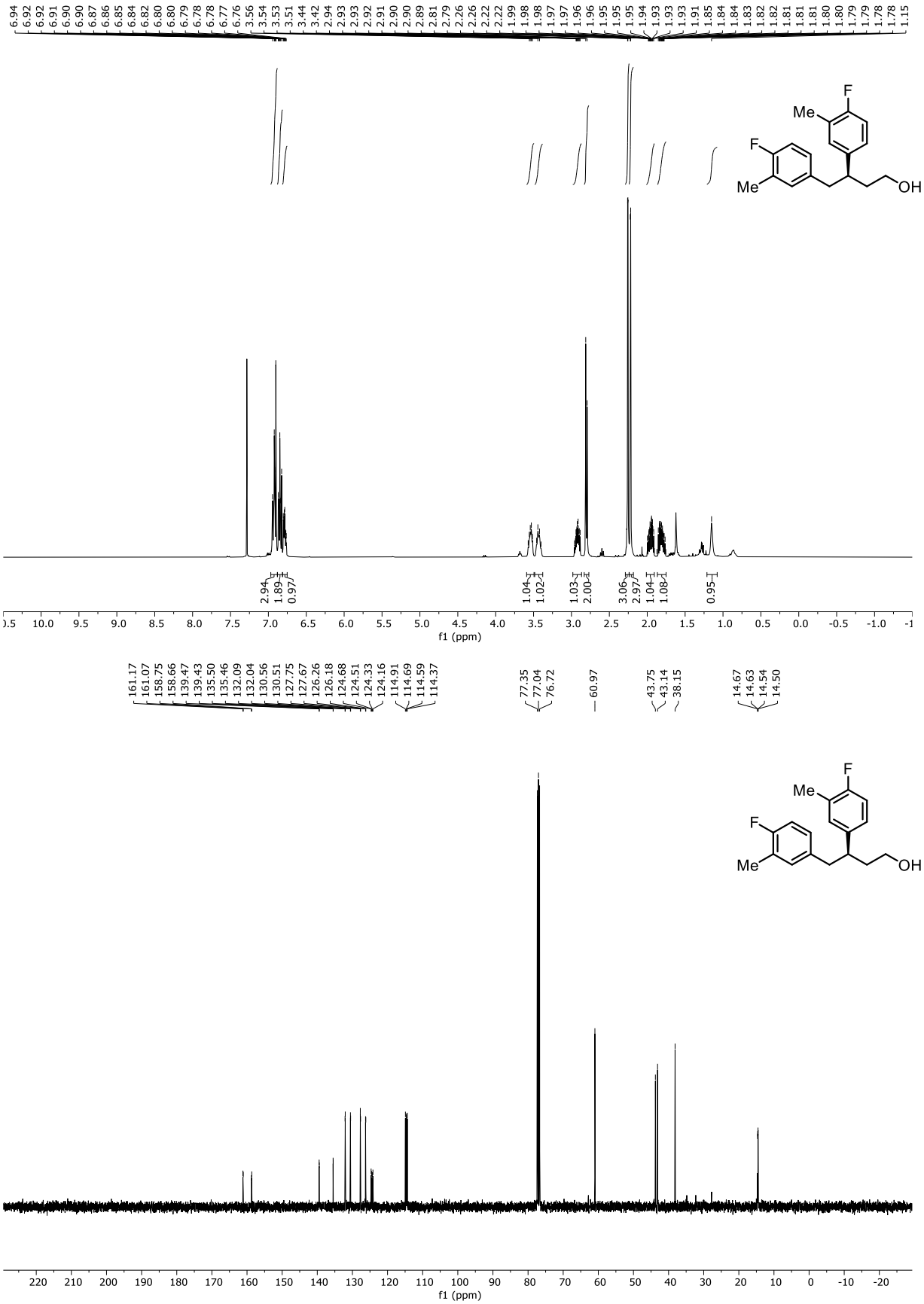

Figure 6.83 (top) ^{1}H NMR (400 MHz) and (bottom) ^{13}C NMR (101 MHz) spectra of **4-9**.

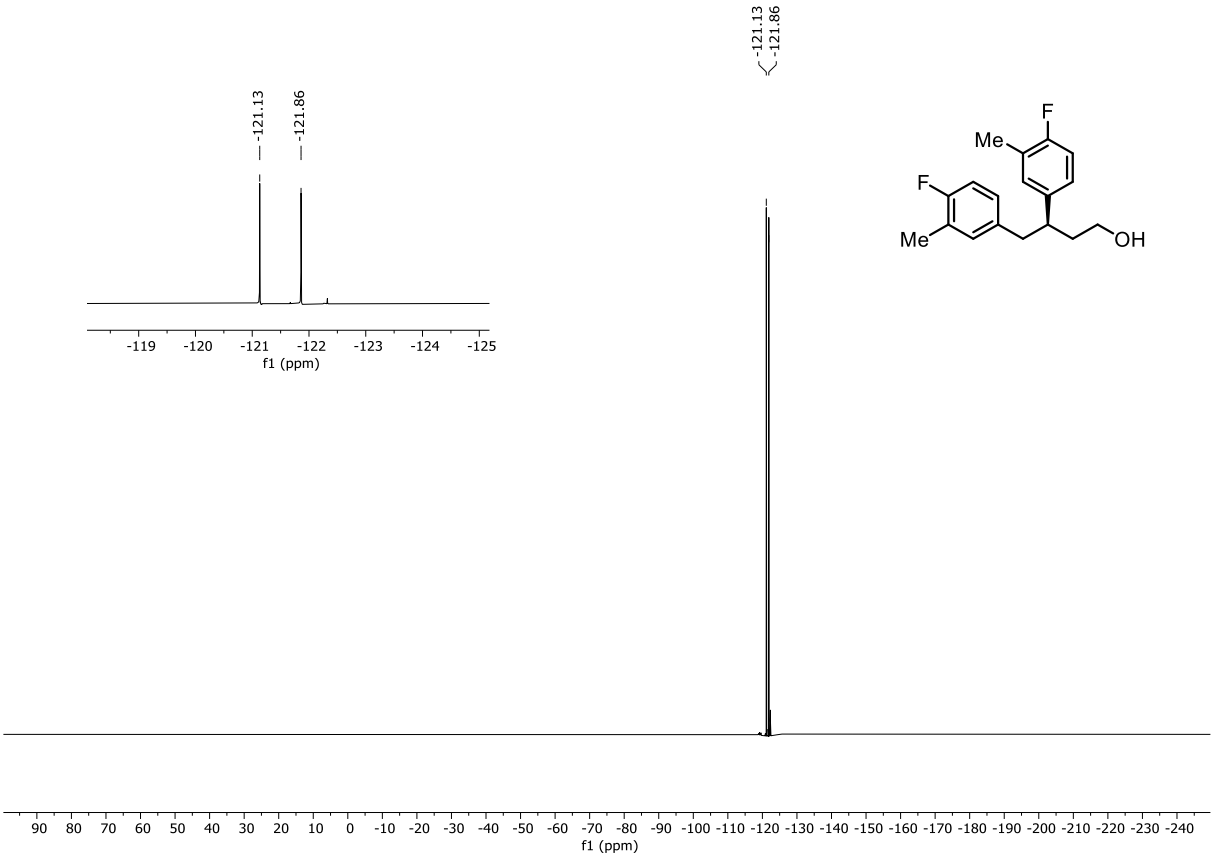

Figure 6.84 ^{19}F (13C)NMR (376 MHz) spectrum of **4-9**.

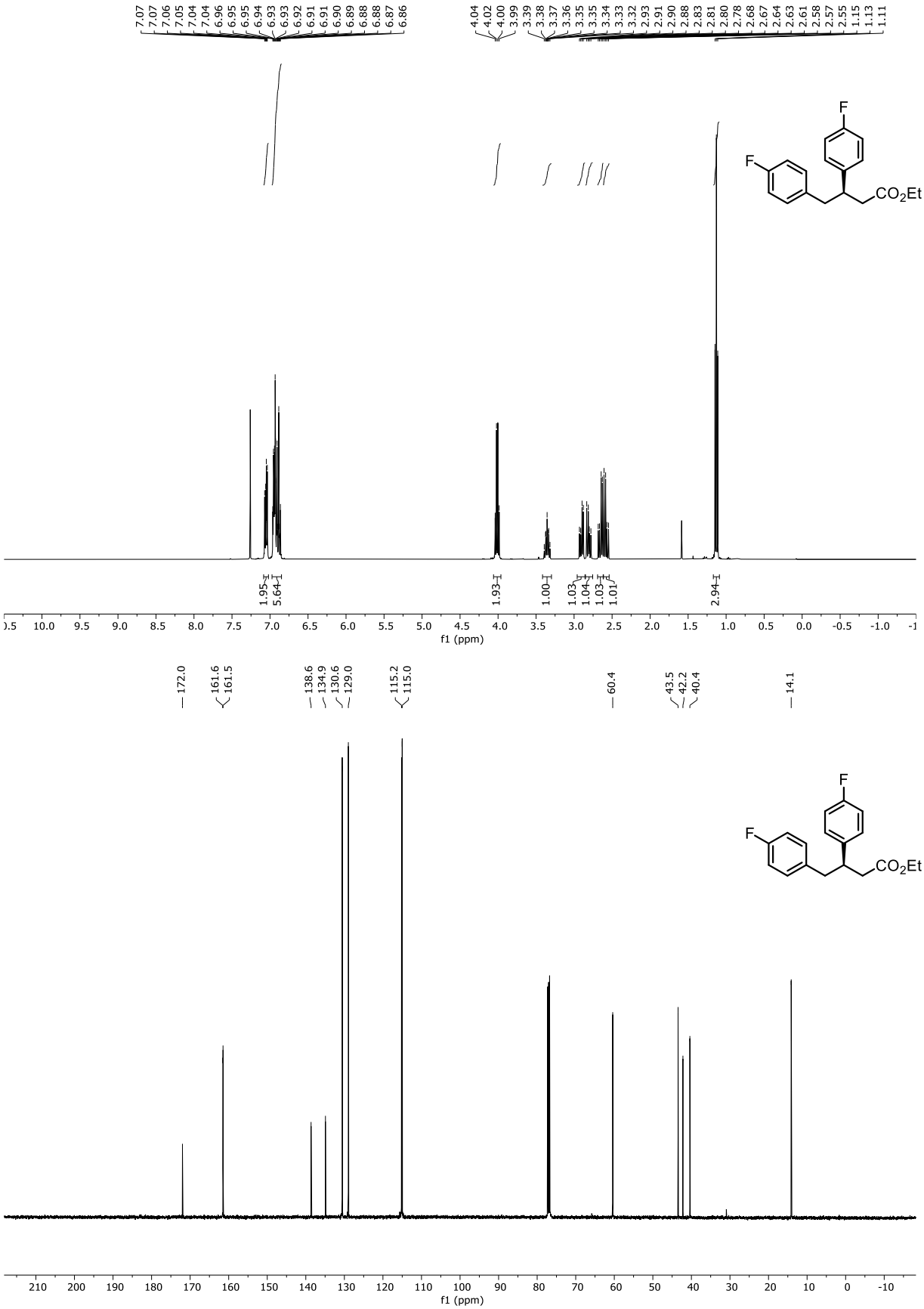

Figure 6.85 (top) ^{1}H NMR (400 MHz) and (bottom) ^{13}C NMR (101 MHz) spectra of **4-7b**.

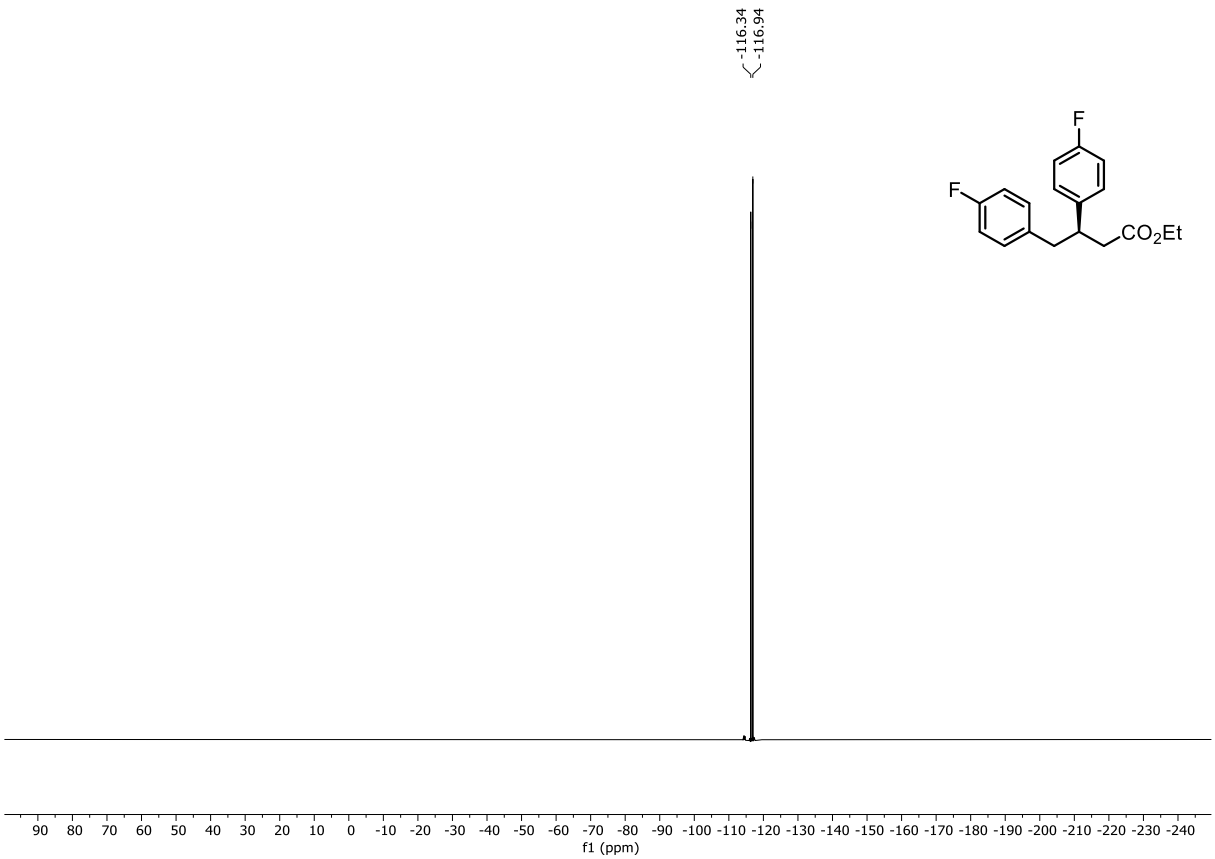

Figure 6.86 ^{19}F (13C)NMR (376 MHz) spectrum of **4-7b**.

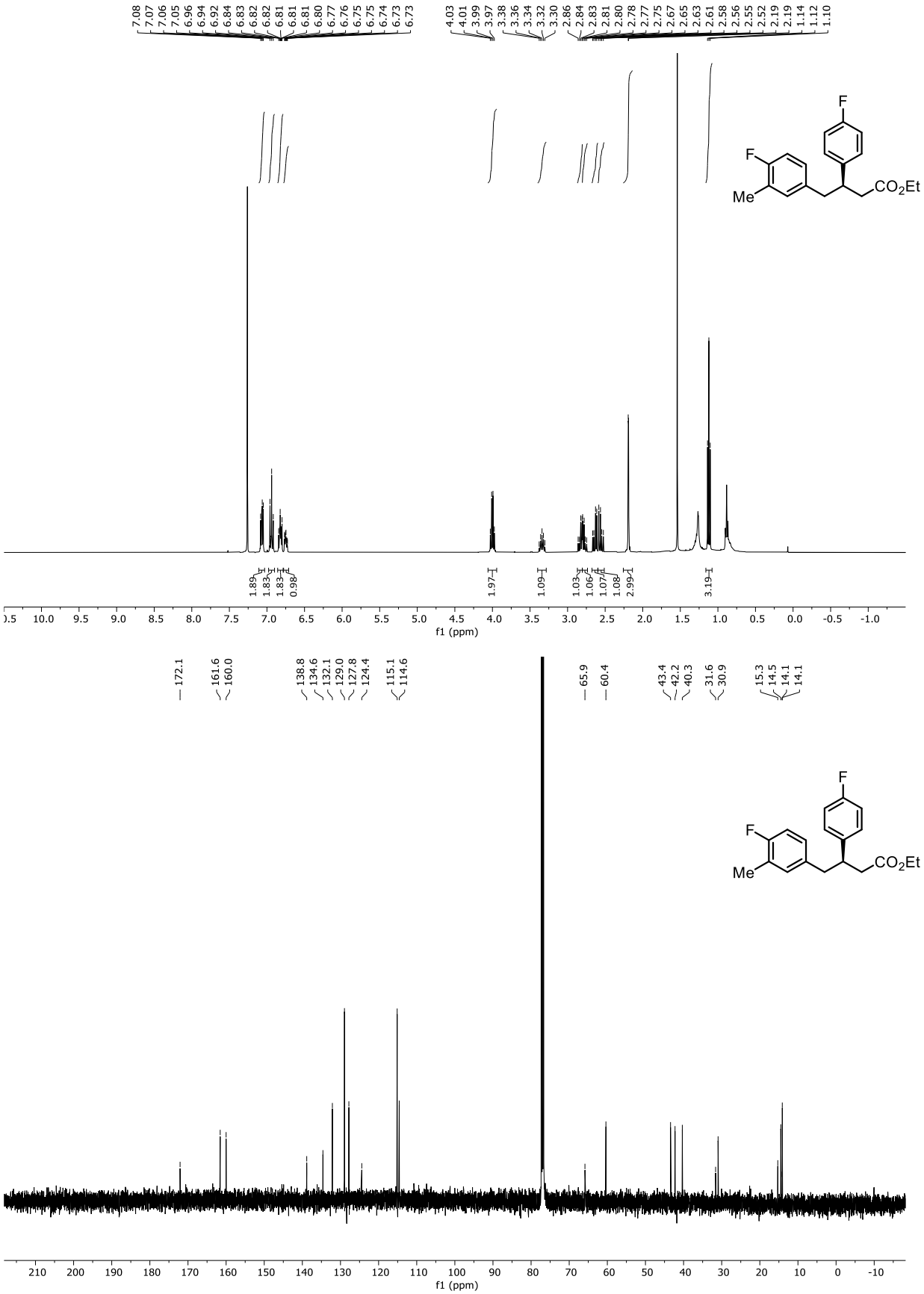

Figure 6.87 (top) ^{1}H NMR (400 MHz) and (bottom) ^{13}C NMR (101 MHz) spectra of **4-11**.

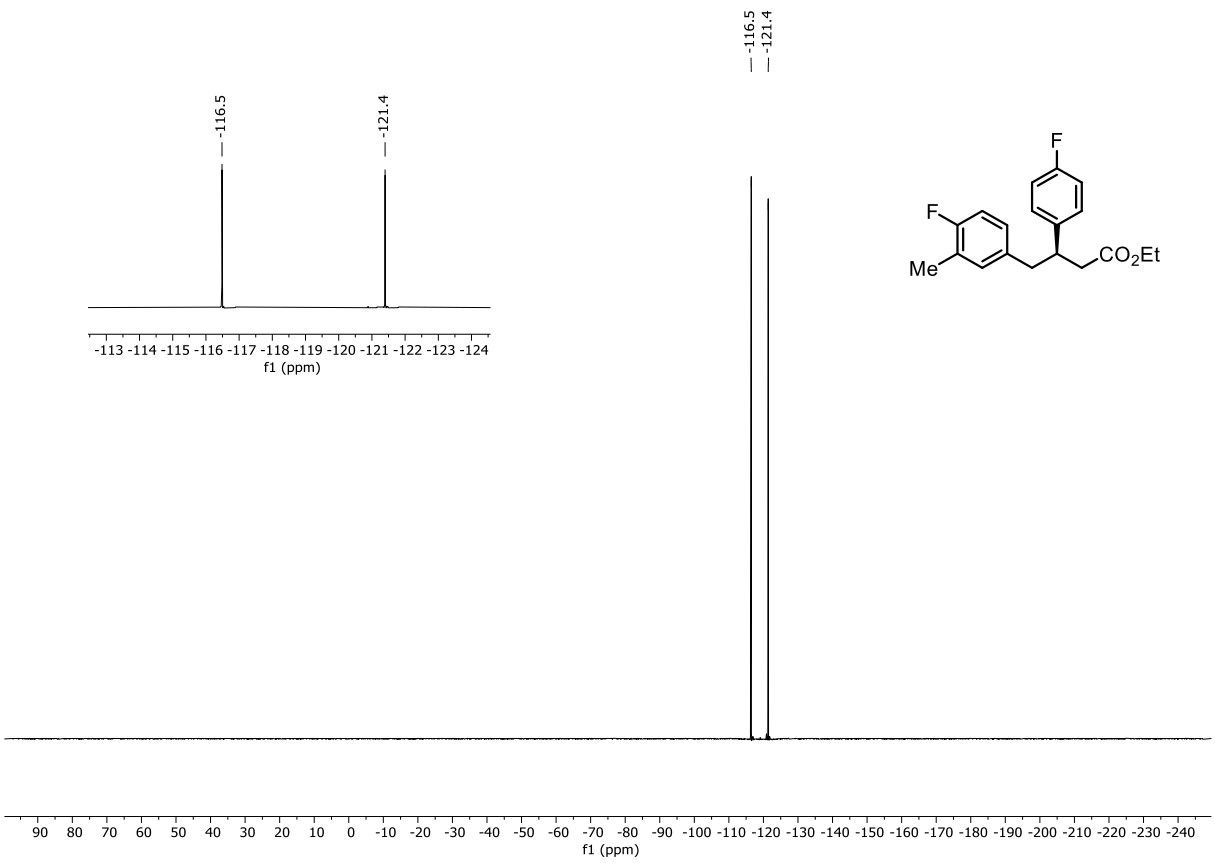

Figure 6.88 ^{19}F (13C)NMR (376 MHz) spectrum of **4-11**.

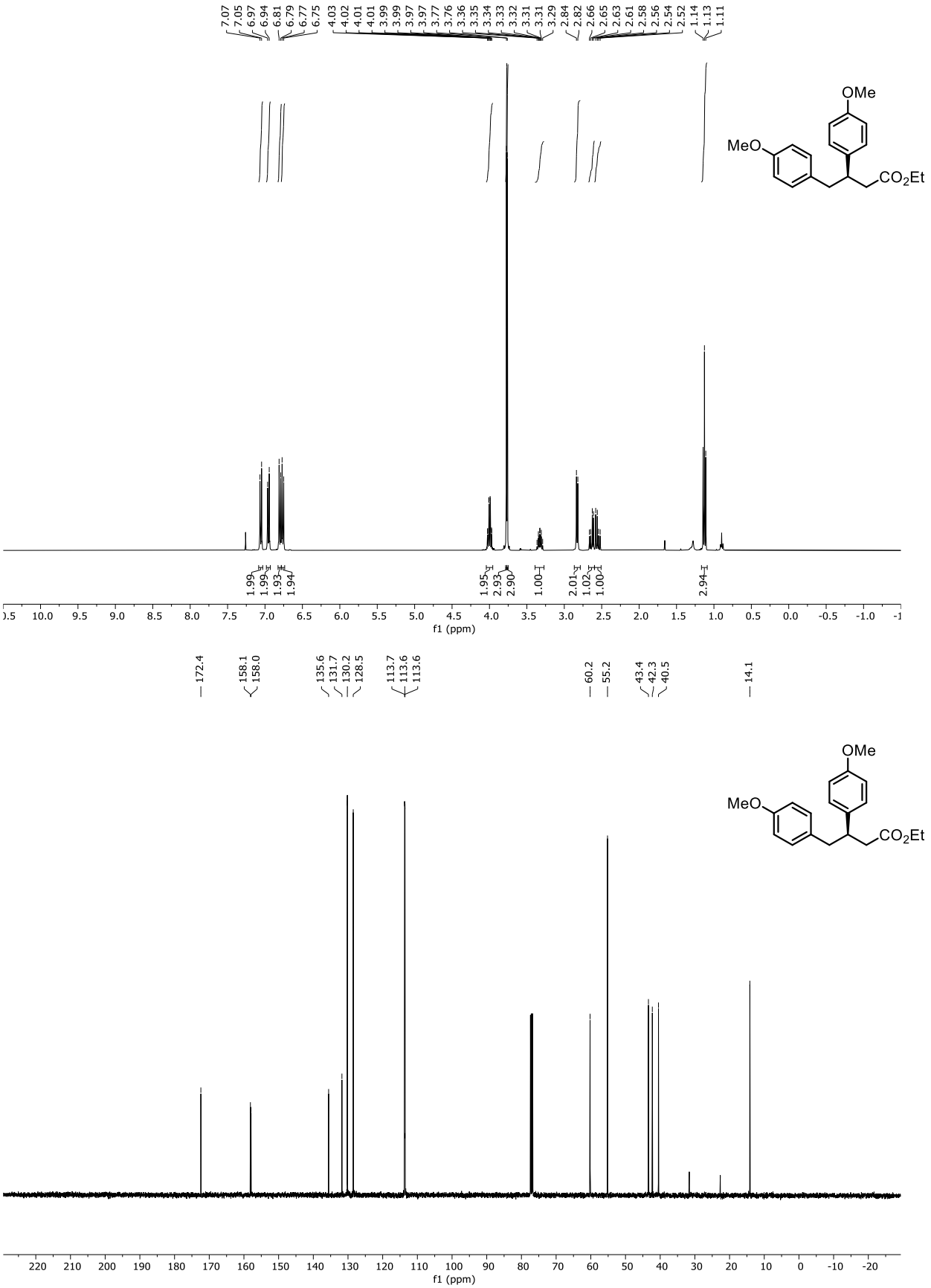

Figure 6.89 (top) ^{1}H NMR (400 MHz) and (bottom) ^{13}C NMR (101 MHz) spectra of **4-7c**.

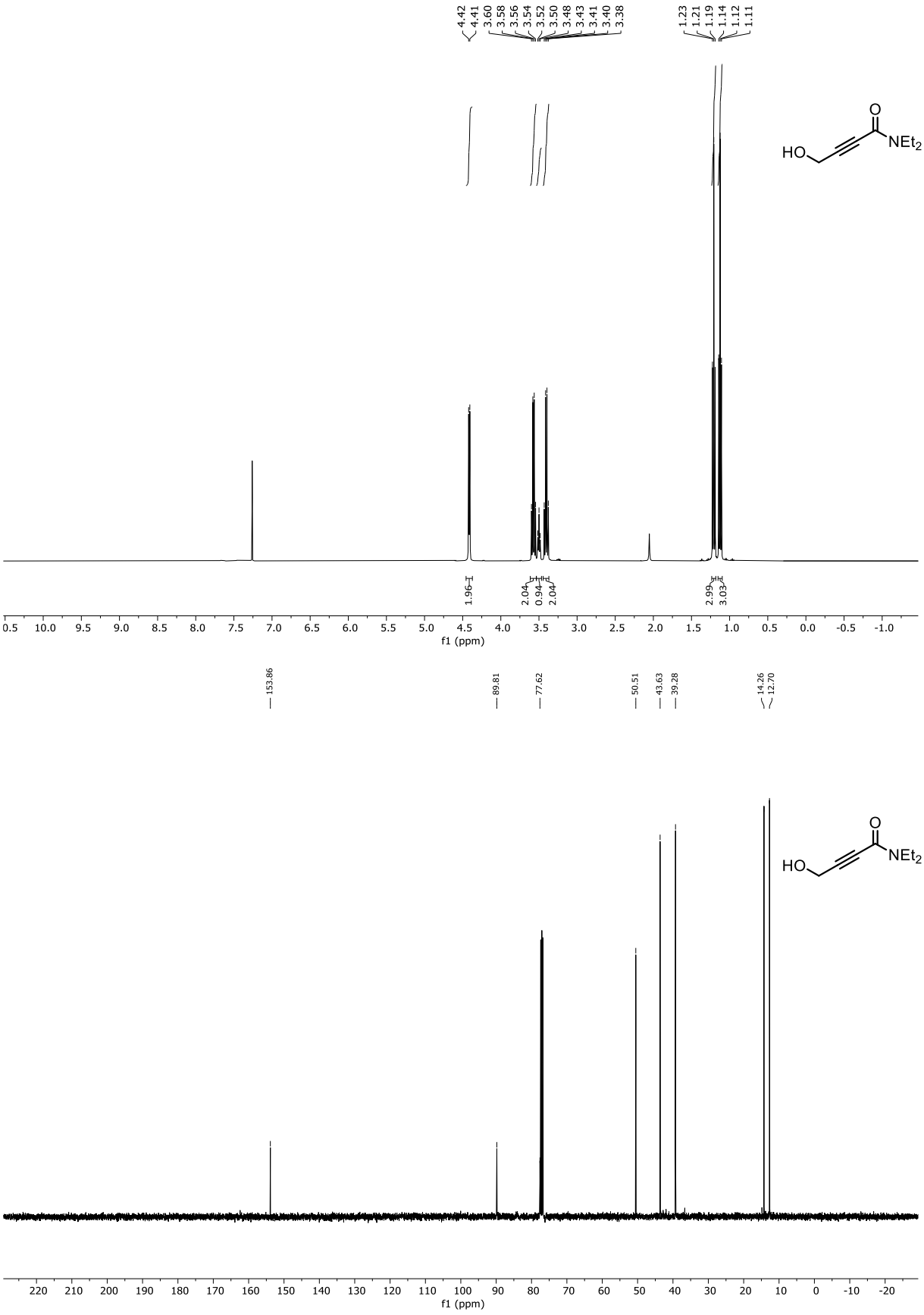

Figure 6.90 (top) ^{1}H NMR (400 MHz) and (bottom) ^{13}C NMR (101 MHz) spectra of **4-12**.

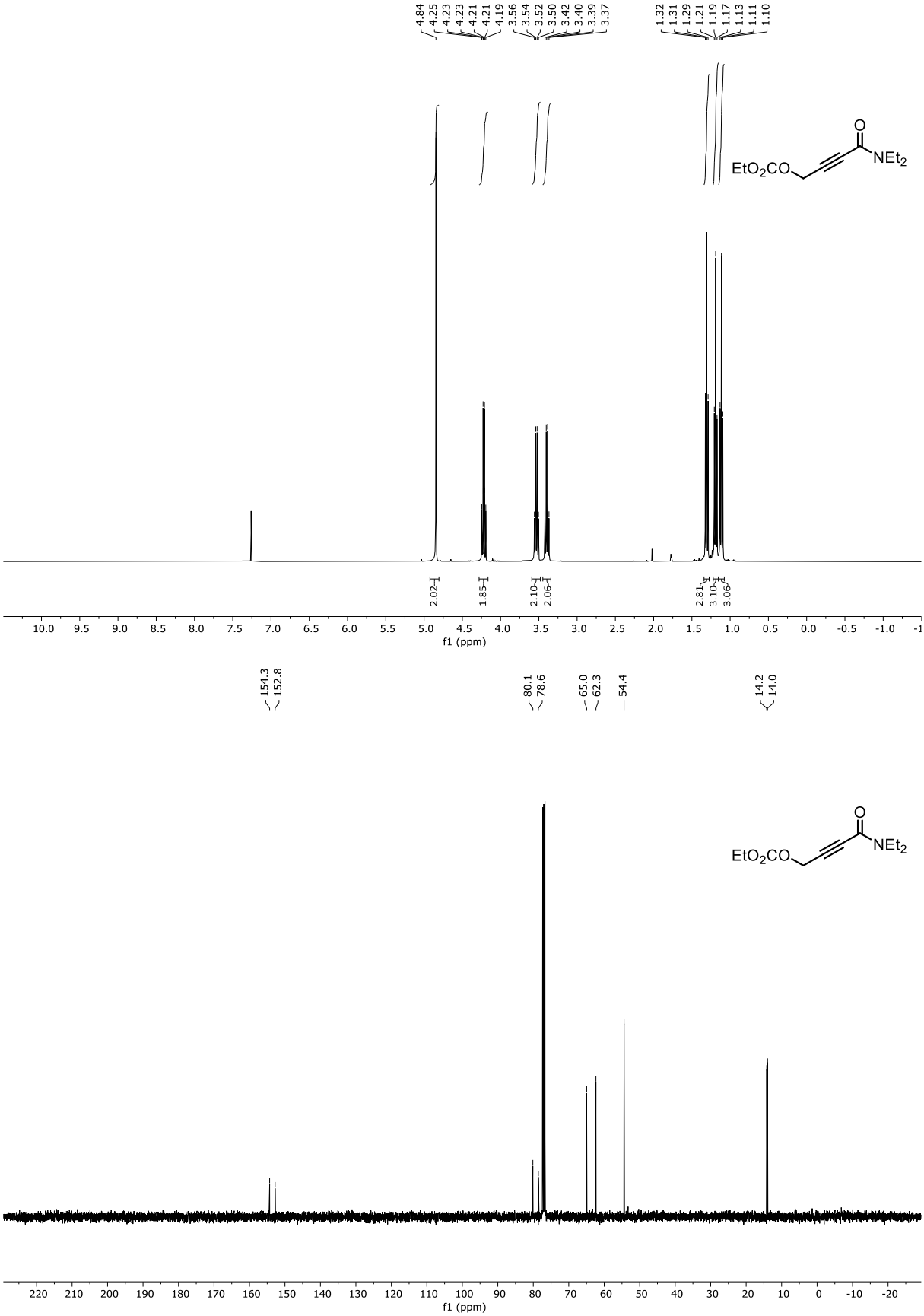

Figure 6.91 (top) ^{1}H NMR (400 MHz) and (bottom) ^{13}C NMR (101 MHz) spectra of **4-13**.

6.2 SFC traces

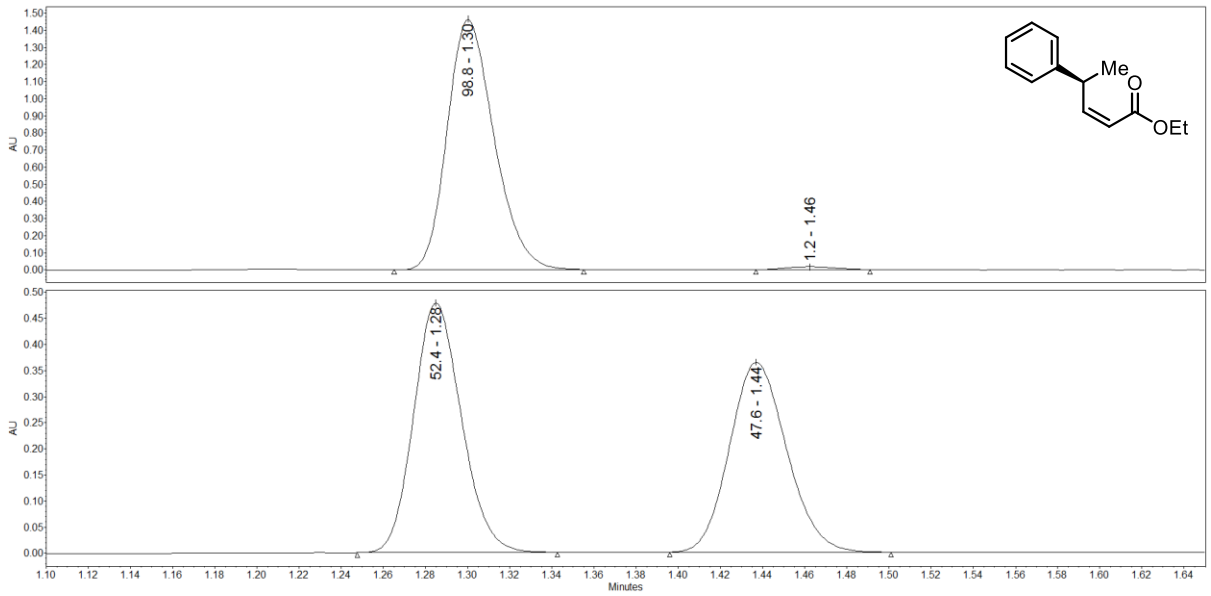

Figure 6.92 SFC trace for (*S*)-*Z*-**2-10a** and (±)-*Z*-**2-10a**.

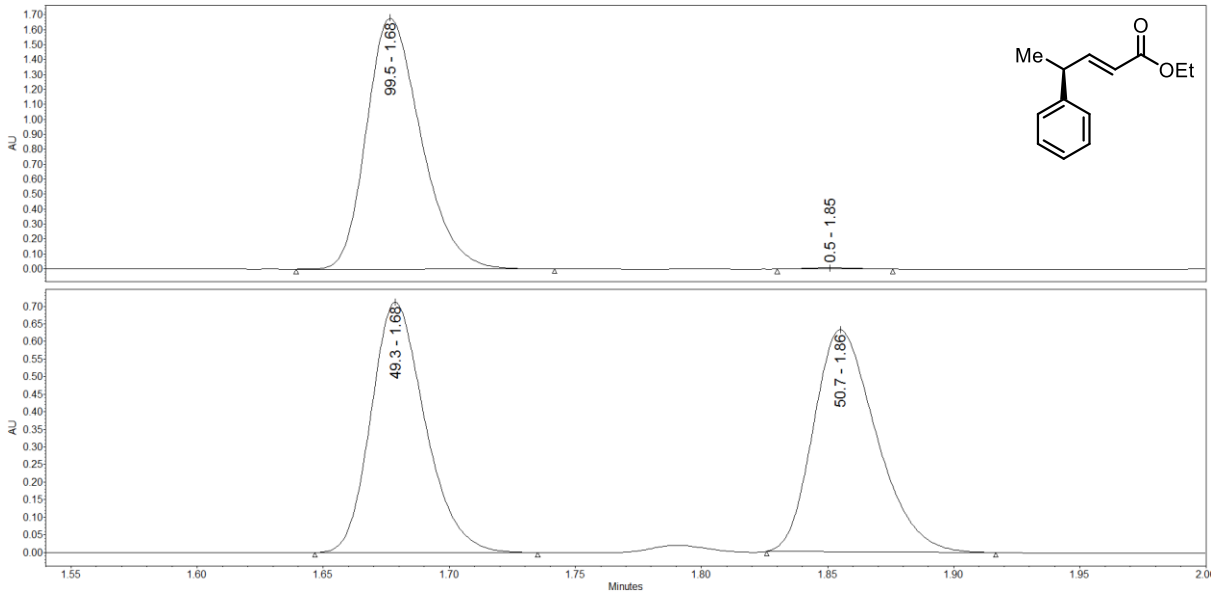

Figure 6.93 SFC trace for (*S*)-*E*-**2-10a** and (±)-*E*-**2-10a**.

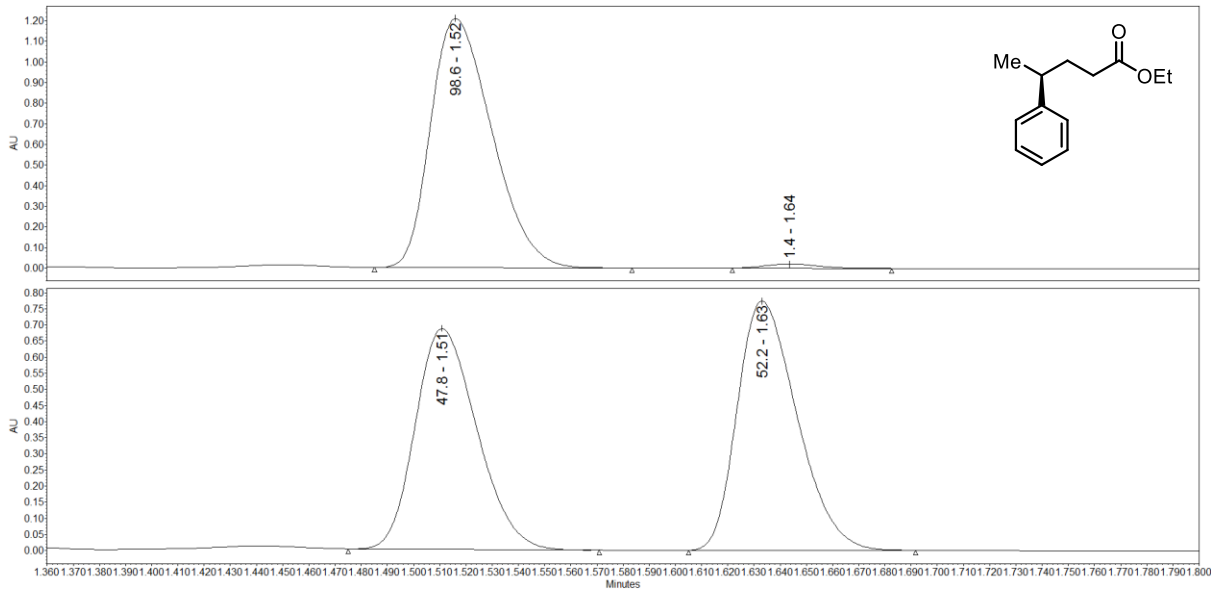

Figure 6.94 SFC trace for (*S*)-*red*-**2-10a** and (±)-*red*-**2-10a**.

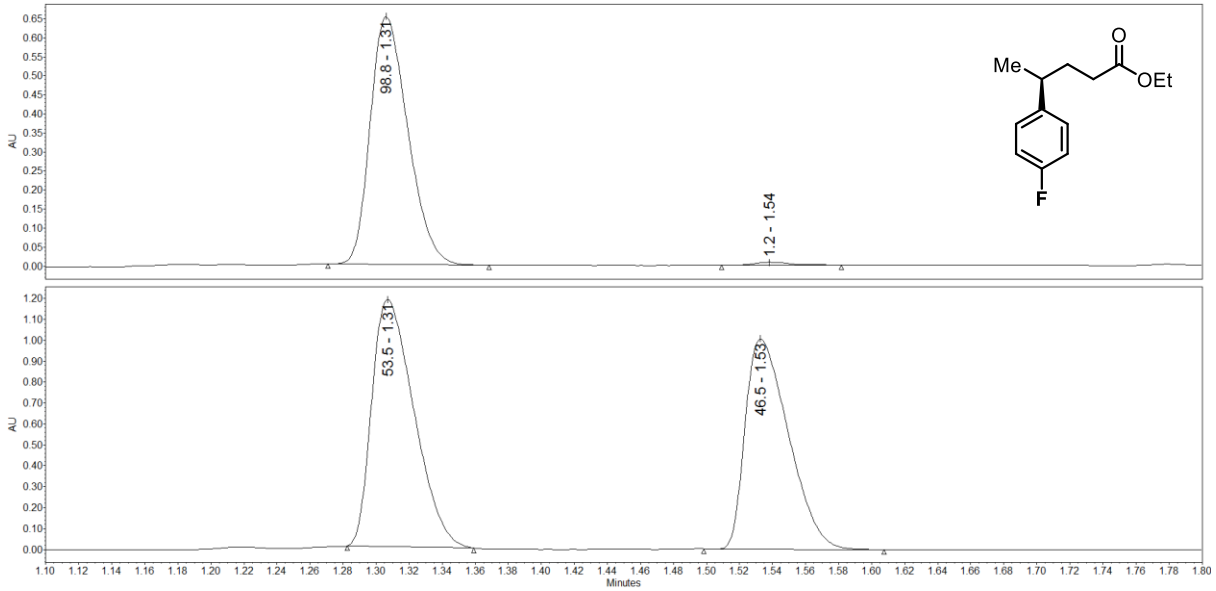

Figure 6.95 SFC trace for (*S*)-*red*-**2-10b** and (±)-*red*-**2-10b**.

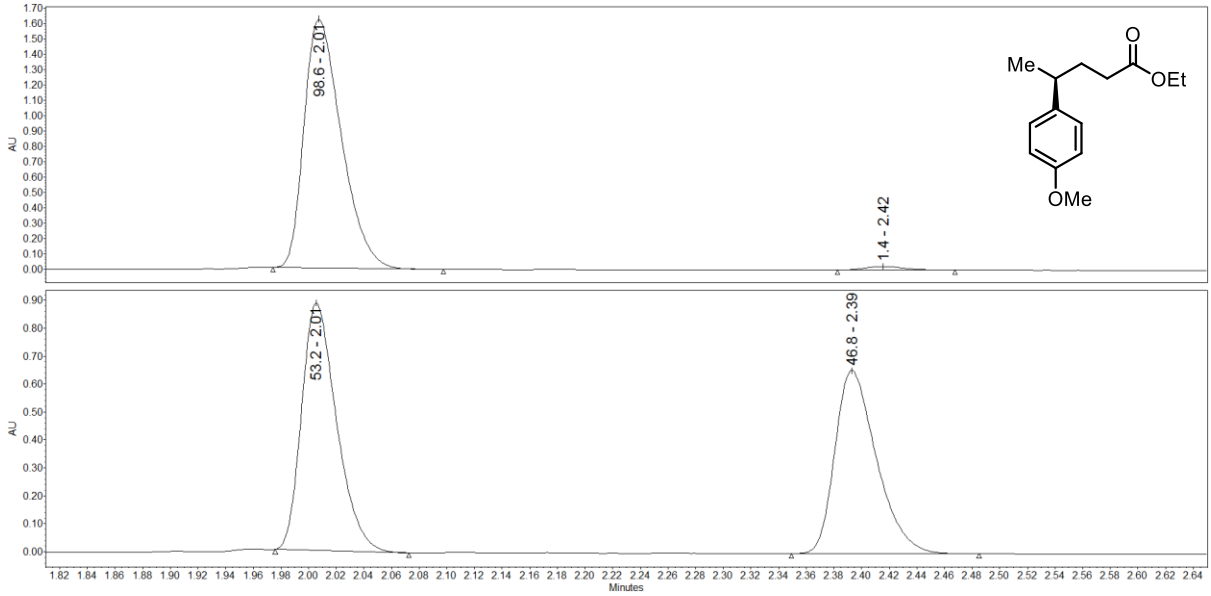

Figure 6.96 SFC trace for (*S*)-*red*-**2-10c** and (±)-*red*-**2-10c**.

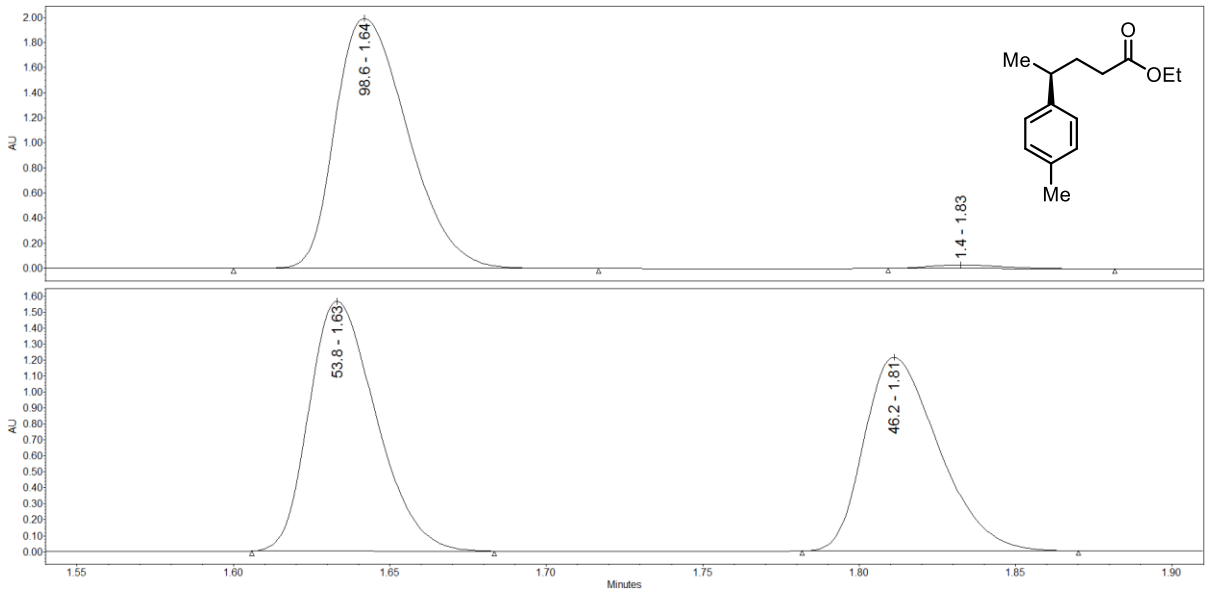

Figure 6.97 SFC trace for (*S*)-*red*-**2-10d** and (±)-*red*-**2-10d**.

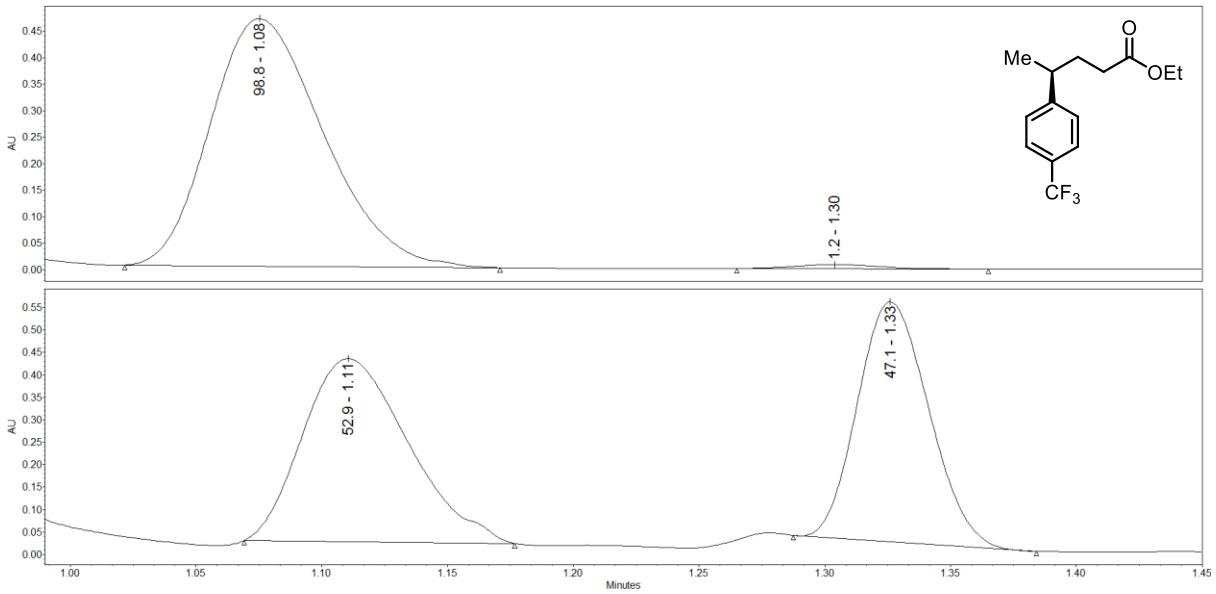

Figure 6.98 SFC trace for (*S*)-*red*-**2-10e** and (±)-*red*-**2-10e**.

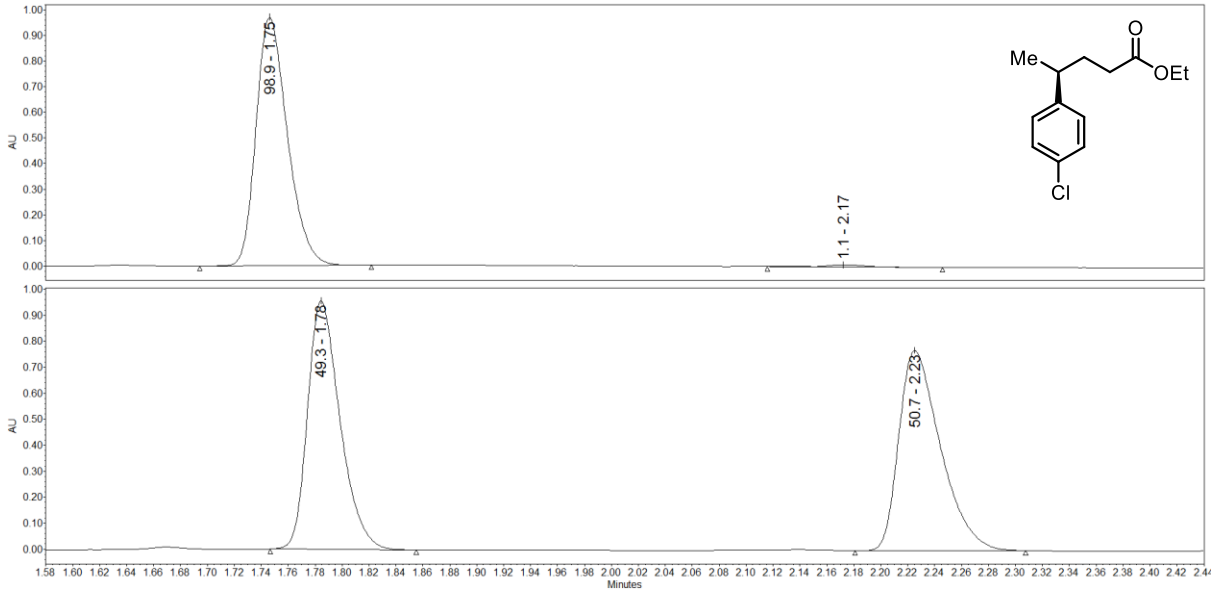

Figure 6.99 SFC trace for (*S*)-*red*-**2-10f** and (±)-*red*-**2-10f**.

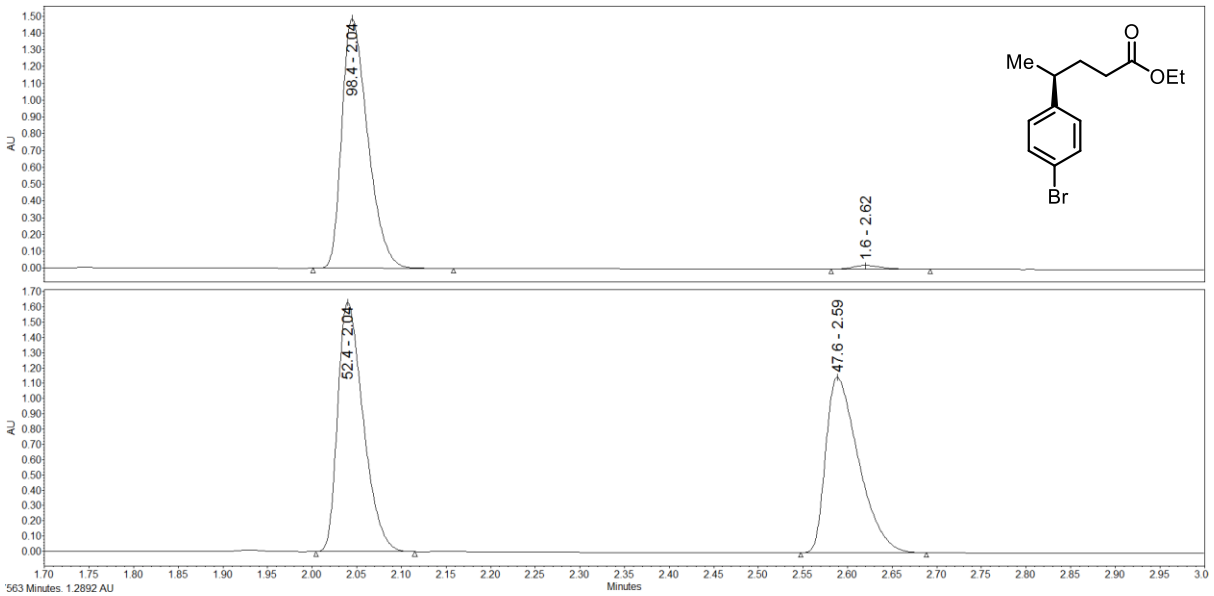

Figure 6.100 SFC trace for (*S*)-*red*-**2-10g** and (±)-*red*-**2-10g**.

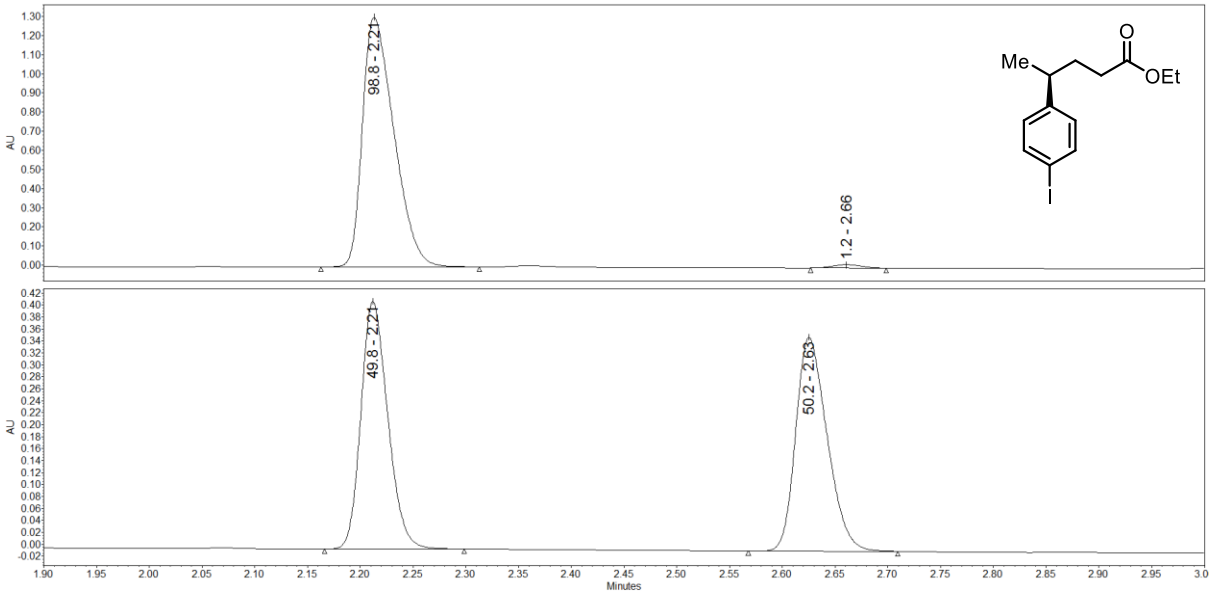

Figure 6.101 SFC trace for (*S*)-*red*-**2-10h** and (±)-*red*-**2-10h**.

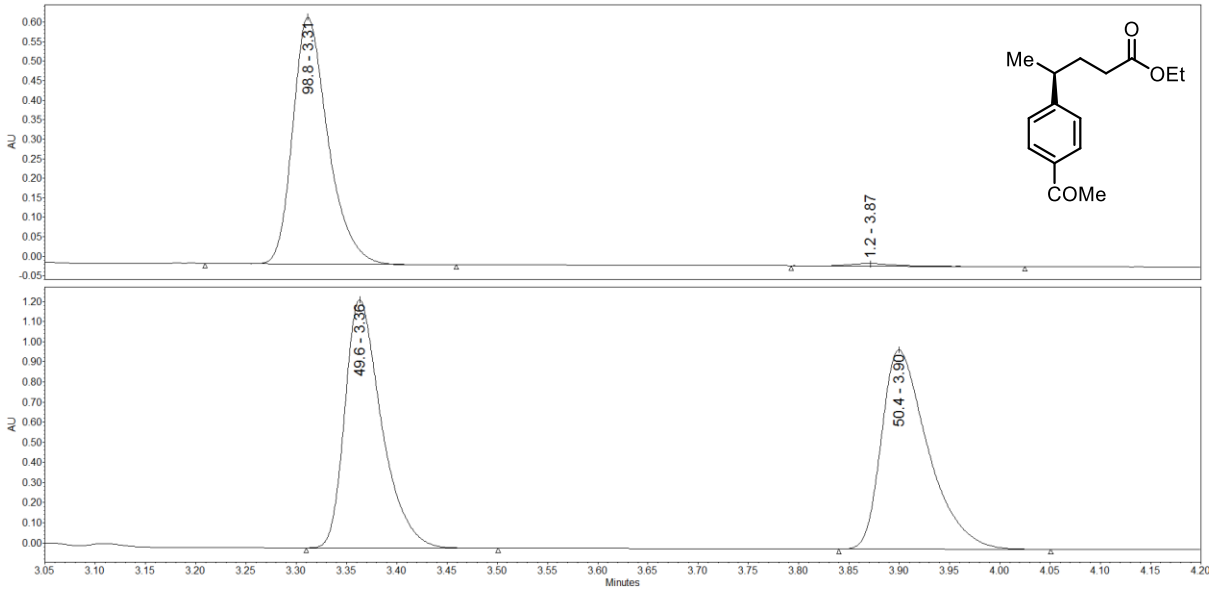

Figure 6.102 SFC trace for (*S*)-*red*-**2-10i** and (±)-*red*-**2-10i**.

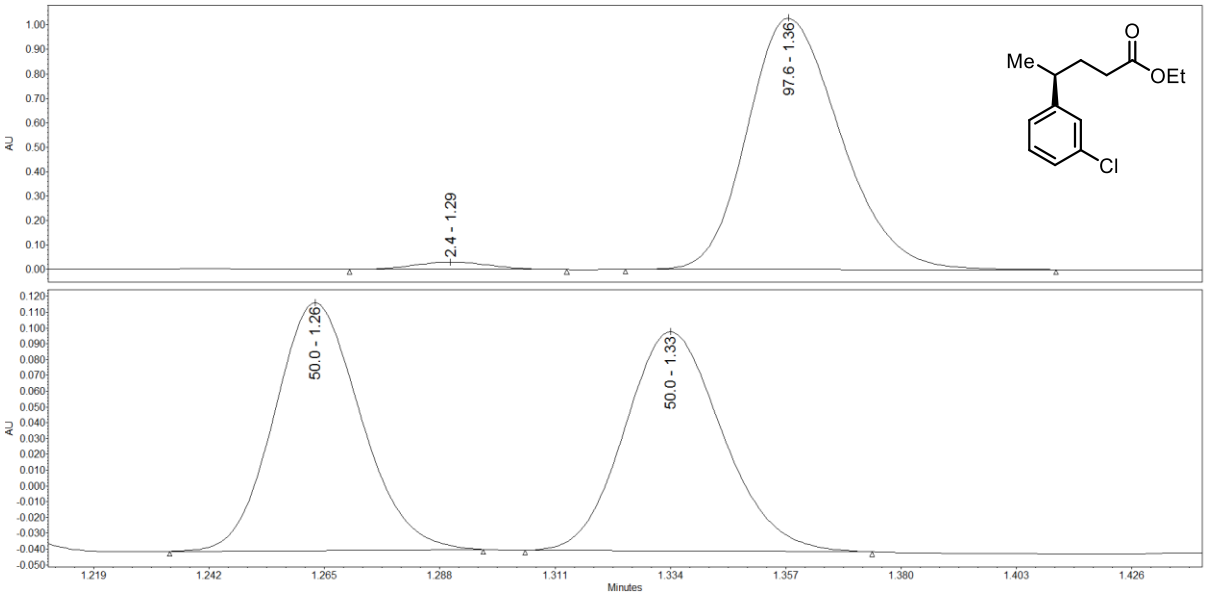

Figure 6.103 SFC trace for (*S*)-*red*-**3j** and (±)-*red*-**3j**.

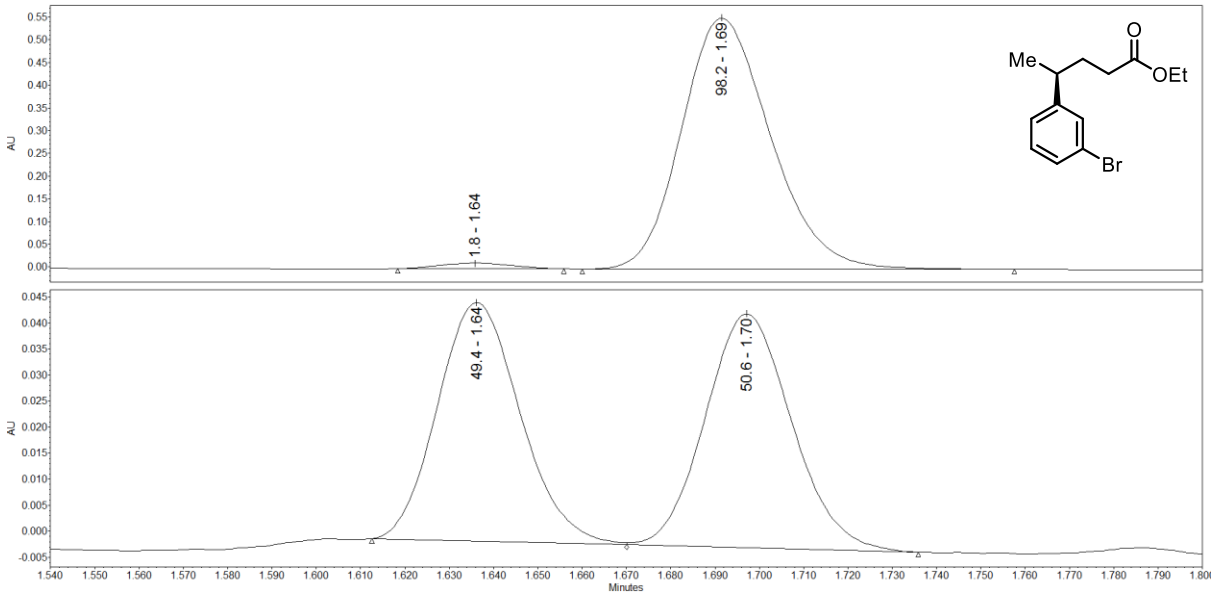

Figure 6.104 SFC trace for (*S*)-*red*-**2-10k** and (±)-*red*-**2-10k**.

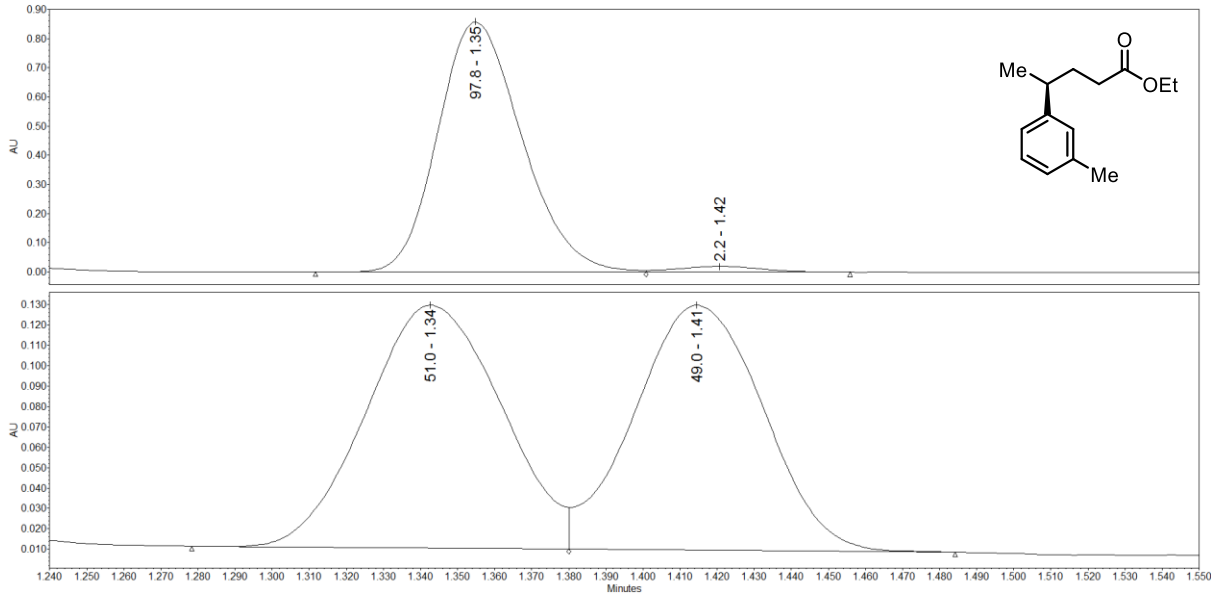

Figure 6.105 SFC trace for (*S*)-*red*-**2-10l** and (±)-*red*-**2-10l**.

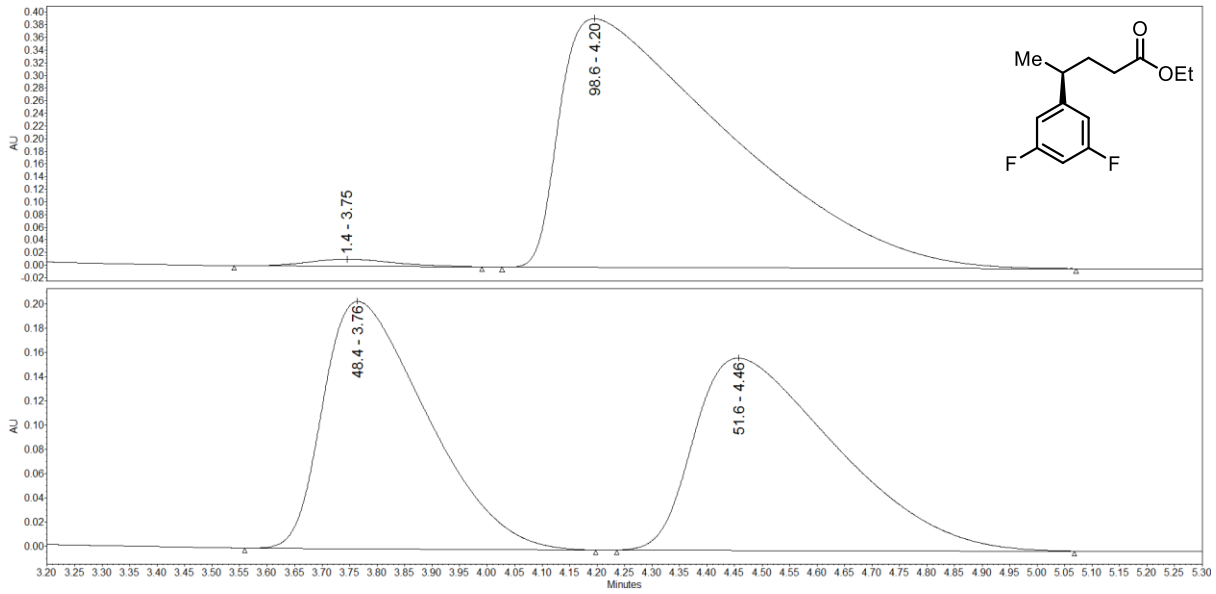

Figure 6.106 SFC trace for (*S*)-*red*-**2-10m** and (±)-*red*-**2-10m**.

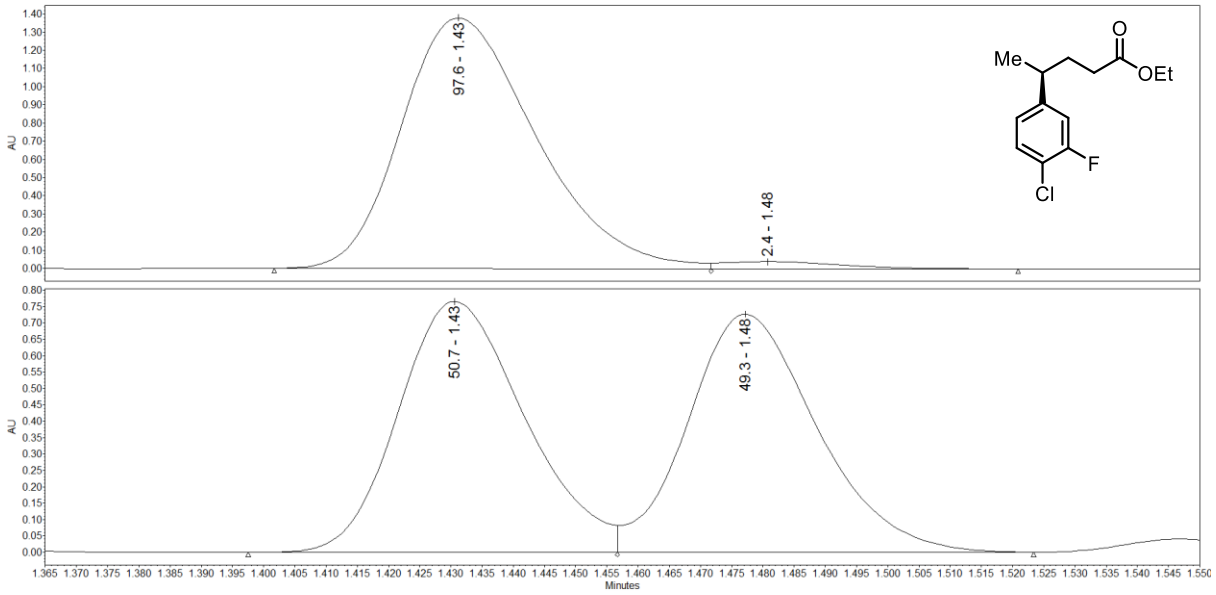

Figure 6.107 SFC trace for (*S*)-*red*-**2-10n** and (±)-*red*-**2-10n**.

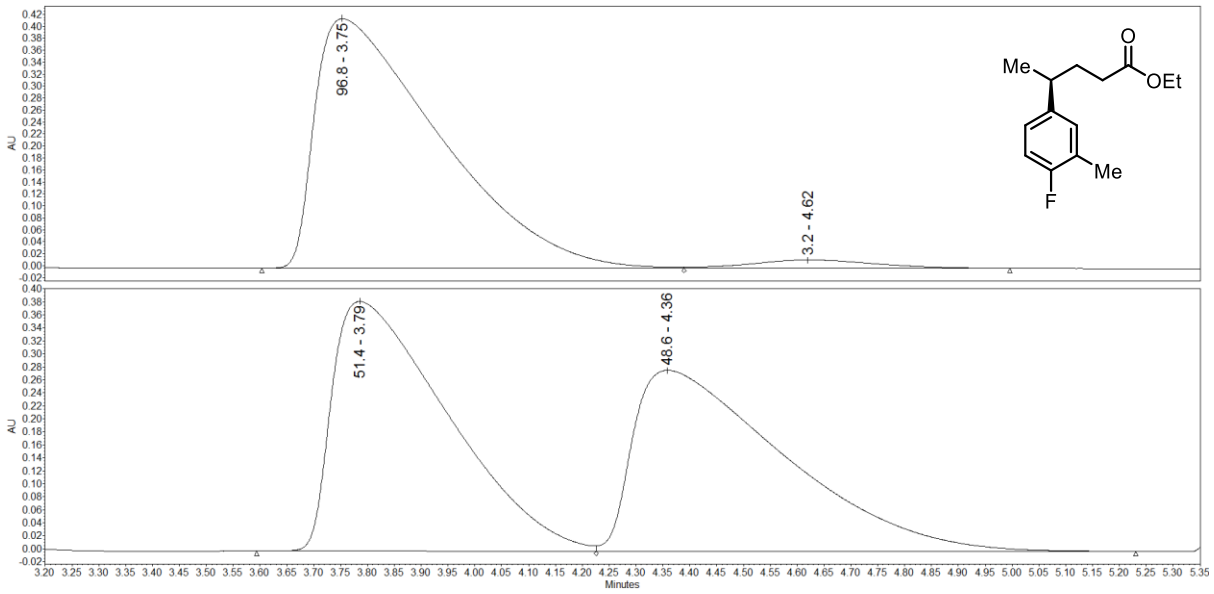

Figure 6.108 SFC trace for (*S*)-*red*-**2-10o** and (±)-*red*-**2-10o**.

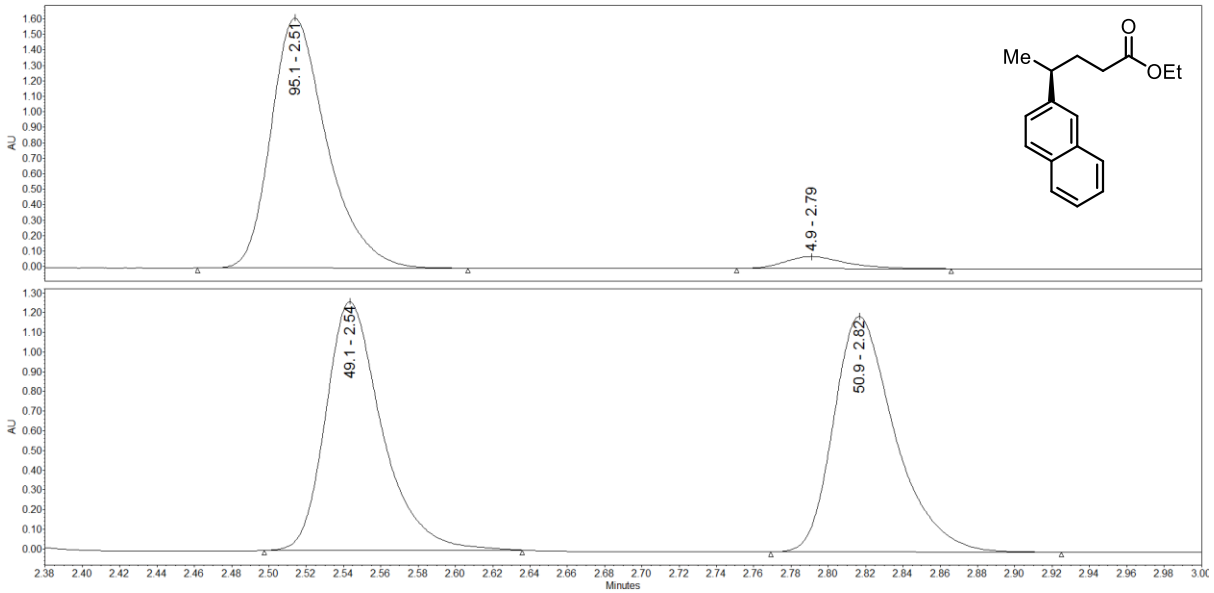

Figure 6.109 SFC trace for (*S*)-*red*-**2-10p** and (±)-*red*-**2-10p**.

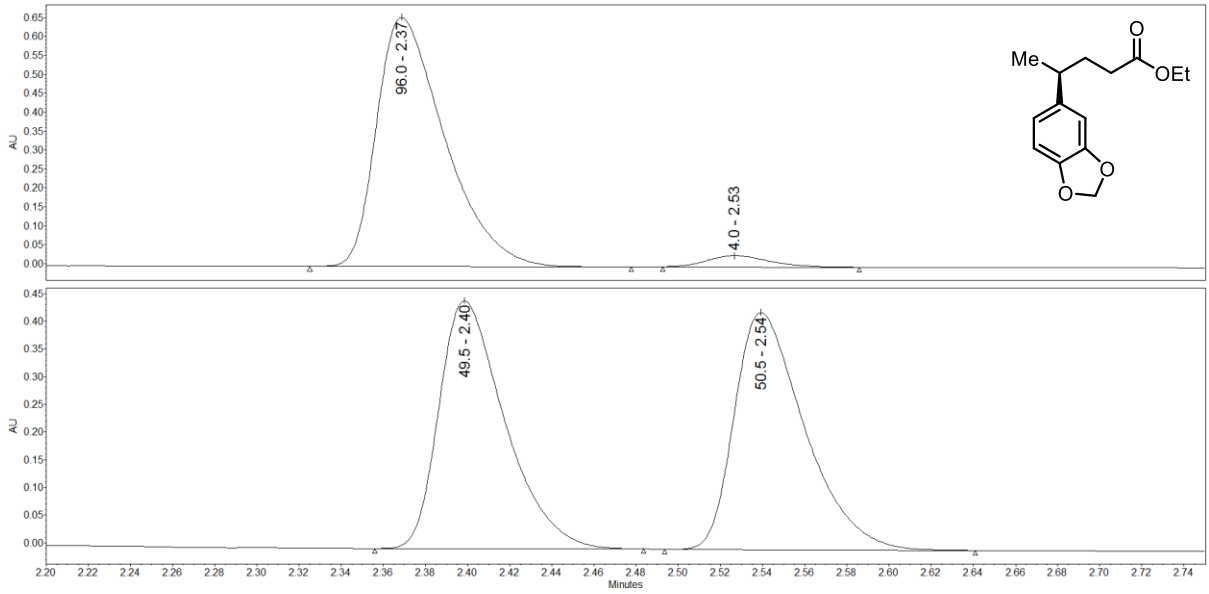

Figure 6.110 SFC trace for (*S*)-*red*-**2-10q** and (±)-*red*-**2-10q**.

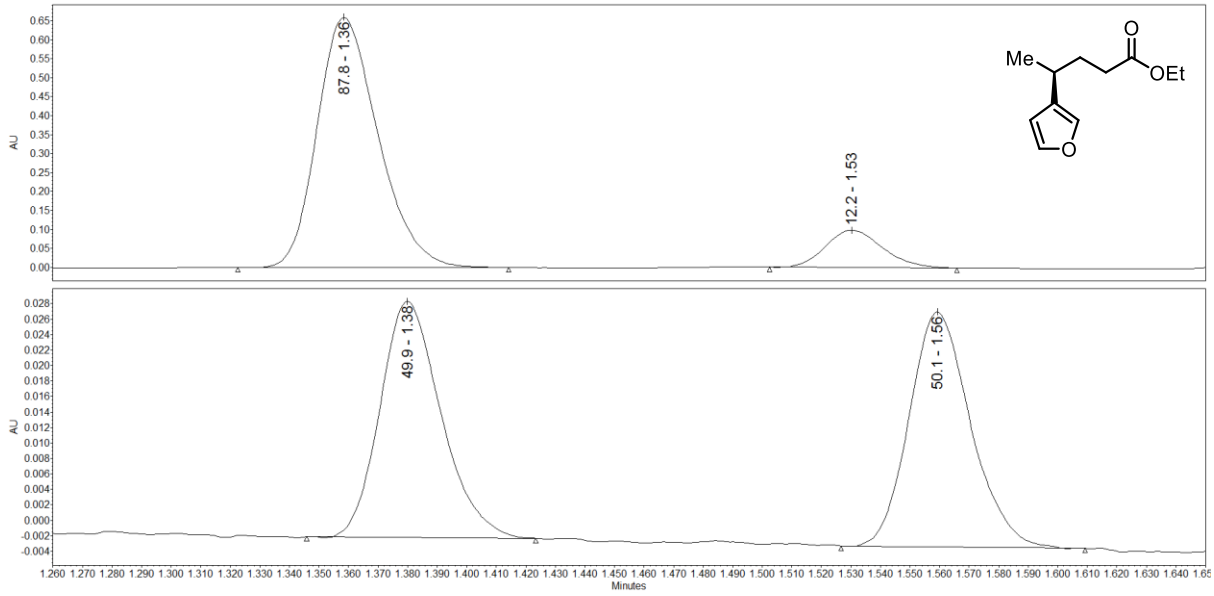

Figure 6.111 SFC trace for (*S*)-*red*-**2-10r** and (±)-*red*-**2-10r**.

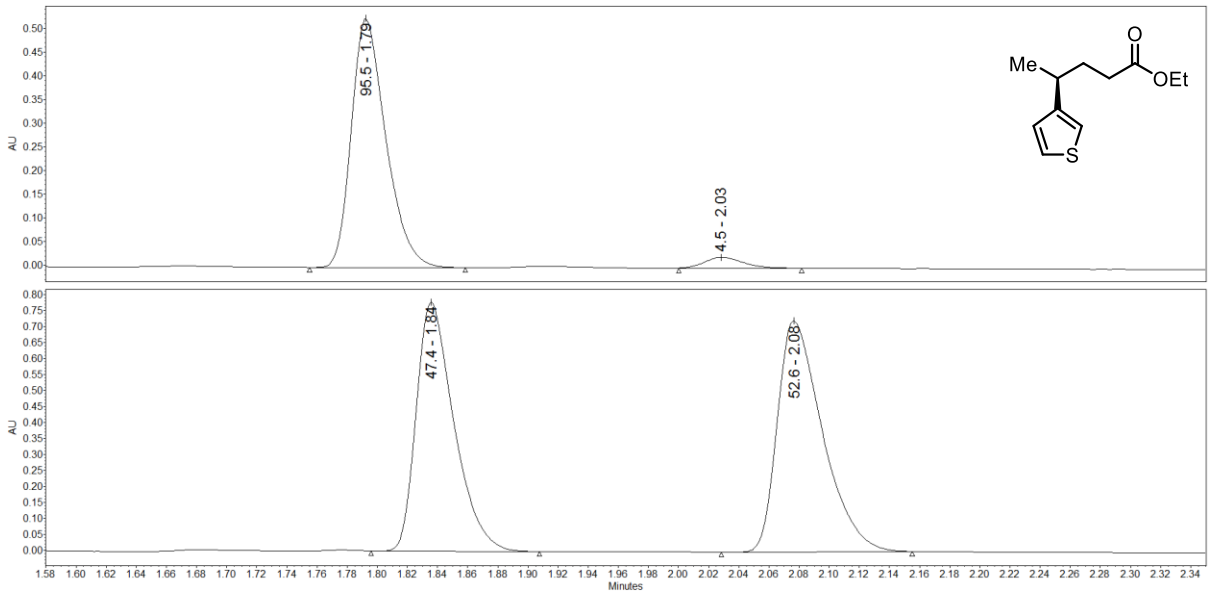

Figure 6.112 SFC trace for (*S*)-*red*-**2-10s** and (±)-*red*-**2-10s**.

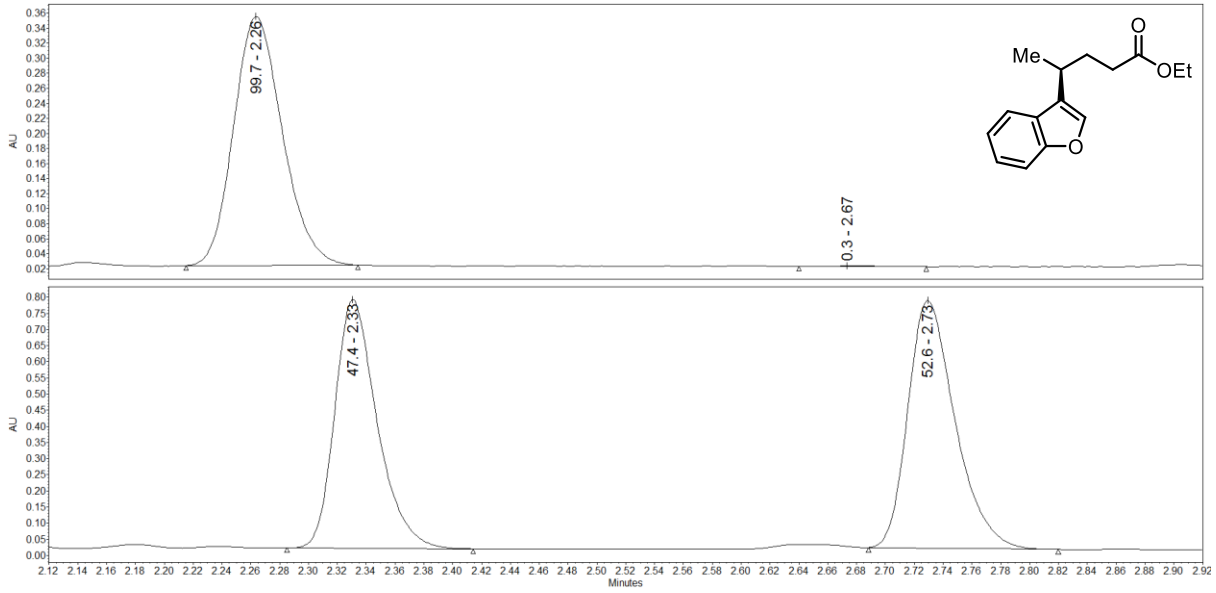

Figure 6.113 SFC trace for (*S*)-*red*-**2-10t** and (±)-*red*-**2-10t**.

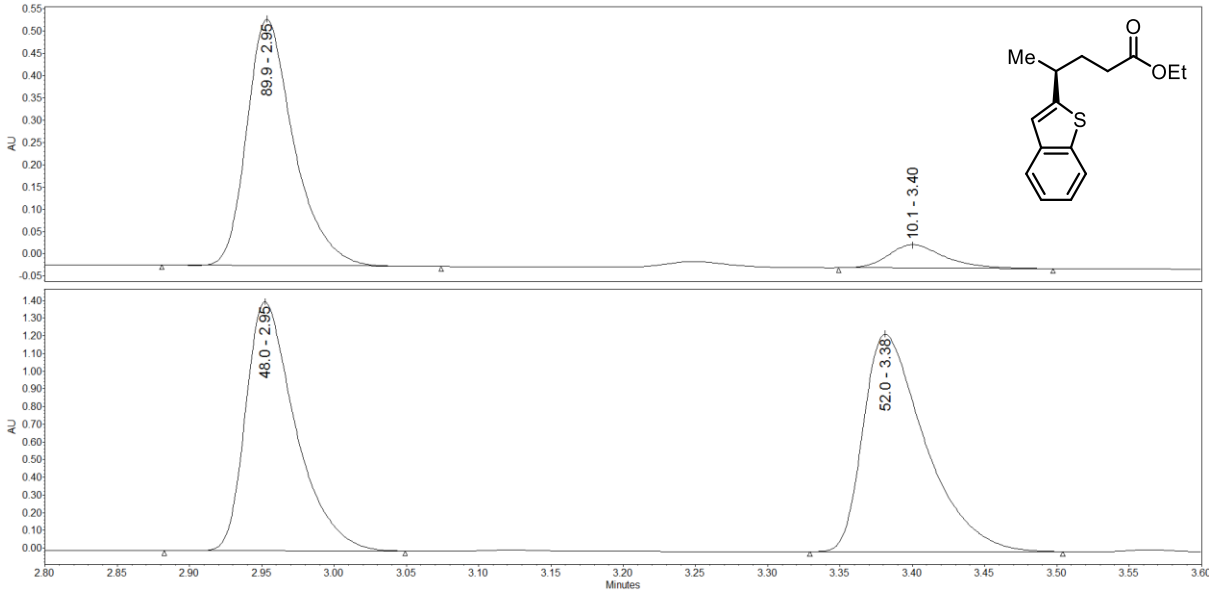

Figure 6.114 SFC trace for (*S*)-*red*-**2-10u** and (±)-*red*-**2-10u**.

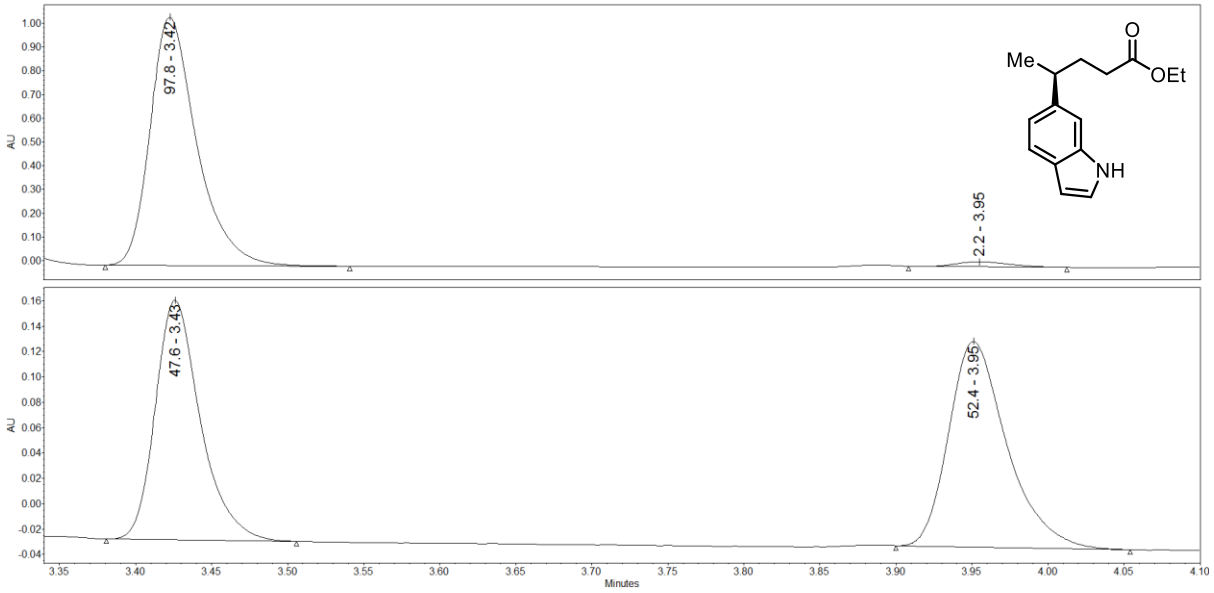

Figure 6.115 SFC trace for (*S*)-*red*-**2-10v** and (±)-*red*-**2-10v**.

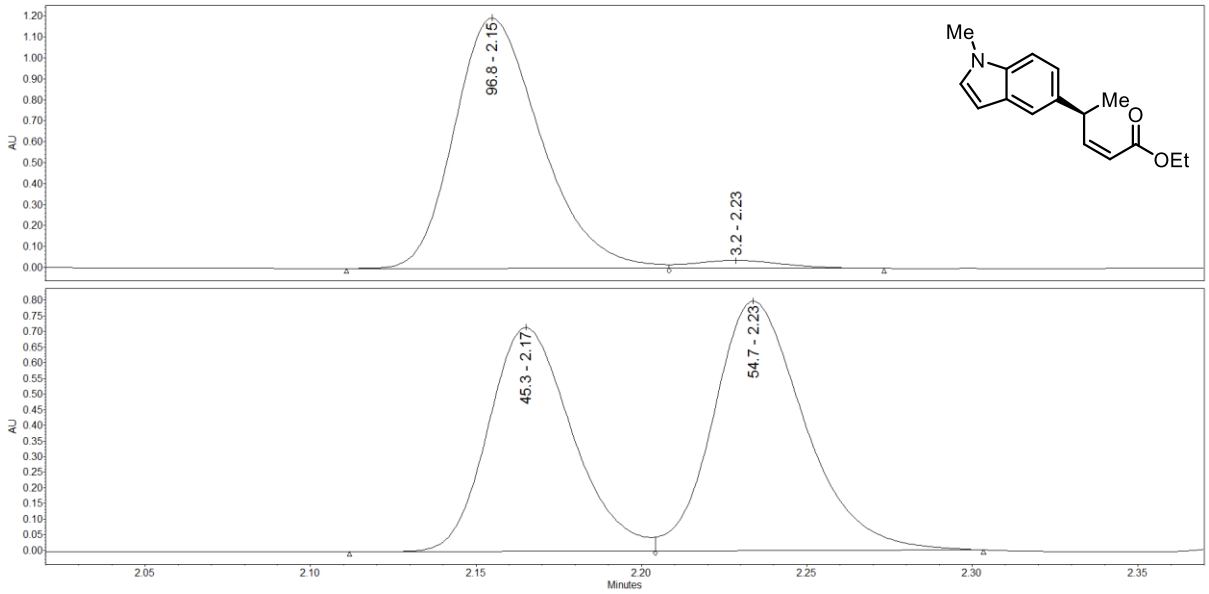

Figure 6.116 SFC trace for (*S*)-*Z*-**2-10w** and (±)-*Z*-**2-10w**.

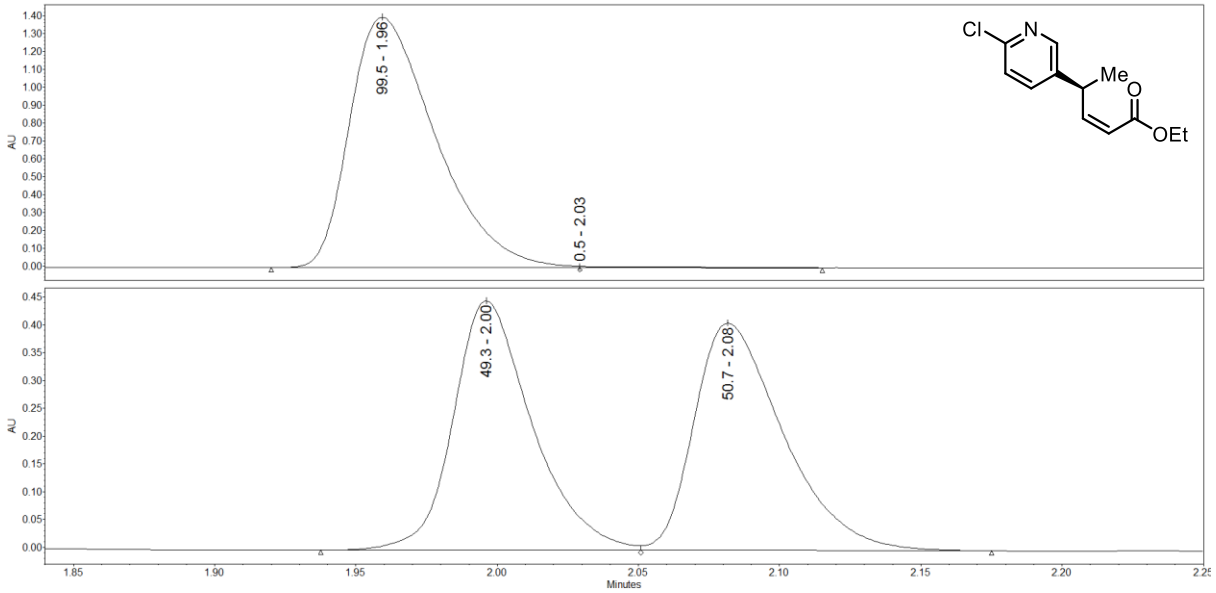

Figure 6.117 SFC trace for (*S*)-*Z*-**2-10x** and (±)-*Z*-**2-10x**.

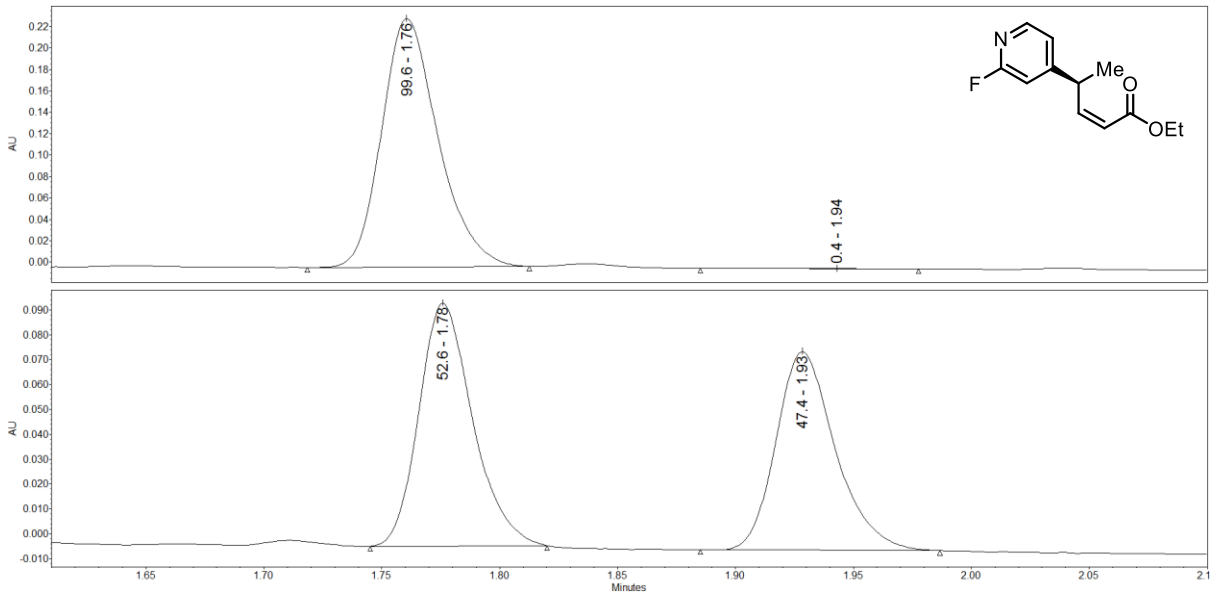

Figure 6.118 SFC trace for (*S*)-*Z*-**2-10y** and (±)-*Z*-**2-10y**.

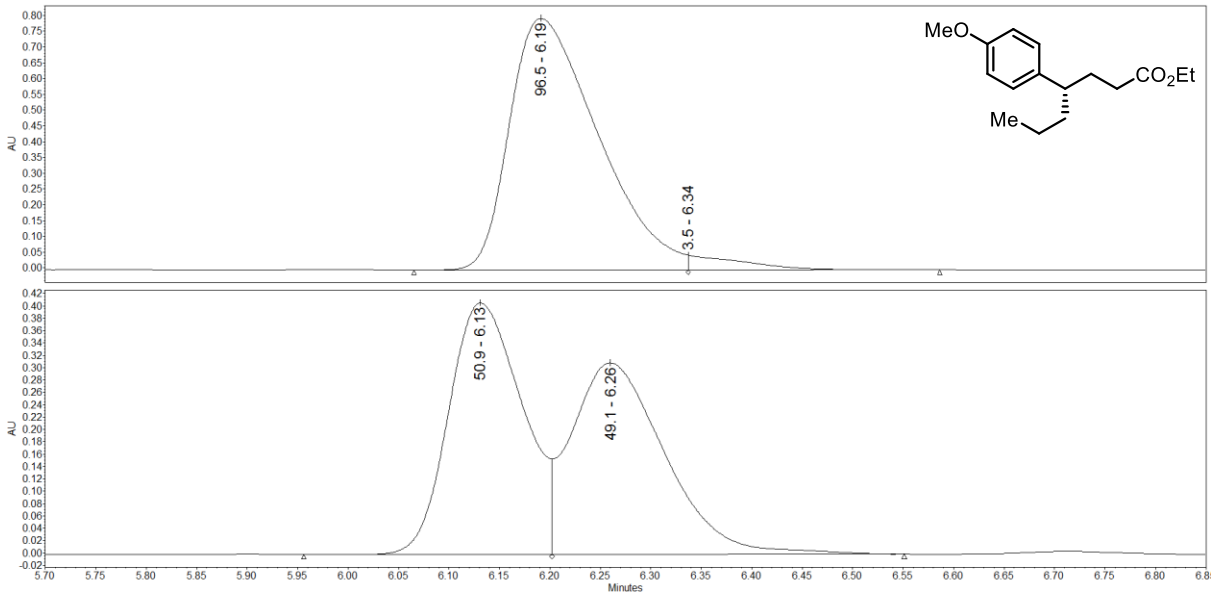

Figure 6.119 SFC trace for (*S*)-*red*-**2-12a** and (±)-*red*-**2-12a**.

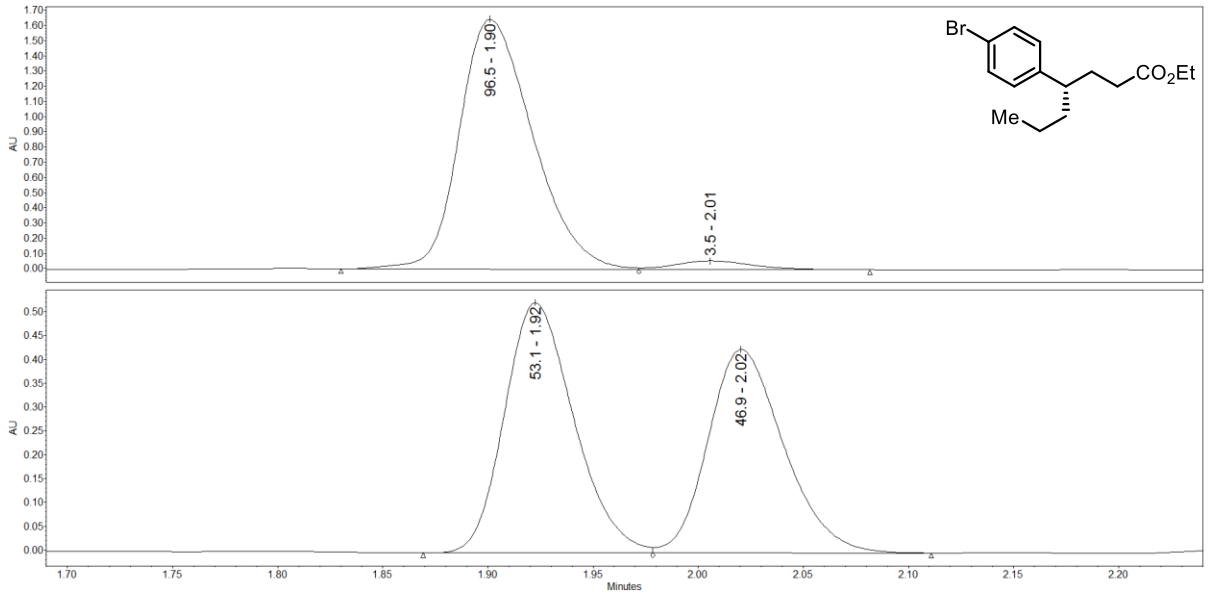

Figure 6.120 SFC trace for (*S*)-*red*-**2-12b** and (±)-*red*-**2-12b**.

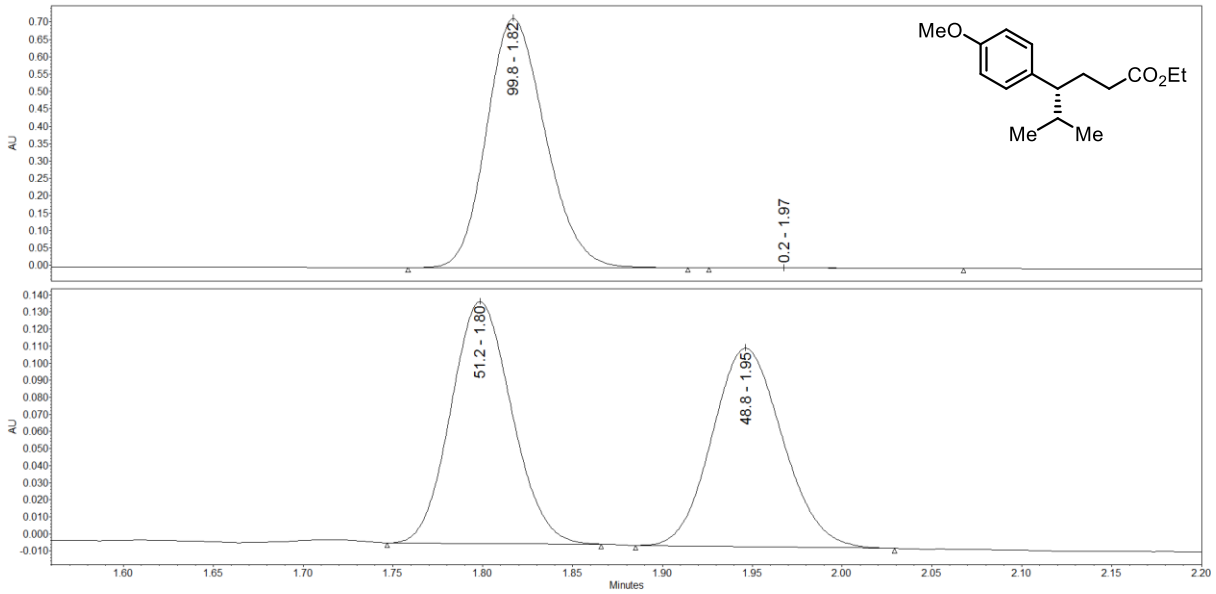

Figure 6.121 SFC trace for (*S*)-*red*-**2-12c** and (±)-*red*-**2-12c**.

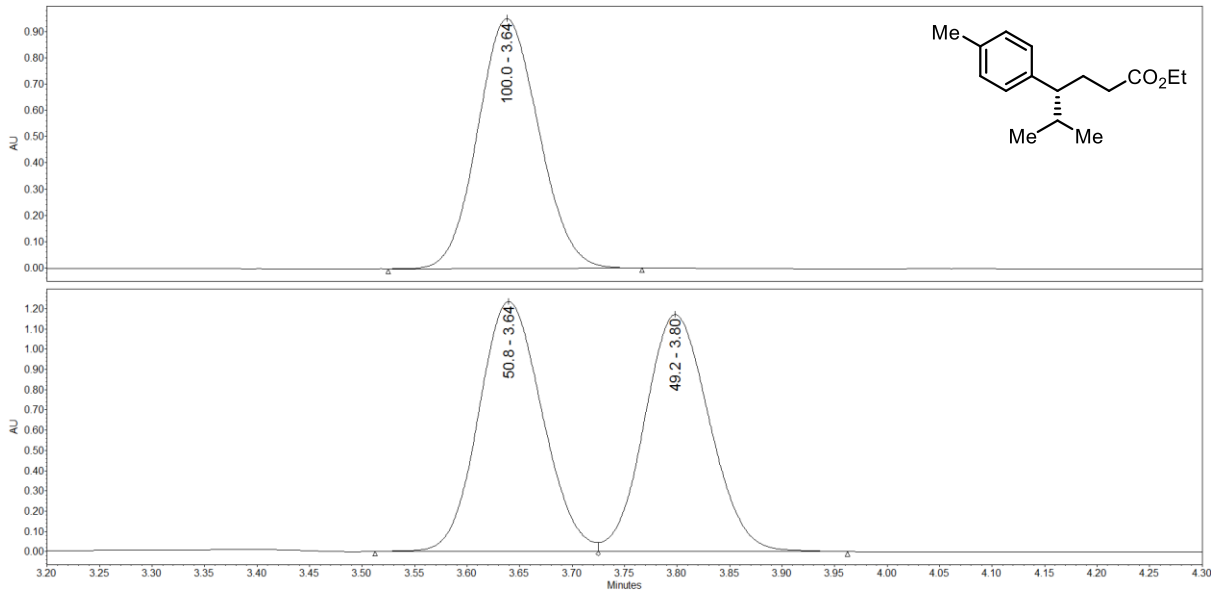

Figure 6.122 SFC trace for (*S*)-*red*-**2-12d** and (±)-*red*-**2-12d**.

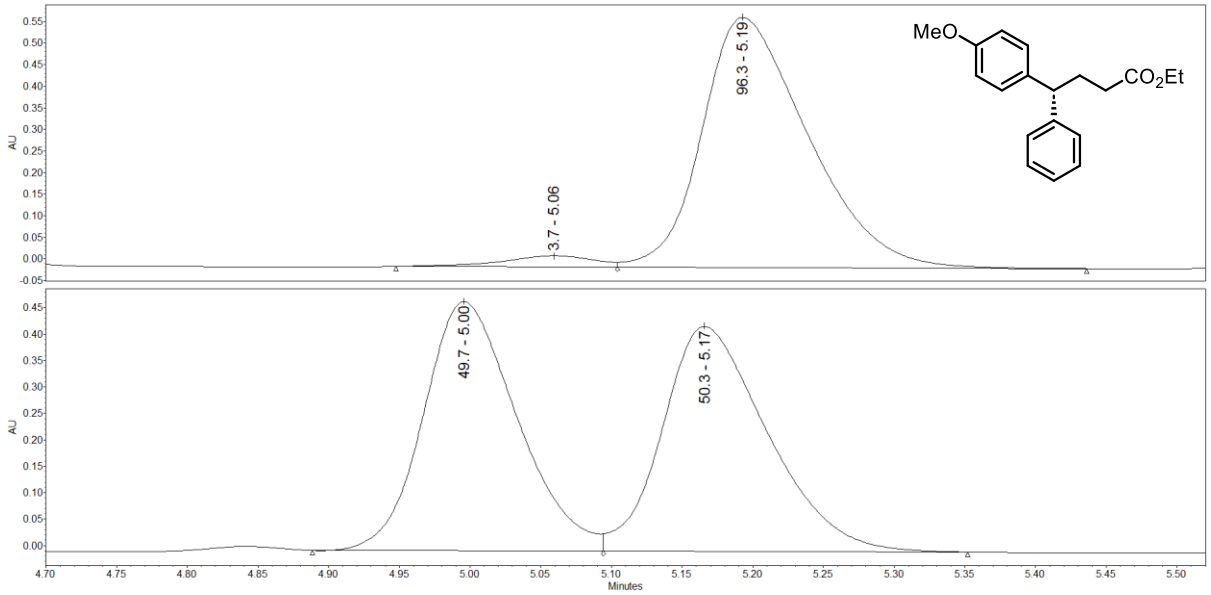

Figure 6.123 SFC trace for (*S*)-*red*-**2-12g** and (±)-*red*-**2-12g**.

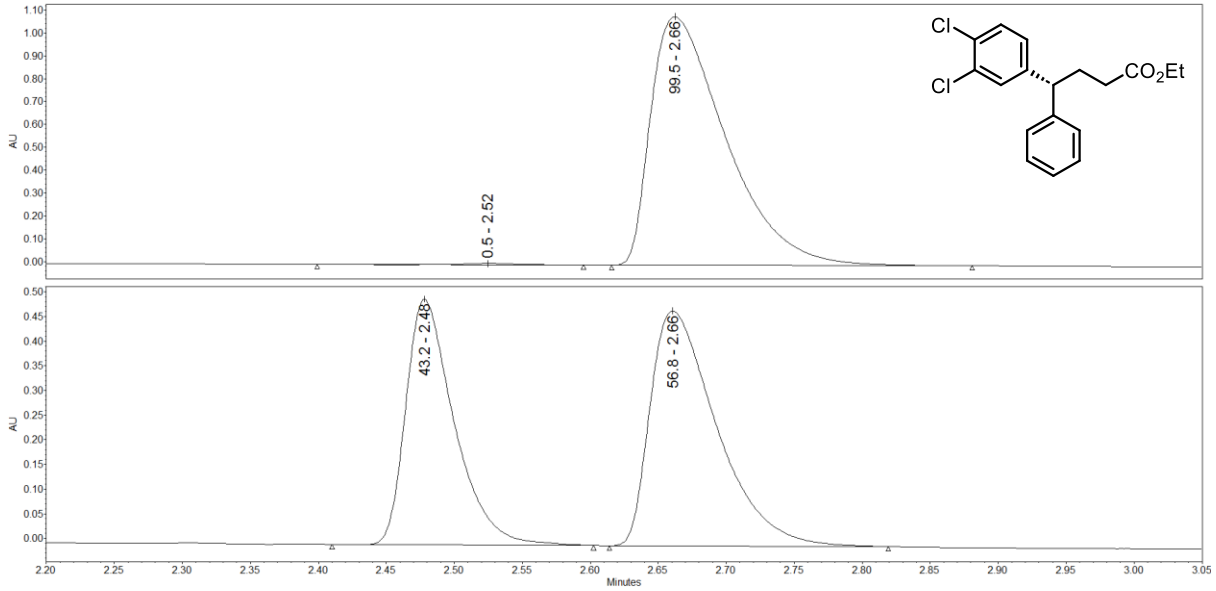

Figure 6.124 SFC trace for (*S*)-*red*-**2-12h** and (±)-*red*-**2-12h**.

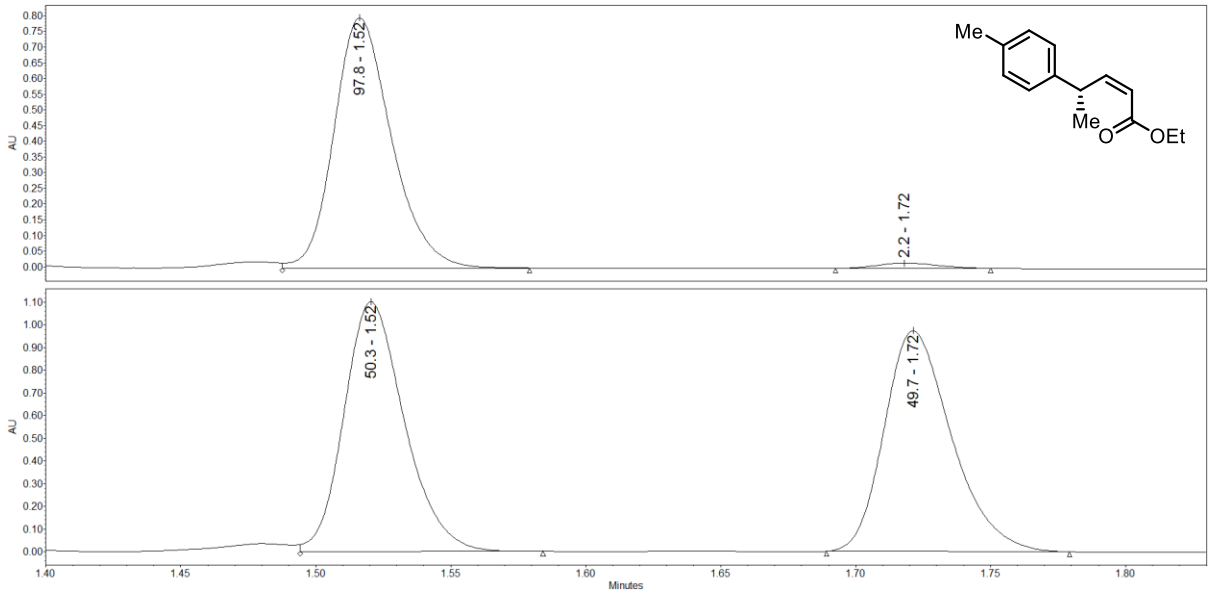

Figure 6.125 SFC trace for (*S*)-*Z*-**2-10d** and (±)-*Z*-**2-10d**.

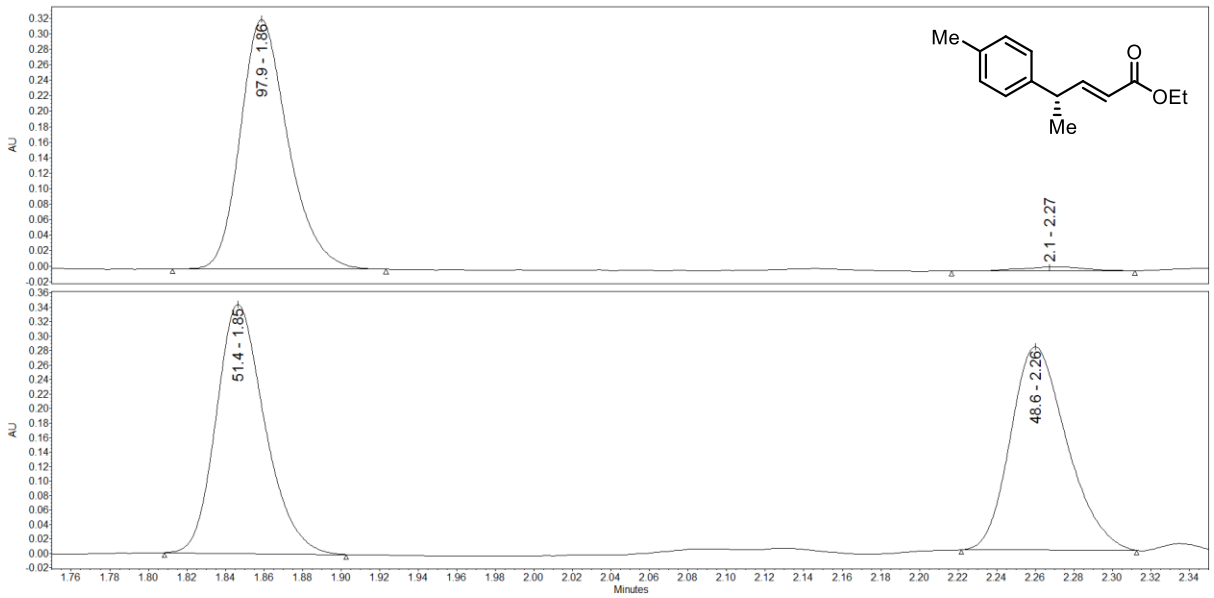

Figure 6.126 SFC trace for (*S*)-*E*-**2-10d** and (±)-*E*-**2-10d**.

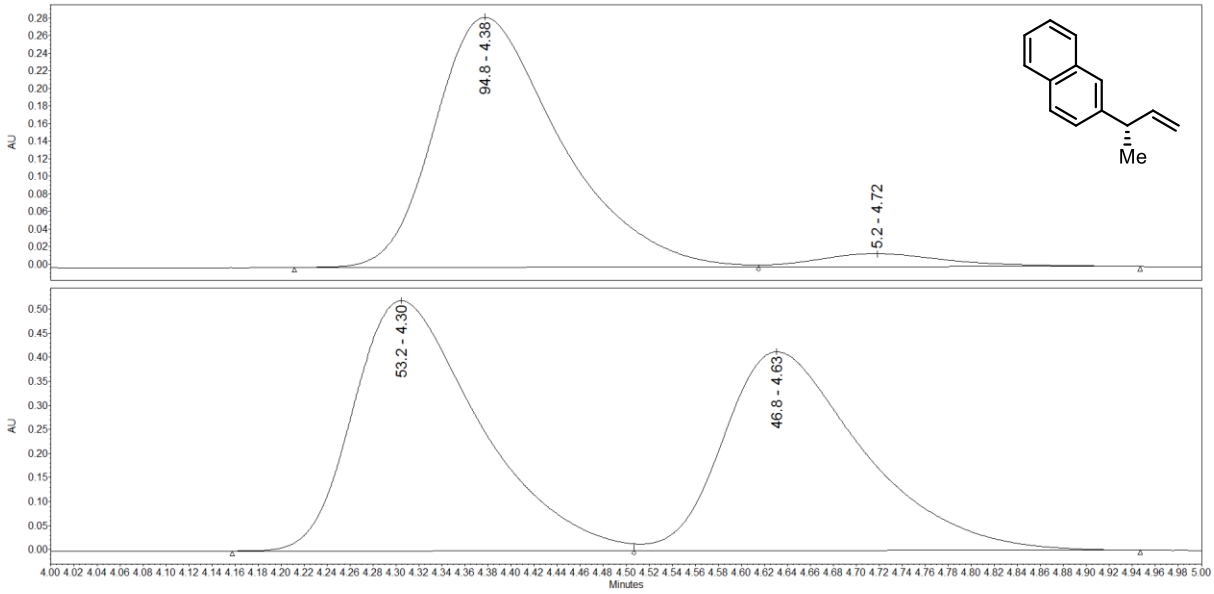

Figure 6.127 SFC trace for (*S*)- **2-15** and (±)-**2-15**.

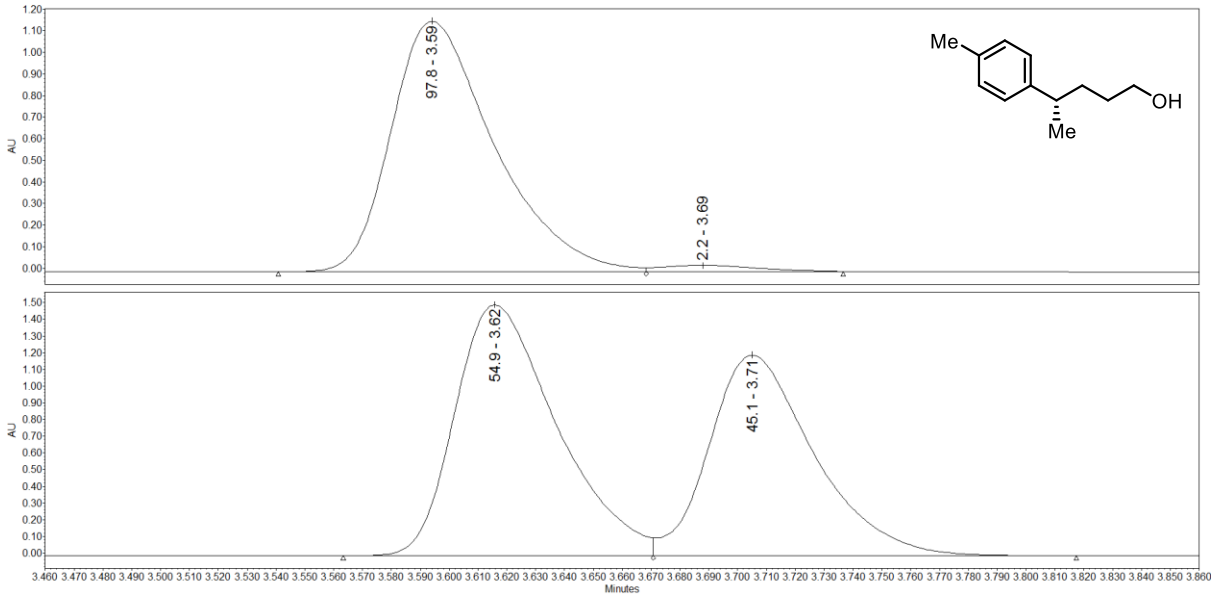

Figure 6.128 SFC trace for (*S*)- **2-16** and (±)-**2-16**.

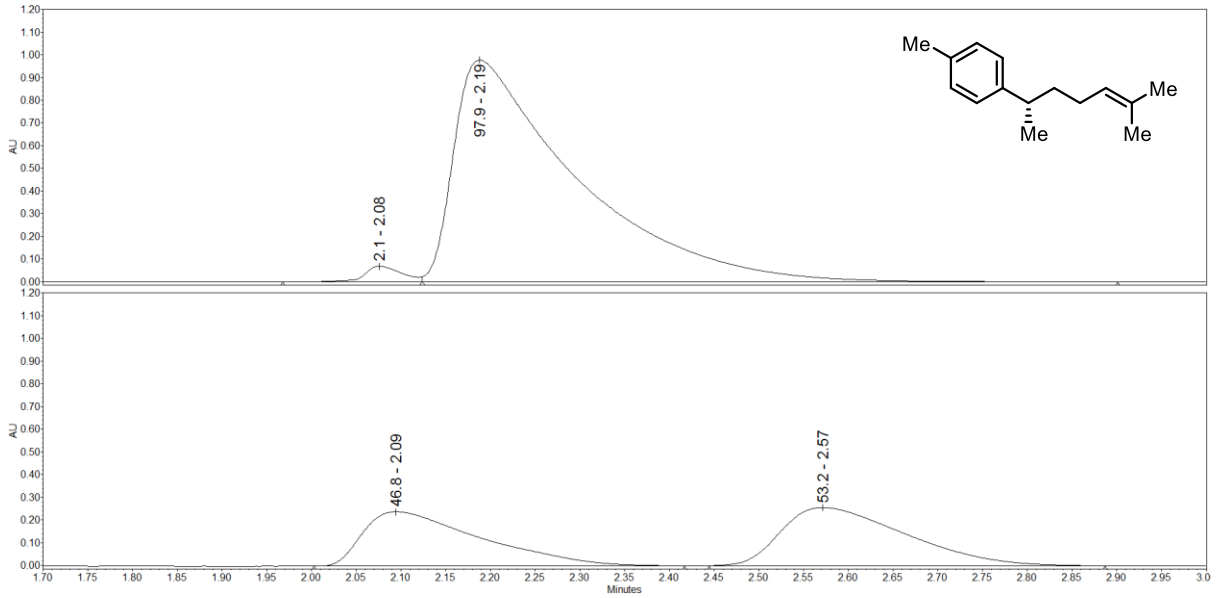

Figure 6.129 SFC trace for (*S*)- **2-17** and (±)-**2-17**.

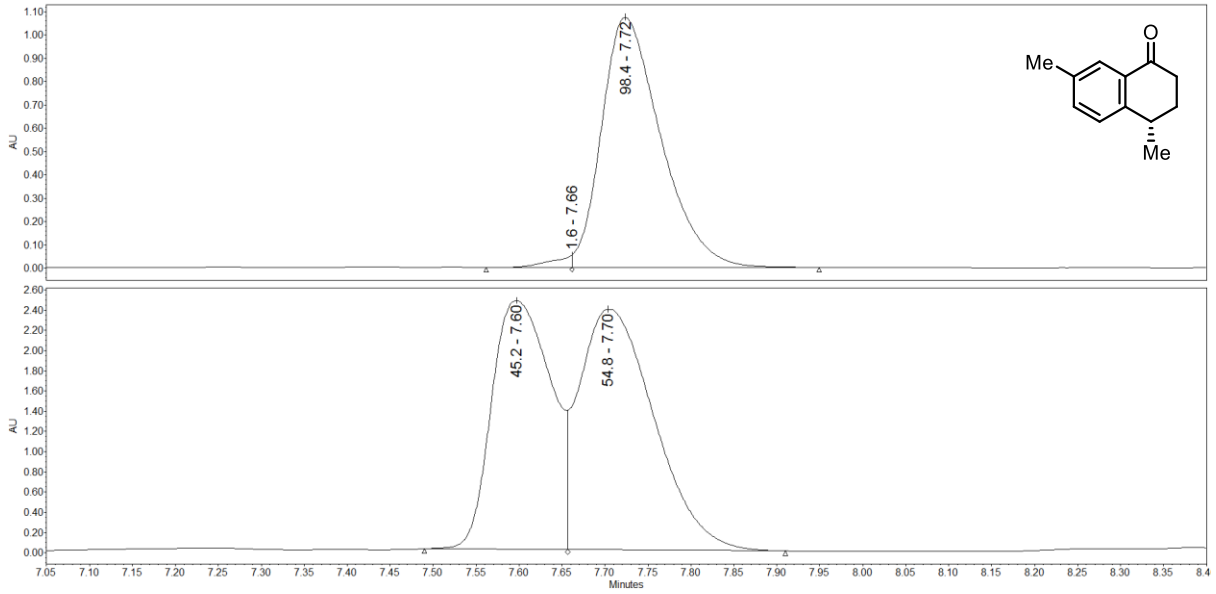

Figure 6.130 SFC trace for (*S*)- **2-19** and (±)-**2-19**.

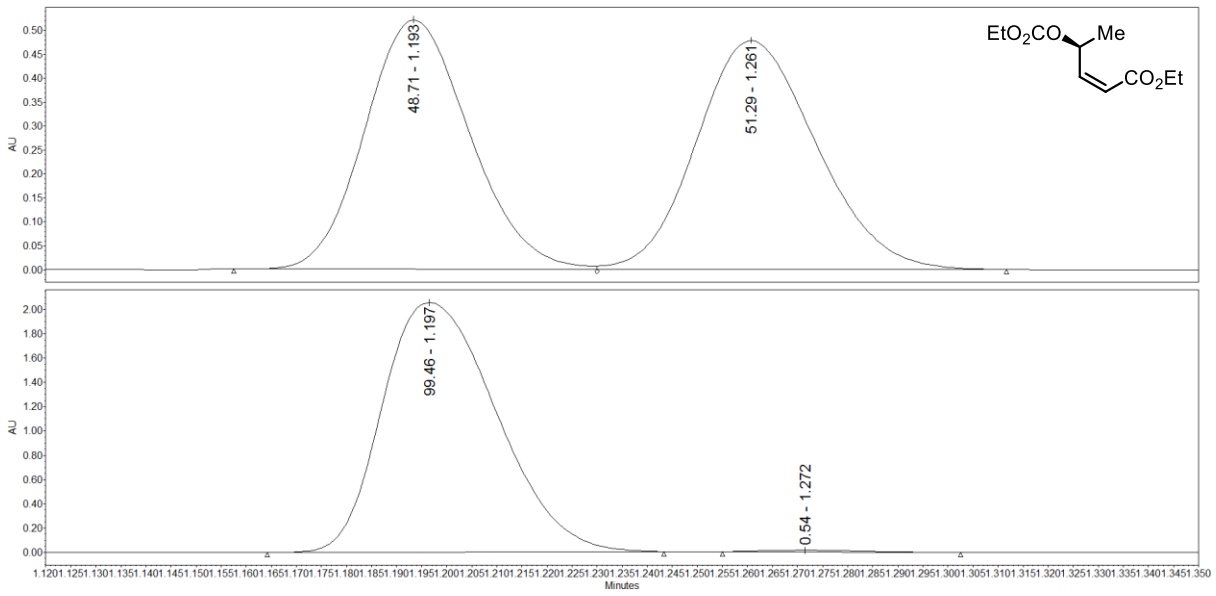

Figure 6.131 SFC trace for (*S*)-**2-9a** (used in mechanistic studies) and (±)-**2-9a**.

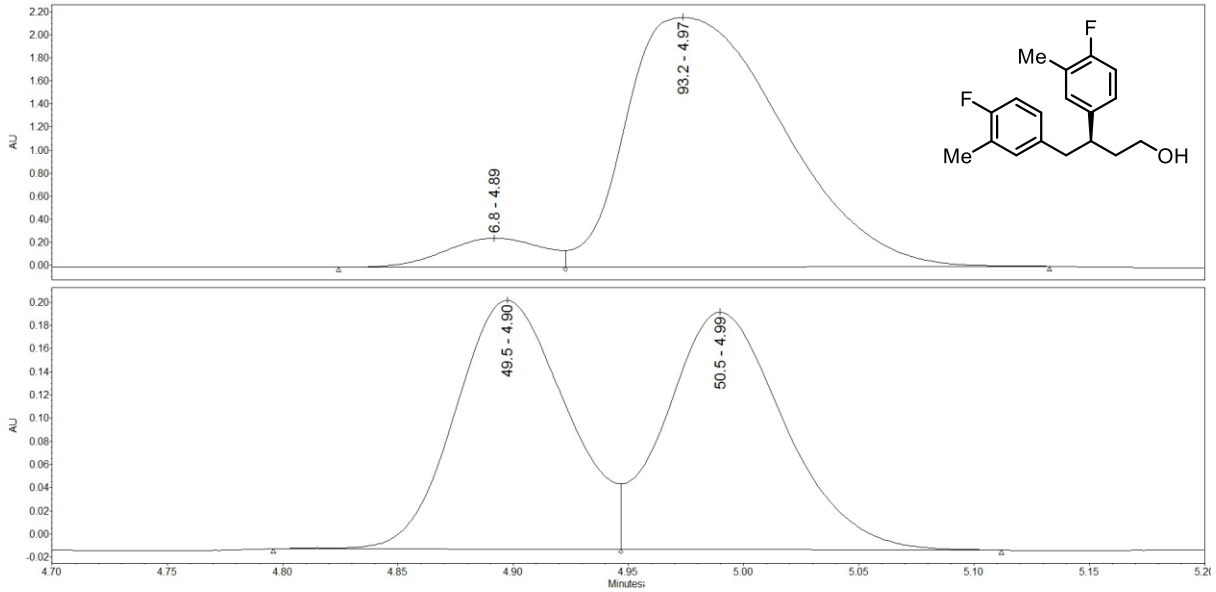

Figure 6.132 SFC trace for (*S*)-**4-9** and (±)-**4-9**.

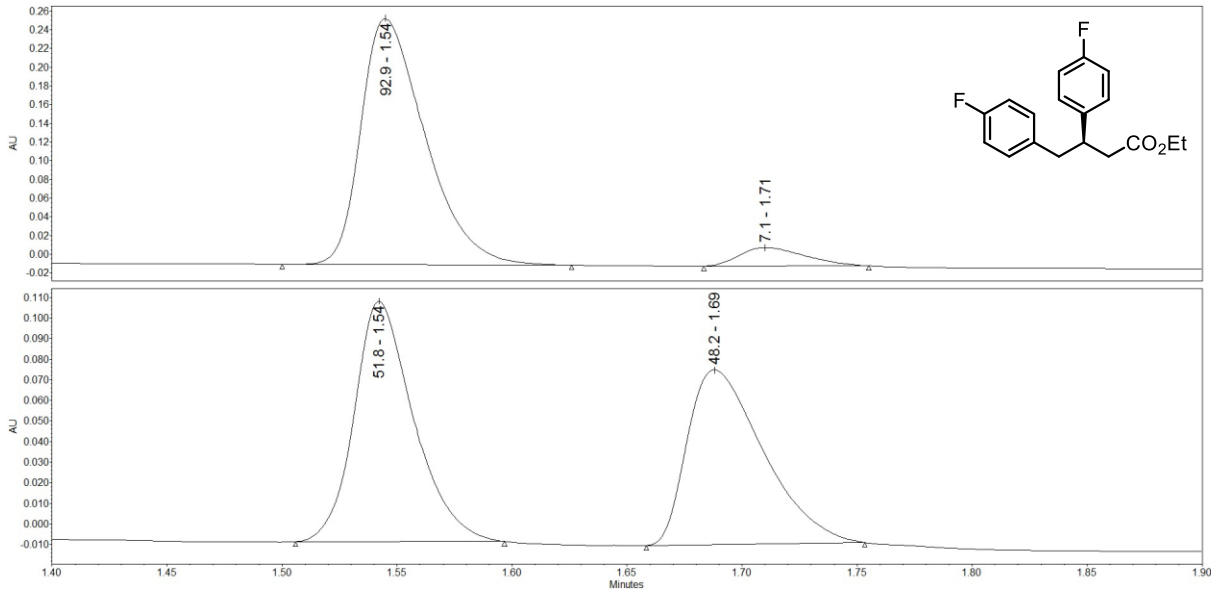

Figure 6.133 SFC trace for (*S*)-**4-7b** and (±)-**4-7b**.

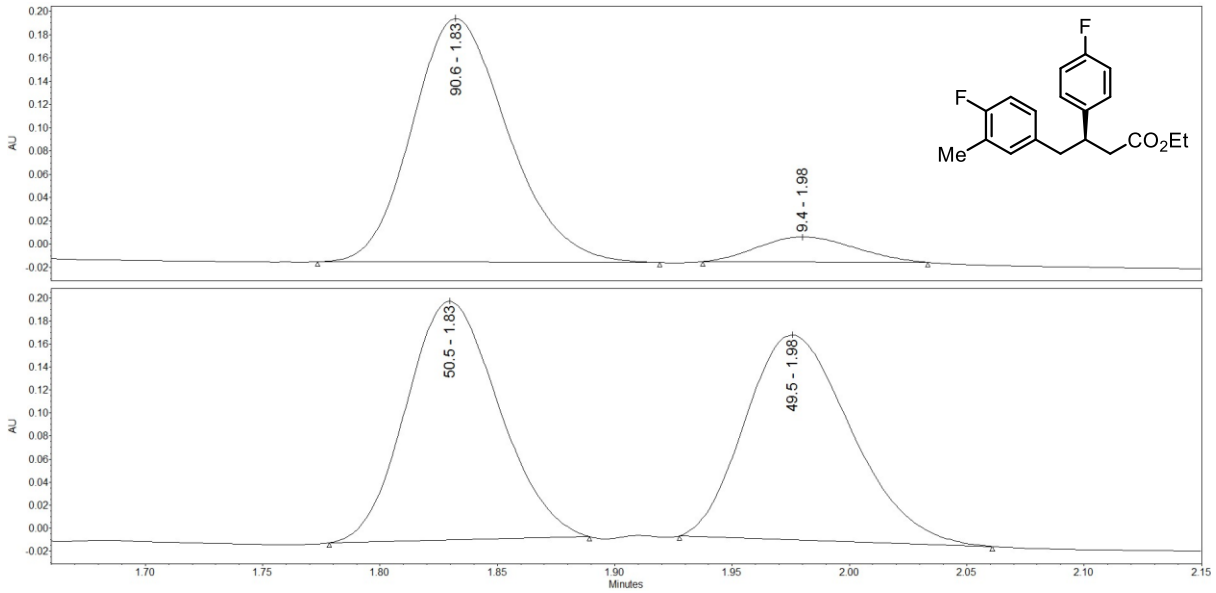

Figure 6.134 SFC trace for (*S*)-**4-11** and (±)-**4-11**.

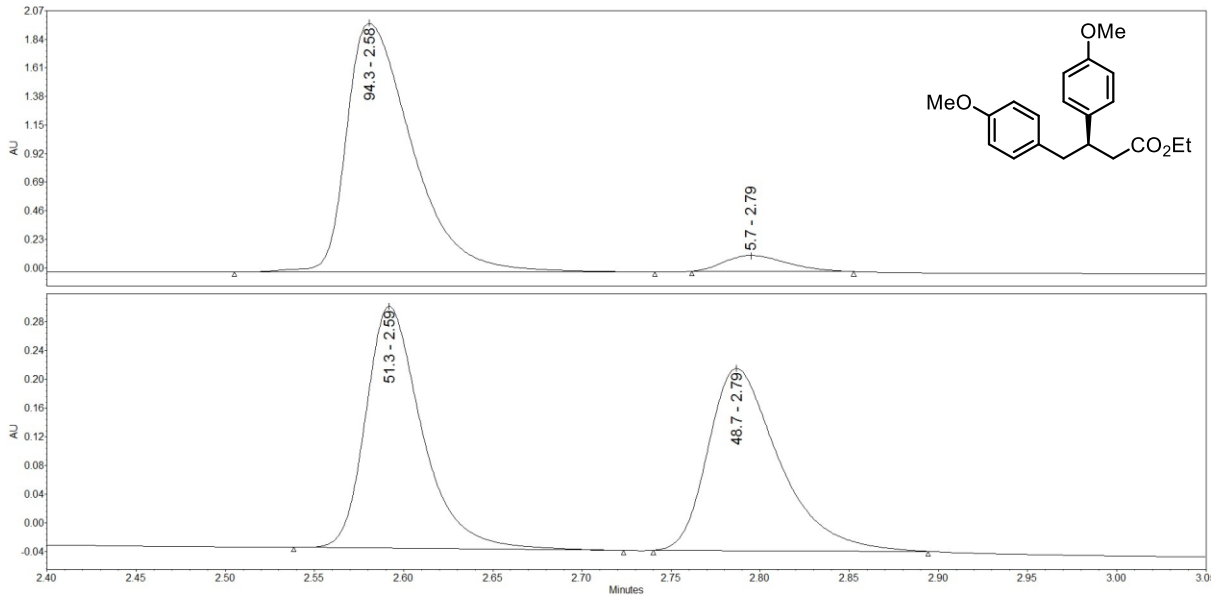

Figure 6.135 SFC trace for (*S*)-**4-7c** and (±)-**4-7c**.

7 References

1 Lovering, F., Bikker, J. & Humblet, C. Escape from flatland: increasing saturation as an approach to improving clinical success. *J. Med. Chem.* **52**, 6752-6756 (2009).
2 Brown, D. G., Gagnon, M. M. & Bostrom, J. Understanding our love affair with p-chlorophenyl: present day implications from historical biases of reagent selection. *J. Med. Chem.* **58**, 2390-2405 (2015).
3 Brown, D. G. & Bostrom, J. Analysis of Past and Present Synthetic Methodologies on Medicinal Chemistry: Where Have All the New Reactions Gone? *J. Med. Chem.* **59**, 4443-4458 (2016).
4 Luker, T. *et al.* Strategies to improve in vivo toxicology outcomes for basic candidate drug molecules. *Bioorg. Med. Chem. Lett.* **21**, 5673-5679 (2011).
5 Ritchie, T. J., Macdonald, S. J., Young, R. J. & Pickett, S. D. The impact of aromatic ring count on compound developability: further insights by examining carbo- and hetero-aromatic and -aliphatic ring types. *Drug Discov. Today* **16**, 164-171 (2011).
6 Talele, T. T. Opportunities for Tapping into Three-Dimensional Chemical Space through a Quaternary Carbon. *J. Med. Chem.* **63**, 13291-13315 (2020).
7 Lipinski, C. & Hopkins, A. Navigating chemical space for biology and medicine. *Nature* **432**, 855-861 (2004).
8 Lovering, F. Escape from Flatland 2: complexity and promiscuity. *MedChemComm* **4**, 515-519 (2013).
9 Meyers, J., Carter, M., Mok, N. Y. & Brown, N. On the origins of three-dimensionality in drug-like molecules. *Future Med. Chem.* **8**, 1753-1767 (2016).
10 Scott, K. A. *et al.* Stereochemical diversity as a source of discovery in chemical biology. *Current Research in Chemical Biology* **2**, 100028 (2022).
11 Bottcher, T. An Additive Definition of Molecular Complexity. *J. Chem. Inf. Model.* **56**, 462-470 (2016).
12 Bottcher, T. From Molecules to Life: Quantifying the Complexity of Chemical and Biological Systems in the Universe. *J. Mol. Evol.* **86**, 1-10 (2018).
13 Demoret, R. M. *et al.* Synthetic, Mechanistic, and Biological Interrogation of Ginkgo biloba Chemical Space En Route to (-)-Bilobalide. *J. Am. Chem. Soc.* **142**, 18599-18618 (2020).
14 Shannon, C. E. A Mathematical Theory of Communication. *Bell System Technical Journal* **27**, 379-423 (1948).
15 Kadu, B. S. Suzuki–Miyaura cross coupling reaction: recent advancements in catalysis and organic synthesis. *Catalysis Science & Technology* **11**, 1186-1221 (2021).
16 Hall, D. G. *Boronic acids: preparation, applications in organic synthesis and medicine*. (John Wiley & Sons, 2006).
17 Yamamoto, Y., Takada, S. & Miyaura, N. Asymmetric Cross-coupling of Potassium 2-Butenyltrifluoroborates with Aryl and 1-Alkenyl Bromides Catalyzed by a Pd(OAc)2/Josiphos Complex. *Chem. Lett.* **35**, 1368-1369 (2006).
18 Yamamoto, Y., Takada, S., Miyaura, N., Iyama, T. & Tachikawa, H. γ-Selective Cross-Coupling Reactions of Potassium Allyltrifluoroborates with Haloarenes Catalyzed by a Pd(0)/D-t-BPF or Pd(0)/Josiphos ((R,S)-CyPF-t-Bu) Complex: Mechanistic Studies on Transmetalation and Enantioselection. *Organometallics* **28**, 152-160 (2008).
19 Zhang, P., Brozek, L. A. & Morken, J. P. Pd-catalyzed enantioselective allyl-allyl cross-coupling. *J. Am. Chem. Soc.* **132**, 10686-10688 (2010).

20 Zhang, P., Le, H., Kyne, R. E. & Morken, J. P. Enantioselective construction of all-carbon quaternary centers by branch-selective Pd-catalyzed allyl-allyl cross-coupling. *J. Am. Chem. Soc.* **133**, 9716-9719 (2011).
21 Ardolino, M. J. & Morken, J. P. Congested C-C bonds by Pd-catalyzed enantioselective allyl-allyl cross-coupling, a mechanism-guided solution. *J. Am. Chem. Soc.* **136**, 7092-7100 (2014).
22 Brozek, L. A., Ardolino, M. J. & Morken, J. P. Diastereocontrol in asymmetric allyl-allyl cross-coupling: stereocontrolled reaction of prochiral allylboronates with prochiral allyl chlorides. *J. Am. Chem. Soc.* **133**, 16778-16781 (2011).
23 Wang, X., Wang, X., Han, Z., Wang, Z. & Ding, K. Palladium-Catalyzed Asymmetric Allylic Allylation of Racemic Morita-Baylis-Hillman Adducts. *Angew. Chem. Int. Ed.* **56**, 1116-1119 (2017).
24 Krautwald, S. & Carreira, E. M. Stereodivergence in Asymmetric Catalysis. *J. Am. Chem. Soc.* **139**, 5627-5639 (2017).
25 Hamilton, J. Y., Sarlah, D. & Carreira, E. M. Iridium-catalyzed enantioselective allylic vinylation. *J. Am. Chem. Soc.* **135**, 994-997 (2013).
26 Hamilton, J. Y., Sarlah, D. & Carreira, E. M. Iridium-catalyzed enantioselective allylic alkynylation. *Angew. Chem. Int. Ed.* **52**, 7532-7535 (2013).
27 Rossler, S. L., Krautwald, S. & Carreira, E. M. Study of Intermediates in Iridium-(Phosphoramidite,Olefin)-Catalyzed Enantioselective Allylic Substitution. *J. Am. Chem. Soc.* **139**, 3603-3606 (2017).
28 Zheng, Y., Yue, B. B., Wei, K. & Yang, Y. R. Iridium-Catalyzed Enantioselective Allyl-Allyl Cross-Coupling of Racemic Allylic Alcohols with Allylboronates. *Org. Lett.* **20**, 8035-8038 (2018).
29 Zhan, M. *et al.* Silver-Assisted, Iridium-Catalyzed Allylation of Bis[(pinacolato)boryl]methane Allows the Synthesis of Enantioenriched Homoallylic Organoboronic Esters. *ACS Catalysis* **6**, 3381-3386 (2016).
30 Lundin, P. M. & Fu, G. C. Asymmetric Suzuki cross-couplings of activated secondary alkyl electrophiles: arylations of racemic alpha-chloroamides. *J. Am. Chem. Soc.* **132**, 11027-11029 (2010).
31 Lu, Z., Wilsily, A. & Fu, G. C. Stereoconvergent amine-directed alkyl-alkyl Suzuki reactions of unactivated secondary alkyl chlorides. *J. Am. Chem. Soc.* **133**, 8154-8157 (2011).
32 Zultanski, S. L. & Fu, G. C. Catalytic asymmetric gamma-alkylation of carbonyl compounds via stereoconvergent Suzuki cross-couplings. *J. Am. Chem. Soc.* **133**, 15362-15364 (2011).
33 Saito, B. & Fu, G. C. Enantioselective alkyl-alkyl Suzuki cross-couplings of unactivated homobenzylic halides. *J. Am. Chem. Soc.* **130**, 6694-6695 (2008).
34 Cong, H. & Fu, G. C. Catalytic enantioselective cyclization/cross-coupling with alkyl electrophiles. *J. Am. Chem. Soc.* **136**, 3788-3791 (2014).
35 Gutierrez, O., Tellis, J. C., Primer, D. N., Molander, G. A. & Kozlowski, M. C. Nickel-catalyzed cross-coupling of photoredox-generated radicals: uncovering a general manifold for stereoconvergence in nickel-catalyzed cross-couplings. *J. Am. Chem. Soc.* **137**, 4896-4899 (2015).
36 Tellis, J. C., Primer, D. N. & Molander, G. A. Dual catalysis. Single-electron transmetalation in organoboron cross-coupling by photoredox/nickel dual catalysis. *Science* **345**, 433-436 (2014).
37 Huang, W., Wan, X. & Shen, Q. Enantioselective Construction of Trifluoromethoxylated Stereogenic Centers by a Nickel-Catalyzed Asymmetric

Suzuki-Miyaura Coupling of Secondary Benzyl Bromides. *Angew. Chem. Int. Ed.* **56**, 11986-11989 (2017).
38 Shields, J. D., Ahneman, D. T., Graham, T. J. & Doyle, A. G. Enantioselective, nickel-catalyzed Suzuki cross-coupling of quinolinium ions. *Org. Lett.* **16**, 142-145 (2014).
39 Sylvester, K. T., Wu, K. & Doyle, A. G. Mechanistic investigation of the nickel-catalyzed Suzuki reaction of N,O-acetals: evidence for boronic acid assisted oxidative addition and an iminium activation pathway. *J. Am. Chem. Soc.* **134**, 16967-16970 (2012).
40 Baslé, O., Denicourt-Nowicki, A., Crévisy, C. & Mauduit, M. Asymmetric Allylic Alkylation. in *Copper-Catalyzed Asymmetric Synthesis* 85-126 (2014).
41 Shido, Y., Yoshida, M., Tanabe, M., Ohmiya, H. & Sawamura, M. Copper-catalyzed enantioselective allylic substitution with alkylboranes. *J. Am. Chem. Soc.* **134**, 18573-18576 (2012).
42 Hojoh, K., Shido, Y., Ohmiya, H. & Sawamura, M. Construction of quaternary stereogenic carbon centers through copper-catalyzed enantioselective allylic cross-coupling with alkylboranes. *Angew. Chem. Int. Ed.* **53**, 4954-4958 (2014).
43 Yasuda, Y., Ohmiya, H. & Sawamura, M. Copper-Catalyzed Enantioselective Allyl-Allyl Coupling between Allylic Boronates and Phosphates with a Phenol/N-Heterocyclic Carbene Chiral Ligand. *Angew. Chem. Int. Ed.* **55**, 10816-10820 (2016).
44 Shintani, R., Takatsu, K., Takeda, M. & Hayashi, T. Copper-catalyzed asymmetric allylic substitution of allyl phosphates with aryl- and alkenylboronates. *Angew. Chem. Int. Ed.* **50**, 8656-8659 (2011).
45 Takeda, M., Takatsu, K., Shintani, R. & Hayashi, T. Synthesis of quaternary carbon stereocenters by copper-catalyzed asymmetric allylic substitution of allyl phosphates with arylboronates. *J. Org. Chem.* **79**, 2354-2367 (2014).
46 Gao, F., Carr, J. L. & Hoveyda, A. H. Copper-catalyzed enantioselective allylic substitution with readily accessible carbonyl- and acetal-containing vinylboron reagents. *Angew. Chem. Int. Ed.* **51**, 6613-6617 (2012).
47 Jung, B. & Hoveyda, A. H. Site- and enantioselective formation of allene-bearing tertiary or quaternary carbon stereogenic centers through NHC-Cu-catalyzed allylic substitution. *J. Am. Chem. Soc.* **134**, 1490-1493 (2012).
48 Shi, Y. & Hoveyda, A. H. Catalytic SN2'- and Enantioselective Allylic Substitution with a Diborylmethane Reagent and Application in Synthesis. *Angew. Chem. Int. Ed.* **55**, 3455-3458 (2016).
49 Shi, Y., Jung, B., Torker, S. & Hoveyda, A. H. N-Heterocyclic Carbene-Copper-Catalyzed Group-, Site-, and Enantioselective Allylic Substitution with a Readily Accessible Propargyl(pinacolato)boron Reagent: Utility in Stereoselective Synthesis and Mechanistic Attributes. *J. Am. Chem. Soc.* **137**, 8948-8964 (2015).
50 Zhou, Y., Shi, Y., Torker, S. & Hoveyda, A. H. S(N)2''-Selective and Enantioselective Substitution with Unsaturated Organoboron Compounds and Catalyzed by a Sulfonate-Containing NHC-Cu Complex. *J. Am. Chem. Soc.* **140**, 16842-16854 (2018).
51 Hoveyda, A. H. *et al.* Sulfonate N-Heterocyclic Carbene-Copper Complexes: Uniquely Effective Catalysts for Enantioselective Synthesis of C-C, C-B, C-H, and C-Si Bonds. *Angew. Chem. Int. Ed.* **59**, 21304-21359 (2020).

52 Menard, F., Chapman, T. M., Dockendorff, C. & Lautens, M. Rhodium-Catalyzed Asymmetric Allylic Substitution with Boronic Acid Nucleophiles. *Org. Lett.* **8**, 4569-4572 (2006).
53 Menard, F., Perez, D., Sustac Roman, D., Chapman, T. M. & Lautens, M. Ligand-controlled selectivity in the desymmetrization of meso cyclopenten-1,4-diols via rhodium(I)-catalyzed addition of arylboronic acids. *J. Org. Chem.* **75**, 4056-4068 (2010).
54 Lautens, M., Yu, B., Menard, F. & Isono, N. Synthesis of Homoallylic Alcohols via Lewis Acid Assisted Enantioselective Desymmetrization. *Synthesis* **2009**, 853-859 (2009).
55 Dong, L. *et al.* Rhodium-Catalyzed Asymmetric Nitroallylation of Arylmetallics with Cyclic Nitroallyl Acetates and Applications in Organic Synthesis. *Eur. J. Org. Chem.* **2006**, 4093-4105 (2006).
56 Kiuchi, H., Takahashi, D., Funaki, K., Sato, T. & Oi, S. Rhodium-catalyzed asymmetric coupling reaction of allylic ethers with arylboronic acids. *Org. Lett.* **14**, 4502-4505 (2012).
57 Iwamoto, T., Okuzono, C., Adak, L., Jin, M. & Nakamura, M. Iron-catalysed enantioselective Suzuki-Miyaura coupling of racemic alkyl bromides. *Chem. Comm.* **55**, 1128-1131 (2019).
58 Huang, W., Wan, X. & Shen, Q. Cobalt-Catalyzed Asymmetric Cross-Coupling Reaction of Fluorinated Secondary Benzyl Bromides with Lithium Aryl Boronates/ZnBr(2). *Org. Lett.* **22**, 4327-4332 (2020).
59 Jiang, S. P. *et al.* Copper-Catalyzed Enantioconvergent Radical Suzuki-Miyaura C(sp(3))-C(sp(2)) Cross-Coupling. *J. Am. Chem. Soc.* **142**, 19652-19659 (2020).
60 Steinreiber, J., Faber, K. & Griengl, H. De-racemization of enantiomers versus de-epimerization of diastereomers--classification of dynamic kinetic asymmetric transformations (DYKAT). *Chemistry* **14**, 8060-8072 (2008).
61 Heravi, M. M. & Zadsirjan, V. Prescribed drugs containing nitrogen heterocycles: an overview. *RSC Adv.* **10**, 44247-44311 (2020).
62 Jampilek, J. Heterocycles in Medicinal Chemistry. *Molecules* **24** (2019).
63 Kerru, N., Gummidi, L., Maddila, S., Gangu, K. K. & Jonnalagadda, S. B. A Review on Recent Advances in Nitrogen-Containing Molecules and Their Biological Applications. *Molecules* **25** (2020).
64 Sidera, M. & Fletcher, S. P. Rhodium-catalysed asymmetric allylic arylation of racemic halides with arylboronic acids. *Nat. Chem.* **7**, 935-939 (2015).
65 Schafer, P., Sidera, M., Palacin, T. & Fletcher, S. P. Asymmetric cross-coupling of alkyl, alkenyl and (hetero)aryl nucleophiles with racemic allyl halides. *Chem. Comm.* **53**, 12499-12511 (2017).
66 Schafer, P., Palacin, T., Sidera, M. & Fletcher, S. P. Asymmetric Suzuki-Miyaura coupling of heterocycles via Rhodium-catalysed allylic arylation of racemates. *Nat. Commun.* **8**, 15762 (2017).
67 Goetzke, F. W., Mortimore, M. & Fletcher, S. P. Enantio- and Diastereoselective Suzuki-Miyaura Coupling with Racemic Bicycles. *Angew. Chem. Int. Ed.* **58**, 12128-12132 (2019).
68 Pàmies, O. *et al.* Recent Advances in Enantioselective Pd-Catalyzed Allylic Substitution: From Design to Applications. *Chem. Rev.* **121**, 4373-4505 (2021).
69 Hoshino, M., Sim, J., Shimizu, K., Nakayama, H. & Koya, A. Effect of AA-2414, a thromboxane A2 receptor antagonist, on airway inflammation in subjects with asthma. *Journal of Allergy and Clinical Immunology* **103**, 1054-1061 (1999).

70 Wu, Z. *et al.* Antioxidative phenolic compounds from a marine-derived fungus Aspergillus versicolor. *Tetrahedron* **72**, 50-57 (2016).
71 Lu, J. *et al.* Sesquiterpene acids from Shellac and their bioactivities evaluation. *Fitoterapia* **97**, 64-70 (2014).
72 Wu, R.-f. *et al.* Neolinulicin A and B from Inula japonica and their anti-inflammatory activities. *Fitoterapia* **152**, 104905 (2021).
73 Wang, H. & Guo, C. Enantioselective γ-Addition of Pyrazole and Imidazole Heterocycles to Allenoates Catalyzed by Chiral Phosphine. *Angew. Chem. Int. Ed.* **58**, 2854-2858 (2019).
74 Zhan, Z.-C. *et al.* Sesquiterpenoids from the Whole Plants of Chloranthus holostegius and Their Anti-inflammatory Activities. *Chin. J. Chem .* **39**, 1168-1174 (2021).
75 Wu, L. *et al.* in *Tetrahedron: Asymmetry* Vol. 27 78-83 (Pergamon, 2016).
76 Du, Z. *et al.* Enantioselective synthesis of (+)-nuciferal, (+)-(E)-nuciferol and (+)-α-curcumene by chiral hydrogenesterification reaction. *J. Chem. Res.* **2004**, 427-429 (2019).
77 Kuninobu, Y. *et al.* Indium-Catalyzed Synthesis of Keto Esters from Cyclic 1,3-Diketones and Alcohols and Application to the Synthesis of Seratrodast. *Chemistry – An Asian Journal* **5**, 941-945 (2010).
78 Yang, S., Zhu, S. F., Guo, N., Song, S. & Zhou, Q. L. Carboxy-directed asymmetric hydrogenation of alpha-alkyl-alpha-aryl terminal olefins: highly enantioselective and chemoselective access to a chiral benzylmethyl center. *Org. Biomol. Chem.* **12**, 2049-2052 (2014).
79 Casalta, C. & Bouzbouz, S. Rhodium(III) Catalyzed Regioselective and Stereospecific Allylic Arylation in Water by β-Fluorine Elimination of the Allylic Fluoride: Toward the Synthesis of Z-Alkenyl-Unsaturated Amides. *Org. Lett.* **22**, 2359-2364 (2020).
80 Chung, K.-G., Miyake, Y. & Uemura, S. Nickel(0)-catalyzed asymmetric cross-coupling reactions of allylic compounds with arylboronic acids. *J. Chem. Soc., Perkin Trans. 1*, 15-18 (2000).
81 Bhat, V., Welin, E. R., Guo, X. & Stoltz, B. M. Advances in Stereoconvergent Catalysis from 2005 to 2015: Transition-Metal-Mediated Stereoablative Reactions, Dynamic Kinetic Resolutions, and Dynamic Kinetic Asymmetric Transformations. *Chem. Rev.* **117**, 4528-4561 (2017).
82 Goetzke, F. W. & Fletcher, S. P. Additions to Racemates: A Strategy for Developing Asymmetric Cross-Coupling Reactions. *Synlett* **32**, 1816-1825 (2021).
83 Hayashi, T. & Yamasaki, K. Rhodium-catalyzed asymmetric 1,4-addition and its related asymmetric reactions. *Chem. Rev.* **103**, 2829-2844 (2003).
84 Heravi, M. M., Dehghani, M. & Zadsirjan, V. Rh-catalyzed asymmetric 1,4-addition reactions to α,β-unsaturated carbonyl and related compounds: an update. *Tetrahedron: Asymmetry* **27**, 513-588 (2016).
85 van Dijk, L. *et al.* Mechanistic investigation of Rh(i)-catalysed asymmetric Suzuki–Miyaura coupling with racemic allyl halides. *Nat. Catal.* **4**, 284-292 (2021).
86 Chen, T. *et al.* Rhodium(I)/Zn(OTf)(2) -Catalyzed Asymmetric Ring Opening/Cyclopropanation of Oxabenzonorbornadienes with Phosphorus Ylides. *Angew. Chem. Int. Ed.* **58**, 15819-15823 (2019).
87 Calvin, J. R., Frederick, M. O., Laird, D. L., Remacle, J. R. & May, S. A. Rhodium-catalyzed and zinc(II)-triflate-promoted asymmetric hydrogenation of tetrasubstituted alpha,beta-unsaturated ketones. *Org. Lett.* **14**, 1038-1041 (2012).

88 Cox, P. A., Leach, A. G., Campbell, A. D. & Lloyd-Jones, G. C. Protodeboronation of Heteroaromatic, Vinyl, and Cyclopropyl Boronic Acids: pH-Rate Profiles, Autocatalysis, and Disproportionation. *J. Am. Chem. Soc.* **138**, 9145-9157 (2016).
89 Cook, X. A. F., de Gombert, A., McKnight, J., Pantaine, L. R. E. & Willis, M. C. The 2-Pyridyl Problem: Challenging Nucleophiles in Cross-Coupling Arylations. *Angew. Chem. Int. Ed.* **60**, 11068-11091 (2021).
90 Jampilek, J. Heterocycles in Medicinal Chemistry. *Molecules* **24**, 3839 (2019).
91 Kerru, N., Gummidi, L., Maddila, S., Gangu, K. K. & Jonnalagadda, S. B. A Review on Recent Advances in Nitrogen-Containing Molecules and Their Biological Applications. *Molecules* **25**, 1909 (2020).
92 Marson, C. M. New and unusual scaffolds in medicinal chemistry. *Chem. Soc. Rev.* **40**, 5514-5533 (2011).
93 Wang, J. *et al.* Rhodium-Catalyzed Asymmetric Arylation of β,γ-Unsaturated α-Ketoamides for the Construction of Nonracemic γ,γ-Diarylcarbonyl Compounds. *Angew. Chem. Int. Ed.* **53**, 6673-6677 (2014).
94 Liu, X., Xiao, Y., Li, J.-Q., Fu, B. & Qin, Z. 1,1-Diaryl compounds as important bioactive module in pesticides. *Molecular Diversity* **23**, 809-820 (2019).
95 Roesner, S., Casatejada, J. M., Elford, T. G., Sonawane, R. P. & Aggarwal, V. K. Enantioselective Syntheses of (+)-Sertraline and (+)-Indatraline Using Lithiation/Borylation–Protodeboronation Methodology. *Org. Lett.* **13**, 5740-5743 (2011).
96 Ohmiya, H., Makida, Y., Li, D., Tanabe, M. & Sawamura, M. Palladium-Catalyzed γ-Selective and Stereospecific Allyl–Aryl Coupling between Acyclic Allylic Esters and Arylboronic Acids. *J. Am. Chem. Soc.* **132**, 879-889 (2010).
97 Reddel, J. C., Lutz, K. E., Diagne, A. B. & Thomson, R. J. Stereocontrolled syntheses of tetralone- and naphthyl-type lignans by a one-pot oxidative [3,3] rearrangement/Friedel-Crafts arylation. *Angew. Chem. Int. Ed.* **53**, 1395-1398 (2014).
98 Davies, H. M. & Manning, J. R. C-H activation as a strategic reaction: enantioselective synthesis of 4-substituted indoles. *J. Am. Chem. Soc.* **128**, 1060-1061 (2006).
99 Byrd, K. M. Diastereoselective and enantioselective conjugate addition reactions utilizing α,β-unsaturated amides and lactams. *Beilstein Journal of Organic Chemistry* **11**, 530-562 (2015).
100 Howell, G. P. Asymmetric and Diastereoselective Conjugate Addition Reactions: C–C Bond Formation at Large Scale. *Org. Process Res. Dev.* **16**, 1258-1272 (2012).
101 Goncalves-Contal, S., Gremaud, L. & Alexakis, A. Enantioselective copper-catalyzed conjugate addition of trimethylaluminum to beta,gamma-unsaturated alpha-ketoamides: efficient access to gamma-methyl-substituted carbonyl compounds. *Angew. Chem. Int. Ed.* **52**, 12701-12704 (2013).
102 Fukuda, M., Ohkoshi, E., Makino, M. & Fujimoto, Y. Studies on the constituents of the leaves of Baccharis dracunculifolia (Asteraceae) and their cytotoxic activity. *Chem. Pharm. Bull.* **54**, 1465-1468 (2006).
103 Davies, H. M., Stafford, D. G. & Hansen, T. Catalytic asymmetric synthesis of diarylacetate and 4,4-diarylbutanoates. A formal asymmetric synthesis of (+)-sertraline. *Org. Lett.* **1**, 233-236 (1999).
104 Marx, L. *et al.* Chemoenzymatic Synthesis of Sertraline. *Eur. J. Org. Chem.* **2020**, 510-513 (2020).

105 Doogan, D. P. & Caillard, V. Sertraline: a new antidepressant. *J. Clin. Psychiatry* **49 Suppl**, 46-51 (1988).
106 Rickels, K. & Schweizer, E. Clinical overview of serotonin reuptake inhibitors. *J. Clin. Psychiatry* **51 Suppl B**, 9-12 (1990).
107 Trevino, L. A., Ruble, M. W., Trevino, K., Weinstein, L. M. & Gresky, D. P. Antidepressant Medication Prescribing Practices for Treatment of Major Depressive Disorder. *Psychiatr. Serv.* **68**, 199-202 (2017).
108 McRae, A. L. & Brady, K. T. Review of sertraline and its clinical applications in psychiatric disorders. *Expert Opin. Pharmacother.* **2**, 883-892 (2001).
109 Heym, J. & Koe, B. K. Pharmacology of sertraline: a review. *J. Clin. Psychiatry* **49 Suppl**, 40-45 (1988).
110 Brar, J., Sidana, A., Chauhan, N. & Bajaj, M. K. A randomized, open-label pilot trial of selective serotonin reuptake inhibitors on neuropsychological functions in patients with obsessive compulsive disorder. *J. Psychiatr. Res.* **151**, 439-444 (2022).
111 Tseng, K. C. *et al.* Antidepressant Sertraline Is a Broad-Spectrum Inhibitor of Enteroviruses Targeting Viral Entry through Neutralization of Endolysosomal Acidification. *Viruses* **14** (2022).
112 Li, W. *et al.* Discovery of Novel Sertraline Derivatives as Potent Anti-Cryptococcus Agents. *J. Med. Chem.* **65**, 6541-6554 (2022).
113 Nykamp, M. J. *et al.* Opportunities for Drug Repurposing of Serotonin Reuptake Inhibitors: Potential Uses in Inflammation, Infection, Cancer, Neuroprotection, and Alzheimer's Disease Prevention. *Pharmacopsychiatry* **55**, 24-29 (2022).
114 Vardanyan, R. & Hruby, V. Antidepressants. in *Synthesis of Best-Seller Drugs* Ch. 7, 111-143 (Academic Press, 2016).
115 Takano, S., Yanase, M., Sugihara, T. & Ogasawara, K. Enantiodivergent route to the aromatic bisabolane sesquiterpenes by regio- and stereo-controlled epoxide opening. *J. Chem. Soc., Chem. Commun.*, 1538-1540 (1988).
116 Takaya, Y., Senda, T., Kurushima, H., Ogasawara, M. & Hayashi, T. Rhodium-catalyzed asymmetric 1,4-addition of arylboron reagents to α,β-unsaturated esters. *Tetrahedron: Asymmetry* **10**, 4047-4056 (1999).
117 Snieckus, V. Directed Ortho Metalation - Tertiary Amide and O-Carbamate Directors in Synthetic Strategies for Polysubstituted Aromatics. *Chem. Rev.* **90**, 879-933 (1990).
118 Cummings, S. R. *et al.* Lasofoxifene in Postmenopausal Women with Osteoporosis. *New England Journal of Medicine* **362**, 686-696 (2010).
119 Gennari, L., Merlotti, D., Stolakis, K. & Nuti, R. Lasofoxifene, from the preclinical drug discovery to the treatment of postmenopausal osteoporosis. *Expert Opinion on Drug Discovery* **6**, 205-217 (2011).
120 Lainé, M. *et al.* Lasofoxifene as a potential treatment for therapy-resistant ER-positive metastatic breast cancer. *Breast Cancer Research* **23**, 54 (2021).
121 Lloyd, M. R., Wander, S. A., Hamilton, E., Razavi, P. & Bardia, A. Next-generation selective estrogen receptor degraders and other novel endocrine therapies for management of metastatic hormone receptor-positive breast cancer: current and emerging role. *Therapeutic Advances in Medical Oncology* **14**, 17588359221113694 (2022).
122 Gennari, L., Merlotti, D. & Nuti, R. Selective estrogen receptor modulator (SERM) for the treatment of osteoporosis in postmenopausal women: focus on lasofoxifene. *Clin. Interv. Aging.* **5**, 19-29 (2010).

123 Zanotti-Gerosa, A., Gazić Smilović, I. & Časar, Z. Acid promoted Ir–P^N complex catalyzed hydrogenation of heavily hindered 3,4-diphenyl-1,2-dihydronaphthalenes: asymmetric synthesis of lasofoxifene tartrate. *Org. Chem. Front.* **4**, 2311-2322 (2017).
124 Biosca, M., Diéguez, M. & Zanotti-Gerosa, A. Chapter Five - Asymmetric hydrogenation in industry. in *Advances in Catalysis* Vol. 68 341-383 (Academic Press, 2021).
125 Kraft, S., Ryan, K. & Kargbo, R. B. Recent Advances in Asymmetric Hydrogenation of Tetrasubstituted Olefins. *J. Am. Chem. Soc.* **139**, 11630-11641 (2017).
126 Schrems, M. G., Neumann, E. & Pfaltz, A. Iridium-Catalyzed Asymmetric Hydrogenation of Unfunctionalized Tetrasubstituted Olefins. *Angew. Chem. Int. Ed.* **46**, 8274-8276 (2007).
127 Li, J.-Q., Quan, X. & Andersson, P. G. Highly Enantioselective Iridium-Catalyzed Hydrogenation of α,β-Unsaturated Esters. *Chemistry – A European Journal* **18**, 10609-10616 (2012).
128 Jagtap, S., Kaji, Y., Fukuoka, A. & Hara, K. High density monolayer of diisocyanide on gold surface as a platform of supported Rh-catalyst for selective 1,4-hydrogenation of α,β-unsaturated carbonyl compounds. *Chem. Comm.* **50**, 5046-5048 (2014).
129 Randad, R. S. & Kulkarni, G. H. Transformations of (+)-Citronellal into Insecticidal Esters Related to Cut-up Chrysanthemates. *Indian J. Chem.* **22**, 795-801 (1983).
130 Wang, W.-T. *et al.* Cooperative catalysis-enabled C–N bond cleavage of biaryl lactams with activated isocyanides. *Chem. Comm.* **58**, 6292-6295 (2022).
131 Tong, X., Schneck, F. & Fu, G. C. Catalytic Enantioselective alpha-Alkylation of Amides by Unactivated Alkyl Electrophiles. *J. Am. Chem. Soc.* **144**, 14856-14863 (2022).
132 Heravi, M. M. & Zadsirjan, V. Oxazolidinones as chiral auxiliaries in asymmetric aldol reactions applied to total synthesis. *Tetrahedron: Asymmetry* **24**, 1149-1188 (2013).
133 Diaz-Muñoz, G., Miranda, I. L., Sartori, S. K., de Rezende, D. C. & Alves Nogueira Diaz, M. Use of chiral auxiliaries in the asymmetric synthesis of biologically active compounds: A review. *Chirality* **31**, 776-812 (2019).
134 Gröger, H. Enzymatic Routes to Enantiomerically Pure Aromatic α-Hydroxy Carboxylic Acids: A Further Example for the Diversity of Biocatalysis. *Adv. Synth. Catal.* **343**, 547-558 (2001).
135 Matsuo, J.-i. & Murakami, M. The Mukaiyama Aldol Reaction: 40 Years of Continuous Development. *Angew. Chem. Int. Ed.* **52**, 9109-9118 (2013).
136 Kan, S. B. J., Ng, K. K. H. & Paterson, I. The Impact of the Mukaiyama Aldol Reaction in Total Synthesis. *Angew. Chem. Int. Ed.* **52**, 9097-9108 (2013).
137 Tang, H. *et al.* Beta-tetrazolyl-propionic acids as metallo-beta-lactamase inhibitors. US patent 9,839,642 (2017).
138 Zuo, Z. *et al.* Dual catalysis. Merging photoredox with nickel catalysis: coupling of alpha-carboxyl sp(3)-carbons with aryl halides. *Science* **345**, 437-440 (2014).
139 Prieto Kullmer, C. N. *et al.* Accelerating reaction generality and mechanistic insight through additive mapping. *Science* **376**, 532-539 (2022).
140 Lingyi Kong, J. L., Chao Han, Xiaobing Wang, Hao Hong. R type resveratrol dimer, preparation method therefor and use thereof in reducing blood sugar. European Patent Office patent EP3009429A1 (2016).

141 Ling, T. & Rivas, F. All-carbon quaternary centers in natural products and medicinal chemistry: recent advances. *Tetrahedron* **72**, 6729-6777 (2016).
142 Bartholow, M. Top 200 drugs of 2011. *Pharmacy Times* **78** (2012).
143 Susse, L. & Stoltz, B. M. Enantioselective Formation of Quaternary Centers by Allylic Alkylation with First-Row Transition-Metal Catalysts. *Chem. Rev.* **121**, 4084-4099 (2021).
144 Wang, Z. X. & Li, B. J. Construction of Acyclic Quaternary Carbon Stereocenters by Catalytic Asymmetric Hydroalkynylation of Unactivated Alkenes. *J. Am. Chem. Soc.* **141**, 9312-9320 (2019).
145 Feng, J., Holmes, M. & Krische, M. J. Acyclic Quaternary Carbon Stereocenters via Enantioselective Transition Metal Catalysis. *Chem. Rev.* **117**, 12564-12580 (2017).
146 Li, B.-J. & Sun, X. Acyclic Quaternary Carbon Stereocenters through Transition-Metal-Catalyzed Enantioselective Functionalization of Unsaturated Hydrocarbons. *Synthesis* **54**, 2103-2118 (2022).
147 Pohlman, M., Kazmaier, U. & Lindner, T. Allylic alkylation versus Michael induced ring closure: chelated enolates as versatile nucleophiles. *J. Org. Chem.* **69**, 6909-6912 (2004).
148 Zhuo, N., Ma, J., Cao, L., Chen, L. & Nan, F. Protecting-Group-Free One-Step Palladium-Catalyzed Coupling on C25 of Cucurbitacin B Expands Chemical Diversity with Improved Cytotoxicity against A549 Cells. *Chin. J. Chem .* **40**, 1662-1666 (2022).
149 Bandyopadhyay, S. *et al.* Substituted cathechols as inhibitors of IL-4 and IL-5 for the treatment of bronchial asthma. United States patent US9302967B2 (2020).
150 Lönn, H. R. *et al.* Certain (2s)-n-[(1s)-1-cyano-2-phenylethyl]-1, 4-oxazepane-2-carboxamides as dipeptidyl peptidase 1 inhibitors. United States patent US20230085620A1 (2023).
151 Sivanandan, S. T., Shaji, A., Ibnusaud, I., Seechurn, C. C. C. J. & Colacot, T. J. Palladium-Catalyzed α-Arylation Reactions in Total Synthesis. *Eur. J. Org. Chem.* **2015**, 38-49 (2015).
152 Landoni, M. F. & Soraci, A. Pharmacology of chiral compounds: 2-arylpropionic acid derivatives. *Curr. Drug. Metab.* **2**, 37-51 (2001).
153 Johansson, C. C. & Colacot, T. J. Metal-catalyzed alpha-arylation of carbonyl and related molecules: novel trends in C-C bond formation by C-H bond functionalization. *Angew. Chem. Int. Ed.* **49**, 676-707 (2010).
154 Bellina, F. & Rossi, R. Transition metal-catalyzed direct arylation of substrates with activated sp3-hybridized C-H bonds and some of their synthetic equivalents with aryl halides and pseudohalides. *Chem. Rev.* **110**, 1082-1146 (2010).
155 Ostrowska, S., Scattolin, T. & Nolan, S. P. N-Heterocyclic carbene complexes enabling the alpha-arylation of carbonyl compounds. *Chem. Comm.* **57**, 4354-4375 (2021).
156 Hao, Y.-J., Hu, X.-S., Zhou, Y., Zhou, J. & Yu, J.-S. Catalytic Enantioselective α-Arylation of Carbonyl Enolates and Related Compounds. *ACS Catal.* **10**, 955-993 (2019).
157 Hossain, M. M., Shaikh, A. C., Moutet, J. & Gianetti, T. L. Photocatalytic α-arylation of cyclic ketones. *Nat. Synth.* **1**, 147-157 (2022).
158 Ruffell, K., Argent, S. P., Ling, K. B. & Ball, L. T. Bismuth-Mediated alpha-Arylation of Acidic Diketones with ortho-Substituted Boronic Acids. *Angew. Chem. Int. Ed.* **61**, e202210840 (2022).

159 Li, J., Bauer, A., Di Mauro, G. & Maulide, N. alpha-Arylation of Carbonyl Compounds through Oxidative C-C Bond Activation. *Angew. Chem. Int. Ed.* **58**, 9816-9819 (2019).
160 Pan, Z. *et al.* Palladium/TY-Phos-Catalyzed Asymmetric Intermolecular alpha-Arylation of Aldehydes with Aryl Bromides. *Angew. Chem. Int. Ed.* **60**, 18542-18546 (2021).
161 van Heerden, P. S., Bezuidenhoudt, B. C. B. & Ferreira, D. Efficient Asymmetric Synthesis of the Four Diastereomers of Diphenacoum and Brodifacoum. *Tetrahedron* **53**, 6045-6056 (1997).
162 Jung, J. C., Lee, J. H., Oh, S., Lee, J. G. & Park, O. S. Synthesis and antitumor activity of 4-hydroxycoumarin derivatives. *Bioorg. Med. Chem. Lett.* **14**, 5527-5531 (2004).
163 Durieux, S. *et al.* Design and synthesis of 3-phenyltetrahydronaphthalenic derivatives as new selective MT2 melatoninergic ligands. Part II. *Bioorg. Med. Chem.* **17**, 2963-2974 (2009).
164 Schwarz, M. *et al.* Exploring the synthetic potential of a marine transaminase including discrimination at a remote stereocentre. *Org. Biomol. Chem.* **19**, 188-198 (2021).
165 Devkota, K. P., Covell, D., Ransom, T., McMahon, J. B. & Beutler, J. A. Growth inhibition of human colon carcinoma cells by sesquiterpenoids and tetralones of Zygogynum calothyrsum. *J. Nat. Prod.* **76**, 710-714 (2013).
166 Izawa, M., Kimata, S., Maeda, A., Kawasaki, T. & Hayakawa, Y. Functional analysis of hatomarubigin biosynthesis genes and production of a new hatomarubigin using a heterologous expression system. *J. Antibiot.* **67**, 159-162 (2014).
167 Wang, K. W., Mao, J. S., Tai, Y. P. & Pan, Y. J. Novel skeleton terpenes from Celastrus hypoleucus with anti-tumor activities. *Bioorg. Med. Chem. Lett.* **16**, 2274-2277 (2006).
168 Loder, J. W., Eibl, R., Falkiner, M. J., Nearn, R. H. & Parr, R. W. Carbocyclic analogues of equol for the immunization of sheep against clover disease. I. Hydroxynaphthalenones. *Aust. J. Chem.* **31**, 1011-1019 (1978).
169 So Ha, L., Sang gi, L., Choong Eui, S., In, O. K. & Bong Young, C. Toward the Development of New Class of Fungicides: Synthesis and Antifungal Activity of 3,4-Diphenylbutanoic acids. *The Korean Journal of Medicinal Chemistry* **7**, 34-40 (1997).
170 Gauni, B., Mehariya, K., Shah, A. & Duggirala, S. M. Tetralone Scaffolds and Their Potential Therapeutic Applications. *Letters in Drug Design & Discovery* **18**, 222-238 (2021).
171 Cui, L. Q., Dong, Z. L., Liu, K. & Zhang, C. Design, synthesis, structure, and dehydrogenation reactivity of a water-soluble o-iodoxybenzoic acid derivative bearing a trimethylammonium group. *Org. Lett.* **13**, 6488-6491 (2011).
172 Yang, T.-F., Wang, K.-Y., Li, H.-W., Tseng, Y.-C. & Lien, T.-C. Synthesis of substituted α-tetralones and substituted 1-naphthols via regioselective ring expansion of 1-acyl-1-indanol skeleton. *Tetrahedron Lett.* **53**, 585-588 (2012).
173 Ishida, N., Sawano, S. & Murakami, M. Synthesis of 3,3-disubstituted alpha-tetralones by rhodium-catalysed reaction of 1-(2-haloaryl)cyclobutanols. *Chem. Comm.* **48**, 1973-1975 (2012).
174 Odagi, M. *et al.* Origin of stereocontrol in guanidine-bisurea bifunctional organocatalyst that promotes alpha-hydroxylation of tetralone-derived beta-ketoesters: asymmetric synthesis of beta- and gamma-substituted tetralone

derivatives via organocatalytic oxidative kinetic resolution. *J. Am. Chem. Soc.* **137**, 1909-1915 (2015).
175 Johnson, K. F., Schmidt, A. C. & Stanley, L. M. Rhodium-Catalyzed, Enantioselective Hydroacylation of ortho-Allylbenzaldehydes. *Org. Lett.* **17**, 4654-4657 (2015).
176 Landwehr, E. M. *et al.* Concise syntheses of GB22, GB13, and himgaline by cross-coupling and complete reduction. *Science* **375**, 1270-1274 (2022).
177 Hayes, H. L. D. *et al.* Protodeboronation of (Hetero)Arylboronic Esters: Direct versus Prehydrolytic Pathways and Self-/Auto-Catalysis. *J. Am. Chem. Soc.* **143**, 14814-14826 (2021).
178 Lennox, A. J. & Lloyd-Jones, G. C. Selection of boron reagents for Suzuki-Miyaura coupling. *Chem. Soc. Rev.* **43**, 412-443 (2014).
179 Hayashi, T., Takahashi, M., Takaya, Y. & Ogasawara, M. Catalytic cycle of rhodium-catalyzed asymmetric 1,4-addition of organoboronic acids. Arylrhodium, oxa-pi-allylrhodium, and hydroxorhodium intermediates. *J. Am. Chem. Soc.* **124**, 5052-5058 (2002).
180 Nishihara, Y., Nishide, Y. & Osakada, K. Synthesis and reactivity of boryloxorhodium complexes. Relevance to intermolecular transmetalation from boron to rhodium in Rh-catalyzed reactions. *Dalton Trans.* **50**, 3610-3615 (2021).
181 Zhao, P., Incarvito, C. D. & Hartwig, J. F. Directly observed transmetalation from boron to rhodium. beta-aryl elimination from Rh(I) arylboronates and diarylborinates. *J. Am. Chem. Soc.* **129**, 1876-1877 (2007).
182 Partyka, D. V. Transmetalation of unsaturated carbon nucleophiles from boron-containing species to the mid to late d-block metals of relevance to catalytic C-X coupling reactions (X = C, F, N, O, Pb, S, Se, Te). *Chem. Rev.* **111**, 1529-1595 (2011).
183 Sakuma, S., Sakai, M., Itooka, R. & Miyaura, N. Asymmetric conjugate 1,4-addition of arylboronic acids to alpha, beta-unsaturated esters catalyzed by Rhodium(I)/(S)-binap. *J. Org. Chem.* **65**, 5951-5955 (2000).
184 Barlaam, B. C. & Piser, T. M. Estrogen receptor-β ligands. United States patent US6518301B1 (2003).
185 Theunissen, C., Ashley, M. A. & Rovis, T. Visible-Light-Controlled Ruthenium-Catalyzed Olefin Metathesis. *J. Am. Chem. Soc.* **141**, 6791-6796 (2019).
186 Aggarwal, V. K., Fulton, J. R., Sheldon, C. G. & de Vicente, J. Generation of phosphoranes derived from phosphites. A new class of phosphorus ylides leading to high E selectivity with semi-stabilizing groups in Wittig olefinations. *J. Am. Chem. Soc.* **125**, 6034-6035 (2003).
187 Brown, S. P. *et al.* Substituted biphenyl GPR40 modulators. United States patent US8030354B2 (2011).
188 Tsuchiya, Y. *et al.* Substituted heterocyclic derivative having squalene epoxidase inhibition action and its use. United States patent US5444084A (1995).
189 Yadav, J. S., Basak, A. K. & Srihari, P. An aldol approach to the synthesis of the anti-tubercular agent erogorgiaene. *Tetrahedron Lett.* **48**, 2841-2843 (2007).
190 Do, H. Q., Chandrashekar, E. R. & Fu, G. C. Nickel/bis(oxazoline)-catalyzed asymmetric Negishi arylations of racemic secondary benzylic electrophiles to generate enantioenriched 1,1-diarylalkanes. *J. Am. Chem. Soc.* **135**, 16288-16291 (2013).
191 Kc, S., Dhungana, R. K., Khanal, N. & Giri, R. Nickel-Catalyzed alpha-Carbonylalkylarylation of Vinylarenes: Expedient Access to gamma,gamma-Diarylcarbonyl and Aryltetralone Derivatives. *Angew. Chem. Int. Ed.* **59**, 8047-8051 (2020).

192 Alexakis, A., Hajjaji, S. E., Polet, D. & Rathgeb, X. Iridium-catalyzed asymmetric allylic substitution with aryl zinc reagents. *Org. Lett.* **9**, 3393-3395 (2007).
193 Fernandes, R. A., Gangani, A. J. & Kunkalkar, R. A. Metal-free annulative hydrosulfonation of propiolate esters: synthesis of 4-sulfonates of coumarins and butenolides. *New J. Chem.* **44**, 3970-3984 (2020).
194 Kojima, N., Nishijima, S., Tsuge, K. & Tanaka, T. Asymmetric alkynylation of aldehydes with propiolates without high reagent loading and any additives. *Org. Biomol. Chem.* **9**, 4425-4428 (2011).
195 Ramón, R. S., Pottier, C., Gómez-Suárez, A. & Nolan, S. P. Gold(I)-Catalyzed Tandem Alkoxylation/Lactonization of γ-Hydroxy-α,β-Acetylenic Esters. *Adv. Synth. Catal.* **353**, 1575-1583 (2011).
196 Trost, B. M. & Quintard, A. Asymmetric catalytic synthesis of the proposed structure of trocheliophorolide B. *Org. Lett.* **14**, 4698-4700 (2012).
197 Tsui, G. C., Villeneuve, K., Carlson, E. & Tam, W. Ruthenium-Catalyzed [2+2] Cycloadditions between Norbornene and Propargylic Alcohols or Their Derivatives. *Organometallics* **33**, 3847-3856 (2014).
198 Downey, C. W., Mahoney, B. D. & Lipari, V. R. Trimethylsilyl Trifluoromethanesulfonate-Accelerated Addition of Catalytically Generated Zinc Acetylides to Aldehydes. *J. Org. Chem.* **74**, 2904-2906 (2009).
199 Du, Z. *et al.* Enantioselective synthesis of (+)-nuciferal, (+)-(E)-nuciferol and (+)-α-curcumene by chiral hydrogenesterification reaction. *J. Chem. Res.* **2004**, 427-429 (2004).
200 Nguyen, T. N. T., Thiel, N. O. & Teichert, J. F. Copper(i)-catalysed asymmetric allylic reductions with hydrosilanes. *Chem. Commun.* **53**, 11686-11689 (2017).
201 Garcia Ruano, J. L., Schopping, C., Alvarado, C. & Aleman, J. Synthesis of unfunctionalized carbonated fragments containing two vicinal chiral centers: stereocontrolled benzylation of vinylsulfones mediated by a remote sulfinyl group. *Chem. Eur. J.* **16**, 8968-8971 (2010).
202 Aggarwal, V. K. *et al.* Application of the lithiation-borylation reaction to the rapid and enantioselective synthesis of the bisabolane family of sesquiterpenes. *Chem. Commun.* **48**, 9230-9232 (2012).
203 Wu, L. *et al.* Asymmetric synthesis of (R)-ar-curcumene, (R)-4,7-dimethyl-l-tetralone, and their enantiomers via cobalt-catalyzed asymmetric Kumada cross-coupling. *Tetrahedron: Asymmetry* **27**, 78-83 (2016).
204 Skotnitzki, J. *et al.* Stereoselective Csp(3)-Csp(2) Cross-Couplings of Chiral Secondary Alkylzinc Reagents with Alkenyl and Aryl Halides. *Angew. Chem. Int. Ed.* **59**, 320-324 (2020).
205 Chavan, S. P. & Khatod, H. S. Enantioselective synthesis of the essential oil and pheromonal component ar-himachalene by a chiral pool and chirality induction approach. *Tetrahedron: Asymmetry* **23**, 1410-1415 (2012).
206 Elford, T. G., Nave, S., Sonawane, R. P. & Aggarwal, V. K. Total synthesis of (+)-erogorgiaene using lithiation-borylation methodology, and stereoselective synthesis of each of its diastereoisomers. *J. Am. Chem. Soc.* **133**, 16798-16801 (2011).
207 Takayama, H. *et al.* Discovery of inhibitors of the Wnt and Hedgehog signaling pathways through the catalytic enantioselective synthesis of an iridoid-inspired compound collection. *Angew. Chem. Int. Ed.* **52**, 12404-12408 (2013).
208 Shimokawa, J., Harada, T., Yokoshima, S. & Fukuyama, T. Total synthesis of gelsemoxonine. *J. Am. Chem. Soc.* **133**, 17634-17637 (2011).

209 Wang, H. Y., Yang, K., Bennett, S. R., Guo, S. R. & Tang, W. Iridium-Catalyzed Dynamic Kinetic Isomerization: Expedient Synthesis of Carbohydrates from Achmatowicz Rearrangement Products. *Angew. Chem. Int. Ed.* **54**, 8756-8759 (2015).
210 Turrini, N. G. *et al.* Biocatalytic access to nonracemic γ-oxo esters via stereoselective reduction using ene-reductases. *Green Chem.* **19**, 511-518 (2017).
211 Brenna, E. *et al.* Biocatalytic synthesis of chiral cyclic γ-oxoesters by sequential C–H hydroxylation, alcohol oxidation and alkene reduction. *Green Chem.* **19**, 5122-5130 (2017).
212 Shukla, K. H. & DeShong, P. Studies on the mechanism of allylic coupling reactions: a hammett analysis of the coupling of aryl silicate derivatives. *J. Org. Chem.* **73**, 6283-6291 (2008).
213 Son, S. & Fu, G. C. Nickel-catalyzed asymmetric Negishi cross-couplings of secondary allylic chlorides with alkylzincs. *J. Am. Chem. Soc.* **130**, 2756-2757 (2008).
214 Rodríguez, S., Vidal, A., Monroig, J. J. & González, F. V. Diastereoselectivity in the epoxidation of γ-hydroxy α,β-unsaturated esters: temperature and solvent effect. *Tetrahedron Lett.* **45**, 5359-5361 (2004).
215 Prudel, C., Huwig, K. & Kazmaier, U. Stereoselective Allylic Alkylations of Amino Ketones and Their Application in the Synthesis of Highly Functionalized Piperidines. *Chem. Eur. J.* **26**, 3181-3188 (2020).
216 Tsai, M.-S., Rao, U. N., Wang, J.-R., Liang, C.-H. & Yeh, M.-C. P. Triphenylphosphine-Mediated Reduction of Electron-Deficient Propargyl Ethers to the Allylic Ethers. *J. Chin. Chem. Soc.* **48**, 869-876 (2001).
217 Reddy, M. P. & Rao, G. S. K. Synthesis of 5-P-Hydroxybenzyl-5,6-Dihydro-2-Naphthol, (+/-)-Sequirin-D. *J. Chem. Soc. Perk. T 1*, 2662-2665 (1981).
218 Xu, S. *et al.* Asymmetric syntheses and bio-evaluation of novel chiral esters derived from substituted tetrafluorobenzyl alcohol. *Bioorg. Med. Chem. Lett.* **24**, 2734-2736 (2014).